Unfolding the Hsp90 Foldasome: Structure-Activity Relationship Studies on EGCG and Development of Isoform-Selective Inhibitors

Unfolding the Hsp90 Foldasome: Structure-Activity Relationship Studies on EGCG and Development of Isoform-Selective Inhibitors

By

Anuj Khandelwal

Submitted to the graduate degree program in Medicinal Chemistry and the Graduate Faculty of the University of Kansas in partial fulfillment of the requirements for the degree of Doctor of Philosophy.

_____

Brian S. J. Blagg, Ph.D.
Chairperson

_____

Ryan A. Altman, Ph.D.

_____

Apurba Dutta, Ph.D.

_____

Paul R. Hanson, Ph.D.

_____

Rick T. Dobrowsky, Ph.D.

Date Defended: June 9th, 2016

The Dissertation Committee for Anuj Khandelwal
certifies that this is the approved version of the following dissertation:

Unfolding the Hsp90 Foldasome: Structure-Activity Relationship Studies on EGCG and Development of Isoform-Selective Inhibitors

_____

Brian S. J. Blagg, Ph.D.
Chairperson

Date approved: June 13th, 2016

Abstract

The 90 kDa heat shock proteins (Hsp90) are critical for the maintenance of cellular homeostasis and mitigate the effects of cellular stress and therefore, play an important role in cell survival. Hsp90, as a molecular chaperone, folds nascent polypeptides and denatured proteins to their biologically relevant conformations. Many of the proteins dependent upon Hsp90 are essential to the growth and proliferation of cancer cells. In fact, proteins associated with all ten hallmarks of cancer are dependent upon the Hsp90 protein folding machinery. Consequently, inhibition of Hsp90 represents a combinatorial approach for the treatment of cancer. 17 small molecule inhibitors of Hsp90 have entered clinical trials, all of which bind Hsp90 N-terminus and exhibit *pan*-inhibitory activity against the four Hsp90 isoforms: Hsp90α, Hsp90β, Grp94, and Trap1. However, lack of isoform selectivity with current clinical candidates appears detrimental as more than 20 clinical trials have failed, citing hepatotoxicity, cardiotoxicity, and peripheral neuropathy amongst other side effects. Additionally, *pan*-inhibition of Hsp90 induces the pro-survival heat shock response, requiring the escalation of patient doses to overcome increased Hsp90 expression. Therefore, alternative approaches for Hsp90 modulation are highly sought after.

Isoform-selective inhibition of Hsp90 provides an opportunity to address the aforementioned detriments associated with pan-Hsp90 N-terminal inhibitors. Hydrolysis of ATP by the N-terminal nucleoside binding pocket is required for the maturation of client protein substrates, and all four Hsp90's share >85% identity within this region. Consequently, the discovery of isoform-selective inhibitors has been challenging. Described herein is the rationale for development of isoform selective inhibitors and the identification of the first isoform selective inhibitors of Hsp90α and Hsp90β-isoforms.

Unlike the N-terminus, inhibition of the Hsp90 C-terminus does not induce the heat shock response and hence, C-terminal inhibitors manifest the desired cytotoxic affect against cancer cells. However, absence of a co-crystal structure and lack of lead compounds, have resulted in limited success towards the development of Hsp90 C-terminal inhibitors. Recently, EGCG, a green tea polyphenol, was shown to bind at the C-terminus of Hsp90. Structure activity relationships studies were conducted on EGCG for improved Hsp90 inhibition and are also presented.

Acknowledgments

I am extremely grateful to those who helped me throughout my graduate career. First, I would like to thank my advisor Dr. Brian S. J. Blagg to giving me the opportunity to work under his supervision. As a mentor, Brian allowed me to work independently but was always available to provide guidance, knowledge, motivation and inspiration when needed.

I would like to acknowledge my family for their undying motivation and encouragement. I am beyond grateful to my parents as they continuously believed in me and supported my decision to pursue a career in research. I would not be where I am today without their support. I am also grateful to my wife Anshul Khandelwal for supporting my passion for research and showing great understanding as I finished my graduate career.

I would also like to thank my fellow lab members Leah Forsberg, Vincent Crowley, Sanket Mishra, and Caitlin Kent, who were a great resource of scientific wisdom but also are great friends outside of laboratory, making my experience at KU enjoyable. Outside of the Blagg laboratory, I am thankful to other department faculty members and graduate students who greatly influenced my career. Specifically, Dr. Ryan Altman for mentoring and Brett Ambler for insightful scientific discussions.

I must thank the department of Medicinal Chemistry for the exemplary training I received during my graduate career. I would also like to thank Dr. Apurba Dutta, Dr. Paul Hanson, Dr. Ryan Altman, and Dr. Rick Dobrowsky for serving on my committee and providing thoughtful suggestions.

I dedicate this work to my uncle Subhash Khandelwal (1965-2010), who always inspired and motivated me to follow my dreams.

Table of Contents

Chapter I
Hsp90 and Its Natural Product-Based Inhibitors

Chapter II
Synthesis and Structure−Activity Relationships of EGCG Analogues

Chapter III
The Development of Grp94-Selective Inhibitors

Chapter IV
Development of the First Hsp90β-Selective N-Terminal Inhibitor

Chapter V
The Development of Hsp90α-Selective Inhibitors

List of Figures:

Chapter I
Hsp90 and Its Natural Product-Based Inhibitors

Chapter II
Synthesis and Structure−Activity Relationships of EGCG Analogues

Chapter III
The Development of Grp94-Selective Inhibitors

Chapter IV
Development of the First Hsp90β-Selective N-Terminal Inhibitor

Chapter V
The Development of Hsp90α-Selective Inhibitors

List of Tables:

Chapter I
Hsp90 and Its Natural Product-Based Inhibitors

Chapter II
Synthesis and Structure−Activity Relationships of EGCG Analogues

Chapter III
The Development of Grp94-Selective Inhibitors

Chapter IV
Development of the First Hsp90β-Selective N-Terminal Inhibitor

Chapter V
The Development of Hsp90α-Selective Inhibitors

List of Schemes:

Chapter II
Synthesis and Structure−Activity Relationships of EGCG Analogues

Chapter III
The Development of Grp94-Selective Inhibitors

Chapter IV
Development of the First Hsp90β-Selective N-Terminal Inhibitor

Chapter V
The Development of Hsp90α-Selective Inhibitors

UNFOLDING THE HSP90 FOLDASOME: STRUCTURE-ACTIVITY RELATIONSHIP STUDIES ON EGCG AND DEVELOPMENT OF ISOFORM-SELECTIVE INHIBITORS

Chapter I

Hsp90 and Its Natural Product-Based Inhibitors

I. 1. Introduction

Molecular chaperones represent a class of proteins that are responsible for the conformational maturation of nascent polypeptides into their biologically active conformation, as well as the rematuration of denatured proteins. Molecular chaperones work together with co-chaperones and other partner proteins to facilitate the folding of protein substrates (foldasomes).[1-3] Many of these chaperones are overexpressed in response to conditions that cause cellular stress, such as hypoxia, acidosis, and increased/decreased temperature. Heat shock proteins, a class of molecular chaperones, were originally identified after cellular exposure to elevated temperatures, which led to their overexpression, to refold proteins that were denatured/aggregated at such temperatures.[4, 5] The 90 kDa heat shock protein (Hsp90) is highly conserved in eukaryotes and represents 1-2% of the total cellular protein at ambient temperatures, but can be overexpressed to comprise 6% in stressed cells.[6-8] Hsp90 is responsible for the maturation of more than 200 client proteins, including several therapeutically sought after anticancer targets, such as Her2, Raf, ALK, Src, and Akt.[6, 9] Due to its central role in oncogenesis, Hsp90 has emerged as a promising target for the development of anti-cancer agents.[4, 10-14]

Geldanamycin (GDA), an ansamycin class of antibiotic, is a classic example of natural product-based drug discovery in medicinal chemistry.[15] Analysis of the biological activity manifested by GDA led to the discovery that its primary biological target is the 90 kDa heat shock protein, Hsp90.[16] Many drug development campaigns with GDA have provided drug candidates that have entered clinical trials and yielded biological probes that have increased the understanding of Hsp90 biology.[17, 18] In the last two decades, other natural products have also been shown to bind

and modulate the Hsp90 chaperone machinery by various mechanisms.[19-31] These natural products have served as a starting point for numerous drug development campaigns, which led to the discovery of highly efficacious Hsp90 inhibitors.[14, 15, 32, 33]

I.2. Hsp90 Structure and Function

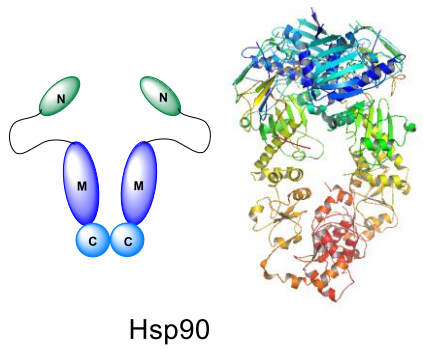

Figure 1. The structure of Hsp90. (PDB: 2CG9).

In cells, Hsp90 exists as a homodimer and each monomer consists of an N-terminal ATP-binding domain, a middle domain connected to the N-terminus by a charged linker, and a C-terminal dimerization motif (Figure 1).[34-37] ATP binds to the highly conserved N-terminus, and its hydrolysis provides the requisite energy to facilitate client protein maturation. The N-terminal ATP-binding site is conserved within the GHKL superfamily of proteins, such as Hsp90, histidine kinase, DNA gyrase B, and MutL.[38] The GHKL superfamily is characterized by the presence of Bergerat ATP-binding fold, in which ATP binds in a unique, bent conformation that is in contrast to the typical extended conformation.[39] The Bergerat motif consists of three α-helices in a helix-sheet-helix orientation and four interstranded β-sheets. The N-terminal ATP-binding site manifests interactions with residues in the loop region that connects to α-helices and β-sheets.[38] The middle domain plays a crucial role in client protein recognition, as well as interactions with co-chaperones and other partner proteins. The C-terminus mediates dimerization and contains a second nucleotide binding site. There are four isoforms of Hsp90 in mammals: Hsp90α and Hsp90β are localized in the cytosol, Grp94 is found in the endoplasmic reticulum and Trap-1 resides in the mitochondria. The Hsp90β isoform is constitutively expressed whereas, the

Hsp90α isoform is inducible upon exposure to cellular stress.[40, 41] In the human genome, there are 17 genes that encode for Hsp90, however, only six of them encode the four functional isoforms.[42]

I.2.1 Hsp90 Chaperone Cycle

The Hsp90 chaperone cycle is complex, but advances in technology and small molecule probes have provided insights into the catalytic cycle. Several other proteins (co-chaperones and partner proteins) associate with Hsp90 during the chaperone cycle and mediate the protein folding process (Table 1).[43-46] The Hsp90-mediated the protein folding process is catalytic and protein maturation is driven by ATP-hydrolysis (Figure 2).[47] Succinctly, the Hsp90 chaperone cycle begins with the delivery of nascent polypeptides to the Hsp90 complex by a Hsp70-Hsp40 complex (Figure 2.3). This process is mediated by the Hsp70-Hsp90 organizing co-chaperone, HOP (Figure 2.2). Upon delivery of the nascent polypeptide, various co-chaperones, immunophilins, and partner proteins interact with Hsp90 to form a heteroprotein complex (Figure 2.4). ATP is recruited to the N-terminus (Figure 2.5) and is then hydrolyzed upon p23 association (Figure 2.7). Association of p23 increases both the rate of ATP hydrolysis and client protein maturation. Following maturation, the client protein is released through opening of the C-terminal dimer interface and the heteroprotein complex dissociates to regenerate the Hsp90 homodimer (Figure 2.1).

I.2.2 Inhibition of Hsp90 Chaperone Cycle

Inhibition of either the N- or C-terminus can disrupt the Hsp90 chaperone cycle. Upon disruption of the chaperone cycle by an inhibitor, the client protein is degraded through the ubiquitin-proteasome pathway (Figure 2.6).[48] Because malignant cells undergo a constant rate of proliferation, increased rates of metabolism and protein synthesis are required for survival. This leads to an increased tumor dependency upon Hsp90. Therefore, Hsp90 exists primarily as the

heteroprotein complex (Figure 2.4) in malignant cells. Conversely, Hsp90 exists as the homodimer (Figure 2.1)

Table 1. Hsp90 co-chaperones and their function's

Co-chaperone/ Partner proteins	**Function**
Aha1	Stimulates ATPase activity
Cdc37	Mediates activation of protein kinase substrates
CHIP	Involved in degradation of unfolded client proteins
Cyclophilin-40	Peptidyl propyl isomerase
FKBP51 and 52	Peptidyl propyl isomerases
HOP	Mediates interaction between Hsp90 and Hsp70
Hsp40	Stabilizes and delivers client proteins to Hsp90 complex
Hsp70	Stabilizes and delivers client proteins to Hsp90 complex
p23	Stabilizes closed, clamped substrate bound conformation
HIP	Inhibits ATPase activity of Hsp70
PP5	Protein phosphatase
Sgt1	Client adaptor, involved in client recruitment
Tom70	Translocation of pre-proteins into mitochondrial matrix
WISp39	Regulates p21 stability

in unstressed or normal cells. Interestingly, the heteroprotein complex possesses more than 200-fold greater affinity for ATP, when compared to the Hsp90 homodimer. Therefore, inhibitors that bind the ATP-binding pocket exhibit an inherent selectivity for the heteroprotein complex, resulting in differential selectivity of ~200-fold for cancer verses normal cells.[11] Not surprisingly, Hsp90 inhibitors accumulate at higher concentrations in tumor tissues than in normal tissues. Hsp90 inhibition exhibits therapeutic potential for the treatment of many different diseases. Most notably, Hsp90 inhibitors are sought after as anti-cancer agents because many Hsp90-dependent client proteins are associated with oncogenic pathways that cause tumor initiation, tumor progression and metastasis. As shown in Table 2, Hsp90 client proteins are present in all 10 hallmarks of cancer, therefore, inhibition of Hsp90 provides a unique opportunity to

simultaneously disrupt multiple oncogenic pathways, and thus provides a multi-dimensional attack on cancer (a complete listing of Hsp90 clients can be found at http://www.picard.ch/downloads/Hsp90interactors.pdf). Hsp90 inhibitors manifest a single drug combination approach toward the treatment of cancer.[49, 50] Stimulation of Hsp's (Hsp70, Hsp40, Hsp27) by non-toxic molecules has potential therapeutic application in diseases caused by misfolded and aggregated proteins. Hence, Hsp90 modulation not only exhibits potential to treat cancer, but also several other unrelated disease states including Alzheimer's, Parkinson's, Amyotrophic lateral sclerosis, multiple sclerosis, Huntington's , and spinal and bulbar muscular atrophy.[51-53]

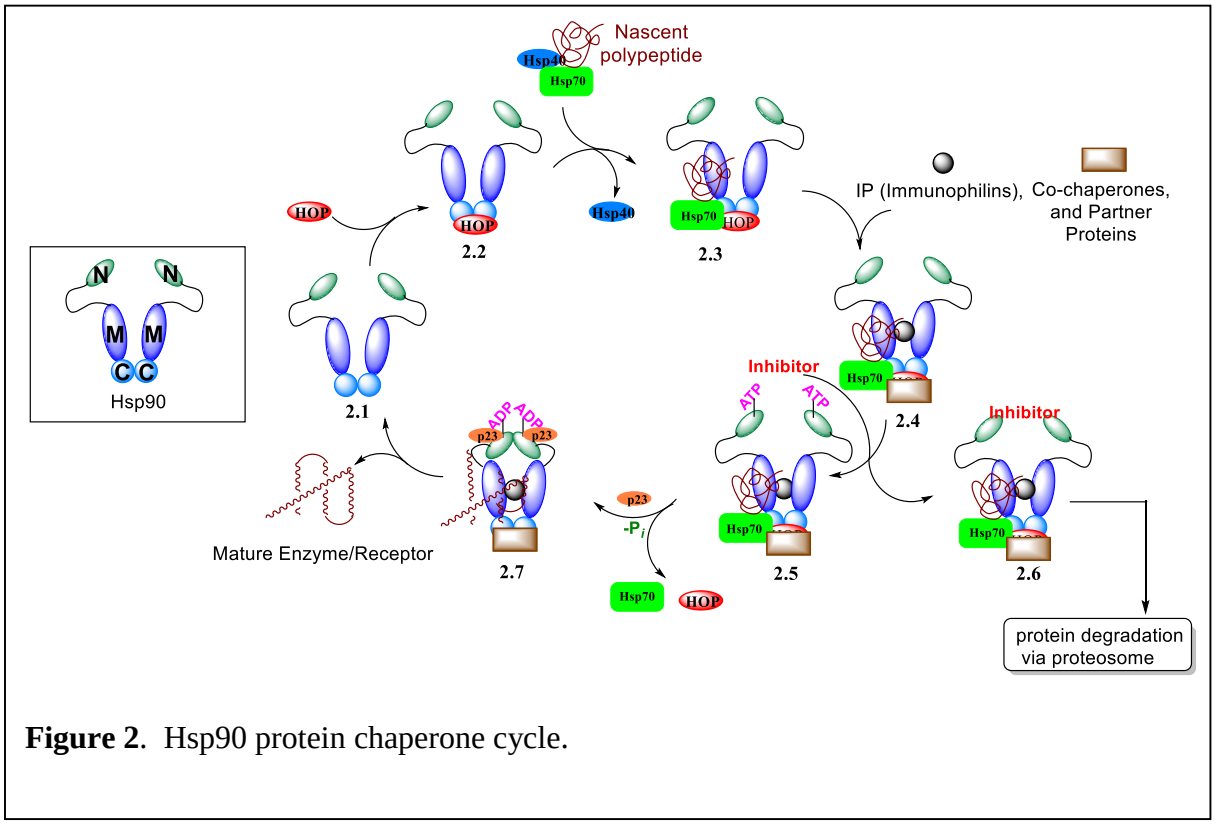

Figure 2. Hsp90 protein chaperone cycle.

Table 2. Ten hallmarks of cancer and associated Hsp90 clients

Hallmarks of Cancer	Hsp90 Client Protein(s)
1. Self-sufficiency in growth signals	Raf-1, AKT, Her2, MEK, Bcr-Abl
2. Insensitivity to anti-growth signals	Plk, Wee1, Myc1, CDK4, CDK6, Myt1
3. Evasion of apoptosis	RIP, AKT, p53, c-MET, Apaf-1, Survivin
4. Limitless replicative potential	Telomerase (h-Tert)
5. Sustained angiogenesis	FAK, AKT, Hif-1α, VEGFR, flt-3
6. Tissue invasion and Metastasis	C-MET
7. Deregulated cellular energetics	ARNT, HIF-1α, HMG1, SREBF1
8. Avoiding immune destruction	IRAK3
9. Tumor-promoting inflammation	IL-6, IL-8, IRAK1, IRAK2, IRAK3
10. Genome instability and mutation	FANCA, MAFG, NEK8, NEK9, NEK11

I.3. Hsp90 Inhibitors

The complexity of the Hsp90 chaperone cycle presents many opportunities to modulate Hsp90's activity. Hsp90 inhibitors can be broadly divided into three classes on the basis of their binding to Hsp90: (1) Hsp90 N-terminal inhibitors; (2) Hsp90 C-terminal inhibitors; and (3) disrupters of co-chaperone interactions (Figure 3).[4, 16, 19, 54-56] Natural products have played an essential role in the development of all three classes of inhibitors. At present, only N-terminal inhibitors have been evaluated in the clinic as anti-cancer agents. While N-terminal inhibition remains the most widely studied and sought after strategy, the latter two approaches are emerging as alternative strategies. [22, 57-59]

I.3.1. N-Terminal Inhibitors

I.3.1.1 Geldanamycin-Based Inhibitors

Geldanamycin (GDA) (Figure 3) was isolated from the *geldanus* variant of the filamentous soil bacterium, *Streptomyces hygroscopicus*, in 1970 and subsequently shown to manifest potent antibiotic and growth inhibitory activity against HeLa derived KB cancer cells.[60] In subsequent years, GDA manifested potent anti-tumor activity against a variety of other cancer cell lines. However, Hsp90 was not identified as the biological target of GDA until 1994, when Whitesell

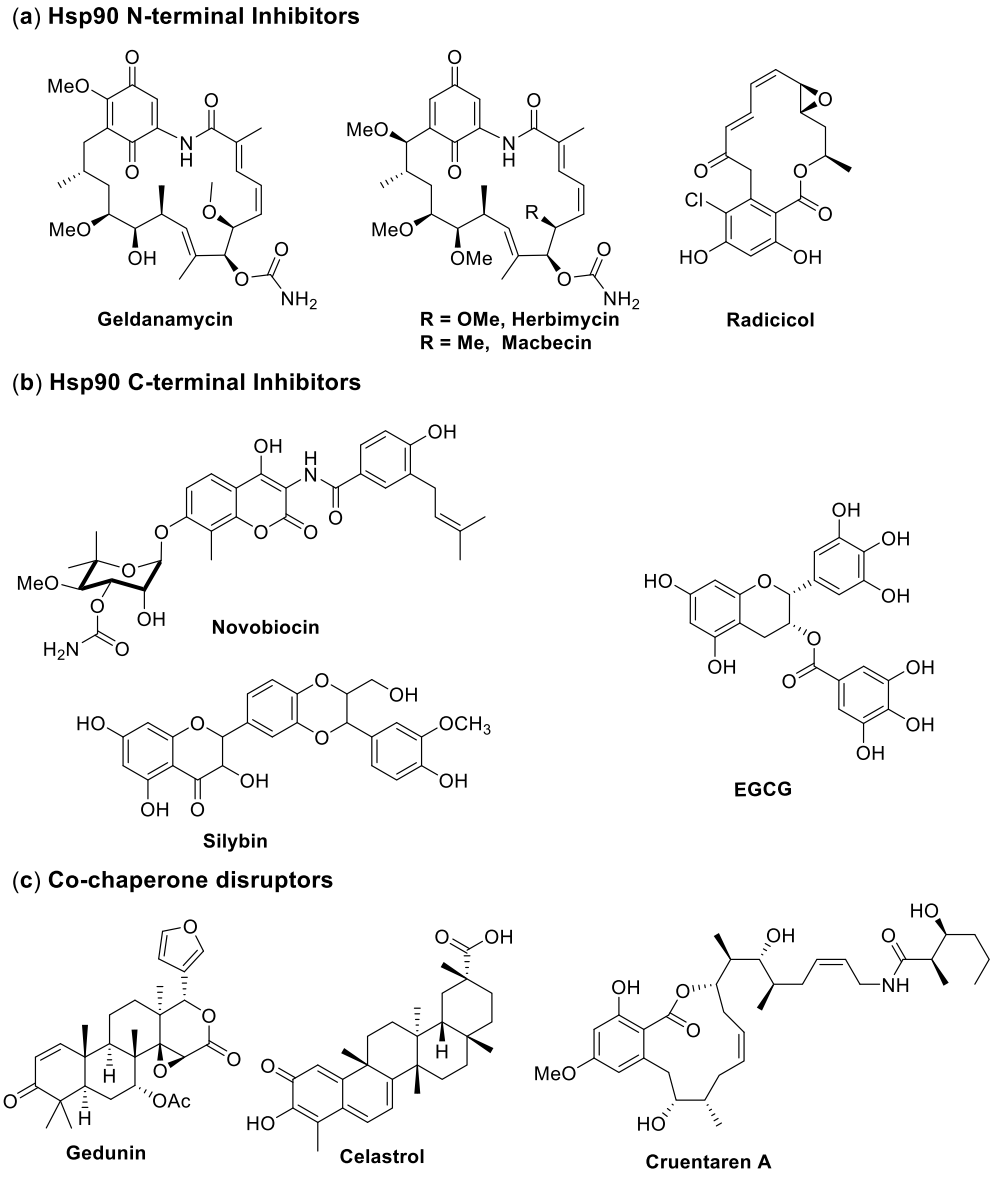

Figure 3. Representative Hsp90 inhibitors.

and co-workers demonstrated that GDA binds Hsp90 to induce the degradation of v-SRC, an oncogenic client protein of Hsp90.[16] Although GDA manifests excellent potency, its hepatotoxicity, low chemical stability, and poor bioavailability prevented it from advancing to clinical trials.[61] In order to produce new analogues with improved pharmacological properties, structure-activity relationship (SAR) studies on GDA have been pursued along with total synthesis, semi-synthesis, and genetic engineering of its biosynthetic pathway. These efforts have led to the development of derivatives that manifest superior pharmacokinetic and pharmacodynamic profiles.

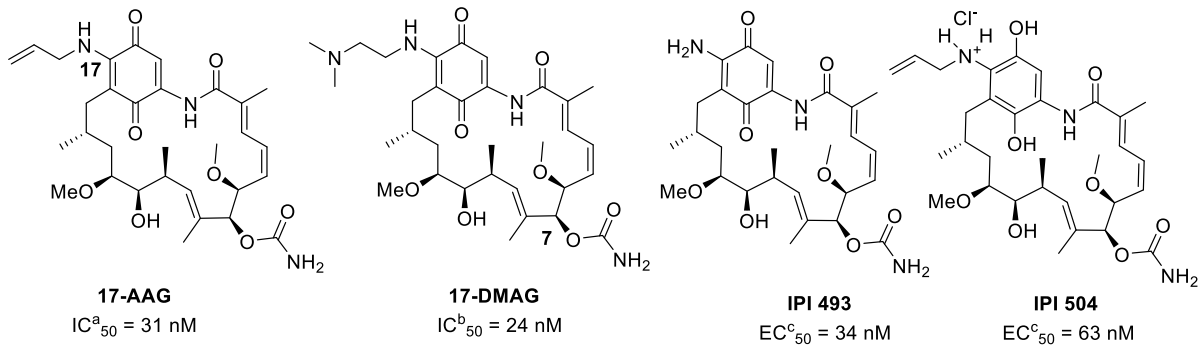

Figure 4. GDA-Analogues for improved Hsp90 inhibition. IC$^{a}_{50}$: Measured in p185 degradation assay (GDA: 70 nM); IC$^{b}_{50}$: measured in competitive binding assay in MCF-7 cell lysate (17-AAG: 20 nM); EC$^{c}_{50}$: measured Her2 degradation assay (GDA 5 nM).

The most efficacious analogues of GDA were produced by semi-synthesis that modified the 17-position.[17, 62-64] Due to the labile nature of the β-methoxy-α,β-unsaturated quinone, the 17-methoxy could be easily substituted with various nucleophiles to provide C-17 substituted analogues. Replacing the 17-methoxy with alkyl amines produced the greatest biological activities, which further stabilized the reactive quinone moiety. These efforts resulted in the development of 17-allylamino-GDA (17-AAG, Figure 4), which became the first Hsp90 inhibitor to enter in clinical trials. [65, 66]

Kosan Biosciences reported the synthesis of more than 60 analogues of the 17-position, as well as the C-7 carbamate during their pursuit of GDA analogues. Modifications to the carbamate decreased potency, as the carbamate provides key hydrogen bonding interactions with the N-terminal ATP-binding site of Hsp90.[67] From these studies, 17-(2-dimethylaminoethyl)amino-17-demethoxygeldanamycin (17-DMAG, Figure 4) was identified as a potent inhibitor of Hsp90 (IC_{50} = 24 nM) with excellent solubility. Subsequently 17-DMAG underwent clinical evaluation. 17-AAG undergoes cytochrome P450 3A4-mediated oxidation of the alpha methylene on the 17-amino substituent, resulting in subsequent hydrolysis of the C-N bond to produce the corresponding amine analogue (IPI-493, Figure 4). This metabolite manifests growth inhibitory activity against breast cancer cells (SKBr3) at 33 nM, which is similar to that of 17-AAG.[68] Consequently, Infinity Pharmaceuticals developed another water soluble GDA analogue, IPI-504 (Figure 4). For IPI-504, the hydroquinone was more water-soluble than the corresponding quinone and upon subsequent preclinical studies, IPI-504 was found to exhibit excellent properties, which led to its clinical evaluation.[69, 70] In 2006, Porter and co-workers reported the hydroquinone analogues (Figure 5). These analogues exhibited increased binding affinity for Hsp90 compared to the corresponding quinone. These studies paralleled prior studies with radicicol and geldanamycin chimeras.[64, 70]

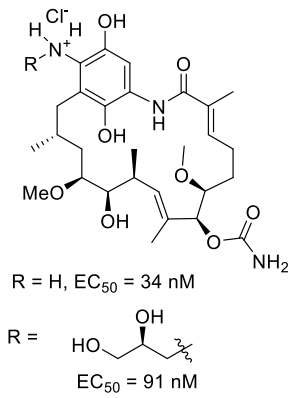

Figure 5. Hydroquinone analogues of GDA. EC_{50} measured in fluorescence polarization assay using BODIPY-GDA as probe (17-AAG: 119 nM).

The biological evaluation of GDA and its derivatives have provided significant insights into Hsp90's biological function, as well as established Hsp90 as a promising anti-cancer target. GDA has served as a starting point for several medicinal chemistry campaigns and as a result

several GDA analogues have advanced into clinical trials.[71-75] The current focus of GDA research has centered on addressing the toxicities associated with the benzoquinone moiety, as well as the use of GDA analogues in combination with other therapies in the clinic.

I.3.1.2. Radicicol-Based Inhibitors

The resorcinol lactone, radicicol (RDC, Figure 6) was originally isolated from *Monosporium bonorden* in 1953.[76] RDC manifested antifungal properties and was later found to exhibit anti-tumor properties. Similar to GDA, RDC was believed to be an inhibitor of the v-Src and Ras-Raf-MAPK signaling pathways.[24, 77] RDC exhibited a similar biological profile as GDA, and in 1998, Schulte and co-workers demonstrated that RDC competes with GDA, for binding to Hsp90. Subsequent experiments showed that, like GDA, RDC binds the N-terminal ATP-binding site of Hsp90; however RDC binds in a different orientation.[78, 79]

RDC manifests greater affinity for Hsp90 than GDA *in vitro* (K_d in ATPase assay, 19 nM vs. 1.2 μM, respectively). However, the administration of RDC *in vivo* does not produce anti-tumor activity, because RDC is rapidly metabolized to inactive metabolites due to its electrophilic nature (allylic epoxide and α,β,γ,δ-unsaturated ketone), which provides no *in vivo* activity.[80] Consequently, RDC was not considered a viable candidate for clinical evaluation.[81] In addition to RDC, less electrophilic natural products (Figure 6) Monocillin I, Pochonins A, and Pochonins D, have also been identified as Hsp90 inhibitors, although they manifest inferior affinity. [82-84]

RDC attracted the attention of several synthetic groups beginning in the early 1990s, and the first total synthesis was reported in 1992. [85, 86] Subsequent routes toward the natural product were also developed by the Winssinger and Danishefsky laboratories.[87-89] These total syntheses allowed for the preparation of the analogues with reduced electrophilicity and enhanced metabolic stability *in vivo*. One strategy to reduce the metabolic susceptibility of RDC was to replace the

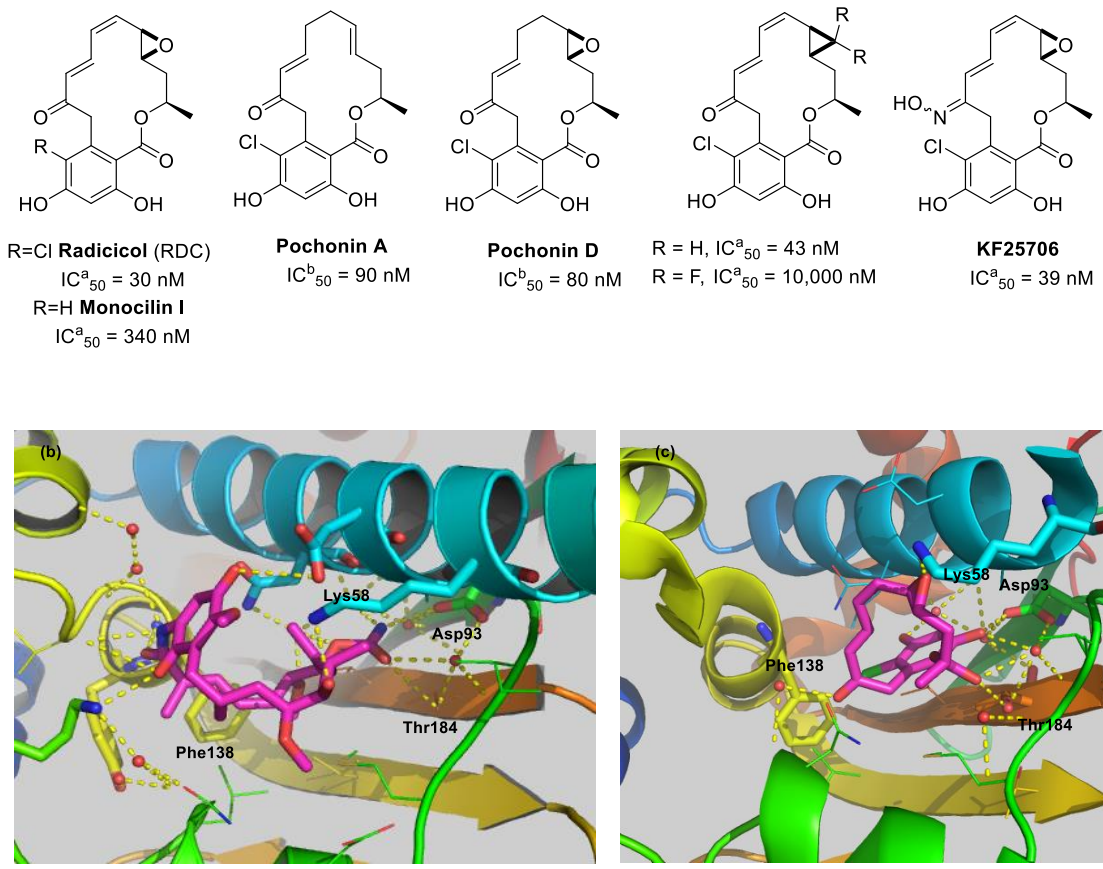

Figure 6. Resorcinol comprising natural products and binding mode of geldanamycin and radicicol. (a) Radicicol and related compounds IC$^{a}_{50}$: represents IC_{50} values of anti-proliferative activity against the MCF-7 breast cancer IC$^{b}_{50}$ represents IC_{50} values of a time-resolved fluorescence resonance energy transfer (TR-FRET) assay. (b) Binding conformation of GDA (PDB: 1YET); (c) binding mode of RDC (PDB: 4EKG).

epoxide with a cyclopropyl ring. Danishefsky and co-workers reported analogues that incorporated the cyclopropyl ring (Figure 6), which resulted in a two-fold loss in cellular efficacy.[90] Additionally, replacement of the epoxide with a difluorocylcopropane ring (Figure 6a) significantly decreased activity. A second strategy to increase the stability of RDC was to modify the 2'-ketone of RDC to the corresponding oxime.[31, 77] The oxime analogues provided the unsubstituted oxime analog, KF25706 (Figure 6a), which manifested comparable potency to RDC against various cancer cell lines. Metabolically stable KF25706 was evaluated in xenograft rodent models of cancer and reduced tumor growth over a 30-day period. Following this work, a series

of substituted oximes was prepared and evaluated for anti-cancer activity. A mixture of *E* and *Z* isomers complicated the development of oxime derivatives. However, it was determined that the *E* isomer possesses higher affinity for Hsp90. Metabolically stable RDC analogues represent a promising method to further develop these natural product inhibitors; however, the synthetic complexity associated with this scaffold renders this compound difficult for large scale production.[91] Fortunately, the data obtained from RDC analogues presented a new pharmacophore that has been successfully utilized to design new Hsp90 inhibitors. [92-97]

The resorcinol ring of RDC serves as a valuable pharmacophore for several highly efficacious Hsp90 inhibitors (Figure 7).[98, 99] Synta pharmaceutical developed the oxazolidinone containing, ganetespib (STA-9090, Figure 7), which is currently in 9 different clinical trial spanning phase I-II evaluation for the treatment of seven types of cancers. STA-9090 manifests greater efficacy than 17-AAG against various lung cancer cell lines (average IC_{50} = 6.5 nM vs. 30.5 nM, respectively), and exhibits greater tumor penetration and an improved toxicity profile in preclinical models. [100-102]

A medicinal chemistry campaign utilizing a structure-based approach led to the development of another clinical candidate, NYP-AUY922 (Figure 7), which is currently in phase II clinical trials for Her-2 positive and estrogen receptor positive metastatic breast cancers. AUY922 was also being evaluated in a phase II trial for non-small cell lung cancer (NSCLC) and produced a 20% response rate.[103-105] AUY922 is also being evaluated for the treatment of patients with multiple myeloma in the presence and absence of the proteasome inhibitor, bortezomib. However, results have not been encouraging, as dose tolerance appears to be an issue when administered in combination with bortezomib.[104, 105] KW-2478 and AT13387 (Figure 7) are additional resorcinol-derived Hsp90 inhibitors that have advanced into clinical trials. KW-2478

was developed by Kyowa Hakko Kirin Pharma in Japan through a unique lead optimization strategy that included the combination of microbial screening, structure-based drug design, cell-based screening, and *in vivo* models.[106] This optimization strategy led to the identification of KW-2478, which manifests 3.8 nM affinity for Hsp90 and low nM anti-proliferative IC_{50} values against various multiple myeloma cell lines. KW-2478 is currently being evaluated in patients with B-cell malignancies (phase I) and relapse or refractory multiple myeloma (phase I-II, in combination with bortezomib).[98] Astex pharmaceuticals developed AT13387 from a fragment-based drug discovery approach. AT13387 manifests an IC_{50} of 0.71 nM via fluorescence polarization and an anti-proliferative IC_{50} of 48 nM against the HCT116 colon cancer cell line. AT13387 is currently in phase I trials for patients with metastatic solid tumors, as well as phase II trial for the treatment of gastrointestinal stromal solid tumors, with or without Imatinib.[107]

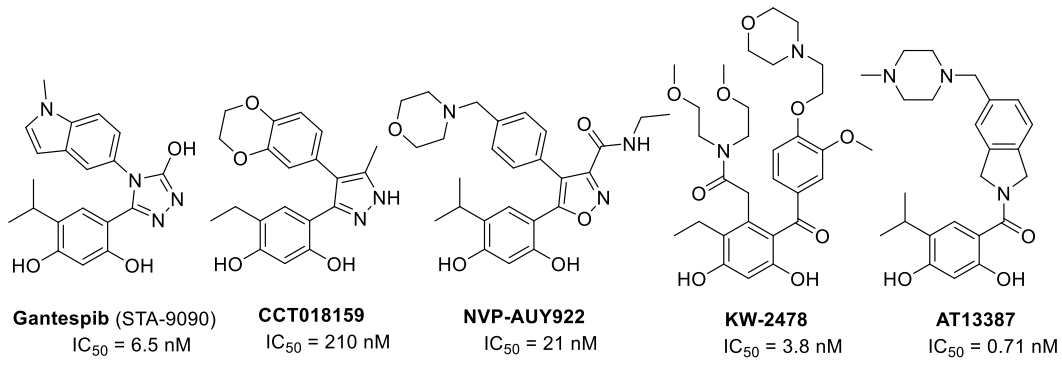

Figure 7. Resorcinol-derived Hsp90 inhibitors. IC_{50} represents anti-proliferation activities.

I.3.1.3. Chimeric Inhibitors

One approach to develop new Hsp90 inhibitory scaffolds is to combine the key structural features found in both GDA and RDC. This approach offers the potential to retain key interactions from both natural products with Hsp90, while simultaneously reducing the structural complexity.

As a result, chimeric inhibitors would allow for identification of structure-activity relationships for each natural product.

The first chimeric inhibitor of Hsp90, radanamycin (Figure 8), focused on maintenance of the resorcinol-mediated hydrogen bonding network.[96] The quinone moiety manifested a key hydrogen bonding network near the solvent-exposed region of the ATP-binding pocket and allowed for selective binding to the Hsp90 heteroprotein complex. Amino acids within this region were responsible for isomerization of the GDA amide bond, which dictated a high differential selectivity for the heteroprotein complex. [14, 93, 108]

Radanamycin was futher modified to generate more effecacious inhibitors using two different linkers to connect the quinone and resorcinol ring systems.[96] The first approach connected the resorcinol ring to the quinone ring via a two carbon-linker containing an amide bond, which yielded radamide (Figure 8).[95] Radamide inhibited Hsp90 ATPase activity at 5.9 μM compared to 2.5 μM for GDA and induced the degradation of Her2, an Hsp90-dependent client protein, in MCF-7 cells. The second approach connected the quinone to the ester linkage of RDC via a two carbon linker (Radester, Figure 8).[109] Radester manifested an anti-proliferative IC_{50} of 13.9 μM against MCF-7 cell line. Hsp90 inhibition by radester was confirmed via degradation of Hsp90 client proteins, Raf and Her2. Importantly, the hydroquinone derivatives of radamide and radester manifested greater affinity for Hsp90 than the corresponding quinones. The hydroquinone derivative of radamide inhibited Hsp90's inherent ATPase activity at 1.8 μM, and induced the degradation of Hsp90 client Her-2 levels in MCF-7 cells. Similarly, the radester-hydroquinone derivative manifested an anti-proliferative IC_{50} of 7.1 μM, and induced the degradation of Her2 and Raf levels. Additionally, the macrocyclic chimera, radanamycin manifested anti-proliferative activity against MCF-7 cells at 1.2 μM and induced the degradation of Hsp90 client proteins, Her2

and Akt. These studies proved important as Infinity Pharmaceuticals developed a hydroquinone derivative of GDA (IPI-504), which is currently undergoing clinical evaluation (see Figure 4).[17]

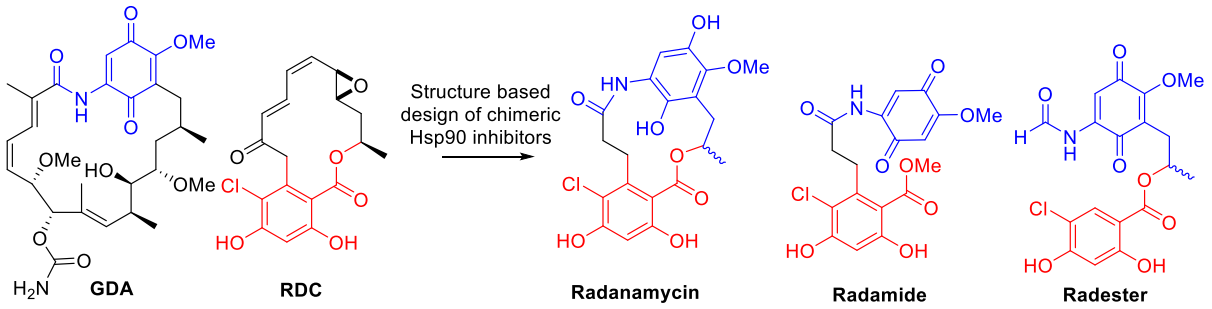

Figure 8. Chimeric Hsp90 N-terminal inhibitors.

I.3.1.4. Purine-Based Inhibitors

In addition to the GDA and RDC, the natural substrate of Hsp90, ATP, has also been used as a starting point for the developing Hsp90 inhibitors.[12, 110, 111] Chiosis and co-workers utilized the purine moiety of ATP as a template to develop small molecule inhibitors that bind the N-terminal ATP-binding site. Using a structure-based approach, the purine moiety was linked to an aryl ring, which mimicked the unique bent shape adopted by ATP within the N-terminal binding pocket. The first inhibitor of this class, PU3 (Figure 9), manifested low micromolar anti-proliferative activity against various breast cancer cell lines. This early study identified a new class of purine based Hsp90 inhibitors and further structure-activity relationship studies resulted in a significant improvement in efficacy.[110, 112] Further optimization of PU3 led to the identification of a more potent compound, PU24FCl (Figure 9). PU24FCl manifested low micromolar anti-proliferative effects against breast, lung, colon, and prostate cancer cell lines, and induced the degradation of Hsp90-dependent client proteins including Her2, Akt, Raf-1 and mutant p53. *In vivo* analysis PU24FCl revealed tumor specific inhibition of Hsp90, as this compound accumulated

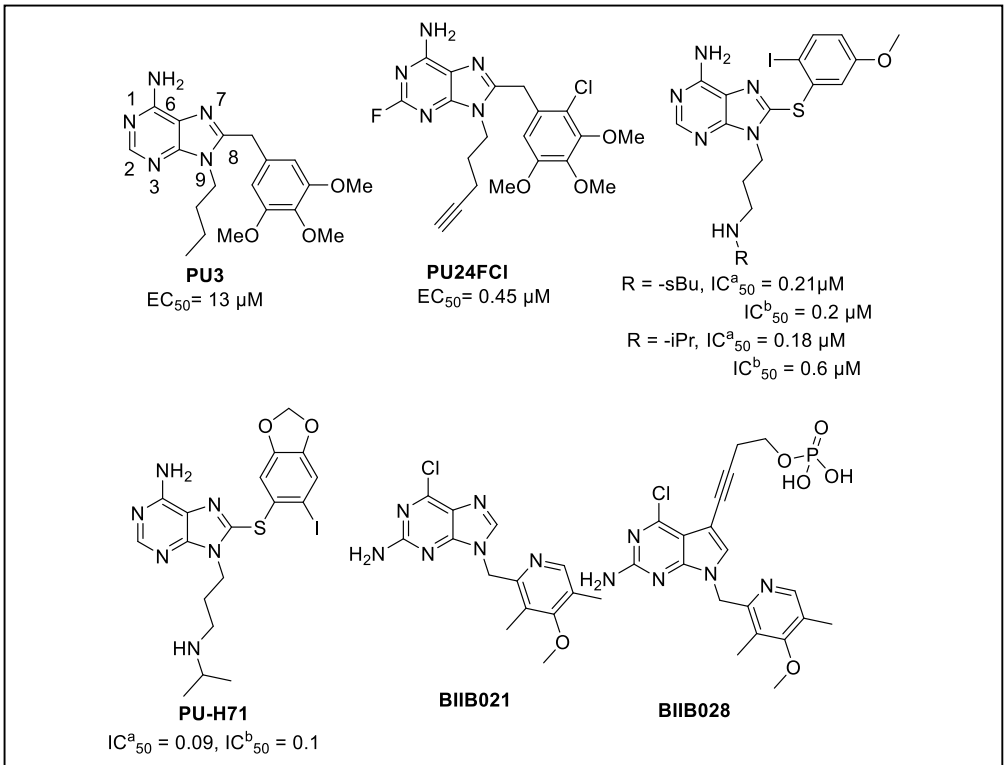

Figure 9. Purine-based Hsp90 N-terminal inhibitors. EC_{50} were determined in a competition assay with GDA. IC^{a}_{50} corresponds to anti-proliferation activity in MTS assay against MCF-7 cell lines. IC^{b}_{50} measured in her2 degradation assay.

in tumor tissues, but rapidly cleared from normal tissue. [113, 114] Administration of PU24FCl decreased tumor volume upon dosing of 200mg/kg i.p. every other day for 30 days. Preliminary structure-activity relationship studies led to the development of more efficacious, second generation of purine analogues. This series of analogues included derivatives of the phenyl ring, and concluded that substituents at the 2-, 4- and 5-positions are important for Hsp90 inhibition (Figure 9).[115, 116] Researchers at Conforma Therapeutics addressed the low bioavailability associated with the purine analogues and incorporated an amino group into the N-9 alkyl chain.[117] Subsequently, phosphoric acid salts of these amines were evaluated in murine tumor xenograft models (Figure 9) and manifested high efficacy. Another important water soluble purine-derived inhibitor (PU-H71, Figure 9) was reported by Chiosis and co-workers, and contained a 3-

isopropylamino-propyl chain.[115] This compound manifested a 16 nM binding affinity for Hsp90 and an IC_{50} of 50 nM in Her2 degradation assays. This analogue manifested significant efficacy *in vivo* and has advanced into clinical trials for the treatment of patients with low-grade non-Hodgkins lymphoma, as well as patients advanced malignancies. Later, Conforma Therapeutics reported analogues with an amine at the 2-position and a chlorine at the 6-position. The most efficacious analogue (BIIB021, Figure 9) also contained a pyridylmethylene group at the 9-position. BIIB021 manifested 9 nM efficacy in Her2 degradation assays and exhibited 333-fold selectivity for tumor cells versus normal cells.[118] After successful preclinical studies, this compound became the first rationally designed Hsp90 inhibitor to enter clinical trials and is currently being evaluated in Phase II trials for gastrointestinal stromal tumors.[119] To increase drug exposure, researchers at Conforma therapeutics also reported the intravenously administered compound, BIIB028 (Figure 9), a phosphate ester prodrug of the homopropargylic alcohol, and it too, is currently under phase I clinical evaluation.[120]

I.3.1.5. Induction of Heat Shock Response

An important consideration, which is often overlooked during development of N-terminal Hsp90 inhibitors, is the induction of the pro-survival heat-shock response.[121, 122] The heat shock response results in increased expression of various Hsp's including, Hsp90, Hsp70, Hsp27, and Hsp42. An Hsp90 bound transcription factor, HSF-1 mediates this pro-survival response. In unstressed/normal cells, HSF-1 is bound to Hsp90 and, is inactive.[123, 124] Under cellular stress, or the administration of an Hsp90 N-terminal inhibitor, heat shock factor-1 (HSF-1) dissociates from Hsp90.[125] Once released, in the cytosol, HSF-1 is trimerized, hyperphophorylated, and then translocated to nucleus, wherein it binds to heat shock element to initiate transcription of Hsp's (Figure 10).[126, 127]

Induction of the heat-shock response is a concern as it negates the cytotoxic effect of Hsp90-inhibitors and results in cytostatic activity. Inhibition of the N-terminus by *pan*-Hsp90 inhibitors results in increased levels of Hsp90 and Hsp70. Clinical trials have demonstrated that induction of the heat-shock response results in both dosing and scheduling issues. In addition, the period of target inhibition remains insufficient to obtain necessary levels of oncogenic client protein degradation. Hence, alternative methods for Hsp90 inhibition are highly desirable.[128, 129]

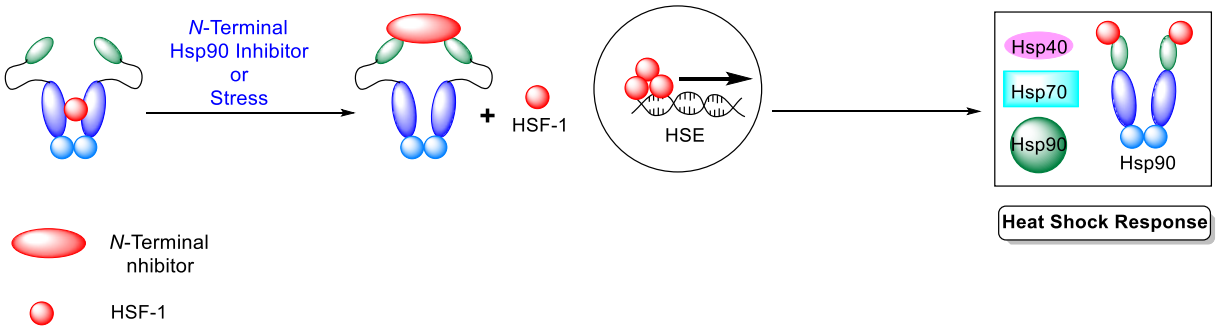

Figure 10. Induction of heat-shock response.

I.3.2. C-Terminal Inhibitors

I.3.2.1. Discovery of Hsp90 C-Terminal Binding Site

Unlike N-terminal inhibitors, Hsp90 C-terminal inhibitors do not induce the heat shock response at the same concentration they induce client protein degradation.[130, 131] The second nucleotide binding site at the C-terminus of Hsp90 was not known until 2000.[131, 132] Pioneering studies by Neckers and co-workers at NCI identified the C-terminal nucleotide binding pocket.[130] Both Hsp90 and DNA gyrase are members of the GHKL superfamily of proteins, and share high similarity in their binding sites. In pursuit of new leads for Hsp90 inhibition, Neckers and co-workers hypothesized that inhibitors of DNA gyrase may also bind Hsp90.[131] Hence, novobiocin was chosen as a probe to test whether it exhibits toxicity against cancer cells. Their hypothesis was confirmed by a concentration-dependent elution of Hsp90 with a novobiocin-sepharose column.

Furthermore, novobiocin eluted Hsp90 in a similar manner from GDA-sepharose column. However, GDA did not elute Hsp90 from a novobiocin-sepharose column, suggesting an alternative binding mode. In their binding studies with purified Hsp90 fragments, novobiocin did not bind the Hsp90 N-terminus of Hsp90. Unexpectedly, novobiocin bound to an Hsp90 fragment that contained the C-terminal amino acids, 580-728. Cellular Hsp90 inhibition by novobiocin was confirmed via western blot analysis of Hsp90 clients. Like N-terminal inhibitors, novobiocin induced the degradation of Raf-1, mutant p53, and her2, at high concentrations (~ 700 μM). Subsequently, via deletion/mutation studies Neckers and co-workers confirmed that novobiocin binds a region that overlaps with the C-terminal dimerization domain. Csermely and co-workers reported that occupancy of the N-terminal binding site is required for C-terminal occupation.[133] In addition, this group determined via oxidative nucleotide cleavage studies, that the C- terminus binds both purine and pyrimidine nucleotides, while the N-terminus only binds the purine class of nucleotides.[134] These studies established the existence of the second ATP-binding site within Hsp90 and suggested an alternative approach to modulate Hsp90.

I.3.2.2. Novobiocin

Novobiocin was identified as a lead compound for Hsp90 C-terminal inhibition and to the date, it is the most studied Hsp90 C-terminal inhibitor.[135-149] Unlike N-terminal inhibitors, there is no co-crystal structure of an inhibitor bound to the Hsp90 C-terminus.[150, 151] Structure-activity relationship studies on novobiocin have provided analogues with improved efficacy, as well as selectivity, over DNA gyrase. A summary of these studies is provided in Figure 11. Removal of the 4-hydroxy group and 3'-carbamante resulted in DHN1 and DHN2 which manifested >300-fold improvement in anti-cancer activity. [152] Importantly, these compounds were selective for Hsp90

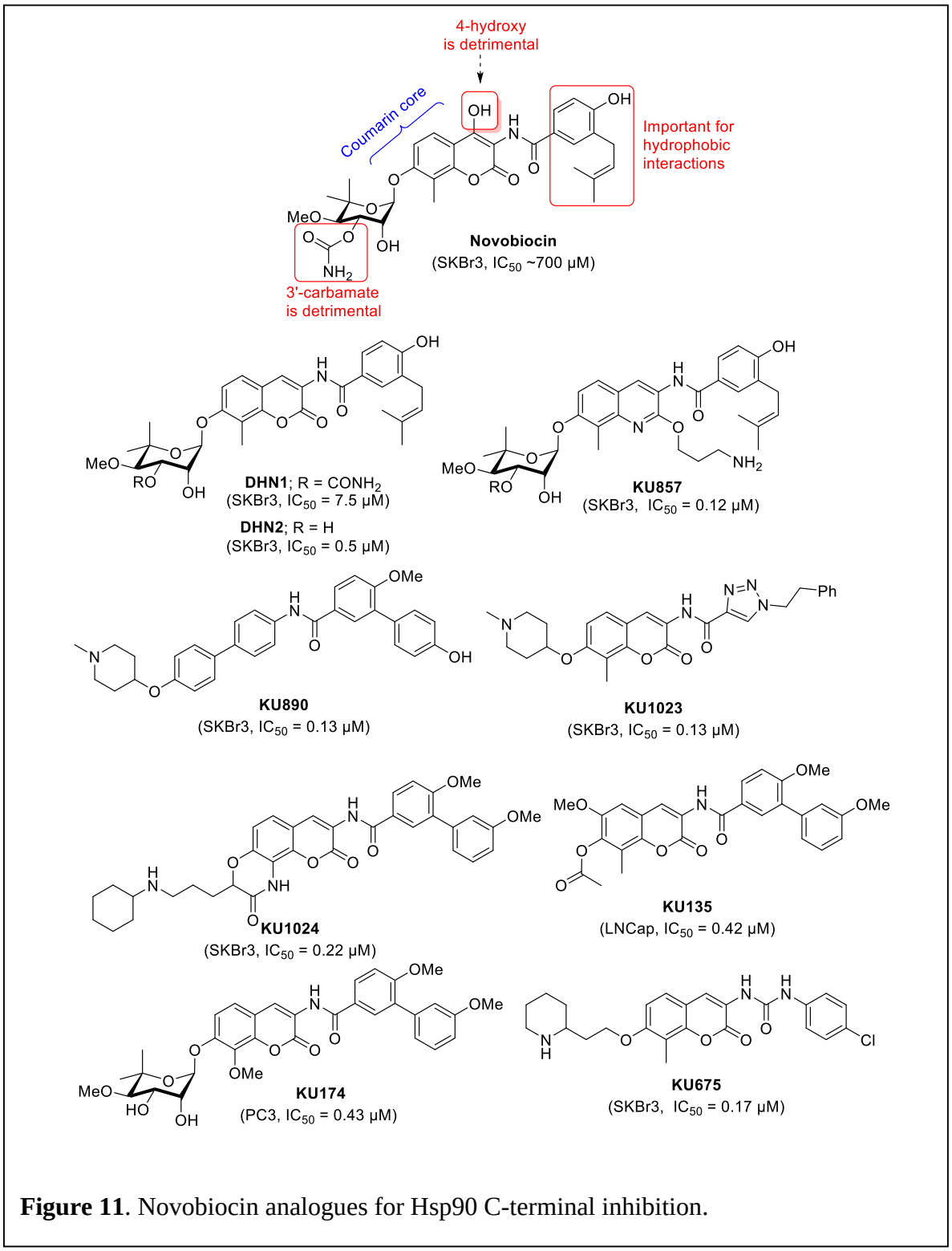

Figure 11. Novobiocin analogues for Hsp90 C-terminal inhibition.

over DNA gyrase. Subsequent, optimization of the coumarin core, noviose sugar, and benzamide side chain resulted in optimal replacements for these moieties.[136, 147, 149, 153] Replacement of coumarin core with other aromatic/heteroaromatic cores (KU857, KU890) improved efficacy and suggested that the central coumarin core serve as a backbone to project the sugar and benzamide side chains within the C-terminal binding pocket.[154-156]. The complex noviose sugar was replaced with alkyl amines. Modification of the benzamides linker with a triazole and urea moiety resulted in improved anti-proliferation activities (KU675, KU1023).[157, 158]

I.3.2.3. Silybin

Silybin is the principal component of the flavonolignan extract isolated from the seed of milk thistle plants (Silybum marianum) (Figure 12).[159] Silybin demonstrated hepato-protective and growth inhibitory activity against various cancer cells. Prior studies demonstrated that silybin induced depletion of CDK2, CDK4, and cyclin D1 proteins in colon cancer cells.[160, 161] Cyclin D1, CDK2 and CDK4 are well-known Hsp90-dependent clients, which led to the assumption that silybin could be an Hsp90 inhibitor. Subsequently, using a luciferase refolding assay Zhao and co-workers demonstrated that Hsp90 is a biochemical target for Silybin.[58, 162] Silybin induced a concentration-dependent degradation of the Hsp90-dependent client proteins Her2, Raf-1, and Akt, without affecting Hsp70 or Hsp90 levels. Further SAR studies in the Blagg laboratory showed that the C-3 and C-23 hydroxyl groups were not required for activity; however, at least one substitution (preferably 4-hydoxyl) on the E-ring was beneficial for activity. The A-ring phenol was not required and its removal led to the development of compounds (Figure 12), that manifested IC_{50}'s of 13 μM and 16 μM against MCF-7 cell lines, respectively. [58]

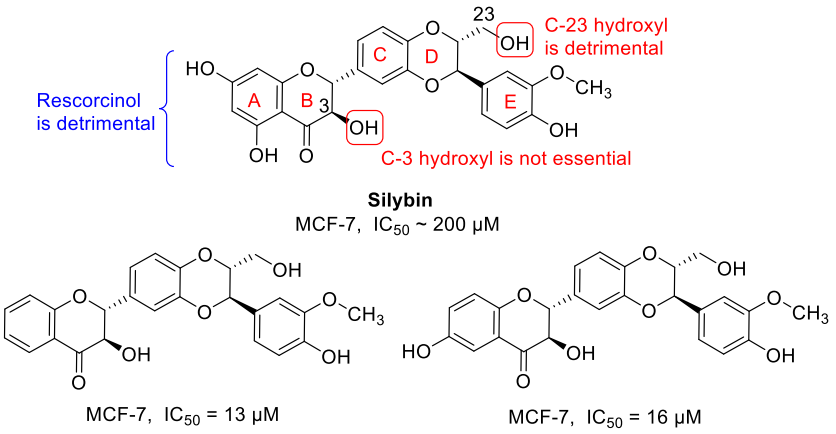

Figure 12. Summary of silybin SAR.

I.3.3. Disruptors of Hsp90 Interaction with Co-Chaperones and Client Proteins

Currently, most Hsp90 inhibitors undergoing clinical evaluation are *pan*-Hsp90 N-terminal inhibitors. To overcome the detrimental side effects of these N-terminal inhibitors, there is growing interest to identify new Hsp90 modulators that exhibit alternative mechanisms of actions. Over the past decade, various natural products have emerged that disrupt interactions between Hsp90 and its co-chaperones.[56, 57, 116] These compounds represent new chemotypes for the development of future Hsp90 inhibitors. Several natural products, such as celastrol, gedunin, and cruentaren A have been shown, amongst a plethora of other biochemical and biological effects, to disrupt interactions between Hsp90 and its partner proteins. Some of these natural products and their mechanisms of action are presented in Figure 13.

I.3.3.1. Celastrol

Celastrol is a pentacyclic quinone methide comprising triterpenoid natural product (Figure 13) is isolated from the root extract of Tripterygium wilfordii Hook F. (also known as Thunder of

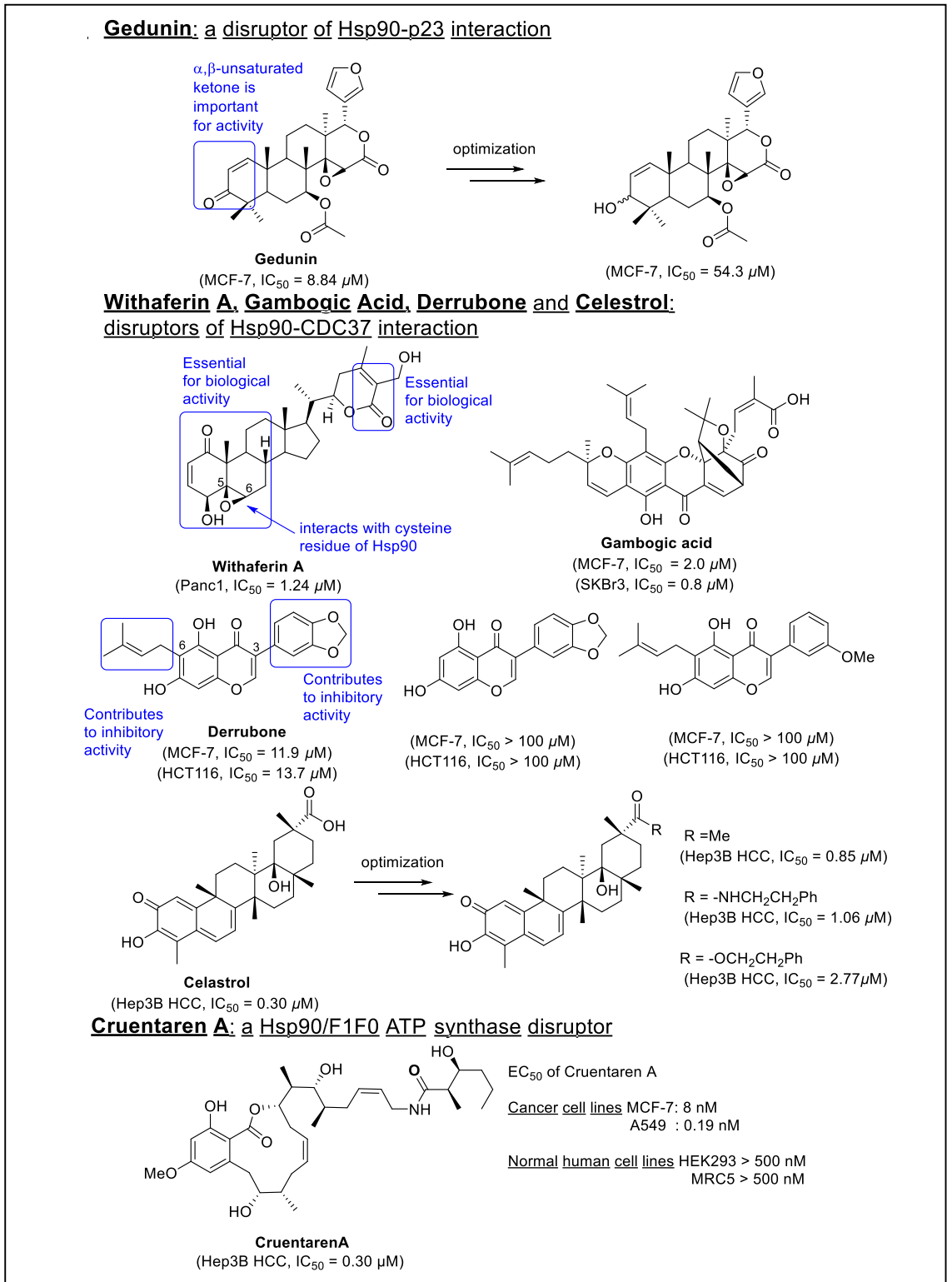

Figure 13. Disruptors of Hsp90 interaction with co-chaperones and client proteins.

God Vine) and has been used in oriental medicine to treat autoimmune disorders and inflammatory diseases.[163, 164] Upon biological evaluation, celastrol exhibited anti-proliferative, anti-metastatic, and pro-apoptotic activities against various cancer cell lines.[165] In 2006, Hieronymus and coworkers reported that celastrol disrupts Hsp90-related pathways, which contributes to its anti-cancer activity, and subsequently it was shown to disrupt association of Hsp90 with co-chaperone cdc37.[30, 166] Celastrol has a high propensity to form covalent adducts with cysteine, which contributes to its promiscuity and limits its utility as an Hsp90 modulator. In addition to celastrol, derrubone, withaferin A and, gambogic acid also inhibit Hsp90's interaction with co-chaperone cdc37.[167-169]

I.3.3.2. Gedunin

Gedunin (Figure 13) is a tetranortriterpenoid isolated from the Indian neem tree (Azadirachta indica, Meliacae). Gedunin has been used for the treatment of infectious diseases in traditional Indian medicine. In addition, gedunin has been shown to exhibited anti-proliferative activity against various cancer cell lines including colon, prostate, and ovarian.[170, 171] In 2006, gedunin was reported to modulate Hsp90's function and shown to induce degradation of Hsp90 client proteins.[166] Subsequently in 2013, Patwardhan and co-workers reported that gedunin binds to Hsp90 co-chaperone p23, and blocks its interaction with Hsp90 and inhibited Hsp90 chaperone cycle.[172] Gedunin exhibited modest efficacy against cancer cell lines. In order to identify key structural features for cytotoxic activity, Brandt and co-workers prepared 19 semisynthetic derivatives.[59] The α,β-unsaturated ketone was found to be important for anti-proliferative activity. However, a more active analog could not be identified.

I.3.3.3. Cruentaren A

Cruentaren A (**12**, Figure 13) is a macrolide isolated from the myxobacterium Byssovorax

and manifests low nM anti-proliferative activity against various cancer cell lines. The biological target of cruentaren A has been identified as F_1F_0-ATP synthase, the enzyme responsible for the mitochondrial production of ATP.[173-176] In 2006, Papathanassiu and coworkers reported that F_1F_0-ATP synthase could act as an Hsp90 co-chaperone that provides the energy required for the maturation of client proteins.[177] Recently, Hall and co-workers demonstrated that incubation of cruentaren A disrupted interactions between Hsp90α and F_1F_0-ATPase synthase.[178] Interestingly, inhibition of F_1F_0-ATPase synthase via cruentaren A induced the degradation of select Hsp90 client proteins without induction of the heat-shock response. Cruentaren A thus represents a novel mechanism to modulate Hsp90 however, limited synthetic accessibility to cruentaren A represents an obstacle that has yet to be overcome.

I. 4. Conclusions & Future Directions

Inhibition of Hsp90's function represents a multifaceted approach to treat cancer due to the fact that Hsp90-dependent client proteins are associated with all ten hallmarks of cancer. Consequently, Hsp90 has attracted the attention of researchers throughout the world. These efforts identified of key interactions within the N-terminal ATP binding pocket, and has led to discovery of new classes of Hsp90 inhibitors. Beginning with the discovery of natural product inhibitors of Hsp90 (GDA and RDC), many analogues have been designed to probe the biological function of Hsp90, 17 of which have advanced into clinical trials. While GDA never advanced into clinical trials, 17-substituted GDA-analogues have proven to be superior candidates, and advanced to the clinic. Likewise, RDC did not advance into clinical trials however, the resorcinol ring of RDC provided a key pharmacophore as several medicinal chemistry campaigns have used the resorcinol moiety as a starting point to produce candidates that are currently undergoing clinical evaluation. The natural substrate of Hsp90, ATP, has also been used to develop purine class of inhibitors that

have advanced into clinical trials. Even though Hsp90 inhibitors have shown promise in clinical trials, no compound has yet been approved by the FDA. These somewhat disappointing results highlight the need to comprehensively understand the biology of Hsp90 and its isoforms. Two major concerns associated with Hsp90 inhibitors are toxicities (ocular-, cardio-, hepato-toxicities), and induction of the heat shock response, as both obstacles resulted in the termination of some trials, suggesting new approaches to Hsp90 inhibition are needed.

One strategy that may prove useful to circumvent the known pitfalls from *pan*-Hsp90 inhibition is the development of isoform-selective inhibitors. By developing selective inhibitors of each isoform, toxicities associated with individual isoforms may be overcome. Furthermore, upon identification of client proteins that are dependent upon each isoform, perhaps more personalized treatments can be developed. An additional strategy involves developing Hsp90 C-terminal inhibitors that do not induce the heat shock response at concentrations needed for client protein degradation, and therefore should address the dosing and scheduling detriments associated with N-terminal inhibitors. Recently, co-chaperone disruptors have emerged as promising alternatives to modulate Hsp90. Hsp90 isoform-selective inhibitors, C-terminal inhibitors and, co-chaperone disruptors represent promising approaches to overcome limitations of current inhibitors.

I. 5. References

1. Li, J.; Soroka, J.; Buchner, J. The Hsp90 chaperone machinery: conformational dynamics and regulation by co-chaperones. *Biochim. Biophys. Acta* **2012**, 1823, 624-635.
2. Li, J.; Buchner, J. Structure, function and regulation of the hsp90 machinery. *Biomed. J.* **2013**, 36, 106-117.
3. Prodromou, C.; Pearl, L. H. Structure and functional relationships of Hsp90. *Curr. Cancer Drug Targets* **2003**, 3, 301-323.
4. Bagatell, R.; Whitesell, L. Altered Hsp90 function in cancer: a unique therapeutic opportunity. *Mol. Cancer Ther.* **2004**, 3, 1021-1030.
5. Schlesinger, M. J. Heat shock proteins. *J. Biol. Chem.* **1990**, 265, 12111-12114.
6. Taipale, M.; Jarosz, D. F.; Lindquist, S. HSP90 at the hub of protein homeostasis: emerging mechanistic insights. *Nat. Rev. Mol. cell Biol.* **2010**, 11, 515-528.

7. Pratt, W. B. The role of heat shock proteins in regulating the function, folding, and trafficking of the glucocorticoid receptor. *J. Biol. Chem.* **1993**, 268, 21455-21458.
8. Csermely, P.; Schnaider, T.; Soti, C.; Prohaszka, Z.; Nardai, G. The 90-kDa molecular chaperone family: structure, function, and clinical applications. A comprehensive review. *Pharmacol. Ther.* **1998**, 79, 129-168.
9. Hong, D. S.; Banerji, U.; Tavana, B.; George, G. C.; Aaron, J.; Kurzrock, R. Targeting the molecular chaperone heat shock protein 90 (HSP90): lessons learned and future directions. *Cancer Treat. Rev.* **2013**, 39, 375-387.
10. Whitesell, L.; Lindquist, S. L. HSP90 and the chaperoning of cancer. *Nat. Rev. Cancer* **2005**, 5, 761-772.
11. Kamal, A.; Thao, L.; Sensintaffar, J.; Zhang, L.; Boehm, M. F.; Fritz, L. C.; Burrows, F. J. A high-affinity conformation of Hsp90 confers tumour selectivity on Hsp90 inhibitors. *Nature* **2003**, 425, 407-410.
12. Workman, P.; Burrows, F.; Neckers, L.; Rosen, N. Drugging the cancer chaperone HSP90: combinatorial therapeutic exploitation of oncogene addiction and tumor stress. *Ann. N.Y. Acad. Sci.* **2007**, 1113, 202-216.
13. Neckers, L.; Trepel, J. B. Stressing the development of small molecules targeting HSP90. *Clin Cancer Res* **2014**, 20, 275-277.
14. Trepel, J.; Mollapour, M.; Giaccone, G.; Neckers, L. Targeting the dynamic HSP90 complex in cancer. *Nat. Rev. Cancer* **2010**, 10, 537-549.
15. Franke, J.; Eichner, S.; Zeilinger, C.; Kirschning, A. Targeting heat-shock-protein 90 (Hsp90) by natural products: geldanamycin, a show case in cancer therapy. *Nat. Prod. Rep.* **2013**, 30, 1299-323.
16. Whitesell, L.; Mimnaugh, E. G.; De Costa, B.; Myers, C. E.; Neckers, L. M. Inhibition of heat shock protein HSP90-pp60v-src heteroprotein complex formation by benzoquinone ansamycins: essential role for stress proteins in oncogenic transformation. *Proc. Natl. Acad. Sci.* **1994**, 91, 8324-8328.
17. Tian, Z. Q.; Liu, Y.; Zhang, D.; Wang, Z.; Dong, S. D.; Carreras, C. W.; Zhou, Y.; Rastelli, G.; Santi, D. V.; Myles, D. C. Synthesis and biological activities of novel 17-aminogeldanamycin derivatives. *Bioorg. Med. Chem.* **2004**, 12, 5317-5329.
18. Waza, M.; Adachi, H.; Katsuno, M.; Minamiyama, M.; Tanaka, F.; Sobue, G. Alleviating neurodegeneration by an anticancer agent: an Hsp90 inhibitor (17-AAG). *Ann. N.Y. Acad. Sci.* **2006**, 1086, 21-34.
19. Bhat, R.; Tummalapalli, S. R.; Rotella, D. P. Progress in the discovery and development of heat shock protein 90 (hsp90) inhibitors. *J. Med. Chem.* **2014**, 57, 8718-8728.
20. Amolins, M. W.; Blagg, B. S. Natural product inhibitors of Hsp90: potential leads for drug discovery. *Mini Rev. Med. Chem.* **2009**, 9, 140-152.
21. Khandelwal, A.; Hall, J. A.; Blagg, B. S. Synthesis and structure-activity relationships of EGCG analogues, a recently identified Hsp90 inhibitor. *J. Org. Chem.* **2013**, 78, 7859-7884.
22. Hall, J. A.; Kusuma, B. R.; Brandt, G. E.; Blagg, B. S. Cruentaren A binds F1F0 ATP synthase to modulate the Hsp90 protein folding machinery. *ACS Chem. Biol.* **2014**, 9, 976-985.
23. Marcu, M. G.; Schulte, T. W.; Neckers, L. Novobiocin and related coumarins and depletion of heat shock protein 90-dependent signaling proteins. *J. Natl. Cancer Inst.* **2000**, 92, 242-248.

24. Schulte, T. W.; Akinaga, S.; Soga, S.; Sullivan, W.; Stensgard, B.; Toft, D.; Neckers, L. M. Antibiotic radicicol binds to the N-terminal domain of Hsp90 and shares important biologic activities with geldanamycin. *Cell Stress Chaperones* **1998**, 3, 100-108.
25. Martin, C. J.; Gaisser, S.; Challis, I. R.; Carletti, I.; Wilkinson, B.; Gregory, M.; Prodromou, C.; Roe, S. M.; Pearl, L. H.; Boyd, S. M.; Zhang, M. Q. Molecular characterization of macbecin as an Hsp90 inhibitor. *J. Med. Chem.* **2008**, 51, 2853-2857.
26. Supko, J. G.; Hickman, R. L.; Grever, M. R.; Malspeis, L. Preclinical pharmacologic evaluation of geldanamycin as an antitumor agent. *Cancer Chemother. Pharmacol.* **1995**, 36, 305-315.
27. Vasko, R. C.; Rodriguez, R. A.; Cunningham, C. N.; Ardi, V. C.; Agard, D. A.; McAlpine, S. R. Mechanistic studies of Sansalvamide A-amide: an allosteric modulator of Hsp90. *ACS Med. Chem. Lett.* **2010**, 1, 4-8.
28. Amolins, M. W.; Peterson, L. B.; Blagg, B. S. J. Synthesis and Evaluation of Electron-Rich Curcumin Analogues. *Bioorg. Med. Chem.* **2009**, 17, 360-367.
29. Patwardhan, C. A.; Fauq, A.; Peterson, L. B.; Miller, C.; Blagg, B. S.; Chadli, A. Gedunin inactivates the co-chaperone p23 protein causing cancer cell death by apoptosis. *J. Biol. Chem.* **2013**, 288, 7313-7325.
30. Zhang, T.; Hamza, A.; Cao, X.; Wang, B.; Yu, S.; Zhan, C. G.; Sun, D. A novel Hsp90 inhibitor to disrupt Hsp90/Cdc37 complex against pancreatic cancer cells. *Mol. Cancer Ther.* **2008**, 7, 162-170.
31. Soga, S.; Neckers, L. M.; Schulte, T. W.; Shiotsu, Y.; Akasaka, K.; Narumi, H.; Agatsuma, T.; Ikuina, Y.; Murakata, C.; Tamaoki, T.; Akinaga, S. KF25706, a novel oxime derivative of radicicol, exhibits in vivo antitumor activity via selective depletion of Hsp90 binding signaling molecules. *Cancer Res.* **1999**, 59, 2931-2938.
32. Khandelwal, A.; Crowley, V. M.; Blagg, B. S. Natural Product Inspired N-Terminal Hsp90 Inhibitors: From Bench to Bedside? *Med. Res. Rev.* **2016**, 36, 92-118.
33. Usmani, S. Z.; Bona, R.; Li, Z. 17 AAG for HSP90 inhibition in cancer-from bench to bedside. *Curr. Mol. Med.* **2009**, 9, 654-664.
34. Krishna, P.; Gloor, G. The Hsp90 family of proteins in Arabidopsis thaliana. *Cell Stress Chaperones* **2001**, 6, 238-246.
35. Nemoto, T.; Sato, N.; Iwanari, H.; Yamashita, H.; Takagi, T. Domain structures and immunogenic regions of the 90-kDa heat-shock protein (HSP90). Probing with a library of anti-HSP90 monoclonal antibodies and limited proteolysis. *J. Biol. Chem.* **1997**, 272, 26179-26187.
36. Prodromou, C.; Pearl, L. H. Structure and functional relationships of Hsp90. *Curr. Cancer Drug Targets* **2003**, 3, 301-323.
37. Young, J. C.; Schneider, C.; Hartl, F. U. In vitro evidence that hsp90 contains two independent chaperone sites. *FEBS Lett.* **1997**, 418, 139-143.
38. Dutta, R.; Inouye, M. GHKL, an emergent ATPase/kinase superfamily. *Trends Biochem. Sci* **2000**, 25, 24-28.
39. Bergerat, A.; de Massy, B.; Gadelle, D.; Varoutas, P. C.; Nicolas, A.; Forterre, P. An atypical topoisomerase II from Archaea with implications for meiotic recombination. *Nature* **1997**, 386, 414-417.
40. Sreedhar, A. S.; Kalmar, E.; Csermely, P.; Shen, Y. F. Hsp90 isoforms: functions, expression and clinical importance. *FEBS Lett.* **2004**, 562, 11-15.

41. Johnson, J. L. Evolution and function of diverse Hsp90 homologs and cochaperone proteins. *Biochim. Biophys. Acta.* **2012**, 1823, 607-613.
42. Chen, B.; Piel, W. H.; Gui, L.; Bruford, E.; Monteiro, A. The HSP90 family of genes in the human genome: insights into their divergence and evolution. *Genomics* **2005**, 86, 627-637.
43. Prodromou, C. The 'Active Life' of Hsp90 Complexes. *Biochim. Biophys. Acta.* **2012,** 1823, 614-623.
44. Rohl, A.; Rohrberg, J.; Buchner, J. The chaperone Hsp90: changing partners for demanding clients. *Trends Biochem. Sci.* **2013**, 38, 253-262.
45. Whitesell, L.; Lindquist, S. L. HSP90 and the Chaperoning of Cancer. *Nat. Rev. Cancer* **2005**, 5, 761-772.
46. Mickler, M.; Hessling, M.; Ratzke, C.; Buchner, J.; Hugel, T. The large conformational changes of Hsp90 are only weakly coupled to ATP hydrolysis. *Nat. Struc. Mol.Biol.* **2009**, 16, 281-286.
47. Prodromou, C.; Panaretou, B.; Chohan, S.; Siligardi, G.; O'Brien, R.; Ladbury, J. E.; Roe, S. M.; Piper, P. W.; Pearl, L. H. The ATPase cycle of Hsp90 drives a molecular 'clamp' via transient dimerization of the N-terminal domains. *EMBO J.* **2000**, 19, 4383-4392.
48. Xu, W.; Marcu, M.; Yuan, X.; Mimnaugh, E.; Patterson, C.; Neckers, L. Chaperone-dependent E3 ubiquitin ligase CHIP mediates a degradative pathway for c-ErbB2/Neu. *Proc. Natl. Acad. Sci.* **2002**, 99, 12847-12852.
49. Hanahan, D.; Weinberg, R. A. Hallmarks of cancer: the next generation. *Cell* **2011**, 144, 646-674.
50. Hanahan, D.; Weinberg, R. A. The hallmarks of cancer. *Cell* **2000**, 100, 57-70.
51. Peterson, L. B.; Blagg, B. S. To fold or not to fold: modulation and consequences of Hsp90 inhibition. *Future Med. Chem.* **2009**, 1, 267-283.
52. Taldone, T.; Gozman, A.; Maharaj, R.; Chiosis, G. Targeting Hsp90: small-molecule inhibitors and their clinical development. *Curr. Opin. Pharmacol.* **2008**, 8, 370-374.
53. Muchowski, P. J.; Wacker, J. L. Modulation of neurodegeneration by molecular chaperones. *Nat. Rev. Neurosci.* **2005**, 6, 11-22.
54. Moulick, K.; Ahn, J. H.; Zong, H.; Rodina, A.; Cerchietti, L.; Gomes DaGama, E. M.; Caldas-Lopes, E.; Beebe, K.; Perna, F.; Hatzi, K.; Vu, L. P.; Zhao, X.; Zatorska, D.; Taldone, T.; Smith-Jones, P.; Alpaugh, M.; Gross, S. S.; Pillarsetty, N.; Ku, T.; Lewis, J. S.; Larson, S. M.; Levine, R.; Erdjument-Bromage, H.; Guzman, M. L.; Nimer, S. D.; Melnick, A.; Neckers, L.; Chiosis, G. Affinity-based proteomics reveal cancer-specific networks coordinated by Hsp90. *Nat. Chem. Biol.* **2011**, 7, 818-826.
55. Whitesell, L.; Bagatell, R.; Falsey, R. The Stress Response; Implications for the Clinical Development of Hsp90 Inhibitors. *Curr. Cancer Drug Targets.* **2003**, 3, 349-358.
56. Brandt, G. E. L.; Blagg, B. S. J. Alternate Strategies of Hsp90 Modulation for the Treatment of Cancer and Other Diseases. *Curr. Top. Med. Chem.* **2009**, 9, 1447-1461.
57. Hall, J. A.; Forsberg, L. K.; Blagg, B. S. Alternative approaches to Hsp90 modulation for the treatment of cancer. *Future Med. Chem.* **2014**, 6, 1587-1605.
58. Zhao, H.; Brandt, G. E.; Galam, L.; Matts, R. L.; Blagg, B. S. J. Identification and Initial SAR of Silybin: an Hsp90 Inhibitor. *Bioorg. Med. Chem. Lett.* **2011**, 21, 2659-2664.
59. Brandt, G. E.; Schmidt, M. D.; Prisinzano, T. E.; Blagg, B. S. Gedunin, a novel hsp90 inhibitor: semisynthesis of derivatives and preliminary structure-activity relationships. *J. Med. Chem.* **2008**, 51, 6495-6502.

60. DeBoer, C.; Meulman, P. A.; Wnuk, R. J.; Peterson, D. H. Geldanamycin, a new antibiotic. . *Antibiot.* **1970**, 23, 442-447.
61. Neckers, L.; Workman, P. Hsp90 Molecular Chaperone Inhibitors: Are We There Yet? *Clin. Cancer Res.* **2012**, 18, 64-76.
62. Ge, J.; Normant, E.; Porter, J. R.; Ali, J. A.; Dembski, M. S.; Gao, Y.; Georges, A. T.; Grenier, L.; Pak, R. H.; Patterson, J.; Sydor, J. R.; Tibbitts, T. T.; Tong, J. K.; Adams, J.; Palombella, V. J. Design, synthesis, and biological evaluation of hydroquinone derivatives of 17-amino-17-demethoxygeldanamycin as potent, water-soluble inhibitors of Hsp90. *J. Med. Chem.* **2006**, 49, 4606-4615.
63. Le Brazidec, J. Y.; Kamal, A.; Busch, D.; Thao, L.; Zhang, L.; Timony, G.; Grecko, R.; Trent, K.; Lough, R.; Salazar, T.; Khan, S.; Burrows, F.; Boehm, M. F. Synthesis and biological evaluation of a new class of geldanamycin derivatives as potent inhibitors of Hsp90. *J. Med. Chem.* **2004**, 47, 3865-3873.
64. Porter, J. R.; Ge, J.; Lee, J.; Normant, E.; West, K. Ansamycin inhibitors of Hsp90: nature's prototype for anti-chaperone therapy. *Curr. Top. Med. Chem.* **2009**, 9, 1386-1418.
65. Schnur, R. C.; Corman, M. L.; Gallaschun, R. J.; Cooper, B. A.; Dee, M. F.; Doty, J. L.; Muzzi, M. L.; DiOrio, C. I.; Barbacci, E. G.; Miller, P. E.; et al. erbB-2 oncogene inhibition by geldanamycin derivatives: synthesis, mechanism of action, and structure-activity relationships. *J. Med. Chem.* **1995**, 38, 3813-3820.
66. Schnur, R. C.; Corman, M. L.; Gallaschun, R. J.; Cooper, B. A.; Dee, M. F.; Doty, J. L.; Muzzi, M. L.; Moyer, J. D.; DiOrio, C. I.; Barbacci, E. G.; et al. Inhibition of the oncogene product p185erbB-2 in vitro and in vivo by geldanamycin and dihydrogeldanamycin derivatives. *J. Med. Chem.* **1995**, 38, 3806-3812.
67. Rastelli, G.; Tian, Z. Q.; Wang, Z.; Myles, D.; Liu, Y. Structure-based design of 7-carbamate analogs of geldanamycin. *Bioorg. Med. Chem. Lett.* **2005**, 15, 5016-5021.
68. Egorin, M. J.; Rosen, D. M.; Wolff, J. H.; Callery, P. S.; Musser, S. M.; Eiseman, J. L. Metabolism of 17-(allylamino)-17-demethoxygeldanamycin (NSC 330507) by murine and human hepatic preparations. *Cancer Res.* **1998**, 58, 2385-2396.
69. Floris, G.; Debiec-Rychter, M.; Wozniak, A.; Stefan, C.; Normant, E.; Faa, G.; Machiels, K.; Vanleeuw, U.; Sciot, R.; Schöffski, P. The Heat Shock Protein 90 Inhibitor IPI-504 Induces KIT Degradation, Tumor Shrinkage, and Cell Proliferation Arrest in Xenograft Models of Gastrointestinal Stromal Tumors. *Mol. Cancer Ther.* **2011**, 10, 1897-1908.
70. Siegel, D.; Jagannath, S.; Vesole, D. H.; Borello, I.; Mazumder, A.; Mitsiades, C.; Goddard, J.; Dunbar, J.; Normant, E.; Adams, J.; Grayzel, D.; Anderson, K. C.; Richardson, P. A phase 1 study of IPI-504 (retaspimycin hydrochloride) in patients with relapsed or relapsed and refractory multiple myeloma. *Leukemia & Lymphoma* **2011**, 52, 2308-2315.
71. Taldone, T.; Ochiana, S. O.; Patel, P. D.; Chiosis, G. Selective targeting of the stress chaperome as a therapeutic strategy. *Trends Pharmacol. Sci.* **2014**, 35, 592-603.
72. Centenera, M. M.; Fitzpatrick, A. K.; Tilley, W. D.; Butler, L. M. Hsp90: still a viable target in prostate cancer. *Biochim. Biophys. Acta* **2013**, 1835, 211-218.
73. Kitson, R. R.; Moody, C. J. An improved route to 19-substituted geldanamycins as novel Hsp90 inhibitors--potential therapeutics in cancer and neurodegeneration. *Chem. Comm.* **2013**, 49, 8441-8443.
74. Li, Z.; Jia, L.; Wang, J.; Wu, X.; Hao, H.; Wu, Y.; Xu, H.; Wang, Z.; Shi, G.; Lu, C.; Shen, Y. Discovery of diamine-linked 17-aroylamido-17-demethoxygeldanamycins as potent Hsp90 inhibitors. *Eur. J. Med. Chem.* **2014**, 87C, 346-363.

75. Whitesell, L.; LIn, N. U. HSP90 as a platform for the assembly of more effective cancer chemotherapy. *Biochim. Biophys. Acta.* **2012,** 1823, 756-766.
76. Delmotte, P.; Delmotte-Plaque, J. A new antifungal substance of fungal origin. *Nature* **1953**, 171, 344.
77. Soga, S.; Shiotsu, Y.; Akinaga, S.; Sharma, S. V. Development of radicicol analogues. *Curr. Cancer Drug Targets.* **2003**, 3, 359-369.
78. Roe, S. M.; Prodromou, C.; O'Brien, R.; Ladbury, J. E.; Piper, P. W.; Pearl, L. H. Structural basis for inhibition of the Hsp90 molecular chaperone by the antitumor antibiotics radicicol and geldanamycin. *J. Med. Chem.* **1999**, 42, 260-266.
79. Schulte, T. W.; Akinaga, S.; Murakata, T.; Agatsuma, T.; Sugimoto, S.; Nakano, H.; Lee, Y. S.; Simen, B. B.; Argon, Y.; Felts, S.; Toft, D. O.; Neckers, L. M.; Sharma, S. V. Interaction of radicicol with members of the heat shock protein 90 family of molecular chaperones. *Mol. Endocrinol.* **1999**, 13, 1435-1448.
80. Prodromou, C.; Nuttall, J. M.; Millson, S. H.; Roe, S. M.; Sim, T. S.; Tan, D.; Workman, P.; Pearl, L. H.; Piper, P. W. Structural basis of the radicicol resistance displayed by a fungal hsp90. *ACS Chem. Biol.* **2009**, 4, 289-297.
81. Proisy, N.; Sharp, S. Y.; Boxall, K.; Connelly, S.; Roe, S. M.; Prodromou, C.; Slawin, A. M.; Pearl, L. H.; Workman, P.; Moody, C. J. Inhibition of Hsp90 with synthetic macrolactones: synthesis and structural and biological evaluation of ring and conformational analogs of radicicol. *Chem. Biol.* **2006**, 13, 1203-1215.
82. Moulin, E.; Barluenga, S.; Winssinger, N. Concise synthesis of pochonin A, an HSP90 inhibitor. *Org. Lett.* **2005**, 7, 5637-5639.
83. Moulin, E.; Zoete, V.; Barluenga, S.; Karplus, M.; Winssinger, N. Design, synthesis, and biological evaluation of HSP90 inhibitors based on conformational analysis of radicicol and its analogues. *J. Am. Chem. Soc.* **2005**, 127, 6999-7004.
84. Turbyville, T. J.; Wijeratne, E. M.; Liu, M. X.; Burns, A. M.; Seliga, C. J.; Luevano, L. A.; David, C. L.; Faeth, S. H.; Whitesell, L.; Gunatilaka, A. A. Search for Hsp90 inhibitors with potential anticancer activity: isolation and SAR studies of radicicol and monocillin I from two plant-associated fungi of the Sonoran desert. *J. Nat. Prod.* **2006**, 69, 178-184.
85. Lampilas, M.; Lett, R. Convergent stereospecific total synthesis of monochiral Monocillin I related macrolides. *Tetrahedron Lett.* **1992**, 33, 773-776.
86. Lampilas, M.; Lett, R. Convergent stereospecific total synthesis of Monocillin I and Monorden (or Radicicol). *Tetrahedron Lett.* **1992**, 33, 777-780.
87. Barluenga, S.; Moulin, E.; Lopez, P.; Winssinger, N. Solution- and solid-phase synthesis of radicicol (monorden) and pochonin C. *Chemistry* **2005**, 11, 4935-52.
88. Yamamoto, K.; Garbaccio, R. M.; Stachel, S. J.; Solit, D. B.; Chiosis, G.; Rosen, N.; Danishefsky, S. J. Total synthesis as a resource in the discovery of potentially valuable antitumor agents: cycloproparadicicol. *Angew. Chem. Int. Ed.* **2003**, 42, 1280-1284.
89. Garbaccio, R. M.; Stachel, S. J.; Baeschlin, D. K.; Danishefsky, S. J. Concise asymmetric syntheses of radicicol and monocillin I. *J. Am. Chem. Soc.* **2001**, 123, 10903-10908.
90. Yang, Z. Q.; Geng, X.; Solit, D.; Pratilas, C. A.; Rosen, N.; Danishefsky, S. J. New efficient synthesis of resorcinylic macrolides via ynolides: establishment of cycloproparadicicol as synthetically feasible preclinical anticancer agent based on Hsp90 as the target. *J. Am. Chem. Soc.* **2004**, 126, 7881-7889.

91. Ikuina, Y.; Amishiro, N.; Miyata, M.; Narumi, H.; Ogawa, H.; Akiyama, T.; Shiotsu, Y.; Akinaga, S.; Murakata, C. Synthesis and antitumor activity of novel O-carbamoylmethyloxime derivatives of radicicol. *J. Med. Chem.* **2003**, 46, 2534-2541.
92. Sgobba, M.; Rastelli, G. Structure-based and in silico design of Hsp90 inhibitors. *ChemMedChem* **2009**, 4, 1399-1409.
93. Hadden, M. K.; Lubbers, D. J.; Blagg, B. S. Geldanamycin, radicicol, and chimeric inhibitors of the Hsp90 N-terminal ATP binding site. *Curr. Top. Med. Chem.* **2006**, 6, 1173-1182.
94. Muth, A.; Crowley, V.; Khandelwal, A.; Mishra, S.; Zhao, J.; Hall, J.; Blagg, B. S. Development of radamide analogs as Grp94 inhibitors. *Bioorg. Med. Chem.* **2014**, 22, 4083-98.
95. Clevenger, R. C.; Blagg, B. S. Design, synthesis, and evaluation of a radicicol and geldanamycin chimera, radamide. *Org. Lett.* **2004**, 6, 4459-4462.
96. Wang, M.; Shen, G.; Blagg, B. S. Radanamycin, a macrocyclic chimera of radicicol and geldanamycin. *Bioorg. Med. Chem. Lett.* **2006**, 16, 2459-2462.
97. Agatsuma, T.; Ogawa, H.; Akasaka, K.; Asai, A.; Yamashita, Y.; Mizukami, T.; Akinaga, S.; Saitoh, Y. Halohydrin and oxime derivatives of radicicol: synthesis and antitumor activities. *Bioorg. Med. Chem.* **2002**, 10, 3445-3454.
98. Jhaveri, K.; Taldone, T.; Modi, S.; Chiosis, G. Advances in the clinical development of heat shock protein 90 (Hsp90) inhibitors in cancers. *Biochim. Biophys. Acta*. **2012**, 1823, 742-755.
99. Messaoudi, S.; Peyrat, J. F.; Brion, J. D.; Alami, M. Heat-shock protein 90 inhibitors as antitumor agents: a survey of the literature from 2005 to 2010. *Expert Opin. Ther. Pat.* **2011**, 21, 1501-1542.
100. Ying, W.; Du, Z.; Sun, L.; Foley, K. P.; Proia, D. A.; Blackman, R. K.; Zhou, D.; Inoue, T.; Tatsuta, N.; Sang, J.; Ye, S.; Acquaviva, J.; Ogawa, L. S.; Wada, Y.; Barsoum, J.; Koya, K. Ganetespib, a unique triazolone-containing Hsp90 inhibitor, exhibits potent antitumor activity and a superior safety profile for cancer therapy. *Mol. Cancer Ther.* **2012**, 11, 475-484.
101. Shimamura, T.; Perera, S. A.; Foley, K. P.; Sang, J.; Rodig, S. J.; Inoue, T.; Chen, L.; Li, D.; Carretero, J.; Li, Y. C.; Sinha, P.; Carey, C. D.; Borgman, C. L.; Jimenez, J. P.; Meyerson, M.; Ying, W.; Barsoum, J.; Wong, K. K.; Shapiro, G. I. Ganetespib (STA-9090), a nongeldanamycin HSP90 inhibitor, has potent antitumor activity in in vitro and in vivo models of non-small cell lung cancer. *Clin. Cancer Res.* **2012**, 18, 4973-4985.
102. Wang, Y.; Trepel, J. B.; Neckers, L. M.; Giaccone, G. STA-9090, a small-molecule Hsp90 inhibitor for the potential treatment of cancer. *Curr. Opin. Investig. Drugs.* **2010**, 11, 1466-1476.
103. Garon, E. B.; Finn, R. S.; Hamidi, H.; Dering, J.; Pitts, S.; Kamranpour, N.; Desai, A. J.; Hosmer, W.; Ide, S.; Avsar, E.; Jensen, M. R.; Quadt, C.; Liu, M.; Dubinett, S. M.; Slamon, D. J. The HSP90 inhibitor NVP-AUY922 potently inhibits non-small cell lung cancer growth. *Mol. Canc. Ther.* **2013**, 12, 890-900.
104. Stuhmer, T.; Zollinger, A.; Siegmund, D.; Chatterjee, M.; Grella, E.; Knop, S.; Kortum, M.; Unzicker, C.; Jensen, M. R.; Quadt, C.; Chene, P.; Schoepfer, J.; Garcia-Echeverria, C.; Einsele, H.; Wajant, H.; Bargou, R. C. Signalling profile and antitumour activity of the novel Hsp90 inhibitor NVP-AUY922 in multiple myeloma. *Leukemia* **2008**, 22, 1604-1612.

105. Garcia-Carbonero, R.; Carnero, A.; Paz-Ares, L. Inhibition of Hsp90 molecular chaperones: moving into the clinic. *Lancet. Oncol.* **2013**, 14, e358-e369.
106. Nakashima, T.; Ishii, T.; Tagaya, H.; Seike, T.; Nakagawa, H.; Kanda, Y.; Akinaga, S.; Soga, S.; Shiotsu, Y. New molecular and biological mechanism of antitumor activities of KW-2478, a novel nonansamycin heat shock protein 90 inhibitor, in multiple myeloma cells. *Clin. Canc. Res.* **2010**, 16, 2792-2802.
107. Woodhead, A. J.; Angove, H.; Carr, M. G.; Chessari, G.; Congreve, M.; Coyle, J. E.; Cosme, J.; Graham, B.; Day, P. J.; Downham, R.; Fazal, L.; Feltell, R.; Figueroa, E.; Frederickson, M.; Lewis, J.; McMenamin, R.; Murray, C. W.; O'Brien, M. A.; Parra, L.; Patel, S.; Phillips, T.; Rees, D. C.; Rich, S.; Smith, D. M.; Trewartha, G.; Vinkovic, M.; Williams, B.; Woolford, A. J. Discovery of (2,4-dihydroxy-5-isopropylphenyl)-[5-(4-methylpiperazin-1-ylmethyl)-1,3-dihydrois oindol-2-yl]methanone (AT13387), a novel inhibitor of the molecular chaperone Hsp90 by fragment based drug design. *J. Med. Chem.* **2010**, 53, 5956-5969.
108. Hadden, M. K.; Hill, S. A.; Davenport, J.; Matts, R. L.; Blagg, B. S. J. Synthesis and Evaluation of Hsp90 inhibitors That Contain the 1,4-naphthoquinone Scaffold. *Bioorg. Med. Chem.* **2009**, 17, 634-640.
109. Shen, G.; Blagg, B. S. Radester, a novel inhibitor of the Hsp90 protein folding machinery. *Org. Lett.* **2005**, 7, 2157-2160.
110. Chiosis, G.; Lucas, B.; Shtil, A.; Huezo, H.; Rosen, N. Development of a purine-scaffold novel class of Hsp90 binders that inhibit the proliferation of cancer cells and induce the degradation of Her2 tyrosine kinase. *Bioorg. Med. Chem.* **2002**, 10, 3555-3564.
111. Chiosis, G.; Timaul, M. N.; Lucas, B.; Munster, P. N.; Zheng, F. F.; Sepp-Lorenzino, L.; Rosen, N. A small molecule designed to bind to the adenine nucleotide pocket of Hsp90 causes Her2 degradation and the growth arrest and differentiation of breast cancer cells. *Chem. Biol.* **2001**, 8, 289-299.
112. Wright, L.; Barril, X.; Dymock, B.; Sheridan, L.; Surgenor, A.; Beswick, M.; Drysdale, M.; Collier, A.; Massey, A.; Davies, N.; Fink, A.; Fromont, C.; Aherne, W.; Boxall, K.; Sharp, S.; Workman, P.; Hubbard, R. E. Structure-activity relationships in purine-based inhibitor binding to HSP90 isoforms. *Chem. Biol.* **2004**, 11, 775-785.
113. Llauger, L.; He, H.; Kim, J.; Aguirre, J.; Rosen, N.; Peters, U.; Davies, P.; Chiosis, G. Evaluation of 8-arylsulfanyl, 8-arylsulfoxyl, and 8-arylsulfonyl adenine derivatives as inhibitors of the heat shock protein 90. *J. Med. Chem.* **2005**, 48, 2892-2905.
114. Vilenchik, M.; Solit, D.; Basso, A.; Huezo, H.; Lucas, B.; He, H.; Rosen, N.; Spampinato, C.; Modrich, P.; Chiosis, G. Targeting wide-range oncogenic transformation via PU24FCl, a specific inhibitor of tumor Hsp90. *Chem. Biol.* **2004**, 11, 787-797.
115. He, H.; Zatorska, D.; Kim, J.; Aguirre, J.; Llauger, L.; She, Y.; Wu, N.; Immormino, R. M.; Gewirth, D. T.; Chiosis, G. Identification of potent water soluble purine-scaffold inhibitors of the heat shock protein 90. *J. Med. Chem.* **2006**, 49, 381-390.
116. Patel, H. J.; Modi, S.; Chiosis, G.; Taldone, T. Advances in the discovery and development of heat-shock protein 90 inhibitors for cancer treatment. *Expert Opin. Drug Disscov.* **2011**, 6, 559-587.
117. Kasibhatla, S. R.; Hong, K.; Biamonte, M. A.; Busch, D. J.; Karjian, P. L.; Sensintaffar, J. L.; Kamal, A.; Lough, R. E.; Brekken, J.; Lundgren, K.; Grecko, R.; Timony, G. A.; Ran, Y.; Mansfield, R.; Fritz, L. C.; Ulm, E.; Burrows, F. J.; Boehm, M. F. Rationally designed

high-affinity 2-amino-6-halopurine heat shock protein 90 inhibitors that exhibit potent antitumor activity. *J. Med. Chem.* **2007**, 50, 2767-2778.

118. Lundgren, K.; Zhang, H.; Brekken, J.; Huser, N.; Powell, R. E.; Timple, N.; Busch, D. J.; Neely, L.; Sensintaffar, J. L.; Yang, Y. C.; McKenzie, A.; Friedman, J.; Scannevin, R.; Kamal, A.; Hong, K.; Kasibhatla, S. R.; Boehm, M. F.; Burrows, F. J. BIIB021, an orally available, fully synthetic small-molecule inhibitor of the heat shock protein Hsp90. *Mol. Cancer Ther.* **2009**, 8, 921-929.
119. Dickson, M. A.; Okuno, S. H.; Keohan, M. L.; Maki, R. G.; D'Adamo, D. R.; Akhurst, T. J.; Antonescu, C. R.; Schwartz, G. K. Phase II study of the HSP90-inhibitor BIIB021 in gastrointestinal stromal tumors. *Ann. Oncol.* **2013**, 24, 252-257.
120. Hong, D.; Said, R.; Falchook, G.; Naing, A.; Moulder, S.; Tsimberidou, A. M.; Galluppi, G.; Dakappagari, N.; Storgard, C.; Kurzrock, R.; Rosen, L. S. Phase I study of BIIB028, a selective heat shock protein 90 inhibitor, in patients with refractory metastatic or locally advanced solid tumors. *Clin. Cancer Res.* **2013**, 19, 4824-4831.
121. Conde, R.; Belak, Z. R.; Nair, M.; O'Carroll, R. F.; Ovsenek, N. Modulation of Hsf1 activity by novobiocin and geldanamycin. *Biochem. Cell Biol.* **2009**, 87, 845-851.
122. McCollum, A. K.; TenEyck, C. J.; Stensgard, B.; Morlan, B. W.; Ballman, K. V.; Jenkins, R. B.; Toft, D. O.; Erlichman, C. P-Glycoprotein-mediated resistance to Hsp90-directed therapy is eclipsed by the heat shock response. *Cancer Res.* **2008**, 68, 7419-7427.
123. Zou, J.; Guo, Y.; Guettouche, T.; Smith, D. F.; Voellmy, R. Repression of heat shock transcription factor HSF1 activation by HSP90 (HSP90 complex) that forms a stress-sensitive complex with HSF1. *Cell* **1998**, 94, 471-480.
124. Shi, Y.; Mosser, D. D.; Morimoto, R. I. Molecular chaperones as HSF1-specific transcriptional repressors. *Genes Dev.* **1998**, 12, 654-666.
125. Bagatell, R.; Paine-Murrieta, G. D.; Taylor, C. W.; Pulcini, E. J.; Akinaga, S.; Benjamin, I. J.; Whitesell, L. Induction of a heat shock factor 1-dependent stress response alters the cytotoxic activity of hsp90-binding agents. *Clin. Cancer Res.* **2000**, 6, 3312-3318.
126. Zuo, J.; Rungger, D.; Voellmy, R. Multiple layers of regulation of human heat shock transcription factor 1. *Mol. Cell Biol.* **1995**, 15, 4319-4330.
127. Xia, W.; Voellmy, R. Hyperphosphorylation of heat shock transcription factor 1 is correlated with transcriptional competence and slow dissociation of active factor trimers. *J. Biol. Chem.* **1997**, 272, 4094-4102.
128. Holzbeierlein, J. M.; Windsperger, A.; Vielhauer, G. Hsp90: a drug target? *Curr. Oncol. Rep.* **2010**, 12, 95-101.
129. Biamonte, M. A.; Van de Water, R.; Arndt, J. W.; Scannevin, R. H.; Perret, D.; Lee, W. C. Heat shock protein 90: inhibitors in clinical trials. *J. Med. Chem.* **2010**, 53, 3-17.
130. Marcu, M. G.; Schulte, T. W.; Neckers, L. Novobiocin and Related Coumarins and Depletion of Heat Shock Protein 90-Dependent Signaling Proteins. *J. Natl. Cancer Inst.* **2000**, 92, 242-248.
131. Marcu, M. G.; Chadli, A.; Bouhouche, I.; Catelli, M.; Neckers, L. M. The heat shock protein 90 antagonist novobiocin interacts with a previously unrecognized ATP-binding domain in the carboxyl terminus of the chaperone. *J. Biol. Chem.* **2000**, 275, 37181-37186.
132. Garnier, C.; Lafitte, D.; Tsvetkov, P. O.; Barbier, P.; Leclerc-Devin, J.; Millot, J.-M.; Briand, C.; Makarov, A. A.; Catelli, M. G.; Peyrot, V. Binding of ATP to heat shock protein 90: evidence for an ATP-binding site in the C-terminal domain. *J. Biol. Chem.* **2002**, 277, 12208-12214.

133. Söti, C.; Rácz, A.; Csermely, P. A Nucleotide-dependent molecular switch controls ATP binding at the C-terminal domain of Hsp90. N-terminal nucleotide binding unmasks a C-terminal binding pocket. *J. Biol. Chem.* **2002**, 277, 7066-7075.
134. Söti, C.; Vermes, Á.; Haystead, T. A. J.; Csermely, P. Comparative analysis of the ATP-binding sites of Hsp90 by nucleotide affinity cleavage: a distinct nucleotide specificity of the C-terminal ATP-binding site. *Eur. J. Biochem.* **2003**, 270, 2421-2428.
135. Bras, G. L.; Radanyi, C.; Peyrat, J.-F.; Brion, J.-D.; Alami, M.; Marsaud, V.; Stella, B.; Renoir, J.-M. New novobiocin analogues as antiproliferative agents in breast cancer cells and potential inhibitors of heat shock protein 90. *J. Med. Chem.* **2007**, 50, 6189-6200.
136. Burlison, J. A.; Avila, C.; Vielhauer, G.; Lubbers, D. J.; Holzbeierlein, J.; Blagg, B. S. J. Development of novobiocin analogues that manifest anti-proliferative activity against several cancer cell lines. *J. Org. Chem.* **2008**, 73, 2130-2137.
137. Donnelly, A.; Blagg, B. S. J. Novobiocin and additional inhibitors of the hsp90 C-terminal nucleotide-binding pocket. *Curr. Med. Chem.* **2008**, 15, 2702-2717.
138. Donnelly, A. C.; Mays, J. R.; Burlinson, J. A.; Nelson, J. T.; Vielhauer, G.; Holzbeierlein, J.; Blagg, B. S. J. The Design, Synthesis and Evaluation of Coumarin Ring Derivatives of the Novobiocin Scaffold that Exhibit Antiproliferative Activity. *J. Org. Chem.* **2008,** 73, 8901-8920.
139. Kusuma, B. R.; Duerfeldt, A. S.; Blagg, B. S. J. Synthesis and Biological Evaluation of Arylated Novobiocin Analogs as Hsp90 Inhibitors. *Bioorg. Med. Chem. Lett.* **2011,** 21, 7170-7174.
140. Kusuma, B. R.; Zhang, L.; Sundstrom, T.; Peterson, L. B.; Dobrowsky, R. T.; Blagg, B. S. Synthesis and evaluation of novologues as C-terminal Hsp90 inhibitors with cytoprotective activity against sensory neuron glucotoxicity. *J. Med. Chem.* **2012,** 55, 5797-5812.
141. Matthews, S. B.; Vielhauer, G. A.; Manthe, C. A.; Chaguturu, V. K.; Szabla, K.; Matts, R. L.; Donnelly, A. C.; Blagg, B. S. J.; Holzbeierlein, J. M. Characterization of a Novel Novobiocin Analogue as a Putative C-Terminal Inhibitor of Heat Shock Protein 90 in Prostate Cancer Cells. *The Prostate* **2010,** 70, 27-36.
142. Peterson, L. B.; Blagg, B. S. J. Click Chemistry to Probe Hsp90: Synthesis and Evaluation of a Series of Triazole-Containing Novobiocin Analogues. *Bioorg. Med. Chem. Lett.* **2010**, 20, 3957-3960.
143. Shelton, S. N.; Shawgo, M. E.; Matthews, S. B.; Lu, Y.; Donnelly, A. C.; Szabla, K.; Tanol, M.; Vielhauer, G. A.; Rajewski, R. A.; Matts, R. L.; Blagg, B. S. J.; Robertson, J. D. KU135, a Novel Novobiocin-Derived C-Terminal Inhibitor of the 90-kDa Heat Shock Protein, Exerts Potent Antiproliferative Effects in Human Leukemic Cells. *Mol. Pharmacol.* **2009**, 76, 1314-1322.
144. Radanyi, C.; Bras, G. L.; Messaoudi, S.; Bouclier, C.; Peyrat, J.-F.; Brion, J.-D.; Marsaud, V.; Renoir, J.-M.; Alami, M. Synthesis and Biological Activity of Simplified Denoviose-Coumarins Related to Novobiocin as Potent Inhibitors of Heat-Shock Protein 90 (hsp90). *Bioorg. Med. Chem. Lett.* **2008**, 18, 2495-2498.
145. Zhao, H.; Blagg, B. S. J. Novobiocin Analogues with Second-Generation Noviose Surrogates. *Bioorg. Med. Chem. Lett.* **2013**, 23, 552-557.
146. Zhao, H.; Donnelly, A. C.; Kusuma, B. R.; Brandt, G. E. L.; Brown, D.; Rajewski, R. A.; Vielhauer, G.; Holzbeierlein, J.; Cohen, M. S.; Blagg, B. S. J. Engineering an Antibiotic to Fight Cancer: Optimization of the Novobiocin Scaffold to Produce Anti-Proliferative Agents. *J. Med. Chem.* **2011**, 54, 3839-3853.

147. Zhao, H.; Kusuma, B. R.; Blagg, B. S. J. Synthesis and Evaluation of Noviose Replacements on Novobiocin that Manifest Anti-proliferative Activity. *ACS Med. Chem. Lett.* **2010**, 1, 311-315.
148. Zhao, H.; Moroni, E.; Yan, B.; Colombo, G.; Blagg, B. S. 3D-QSAR Assisted Design, Synthesis and Evaluation of Novobiocin Analogues. *ACS Med. Chem. Lett.* **2012**, 4, 57-62.
149. Zhao, H.; Yan, B.; Peterson, L. B.; Blagg, B. S. J. 3-Arylcoumarin Derivatives Manifest Anti-proliferative Activity through Hsp90 Inhibition. *ACS Med. Chem. Lett.* **2012**, 3, 327-331.
150. Matts, R. L.; Dixit, A.; Peterson, L. B.; Sun, L.; Voruganti, S.; Kalyanaraman, P.; Hartson, S. D.; Verkhivker, G. M.; Blagg, B. S. J. Elucidation of the Hsp90 C-Terminal Inhibitor Binding Site. *ACS Chem. Biol.* **2011**, 6, 800-807.
151. Dixit, A.; Verkhivker, G. M. Probing Molecular Mechanisms of the Hsp90 Chaperone: Biophysical Modeling Identifies Key Regulators of Functional Dynamics. *PloS one* **2012**, 7, e37605.
152. Burlison, J. A.; Neckers, L.; Smith, A. B.; Maxwell, A.; Blagg, B. S. J. Novobiocin: Redesigning a DNA Gyrase Inhibitor for Selective Inhibitor of Hsp90. *J. Am. Chem. Soc.* **2006**, 128, 15529-15536.
153. Kusuma, B. R.; Peterson, L. B.; Zhao, H.; Vielhauer, G.; Holzbeierlein, J.; Blagg, B. S. J. Targeting the Heat Shock Protein 90 Dimer with Dimeric Inhibitors. *J. Med. Chem.* **2011**, 54, 6234-6253.
154. Kusuma, B. R.; Khandelwal, A.; Gu, W.; Brown, D.; Liu, W.; Vielhauer, G.; Holzbeierlein, J.; Blagg, B. S. J. Synthesis and Biological Evaluation of Coumarin Replacements of Novobiocin as Hsp90 Inhibitors. *Bioorg. Med. Chem.* **2014**, 22, 1441-1449.
155. Moroni, E.; Zhao, H.; Blagg, B. S.; Colombo, G. Exploiting Conformational Dynamics in Drug Discovery: Design of C-Terminal Inhibitors of Hsp90 with Improved Activities. *J. Chem. Infor. Model.* **2014**, 54, 195-208.
156. Zhao, H.; Moroni, E.; Colombo, G.; Blagg, B. S. J. Identification of a New Scaffold for Hsp90 C-Terminal Inhibition. *ACS Med. Chem. Lett.* **2014**, 5, 84-88.
157. Zhao, J.; Zhao, H.; Hall, J. A.; Brown, D.; Brandes, E.; Bazzill, J.; Grogan, P. T.; Subramanian, C.; Vielhauer, G.; Cohen, M. S.; Blagg, B. S. Triazole Containing Novobiocin and Biphenyl Amides as Hsp90 C-Terminal Inhibitors. *Med. Chem. Comm.* **2014**, 5, 1317-1323.
158. Liu, W.; Vielhauer, G. A.; Holzbeierlein, J. M.; Zhao, H.; Ghosh, S.; Brown, D.; Lee, E.; Blagg, B. S. KU675, a Concomitant Heat-Shock Protein Inhibitor of Hsp90 and Hsc70 that Manifests Isoform Selectivity for Hsp90α in Prostate Cancer Cells. *Mol. Pharmacol.* **2015,** 88, 121-130.
159. Gazak, R.; Walterova, D.; Kren, V. Silybin and Silymarin--New and Emerging Applications in Medicine. *Curr. Med. Chem.* **2007**, 14, 315-338.
160. Agarwal, C.; Singh, R. P.; Dhanalakshmi, S.; Tyagi, A. K.; Tecklenburg, M.; Sclafani, R. A.; Agarwal, R. Silibinin upregulates the expression of cyclin-dependent kinase inhibitors and causes cell cycle arrest and apoptosis in human colon carcinoma HT-29 cells. *Oncogene* **2003**, 22, 8271-8282.
161. Yang, L. X.; Huang, K. X.; Li, H. B.; Gong, J. X.; Wang, F.; Feng, Y. B.; Tao, Q. F.; Wu, Y. H.; Li, X. K.; Wu, X. M.; Zeng, S.; Spencer, S.; Zhao, Y.; Qu, J. Design, Synthesis, and

Examination of Neuron Protective Properties of Alkenylated and Amidated Dehydro-Silybin Derivatives. *J. Med. Chem.* **2009**, 52, 7732-7752.
162. Matts, R. L.; Brandt, G. E. L.; Lu, Y.; Dixit, A.; Mollapour, M.; Wang, S.; Donnelly, A. C.; Neckers, L.; Verkhivker, G.; Blagg, B. S. J. A Systematic Protocol for the Characterization of Hsp90 Modulators. *Bioorg. Med. Chem.* **2011**, 19, 684-692.
163. Yang, H.; Chen, D.; Cui, Q. C.; Yuan, X.; Dou, Q. P. Celastrol, a triterpene extracted from the Chinese "Thunder of God Vine," is a potent proteasome inhibitor and suppresses human prostate cancer growth in nude mice. *Cancer Res.* **2006**, 66, 4758-4765.
164. Sethi, G.; Ahn, K. S.; Pandey, M. K.; Aggarwal, B. B. Celastrol, a novel triterpene, potentiates TNF-induced apoptosis and suppresses invasion of tumor cells by inhibiting NF-kappaB-regulated gene products and TAK1-mediated NF-kappaB activation. *Blood* **2007**, 109, 2727-2735.
165. Allison, A. C.; Cacabelos, R.; Lombardi, V. R.; Alvarez, X. A.; Vigo, C. Celastrol, a potent antioxidant and anti-inflammatory drug, as a possible treatment for Alzheimer's disease. *Prog. Neuropsycho. Pharmacol. Biol. Psychiatry.* **2001**, 25, 1341-1357.
166. Hieronymus, H.; Lamb, J.; Ross, K. N.; Peng, X. P.; Clement, C.; Rodina, A.; Nieto, M.; Du, J.; Stegmaier, K.; Raj, S. M.; Maloney, K. N.; Clardy, J.; Hahn, W. C.; Chiosis, G.; Golub, T. R. Gene expression signature-based chemical genomic prediction identifies a novel class of HSP90 pathway modulators. *Cancer Cell.* **2006**, 10, 321-330.
167. Davenport, J.; Manjarrez, J. R.; Peterson, L.; Krumm, B.; Blagg, B. S.; Matts, R. L. Gambogic acid, a natural product inhibitor of Hsp90. *J. Nat. Prod.* **2011**, 74, 1085-1092.
168. Hadden, M. K.; Galam, L.; Gestwicki, J. E.; Matts, R. L.; Blagg, B. S. Derrubone, an inhibitor of the Hsp90 protein folding machinery. *J. Nat. Prod.* **2007**, 70, 2014-2018.
169. Yu, Y.; Hamza, A.; Zhang, T.; Gu, M.; Zou, P.; Newman, B.; Li, Y.; Gunatilaka, A. A.; Zhan, C. G.; Sun, D. Withaferin A targets heat shock protein 90 in pancreatic cancer cells. *Biochem. Pharmacol.* **2010**, 79, 542-551.
170. Kamath, S. G.; Chen, N.; Xiong, Y.; Wenham, R.; Apte, S.; Humphrey, M.; Cragun, J.; Lancaster, J. M. Gedunin, a novel natural substance, inhibits ovarian cancer cell proliferation. *Int. J. Gynecol. Cancer.* **2009**, 19, 1564-1569.
171. Lamb, J.; Crawford, E. D.; Peck, D.; Modell, J. W.; Blat, I. C.; Wrobel, M. J.; Lerner, J.; Brunet, J. P.; Subramanian, A.; Ross, K. N.; Reich, M.; Hieronymus, H.; Wei, G.; Armstrong, S. A.; Haggarty, S. J.; Clemons, P. A.; Wei, R.; Carr, S. A.; Lander, E. S.; Golub, T. R. The Connectivity Map: using gene-expression signatures to connect small molecules, genes, and disease. *Science* **2006**, 313, 1929-1935.
172. Patwardhan, C. A.; Fauq, A.; Peterson, L. B.; Miller, C.; Blagg, B. S.; Chadli, A. Gedunin inactivates the co-chaperone p23 protein causing cancer cell death by apoptosis. *J. Biol. Chem.* **2013**, 288, 7313-7325.
173. Kunze, B.; Sasse, F.; Wieczorek, H.; Huss, M. Cruentaren A, a highly cytotoxic benzolactone from Myxobacteria is a novel selective inhibitor of mitochondrial F1-ATPases. *FEBS Lett.* **2007**, 581, 3523-3527.
174. Kunze, B.; Steinmetz, H.; Hofle, G.; Huss, M.; Wieczorek, H.; Reichenbach, H. Cruentaren, a new antifungal salicylate-type macrolide from Byssovorax cruenta (myxobacteria) with inhibitory effect on mitochondrial ATPase activity. Fermentation and biological properties. *J. Antibiot.* **2006,** 59, 664-668.
175. Bindl, M.; Jean, L.; Herrmann, J.; Muller, R.; Furstner, A. Preparation, modification, and evaluation of cruentaren A and analogues. *Chemistry* **2009**, 15, 12310-12319.

176. Vintonyak, V. V.; Cala, M.; Lay, F.; Kunze, B.; Sasse, F.; Maier, M. E. Synthesis and biological evaluation of cruentaren A analogues. *Chemistry* **2008**, 14, 3709-3720.
177. Papathanassiu, A. E.; MacDonald, N. J.; Bencsura, A.; Vu, H. A. F1F0-ATP synthase functions as a co-chaperone of Hsp90-substrate protein complexes. *Biochem. Biophys. Res. Commun.* **2006**, 345, 419-429.
178. Hall, J. A.; Kusuma, B. R.; Brandt, G. E.; Blagg, B. S. Cruentaren A binds F1F0 ATP synthase to modulate the Hsp90 protein folding machinery. *ACS Chem. Biol.* **2014**, 9, 976-985.

Chapter II

Synthesis and Structure−Activity Relationships of EGCG Analogues

II.1. Introduction to EGCG

Green tea is one of the most popular beverages consumed worldwide and its consumption has been associated with many health benefits.[1-6] Green tea is composed of alkaloids (caffeine, theophylline, and theobromine), amino acids, proteins, carbohydrates, volatile organic compounds, and polyphenols.[7] The catechins (Figure 14), which are responsible for the some of the health benefits attributed to the consumption of green tea polyphenols, are part of the polyphenolic component of the green tea.[8-10] Epigallocatechin-3-gallate (EGCG) is the most abundant catechin found in the green tea (Table 3), and exhibits both antioxidant activity and anticancer activity *in vitro* and *in vivo*.[8, 11-14] Additionally, EGCG exhibits beneficial effects in several diseases including diabetes, Parkinson's, Alzheimer's, and obesity.[15-20]

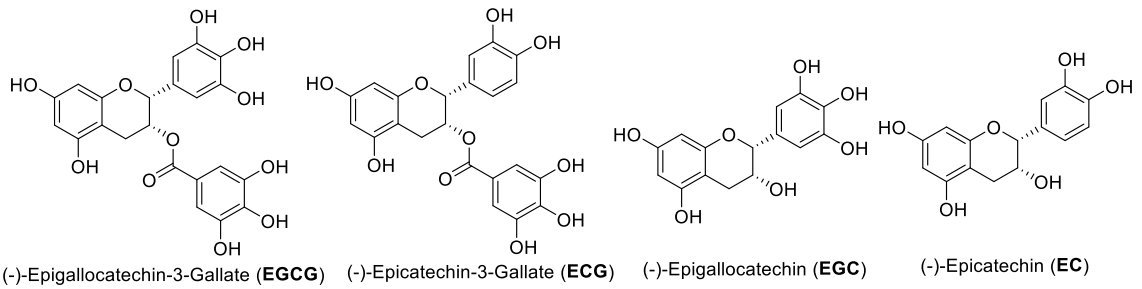

Figure 14. Structure of green tea catechins.

EGCG has been shown to be an efficacious agent in cancer chemoprevention against a broad range of carcinogens. EGCG acts on multiple signal transduction pathways associated with differentiation, apoptosis, inflammation, angiogenesis and metastasis.[1, 6, 7, 16] Recent studies have provided additional mechanistic insights and revealed that EGCG suppresses the levels of various cancer biomarkers.[20-24] As a result, EGCG is currently undergoing multiple clinical trials to evaluate its chemopreventive activity.[25-32] Results from these studies have been encouraging, as

daily consumption of EGCG delays the onset of cancer and lower the rate of recurrence in breast cancer patients.

Table 3. Catechin concentrations in green tea

Catechin in green tea infusion	Catechin Concentration (mg/L)	Catechin Concentration (mg/8 fl oz)
EGCG	117-442	25-106
EGC	203-471	49-113
ECG	17-150	4-36
EC	25-81	6-19

EGCG also manifests anti-proliferative effects against various types of cancer including breast, colon, lung, blood, and skin cancers. EGCG inhibits tumor growth via multiple mechanisms of action (Table 4).[18, 30, 33-36] In oral cancer cells, EGCG blocked cell division in the G1 phase and suppressed mitogenic signal transduction by prohibiting the binding of growth factors to their receptors.[37] Similarly, EGCG also induced cell cycle arrest in the G0/G1 phase in MCF-7 cells at 30 μM.[38] In human lymphoid leukemia cells, EGCG inhibited cell proliferation and induced apoptosis.[39] Additionally, EGCG has been shown to modulate aberrant epigenetic alternations associated with tumor initiation and progression, including DNA methylation. EGCG blocked DNA methylation via inhibition of DNA methyltransferases (DNMT's) in colon cancer (HT-29) cells, esophageal cancer (KYSE-150), and prostate cancer (PC3).[40-44] EGCG exhibited efficacy in xenograft model of breast and pancreatic cancer, and manifested anti-cancer activity in a human prostate cancer progression model.[10, 45]

In recent years, an increasing number of studies have been conducted to evaluate EGCG as an adjuvant for cancer chemotherapy.[9] For example, the co-administration of EGCG with traditional cancer chemotherapeutics have resulted in additive or synergistic effects; cisplatin,

tamoxifen, 5-flurouracil, temozolamide exhibited enhanced activity when given in combination with EGCG.[46-49] These activities likely result from EGCG's ability to act as a chemosensitizer and to modulate the pharmacokinetics of drugs by inhibition of the P-glycoprotein efflux pumps.[10]

Table 4. Molecular Mechanisms of EGCG.

Molecular Mechanism	Molecular Targets	References
Induction of cell cycle arrest	CyclinD, Cyclin E, CDK1, CDK2, CDK4, CDK6	45, 50-52
Induction of apoptosis	Survivin, c-IAP1, c-IAP2, Bcl-xl,*Caspase-3*, *Caspase-9*	13, 53-56
Inhibition of proliferation and Inflammation	PI3K, EGFR, COX-2, HIF-1a, AKT, ERK,	45, 57-60
Angiogenesis	HIF-1a, Erb2, VEGFR1 & 2	61-63
Metastasis	MMP2-9, MMP-2, lamanin	64-66
Epigenetic modifier	DNMT's, HAT,	40, 42, 67
Proteasomal activity	20S/26S proteasome complex	68, 69

II.1.1. Binding of EGCG to Hsp90

While EGCG exerts anticancer effects for decades, its association with Hsp90 was not identified until recently. Studies on EGCGs chemoprevention effect led to the identification of Hsp90 as one of its biological target. In 2005, Palermo and co-workers showed that EGCG blocked (AhR)-mediated transcription induced by a potent carcinogen 2,3,7,8-Tetrachlorodibenzodioxin (TCDD), by a mechanism that involves Hsp90.[70] Aryl hydrocarbon receptor (AhR) is a ligand activated transcription factor that mediates toxic effects of numerous toxins including polycyclic aryl hydrocarbons (PAH's), which binds to the AhR. In cytosol, AhR exists in a protein complex with Hsp90, p23, and XAP2. Upon binding of PAH's to AhR, XAP2 is dissociated from the complex and the Hsp90-AhR complex translocated to nucleus. Subsequent events lead to the

generation of DNA adducts that facilitate carcinogenesis. EGCG exhibited its chemo-preventive activity and inhibited the AhR-mediated carcinogenesis, however, it did not compete for binding to AhR. This study led to the discovery of an indirect mechanism of AhR modulation that involved the binding of EGCG to the Hsp90 C-terminus. Subsequent affinity purification studies demonstrated that EGCG binds to amino acids 538-728 within the Hsp90 C-terminus to inhibit AhR-mediated transcription. Additionally, EGCG induced the degradation of other Hsp90 clients as well, including Raf1, Her2, and Akt, while levels of Hsp90 and Hsp70 remained unchanged.[71]

While EGCG manifests modest efficacy against various cancer cell lines, the poor bioavailability and lipophilicity of EGCG along with its metabolically labile functionalities make EGCG a poor lead compound for clinical development.[72, 73] At the time, only two natural products novobiocin and silybin were known to bind the Hsp90 C-terminus, and therefore EGCG was pursued as a probe to further investigate the mechanism by which C-terminal inhibitors modulate the Hsp90 protein folding machinery.

II.2. Proposed EGCG Analogues

EGCG exhibits antioxidant activity both *in vitro* and *in vivo*, which also leads to epimerization and/or dimerization (Figure 15) and contributes to its low efficacy and metabolic instability.[74-77] Epimerization of the methine hydrogen leads to formation of the thermodynamically more stable anti product, GCG (Figure 15a), whose activity against Hsp90 has not been investigated. EGCG is prone to autoxidation and dimerizes to give theasinensin A, and P2 (Figure 15b). Studies by Suzuki and co-workers have shown that phenols on the B-ring facilitates epimerization at C-2, whereas O-methylated derivatives of the 4-phenols prevent epimerization.[77] Therefore, the design of new EGCG analogues must take these prior studies into account in an effort to produce stable derivatives that are not prone to oxidation/epimerization.

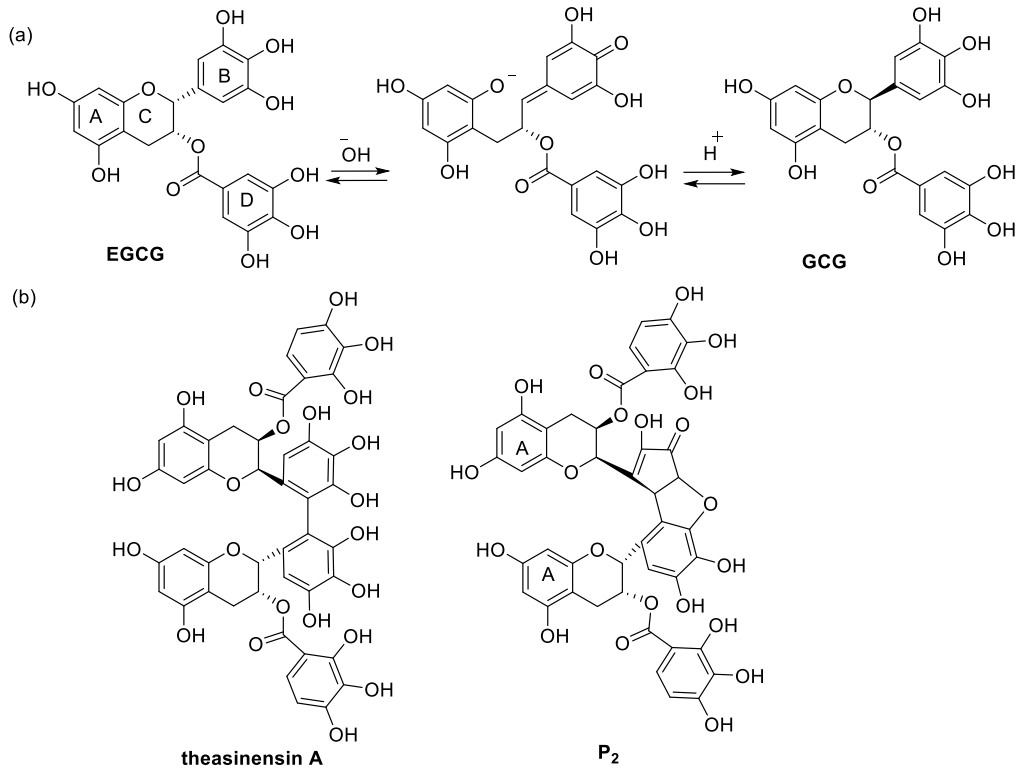

Figure 15. Chemical instability of EGCG: (a) Mechanism of epimerization of EGCG; (b) autoxidation products of EGCG.

To probe EGCG's structure-activity relationships with Hsp90, three series of analogues (Figure 16) were pursued; (I) 3',4',5'-trimethoxy groups were incorporated into the B-ring, (II) compounds omitting substituents on the B-ring were prepared, and (III) compounds lacking the B-ring were also constructed. Furthermore, the phenols on the A-ring were converted to methyl ethers for biological evaluation and finally, the gallic acid moiety (D-ring) of EGCG was replaced with various aryl acids for elucidation of additional SAR trends. These aryl acids were chosen to probe the effect of substitution at the 3- and 4-position of the D-ring and to incorporate optimized novobiocin appendages to evaluate their potential for overlapping binding modes.[78-81]

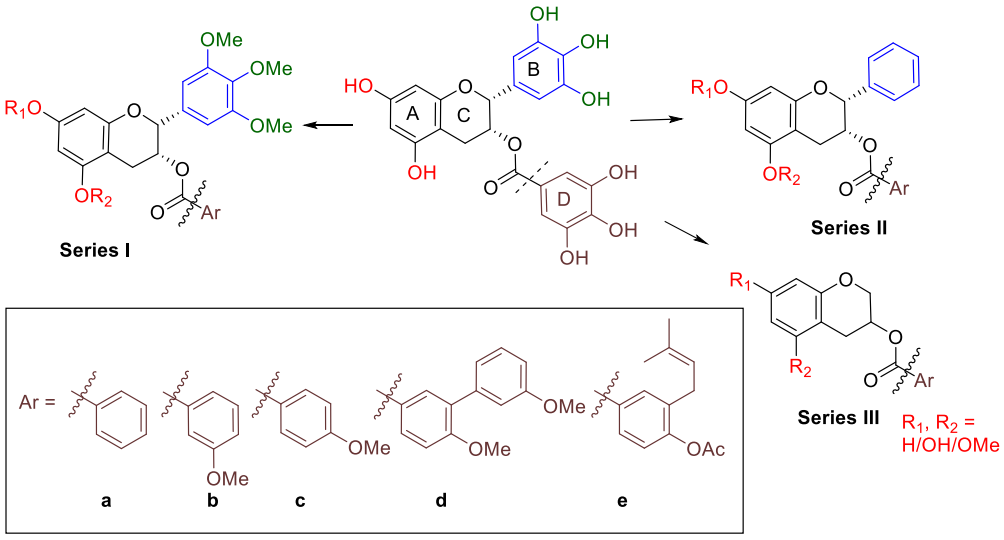

Figure 16. Three different series of EGCG analogues.

II.3. Synthesis and Evaluation of Series I and Series II EGCG Analogues

II.3.1 Synthesis of Series I Analogues

Syntheses of the A-, B- and D-ring modified compounds (**7a–e** and **8a–e**) are described in Scheme 1. Prior work by Li and co-workers provided rapid access towards preparation of the flavon-3-ol core, enlisting the use of a silica/sulfuric acid catalyst to couple electron rich phenols (**1a–b**) with (E)-3-(3,4,5-trimethoxyphenyl)prop-2-en-1-ol, which worked surprisingly well and led to various substituted A-ring analogues (**2a–b**).[82] Dihydroxylation of the resulting alkenes (**2a–b**) with catalytic osmium tetroxide and excess N-methylmorpholine-N-oxide gave the corresponding diol's, **3a–b**.[83] Various methods have been reported for cyclization and construction of the benzopyran core; however, stereochemical control at the 2,3-ring junction depends upon substituents on the B-ring.[84] Therefore, cyclization of diol's **3a–b** to furnish the 2,3-dihydrobenzopyran core in a stereoselective manner was pursued via two steps. Treatment of **3a–b** with trimethylorthoacetate in the presence of catalytic pyridinium *p*-toluenesulfonate, formed

the corresponding orthoesters, which upon the addition of 10% boron trifluoride diethyl etherate produced the desired cyclic products. Without purification, the cyclized products were subjected to solvolysis conditions to furnish alcohols **4a–b** in high yields and with the anti-configuration. The 2,3-syn products, **5a–b**, were established by Dess-Martin oxidation of the secondary alcohols

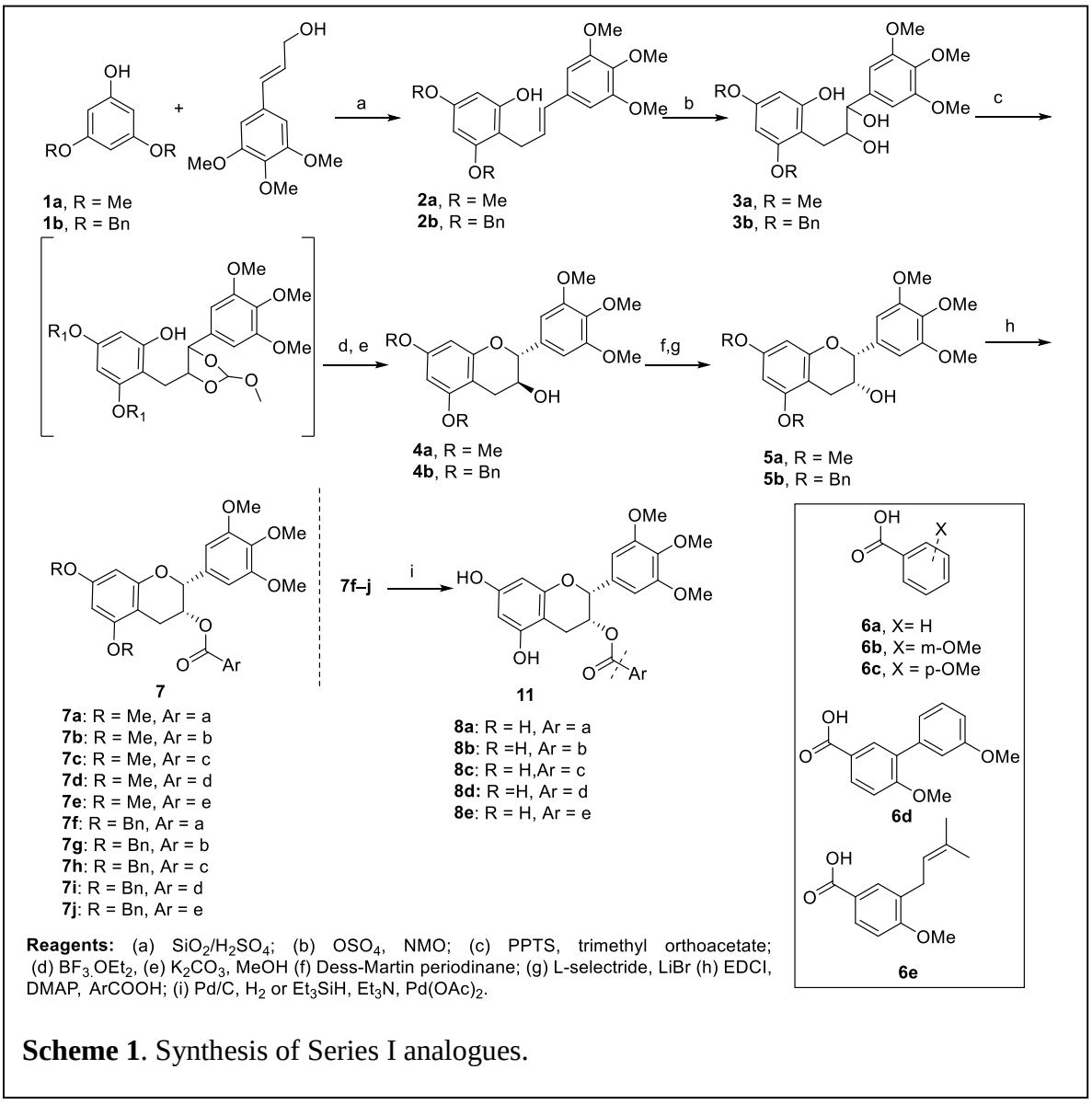

Scheme 1. Synthesis of Series I analogues.

(**4a–b**) to the corresponding ketones, which underwent subsequent reduction with L-selectride to give *syn* products, **5a–b**, respectively.[85] These flavon-3-ol moieties (**5a–b**) served as late stage intermediates to incorporate additional substitutions onto the D-ring. Aryl acids **6a–e** were chosen

as replacements for the metabolically labile, gallic ester moiety of EGCG and also represent optimized side chains identified from prior studies with the other Hsp90 C-terminal inhibitor, novobiocin. Acids **6a–c** were purchased from commercial sources and **6d** and **6e** were synthesized following literature procedures. Coupling of the alcohols (**5a–b**) with aromatic acids **6a–e** enlisting 1-ethyl-3-(3-dimethylaminopropyl) carbodiimide (EDCI) and 4-dimethylaminopyrine (DMAP) gave the corresponding esters, **7a–j**. Hydrogenolysis of **7f–i** with palladium/carbon and hydrogen gas gave **8a–d** in high yield**.** Cleavage of benzyl ethers of **7j** was accomplished using transfer hydrogenation using triethylsilane to give the desired **8e**.[86]

II.3.2. Synthesis of Series II Analogues

Syntheses of compounds omitting substitution on the B-ring (**13a–e** and **14a–e**) are described in Scheme 2. These compounds were synthesized similar to Series I compounds starting from commercially available cinnamyl alcohol and phenols **1a** and **1b**.

II.3.3. Biological Evaluation of Series I and Series II Analogues

Upon preparation of the A-, the D-ring modified B-ring substituted EGCG analogues (**7a–e**, **8a–e** and, **13a–e**, **14a–e**), these compounds were evaluated against MCF-7 and SKBr3 breast cancer cell lines for determination of their anti-proliferative activities (Table 5). The SkBr3 (estrogen receptor negative, Her2 overexpressing) and the MCF-7 (estrogen receptor positive) cell lines were chosen due to the fact that both Her2 and the estrogen receptor are Hsp90-dependent client proteins. Four of the D-ring analogues that contain two methoxy groups on the A-ring and no substituents on the B-ring (**13a–d**) were inactive against both MCF-7 and SKBr3 cell lines. Only compound **13e** manifested significant anti-proliferative activity with an IC_{50} value of 25.35 ± 5.25 μM against MCF-7 and 36.1 ± 2.51 μM against SKBr3 cell lines. Similar trends were observed for compounds (**7a–e**) containing the 3,4,5-trimethoxy substituents on the B-ring, as only

7e was found to be potent with IC_{50} values of 19.48 ± 2.5 μM and 24.87 ± 3.29 μM against MCF-7 and SKBr-3 cell lines, respectively. Analogues **14a–e** containing phenols on the A-ring were more potent when compared to EGCG and analogues with methyl ethers (**13a–e)**. Incorporation of a methoxy group at the *meta*- and the *para*-positions of the D-ring (**14b** and **14c**) did not alter activity when compared to unsubstituted analogue, **14a**. Compound **14e** was found to be the most potent of this series and displayed an IC_{50} value of 3.99 ± 1.4 μM against the MCF-7 cell line. In contrast, compounds with 3-,4-,5-trimethoxy groups on the B-ring (**8a–e**) were less active when compared to analogues without substitution on the B-ring (**14a–e**). This data suggests that substitutions on the B-ring are detrimental to activity, whereas replacement of the gallate ester moiety with prenyl benzoate enhances potency. In addition, the MCF-7 cell line was more sensitive than the SKBr3 cell line upon administration of these analogues.

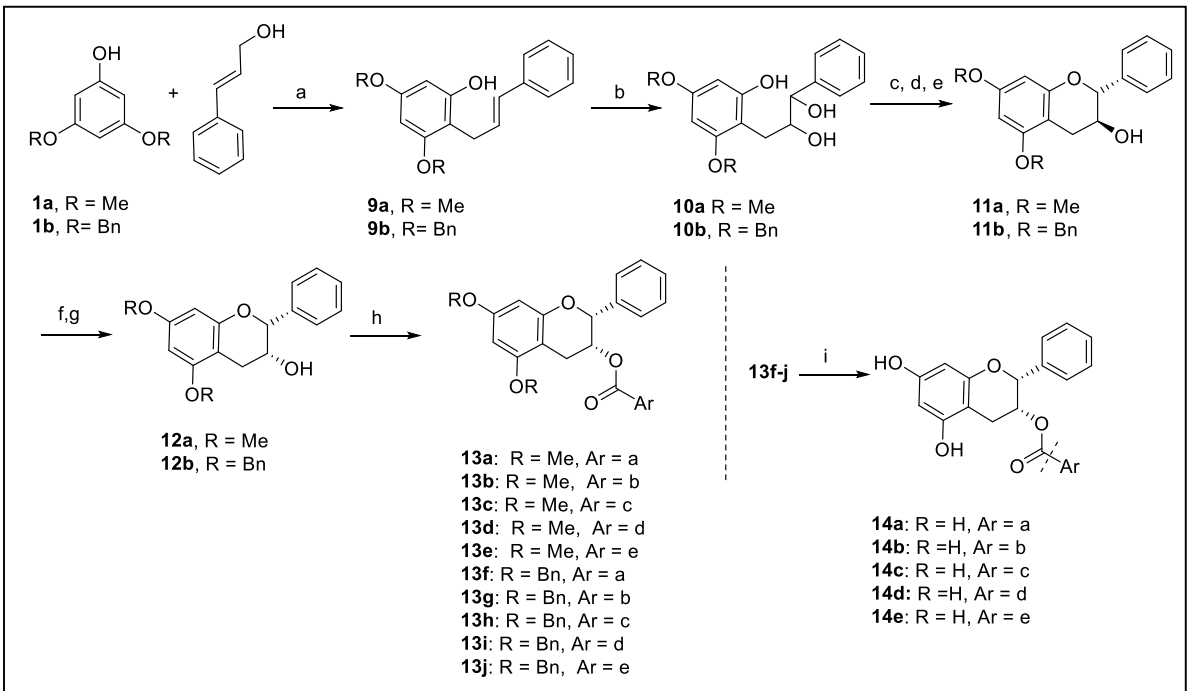

Scheme 2. Synthesis of Series II analogues.

Table 5. Anti-proliferative activities produced by A-, B- and the D-ring modified EGCG analogues

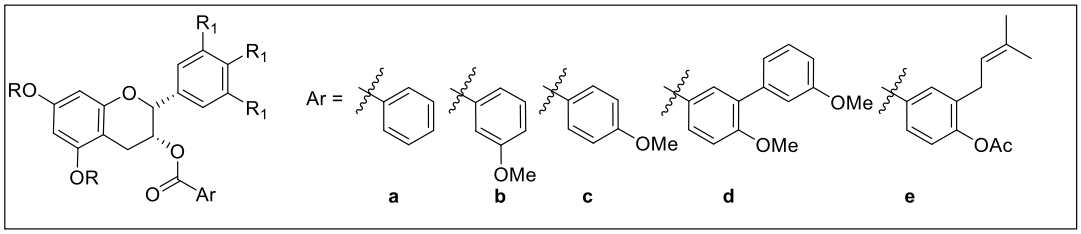

Entry	R	R_1	Ar	MCF-7 (IC_{50}, μM)	SKBr3 (IC_{50}, μM)
EGCG	-	-	-	74.4 ± 2.19	100.16 ± 0.03
GDA	-	-	-	0.05 ± 0.03	0.008 ± 0.02
13a	Me	H	a	>100	>100
13b	Me	H	b	>100	>100
13c	Me	H	c	>100	>100
13d	Me	H	d	>100	>100
13e	Me	H	e	25.35 ± 5.25	36.1 ± 2.51
7a	Me	OMe	a	>100	>100
7b	Me	OMe	b	91.18 ± 0.76	>100
7c	Me	OMe	c	>100	>100
7d	Me	OMe	d	88.7 ± 11.31	>100
7e	Me	OMe	e	19.48 ± 2.5	24.87 ± 3.29
14a	OH	H	a	15.26 ± 0.57	18.67 ± 0.82
14b	OH	H	b	13.10 ± 0.86	15.42 ± 1.04
14c	OH	H	c	13.12 ± 0.54	17.26 ± 2.27
14d	OH	H	d	14.14 ± 0.73	19.88 ± 3.22
14e	OH	H	e	3.99 ± 1.49	21.45 ± 4.75
8a	OH	OMe	a	65.88 ± 2.15	>100
8b	OH	OMe	b	45.72 ± 0.41	37.92 ± 4.08
8c	OH	OMe	c	42.80 ± 7.30	62.90 ± 0.70
8d	OH	OMe	d	47.31 ± 3.39	71.9 ± 2.76
8e	OH	OMe	e	42.08 ± 1.85	50.4 ± 1.39

II.4. Synthesis and Evaluation of Series III Analogues

Biological evolution of Series-I and Series-II analogues established that substituents on the B-ring of EGCG are not essential for efficacy. In addition, phenols on the A-ring were more efficacious that the corresponding methyl ethers. To probe the necessity of the B-ring, a new series of compounds was proposed (Series III) than lack the B-ring. As shown in Figure 17, the proposed

analogues would also probe the role of individual A-ring phenols. Aryl acids **6a–e** were used as gallic acid replacements. Additionally, phenols were also incorporated on the D-ring for evaluation.

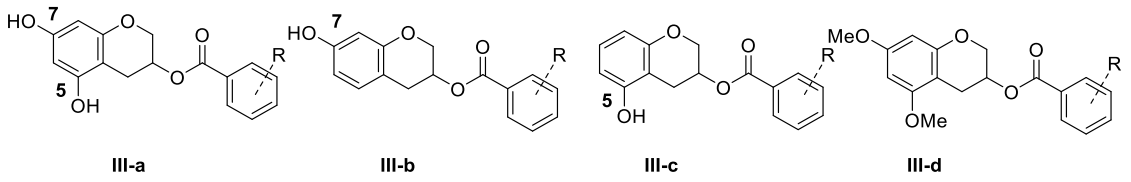

Figure 17. Proposed series-III analogues lacking the B-ring of EGCG.

II.4.1. Syntheses of Series IIIa-c Analogues

Syntheses of analogues that lack the B-ring and contain phenols on the A-ring were commenced by the treatment of 3,5-dibenzyloxyphenol (**1b**, Scheme 3) with allyl bromide in the presence of potassium carbonate to give allyl ether **16a**.[87] 3,3-Sigmatropic rearrangement of the O-allylated product (**16a**) gave **17a** in high yield. Upjohn dihydroxylation of the resulting olefin afforded diol **18a**.[88] Unfortunately, attempts to cyclize via the orthoester were unsuccessful as only the 5-membered benzofuran ring containing product was formed. Therefore, an alternative strategy for the cyclization of **19a** was pursued. Treatment of the primary alcohol present in **19a** with *p*-toluenesulfonyl chloride formed of the corresponding *p*-toluenesulfonic ester, which underwent intramolecular cyclization upon exposure to potassium carbonate to give a 1:1 mixture of 5- and 6-membered rings that were separated by silica gel chromatography. Subsequent coupling of **20a** with various substituted benzoic acids produced the requisite esters, which underwent hydrogenolysis to afford **21a–i**, respectively.

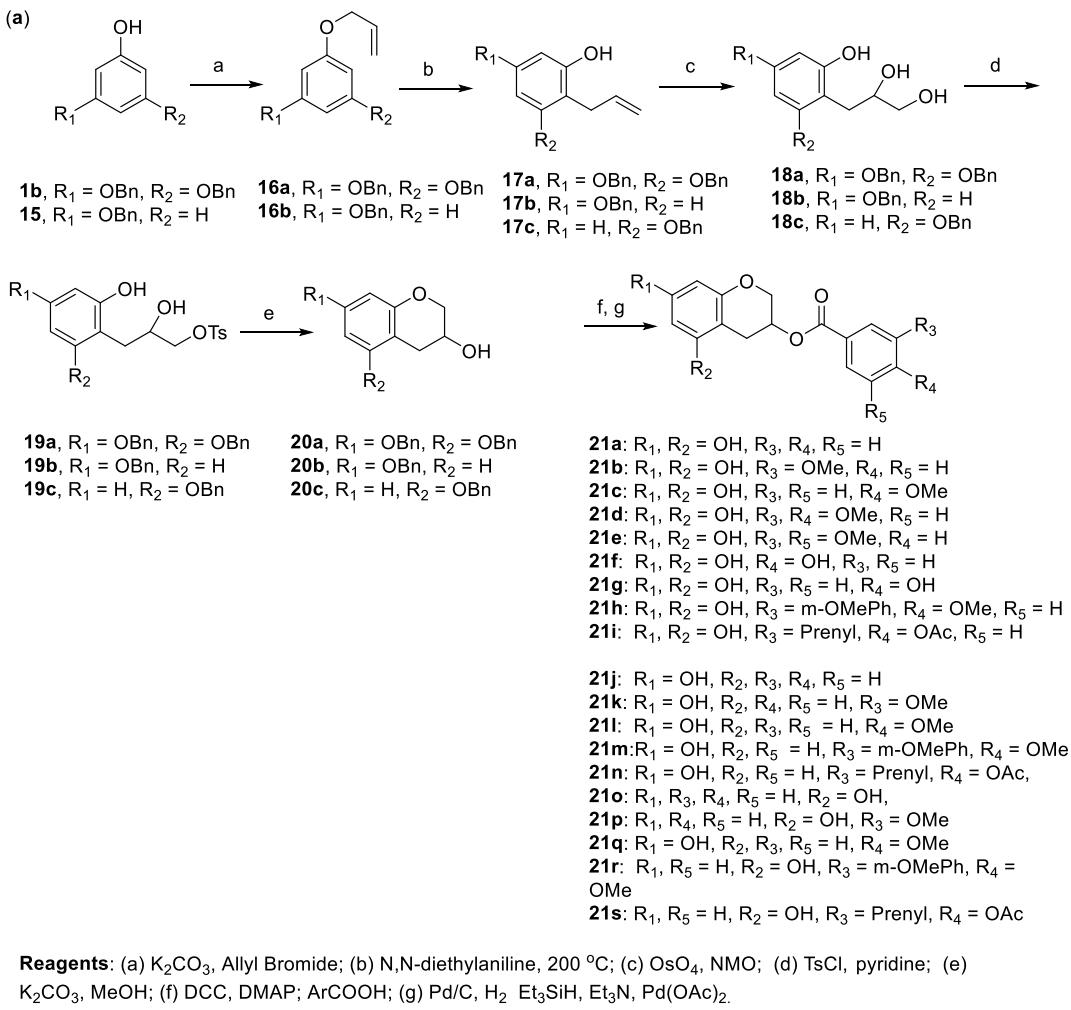

Scheme 3. Synthesis of B-ring lacking Series IIIa-c analogues.

Upon construction of analogues that lack the B-ring, each phenol on the A-ring was systematically investigated. Therefore, derivatives **21i–s** that contain only one phenol at either the 5- or the 7-positions were pursued similar to that described above. Allylation of the phenol (**15**) gave ally ether, **16b**. 3,3-Rearrangement of the allyl ether (**16b**) gave a mixture of two regioisomers, **17b** and **17c**, which upon dihydroxylation and subsequent ring closure gave **20b** and **20c,** respectively.

II.4.2. Biological Evaluation of Series IIIa-c Analogues

Table 6. Anti-proliferative activities produced by 3,5-dihydroxychroman-3-ol esters.

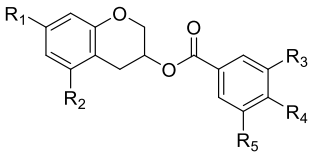

Entry	R_1	R_2	R_3	R_4	R_5	MCF-7 (IC_{50}, μM)	SKBr3 (IC_{50}, μM)
21a	OH	OH	H	H	H	98.24 ± 1.76	>100
21b	OH	OH	OMe	H	H	57.75 ± 3.12	50
21c	OH	OH	H	OMe	H	>100	>100
21d	OH	OH	OMe	OMe	H	>100	>100
21e	OH	OH	OMe	H	OMe	96.50 ± 3.51	>50
21f	OH	OH	OH	H	H	61.94 ± 6.85	85.30 ± 5.36
21g	OH	OH	H	OH	H	>100	>100
21h	OH	OH	*m*-OMePh	OMe	H	21.93 ± 2.27	34.84 ± 16.29
21i	OH	OH	Prenyl	OAc	H	10.66 ± 1.09	23. 15 ± 0.25
21j	OH	H	H	H	H	>100	>100
21k	OH	H	OMe	H	H	>100	>100
21l	OH	H	H	OMe	H	>100	>100
21m	OH	H	*m*-OMePh	OMe	H	55.09 ± 5.53	57.73 ± 4.28
21n	OH	H	Prenyl	OAc	H	15.94 ± 1.86	25.25 ± 4.05
21o	H	OH	H	H	H	>100	>100
21p	H	OH	OMe	H	H	>100	>100
21q	H	OH	H	OMe	H	>100	>100
21r	H	OH	*m*-OMePh	OMe	H	21.6 ± 2.55	41.72 ± 0.34
21s	H	OH	Prenyl	OAc	H	60 ± 7.38	>100

Results from the anti-proliferative studies with compounds **21a–s** are summarized in Table 6. In addition to previously investigated substituents, the effect of hydroxyl substitution on the D-ring was also explored. Many of the compounds were more potent than EGCG itself. This data suggests that methoxy substituents on the D-ring are more beneficial than the naturally occurring phenols, and corresponds to an overall pattern represented by O-alkyl substitutions at the 3'-position being more active than those at the 4'-position. Data also suggested that aryl and prenyl substitution on the D-ring enhanced efficacy, as **21h** manifested an IC_{50} value of 21.93 ± 2.27 μM against MCF-7 cells and 41.72 ± 0.34 μM against SKBr3 cells. Compounds containing only one

phenolic group at the 5-position on the A-ring showed decreased activity, except for **21s.** Similarly, compounds with a 7-hydroxyl substitution on the A-ring showed decreased activity with the exception of **21n**, which manifested enhanced activity and an IC_{50} value of 55.09 ± 5.53μM against the MCF-7 cell line. Similar to the most active analogue produced from the B-ring series, **14e**, the most active analogue identified in this series was **21i** (IC_{50} ~ 10 μM in MCF-7 cell line), which also incorporated the prenylated benzoic ester side chain.

II.4.3. Synthesis of Series III-d Analogues

In an effort to further investigate the A-ring, the free phenols were replaced with methyl ethers. 5,7-Dimethoxychroman-3-ol (**24**) was synthesized in two steps using a gold(III)- mediated procedure as described by Zhangjie and co-workers (Scheme 4).[89] Commencing with commercially available 3,5-dimethoxyphenol and enlistment of epichlorohydrin and sodium hydride, oxirane **23** was produced, which was treated with gold(III) chloride/silver trifluormethanesulfonate catalyst to yield **24**. Upon construction of the chroman-3-ol core (**24**), subsequent coupling with various substituted aryl acids furnished the corresponding esters, **25a–m**. Hydrogenolysis of **25i–m** produced the final products **26a–e**.

II.4.4. Biological Evaluation of Series III-d Analogues

Results from anti-proliferative studies for compounds lacking the B-ring are summarized in Table 7. The 3-methoxy substituted compound **26b** was the most active compound against the MCF-7 and the SKBr3 cell lines, and manifested IC_{50} values 0.78 ± 0.02 μM and 0.88 ± 0.06 μM, respectively. Increasing the length of the side chain decreased activity for compound **25h**. The phenol was more beneficial at the 4'-position in lieu of the 3'-position. Unfortunately, the combination of 3-methoxy and 4-hydroxyl substitutions on the D-ring (**26e**) did not improve anti-proliferative activity. Once again, MCF-7 cells exhibited greater sensitivity to these compounds.

The IC_{50} values for **25d** and **25e** correlated directly with prior studies using novobiocin, suggesting a beneficial effect for inclusion of an aryl or prenyl group on the D-ring.

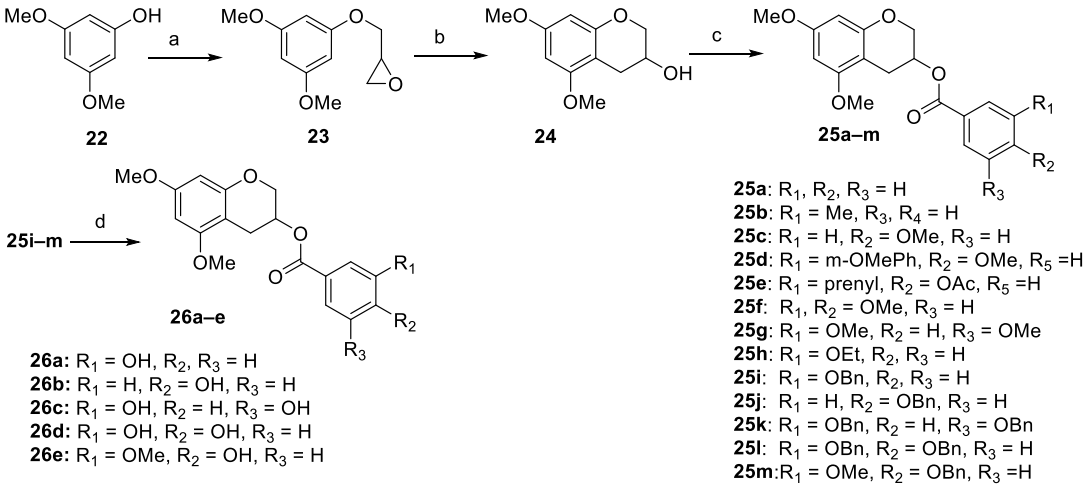

Scheme 4. Syntheses of series III-d.

Table 7. Biological evaluation of series III-d.

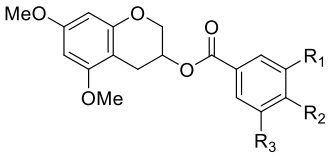

Entry	R_1	R_2	R_3	MCF-7 (μM)	SKBr3 (μM)
25a	H	H	H	14.02 ± 0.91	44.605 ± 5.40
25b	OMe	H	H	0.77 ± .02	0.88 ± 0.06
25c	H	OMe	H	32.89 ± 2.05	50.40 ± 1.39
25d	m-OMePh	OMe	H	31.20 ± 18.17	80.13 ± 9.67
25e	Prenyl	OAc	H	38.66 ± 7.71	47.90 ± 0.71
25f	OMe	OMe	H	10.89 ± 0.27	36.98 ± 5.24
25g	OMe	H	OMe	21.8 ± 3.08	29.5 ± 1.5
25h	OEt	H	H	8.19 ± 0.16	33.35 ± 4.81
26a	OH	H	H	37.72 ± 6.75	64.11 ± 13.95
26b	H	OH	H	17.51 ± 0.86	17.73 ± 5.97
26c	OH	H	OH	>100	>100
26d	OH	OH	H	22.12 ± 1.01	30.63 ± 11.89
26e	OMe	OH	H	51.29 ± 1.13	76.50 ± 1.10

II.5. Optimization of Linker

II.5.1. Synthesis of Amide Linker Analogues

In addition, investigation of the linker connecting the B- and D-rings was pursued. The ester linker was replaced with an amide. These amide-based analogues were prepared from previously synthesized alcohol **22**, which was transformed into azide **27** via Mitsunobu conditions with diisopropyl azodicarboxylate, triphenylphosphine and diphenylphosphoryl azide. Azide formation was followed by Staudinger reduction with triphenylphosphine to afford amine **28** (Scheme-5).[90] Subsequent coupling of amine **28** with the optimal aryl acids gave the corresponding amides, **29a–d**.[91] Furthermore, the anti-isomer of **13e** was also synthesized from **12a**.

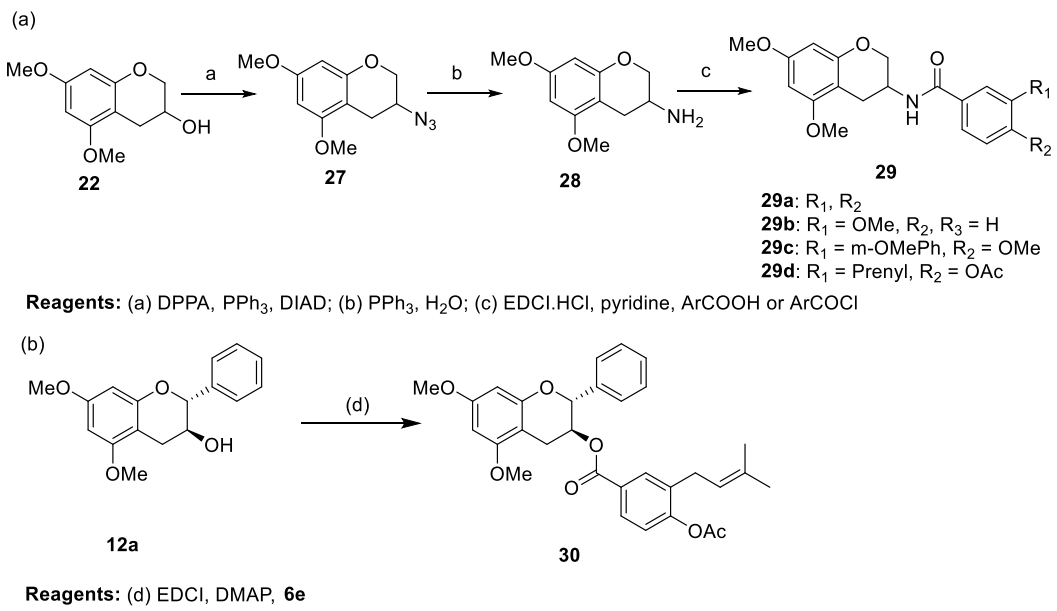

Scheme 5. Synthesis of linker analogues. (a) amide linker analogues; (b) anti-stereochemistry containing analogues.

II.5.2. Biological Evaluation of Amide Linker Analogues

The results from biological evaluation of the linker are summarized in table 8. The linker between the B- and D-ring was also evaluated and replacement of the ester with an amide (**29a–d**) was found detrimental. The anti-isomer of **13e**, **30** was also evaluated and found to be less active

(IC_{50} = 33.7 ± 1.8 against MCF-7 cell line), suggesting that *syn*-stereochemistry is important for inhibitory activity

Table 8. Anti-proliferative activity produced by analogues containing amide linkers.

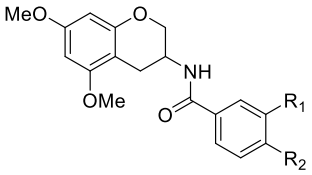

Entry	R_1	R_2	MCF-7 (IC_{50}, μM)	SKBr3 (IC_{50}, μM)
29a	H	H	>100	>100
29b	OMe	H	>100	>100
29c	m-OMePh	OMe	>100	>100
29d	Prenyl	OAc	54.5 ± 0.6	55.2 ± 1.2

II.6. Western Blots Analyses

After determination of anti-proliferative activity for EGCG analogues, four representative compounds were chosen for subsequent western blot analyses to confirm Hsp90 inhibition, based on each class of scaffold investigated. Since Hsp90 inhibition induces client protein degradation via the ubiquitin-proteasome pathway, immunoblots were used to confirm Hsp90 inhibitory activity. As shown in Figure 18, **14e**, **25e** and **13e** induced the degradation of Hsp90 client proteins Her2, Raf and p-Akt at concentrations that mirrored the concentration needed to exhibit anti-proliferative activity, thereby linking Hsp90 inhibition to cell viability. Analogue **25b** failed to induce client protein degradation, demonstrating that this compound manifests anti-proliferative activity through a mechanism independent of Hsp90 inhibition. However, a related compound containing the prenylated benzoate side chain, **25e**, did exhibit Hsp90 inhibitory activity. Further investigation of **14e** at increasing concentrations demonstrated client protein degradation in a dose-dependent manner, while actin levels remained the same. Actin is not an Hsp90-dependent protein

and is therefore unaffected by Hsp90 inhibition. Similar to other Hsp90 C-terminal inhibitors, the levels of Hsp90 were unchanged.

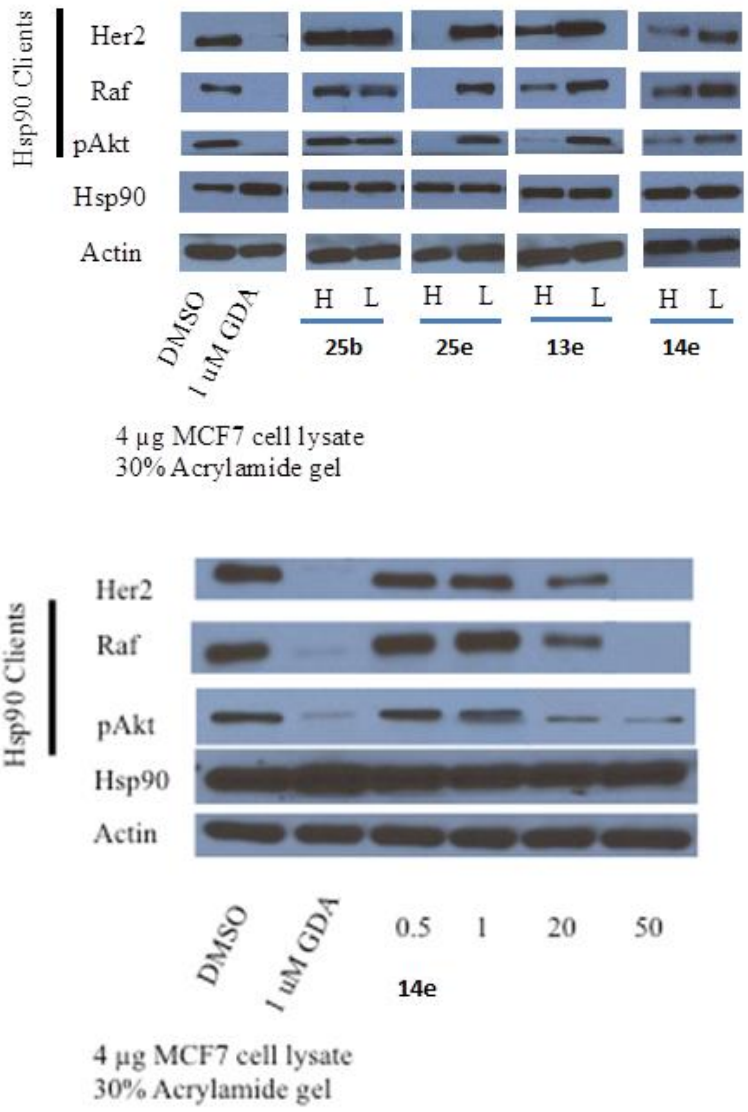

Figure 18. Western blot analyses to confirm Hsp90 inhibition. "H" (high) represents a concentration 5 × IC_{50} value, whereas and "L" (low) represents a concentration at one-half the IC_{50} value as determined by anti-proliferative studies. Concentrations are represented in µM. Geldanamycin (GDA) was used as a positive control.

II.7. Conclusion and Future Directions

In summary, the first structure-activity relationships between EGCG and Hsp90 have been produced (Figure 19).[92] The results obtained suggest that phenols on the A-ring are beneficial for Hsp90 inhibition, while phenols on the D-ring are detrimental. Similar to EGCG, novobiocin also binds Hsp90 within amino acids 538-578 and represents another naturally occurring C-terminal inhibitor. The inclusion of a novobiocin-derived prenylated benzoic ester was found to be a suitable replacement for the gallic acid moiety present on EGCG, and suggests that both novobiocin and the EGCG may bind similarly to the Hsp90 C-terminus. Results from these studies have led to the development of analogue **14e**, which exhibits an 18-fold improvement over EGCG and can serve as a probe for further biological investigations.

The optimized analogue resulting from this work lacks the structural detriments associated with EGCG and can be further developed for increased Hsp90 inhibition and better understating of the C-terminal binding pocket. The central benzopyran core of EGCG allows for modifications that are inaccessible with the coumarin core of novobiocin. The most efficacious analogue (**14e**) can allow for modification at the 1-, 2-, and 4-positions of the chromane core, which corresponding are not amiable for modification with the coumarin ring. The chromane core can further be replaced with to 1,2,3,4-tetrahydroquinoline core to probe the binding pocket. Lead compound, **14e**, represents a new scaffold to probe the Hsp90 C-terminal binding pocket and its further optimization is currently under investigation.

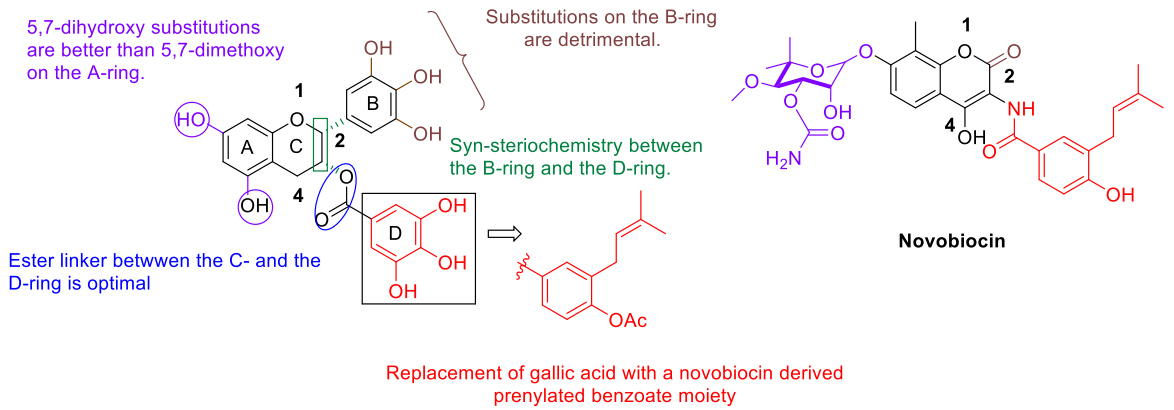

Figure 19. Summary of EGCG structure-activity relationship studies.

II.8. Methods and Experiments

All reactions were performed in oven-dried glassware under argon atmosphere unless otherwise stated. Dichloromethane (DCM), tetrahydrofuran (THF), and toluene were passed through a column of activated alumina prior to use. Anhydrous methanol, acetonitrile, *N*,*N*-dimethylformamide (DMF), and dimethoxyethane (DME) were purchased and used without further purification. (−)-EGCG was purchased from Sigma-Aldrich and used as obtained. Flash column chromatography was performed using silica gel (40−63 μm particle size). The ^{1}H (500 and 400 MHz) and ^{13}C NMR (125 and 100 MHz) spectra were recorded on 500 and 400 MHz spectrometer. Data are reported as p = pentet, q = quartet, t = triplet, d = doublet, s = singlet, br s = broad singlet, m = multiplet; coupling constant(s) in Hz. Infrared spectra were obtained using FT/IR spectrometer. High resolution mass spectral data were obtained on a time-of-flight mass spectrometer and analysis was performed using electrospray ionization.

Anti-proliferation Assay

MCF-7 and SKBr3 cells were maintained in advanced DMEM/F12 (Gibco) supplemented with l-glutamine (2 mM), streptomycin (500 μg/mL), penicillin (100 units/mL), and 10% FBS.

Cells were grown to confluence in a humidified atmosphere (37 °C, 5% CO_2) and seeded (2000/well, 100 μL) in 96-well plates, and allowed to attach for 24 h. Compounds or geldanamycin at 6 increasing concentrations in DMSO (1% DMSO final concentration) were added, and cells were returned to the incubator for 72 h. At 72 h, the cell growth was determined using an MTS/PMS cell proliferation kit (Promega) per the manufacturer's instructions. Cells incubated in 1% DMSO were used as 100% proliferation, and values were adjusted accordingly. IC_{50} values were calculated from minimum two separate experiments performed in triplicate using GraphPad Prism program.

Western Blot Analysis

MCF-7 cells were cultured as described previously and treated with various concentrations of the compound to be tested, geldanamycin in DMSO (1% DMSO final concentration), or vehicle (DMSO) for 24 h. Cells were harvested in cold PBS and lysed in M-PER lysis buffer (Sigma) containing protease and phosphatase inhibitors (Roche) on ice for 1 h. Lysates were clarified at 14000*g* for 15 min at 4 °C. Protein concentrations were determined by using the Pierce BCA assay kit per the manufacturer's instructions. Equal amounts of proteins were electrophoresed under reducing conditions, transferred to a PVDF membrane, and immunoblotted with the corresponding specific antibodies. Membranes were incubated with an appropriate horseradish peroxidase-labeled secondary antibody, developed with chemiluminescent substrate, and visualized.

Compound **1b**, **22**, **6d**, and **6e** were synthesized following reported procedures.[80, 85, 89]

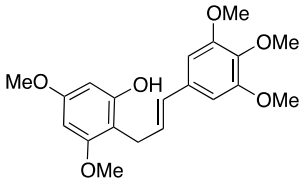

(*E*)-3,5-Dimethoxy-2-(3-(3,4,5-trimethoxyphenyl)allyl)phenol (**2a**): A solution of 3,5-dimethoxyphenol (2.06 g, 13.4 mmol) and (*E*)-3,4,5-trimethoxycinnamyl alcohol (3.0 g, 13.4 mmol) in a solvent mixture of dichloromethane (26 mL) and carbon disulfide (26 mL) was treated with 25% H_2SO_4/SiO_2 catalyst (2.2g, 5.36 mmol) at rt. The resulting mixture was stirred for 4 h and then filtered through a plug of SiO_2. Solvent was removed and the residue purified by flash chromatography (SiO_2, 1:2 EtOAc/hexanes) to give **2a** as an amorphous light yellow solid (1.660 g, 39.4%): ^{1}H NMR (500 MHz, $CDCl_3$) δ 6.56 (s, 2H), 6.38 (dt, *J* = 15.8, 1.7 Hz, 1H), 6.23 (dt, *J* = 15.8, 6.2 Hz, 1H), 6.14 (d, *J* = 2.4 Hz, 1H), 6.10 (d, *J* = 2.3 Hz, 1H), 5.09 (s, 1H), 3.85 (s, 6H), 3.83 (s, 3H), 3.81 (s, 3H), 3.79 (s, 3H), 3.54 (dd, *J* = 6.2, 1.7 Hz, 2H); ^{13}C NMR (125 MHz, $CDCl_3$) δ 159.9, 159.0, 155.9, 153.4 (2), 137.6, 133.2, 130.4, 128.1, 106.1, 103.3 (2), 93.9, 91.7, 61.1, 56.2 (2), 56.0, 55.5, 26.2; IR (KBr) ν_{max} 3379, 3379, 2937, 1620, 1593, 1506, 1421, 1361, 1330, 1201, 1147, 1053, 817, 707 cm^{-1}; HRMS (ESI+) *m*/*z* [M + H$^+$] calcd for $C_{20}H_{25}O_6$, 361.1651, found 361.1657.

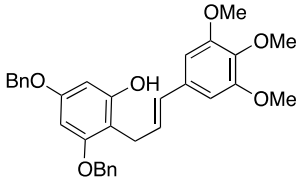

(*E*)-3,5-Bis(benzyloxy)-2-(3-(3,4,5-trimethoxyphenyl)allyl)phenol (**2b**): A solution 3,5-bis(benzyloxy)phenol (5.2 g, 6.97 mmol) and (E)-3,4,5 trimethoxycinnamyl alcohol (3.81 g, 16.97 mmol) in a solvent mixture of dichloromethane (33 mL) and carbon disulfide (33 mL) was treated with 25% H_2SO_4/SiO_2 catalyst (1.11 g, 2.8 mmol) at rt. The resulting mixture was stirred for 4 h and then filtered through a plug of SiO_2. Solvent was removed and the residue purified by flash chromatography (SiO_2, 1:3 EtOAc/hexanes) to give **2b** (1.970 g, 22.6%) as an amorphous light yellow solid: ^{1}H NMR (500 MHz, $CDCl_3$) δ 7.47–7.28 (m, 10H), 6.54 (s, 2H), 6.39 (dt, *J* = 15.8,

1.7 Hz, 1H), 6.30 (d, *J* = 2.3 Hz, 1H), 6.24 (dt, *J* = 15.8, 6.3 Hz, 1H), 6.19 (d, *J* = 2.3 Hz, 1H), 5.05 (s, 2H), 5.03 (s, 1H), 5.02 (s, 2H), 3.90–3.80 (m, 9H), 3.65–3.56 (m, 2H); ^{13}C NMR (125 MHz, $CDCl_3$) δ 159.1, 158.2, 155.9, 153.5 (2), 137.6, 137.3, 137.1, 133.3, 130.7, 128.9 (2), 128.8 (2), 128.7, 128.3 (2), 128.1 (2), 127.8 (2), 127.5, 107.0, 103.4, 95.3, 93.9, 70.6, 70.4, 61.2, 56.3 (2), 26.6; IR (KBr) ν_{max} 3400, 2937, 1614, 1585, 1454, 1328, 1238, 1126, 1001, 736, 696 cm^{-1}; HRMS (ESI+) *m*/*z* [M + Na^+] calcd for $C_{32}H_{32}NaO_6$, 535.2097, found 535.2100.

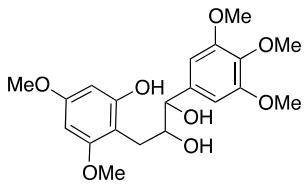

3-(2-Hydroxy-4,6-dimethoxyphenyl)-1-(3,4,5-trimethoxyphenyl)propane-1,2-diol (3a): *N*-Methylmorpholine *N*-oxide (702 mg, 6 mmol) was added to a solution of **2a** (1.350 g, 3.75 mmol) in a solvent mixture of tetrahydrofuran (12 mL) and H_2O (8 mL). The resulting solution was stirred for 15 min at rt before the addition osmium tetraoxide (0.04 mmol, 4% solution in water). The mixture was stirred for 14 h at rt before quenching with 20% of sodium metabisulfite (12 mL). The aqueous layer was extracted with EtOAc (3 × 25 mL), and the combined organic layers were washed with saturated sodium chloride solution (50 mL), dried over anhydrous Na_2SO_4, filtered, and concentrated. The residue was purified by flash chromatography (SiO_2, 1:10 acetone/dichloromethane) to afford **3a** (1.33 g, 90.4%) as a colorless oil: ^{1}H NMR (500 MHz, $CDCl_3$) δ 8.08 (s, 1H), 6.54 (s, 2H), 6.14 (d, *J* = 2.4 Hz, 1H), 6.03 (d, *J* = 2.4 Hz, 1H), 4.47 (d, *J* = 6.0 Hz, 1H), 3.98 (ddd, *J* = 8.0, 6.1, 3.8 Hz, 1H), 3.84 (s, 6H), 3.82 (s, 3H), 3.75 (s, 3H), 3.62 (s, 3H), 3.44 (br s, 1 H), 3.10–2.92 (m, 1H), 2.85 (dd, *J* = 14.7, 3.8 Hz, 1H), 2.73 (dd, *J* = 14.7, 7.8 Hz, 1H); ^{13}C NMR (125 MHz, $CDCl_3$) δ 160.1, 159.0, 157.3, 153.4 (2), 137.6, 136.5, 105.6, 103.9 (2), 94.6, 91.4, 76.9, 76.7, 61.0, 56.3 (2), 55.7, 55.5, 26.5; IR (KBr) ν_{max} 3405, 2932, 1620,

1591, 1498, 1439, 1379, 1218, 1146, 1029, 817 cm^{-1}; HRMS (ESI+) *m*/*z* [M + H^+] calcd for $C_{20}H_{27}O_8$, 395.1706, found 395.1719.

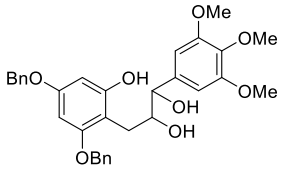

3-(2,4-Bis(benzyloxy)-6-hydroxyphenyl)-1-(3,4,5-trimethoxyphenyl)propane-1,2-diol (**3b**): *N*-Methylmorpholine *N*-oxide (444 mg, 3.79 mmol) was added to a solution of **2b** (1.0 g, 2.36 mmol) in a solvent mixture of tetrahydrofuran (7.5 mL) and H_2O (5 mL). The resulting solution was stirred for 15 min at rt before the addition of osmium tetraoxide (0.02 mmol, 4% solution in water). The mixture was stirred for 14 h at rt before quenching with 20% of sodium metabisulfite (10 mL). The aqueous layer was extracted with ethyl acetate (3 × 20 mL), and the combined organic layers were washed with saturated sodium chloride solution (40 mL), dried over anhydrous Na_2SO_4, filtered, and concentrated. The residue was purified by flash chromatography (SiO_2, 1:10 acetone/dichloromethane) to afford **3b** (595 g, 56.7%) as an amorphous light yellow solid: ^{1}H NMR (500 MHz, $CDCl_3$) δ 8.00 (br s, 1 H), 7.47–7.28 (m, 10H), 6.54 (s, 2H), 6.28 (d, *J* = 2.3 Hz, 1H), 6.22 (d, *J* = 2.3 Hz, 1H), 5.06–4.95 (m, 4H), 4.91 (d, *J* = 3.0 Hz, 1H), 4.52 (d, *J* = 6.0 Hz, 1H), 3.77 (d, *J* = 10.2 Hz, 9H), 3.25 (b rs, 1 H), 3.01–2.95 (m, 1H), 2.83 (dd, *J* = 14.6, 8.3 Hz, 1H), 2.74 (br s, 1 H); ^{13}C NMR (125 MHz, $CDCl_3$) δ 159.4, 158.1, 157.6, 153.5 (2), 137.1, 137.0, 136.4, 129.0, 128.8, 128.7, 128.5, 128.4, 128.3 (2), 128.1, 127.8, 127.5, 127.4, 127.3, 126.9, 106.3, 103.8 (2), 96.2, 93.7, 70.3 (2), 61.0, 56.3, 56.3, 27.0; IR (KBr) ν_{max} 3446, 2935, 2837, 1591, 1498, 1456, 1328, 1232, 1126, 1004, 736 cm^{-1}; HRMS (ESI+) *m*/*z* [M + H^+] calcd for $C_{32}H_{35}O_8$, 547.2332, found 547.2347.

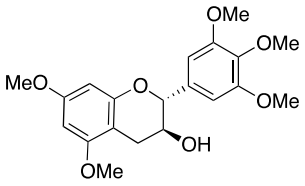

5,7-Dimethoxy-2-(3,4,5-trimethoxyphenyl)chroman-3-ol (**4a**): Trimethyl orthoacetate (1.92 mmol, 250 μL) and pyridinium *p*-toluenesulfonate (10 mg, 0.032 mmol) were added to a solution of **3a** (620 mg, 1.6 mmol) in dichloromethane (32 mL) at rt. The resulting mixture was stirred for 30 min at rt and then cooled to 0 °C before the dropwise addition of boron trifluoride diethyl etherate (20 μL, 0.16 mmol). The reaction mixture was warmed to rt and stirred for another 15 min before quenching with aqueous acetone (4 mL). Solvent was removed and the residue dissolved in methanol (32 mL). Potassium carbonate (240 mg, 1.76 mmol) was added and the mixture stirred for 6 h at rt. Methanol was removed, water (25 mL) was added, and the products were extracted with ethyl acetate (2 × 30 mL). The combined organic layers were washed with saturated sodium chloride solution (50 mL). The organic phase was dried over anhydrous Na_2SO_4 and filtered. Solvent was removed and the residue was purified via flash chromatography (SiO_2, 1:4 EtOAc/hexanes) to yield compound **4a** (460 mg, 77.8) as a colorless oil: ^{1}H NMR (500 MHz, $CDCl_3$) δ 6.68 (s, 2H), 6.15 (d, *J* = 2.3 Hz, 1H), 6.12 (d, *J* = 2.3 Hz, 1H), 4.63 (d, *J* = 8.5 Hz, 1H), 4.07 (ddd, *J* = 9.3, 8.5, 5.8 Hz, 1H), 3.87 (s, 6H), 3.85 (s, 3H), 3.82 (s, 3H), 3.76 (s, 3H), 3.11 (dd, *J* = 16.3, 5.8 Hz, 1H), 2.60 (dd, *J* = 16.3, 9.3 Hz, 1H), 1.95 (br s, 1 H); ^{13}C NMR (125 MHz, $CDCl_3$) δ 159.9, 158.9, 155.4, 153.7 (2), 138.2, 133.6, 104.3 (2), 101.9, 93.2, 92.2, 82.4, 68.5, 61.0, 56.3 (2), 55.7, 55.6, 28.0; IR (KBr) ν_{max} 3438, 3001, 2916, 2848, 1622, 1593, 1496, 1622, 2593, 1456, 1361, 1215, 1145, 1120, 810, 667 cm^{-1}; HRMS (ESI+) *m*/*z* [M + Na$^+$] calcd for $C_{20}H_{24}NaO_7$, 399.1420, found 399.1414.

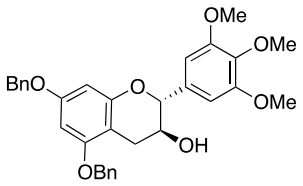

5,7-Bis(benzyloxy)-2-(3,4,5-trimethoxyphenyl)chroman-3-ol (**4b**): Trimethyl orthoacetate (0.94 mmol, 120 μL) and pyridinium *p*-toluene sulfonate (4 mg, 0.016 mmol) were added to a solution of **3b** (425 mg, 0.78 mmol) in dichloromethane (16 mL) at rt. The resulting mixture was stirred for 30 min at rt and then cooled to 0 °C before the dropwise addition of borontrifluoride diethyletherate (11 μL, 0.08 mmol) dropwise. The reaction mixture was warmed to rt and stirred for another 15 min before quenching with aqueous acetone (3 mL). Solvent was removed and the residue dissolved in methanol (16 mL). Potassium carbonate (118 mg, 0.85 mmol) was added and mixture stirred for 6 h at rt. Methanol was removed, water (20 mL) was added, and the products were extracted with ethyl acetate (2 × 25 mL). The combined organic layers were washed with saturated sodium chloride solution (30 mL). The organic phase was dried over anhydrous Na_2SO_4 and filtered. Solvent was removed, and the residue was purified via flash chromatography (SiO_2, 1:4 EtOAc/hexanes) to afford **4b** (265 mg, 63.3%) as a pale yellow oil: ^{1}H NMR (500 MHz, $CDCl_3$) δ 7.49–7.37 (m, 8H), 7.37–7.30 (m, 2H), 6.69 (s, 2H), 6.30 (d, *J* = 2.3 Hz, 1H), 6.26 (d, *J* = 2.3 Hz, 1H), 5.11–4.96 (m, 4H), 4.65 (d, *J* = 8.5 Hz, 1H), 4.10 (td, *J* = 8.9, 5.8 Hz, 1H), 3.88 (s, 6H), 3.86 (s, 3H), 3.22 (dd, *J* = 16.3, 5.8 Hz, 1H), 2.69 (dd, *J* = 16.4, 9.3 Hz, 1H), 1.82 (s, 1H); ^{13}C NMR (125 MHz, $CDCl_3$) δ 159.0, 157.9, 155.4, 153.7 (2), 137.1, 137.0 (2), 133.5, 128.8 (2), 128.7 (2), 128.2, 128.1, 127.7, 127.3 (3), 104.3 (2), 102.6, 94.5, 94.1, 82.4, 70.3, 70.1, 68.5, 61.0, 56.3 (2), 28.2; IR (KBr) ν_{max} 3481, 2935, 1618, 1593, 1498, 1460, 1421, 1346, 1145, 1128, 1022, 829, 752, 734 cm^{-1}; HRMS (ESI+) *m*/*z* [M + H$^+$] calcd for $C_{32}H_{33}O_7$, 529.2226, found 529.2234.

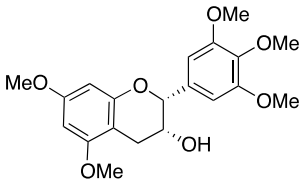

5,7-Dimethoxy-2-(3,4,5-trimethoxyphenyl)chroman-3-ol (5a): Dess-Martin periodinane 687 mg, 1.62 mmol, 1.5 eq.) was added to a solution of **4a** (421 mg, 1.08 mmol, 1.0 eq.) in dichloromethane (10 mL). The resulting mixture was stirred for 2 h before quenching with 15 % aqueous solution of sodium thiosulfate (3 mL) and saturated sodium bicarbonate (3 mL). The aqueous layer was extracted with dichloromethane (3 × 5 mL) and the combined organic layers were washed with saturated sodium chloride solution (15 mL), dried over anhydrous sodium sulfate, filtered, and concentrated. The residue was purified via flash chromatography (SiO_2, 1:3 EtOAc/hexanes) to yield the corresponding ketone which was used further as obtained. A solution of the ketone in tetrahydrofuran (2 mL) was added dropwise to a solution of lithium bromide (487 mg, 5.61 mmol, 5.2 eq.) and L-selectride (1 M solution) (1.41 mL, 1.41 mmol, 1.3 eq.) in tetrahydrofuran (8 mL) at -78 °C. The resulting mixture was stirred for 6 h at -78 °C, warmed to rt, and quenched with 2.5 M sodium hydroxide solution (5.0 mL), followed by the addition of ethanol (3.9 mL) and 35% aqueous hydrogen peroxide solution (1.3 mL). The resulting mixture was stirred for 14 h before the addition of ethyl acetate (15 mL). The aqueous layer was extracted with ethyl acetate (2 × 10 mL) and the combined organic layers washed with saturated sodium chloride solution (20 mL), dried over anhydrous sodium sulfate, filtered, and concentrated. The residue purified via flash chromatography (SiO_2, 1:2 EtOAc/hexanes) to yield compound **5a** as a colorless oil (175 mg, 43%). ^{1}H NMR (500 MHz, $CDCl_3$) δ 6.75 (s, 2H), 6.21 (d, J = 2.3 Hz, 1H), 6.12 (d, J = 2.4 Hz, 1H), 4.93 (s, 1H), 4.44–4.23 (m, 1H), 3.89 (s, 6H), 3.85 (s, 3H), 3.80 (s, 3H), 3.78 (s, 3H), 3.00–2.93 (m, 1H), 2.89 (dd, J = 17.3, 4.4 Hz, 1H), 1.88 (br s, 1 H); ^{13}C NMR (125

MHz, $CDCl_3$) δ 159.8, 159.4, 155.2, 153.6 (2), 137.5, 134.2, 103.4 (2), 100.4, 93.5, 92.4, 78.8, 66.6, 61.0, 56.3 (2), 55.6, 55.5, 28.2; IR (KBr) ν_{max} 3460, 2997, 2939, 2839, 1620, 1593, 1498, 1456, 1419, 1357, 1330, 1317, 1236, 1197, 1145, 1120, 1081, 939, 815, 729 cm^{-1}; HRMS (ESI+) *m*/*z* [M + H^+] calcd for $C_{20}H_{25}O_7$, 377.1600, found 377.1593.

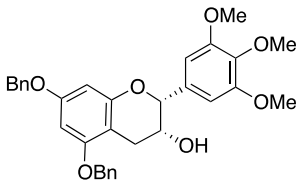

5,7-Bis(benzyloxy)-2-(3,4,5-trimethoxyphenyl)chroman-3-ol (5b): Dess-Martin periodinane 127 mg, 0.30 mmol, 1.5 eq.) was added to a solution of **4b** (106 mg, 0.20 mmol, 1.0 eq.) in dichloromethane (2 mL). The resulting mixture was stirred for 2 h before quenching with 15 % aqueous solution of sodium thiosulfate (1 mL) and saturated sodium bicarbonate (1mL). The aqueous layer was extracted with dichloromethane (3 × 2 mL) and the combined organic layers were washed with saturated sodium chloride solution (5 mL), dried over anhydrous sodium sulfate, filtered, and concentrated. The residue was purified via flash chromatography (SiO_2, 1:3 EtOAc/hexanes) to yield the corresponding ketone which was used further as obtained. A solution of the ketone in tetrahydrofuran (0.5 mL) was added dropwise to a solution of lithium bromide (90 mg, 1.04 mmol, 5.2 eq.) and L-selectride (1 M solution) (0.26 mL, 0.26 mmol, 1.3 eq.) in tetrahydrofuran (1.5 mL) at -78 °C. The resulting mixture was stirred for 6 h at -78 °C, warmed to rt, and quenched with 2.5 M sodium hydroxide solution (1.0 mL), followed by the addition of ethanol (1.35 mL) and 35% aqueous hydrogen peroxide solution (0.45 mL). The resulting mixture was stirred for 14 h before the addition of ethyl acetate (4 mL). The aqueous layer was extracted with ethyl acetate (2 × 5 mL) and the combined organic layers washed with saturated sodium chloride solution (10 mL), dried over anhydrous sodium sulfate, filtered, and concentrated. The

residue purified via flash chromatography (SiO_2, 1:2 EtOAc/hexanes) to yield compound **5b**. Obtained as an amorphous pale yellow solid (72 mg, 68%): ^{1}H NMR (500 MHz, $CDCl_3$) δ 7.44–7.34 (m, 10H), 6.75 (s, 2H), 6.32 (d, *J* = 2.3 Hz, 1H), 6.30 (d, *J* = 2.3 Hz, 1H), 5.06–5.00 (m, 4H), 4.97 (s, 1H), 4.30 (d, *J* = 4.3 Hz, 1H), 3.91 (s, 6H), 3.87 (s, 3H), 3.07 (dd, *J* = 17.4, 2.5 Hz, 1H), 2.98 (dd, *J* = 17.3, 4.5 Hz, 1H), 1.78 (br s, 1 H); ^{13}C NMR (125 MHz, $CDCl_3$) δ 159.0, 158.5, 155.3, 153.7 (2), 137.2 (2), 137.1, 134.1, 128.8 (2), 128.7 (2), 128.2, 128.1, 127.8 (2), 127.4 (2), 103.4 (2), 101.1, 94.9, 94.4, 78.9, 70.4, 70.2, 66.8, 61.1, 56.4 (2), 28.5; IR (KBr) ν_{max} 3461, 2925, 2834, 1593, 1458, 1375, 1236, 1145, 1126, 1078, 1010, 813, 738, 696 cm^{-1}; HRMS (ESI+) *m*/*z* [M + H$^+$] calcd for $C_{32}H_{33}O_7$, 529.2226, found 529.2234.

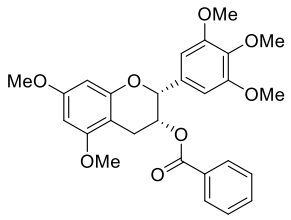

5,7-Dimethoxy-2-(3,4,5-trimethoxyphenyl)chroman-3-yl Benzoate (7a): Benzoyl chloride (14 μL, 0.12 mmol) in dichloromethane (0.5 mL) was added to a solution of **5a** (15 mg, 0.04 mmol) and 4-dimethylaminopyridine (24 mg, 0.2 mmol) in dichloromethane 1 (mL) at 0 °C and stirred for 6 h at rt. The solvent was removed and the residue purified via flash chromatography (SiO_2, 1:4 EtOAc/hexanes) to give the desired ester **7a** (17 mg, 89.4%) as a colorless oil: ^{1}H NMR (500 MHz, $CDCl_3$) δ 8.02–7.89 (m, 2H), 7.59–7.47 (m, 1H), 7.42–7.33 (m, 2H), 6.72 (s, 2H), 6.27 (d, *J* = 2.3 Hz, 1H), 6.14 (d, *J* = 2.3 Hz, 1H), 5.69 (td, *J* = 3.5, 1.3 Hz, 1H), 5.09 (t, *J* = 1.0 Hz, 1H), 3.82 (s, 3H), 3.80 (d, *J* = 1.7 Hz, 6H), 3.71 (s, 6H), 3.10–3.05 (m, 2H); ^{13}C NMR (125 MHz, $CDCl_3$) δ 165.5, 159.6, 158.9, 155.5, 153.1 (2), 137.7, 133.3, 133.1, 130.0, 129.7 (3), 128.3 (2), 103.8 (2), 100.2, 93.4, 92.0, 78.0, 68.5, 60.8, 55.9, 55.4 (2), 26.1; IR (KBr) ν_{max} 2910, 2848, 1718,

1595, 1461, 1271, 1118 cm^{-1}; HRMS (ESI+) *m*/*z* [M + H^+] calcd for $C_{27}H_{29}O_8$, 481.1862 found 481.1863.

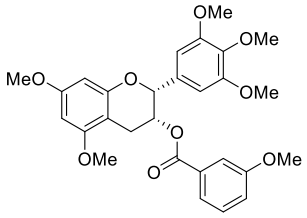

5,7-Dimethoxy-2-(3,4,5-trimethoxyphenyl)chroman-3-yl 3-Methoxybenzoate (**7b**): A solution of **5a** (12 mg, 0.03 mmol) in dichloromethane (0.5 mL) was added to a solution of 3-methoxybenzoic acid (10 mg, 0.06 mmol), *N*-(3-dimethylaminopropyl)-*N′*-ethylcarbodiimide hydrochloride (13 mg, 0.06 mmol), and 4-dimethylaminopyridine (8 mg, 0.06 mmol) in dichloromethane (1 mL) at 0 °C. The resulting mixture was stirred for 6 h at rt, diluted with dichloromethane (5 mL) and washed with saturated sodium bicarbonate (2 × 4 mL) solution. The organic layer was dried over anhydrous sodium sulfate, filtered, and concentrated. The residue was purified via flash chromatography (SiO_2, 1:3 EtOAc/hexanes) to give the desired ester product **7b** as a colorless oil (13 mg, 80.4%): ^{1}H NMR (500 MHz, $CDCl_3$) δ 7.56 (dt, *J* = 7.7, 1.2 Hz, 1H), 7.48 (dd, *J* = 2.7, 1.5 Hz, 1H), 7.30–7.26 (m, 1H) 7.05 (ddd, *J* = 8.3, 2.7, 1.0 Hz, 1H), 6.72 (s, 2H), 6.26 (d, *J* = 2.3 Hz, 1H), 6.13 (d, *J* = 2.4 Hz, 1H), 5.67 (td, *J* = 3.6, 1.3 Hz, 1H), 5.08 (s, 1H), 3.81 (s, 3H), 3.81–3.78 (m, 9H), 3.73 (s, 6H), 3.07 (d, *J* = 3.5 Hz, 2H); ^{13}C NMR (125 MHz, $CDCl_3$) δ 165.4, 159.6, 158.9, 155.5, 153.1 (2), 137.7, 133.3, 131.3, 129.3 (2), 122.0, 119.1, 114.7, 103.8 (2), 100.1, 93.4, 92.0, 78.0, 68.6, 60.8, 55.9 (2), 55.4 (3), 26.0; IR (KBr) ν_{max} 2937, 1718, 1622, 1593, 1498, 1456, 1274, 1218, 1124, 1047, 754 cm^{-1}; HRMS (ESI+) *m*/*z* [M + H^+] calcd for $C_{28}H_{31}O_9$, 511.1968, found 511.1977.

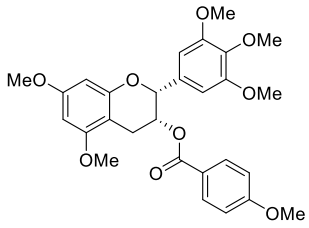

5,7-Dimethoxy-2-(3,4,5-trimethoxyphenyl)chroman-3-yl 4-Methoxybenzoate (**7c**): 4-Methoxybenzoyl chloride (10 μL, 0.07 mmol) in dichloromethane (0.5 mL) was added to a solution of **5a** (13 mg, 0.035 mmol) and 4-dimethylaminopyridine (13 mg, 0.1 mmol) in dichloromethane 0.7 (mL)–pyridine (0.3 mL) at 0 °C. The resulting mixture was stirred for 6 h at rt, solvent was removed, and the residue was purified via flash chromatography (SiO_2, 1:3 EtOAc/hexanes) to give the desired ester **7c** (15 mg, 87.4%) as a colorless oil: ^{1}H NMR (500 MHz, $CDCl_3$) δ 7.77–7.55 (m, 2H), 6.66–6.53 (m, 2H), 6.46 (s, 2H), 6.01 (d, *J* = 2.3 Hz, 1H), 5.88 (d, *J* = 2.3 Hz, 1H), 5.41 (td, *J* = 3.5, 1.3 Hz, 1H), 4.82 (s, 1H), 3.58 (s, 3H), 3.57 (s, 3H), 3.55 (s, 3H), 3.54 (s, 3H), 3.48 (s, 6H), 2.80 (d, *J* = 3.5 Hz, 2H); ^{13}C NMR (125 MHz, $CDCl_3$) δ 165.2, 163.4, 159.6, 158.9, 155.5, 153.1 (2), 133.4, 131.8 (2), 122.4, 113.5 (2), 103.9 (2), 100.3, 93.4, 91.9, 78.1, 68.0, 60.8, 55.9 (2), 55.4 (4), 26.1; IR (KBr) ν_{max} 2927, 1731, 1604, 1591, 1508, 1458, 1458, 1419, 1373, 1326, 1255, 1234, 1126, 1099, 846, 763 cm^{-1}; HRMS (ESI+) *m*/*z* [M + H^+] calcd for $C_{28}H_{31}O_9$, 511.1968, found 511.1961.

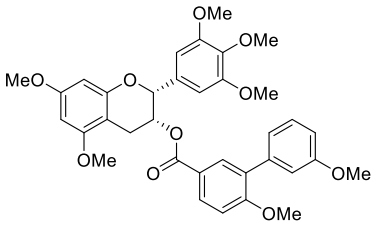

5,7-Dimethoxy-2-(3,4,5-trimethoxyphenyl)chroman-3-yl 3′,6-dimethoxy-[1,1′-biphenyl]-3-carboxylate (**7d**): A solution of **5a** (15 mg, 0.04 mmol) in dichloromethane (0.5 mL) was added

to a solution of 3′,6-dimethoxy-[1,1′-biphenyl]-3-carboxylic acid (21 mg, 0.08 mmol), *N*-(3-dimethylaminopropyl)-*N*′-ethylcarbodiimide hydrochloride (16 mg, 0.08 mmol), and 4-dimethylaminopyridine (9.6 mg, 0.08 mmol) in dichloromethane (1 mL) at 0 °C. The resulting mixture was stirred for 6 h at rt, diluted with dichloromethane (5 mL), and washed saturated sodium bicarbonate (2 × 4 mL) solution. The organic layer was dried over anhydrous sodium sulfate, filtered and concentrated. The residue was purified via flash chromatography (SiO_2, 1:3 EtOAc/hexanes) to give the desired ester **7d** (15 mg, 62.5%) as a colorless oil: ^{1}H NMR (500 MHz, $CDCl_3$) δ 7.95 (dd, *J* = 8.6, 2.3 Hz, 1H), 7.92 (d, *J* = 2.2 Hz, 1H), 7.32 (t, *J* = 7.9 Hz, 1H), 7.02 (ddd, *J* = 7.6, 1.6, 1.0 Hz, 1H), 6.99 (dd, *J* = 2.6, 1.6 Hz, 1H), 6.93 (d, *J* = 8.7 Hz, 1H), 6.90 (ddd, *J* = 8.3, 2.6, 1.0 Hz, 1H), 6.75 (s, 2H), 6.25 (d, *J* = 2.3 Hz, 1H), 6.13 (d, *J* = 2.3 Hz, 1H), 5.65 (ddd, *J* = 4.2, 2.9, 1.3 Hz, 1H), 5.16–5.02 (m, 1H), 3.84 (s, 3H), 3.83 (s, 3H), 3.81 (s, 3H), 3.80 (s, 3H), 3.79 (s, 3H), 3.69 (s, 6H), 3.07 (t, *J* = 3.3 Hz, 2H); ^{13}C NMR (125 MHz, $CDCl_3$) δ 165.3, 160.3, 159.6, 159.3, 158.9, 155.5, 153.1 (2), 138.7, 133.4, 132.4, 131.0, 130.4 (2), 129.1, 122.5, 121.9, 115.1, 113.0, 110.5, 103.8 (2), 100.3, 93.4, 92.0, 78.0, 68.4, 60.8, 55.9 (2), 55.8, 55.4 (2), 55.3, 26.1; IR (KBr) ν_{max} 2927,2848, 1716, 1593, 1496, 1456, 1361, 1238, 1126, 771 cm^{-1}; HRMS (ESI+) *m*/*z* [M + H$^+$] calcd for $C_{35}H_{37}O_{10}$, 617.2387, found 617.2382.

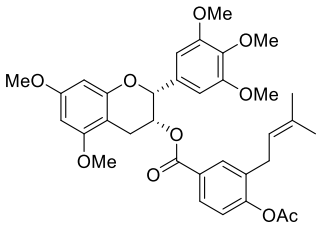

5,7-Dimethoxy-2-(3,4,5-trimethoxyphenyl)chroman-3-yl 4-Acetoxy-3-(3-methylbut-2-en-1-yl)benzoate (**7e**): A solution of **5a** (24 mg, 0.064 mmol) in dichloromethane (0.5 mL) was added to a solution of 4-acetoxy-3-(3-methylbut-2-en-1-yl)benzoic acid (32 mg, 0.13 mmol), *N*-(3-

dimethylamino-propyl)-*N′*-ethylcarbodiimide hydrochloride (26 mg, 0.13 mmol), and 4-dimethylaminopyridine (15 mg, 0.13 mmol) in dichloromethane (1 mL) at 0 °C. The resulting mixture was stirred for 6 h at rt, diluted with dichloromethane (5 mL) and washed saturated sodium bicarbonate solution (2 × 4 mL). The organic layer was dried over anhydrous sodium sulfate, filtered, and concentrated. The residue was purified via flash chromatography (SiO_2, 1:4 EtOAc/hexanes) to give the desired ester **7e** (28 mg, 72.5%) as a colorless oil: ^{1}H NMR (500 MHz, $CDCl_3$) δ 7.84 (d, *J* = 2.1 Hz, 1H), 7.81 (dd, *J* = 8.3, 2.2 Hz, 1H), 7.02 (d, *J* = 8.3 Hz, 1H), 6.69 (s, 2H), 6.26 (d, *J* = 2.3 Hz, 1H), 6.13 (d, *J* = 2.4 Hz, 1H), 5.67 (td, *J* = 3.4, 1.2 Hz, 1H), 5.14 (dddd, *J* = 7.3, 5.8, 2.9, 1.4 Hz, 1H), 5.08 (br s, 1 H), 3.81 (s, 3H), 3.80 (s, 3H), 3.79 (s, 3H), 3.71 (s, 6H), 3.21 (d, *J* = 7.2 Hz, 2H), 3.05 (d, *J* = 3.3 Hz, 2H), 2.30 (s, 3H), 1.72 (s, 3H), 1.66 (s, 3H); ^{13}C NMR (125 MHz, $CDCl_3$) δ 168.8, 164.9, 159.6, 158.9, 155.4, 153.1 (2), 152.7, 137.8, 134.0, 133.9, 133.3, 131.8, 128.6, 127.8, 122.4, 120.7, 103.8 (2), 100.0, 93.3, 92.0, 77.9, 68.4, 60.8, 56.0, 55.4 (3), 28.6, 25.7 (2), 20.9, 17.8; IR (KBr) ν_{max} 2921, 2850, 1716, 1593, 1458, 1282, 1201, 1142, 1010, 948, 813 cm^{-1}; HRMS (ESI+) *m/z* [M + H$^+$] calcd for $C_{34}H_{39}O_{10}$, 607.2543, found 607.2541.

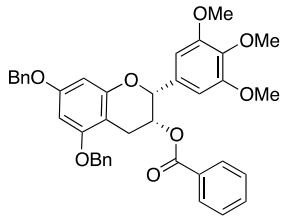

5,7-Bis(benzyloxy)-2-(3,4,5-trimethoxyphenyl)chroman-3-yl Benzoate (**7f**): Benzoyl chloride (8 μL, 0.064 mmol) in dichloromethane (0.5 mL) was added to a solution of **5b** (17 mg, 0.032 mmol) and 4-dimethylaminopyridine (12 mg, 0.092 mmol) in dichloromethane (0.7 mL) with pyridine (0.3 mL) at 0 °C. The solvent was removed and the residue purified via flash chromatography (SiO_2, 1:8 EtOAc/hexanes) to give the desired ester, **7f** (16 mg, 83.5%), as an

amorphous white solid: ^{1}H NMR (500 MHz, $CDCl_3$) δ 8.01–7.96 (m, 2H), 7.63 (d, *J* = 1.7 Hz, 1H), 7.53–7.34 (m, 12H), 6.72 (s, 2H), 6.38 (d, *J* = 2.3 Hz, 1H), 6.32 (d, *J* = 2.3 Hz, 1H), 5.71 (ddd, *J* = 4.1, 3.0, 1.3 Hz, 1H), 5.10 (d, *J* = 3.8 Hz, 1H), 5.08–5.01 (m, 4H), 3.80 (s, 3H), 3.71 (s, 6H), 3.18–3.10 (m, 2H); ^{13}C NMR (125 MHz, $CDCl_3$) δ 172.0, 165.5, 158.8, 158.0, 155.6, 153.1, 137.7, 136.9, 136.8, 133.8, 133.3, 133.2, 130.2, 130.0, 129.8 (2), 129.3, 128.6 (2), 128.6, 128.5, 128.3 (2), 128.0, 127.9 (2), 127.6, 127.2, 100.9, 94.8, 94.0, 78.1, 70.2, 70.0, 68.5, 60.8, 55.9 (2), 26.3; IR (KBr) ν_{max} 2929,, 2839, 1716, 1616, 1591, 1506, 1456, 1361, 1226, 1149, 1126, 1041, 811, 754 cm^{-1}; HRMS (ESI+) *m*/*z* [M + Na^+] calcd for $C_{39}H_{36}NaO_8$, 655.2308, found 655.2307.

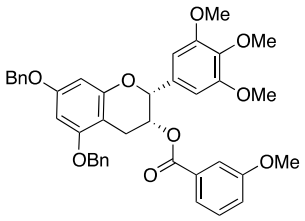

5,7-Bis(benzyloxy)-2-(3,4,5-trimethoxyphenyl)chroman-3-yl 3-Methoxybenzoate (**7g**): 3-Methoxybenzoyl chloride (9 μL, 0.064 mmol) in dichloromethane (0.5 mL) was added to a solution of **5b** (17 mg, 0.032 mmol) and 4-dimethylaminopyridine (12 mg, 0.092 mmol) in dichloromethane 0.7 (mL) with pyridine (0.3 mL) at 0 °C. The resulting mixture was stirred for 6 h at rt. The resulting mixture was stirred for 6 h at rt. The solvent was removed and the residue purified via flash chromatography (SiO_2, 1:8 EtOAc/hexanes) to give the desired ester **7g** (16 mg, 85.1%) as an amorphous white solid: ^{1}H NMR (500 MHz, $CDCl_3$) δ 7.58 (dt, *J* = 7.7, 1.2 Hz, 1H), 7.50–7.30 (m, 12H), 7.07 (ddd, *J* = 8.2, 2.7, 1.0 Hz, 1H), 6.72 (s, 2H), 6.37 (d, *J* = 2.3 Hz, 1H), 6.31 (d, *J* = 2.3 Hz, 1H), 5.68 (ddd, *J* = 4.2, 3.0, 1.3 Hz, 1H), 5.17–5.03 (m, 4H), 5.03 (s, 1H), 3.80 (s, 6H), 3.73 (s, 6H), 3.17–3.11 (m, 2H); ^{13}C NMR (125 MHz, $CDCl_3$) δ 165.4, 159.5, 158.8, 158.0, 155.6, 153.1 (2), 137.7, 136.9, 136.8, 133.3, 131.3, 129.3, 128.6 (3), 128.5, 128.0, 127.9

(3), 127.6, 127.2 (2), 122.1, 119.1, 114.7, 103.8 (2), 100.8, 94.8, 94.0, 78.0, 70.2, 70.0, 68.6, 60.8, 55.9, 55.4, 26.2; IR (KBr) ν_{max} 2931, 2664, 1716, 1593, 1506, 1456, 1361, 1269, 1217, 1126, 1070. 1008 cm^{-1}; HRMS (ESI+) *m*/*z* [M + Na+] calcd for $C_{40}H_{38}NaO_9$, 685.2414, found 685.2401.

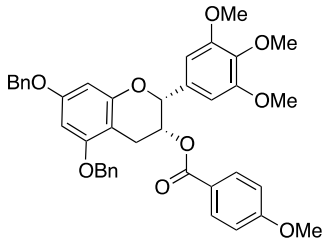

5,7-Bis(benzyloxy)-2-(3,4,5-trimethoxyphenyl)chroman-3-yl 4-Methoxybenzoate (**7h**): 4-Methoxybenzoyl chloride (9 μL, 0.064 mmol) in dichloromethane (0.7 mL) was added to a solution of **5b** (17 mg, 0.032 mmol) and 4-dimethylaminopyridine (12 mg, 0.092 mmol) in dichloromethane (0.7 mL) with pyridine (0.3 mL) at 0 °C. The resulting mixture was stirred for 6 h at rt. The solvent was removed and the residue purified via flash chromatography (SiO_2, 1:8 EtOAc/hexanes) to give the desired ester product **7h** (17 mg, 87.4%) as an amorphous white solid: ^{1}H NMR (500 MHz, $CDCl_3$) δ 7.98–7.89 (m, 2H), 7.49–7.44 (m, 2H), 7.44–7.31 (m, 8H), 6.88–6.84 (m, 2H), 6.71 (s, 2H), 6.37 (d, *J* = 2.3 Hz, 1H), 6.31 (d, *J* = 2.3 Hz, 1H), 5.68 (tt, *J* = 3.1, 1.2 Hz, 1H), 5.08 (s, 1H), 5.08–5.01 (m, 4H), 3.84 (s, 3H), 3.80 (s, 3H), 3.72 (s, 6H), 3.12 (t, *J* = 3.0 Hz, 2H); ^{13}C NMR (125 MHz, $CDCl_3$) δ 165.2, 163.5, 158.7, 158.0, 155.6, 153.1, 137.7, 136.9, 136.8, 133.3 (2), 131.8, 128.6 (2), 128.5 (2), 128.0 (2), 127.9 (2), 127.6 (2), 127.2, 122.4, 113.5 (2), 103.9 (2), 101.0, 94.8, 93.9, 78.1, 70.2, 70.0, 68.0, 60.8, 60.0, 55.9, 55.5, 26.4; IR (KBr) ν_{max} 3348, 2952, 2927, 1716, 1506, 1417, 1257, 1168, 1126, 1035, 821 cm^{-1}; HRMS (ESI+) *m*/*z* [M + H^+] calcd for $C_{40}H_{39}O_9$, 663.2594, found 663. 2608.

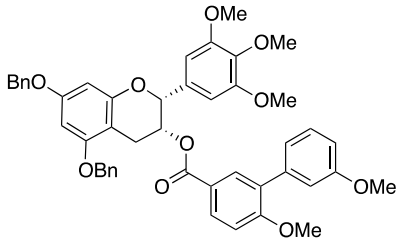

5,7-Bis(benzyloxy)-2-(3,4,5-trimethoxyphenyl)chroman-3-yl 3′,6-Dimethoxy-[1,1′-biphenyl]-3-carboxylate (**7i**): A solution of 3′,6-dimethoxy-[1,1′-biphenyl]-3-carboxylic acid (35 mg, 0.135 mmol) in THF (5 mL) was treated with thionyl chloride (20 μL, 0.27 mmol). The resulting solution was heated at reflux for 3 h, cooled to rt before the solvent was removed. The crude was dissolved in dichloromethane (0.5 mL) and added to a solution of **5b** (18 mg, 0.045 mmol) and 4-dimethylaminopyridine (22 mg, 0.18 mmol) in dichloromethane (0.7 mL) with pyridine (0.3 mL) at 0 °C. The resulting mixture was stirred for 6 h at rt, the solvent was removed, and the residue was purified via flash chromatography (SiO_2, 1:3 EtOAc/hexanes) to give the desired ester, **7i** (28 mg, 83%) as a colorless oil: ^{1}H NMR (500 MHz, $CDCl_3$) δ 7.97 (dd, *J* = 8.6, 2.2 Hz, 1H), 7.93 (d, *J* = 2.2 Hz, 1H), 7.44 (d, *J* = 1.3 Hz, 1H), 7.43–7.29 (m, 10H), 7.03 (dt, *J* = 7.7, 1.2 Hz, 1H), 7.00 (dd, *J* = 2.6, 1.5 Hz, 1H), 6.94 (d, *J* = 8.7 Hz, 1H), 6.91 (ddd, *J* = 8.3, 2.6, 1.0 Hz, 1H), 6.71 (s, 2H), 6.37 (d, *J* = 2.3 Hz, 1H), 6.30 (d, *J* = 2.3 Hz, 1H), 5.67 (td, *J* = 3.6, 1.4 Hz, 1H), 5.10 (s, 1H), 5.07–5.01 (m, 4H), 3.86–3.79 (m, 9H), 3.69 (s, 6H), 3.15 (d, *J* = 3.6 Hz, 2H); ^{13}C NMR (125 MHz, $CDCl_3$) δ 165.6, 160.6, 159.5, 159.0, 158.2, 155.8, 153.3 (2), 138.9, 137.1, 137.1, 133.6, 132.6, 131.3, 130.7, 129.3, 128.9, 128.8 (2), 128.3 (2), 128.2 (2), 127.8 (2), 127.4 (2), 122.7, 122.1, 115.4, 113.2, 110.7, 104.0 (2), 101.3, 95.0, 94.2, 78.3, 70.4, 70.2, 68.6, 61.1, 56.2, 56.1 (2), 55.5, 26.5; IR (KBr) ν_{max} 3434, 2929, 1712, 1616, 1593, 1500, 1456, 2440, 2303, 1238, 1149, 1126, 1027, 821, 736,698 cm^{-1}; HRMS (ESI+) *m/z* [M + Na^+] calcd for $C_{47}H_{44}NaO_{10}$, 791.2832, found 791.2766.

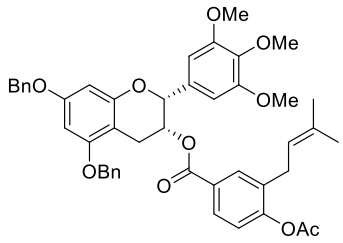

5,7-Bis(benzyloxy)-2-(3,4,5-trimethoxyphenyl)chroman-3-yl 4-Acetoxy-3-(3-methylbut-2-en-1-yl)benzoate (7j): A solution of 4-acetoxy-3-(3-methylbut-2-en-1-yl)benzoic acid (33.5 mg, 0.135 mmol) in THF (5 mL) was treated with thionyl chloride (20 μL, 0.27 mmol). The resulting solution was heated at 70 °C for 3 h and cooled to rt and concentrated. The residue was dissolved in dichloromethane (0.5 mL) and added to a solution of **5b** (18 mg, 0.045 mmol) and 4-dimethylaminopyridine (22 mg, 0.18 mmol) in dichloromethane (0.7 mL) with pyridine (0.3 mL) at 0 °C. The resulting mixture was stirred for 6 h at rt. The solvent was removed and the residue purified via flash chromatography (SiO_2, 1:3 EtOAc/hexanes) to give the desired ester, **7j** (26.6 mg, 78%), as a colorless oil: ^{1}H NMR (500 MHz, $CDCl_3$) δ 7.78 (d, *J* = 2.1 Hz, 1H), 7.74 (dd, *J* = 8.4, 2.2 Hz, 1H), 7.52–7.46 (m, 2H), 7.44–7.36 (m, 2H), 7.39–7.28 (m, 6H), 7.01 (d, J = 8.4 Hz, 1H), 6.79 (s, 2H), 6.29–6.37 (m, 2H), 5.76 (ddd, J = 4.3, 2.9, 1.4 Hz, 1H), 5.22 (m, 1H), 5.15 (m, 3H), 5.00 (s, 2H), 3.81 (s, 3H), 3.77 (s, 6H), 3.20 (d, *J* = 7.4 Hz, 2H), 3.19–3.06 (m, 2H), 2.31 (s, 3H), 1.71 (d, 1.6 Hz, 3H), 1.66 (d, *J* = 1.4 Hz, 3H); ^{13}C NMR (125 MHz, $CDCl_3$) δ 169.0, 165.1, 156.7, 155.1, 153.3, 152.9 (2), 152.1, 137.7, 136.9, 136.6, 134.3, 134.1, 133.0, 132.0, 128.9, 128.8 (2), 128.3 (2), 128.2 (2), 127.8 (1), 127.4 (2), 127.3 (2), 122.6, 120.8, 103.5 (2), 102.6, 93.0, 92.9, 78.2, 71.5, 70.5, 68.0, 61.0, 56.2 (2), 28.8, 26.5, 25.9, 21.0, 18.0; IR (KBr) ν_{max} 2960, 2925, 1714, 1604, 1456, 1353, 1261, 1236, 1174, 1126, 1012, 819 cm^{-1}; HRMS (ESI+) *m*/*z* [M + H^+] calcd for $C_{46}H_{47}O_{10}$, 759.3169, found 759.3195.

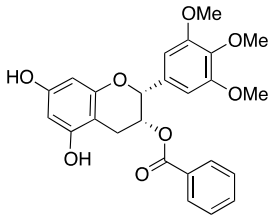

5,7-Dihydroxy-2-(3,4,5-trimethoxyphenyl)chroman-3-yl benzoate (**8a**): Compound **7f** (15 mg, 0.023 mmol) and palladium/carbon (10%) were suspended in tetrahydrofuran (2 mL) and stirred for 18 h under a hydrogen atmosphere. The suspension was filtered through a small pad of celite. The eluent was concentrated and the residue purified by flash chromatography (SiO_2, acetone/dichloromethane 1:8) to give the desired product **8a** (9.5 mg, 88.5%) as a colorless oil: ^{1}H NMR (500 MHz, $CDCl_3$) δ 7.99–7.86 (m, 2H), 7.53 (ddt, *J* = 8.7, 7.2, 1.3 Hz, 1H), 7.45–7.33 (m, 2H), 6.70 (s, 2H), 6.19 (d, *J* = 2.3 Hz, 1H), 5.98 (d, *J* = 2.3 Hz, 1H), 5.70 (ddd, *J* = 4.3, 2.8, 1.3 Hz, 1H), 5.09 (br s, 1H), 3.80 (s, 3H), 3.70 (s, 6H), 3.15–3.00 (m, 2H); ^{13}C NMR (125 MHz, $CDCl_3$) δ 165.6, 156.1, 155.3 (2), 155.1 (2), 153.1, 137.7, 133.3, 129.8(2), 129.7 (3), 128.4, 103.8 (2), 98.9, 96.5, 96.1, 77.9, 68.3, 60.9, 55.9 (2), 25.8 cm^{-1}; IR (KBr) ν_{max} 3421, 2931, 2850, 1717, 1596, 1465, 1276, 1126, 756 cm^{-1}; HRMS (ESI-) *m*/*z* [M – H$^+$] calcd for $C_{25}H_{23}O_8$, 451.1393, found 451.1412.

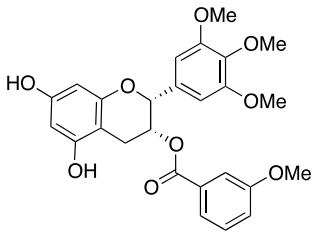

5,7-Dihydroxy-2-(3,4,5-trimethoxyphenyl)chroman-3-yl 3-Methoxybenzoate (**8b**): Compound **7g** (14 mg, 0.021 mmol) and palladium/carbon (10%) were suspended in tetrahydrofuran (2 mL) and stirred for 18 h under a hydrogen atmosphere. The suspension was

filtered through a small pad of celite. The eluent was concentrated and the residue purified by flash chromatography (SiO_2, acetone/dichloromethane 1:8) to afford **8b** (9 mg, 89%) as a colorless oil: ^{1}H NMR (500 MHz, $CDCl_3$) δ 7.55 (dt, *J* = 7.7, 1.2 Hz, 1H), 7.45 (dd, *J* = 2.7, 1.5 Hz, 1H), 7.30–7.26 (m, 1H), 7.06 (ddd, *J* = 8.3, 2.7, 1.0 Hz, 1H), 6.70 (s, 2H), 6.18 (d, *J* = 2.3 Hz, 1H), 5.94 (d, *J* = 2.3 Hz, 1H), 5.68 (ddd, *J* = 4.2, 2.8, 1.3 Hz, 1H), 5.43 (s, 1H), 5.29 (s, 1H), 5.13–5.06 (m, 1H), 3.80 (s, 3H), 3.77 (s, 3H), 3.70 (s, 6H), 3.20–3.02 (m, 2H); ^{13}C NMR (125 MHz, $CDCl_3$) δ 165.6, 159.5, 156.0, 155.4, 155.2, 153.1 (2), 137.6, 133.4, 131.1, 129.4, 122.0, 119.4, 114.6, 103.8 (2), 98.8, 96.3, 96.1, 77.9, 68.6, 60.8, 55.9, 55.4 (2), 25.7; IR (KBr) ν_{max} 3419, 3404, 3010, 2927, 2852, 1716, 1596, 1463, 1274, 1128,1105, 754 cm^{-1}; HRMS (ESI+) *m*/*z* [M – H$^+$] calcd for $C_{26}H_{25}O_9$, 481.1499, found 481.1509.

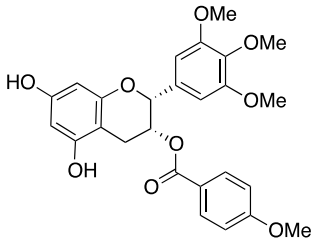

5,7-Dihydroxy-2-(3,4,5-trimethoxyphenyl)chroman-3-yl 4-Methoxybenzoate (**8c**): **7h** (14 mg, 0.021 mmol) and palladium/carbon (10%) were suspended in tetrahydrofuran (2 mL) and stirred for 18 h under a hydrogen atmosphere. The suspension was filtered through a small pad of celite. The eluent was concentrated and the residue purified by flash chromatography (SiO_2, acetone/dichloromethane 1:8) to give **8c** (9 mg, 89%) as a colorless oil: ^{1}H NMR (500 MHz, CD_3OD) δ 7.93–7.76 (m, 2H), 6.98–6.90 (m, 2H), 6.79 (s, 2H), 6.00 (q, *J* = 2.3 Hz, 2H), 5.63 (ddd, *J* = 4.7, 2.3, 1.2 Hz, 1H), 5.14 (s, 1H), 3.83 (s, 3H), 3.70 (s, 3H), 3.67 (s, 6H), 3.07 (dd, *J* = 17.4, 4.6 Hz, 1H), 2.95–2.86 (m, 1H); ^{13}C NMR (125 MHz, $CDCl_3$) δ 165.2, 163.8, 156.2, 155.5, 155.3, 153.3, 137.3, 133.5, 132.0 (3),122.4, 113.8 (2), 104.0 (2), 99.2, 96.6, 96.2, 78.2, 68.1, 63.0,

56.1, 55.7 (2), 26.0; IR (KBr) ν_{max} 3419, 2931, 2842, 1701, 1604, 1506, 1458, 1361, 1257, 1166, 1126, 1101, 1018 cm^{-1} ; HRMS (ESI-) *m*/*z* [M – H^+] calcd for $C_{26}H_{25}O_9$, 481.1499, found 481.1518.

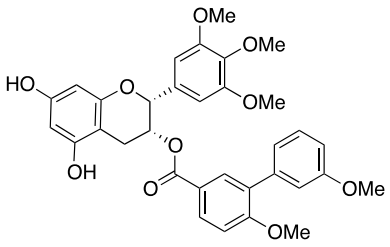

5,7-Dihydroxy-2-(3,4,5-trimethoxyphenyl)chroman-3-yl 3′,6-Dimethoxy-[1,1′-biphenyl]-3-carboxylate (**8d**): Compound **7i** (25 mg, 0.032 mmol) and palladium/carbon (10%) were suspended in tetrahydrofuran (2 mL) and stirred for 18 h under a hydrogen atmosphere. The suspension was filtered through a small pad of celite. The eluent was concentrated and the residue purified by flash chromatography (SiO_2, acetone/dichloromethane 1:8) to give **8d** (17.4 mg, 91%) as a colorless oil: ^{1}H NMR (500 MHz, $CDCl_3$) δ 8.00–7.85 (m, 2H), 7.32 (t, *J* = 7.9 Hz, 1H), 7.07–6.96 (m, 2H), 6.96–6.85 (m, 2H), 6.69 (s, 2H), 6.16 (d, *J* = 2.3 Hz, 1H), 5.96 (d, *J* = 2.3 Hz, 1H), 5.71–5.62 (m, 2H), 5.52 (s, 1H), 5.09 (s, 1H), 3.83 (d, *J* = 3.7 Hz, 6H), 3.79 (d, *J* = 0.6 Hz, 3H), 3.67 (s, 6H), 3.09 (d, *J* = 3.4 Hz, 2H); ^{13}C NMR (125 MHz, $CDCl_3$) δ 165.7, 160.6, 159.4, 156.2, 155.6, 155.4, 153.3 (2), 138.8, 133.6, 132.6, 131.2, 130.6, 129.3 (2), 122.5, 122.1, 115.3, 113.2, 110.7, 103.9 (2), 99.2, 96.6, 96.3, 78.1, 68.5, 61.0, 56.1, 56.0, 55.5, 53.6, 29; IR (KBr) ν_{max} 3429, 2931, 2851, 1699, 1604, 1508, 1476, 1248, 1166, 1145, 1098, cm^{-1}; HRMS (ESI+) *m*/*z* [M + H^+] calcd for $C_{33}H_{33}O_{10}$, 589.2074 found 589.2057

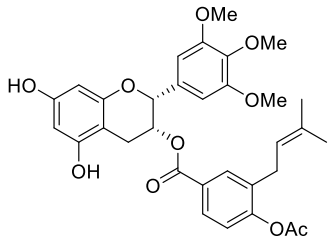

5,7-Dihydroxy-2-(3,4,5-trimethoxyphenyl)chroman-3-yl 4-Acetoxy-3-(3-methylbut-2-en-1-yl)benzoate (8e): A solution of palladium acetate (1 mg, 0.004 mmol), trimethylamine (7 μL, 0.047 mmol), triethylsilane (34 μL, 0.208 in dichloromethane (0.5 mL) was stirred for 15 min before the addition of **7j** (20 mg, 0.026 mmol) in dichloromethane (0.4 mL). The resulting mixture was stirred for 15 h, quenched with saturated ammonium chloride (2 mL), and extracted with diethyl ether (3 × 4 mL). The combined organic layers were washed with saturated sodium chloride solution and dried over anhydrous Na_2SO_4. Solvent was removed, and the residue was purified via flash chromatography (SiO_2, 5:95 MeOH/DCM) to give **8e** (4 mg, 18.9%) as a colorless oil: ^{1}H NMR (500 MHz, $CDCl_3$) δ 7.71 (dd, *J* = 6.4, 2.4 Hz, 2H), 6.67 (s, 3H), 6.43 (d, *J* = 2.2 Hz, 1H), 6.23 (d, *J* = 2.2 Hz, 1H), 5.74 (s, 1H), 5.66–5.59 (m, 1H), 5.36 (br s, 1 H), 5.22 (dddt, *J* = 7.3, 5.8, 2.9, 1.5 Hz, 1H), 4.97 (s, 1H), 3.80 (s, 3H), 3.73 (s, 3H), 3.32 (d, *J* = 7.4 Hz, 2H), 3.07–2.99 (m, 2H), 2.30 (d, *J* = 5.3 Hz, 3H), 1.80–1.64 (m, 6H); ^{13}C NMR (125 MHz, $CDCl_3$) δ 170.1, 165.6, 159.2, 156.0, 155.0, 153.3 (2), 150.0, 137.9, 136.0, 133.2, 132.2, 130.0, 127.1 (2), 122.2, 121.0, 115.7, 104.8, 103.9 (2), 103.1, 102.1, 78.2, 67.7, 61.0, 56.2, 29.7, 26.0 (2), 21.4, 18.1; IR (KBr) ν_{max} 3412, 2937, 2843, 1715, 1693, 1562, 1473, 1126 cm^{-1}; HRMS (ESI-) *m*/*z* [M – H$^+$] calcd for $C_{32}H_{33}O_{10}$, 577.2074, found 577.2079.

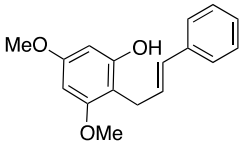

2-Cinnamyl-3,5-dimethoxyphenol (**9a**): A solution of 3,5-dimethoxy phenol (**1a**) (2.3 g, 14.91 mmol) and cinnamyl alcohol (2.0 g, 14.91 mmol) in a solvent mixture of dichloromethane (30 mL) and carbon disulfide (30 mL) was treated with 25% H_2SO_4/SiO_2 catalyst (2.4 g, 5.96 mmol) at rt. The resulting mixture was stirred for 4 h and then filtered through a plug of SiO_2. Solvent was removed and the residue purified by flash chromatography (SiO_2, 1:9 EtOAc/hexanes) to give **9a** (1.735 g, 43.15%) as an amorphous light yellow solid: ^{1}H NMR (500 MHz, $CDCl_3$) δ 7.37–7.26 (m, 2H), 7.30 (dd, *J* = 7.2, 1.7 Hz, 2H), 7.23–7.17 (m, 1H), 6.48 (dt, *J* = 16.0, 1.7 Hz, 1H), 6.34 (dt, *J* = 15.9, 6.3 Hz, 1H), 6.15 (d, *J* = 2.3 Hz, 1H), 6.11 (d, *J* = 2.3 Hz, 1H), 5.06 (s, 1H), 3.82 (s, 3H), 3.80 (s, 3H), 3.56 (d, *J* = 1.6 Hz, 1H), 3.55 (d, *J* = 1.6 Hz, 1H); ^{13}C NMR (125 MHz, $CDCl_3$) δ 159.9, 159.0, 155.9, 137.4, 130.6, 128.6 (2), 128.6, 128.5, 127.3, 126.3, 106.1, 93.9, 91.8, 56.0, 55.5, 26.4; IR (KBr) ν_{max} 3367, 1614, 1596, 1454, 1423, 1201, 1147, 1097, 1053, 811, 736, 692 cm^{-1}; HRMS (ESI+) *m*/*z* [M + H^+] calcd for $C_{17}H_{19}O_3$, 271.1334, found 271.1336.

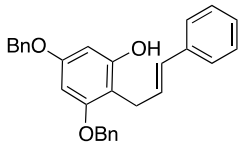

3,5-bis(benzyloxy)-2-cinnamylphenol (**9b**): A solution of 3,5-bis(benzyloxy)phenol (**1b**) (3.3 g, 9.98 mmol) and cinnamyl alcohol (1.34 g, 9.98 mmol) in a solvent mixture of dichloromethane (20 mL) and carbon disulfide (20 mL) was treated with 25% H_2SO_4/SiO_2 catalyst (1.59g, 3.99 mmol) at rt. The resulting mixture was stirred for 4 h and then filtered through a plug of SiO_2. Solvent was removed and the residue purified by flash chromatography (SiO_2, 1:8 EtOAc/hexanes) to give **9b** (1.425 g, 33.7%) as an amorphous light yellow solid: ^{1}H NMR (400 MHz, $CDCl_3$) δ 7.48–7.29 (m, 15H), 6.53–6.44 (m, 1H), 6.39–6.30 (m, 1H), 6.29 (d, *J* = 2.2 Hz, 1H), 6.18 (d, *J* = 2.3 Hz, 1H), 5.03 (m, 5H), 3.60 (dd, *J* = 6.5, 1.6 Hz, 2H); ^{13}C NMR (125 MHz, $CDCl_3$) δ 159.0,

158.1, 155.9, 137.5, 137.2, 137.0 (2), 128.8 (2), 128.7 (2), 128.6 (3), 128.5, 128.2, 128.0, 127.8, 127.5 (2), 127.3, 126.3 (2), 107.0, 95.3, 93.9, 70.5, 70.3, 26.7; IR (KBr) ν_{max} 3419, 3028, 2925, 1618, 1596, 1452, 1436,1375, 1147, 1091, 734, 696 cm^{-1}; HRMS (ESI+) *m*/*z* [M + H^+] calcd for $C_{29}H_{27}O_3$, 423.1960, found 423.1966.IR (KBr) ν_{max} cm^{-1}.

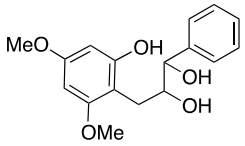

3-(2-Hydroxy-4,6-dimethoxyphenyl)-1-phenylpropane-1,2-diol (**10a**): N-Methylmorpholine *N*-oxide (1.26g, 10.76 mmol) was added to a solution of **9a** (1.7g, 6.33 mmol) in a solvent mixture of tetrahydrofuran (18 mL) and H_2O (12 mL). The resulting solution was stirred for 15 min at rt before the addition osmium tetraoxide (0.1 mmol, 4% solution in water). The mixture was stirred for 14 h at rt before quenching with 20% of sodium metabisulfite (15 mL). The aqueous layer was extracted with ethyl acetate (3 × 25 mL) and the combined organic layers were washed with saturated sodium chloride solution (50 mL), dried over anhydrous Na_2SO_4, filtered and concentrated. The residue was purified by flash chromatography (SiO_2, 1:2 EtOAc/hexanes) to afford **10a** (1.55 g, 81%) as a colorless oil: ^{1}H NMR (500 MHz, $CDCl_3$) δ 7.98 (br s, 1 H), 7.43–7.37 (m, 2H), 7.37–7.32 (m, 3H), 6.17 (d, *J* = 2.4 Hz, 1H), 6.03 (d, *J* = 2.4 Hz, 1H), 4.55 (d, *J* = 6.6 Hz, 1H), 4.04 (ddd, *J* = 7.4, 6.5, 3.8 Hz, 1H), 3.77 (s, 3H), 3.59 (s, 3H), 3.23 (br s, 1 H), 2.84 (dd, *J* = 14.8, 3.8 Hz, 1H), 2.74 (dd, *J* = 14.8, 7.4 Hz, 1H), 2.46 (br s, 1 H); ^{13}C NMR (125 MHz, $CDCl_3$) δ 160.2, 158.9, 157.5, 140.6, 128.7 (2), 128.5 (2), 127.2, 105.5, 76.9, 76.5, 94.6, 91.5, 55.5 (2), 26.2; IR (KBr) ν_{max} 3348, 2837, 1622, 1593, 1496, 1456, 1338, 1199, 1147, 1105, cm^{-1}; HRMS (ESI-) *m*/*z* [M – H^-] calcd for $C_{17}H_{19}O_5$, 303.1233, found 303.1227.

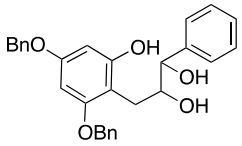

3-(2,4-Bis(benzyloxy)-6-hydroxyphenyl)-1-phenylpropane-1,2-diol (10b): *N*-Methylmorpholine *N*-oxide (393 mg, 3.36 mmol) was added to a solution of **9b** (0.9g, 2.1 mmol) in a solvent mixture of tetrahydrofuran (9 mL) and H_2O (6 mL). The resulting solution was stirred for 15 min at rt before the addition osmium tetraoxide (0.02 mmol, 4% solution in water). The mixture was stirred for 14 h at rt before quenching with 20% of sodium metabisulfite (10 mL). The aqueous layer was extracted with ethyl acetate (3 × 20 mL) and the combined organic layers were washed with saturated sodium chloride solution (40 mL), dried over anhydrous Na_2SO_4, filtered, and concentrated. The residue was purified by flash chromatography (SiO_2, 1:3 EtOAc/hexanes) to afford **10b** (0.78g, 80.1%) as a colorless oil: ^{1}H NMR (500 MHz, $CDCl_3$) δ 8.03 (s, 1H), 7.46–7.36 (m, 5H), 7.36–7.29 (m, 6H), 7.27–7.25 (m, 2H), 7.19–7.06 (m, 2H), 6.29 (d, *J* = 2.3 Hz, 1H), 6.21 (d, *J* = 2.4 Hz, 1H), 5.01 (s, 2H), 4.90–4.82 (m, 2H), 4.56 (d, *J* = 6.8 Hz, 1H), 4.04 (ddd, *J* = 8.5, 6.7, 3.5 Hz, 1H), 3.32 (s, 1H), 2.93 (dd, *J* = 14.7, 3.5 Hz, 1H), 2.75 (dd, *J* = 14.6, 8.4 Hz, 1H), 2.46 (s, 1H); ^{13}C NMR (125 MHz, $CDCl_3$) δ 159.3, 158.0, 157.7, 140.4, 137.1, 137.0, 128.8 (5), 128.7 (2), 128.6, 128.2, 127.8 (4), 127.2 (2), 127.0 (2), 106.3, 96.1, 93.6, 70.3 (2), 26.6; IR (KBr) ν_{max} 3363, 3330 3087, 3031, 1701, 1620, 1598, 1452, 1375, 1147, 1099, 815, 698 cm-^{1}; HRMS (ESI+) *m*/*z* [M + H^+] calcd for $C_{29}H_{29}O_5$, 457.2015, found 457.2028.

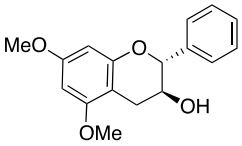

5,7-Dimethoxy-2-phenylchroman-3-ol (**11a**): Trimethyl orthoacetate (2.50 mmol, 300 μL) and pyridinium *p*-toluenesulfonate (9 mg, 0.036 mmol) were added to a solution of **10a** (600 mg, 1.92

mmol) in dichloromethane (36 mL) at rt. The resulting mixture was stirred for 30 min at rt and then cooled to 0 °C before the dropwise addition of boron trifluoride diethyl etherate (25 μL, 0.192 mmol). The reaction mixture was warmed to rt and stirred for another 15 min before quenching with aqueous acetone (4 mL). Solvent was removed and the residue was dissolved in methanol (32 mL). Potassium carbonate (225 mg, 1.84 mmol) was added and the mixture stirred for 6 h at rt. Methanol was removed, water (25 mL) was added, and the products were extracted with ethyl acetate (2 × 30 mL). The organic layers were combined and washed with saturated sodium chloride solution (60 mL). The organic phase was dried over anhydrous Na_2SO_4 and filtered. Solvent was removed, and the residue was purified via flash chromatography (SiO_2, 1:4 EtOAc/hexanes) to yield compound **11a** (422 mg, 77.7%) as a colorless oil: ^{1}H NMR (500 MHz, $CDCl_3$) δ 7.47–7.34 (m, 5H), 6.16 (d, *J* = 2.3 Hz, 1H), 6.12 (d, *J* = 2.3 Hz, 1H), 4.79 (d, *J* = 7.8 Hz, 1H), 4.11 (td, *J* = 8.1, 5.5 Hz, 1H), 3.81 (s, 3H), 3.77 (s, 3H), 3.00 (dd, *J* = 16.4, 5.5 Hz, 1H), 2.63 (dd, *J* = 16.4, 8.4 Hz, 1H), 1.71 (s, 1H); ^{13}C NMR (125 MHz, $CDCl_3$) δ 159.7, 158.8, 155.1, 138.1, 128.8 (2), 128.6 (2), 127.1, 101.4, 93.0, 91.9, 81.7, 68.2, 55.5, 55.4, 27.2; IR (KBr) ν_{max} 3446, 2937, 2839, 1618, 1593, 1496, 1213, 1143, 1120, 1051, 1022, 813, 761, 689 cm^{-1}; HRMS (ESI+) *m*/*z* [M + H$^+$] calcd for $C_{17}H_{19}O_4$, 287.1283, found 287.1270.

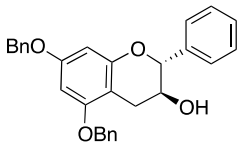

5,7-Bis(benzyloxy)-2-phenylchroman-3-ol (**11b**): Trimethyl orthoacetate (1.48 mmol, 188 μL) and pyridinium p-toluenesulfonate (6 mg, 0.012 mmol) were added to a solution of **10b** (560 mg, 1.22 mmol) in dichloromethane (24 mL) at rt. The resulting mixture was stirred for 30 min and cooled to 0 °C before the addition of borontrifluoride diethyletherate (18 μL, 0.24 mmol) dropwise. The reaction mixture was warmed to rt and stirred for another 15 min before quenching with

aqueous acetone (4 mL). Solvent was removed, and the residue was dissolved in methanol (18 mL). Potassium carbonate (185 mg, 1.34 mmol) was added and mixture stirred for 6 h at rt. Methanol was removed, water (20 mL) was added and the products extracted with ethyl acetate (2 × 25 mL). The combined organic layers were washed with saturated sodium chloride solution (60 mL). The organic phase was dried over anhydrous Na_2SO_4 and filtered. Solvent was removed and the residue was purified via flash chromatography (SiO_2, 1:4 EtOAc/hexanes) to yield compound **11b** (420 mg, 78.2%) as a pale yellow oil: ^{1}H NMR (400 MHz, $CDCl_3$) δ 7.61–7.23 (m, 15H), 6.28–6.09 (m, 2H), 5.09–4.76 (m, 4H), 4.73 (d, *J* = 7.9 Hz, 1H), 4.07 (td, *J* = 8.4, 5.6 Hz, 1H), 3.05 (dd, *J* = 16.5, 5.5 Hz, 1H), 2.65 (dd, *J* = 16.4, 8.6 Hz, 1H); IR (KBr) ν_{max} 3460, 2912, 1617, 1592, 1375, 1145, 1126, 1076, 973, 813, 696 cm^{-1}; HRMS (ESI+) *m/z* [M + H^+] calcd for $C_{29}H_{27}O_4$, 439.1909, found 439.1897.

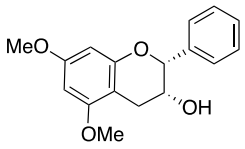

5,7-Dimethoxy-2-phenylchroman-3-ol (**12a**): Dess-Martin periodinane (937 mg, 2.20 mmol, 1.5 eq.) was added to a solution of **11a** (421 mg, 1.47 mmol, 1.0 eq.) in dichloromethane (15 mL). The resulting mixture was stirred for 2 h before quenching with 15 % aqueous solution of sodium thiosulfate (5 mL) and saturated sodium bicarbonate (5 mL). The aqueous layer was extracted with dichloromethane (3 × 10 mL) and the combined organic layers were washed with saturated sodium chloride solution (15 mL), dried over anhydrous sodium sulfate, filtered, and concentrated. The residue was purified via flash chromatography (SiO_2, 1:4 EtOAc/hexanes) to yield the corresponding ketone which was used further as obtained. A solution of the ketone in tetrahydrofuran (3 mL) was added dropwise to a solution of lithium bromide (663 mg, 7.64 mmol, 5.2 eq.) and L-selectride (1 M solution) (1.91 mL, 1.91 mmol, 1.3 eq.) in tetrahydrofuran at -78

°C. The resulting mixture was stirred for 6 h at -78 °C, warmed to rt, and quenched with 2.5 M sodium hydroxide solution (6.86 mL), followed by the addition of ethanol (5.10 mL) and 35% aqueous hydrogen peroxide solution (1.70 mL). The resulting mixture was stirred for 14 h before the addition of ethyl acetate (20 mL). The aqueous layer was extracted with ethyl acetate (2 × 15 mL) and the combined organic layers washed with saturated sodium chloride solution (30 mL), dried over anhydrous sodium sulfate, filtered, and concentrated. The residue purified via flash chromatography (SiO_2, 1:4 EtOAc/hexanes) to yield compound **12a** as a colorless oil (232 mg, 55%): ^{1}H NMR (400 MHz, $CDCl_3$) δ 7.58–7.52 (m, 2H), 7.45 (dd, *J* = 8.4, 6.7 Hz, 2H), 7.43–7.33 (m, 1H), 6.23 (d, *J* = 2.3 Hz, 1H), 6.15 (d, *J* = 2.3 Hz, 1H), 5.05 (s, 1H), 4.34 (s, 1H), 3.82 (s, 3H), 3.80 (d, *J* = 0.7 Hz, 3H), 3.04–2.82 (m, 2H), 1.73 (br s, 1 H); ^{13}C NMR (125 MHz, $CDCl_3$) δ 159.9, 159.5, 155.4, 138.4, 129.0, 128.8, 128.3, 126.5, 126.4, 100.4, 93.5, 92.4, 78.8, 66.6, 55.7, 55.6, 28.3; IR (KBr) ν_{max} 3451, 1952, 2923, 2854, 1618, 1593, 1203, 1145, 1118, 1058, 968, 811, 746, 700 cm^{-1}; HRMS (ESI+) *m/z* [M + H$^+$] $C_{17}H_{19}O_4$, 287.1283, found 287.1277.

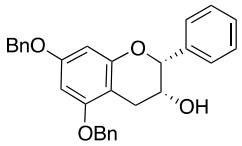

5,7-Bis(benzyloxy)-2-phenylchroman-3-ol (**12b**): Dess-Martin periodinane (609 mg, 1.44 mmol, 1.5 eq.) was added to a solution of **11b** (421 mg, 0.96 mmol, 1.0 eq.) in dichloromethane (10 mL). The resulting mixture was stirred for 2 h before quenching with 15 % aqueous solution of sodium thiosulfate (3 mL) and saturated sodium bicarbonate (3 mL). The aqueous layer was extracted with dichloromethane (3 × 10 mL) and the combined organic layers were washed with saturated sodium chloride solution (10 mL), dried over anhydrous sodium sulfate, filtered, and concentrated. The residue was purified via flash chromatography (SiO_2, 1:3 EtOAc/hexanes) to yield the corresponding ketone which was used further as obtained. A solution of the ketone in

tetrahydrofuran (2 mL) was added dropwise to a solution of lithium bromide (429 mg, 4.99 mmol, 5.2 eq.) and L-selectride (1 M solution) (1.24 mL, 1.24 mmol, 1.3 eq.) in tetrahydrofuran at -78 °C. The resulting mixture was stirred for 6 h at -78 °C, warmed to rt, and quenched with 2.5 M sodium hydroxide solution (4.45 mL), followed by the addition of ethanol (3.30 mL) and 35% aqueous hydrogen peroxide solution (1.10 mL). The resulting mixture was stirred for 14 h before the addition of ethyl acetate (14 mL). The aqueous layer was extracted with ethyl acetate (2 × 10 mL) and the combined organic layers washed with saturated sodium chloride solution (20 mL), dried over anhydrous sodium sulfate, filtered, and concentrated. The residue purified via flash chromatography (SiO_2, 1:3 EtOAc/hexanes) to yield compound **11b** as a pale yellow oil (198 mg, 47%). ^{1}H NMR (400 MHz, $CDCl_3$) δ 7.91 (s, 1H), 7.65–7.31 (m, 15H), 6.23 (d, *J* = 2.3 Hz, 1H), 6.16 (d, *J* = 2.3 Hz, 1H), 5.62 (dt, *J* = 7.6, 4.9 Hz, 1H), 5.13 (d, *J* = 5.3 Hz, 1H), 4.99 (d, *J* = 1.9 Hz, 4H), 3.25 (dd, *J* = 14.6, 4.9 Hz, 1H), 2.89 (dd, *J* = 14.6, 8.0 Hz, 1H), 1.75 (br s, 1 H); IR (KBr) ν_{max} 3449, 2954, 2842, 1618, 1593, 1498, 1458, 1198, 1145, 1120, 1080, 729 cm^{-1}; HRMS (ESI+) *m*/*z* [M + Na^+] calcd for $C_{29}H_{26}NaO_4$, 461.1729, found 461.1724.

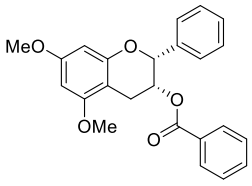

5,7-Dimethoxy-2-phenylchroman-3-yl benzoate (13a): Benzoyl chloride (8 μL, 0.07 mmol) in dichloromethane (0.5 mL) was added to a solution of **12a** (10 mg, 0.035 mmol) and 4-dimethylaminopyridine (11 mg, 0.08 mmol) in dichloromethane (1 mL) at 0 °C. The resulting mixture was stirred for 6 h at rt. Solvent was removed and the residue purified via flash chromatography (SiO_2, 1:8 EtOAc/hexanes) to give the desired ester **13a** as an amorphous white solid: (11 mg, 88.8%): ^{1}H NMR (500 MHz, $CDCl_3$) δ 7.95–7.87 (m, 2H), 7.56–7.47 (m, 3H), 7.41–

7.28 (m, 5H), 6.27 (d, *J* = 2.3 Hz, 1H), 6.12 (d, *J* = 2.3 Hz, 1H), 5.69 (ddd, *J* = 4.1, 3.2, 1.4 Hz, 1H), 5.21 (m, 1H), 3.82 (s, 3H), 3.78 (s, 3H), 3.15–3.02 (m, 2H); ^{13}C NMR (125 MHz, $CDCl_3$) δ 165.9, 159.9, 159.1, 155.7, 138.0, 133.1, 130.2, 129.9 (2), 128.5 (4), 128.3 (2), 126.7, 100.4, 93.5, 92.1, 78.0, 68.8, 55.6 (2), 26.1; IR (KBr) ν_{max} 2956, 1935, 2839, 1714, 1593, 1458, 1419, 1361, 1257, 1147, 1124, 1101, 1029, 1006, 846, 813, 769 cm^{-1}; HRMS (ESI+) *m*/*z* [M + H^+] calcd for $C_{24}H_{23}O_5$, 391.1545, found 391.1538.

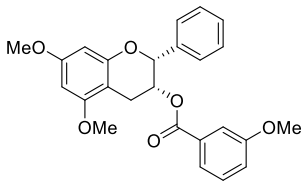

5,7-Dimethoxy-2-phenylchroman-3-yl 3-Methoxybenzoate (**13b**): A solution of **12a** (8 mg, 0.027 mmol) in dichloromethane (0.5 mL) was added to a solution of 3-methoxybenzoic acid (8 mg, 0.05 mmol), *N*-(3-dimethylamino-propyl)-*N*′-ethylcarbodiimide hydrochloride (9.5 mg, 0.05 mmol), and 4-dimethylaminopyridine (6 mg, 0.05 mmol) in dichloromethane (1 mL) at 0 °C. The resulting mixture was stirred for 6 h at rt and then diluted with dichloromethane (5 mL). The organic phase was washed with saturated sodium bicarbonate solution (2 × 4 mL). The organic layer was dried over anhydrous sodium sulfate, filtered and solvent removed. The residue was purified via flash chromatography (SiO_2, 1:8 EtOAc/hexanes) to give the desired ester **13b** (9 mg, 76.9%) as a colorless oil: ^{1}H NMR (500 MHz, $CDCl_3$) δ 7.56–7.46 (m, 3H), 7.42 (dd, *J* = 2.7, 1.5 Hz, 1H), 7.38–7.30 (m, 2H), 7.29 (t, *J* = 2.6 Hz, 1H), 7.27–7.21 (m, 1H), 7.04 (ddd, *J* = 8.3, 2.7, 1.0 Hz, 1H), 6.26 (d, *J* = 2.3 Hz, 1H), 6.12 (d, *J* = 2.3 Hz, 1H), 5.67 (ddd, *J* = 4.1, 3.2, 1.4 Hz, 1H), 5.21 (s, 1H), 3.81 (s, 3H), 3.80 (s, 3H), 3.78 (s, 3H), 3.10–3.04 (m, 2H); ^{13}C NMR (125 MHz, $CDCl_3$) δ 165.8, 159.9, 159.6, 159.1, 155.7, 138.0, 131.5, 129.5 (2), 128.5 (2), 128.3, 126.7, 122.3, 119.6, 114.4, 100.3, 93.5, 92.1, 77.9, 69.0, 55.6 (3), 26.0; IR (KBr) ν_{max} 2925, 2837, 1718, 1618,

1593, 1319, 1274, 1220, 1147, 1105, 1041, 958, 910, 811, 752, 696 cm^{-1}; HRMS (ESI+) *m*/*z* [M + H^+] calcd for $C_{25}H_{25}O_6$, 421.1651, found 421.1642

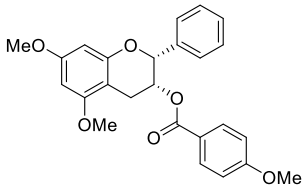

5,7-Dimethoxy-2-phenylchroman-3-yl 4-methoxybenzoate (**13c**): A solution of **12a** (10 mg, 0.035 mmol) in dichloromethane (0.5 mL) was added to a solution 4-methoxybenzoic acid (18 mg, 0.07 mmol), *N*-(3-Dimethylamino-propyl)-*N*′-ethylcarbodiimide hydrochloride (13.5 mg, 0.07 mmol), and 4-dimethylaminopyridine (9 mg, 0.07 mmol) in dichloromethane (1 mL) at 0 °C. The resulting mixture was stirred for 6 h at rt and then diluted with dichloromethane (5 mL). The organic phase was washed with saturated sodium bicarbonate solution (2 × 4 mL). The organic layer was dried over anhydrous sodium sulfate, filtered and the solvent removed. The residue was purified via flash chromatography (SiO_2, 1:8 EtOAc/hexanes) to give the desired ester **13c** as a colorless oil (9.5 mg, 81.1%): ^{1}H NMR (500 MHz, $CDCl_3$) δ 7.93–7.83 (m, 2H), 7.57–7.49 (m, 2H), 7.36–7.30 (m, 2H), 7.28 (d, *J* = 7.0 Hz, 1H), 6.87–6.82 (m, 2H), 6.26 (d, *J* = 2.3 Hz, 1H), 6.12 (d, *J* = 2.3 Hz, 1H), 5.66 (td, *J* = 3.7, 1.5 Hz, 1H), 5.20 (s, 1H), 3.82 (s, 3H), 3.81 (s, 3H), 3.78 (s, 3H), 3.08–3.04 (m, 2H); ^{13}C NMR (125 MHz, $CDCl_3$) δ 165.6, 163.5, 159.8, 159.1, 155.7, 138.1, 131.9 (2), 128.5 (2), 128.2 (2), 126.7, 122.6, 113.7 (2), 100.5, 93.5, 92.1, 78.0, 68.4, 55.6 (3), 26.1; IR (KBr) ν_{max} 2958, 2935, 2839, 1716, 1618, 1255, 1203, 1147, 1101, 1029, 906, 846, 700 cm^{-1}; HRMS (ESI+) *m*/*z* [M + H^+] calcd for $C_{25}H_{25}O_6$, 421.1651, found 421.1644.

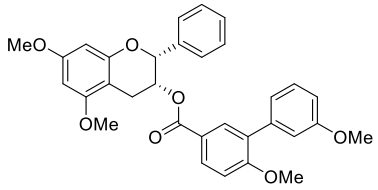

(5,7-Dimethoxy-2-phenylchroman-3-yl 3′,6-dimethoxy-[1,1′-biphenyl]-3-carboxylate (**13d**): A solution of **12a** (10 mg, 0.035 mmol) in dichloromethane (0.5 mL) was added to a solution of 3′,6-dimethoxy-[1,1′-biphenyl]-3-carboxylic acid (18 mg, 0.07 mmol), *N*-(3-dimethylamino-propyl)-*N*′-ethylcarbodiimide hydrochloride (13.5 mg, 0.07 mmol), and 4-dimethylaminopyridine (9 mg, 0.07 mmol) in dichloromethane (1 mL) at 0 °C. The resulting mixture was stirred for 6 h at rt and then diluted with dichloromethane (5 mL). The organic phase was washed with saturated sodium bicarbonate solution (2 × 4 mL), dried over anhydrous sodium sulfate, filtered and concentrated. The residue was purified via flash chromatography (SiO_2, 1:7 EtOAc/hexanes) to give the desired ester **13d** (14 mg, 76%) as a colorless oil: ^{1}H NMR (500 MHz, $CDCl_3$) δ 7.94–7.84 (m, 2H), 7.58–7.48 (m, 2H), 7.38–7.31 (m, 3H), 7.31–7.28 (m, 1H), 7.05 (ddd, *J* = 7.6, 1.6, 1.0 Hz, 1H), 7.01 (dd, *J* = 2.6, 1.6 Hz, 1H), 6.96–6.87 (m, 2H), 6.24 (d, *J* = 2.3 Hz, 1H), 6.11 (d, *J* = 2.3 Hz, 1H), 5.65 (td, *J* = 3.7, 1.5 Hz, 1H), 5.21 (s, 1H), 3.84 (d, *J* = 0.7 Hz, 6H), 3.80 (s, 3H), 3.78 (s, 3H), 3.11–3.04 (m, 2H); ^{13}C NMR (125 MHz, $CDCl_3$) δ 165.5, 160.2, 159.6, 159.3, 158.9, 155.5, 138.8, 137.9, 132.5, 131.0, 130.2, 129.0 (2), 128.3, 128.1 (2), 126.5, 122.5, 122.0, 115.2, 112.9, 110.5, 100.2, 93.3, 91.9, 77.8, 68.5, 55.8, 55.4 (2), 55.3, 25.8; IR (KBr) ν_{max} 2933, 1716, 1616, 1595, 1298, 1245, 1205, 1147, 1108, 1027, 918, 813, 696, 649 cm^{-1}; HRMS (ESI+) *m*/*z* [M + Na^+] calcd for $C_{32}H_{30}NaO_7$, 549.1889, found 549.1863.

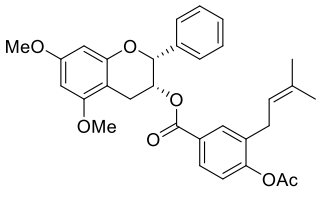

5,7-Dimethoxy-2-phenylchroman-3-yl 4-Acetoxy-3-(3-methylbut-2-en-1-yl)benzoate (**13e**): A solution of **12a** (20 mg, 0.07 mmol) in dichloromethane (0.5 mL) was added to a solution of 4-acetoxy-3-(3-methylbut-2-en-1-yl)benzoic acid (35 mg, 0.14 mmol), N-(3-dimethylamino-propyl)-N′-ethylcarbodiimide hydrochloride (27 mg, 0.14 mmol) and 4-dimethylaminopyridine (25 mg, 0 0.21 mmol) in dichloromethane (1 mL) at 0 °C. The resulting mixture was stirred for 6 h at rt, diluted with dichloromethane (5 mL) and washed saturated sodium bicarbonate solution (2 × 4 mL). The organic layer was dried over anhydrous sodium sulfate, filtered and the solvent removed. The residue was purified via flash chromatography (SiO_2, 1:7 EtOAc/hexanes) to give the desired ester **13e** (20 mg, 55.5%) as a colorless oil: ^{1}H NMR (400 MHz, $CDCl_3$) δ 7.80 (d, *J* = 2.1 Hz, 1H), 7.76 (dd, *J* = 8.4, 2.1 Hz, 1H), 7.50 (dd, *J* = 7.9, 1.4 Hz, 2H), 7.34 (m, 3H), 7.01 (d, *J* = 8.4 Hz, 1H), 6.25 (d, *J* = 2.3 Hz, 1H), 6.11 (d, *J* = 2.3 Hz, 1H), 5.68–5.57 (m, 1H), 5.22–5.15 (m, 2H), 3.81 (s, 3H), 3.78 (s, 3H), 3.21 (d, *J* = 7.3 Hz, 2H), 3.05 (d, *J* = 3.5 Hz, 2H), 2.31 (s, 3H), 1.75 (d, *J* = 1.5 Hz, 3H), 1.71–1.62 (m, 3H); ^{13}C NMR (125 MHz, $CDCl_3$) δ 170.10, 155.48, 154.11, 151.35, (2), 136.7 (2), 128.4 (5), 128.3(5), 126.14, 111.2 (2), 104.6, 102.9, 78.23, 66.5, 60.7, 60.4 (2), 31.0, 29.7, 26.8, 20.7; IR (KBr) ν_{max} 2925, 1760, 1716, 1593, 1369, 1201, 1147, 1108, 813 cm^{-1}; HRMS (ESI+) *m*/*z* [M + H$^+$] calcd for $C_{31}H_{33}O_7$, 517.2226, found 517.2215.

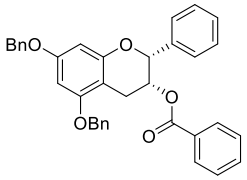

5,7-Bis(benzyloxy)-2-phenylchroman-3-yl benzoate (**13f**): A solution of **12b** (20 mg, 0.046 mmol) in dichloromethane (0.5 mL) was added to a solution of benzoic acid (11 mg, 0.09 mmol), N-(3-dimethylamino-propyl)-N′-ethylcarbodiimide hydrochloride (18 mg, 0.09 mmol) and 4-dimethylaminopyridine (12 mg, 0.09 mmol) in dichloromethane (1 mL) at 0 °C. The resulting

mixture was stirred for 6 h at rt, diluted with dichloromethane (5 mL) and washed with saturated sodium bicarbonate (2 × 4 mL) solution. The organic layer was dried over anhydrous sodium sulfate, filtered and concentrated. The residue was purified via flash chromatography (SiO_2, 1:7 EtOAc/hexanes) to give the desired ester **13f** (23 mg, 93%) as a colorless oil: ^{1}H NMR (500 MHz, $CDCl_3$) δ 7.97–7.91 (m, 2H), 7.55–7.51 (m, 3H), 7.50–7.44 (m, 2H), 7.42–7.30 (m, 13H), 6.38 (d, *J* = 2.3 Hz, 1H), 6.31 (d, *J* = 2.3 Hz, 1H), 5.72 (ddd, *J* = 4.4, 2.9, 1.4 Hz, 1H), 5.22 (s, 1H), 5.06 (d, *J* = 4.9 Hz, 2H), 5.02 (d, *J* = 2.6 Hz, 2H), 3.21–3.08 (m, 2H); ^{13}C NMR (125 MHz, $CDCl_3$) δ 165.7, 158.8, 158.0, 155.6, 137.7, 136.9, 136.8, 133.0, 129.9 (2), 129.7 (2), 128.6 (2), 128.5 (2), 128.3 (4), 128.1, 128.0, 127.9, 127.6 (2), 127.2 (2), 126.5, 100.9, 94.7, 93.9, 77.8, 70.2, 70.0, 68.6, 26.1; IR (KBr) ν_{max} 2952, 2923, 2852, 1716, 1616, 1269, 1147, 1107, 1027, 1002, 906, 811, 739 cm^{-1}; HRMS (ESI+) *m*/*z* [M + Na^+] calcd for $C_{36}H_{30}NaO_5$, 565.1991, found 565.1998.

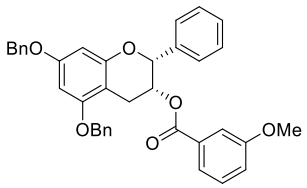

5,7-Dimethoxy-2-(3,4,5-trimethoxyphenyl)chroman-3-yl 3-Methoxybenzoate (**13g**):A solution of **12b** (12 mg, 0.03 mmol) in dichloromethane (0.5 mL) was added to a solution of 3-methoxybenzoic acid (10 mg, 0.06 mmol), *N*-(3-dimethylaminopropyl)-*N′*-ethylcarbodiimide hydrochloride (13 mg, 0.06 mmol), and 4-dimethylaminopyridine (8 mg, 0.06 mmol) in dichloromethane (1 mL) at 0 °C. The resulting mixture was stirred for 6 h at rt, diluted with dichloromethane (5 mL) and washed with saturated sodium bicarbonate (2 × 4 mL) solution. The organic layer was dried over anhydrous sodium sulfate, filtered, and concentrated. The residue was purified via flash chromatography (SiO_2, 1:3 EtOAc/hexanes) to give the desired ester product **13g** as a colorless oil (13 mg, 80.4%): ^{1}H NMR (500 MHz, $CDCl_3$) δ 7.56 (dt, *J* = 7.7, 1.2 Hz, 1H),

7.48 (dd, *J* = 2.7, 1.5 Hz, 1H), 7.30–7.26 (m, 1H) 7.05 (ddd, *J* = 8.3, 2.7, 1.0 Hz, 1H), 6.72 (s, 2H), 6.26 (d, *J* = 2.3 Hz, 1H), 6.13 (d, *J* = 2.4 Hz, 1H), 5.67 (td, *J* = 3.6, 1.3 Hz, 1H), 5.08 (s, 1H), 3.81 (s, 3H), 3.81–3.78 (m, 9H), 3.73 (s, 6H), 3.07 (d, *J* = 3.5 Hz, 2H); ^{13}C NMR (125 MHz, $CDCl_3$) δ 165.4, 159.6, 158.9, 155.5, 153.1 (2), 137.7, 133.3, 131.3, 129.3 (2), 122.0, 119.1, 114.7, 103.8 (2), 100.1, 93.4, 92.0, 78.0, 68.6, 60.8, 55.9 (2), 55.4 (3), 26.0; IR (KBr) ν_{max} 2937, 1718, 1622, 1593, 1498, 1456, 1274, 1218, 1124, 1047, 754 cm^{-1}; HRMS (ESI+) *m*/*z* [M + H^+] calcd for $C_{28}H_{31}O_9$, 511.1968, found 511.1977.

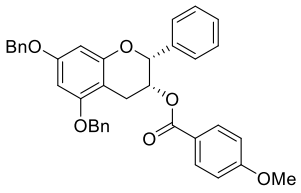

5,7-Bis(benzyloxy)-2-phenylchroman-3-yl 4-Methoxybenzoate (**13h**): A solution of **12b** (20 mg, 0.046 mmol) in dichloromethane (0.5 mL) was added to a solution of 4-methoxybenzoic acid (14 mg, 0.09 mmol), *N*-(3-dimethylaminopropyl)-*N*′-ethylcarbodiimide hydrochloride (18 mg, 0.09 mmol), and 4-dimethylaminopyridine (12 mg,0 0.09 mmol) in dichloromethane (1 mL) at 0 °C. The resulting mixture was stirred for 6 h at rt and then diluted with dichloromethane (5 mL). The organic phase was washed with saturated sodium bicarbonate solution (2 × 4 mL), dried over anhydrous sodium sulfate, filtered, and concentrated. The residue was purified via flash chromatography (SiO_2, 1:7 EtOAc/hexanes) to give the desired ester **13h** (22 mg, 85%) as a colorless oil: ^{1}H NMR (500 MHz, $CDCl_3$) δ 7.89 (d, *J* = 2.0 Hz, 1H), 7.89–7.85 (m, 1H), 7.53–7.49 (m, 2H), 7.49–7.44 (m, 2H), 7.44–7.30 (m, 11H), 6.86 (d, *J* = 2.0 Hz, 1H), 6.85 (d, *J* = 2.1 Hz, 1H), 6.37 (d, *J* = 2.3 Hz, 1H), 6.30 (d, *J* = 2.3 Hz, 1H), 5.69 (ddd, *J* = 4.5, 2.9, 1.5 Hz, 1H), 5.21 (br s, 1 H), 5.06 (d, *J* = 4.8 Hz, 2H), 5.04–5.00 (m, 2H), 3.83 (s, 3H), 3.19–3.05 (m, 2H); ^{13}C NMR (125 MHz, $CDCl_3$) δ 165.4, 163.4, 158.8, 158.0, 155.6, 137.8, 136.9, 136.8, 131.8, 128.6,

128.5 (3), 128.3 (3), 128.1 (2), 128.0, 127.9 (2), 127.6 (2), 127.2, 126.5, 122.4, 113.5 (2), 101.0, 94.7, 93.8, 77.9, 70.2, 69.9, 68.2, 55.4, 26.1; IR (KBr) ν_{max} 2925, 2852, 1716, 1147, 1095, 1026, 798, cm^{-1}; HRMS (ESI+) *m*/*z* [M + Na^+] calcd for $C_{37}H_{32}NaO_6$, 595.2097, found 595.2109.

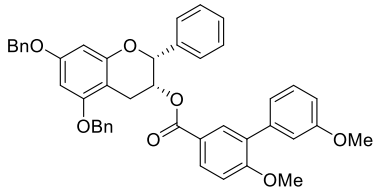

5,7-Bis(benzyloxy)-2-phenylchroman-3-yl 3′,6-Dimethoxy-[1,1′-biphenyl]-3-carboxylate (**13i**): A solution of **12b** (20 mg, 0.045 mmol) in dichloromethane (0.5 mL) was added to a solution of 3′,6-dimethoxy-[1,1′-biphenyl]-3-carboxylic acid (25 mg, 0.09 mmol), *N*-(3-dimethylaminopropyl)-*N*′-ethylcarbodiimide hydrochloride (18 mg, 0.09 mmol), and 4-dimethylaminopyridine (11 mg, 0.09 mmol) in dichloromethane (1 mL) at 0 °C. The resulting mixture was stirred for 6 h at rt and the diluted with dichloromethane (5 mL). The organic phase was washed with saturated sodium bicarbonate solution. The organic layer was dried over anhydrous sodium sulfate, filtered, and concentrated. The residue was purified via flash chromatography (SiO_2, 1:4 EtOAc/hexanes) to give the desired ester **13i** (27 mg, 90%) as a colorless oil: ^{1}H NMR (500 MHz, $CDCl_3$) δ 7.94–7.89 (m, 2H), 7.55–7.52 (m, 2H), 7.48–7.44 (m, 2H), 7.42–7.29 (m, 12H), 7.09–7.04 (m, 1H), 7.03 (dd, *J* = 2.6, 1.5 Hz, 1H), 6.96–6.89 (m, 2H), 6.36 (d, *J* = 2.3 Hz, 1H), 6.30 (d, *J* = 2.3 Hz, 1H), 5.68 (ddd, *J* = 4.3, 3.1, 1.5 Hz, 1H), 5.22 (br s, 1 H), 5.04 (d, *J* = 3.5 Hz, 2H), 5.02 (d, *J* = 2.2 Hz, 2H), 3.85 (s, 3H), 3.84 (s, 3H), 3.20–3.11 (m, 2H); ^{13}C NMR (125 MHz, $CDCl_3$) δ 165.5, 160.2, 159.2, 158.7, 157.9, 155.6, 138.8, 137.9, 136.9, 136.8, 132.5, 131.0, 130.2, 129.0, 128.6 (3), 128.5 (2), 128.3, 128.1, 128.0, 127.9 (2), 127.6 (2), 127.2, 126.5, 122.4, 122.0, 115.2 (2), 112.9, 110.5, 101.0, 94.7, 93.8, 77.8, 70.2, 69.9, 68.5, 55.8,

55.3, 26.0; IR (KBr) ν_{max} 2952, 2923, 2852, 1716, 1558, 1456, 1245, 1145, 1101, 1026, 798 cm^{-1}; HRMS (ESI+) *m*/*z* [M + H^+] calcd for $C_{44}H_{39}O_7$, 679.2696, found 679.2682.

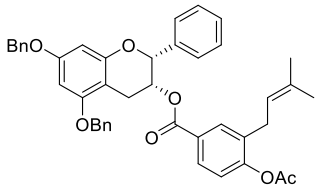

5,7-Bis(benzyloxy)-2-phenylchroman-3-yl 4-Acetoxy-3-(3-methylbut-2-en-1-yl)benzoate (**13j**): A solution of 4-acetoxy-3-(3-methylbut-2-en-1-yl)benzoic acid (34 mg, 0.138 mmol) in THF (5 mL) was treated with thionyl chloride (20 μL, 0.276 mmol). The resulting solution was heated at 70 °C for 3 h, cooled to rt, and concentrated. The residue was dissolved in dichloromethane (0.5 mL) and added to a solution of **12b** (20 mg, 0.046 mmol) and 4-dimethylaminopyridine (22 mg, 0.184 mmol) in dichloromethane (1 mL) 0 °C. The resulting mixture was stirred for 6 h at rt. The solvent was removed, and the residue was purified via flash chromatography (SiO_2, 1:7 EtOAc/hexanes) to give the ester **13j** (22.5 mg, 83.5%) as a colorless oil: ^{1}H NMR (500 MHz, $CDCl_3$) δ 7.73 (d, *J* = 2.2 Hz, 1H), 7.69 (dd, *J* = 8.4, 2.2 Hz, 1H), 7.46–7.35 (m, 5H), 7.34–7.22 (m, 10H), 6.94 (d, *J* = 8.4 Hz, 1H), 6.28 (d, *J* = 2.3 Hz, 1H), 6.21 (d, *J* = 2.3 Hz, 1H), 5.58 (ddd, *J* = 4.3, 3.1, 1.5 Hz, 1H), 5.17–5.06 (m, 2H), 5.00–4.89 (m, 4H), 3.13 (d, *J* = 7.5 Hz, 2H), 3.04 (t, *J* = 2.6 Hz, 2H), 2.23 (s, 3H), 1.67 (q, *J* = 1.3 Hz, 3H), 1.60 (d, *J* = 1.3 Hz, 3H); ^{13}C NMR (125 MHz, $CDCl_3$) δ 168.9, 165.1, 158.8, 158.0, 155.5, 152.5, 137.8, 136.9, 136.8, 134.0, 133.7, 131.9, 128.7, 128.6 (2), 128.5 (2), 128.4 (2), 128.1, 128.0, 127.9 (2), 127.8 (2), 127.6 (2), 127.2, 126.4, 122.3, 120.8, 100.8, 94.6, 93.8, 77.7, 70.2, 70.0, 68.7, 29.7, 28.5, 26.1, 20.9, 17.84; IR (KBr) ν_{max} 2921, 2852, 1760, 1716, 1616, 1373, 1257, 1201, 1149, 1114, 1027, 736 cm^{-1}; HRMS (ESI+) *m*/*z* [M + Na^+] calcd for $C_{43}H_{40}NaO_7$, 691.2672, found 691.2682.

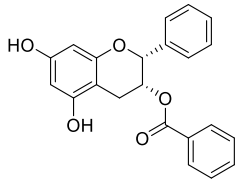

5,7-Dihydroxy-2-phenylchroman-3-yl Benzoate (**14a**): Compound **13f** (20 mg, 0.036 mmol) and palladium/carbon (10%) were suspended in tetrahydrofuran (2 mL) and stirred for 18 h under a hydrogen atmosphere. The suspension was filtered through a small pad of celite. The eluent was concentrated and the residue purified by flash chromatography (SiO_2, Acetone/dichloromethane 1:12) to give **14a** (12 mg, 90%) as a colorless oil: ^{1}H NMR (500 MHz, CD_3OD) δ 7.87–7.79 (m, 2H), 7.56–7.47 (m, 3H), 7.43–7.34 (m, 2H), 7.31–7.19 (m, 3H), 6.01 (d, *J* = 2.3 Hz, 1H), 5.98 (d, *J* = 2.3 Hz, 1H), 5.66 (ddd, *J* = 4.6, 2.4, 1.3 Hz, 1H), 5.23 (s, 1H), 3.08 (dd, *J* = 17.5, 4.6 Hz, 1H), 2.93 (ddd, *J* = 17.6, 2.5, 0.9 Hz, 1H); ^{13}C NMR (125 MHz, CD_3OD) δ 167.1, 158.0, 157.9, 157.1, 139.9, 134.2, 131.2, 130.5, 129.5 (2), 129.1 (2), 128.8 (2), 127.5 (2), 99.1, 96.7, 95.8, 78.6, 70.6, 26.7; IR (KBr) ν_{max} 3427, 2921, 2848, 1701, 1560, 1473, 1271, 1097 cm^{-1}; HRMS (ESI+) *m*/*z* [M + H$^+$] calcd for $C_{22}H_{19}O_5$, 363.1232, found 363.1241.

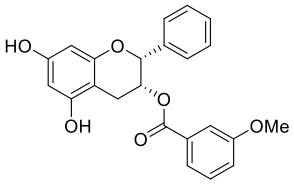

5,7-Dihydroxy-2-phenylchroman-3-yl 3-Methoxybenzoate (**14b**): Compound **13g** (20 mg, 0.034 mmol) and palladium/carbon (10%) were suspended in tetrahydrofuran (2 mL) and stirred for 18 h under a hydrogen atmosphere. The suspension was filtered through a small pad of celite. The eluent was concentrated and the residue purified by flash chromatography (SiO_2, acetone/dichloromethane 1:10) to give **14b** (20 mg, 89%) as a colorless oil: ^{1}H NMR (500 MHz,

$CDCl_3$) δ 7.50 (dt, *J* = 7.7, 1.2 Hz, 3H), 7.41 (dd, *J* = 2.7, 1.5 Hz, 1H), 7.38–7.30 (m, 2H), 7.31–7.27 (m, 2H), 7.05 (ddd, *J* = 8.3, 2.7, 1.0 Hz, 1H), 6.17 (d, *J* = 2.4 Hz, 1H), 5.99 (d, *J* = 2.4 Hz, 1H), 5.67 (ddd, *J* = 4.4, 2.9, 1.5 Hz, 1H), 5.21 (br s, 1 H), 5.18 (br s, 1 H), 5.05 (br s, 1 H), 3.79 (s, 3H), 3.22–3.00 (m, 2H); ^{13}C NMR (125 MHz, $CDCl_3$) δ 166.0, 159.6, 156.2, 155.5, 155.3, 137.8, 131.3, 129.6, 128.5, 128.4 (2), 126.6 (2), 122.3, 119.7, 114.4, 99.1, 96.5, 96.2, 77.8, 68.9, 55.6, 25.7; IR (KBr) ν_{max} 3359, 2923, 2852, 1714, 1631, 1461, 1274, 1103, 754, cm^{-1}; HRMS (ESI-) *m*/*z* [M – H^+] calcd for $C_{23}H_{19}O_6$, 391.1182, found 391.1181.

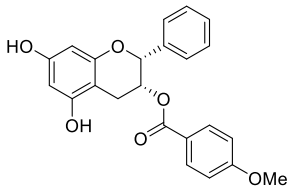

5,7-Dihydroxy-2-phenylchroman-3-yl 4-Methoxybenzoate (**14c**): Compound **13h** (16 mg, 0.027 mmol) and palladium/carbon (10%) were suspended in tetrahydrofuran (2 mL) and stirred for 18 h under a hydrogen atmosphere. The suspension was filtered through a small pad of Celite. The eluent was concentrated and the residue purified by flash chromatography (SiO_2, acetone/dichloromethane 1:10) to afford **14c** (10 mg, 91%) as a colorless oil: ^{1}H NMR (500 MHz, $(CD_3)_2CO$) δ 8.20 (d, *J* = 1.3 Hz, 1H), 8.00 (d, *J* = 1.2 Hz, 1H), 7.72–7.67 (m, 2H), 7.51–7.41 (m, 2H), 7.25–7.16 (m, 2H), 7.16–7.08 (m, 1H), 6.84–6.79 (m, 2H), 5.95 (s, 2H), 5.53 (ddd, *J* = 4.7, 2.4, 1.4 Hz, 1H), 5.21 (s, 1H), 3.71 (s, 3H), 2.99 (dd, *J* = 17.7, 4.4 Hz, 1H), 2.87 (ddd, *J* = 17.4, 2.4, 0.9 Hz, 1H); ^{13}C NMR (125 MHz, $(CD_3)_2CO$) δ 165.7, 164.6, 158.0, 157.6, 156.9, 139.9, 132.3 (2), 129.0 (2), 128.6 (2), 127.5, 123.4, 114.7 (2), 98.9, 96.7, 95.9, 78.2, 69.6, 56.0, 26.6; IR (KBr) ν_{max} 3369, 2925, 2852, 1714, 1604, 1512, 1456, 1257, 1168, 1101, 1029, 667 cm^{-1}; HRMS (ESI-) *m*/*z* [M – H^+] calcd for $C_{23}H_{19}O_6$, 391.1182, found 391.1175.

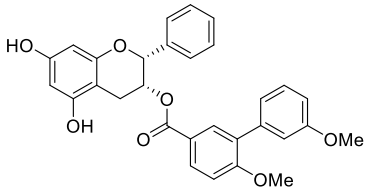

5,7-Dihydroxy-2-phenylchroman-3-yl 3′,6-Dimethoxy-[1,1′-biphenyl]-3-carboxylate (**14d**): Compound **13i** (20 mg, 0.029 mmol) and palladium/carbon (10%) were suspended in tetrahydrofuran (2 mL) and stirred for 18 h under hydrogen atmosphere. The suspension was filtered through a small pad of Celite. The eluent was concentrated and the residue purified by flash chromatography (SiO_2, acetone/dichloromethane 1:9) to give **14d** (13 mg, 89%) as a colorless oil: (500 MHz, $CDCl_3$) ^{1}H NMR δ 7.83–7.78 (m, 2H), 7.45–7.39 (m, 2H), 7.31–7.22 (m, 3H), 7.23–7.20 (m, 1H), 6.98 (ddd, *J* = 7.6, 1.6, 1.0 Hz, 1H), 6.93 (dd, *J* = 2.6, 1.6 Hz, 1H), 6.88–6.80 (m, 2H), 6.08 (d, *J* = 2.2 Hz, 1H), 5.91 (d, *J* = 2.4 Hz, 1H), 5.57 (tt, *J* = 3.3, 1.5 Hz, 1H), 5.13 (s, 1H), 5.01 (s, 1H), 4.91 (s, 1H), 3.76 (d, *J* = 1.4 Hz, 6H), 3.08–2.95 (m, 2H); ^{13}C NMR (125 MHz, $CDCl_3$) δ 165.8, 160.5, 159.4, 156.2, 155.5, 155.3, 138.9, 137.9, 132.7, 131.2, 130.5, 129.2, 128.5 (2), 128.3 (2), 126.7, 122.5, 122.2, 115.5, 113.1, 110.7, 99.2, 96.6, 96.2, 77.9, 68.6, 56.0, 55.5, 25.7; IR (KBr) ν_{max} 3374, 2952, 2852, 1714, 1558, 1456, 1271, 1101, 1026 cm^{-1}; HRMS (ESI+) *m*/*z* [M + H$^+$] calcd for $C_{30}H_{27}O_7$, 499.1757, found 499.1744.

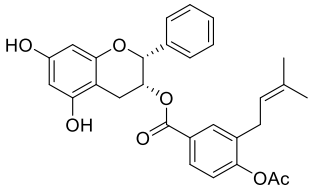

5,7-Dihydroxy-2-phenylchroman-3-yl 4-Acetoxy-3-(3-methylbut-2-en-1-yl)benzoate (**14e**): A solution of palladium acetate (2 mg, 0.008 mmol), trimethylamine (13 μL, 0.09 mmol), and triethylsilane (64 μL, 0.405) in dichloromethane (0.8 mL) was stirred for 15 min before the

addition of **13j** (30 mg, 0.045 mmol) in dichloromethane (0.4 mL). The resulting mixture was stirred for 15 h, quenched with saturated ammonium chloride (2 mL), and extracted with diethyl ether (3 × 4 mL). The combined organic layers were washed with saturated sodium chloride solution and dried over anhydrous Na_2SO_4. The solvent was removed and residue purified via flash chromatography (SiO_2, 5:95 MeOH/DCM) to give **14e** (4 mg, 18.9%) as a colorless oil: ^{1}H NMR (500 MHz, $CDCl_3$) δ 7.71–7.63 (m, 2H), 7.51–7.45 (m, 2H), 7.33–7.25(m, 3H), 6.69 (d, *J* = 8.2 Hz, 1H), 6.42 (d, *J* = 2.2 Hz, 1H), 6.22 (d, *J* = 2.2 Hz, 1H), 5.68–5.56 (m, 2H), 5.26 (m, 2H), 5.13 (d, *J* = 1.2 Hz, 1H), 3.32 (d, *J* = 7.2 Hz, 2H), 3.06 (t, *J* = 3.2 Hz, 2H), 2.30 (s, 3H), 1.81–1.72 (m, 6H); ^{13}C NMR (125 MHz, $CDCl_3$) δ 170.0, 165.8, 158.9, 156.0, 154.9, 150.0, 137.7, 135.9, 132.2, 130.0 (2), 128.5 (2), 128.3 (2), 126.9, 126.6, 122.2, 121.1, 115.7, 104.7, 103.0, 101.9, 78.0, 67.9, 29.6, 26.1 (2), 21.4, 18.1; IR (KBr) ν_{max} 3432, 2922, 1701, 1562, 1471, 1101, 1271, 1093 cm^{-1}; HRMS (ESI-) *m*/*z* [M – H$^+$] calcd for $C_{29}H_{27}O_7$, 487.1757, found 487.1755.

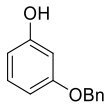

3-(Benzyloxy)phenol (**15**): A solution of resorcinol (4g, 36.3 mmol), potassium carbonate (12.5 g, 90.7 mmol), and benzyl bromide (4.75 mL, 40 mmol) in acetonitrile (130 mL) heated as reflux for 12 h. Solvent was removed, water (100 mL) was added, and the mixture was extracted with ethyl acetate (3 × 100 mL). The combined organic layers were washed with saturated sodium chloride solution (200 mL), dried over anhydrous Na_2SO_4, filtered, and concentrated. The residue was purified by flash chromatography (SiO_2, 1:6 EtOAc/Hexaes) to afford **17** as colorless oil (3.5 g, 21.7%): ^{1}H NMR (500 MHz, $CDCl_3$) δ 7.48 −7.31 (m, 5H), 7.15 (t, *J* = 8.2 Hz, 1H), 6.58 (ddd, *J* = 8.3, 2.4, 0.9 Hz, 1H), 6.50 (t, *J* = 2.3 Hz, 1H), 6.45 (ddd, *J* = 8.0, 2.4, 0.9 Hz, 1H), 5.05 (s, 2H); 4.71 (s, 1H); ^{13}C NMR (125 MHz, $CDCl_3$) δ 160.37, 156.83, 137.06, 130.39, 128.81, 128.20 (2),

127.69 (2), 108.21, 107.56, 102.63, 70.22; IR (KBr) ν_{max} 3309, 2925, 2869, 1595, 1488, 1456, 1380, 1284, 1215, 1147, 1026, 837, 763, 736 cm^{-1}; HRMS (ESI+) *m*/*z* [M + H^+] calcd for $C_{13}H_{13}O_2$, 201.0916; found 201.0916.

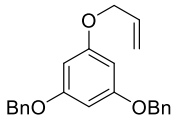

(((5-(Allyloxy)-1,3-phenylene)bis(oxy))bis(methylene))dibenzene (16a): A solution of **1b** (1.2 g, 3.9 mmol), potassium carbonate (2.17g, 15.7 mmol), and allyl bromide (0.44 mL, 5.1 mmol) in dimethylformamide (40 mL) was heated at 90 °C for 12 h. The reaction mixture was cooled to rt, diluted with ethyl acetate (200 mL), and washed with water (3 × 100 mL) and then saturated sodium chloride solution (100 mL). The organic phase was dried over anhydrous sodium sulfate, filtered, and concentrated. The residue was purified by flash chromatography (SiO_2 1:9 EtOAc/hexanes) to give **16a** (1.62 g, 89%) as a light yellow oil: ^{1}H NMR (400 MHz, $CDCl_3$) δ 7.51–7.29 (m, 10H), 6.27 (t, *J* = 2.2 Hz, 1H), 6.21 (d, *J* = 2.1 Hz, 2H), 6.04 (ddt, *J* = 17.2, 10.6, 5.4 Hz, 1H), 5.40 (dq, *J* = 17.3, 1.6 Hz, 1H), 5.29 (dq, *J* = 10.5, 1.4 Hz, 1H), 5.01 (s, 4H), 4.49 (dt, *J* = 5.4, 1.5 Hz, 2 H); ^{13}C NMR (125 MHz, $CDCl_3$) δ 160.8 (2), 160.6, 137.0 (2), 133.3, 128.8 (4), 128.2 (2), 127.8 (4), 118.0, 95.0, 94.9 (2), 70.3 (2), 69.1; IR (KBr) ν_{max} 3390, 2975, 2908, 2864, 1622, 1591, 1506, 1434, 1213, 1159, 1110, 1066, 1043, 933, 810, 703 cm^{-1}; HRMS (ESI+) *m*/*z* [M + H^+] calcd for $C_{23}H_{23}O_3$, 347.1647, found 347.1647.

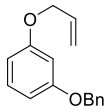

1-(Allyloxy)-3-(benzyloxy)benzene (**16b**): A solution of **15** (2.45g, 12.3 mmol), potassium carbonate (6.62g, 49.2 mmol), allyl bromide (1.34 mL, 16 mmol), and dimethylformamide (60

mL) was stirred for 12 h at 90 °C. The reaction mixture was cooled to rt, diluted with EtOAc (200 mL), and washed with water (3 × 100 mL times) and saturated sodium chloride solution (100 mL). The organic phase was dried over anhydrous sodium sulfate, filtered, and concentrated. The residue was purified by flash chromatography (SiO_2, 1:9 EtOAc/hexanes) to give **16b** (2.8g, 95.2%) as light yellow oil: ^{1}H NMR (500 MHz, $CDCl_3$) δ 7.47–7.43 (m, 2H), 7.42–7.38 (m, 2H), 7.37–7.32 (m, 1H), 7.19 (t, *J* = 8.1 Hz, 1H), 6.63–6.57 (m, 2H), 6.55 (ddd, *J* = 8.2, 2.3, 0.9 Hz, 1H), 6.06 (ddt, *J* = 17.2, 10.6, 5.3 Hz, 1H), 5.42 (dq, *J* = 17.2, 1.6 Hz, 1H), 5.29 (dq, *J* = 10.5, 1.4 Hz, 1H), 5.06 (s, 2H), 4.53 (dt, *J* = 5.3, 1.5 Hz, 2H); ^{13}C NMR (125 MHz, $CDCl_3$) δ 160.2, 160.0, 137.3, 133.4, 130.1, 128.8 (2), 128.2 (2), 127.7, 117.9, 107.5, 107.4, 102.3, 70.2, 69.0; IR (KBr) ν_{max} 3031, 2866, 1591, 1490, 1454, 1379, 1288, 1261, 1178, 1149, 1039, 1027, 927, 835, 734, 696 cm^{-1}; HRMS (ESI+) *m*/*z* [M + Na$^+$] calcd for $C_{16}H_{16}NaO_2$, 263.1048, found 263.1053.

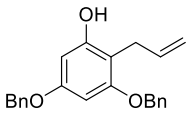

2-Allyl-3,5-bis(benzyloxy)phenol (17a): Compound **16a** (1.62 g, 4.66 mmol) was dissolved in *N*,*N*-diethylaniline (23 mL) and heated at 210 °C for 12 h. The reaction mixture was cooled to rt, diluted with ethyl acetate (200 mL), and washed with 1 N HCl (3 × 100 mL) and then saturated sodium chloride solution. The organic layer was dried over anhydrous sodium sulfate, filtered, and concentrated. The residue was purified by flash chromatography (SiO_2, 1:8 EtOAc/hexanes) to afford **17a** (1.215g, 75%) as a pale yellow oil: ^{1}H NMR (400 MHz, $CDCl_3$) δ 7.47–7.32 (m, 10H), 6.27 (d, *J* = 2.3 Hz, 1H), 6.19 (d, *J* = 2.3 Hz, 1H), 5.98 (ddt, *J* = 16.3, 10.0, 6.1 Hz, 1H), 5.18 (q, *J* = 1.8 Hz, 1H), 5.13 (dq, *J* = 5.0, 1.7 Hz, 1H), 5.07 (s, 1H), 5.02 (s, 2H), 5.01 (s, 2H), 3.46 (dt, *J* = 6.2, 1.7 Hz, 2H); ^{13}C NMR (125 MHz, $CDCl_3$) δ 161.9, 160.5, 158.3, 137.0 (2), 136.9, 128.8 (4), 128.2 (2), 127.8 (4), 116.0, 106.3, 95.0, 92.9, 70.3, 69.1, 26.3; IR (KBr) ν_{max} 2925, 2867, 1596,

1456, 1375, 1213, 1153, 1058, 927, 817, 736 cm^{-1}; HRMS (ESI-) *m*/*z* [M – H^+] calcd for $C_{23}H_{21}O_3$, 345.1491, found 345.1503.

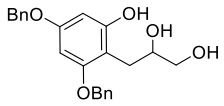

3-(2,4-Bis(benzyloxy)-6-hydroxyphenyl)propane-1,2-diol (18a): A solution of **17a** (1.062g, 3.1 mmol), osmium tetraoxide (0.03 mmol, 4% aqueous solution), and *N*-methylmorphline *N*-oxide (575 mg, 4.9 mmol) in tetrahydrofuran-water (13 mL-9 mL) was stirred for 12 h before quenching with 10% aqueous sodium metabisulfite. The aqueous layer was extracted with ethyl acetate (3 × 50 mL), and the combined organic layers were washed with saturated sodium chloride solution (100 mL). The solvent was removed and the residue purified by flash chromatography (SiO_2, 2:5 EtOAc/hexanes) to afford **18a** (744 mg, 64%) as a colorless oil: ^{1}H NMR (500 MHz, $(CD_3)_2CO$) δ 8.77 (s, 1H), 7.50 (dd, *J* = 8.1, 1.4 Hz, 2H), 7.48–7.44 (m, 2H), 7.39 (td, *J* = 7.9, 7.5, 1.5 Hz, 4H), 7.36–7.30 (m, 2H), 6.32 (d, *J* = 2.3 Hz, 1H), 6.20 (d, *J* = 2.3 Hz, 1H), 5.10 (s, 2H), 5.05 (s, 2H), 4.65 (d, *J* = 5.2 Hz, 1H), 3.91 (br s, 1 H), 3.81 (d, *J* = 6.1 Hz, 1H), 3.53 (br s, 1 H), 3.41 (dd, *J* = 11.3, 6.4 Hz, 1H), 2.96 (dd, *J* = 14.1, 5.0 Hz, 1H), 2.79 (dd, *J* = 14.1, 6.8 Hz, 1H); ^{13}C NMR (125 MHz, $(CD_3)_2CO$) δ 159.9, 159.1 (2), 138.7 (2), 129.4 (2), 129.3 (2), 128.9, 128.7, 128.6, 128.5, 128.2, 107.6, 96.8, 96.8, 93.6, 74.1, 70.9, 70.5, 66.6, 27.8; IR (KBr) ν_{max} 3298, 1616, 1598, 1452, 1436, 1375, 1217, 1147, 1105, 1045, 1027, 908, 813, 736, 696, 649 cm^{-1}; HRMS (ESI+) *m*/*z* [M + H^+] calcd for $C_{23}H_{25}O_5$, 381.1702, found 381.1709.

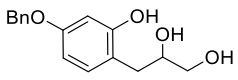

3-(4-(Benzyloxy)-2-hydroxyphenyl)propane-1,2-diol (**18b**): Compound **16b** (2.7g, 11.23 mmol) was dissolved in *N*,*N*-diethylaniline (70 mL) and heated at 210 °C for 12 h. The reaction mixture

was cooled to rt, diluted with ethyl acetate (200 mL), and washed with 1 N HCl (3 × 100 mL) and then with saturated sodium chloride solution. The organic layer was dried over anhydrous Na_2SO_4, filtered and concentrated. The residue was purified by flash chromatography (SiO_2, 1:8 EtOAc/hexanes) to give a mixture of **17b** and **17c.** A solution of the mixture of **17b** and **17c** (2.02g, 8.41 mmol), osmium tetraoxide (0.168 mmol, 4% aqueous solution), and *N*-methylmorphline *N*-oxide (1.67g, 14.29 mmol) in tetrahydrofuran–water (18 mL–12 mL) was stirred for 12 h before quenching with 10% aqueous sodium metabisulfite. The aqueous phase was extracted with ethyl acetate (3 × 200 mL), the combined organic layers were washed with saturated sodium chloride solution, and solvent was removed. The residue was purified by flash chromatography (1:5 acetone–DCM) to afford **18b** (1.24g) as a colorless oil: ^{1}H NMR (500 MHz, $(CD_3)_2CO$) δ 7.49–7.43 (m, 2H), 7.427.35 (m, 2H), 7.34–7.27 (m, 1H), 6.99 (d, *J* = 8.3 Hz, 1H), 6.49 (d, *J* = 2.6 Hz, 1H), 6.45 (dd, *J* = 8.2, 2.5 Hz, 1H), 5.06 (s, 2H), 3.90 (tt, *J* = 6.9, 4.4 Hz, 1H), 3.54–3.49 (m, 1H), 3.47–3.40 (m, 1H), 2.83–2.75 (m, 1H), 2.74–2.66 (m, 1H); ^{13}C NMR (125 MHz, $(CD_3)_2CO$) δ 159.6, 157.7, 138.6, 132.6, 129.2, 129.1, 128.4 (2), 128.2, 118.8, 106.7, 103.8, 74.2, 70.2, 66.2, 35.3; IR (KBr) ν_{max} 3311, 2931, 1618, 1585, 1506, 1454, 1279, 1286, 1166, 1108, 1024, 842, 736, 696 cm^{-1}; HRMS (ESI-) *m*/*z* [M – H$^+$] calcd for $C_{16}H_{17}O_4$, 273.1127, found 273.1129.

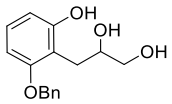

3-(2-(Benzyloxy)-6-hydroxyphenyl)propane-1,2-diol (18c): A solution of the mixture of **17b** and **17c** (2.02g, 8.41 mmol), osmium tetraoxide (0.168 mmol, 4% aqueous solution), and *N*-methylmorphline *N*-oxide (1.67g, 14.29 mmol) in tetrahydrofuran–water (18 mL–12 mL) was stirred 12 h before quenching with 10% aqueous sodium metabisulfite. The aqueous phase was extracted with ethyl acetate (3 × 200 mL), and the combined organic layers were washed with

saturated sodium chloride solution. The solvent was removed and the residue purified by flash chromatography (1:5 acetone–DCM) to afford **18c** (0.8 g) as a colorless oil which was used as is in the next step: ^{1}H NMR (500 MHz, $(CD_3)_2CO$) δ 8.70 (s, 1H), 7.53–7.48 (m, 2H), 7.42–7.35 (m, 2H), 7.35–7.29 (m, 1H), 7.02 (t, *J* = 8.2 Hz, 1H), 6.59 (dd, *J* = 8.3, 1.0 Hz, 1H), 6.52 (dd, *J* = 8.1, 1.0 Hz, 1H), 5.10 (s, 2H), 4.86–4.48 (m, 1H), 3.97 (tdd, *J* = 6.7, 5.3, 4.0 Hz, 1H), 3.83 (br s, 1 H), 3.55 (dd, *J* = 11.2, 4.0 Hz, 1H), 3.43 (dd, *J* = 11.2, 6.6 Hz, 1H), 3.04 (dd, *J* = 13.8, 5.3 Hz, 1H), 2.89 (dd, *J* = 13.8, 6.7 Hz, 1H); ^{13}C NMR (100 MHz, $CDCl_3$) δ 157.47, 156.58, 136.82, 128.69 (2), 128.10 (2), 127.40 (2), 112.99, 110.56, 104.13, 72.83, 70.54, 65.24, 26.59; IR (KBr) ν_{max} 3334, 2929, 1618, 1583, 1506, 1454, 1279, 1286, 1217, 1166, 1045, 1025, 849 cm^{-1}; HRMS (ESI-) *m*/*z* [M – H^{+}] calcd for $C_{16}H_{17}O_4$, 273.1127, found 273.1127.

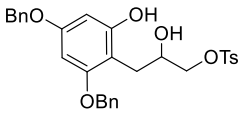

3-(2,4-Bis(benzyloxy)-6-hydroxyphenyl)-2-hydroxypropyl 4-Methylbenzenesulfonate (19a): Pyridine (0.46 mL, 5.8 mmol) was added to a solution of **18a** (500 mg, 1.37 mmol) and *p*-toluenesulfonyl chloride (282 mg, 1.5 mmol) in dichloromethane (14 mL) at 0 °C. The resulting mixture was stirred for 12 h at rt before quenching with 2 N HCl (20 mL). The aqueous layer was extracted with dichloromethane (2 × 30 mL). The combined organic layers were washed with saturated sodium chloride solution, dried over anhydrous Na_2SO_4, filtered, and concentrated. The residue was purified by flash chromatography (SiO_2, 2:5 EtOAc/hexanes) to give **19a** (427 mg, 58%) as a pale yellow oil: ^{1}H NMR (500 MHz, $(CD_3)_2CO$) δ 8.51 (s, 1H), 7.72–7.67 (m, 2H), 7.50–7.44 (m, 4H), 7.43–7.37 (m, 6H), 7.37–7.30 (m, 2H), 6.31 (d, *J* = 2.4 Hz, 1H), 6.19 (d, *J* = 2.3 Hz, 1H), 5.07 (s, 2H), 5.04 (s, 2H), 4.84 (d, *J* = 4.5 Hz, 1H), 4.11–3.94 (m, 2H), 3.95–3.70 (m, 1H), 2.42 (s, 3H); ^{13}C NMR (125 MHz, $(CD_3)_2CO$) δ 160.0, 159.1, 158.0, 145.7, 138.4 (2), 130.8

(2), 129.4 (2), 129.3 (2), 128.6 (5), 128.5 (2), 128.1 (2), 106.1, 96.2, 93.3, 75.2, 70.6, 70.4, 70.2, 28.0, 21.5; IR (KBr) ν_{max} 3334, 2925, 1625, 1506, 1361, 1174, 1108, 1095, 975 cm^{-1}; HRMS (ESI+) *m*/*z* [M + H^+] calcd for $C_{30}H_{31}O_7S$, 535.1790, found 535.1773.

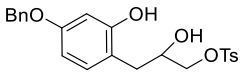

3-**(4-(Benzyloxy)-2-hydroxyphenyl)-2-hydroxypropyl 4-Methylbenzenesulfonate** (**19b**): Pyridine (0.46 mL, 5.8 mmol) was added to a solution of **18b** (500 mg, 1.37 mmol) and *p*-toluenesulfonyl chloride (282 mg, 1.5 mmol) in dichloromethane (14 mL) at 0 °C. The resulting mixture was stirred for 12 h at rt before quenching with 2 N HCl (20 mL). The aqueous layer was extracted with dichloromethane (2 × 30 mL). The combined organic layers were washed with saturated sodium chloride solution (40 mL), dried over anhydrous sodium sulfate, filtered, and concentrated. The residue was purified by flash chromatography (SiO_2, 2:5 EtOAc/hexanes) to give **19b** (0.97g, 58.6%) as a pale yellow oil: ^{1}H NMR (500 MHz, $(CD_3)_2CO$) δ 8.50 (br s, 1 H), 7.82–7.74 (m, 2H), 7.50–7.43 (m, 4H), 7.43–7.2 (m, 3H), 6.92 (d, *J* = 8.2 Hz, 1H), 6.48 (d, *J* = 2.5 Hz, 1H), 6.42 (dd, *J* = 8.3, 2.5 Hz, 1H), 5.03 (s, 2H), 4.17–3.97 (m, 3H), 3.89 (dd, *J* = 9.9, 6.7 Hz, 1H), 2.76–2.67 (m, 2H), 2.45 (s, 3H); ^{13}C NMR (125 MHz, $(CD_3)_2CO$) δ 159.8 (2), 145.8, 138.6, 134.1, 132.8, 130.9, 130.8, 129.3 (2), 128.8, 128.7, 128.6 (2), 117.56, 128.4, 106.8, 103.5, 74.3, 70.4, 70.3, 34.9, 21.5; IR (KBr) ν_{max} 3348, 2928, 1627, 1361, 1174, 1108, 1096 cm^{-1}; HRMS (ESI+) *m*/*z* [M + H^+] calcd for $C_{23}H_{25}O_6S$, 429.1372, found 429.1383.

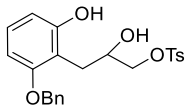

3-(2-(Benzyloxy)-6-hydroxyphenyl)-2-hydroxypropyl 4-Methylbenzenesulfonate (19c): Pyridine (0.47 mL, 15.4 mmol) was added to a solution of **28c** (410 mg, 1.5 mmol) and *p*-toluenesulfonyl chloride (310 mg, 1.7 mmol) in dichloromethane (14 mL) at 0 °C. The resulting mixture was stirred for 12 h at rt before quenching with 2 N HCl (20 mL). The aqueous layer was extracted with dichloromethane (2 × 30 mL). The combined organic layers were washed with saturated sodium chloride solution (40 mL), dried over anhydrous Na_2SO_4, filtered, and concentrated. The residue was purified by flash chromatography (SiO_2, 2:5 EtOAc/hexanes) to give **19c** (367 mg, 57%) as a pale yellow oil and was used as is in the next step.

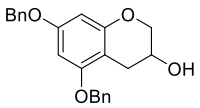

5,7-Bis(benzyloxy)chroman-3-ol (20a): Potassium carbonate (115 mg, 0.83 mmol) was added to a solution of **19a** (277 mg, 0.58 mmol) in methanol (2.6 mL), and the resulting mixture was stirred for 6 h at rt. Methanol was removed, and the residue was partitioned between water (5 mL) and dichloromethane (5 mL) The aqueous layer was extracted with dichloromethane (2 × 5 mL). The combined organic layers were washed with saturated sodium chloride solution, dried over anhydrous Na_2SO_4, filtered, and concentrated. The residue was purified by flash chromatography (SiO_2, 1:5 EtOAc/hexanes) to give **20a** (86 mg, 46%) as a colorless oil: ^{1}H NMR (500 MHz, $CDCl_3$) δ 7.45–7.37 (m, 8H), 7.34 (ddt, *J* = 7.4, 4.0, 1.7 Hz, 2H), 6.26 (d, *J* = 2.3 Hz, 1H), 6.18 (d, *J* = 2.3 Hz, 1H), 5.02 (s, 2H), 5.01 (s, 2H), 4.33–4.15 (m, 1H), 4.15–3.97 (m, 2H), 2.93 (dd, *J* = 17.0, 5.0 Hz, 1H), 2.75 (dd, *J* = 17.0, 4.5 Hz, 1H), 1.89 (br s, 1 H); ^{13}C NMR (125 MHz, $CDCl_3$) δ 158.9, 158.4, 155.2, 137.1, 137.1, 128.8 (2), 128.7, 128.7, 128.2, 128.1, 127.8, 127.7, 127.4 (2), 101.6, 94.8, 94.0, 70.3, 70.1, 69.8, 63.2, 28.4; IR (KBr) ν_{max} 3392, 2925, 2871, 1616, 1591, 1496,

1456, 1145, 1122, 1062, 1027, 811, 696 cm^{-1}; HRMS (ESI+) *m*/*z* [M + H^+] calcd for $C_{23}H_{23}O_4$, 363.1596, found 363.1596.

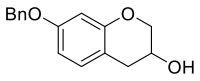

7-(Benzyloxy)chroman-3-ol (**20b**): Potassium carbonate (440 mg, 3.18 mmol) was added to a solution of **19b** (830 mg, 1.98 mmol) in methanol (5 mL), and the resulting solution was stirred for 6 h at rt. Methanol was removed, and the residue was partitioned between water (10 mL) and dichloromethane (10 mL). The aqueous layer was extracted with dichloromethane (2 × 10 mL). The combined organic layers were washed with saturated sodium chloride solution, dried over anhydrous sodium sulfate, filtered, and concentrated. The residue was purified by flash chromatography (SiO_2, 1:5 EtOAc/hexanes) to give the desired product **20b** (200 mg, 40%) as a colorless oil: ^{1}H NMR (500 MHz, $CDCl_3$) δ 7.51–7.30 (m, 5H), 7.04 (d, *J* = 8.0 Hz, 1H), 6.52–6.45 (m, 2H), 5.03 (s, 2H), 4.98–4.80 (m, 1H), 3.84 (dd, *J* = 12.0, 3.3 Hz, 1H), 3.74 (dd, *J* = 12.0, 6.4 Hz, 1H), 3.19 (dd, *J* = 15.1, 9.4 Hz, 1H), 2.94 (ddd, *J* = 15.1, 7.2, 1.2 Hz, 1H), 2.07 (br s, 1 H); ^{13}C NMR (125 MHz, $CDCl_3$) δ 161.4, 159.7, 137.2, 128.8 (2), 128.1 (2), 127.6, 125.2, 118.9, 107.3, 97.5, 84.3, 70.5, 65.2, 30.8; IR (KBr) ν_{max} 3382, 2927, 1614, 1494, 1145, 1029 cm^{-1}; HRMS (ESI+) *m*/*z* [M + Na^+] calcd for $C_{16}H_{16}NaO_3$, 279.0097, found 279.1002.

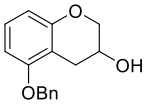

5-(Benzyloxy)chroman-3-ol (20c): Potassium carbonate (262 mg, 0.61 mmol) was added to a solution of **19c** (135 mg, 0.98 mmol) in methanol (2 mL), and the resulting solution was stirred for 6 h at rt. Methanol was removed, the residue was partitioned between water (5 mL) and

dichloromethane (5 mL) The aqueous layer was extracted with dichloromethane (2 × 5 mL). The combined organic layers were washed with saturated sodium chloride solution, dried over anhydrous Na_2SO_4, filtered, and concentrated. The residue was purified by flash chromatography (SiO_2, 1:5 EtOAc/hexanes) to give the desired product **20c** (70 mg, 45%) as a colorless oil: ^{1}H NMR (500 MHz, CD_3OD) δ 7.49–7.43 (m, 2H), 7.37 (ddd, *J* = 7.7, 6.4, 1.2 Hz, 2H), 7.30 (td, *J* = 7.1, 1.4 Hz, 1H), 7.01 (t, *J* = 8.2 Hz, 1H), 6.55 (dd, *J* = 8.3, 1.1 Hz, 1H), 6.43 (dd, *J* = 8.1, 1.1 Hz, 1H), 5.07 (s, 2H), 4.15 (qd, *J* = 5.8, 2.6 Hz, 1H), 4.08 (ddd, *J* = 10.8, 2.7, 1.5 Hz, 1H), 3.88 (ddd, *J* = 10.7, 6.4, 1.5 Hz, 1H), 2.99 (ddd, *J* = 17.3, 5.3, 1.6 Hz, 1H), 2.66 (dd, *J* = 17.1, 5.9 Hz, 1H); ^{13}C NMR (125 MHz, CD_3OD) δ 158.8, 156.3, 139.0, 129.5, 128.8, 128.3, 128.1 (2), 110.5, 110.3, 104.8 (2), 71.0, 70.3, 63.7, 29.3; IR (KBr) ν_{max} 3388, 2928, 1616, 1591, 1496, 1146, 1061, 1027 cm^{-1}; HRMS (ESI+) *m*/*z* [M + Na^+] calcd for $C_{16}H_{16}NaO_3$, 279.0997, found 279.0993.

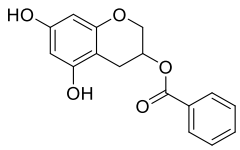

5,7-Dihydroxychroman-3-yl Benzoate (21a): A solution of **20a** (14 mg, 0.04 mmol) in dichloromethane (0.5 mL) was added to a stirred solution of benzoic acid (10 mg, 0.08 mmol), *N*,*N*′-dicyclohexylcarbodiimide (17 mg, 0.08 mmol), and 4-dimethylaminopyridine (4.8 mg, 0.04 mmol) in dichloromethane (1 mL) at 0 °C. The resulting solution was stirred for 6 h at rt and then filtered. The eluent was diluted with dichloromethane (5 mL) and washed with 0.5 N HCl (2 × 4 mL) and then saturated sodium bicarbonate (2 × 4 mL) solution. The combined organic layers were washed with saturated sodium chloride solution (4 mL), dried over anhydrous sodium sulfate, filtered, and concentrated. The residue was purified by flash chromatography (SiO_2, 1:4 EtOAc/hexanes) to afford 5,7-bis(benzyloxy)chroman-3-yl benzoate (16.2 mg, 90%) as a colorless

oil, which was used as is for hydrogenolysis: ^{1}H NMR (500 MHz, $CDCl_3$) δ 8.10–7.99 (m, 2H), 7.65–7.48 (m, 1H), 7.47–7.29 (m, 11H), 6.28 (d, *J* = 2.3 Hz, 1H), 6.22 (d, *J* = 2.3 Hz, 1H), 5.54 (d, *J* = 6.6 Hz, 1H), 4.32 (ddd, *J* = 11.4, 4.9, 1.8 Hz, 1H), 4.26–4.17 (m, 1H), 3.10 (ddd, *J* = 17.5, 5.4, 1.2 Hz, 1H), 3.00–2.90 (m, 1H); ^{13}C NMR (125 MHz, $CDCl_3$) δ 166.2, 158.9, 158.1, 155.4,137.1 (2), 133.3, 130.0, 128.8, 128.8 (2), 128.5 (3), 128.2, 128.1, 127.8 (3), 127.4 (2), 101.4, 94.8, 93.9, 70.4, 70.2, 67.0, 66.1, 25.3. 5,7-Bis(benzyloxy)chroman-3-yl benzoate (16.2 mg, 0.034 mmol) and palladium/carbon (10%) were suspended in tetrahydrofuran (2 mL) and stirred for 18 h under a hydrogen atmosphere. The suspension was filtered through a small pad of celite. The eluent was concentrated and the residue purified by flash chromatography (SiO_2, 1:1 EtOAc/hexanes) to give **21a** (8 mg, 81.6%) as a colorless oil: ^{1}H NMR (500 MHz, $(CD_3)_2CO$) δ 8.32 (s, 1H), 8.05 (s, 1H), 8.02–7.91 (m, 2H), 7.71–7.59 (m, 1H), 7.57 - 7.44 (m, 2H), 6.05 (d, *J* = 2.3 Hz, 1H), 5.91 (d, *J* = 2.3 Hz, 1H), 5.60–5.41 (m, 1H), 4.34–4.31 (m, 1H), 4.23–4.20 (m, 1H), 3.02 (ddd, *J* = 17.1, 5.3, 1.2 Hz, 1H), 2.90–2.83 (m, 1H); ^{13}C NMR (125 MHz, $(CD_3)_2CO$) δ 166.4, 157.9, 157.5, 156.5, 134.1, 131.3 (2), 130.3 (2), 129.5, 99.2, 96.5, 95.8, 67.4, 67.3, 25.6; IR (KBr) ν_{max} 3385, 2933, 2840, 1716, 1622, 1593, 1496, 1452, 1272, 1201, 1145, 1056, 813, 711 cm^{-1}; HRMS (ESI+) *m*/*z* [M + H^+] calcd for $C_{16}H_{14}O_5$, 287.0919, found 287.0912.

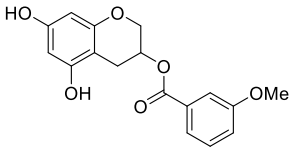

5,7-Dihydroxychroman-3-yl 3-Methoxybenzoate (21b): A solution of **20a** (14 mg, 0.04 mmol) in dichloromethane (0.5 mL) was added to a stirred solution of 3-methoxybenzoic acid (12 mg, 0.08 mmol), *N*,*N*′-dicyclohexylcarbodiimide (17 mg, 0.08 mmol), and 4-dimethylaminopyridine (4.8 mg, 0.04 mmol) in dichloromethane (1 mL) at 0 °C. The resulting solution was stirred for 6 h

at rt and then filtered. The eluent was diluted with dichloromethane (5 mL) and washed with 0.5 N HCl (2 × 4 mL) and then with saturated sodium bicarbonate (2 × 4 mL) solution. The combined organic layers were washed with saturated sodium chloride solution (4 mL), dried over anhydrous sodium sulfate, filtered, and concentrated. The residue was purified by flash chromatography (SiO_2, 1:4 EtOAc/hexanes) to afford 5,7-bis(benzyloxy)chroman-3-yl 3-methoxybenzoate (18 mg, 89%) as a colorless oil, which was used as is for hydrogenolysis: ^{1}H NMR (500 MHz, $CDCl_3$) δ 7.58 (dt, *J* = 7.7, 1.2 Hz, 1H), 7.51 (dd, *J* = 2.7, 1.5 Hz, 1H), 7.43–7.25 (m, 11H), 7.06 (ddd, *J* = 8.2, 2.7, 1.0 Hz, 1H), 6.23 (d, *J* = 2.3 Hz, 1H), 6.17 (d, *J* = 2.2 Hz, 1H), 5.48 (ddq, *J* = 6.6, 5.1, 2.2 Hz, 1H), 4.98 (s, 4H), 4.30–4.22 (m, 1H), 4.21–4.14 (m, 1H), 3.80 (s, 3H), 3.11–3.01 (m, 1H), 2.94–2.84 (m, 1H); ^{13}C NMR (125 MHz, $CDCl_3$) δ 166.4, 159.9, 159.2, 158.3, 155.6, 137.3 (2), 131.8, 129.8, 129.1, 129.0 (2), 128.5, 128.4, 128.1 (2), 127.7 (2), 122.7, 119.9, 114.8, 101.7, 95.0, 94.1, 70.6, 70.4, 67.3, 66.5, 55.9, 25.6. 5,7-Bis(benzyloxy)chroman-3-yl 3-methoxybenzoate (18 mg, 0.036 mmol) and palladium/carbon (10%) were suspended in tetrahydrofuran (2 mL) and stirred for 18 h under hydrogen atmosphere. The suspension was filtered through a small pad of celite. The eluent was concentrated and the residue purified by flash chromatography (SiO_2, 1:1 EtOAc/hexanes) to give **21b** (11 mg, 96%) as a colorless oil: ^{1}H NMR (500 MHz, $CDCl_3$) δ 7.60 (ddd, *J* = 7.7, 1.5, 1.0 Hz, 1H), 7.53 (dd, *J* = 2.7, 1.5 Hz, 1H), 7.32 (t, *J* = 8.0 Hz, 1H), 7.09 (ddd, *J* = 8.3, 2.7, 1.0 Hz, 1H), 6.03 (d, *J* = 2.3 Hz, 1H), 5.99 (d, *J* = 2.4 Hz, 1H), 5.54–5.45 (m, 1H), 5.43–5.33 (m, 1H), 5.24 (s, 1H), 4.29 (ddd, *J* = 11.4, 5.0, 1.8 Hz, 1H), 4.20 (ddd, *J* = 11.4, 2.3, 1.0 Hz, 1H), 3.83 (s, 3H), 3.04 (ddd, *J* = 16.9, 5.4, 1.2 Hz, 1H), 2.88 (ddd, *J* = 16.9, 4.5, 1.7 Hz, 1H); ^{13}C NMR (125 MHz, $CDCl_3$) δ 166.3, 159.7, 155.7, 155.4, 155.3, 131.3, 129.7, 122.4, 119.8, 114.6, 99.5, 96.3, 96.1, 66.9, 66.2, 55.7, 24.9; IR (KBr) ν_{max} 3404, 2960, 1716, 1596, 1469, 1278,

1224, 1099, 933, 752 cm^{-1}; HRMS (ESI-) *m*/*z* [M – H^+] calcd for $C_{17}H_{15}O_6$, 315.0869, found 315.0830.

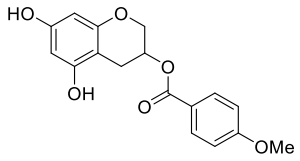

5,7-Dihydroxychroman-3-yl 4-Methoxybenzoate (21c): A solution of **20a** (13 mg, 0.036 mmol) in dichloromethane (0.5 mL) was added to a stirred solution of 4-methoxybenzoic acid (11 mg, 0.072 mmol), *N*,*N*′-dicyclohexylcarbodiimide (17 mg, 0.08 mmol), and 4-dimethylaminopyridine (4.8 mg, 0.04 mmol) in dichloromethane (1 mL) at 0 °C. The resulting solution was stirred for 6 h at rt and then filtered. The eluent was diluted with dichloromethane (5 mL) and washed with 0.5 N HCl (2 × 4 mL) and then with saturated sodium bicarbonate (2 × 4 mL) solution. The combined organic layers were washed with saturated sodium chloride solution (4 mL), dried over anhydrous sodium sulfate, filtered, and concentrated. The residue was purified by flash chromatography (SiO_2, 1:4 EtOAc/hexanes) to afford 5,7-bis(benzyloxy)chroman-3-yl 4-methoxybenzoate (16.7 mg, 93.8%) as a colorless oil, which was used as is for hydrogenolysis: ^{1}H NMR (500 MHz, $CDCl_3$) δ 8.01–7.96 (m, 2H), 7.52–7.29 (m, 10H), 6.94–6.85 (m, 2H), 6.27 (d, *J* = 2.3 Hz, 1H), 6.21 (d, *J* = 2.3 Hz, 1H), 5.57–5.46 (m, 1H), 5.02 (s, 4H), 4.30 (ddd, *J* = 11.4, 5.0, 1.8 Hz, 1H), 4.24–4.17 (m, 1H), 3.86 (s, 3H), 3.08 (ddd, *J* = 17.4, 5.5, 1.2 Hz, 1H), 2.98–2.88 (m, 1H); ^{13}C NMR (125 MHz, $CDCl_3$) δ 165.9, 163.7, 158.8, 158.1, 155.4, 137.1 (2), 132.7, 131.4, 130.6, 129.3, 128.8, 128.8, 128.2, 128.1, 127.8 (2), 127.4 (2), 122.6, 113.7 (2), 101.5, 94.7, 93.8, 76.9, 70.3, 67.1, 65.9, 55.5, 25.4. 5,7-Bis(benzyloxy)chroman-3-yl 4-methoxybenzoate (16.2 mg, 0.033 mmol) and palladium/carbon (10%) were suspended in tetrahydrofuran (2 mL) and stirred for 18 h under a hydrogen atmosphere. The suspension was filtered through a small pad of celite. The

eluent was concentrated and the residue purified by flash chromatography (SiO_2, 1:1 EtOAc/hexanes) to give **21c** (10 mg, 98%) as a colorless oil: ^{1}H NMR (500 MHz, $(CD_3)_2CO$) δ 8.30 (s, 1H), 8.04 (s, 1H), 7.99–7.88 (m, 2H), 7.03–6.94 (m, 2H), 6.05 (d, *J* = 2.3 Hz, 1H), 5.90 (d, *J* = 2.3 Hz, 1H), 5.42 (dtd, *J* = 5.4, 4.5, 2.2 Hz, 1H), 4.24 (ddd, *J* = 11.4, 4.7, 1.9 Hz, 1H), 4.19 (ddt, *J* = 11.5, 1.9, 0.9 Hz, 1H), 3.86 (s, 3H), 3.00 (ddd, *J* = 17.2, 5.3, 1.2 Hz, 1H), 2.83 (ddd, *J* = 17.2, 4.4, 1.9 Hz, 1H); ^{13}C NMR (125 MHz, $(CD_3)_2CO$) δ 166.1 (2), 164.6, 157.8, 157.5, 156.5, 132.4 (2), 123.5, 114.7, 99.2, 96.5, 95.7, 67.3, 66.9, 56.0, 25.6; IR (KBr) ν_{max} 3404, 2958, 1716, 1596, 14266, 1284 1224, 1098 cm^{-1}; HRMS (ESI+) *m*/*z* [M + H$^+$] calcd for $C_{17}H_{17}O_6$, 317.1025, found 317.1029.

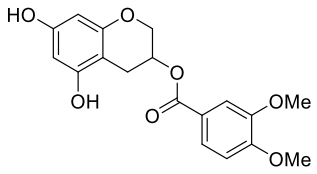

5,7-Dihydroxychroman-3-yl 3,4-Dimethoxybenzoate (21d): A solution of **20a** (12 mg, 0.033 mmol) in dichloromethane (0.5 mL) was added to a stirred solution of 4-methoxybenzoic acid 3,4-methoxybenzoic acid (14 mg, 0.066 mmol), *N*,*N*′-dicyclohexylcarbodiimide (14 mg, 0.066 mmol), and 4-dimethylaminopyridine (4.8 mg, 0.04 mmol) in dichloromethane (1 mL) at 0 °C. The resulting solution was stirred for 6 h at rt and then filtered. The eluent was diluted with dichloromethane (5 mL) and washed with 0.5 N HCl (2 × 4 mL) and then with saturated sodium bicarbonate (2 × 4 mL) solution. The combined organic layers were washed with saturated sodium chloride solution (4 mL), dried over anhydrous sodium sulfate, filtered, and the solvent was removed. The residue was purified by flash chromatography (SiO_2, 1:4 EtOAc/hexanes) to afford 5,7-bis(benzyloxy)chroman-3-yl 3,4-methoxybenzoate (17 mg, 95%) as a colorless oil which was used as for hydrogenolysis: ^{1}H NMR (500 MHz, $CDCl_3$) δ 7.66 (dd, *J* = 8.5, 2.0 Hz, 1H), 7.52 (d,

J = 2.0 Hz, 1H), 7.50–7.29 (m, 10H), 6.85 (d, *J* = 8.4 Hz, 1H), 6.27 (d, *J* = 2.3 Hz, 1H), 6.21 (d, *J* = 2.3 Hz, 1H), 5.51 (qd, *J* = 5.1, 2.4 Hz, 1H), 5.02 (d, *J* = 2.1 Hz, 4H), 4.29 (ddd, *J* = 11.3, 5.2, 1.7 Hz, 1H), 4.24 (s, 1H), 3.93 (s, 3H), 3.91 (s, 3H), 3.10 (ddd, *J* = 17.3, 5.6, 1.1 Hz, 1H), 2.93 (ddd, *J* = 17.3, 4.6, 1.6 Hz, 1H); ^{13}C NMR (125 MHz, $CDCl_3$) δ 166.1, 158.9, 158.1, 155.4, 153.4, 148.8, 137.1 (2), 128.9 (2), 128.8, 128.3 (2), 128.2 (2), 127.8, 127.5 (2), 124.2, 122.7, 112.3, 110.4, 101.6, 94.8, 93.9, 70.4, 70.2, 67.2, 66.0, 56.3 (2), 25.4. 5,7-Bis(benzyloxy)chroman-3-yl 3,4-methoxybenzoate (17 mg, 0.032 mmol) and palladium/carbon (10%) were suspended in tetrahydrofuran (2 mL) and stirred for 18 h under a hydrogen atmosphere. The suspension was filtered through a small pad of celite. The eluent was concentrated and the residue purified by flash chromatography (SiO_2, 1:1 EtOAc/hexanes) to give **21d** (9.5 mg, 86%) as colorless oil: ^{1}H NMR (500 MHz, $(CD_3)_2CO$) δ 8.30 (s, 1H), 8.04 (s, 1H), 7.58 (dd, *J* = 8.5, 2.0 Hz, 1H), 7.50 (d, *J* = 2.0 Hz, 1H), 7.02 (d, *J* = 8.5 Hz, 1H), 6.05 (d, *J* = 2.3 Hz, 1H), 5.90 (d, *J* = 2.3 Hz, 1H), 5.41 (qd, *J* = 4.7, 2.5 Hz, 1H), 4.21 (td, *J* = 4.2, 3.5, 1.4 Hz, 2H), 3.87 (s, 3H), 3.83 (s, 3H), 3.01 (ddd, *J* = 17.1, 5.3, 1.1 Hz, 1H), 2.88–2.73 (m, 1H); ^{13}C NMR (125 MHz $(CD_3)_2CO$) δ 166.2, 157.9, 157.5, 156.6, 154.7, 150.0, 124.4, 123.5, 113.2, 111.8, 99.3, 96.5, 95.7, 78.1, 67.1, 56.3, 56.2, 25.7; IR (KBr) ν_{max} 3404, 2921, 1699, 1515, 1271, 1145, 1022, 761, 667 cm^{-1}; HRMS (ESI+) *m*/*z* [M + H$^+$] calcd for $C_{18}H_{19}O_7$, 347.1131, found 347.1128.

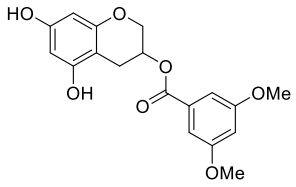

5,7-Dihydroxychroman-3-yl 3,5-Dimethoxybenzoate (21e): A solution of **20a** (13 mg, 0.036 mmol) in dichloromethane (0.5 mL) was added to a stirred solution of 4-methoxybenzoic acid 3,5-dimethoxybenzoic acid (13 mg, 0.072 mmol), *N*,*N*′-dicyclohexylcarbodiimide (17 mg, 0.08

mmol), and 4-dimethylaminopyridine (4.8 mg, 0.04 mmol) in dichloromethane (1 mL) at 0 °C. The resulting solution was stirred for 6 h at rt and then filtered. The eluent was diluted with dichloromethane (5 mL) and washed with 0.5 N HCl (2 × 4 mL), and then with saturated sodium bicarbonate (2 × 4 mL) solution. The combined organic layers were washed with saturated sodium chloride solution (4 mL), dried over anhydrous sodium sulfate, filtered, and concentrated. The residue was purified by flash chromatography (SiO_2, 1:4 EtOAc/hexanes) to afford 5,7-bis(benzyloxy)chroman-3-yl 3,5-dimethoxybenzoate (17.8 mg, 94.6%) as a colorless oil, which was used as is for hydrogenolysis: ^{1}H NMR (500 MHz, $CDCl_3$) δ 7.46–7.32 (m, 10H), 7.17 (d, *J* = 2.4 Hz, 2H), 6.64 (t, *J* = 2.4 Hz, 1H), 6.27 (d, *J* = 2.3 Hz, 1H), 6.20 (d, *J* = 2.2 Hz, 1H), 5.50 (qd, *J* = 5.1, 2.3 Hz, 1H), 5.02 (d, *J* = 2.4 Hz, 4H), 4.28 (ddd, *J* = 11.3, 5.3, 1.7 Hz, 1H), 4.25–4.18 (m, 1H), 3.81 (s, 6H), 3.16–3.04 (m, 1H), 2.92 (ddd, *J* = 17.3, 4.6, 1.6 Hz, 1H); ^{13}C NMR (125 MHz, $CDCl_3$) δ 166.1, 160.8 (2), 158.9, 158.1, 155.4, 137.1 (2), 132.1, 128.9 (2), 128.8 (2), 128.3, 128.2 (2), 127.8 (2), 127.5, 107.7 (2), 105.8, 101.4, 94.8, 93.9, 70.4, 70.2, 67.0, 66.4, 55.8 (2), 25.4. 5,7-Bis(benzyloxy)chroman-3-yl 3,5-dimethoxybenzoate (17 mg, 0.032 mmol) and palladium/carbon (10%) were suspended in tetrahydrofuran (2 mL) and stirred for 18 h under a hydrogen atmosphere. The suspension was filtered through a small pad of celite. The eluent was concentrated and the residue purified by flash chromatography (SiO_2, 1:1 EtOAc/hexanes) to give **21e** (9.5 mg, 86%) as a colorless oil: ^{1}H NMR (500 MHz, $(CD_3)_2CO$) δ 8.31 (s, 1H), 8.04 (s, 1H), 7.10 (d, *J* = 2.4 Hz, 2H), 6.72 (t, *J* = 2.4 Hz, 1H), 6.05 (d, *J* = 2.3 Hz, 1H), 5.90 (d, *J* = 2.3 Hz, 1H), 5.53–5.35 (m, 1H), 4.32–4.16 (m, 2H), 3.81 (s, 6H), 3.15–2.95 (m, 1H), 2.86–2.82 (m, 1H); ^{13}C NMR (125 MHz, $(CD_3)_2CO$) δ 166.1, 161.8 (2), 157.8, 157.4, 156.4, 133.2, 108.1 (2), 105.6, 99.1, 96.4, 95.6, 77.1, 67.5, 67.2, 55.9, 25.5; IR (KBr) ν_{max} 1916, 2848, 1702, 1683, 1558, 1244, 1145, 1103, cm^{-1}; HRMS (ESI+) *m/z* [M + Na^+] calcd for $C_{18}H_{18}NaO_7$, 369.0950, found 369.0962.

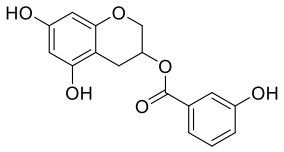

5,7-Dihydroxychroman-3-yl 3-Hydroxybenzoate (21f): A solution of **20a** (14 mg, 0.039 mmol) in dichloromethane (0.5 mL) was added to a stirred solution of 4-(benzyloxy)benzoic acid (13 mg, 0.072 mmol), *N*,*N*′-dicyclohexylcarbodiimide (16 mg, 0.077 mmol), and 4-dimethylaminopyridine (4.8 mg, 0.04 mmol) in dichloromethane (1 mL) at 0 °C. The resulting solution was stirred for 6 h at rt and then filtered. The eluent was diluted with dichloromethane (5 mL) and washed with 0.5 N HCl (2 × 4 mL) and saturated sodium bicarbonate (2 × 4 mL) solution. The combined organic layers were washed with saturated sodium chloride solution (4 mL), dried over anhydrous sodium sulfate, filtered, and concentrated. The residue was purified by flash chromatography (SiO_2, 1:4 EtOAc/hexanes) to afford 5,7-bis(benzyloxy)chroman-3-yl 3-(benzyloxy)benzoate (19 mg, 86.3%), which was used further as obtained: ^{1}H NMR (500 MHz, $CDCl_3$) δ 7.63 (ddd, *J* = 5.7, 2.5, 1.2 Hz, 2H), 7.46–7.30 (m, 16H), 7.16 (ddd, *J* = 8.3, 2.6, 1.1 Hz, 1H), 6.28 (d, *J* = 2.3 Hz, 1H), 6.21 (d, *J* = 2.3 Hz, 1H), 5.69–5.44 (m, 1H), 5.09 (s, 2H), 5.02 (d, *J* = 5.2 Hz, 4H), 4.30 (ddd, *J* = 11.5, 5.0, 1.8 Hz, 1H), 4.25–4.13 (m, 1H), 3.09 (ddd, *J* = 17.5, 5.6, 1.2 Hz, 1H), 2.93 (ddd, *J* = 17.5, 4.4, 1.7 Hz, 1H); ^{13}C NMR (125 MHz, $CDCl_3$) δ 166.1, 158.9, 158.8, 158.1, 155.4, 137.0 (2), 136.7, 131.5, 129.6 (2), 128.8 (3), 128.7, 128.3, 128.2, 128.1 (2), 127.9 (2), 127.8 (2), 127.4 (2), 122.7, 120.4, 115.6, 101.4, 94.8, 93.9, 70.4 (2), 70.2, 67.0, 66.3, 25.3. 5,7-Bis(benzyloxy)chroman-3-yl 3-(benzyloxy)benzoate (18 mg, 0.031 mmol) and palladium/carbon (10%) were suspended in tetrahydrofuran (2 mL) and stirred for 18 h under a hydrogen atmosphere. The suspension was filtered through a small pad of celite. The eluent was concentrated and the residue purified by flash chromatography (SiO_2, 1:9 acetone/dichloromethane) to give **21f** (8.6 mg, 92.6%) as a colorless oil: ^{1}H NMR (500 MHz, MeOD) δ 7.83 (d, *J* = 8.8 Hz, 2H), 6.79 (d, *J*

= 8.8 Hz, 2H), 5.94 (d, *J* = 2.3 Hz, 1H), 5.84 (d, *J* = 2.3 Hz, 1H), 5.37 (ddd, *J* = 5.3, 4.5, 2.7 Hz, 1H), 4.19 (ddd, *J* = 11.4, 4.9, 1.8 Hz, 1H), 4.14 (dd, *J* = 11.4, 2.1 Hz, 1H), 2.95 (ddd, *J* = 17.1, 5.4, 1.1 Hz, 1H), 2.77 (ddd, *J* = 17.1, 4.5, 1.7 Hz, 1H); ^{13}C NMR (125 MHz, $(CD_3)_2CO$) δ 166.2, 158.3, 157.7, 157.4, 156.4, 132.6, 130.5, 121.5, 121.0, 116.7, 99.1, 96.3, 95.6, 67.6, 67.2, 25.5; IR (KBr) ν_{max} 3384, 2910, 1848, 1699, 1436, 1290, 1145 cm^{-1}; HRMS (ESI-) *m*/*z* [M – H$^-$] calcd for $C_{16}H_{13}O_6$, 301.0712, found 301.0717.

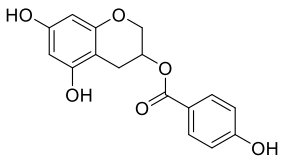

5,7-Bis(benzyloxy)chroman-3-yl 4-hydroxybenzoate (21g): A solution of **20a** (14 mg, 0.039 mmol) in dichloromethane (0.5 mL) was added to a stirred solution of 4-(benzyloxy)benzoic acid (13 mg, 0.072 mmol), *N*,*N*′-dicyclohexylcarbodiimide (16 mg, 0.077 mmol), and 4-dimethylaminopyridine (4.8 mg, 0.04 mmol) in dichloromethane (1 mL) at 0 °C. The resulting solution was stirred for 6 h at rt and filtered. The eluent was diluted with dichloromethane (5 mL) and washed with 0.5 N HCl (2 × 4 mL) and then with saturated sodium bicarbonate (2 × 4 mL) solution. The combined organic layers were washed with saturated sodium chloride solution (4 mL), dried over anhydrous sodium sulfate, filtered, and concentrated. The residue was purified by flash chromatography (SiO_2, 1:4 EtOAc/hexanes) to afford 5,7-bis(benzyloxy)chroman-3-yl 4-(benzyloxy)benzoate (20 mg, 90.4%) as a colorless oil, which was used as is for hydrogenolysis: ^{1}H NMR (500 MHz, $CDCl_3$) δ 8.06–7.90 (m, 2H), 7.50–7.30 (m, 15H), 7.02–6.91 (m, 2H), 6.27 (d, *J* = 2.3 Hz, 1H), 6.21 (d, *J* = 2.3 Hz, 1H), 5.50 (dp, *J* = 7.0, 2.4 Hz, 1H), 5.12 (s, 2H), 5.02 (s, 4H), 4.30 (ddd, *J* = 11.4, 5.0, 1.8 Hz, 1H), 4.20 (dd, *J* = 11.2, 2.4 Hz, 1H), 3.08 (ddd, *J* = 17.5, 5.5, 1.1 Hz, 1H), 2.92 (ddd, *J* = 17.5, 4.4, 1.7 Hz, 1H); ^{13}C NMR (125 MHz, $CDCl_3$) δ 165.9, 162.8,

158.8, 158.1, 155.4, 137.1 (2), 136.4, 132.1(2), 128.9 (4), 128.8 (2), 128.4, 128.2, 128.1, 127.8, 127.7, 127.4 (4), 122.8. 114.6 (2), 101.5, 94.8, 93.8, 70.4, 70.3, 70.1, 67.1, 65.8, 25.3. Bis(benzyloxy)chroman-3-yl 4-(benzyloxy)benzoate (18 mg, 0.031 mmol) and palladium/carbon (10%) were suspended in tetrahydrofuran (2 mL) and stirred for 18 h under a hydrogen atmosphere. The suspension was filtered through a small pad of celite. The eluent was concentrated and the residue purified by flash chromatography (SiO_2, 1:1 EtOAc/hexanes) to give **21g** (9.8 mg, 97%) as a colorless oil: ^{1}H NMR (500 MHz, $(CD_3)_2CO$) δ 9.15 (s, 1H), 8.29 (s, 1H), 8.03 (s, 1H), 7.85 (d, *J* = 8.7 Hz, 2H), 6.97–6.83 (m, 2H), 6.05 (d, *J* = 2.3 Hz, 1H), 5.90 (d, *J* = 2.3 Hz, 1H), 5.57–5.28 (m, 1H), 4.23 (ddd, *J* = 11.4, 4.7, 1.8 Hz, 1H), 4.18 (ddt, *J* = 11.4, 2.1, 0.9 Hz, 1H), 2.99 (ddd, *J* = 17.0, 5.4, 1.1 Hz, 1H), 2.82 (ddd, *J* = 17.0, 4.4, 1.7 Hz, 1H); ^{13}C NMR (125 MHz, $(CD_3)_2CO$) δ 166.2, 160.7, 159.8, 159.4, 156.1, 133.1, 108.7, 108.1, 101.1, 94.2, 92.2, 67.3, 66.8, 55.8, 55.5, 25.3; IR (KBr) ν_{max} 3363, 2962, 2927, 1683, 1608, 1355, 1272, 1166, 1143, 1099, 1014, 769 cm^{-1}; HRMS (ESI+) *m*/*z* [M + H$^+$] calcd for $C_{16}H_{15}O_6$, 303.0869, found 303.0878.

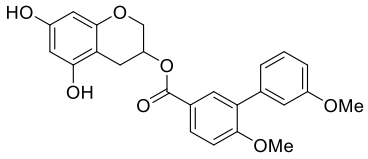

5,7-Dihydroxychroman-3-yl 3′,6-Dimethoxy-[1,1′-biphenyl]-3-carboxylate (21h): A solution of **20a** (11 mg, 0.03 mmol) in dichloromethane (0.5 mL) was added to a stirred solution of 3′,6-dimethoxy-[1,1′-biphenyl]-3-carboxylic acid (16 mg, 0.06 mmol), *N*,*N*′-dicyclohexylcarbodiimide (13 mg, 0.06 mmol), and 4-dimethylaminopyridine (4.8 mg, 0.04 mmol) in dichloromethane (1 mL) 0 °C. The resulting solution was stirred for 6 h at rt and filtered. The eluent was diluted with dichloromethane (5 mL) and washed with 0.5 N HCl (2 × 4 mL) and then with saturated sodium bicarbonate (2 × 4 mL) solution. The combined organic layers were washed with saturated sodium

chloride solution (4 mL), dried over anhydrous sodium sulfate, filtered, and concentrated. The residue was purified by flash chromatography (SiO_2, EtOAc/hexanes) to afford 5,7-bis(benzyloxy)chroman-3-yl 3′,6-dimethoxy-[1,1′-biphenyl]-3-carboxylate (17.5 mg, 96.1%) as a colorless oil, which was used as is for hydrogenolysis: ^{1}H NMR (500 MHz, $CDCl_3$) δ 8.14–7.87 (m, 2H), 7.49–7.29 (m, 11H), 7.09 (dt, *J* = 7.7, 1.3 Hz, 1H), 7.04 (dd, *J* = 2.6, 1.5 Hz, 1H), 6.97 (d, *J* = 8.6 Hz, 1H), 6.91 (ddd, *J* = 8.3, 2.6, 1.0 Hz, 1H), 6.26 (d, *J* = 2.3 Hz, 1H), 6.20 (d, *J* = 2.3 Hz, 1H), 5.51 (dd, *J* = 5.2, 2.3 Hz, 1H), 5.01 (d, *J* = 4.2 Hz, 4H), 4.34–4.25 (m, 1H), 4.24–4.19 (m, 1H), 3.71 (s, 3H), 3.79 (s, 3H), 3.10 (ddd, *J* = 17.3, 5.7, 1.2 Hz, 1H), 2.92 (ddd, *J* = 17.3, 4.7, 1.6 Hz, 1H); ^{13}C NMR (125 MHz, $CDCl_3$) δ 166.0, 160.5, 159.4, 158.9, 158.1, 155.4, 139.0, 137.1 (2), 132.7, 131.4, 130.6, 129.3 (2), 128.8 (3), 128.2, 128.1 (3), 127.8, 127.4, 122.6, 122.2, 115.4, 113.1, 110.7, 101.6, 94.7, 93.8, 77.0, 70.4, 67.1, 65.9, 56.0, 55.5, 25.4. 5,7-Bis(benzyloxy)chroman-3-yl 3′,6-dimethoxy-[1,1′-biphenyl]-3-carboxylate (17 mg, 0.028 mmol) and palladium/carbon (10%) were suspended in tetrahydrofuran (2 mL) and stirred for 18 h under a hydrogen atmosphere. The suspension was filtered through a small pad of celite. The eluent was concentrated and the residue purified by flash chromatography (SiO_2, 1:1 EtOAc/hexanes) to give **21h** (11.1 mg, 93.2%) as a colorless oil: ^{1}H NMR (500 MHz, $(CD_3)_2CO$) δ 8.3 (br s , 1 H), 8.03 (br s, 1 H), 7.97 (dd, *J* = 8.7, 2.2 Hz, 1H), 7.92 (d, *J* = 2.2 Hz, 1H), 7.37–7.29 (m, 1H), 7.19 (d, *J* = 8.7 Hz, 1H), 7.10–7.00 (m, 2H), 6.91 (ddd, *J* = 8.3, 2.6, 1.1 Hz, 1H), 6.04 (d, *J* = 2.3 Hz, 1H), 5.89 (d, *J* = 2.3 Hz, 1H), 5.50–5.35 (m, 1H), 4.33–4.23 (m, 1H), 4.22–4.18 (m, 1H), 3.89 (s, 3H), 3.81 (s, 3H), 3.01 (ddd, *J* = 17.1, 5.3, 1.2 Hz, 1H), 2.92–2.80 (m, 1H); ^{13}C NMR (125 MHz, $(CD_3)_2CO$) δ 166.0, 161.4, 160.4, 157.8, 157.4, 156.5, 139.9, 132.7, 131.7, 131.3, 129.9, 123.5, 122.5, 116.0, 113.6, 112.1, 99.2, 96.4, 95.7, 67.3, 67.0, 55.5 (2), 25.6; IR (KBr) ν_{max} 3355, 2923,

1701, 1606,1458, 1251, 1145, 1031, 752, 667 cm^{-1}; HRMS (ESI+) *m*/*z* [M + H^+] calcd for $C_{24}H_{23}O_7$, 423.1444, found 423.1454.

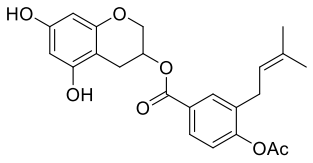

5,7-Dihydroxychroman-3-yl 4-acetoxy-3-(3-methylbut-2-en-1-yl)benzoate (21i): 4-Acetoxy-3-(3-methylbut-2-en-1-yl)benzoic acid (34 mg, 0.137 mmol) and thionyl chloride (33 μL, 0.27 mmol) in tetrahydrofuran (5 mL) were heated at reflux for 3 h, cooled to rt and concentrated. The residue was dissolved in dichloromethane (0.5 mL) and added to a stirred solution of **20a** (25 mg, 0.069 mmol) in dichloromethane (0.7 mL) with trimethylamine (0.3 mL) under at 0 °C. The resulting mixture was stirred for 6 h and concentrated, and the residue was purified by flash chromatography (SiO_2, 1:4 EtOAc/hexanes) to give 5,7-bis(benzyloxy)chroman-3-yl 4-acetoxy-3-(3-methylbut-2-en-1-yl)benzoate (34 mg, 85%) as a colorless oil, which was used as is for hydrogenolysis: ^{1}H NMR (500 MHz, $CDCl_3$) δ 7.91 (d, *J* = 2.1 Hz, 1H), 7.87 (dd, *J* = 8.4, 2.2 Hz, 1H), 7.47–7.31 (m, 10H), 7.07 (d, *J* = 8.4 Hz, 1H), 6.27 (d, *J* = 2.3 Hz, 1H), 6.20 (d, *J* = 2.3 Hz, 1H), 5.51 (dp, *J* = 7.2, 2.5 Hz, 1H), 5.19 (tdt, *J* = 5.9, 2.9, 1.4 Hz, 1H), 5.02 (s, 4H), 4.30 (ddd, *J* = 11.4, 5.0, 1.8 Hz, 1H), 4.20 (dd, *J* = 11.3, 2.1 Hz, 1H), 3.25 (d, *J* = 7.2 Hz, 2H), 3.07 (ddd, *J* = 17.6, 5.4, 1.2 Hz, 1H), 2.93 (ddd, *J* = 17.3, 4.4, 1.7 Hz, 1H), 2.32 (s, 3H), 1.72 (d, *J* = 1.6 Hz, 3H), 1.68 (s, 3H); ^{13}C NMR (125 MHz, $CDCl_3$) δ 169.0, 165.6, 158.9, 158.1, 155.3, 152.9, 137.1, 137.0, 134.1, 134.0, 132.2, 129.0, 128.8, 128.7, 128.2 (2), 128.1 (2), 127.8 (4), 127.4 (2), 122.6, 121.1, 101.4, 94.7, 93.8, 70.4, 70.2, 67.0, 66.1, 29.9, 28.9, 25.9, 21.1, 18.1. A solution of palladium acetate (5 mg, 0.023 mg), trimethylamine (15 μL, 0.108 mmol), triethylsilane (82 μL, 0.108) in dichloromethane (0.8 mL) was stirred for 15 min before the slow addition of a solution of 5,7-

bis(benzyloxy)chroman-3-yl 4-acetoxy-3-(3-methylbut-2-en-1-yl)benzoate (34 mg, 0.057 mmol) in dichloromethane (0.4 mL). The resulting mixture was stirred for 15 h, quenched with saturated ammonium chloride (2 mL) and extracted with ether (3 × 4 mL). The combined organic layers were washed with saturated sodium chloride solution, dried over anhydrous sodium sulfate, filtered, and concentrated. The residue was purified by flash chromatography (silica, 5:95 MeOH/DCM) to afford **21i** (15.2 mg, 54.8%) as a colorless oil: ^{1}H NMR (500 MHz, $CDCl_3$): δ 7.92 (dd, *J* = 13.7, 2.2 Hz, 1H), 7.86 (dd, *J* = 8.4, 2.2 Hz, 1H), 7.06 (d, *J* = 8.4 Hz, 1H), 6.03–5.99 (m, 1H), 5.96 (d, *J* = 2.4 Hz, 1H), 5.50 (ddt, *J* = 7.2, 4.8, 2.4 Hz, 1H), 5.18 (dddd, *J* = 7.3, 5.8, 2.9, 1.5 Hz, 1H), 4.29 (ddd, *J* = 11.5, 4.9, 1.9 Hz, 1H), 4.24–4.14 (m, 1H), 3.25 (d, *J* = 7.2 Hz, 2H), 3.07–2.98 (m, 1H), 2.87 (ddd, *J* = 16.9, 4.4, 1.8 Hz, 1H), 2.32 (s, 3H), 1.72 (q, *J* = 1.3 Hz, 3H), 1.68 (d, *J* = 1.4 Hz, 3H); ^{13}C NMR (125 MHz, $CDCl_3$) δ 169.1, 165.7, 155.4, 155.3 (2), 152.9, 134.2, 134.1, 132.2, 129.0, 127.9, 122.6, 121.0, 99.4, 96.3, 96.0, 66.9, 65.9, 28.9, 25.9, 24.9, 21.1, 18.1; IR (KBr) ν_{max} 3363, 2921, 1703, 1606, 1252, 1146 cm^{-1}; HRMS (ESI+) *m*/*z* [M + H^{+}] calcd for $C_{23}H_{25}O_7$, 413.1600, found 413.1617.

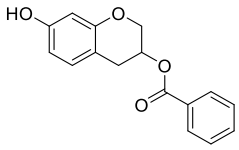

7-Hydroxychroman-3-yl Benzoate (21j): A solution of **20b** (15 mg, 0.06 mmol) in dichloromethane (0.5 mL) was added to a stirred solution benzoic acid (14 mg, 0.12 mmol), *N*,*N*′-dicyclohexylcarbodiimide (24 mg, 0.12 mmol), and 4-dimethylaminopyridine (7.2 mg, 0.06 mmol) at 0 °C. The resulting solution was stirred for 6 h at rt and then filtered. The eluent was diluted with dichloromethane (5 mL) and washed with 0.5 N HCl (2 × 4 mL) and then with saturated sodium bicarbonate (2 × 4 mL) solution. The combined organic layers were washed with

saturated sodium chloride solution (4 mL), dried over anhydrous sodium sulfate, filtered, and concentrated. The residue was purified by flash chromatography (SiO_2, 1:8 EtOAc/hexanes) to afford 7-(benzyloxy)chroman-3-yl benzoate as a colorless oil (21 mg, 90%), which was used as is for hydrogenolysis: ^{1}H NMR (500 MHz, $CDCl_3$) δ 8.04–7.93 (m, 2H), 7.56 (ddt, *J* = 8.8, 7.2, 1.3 Hz, 1H), 7.47–7.37 (m, 6H), 7.37–7.31 (m, 1H), 6.98 (dt, *J* = 8.4, 1.0 Hz, 1H), 6.60 (dd, *J* = 8.4, 2.5 Hz, 1H), 6.54 (d, *J* = 2.5 Hz, 1H), 5.51 (qd, *J* = 4.8, 2.2 Hz, 1H), 5.04 (s, 2H), 4.34 (ddd, *J* = 11.5, 4.9, 1.9 Hz, 1H), 4.25 (ddd, *J* = 11.5, 2.1, 1.1 Hz, 1H), 3.22 (ddt, *J* = 16.6, 5.1, 1.2 Hz, 1H), 2.98 (ddd, *J* = 16.8, 4.5, 1.9 Hz, 1H); ^{13}C NMR (125 MHz, $CDCl_3$) δ 166.2, 158.7, 154.7, 137.2, 133.4, 130.7, 130.1, 130.0 (2), 128.8 (2), 128.6 (2), 128.2 (2), 127.7, 111.4, 108.9, 102.7, 70.3, 67.1, 66.4, 29.9. 7-(Benzyloxy)chroman-3-yl benzoate (14 mg, 0.04 mmol) and palladium/carbon (10%) were suspended in tetrahydrofuran (2 mL) and stirred for 18 h under a hydrogen atmosphere. The suspension was filtered through a small pad of celite. The eluent was concentrated and the residue purified by flash chromatography (SiO_2, 1:1 EtOAc/hexanes) to give **21j** (11.1 mg, 90.4%) as a colorless oil: ^{1}H NMR (500 MHz, $CDCl_3$) δ 8.04–7.93 (m, 2H), 7.54 (ddt, *J* = 8.7, 7.7, 1.3 Hz, 1H), 7.40 (ddt, *J* = 7.3, 6.3, 1.0 Hz, 2H), 6.92 (dt, *J* = 8.1, 0.9 Hz, 1H), 6.42 (dd, *J* = 8.2, 2.6 Hz, 1H), 6.38 (d, *J* = 2.5 Hz, 1H), 5.49 (qd, *J* = 4.8, 2.2 Hz, 1H), 4.71 (s, 1H), 4.32 (ddd, *J* = 11.5, 4.8, 1.9 Hz, 1H), 4.23 (dtd, *J* = 11.5, 1.5, 0.8 Hz, 1H), 3.18 (ddt, *J* = 16.6, 5.1, 1.1 Hz, 1H), 3.02–2.89 (m, 1H); ^{13}C NMR (125 MHz, $CDCl_3$) δ 166.3, 155.3, 154.8, 133.4, 130.8 (2), 130.1, 130.0, 128.6 (2), 111.4, 108.9, 103.5, 67.1, 66.4, 29.8; IR (KBr) ν_{max} 3392, 2925, 1716, 1699, 1519, 1456, 1272, 1145, 1027, 1016, 821, 711 cm^{-1}; HRMS (ESI+) *m*/*z* [M + H$^+$] calcd for $C_{16}H_{15}O_4$, 271.0970, found 271.0966.

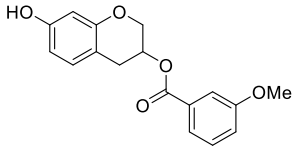

7-Hydroxychroman-3-yl 3-Methoxybenzoate (21k): A solution of **20b** (11 mg, 0.04 mmol) in dichloromethane (0.5 mL) was added to a stirred solution 3-methoxybenzoic acid (12 mg, 0.08 mmol), *N*,*N*′-dicyclohexylcarbodiimide (17 mg, 0.08 mmol), and 4-dimethylaminopyridine (5 mg, 0.04 mmol) under argon at 0 °C. The resulting solution was stirred for 6 h at rt and then filtered. The eluent was diluted with dichloromethane (5 mL) and washed with 0.5 N HCl (2 × 4 mL) and saturated sodium bicarbonate (2 × 4 mL) solution. The combined organic layers were washed with saturated sodium chloride solution (4 mL), dried over anhydrous Na_2SO_4, filtered, and concentrated. The residue was purified by flash chromatography (SiO_2, 1:8 EtOAc/hexanes) to afford 7-(benzyloxy)chroman-3-yl 3-methoxybenzoate (15 mg, 89.5) as a colorless oil, which was used as is for hydrogenolysis: ^{1}H NMR (500 MHz, $CDCl_3$) δ 7.59 (dt, *J* = 7.7, 1.2 Hz, 1H), 7.53 (dd, *J* = 2.7, 1.5 Hz, 1H), 7.48–7.43 (m, 2H), 7.42–7.36 (m, 2H), 7.37–7.30 (m, 2H), 7.10 (ddd, *J* = 8.3, 2.7, 1.0 Hz, 1H), 6.98 (dt, *J* = 8.5, 0.9 Hz, 1H), 6.59 (dd, *J* = 8.4, 2.5 Hz, 1H), 6.53 (d, *J* = 2.5 Hz, 1H), 5.50 (qd, *J* = 4.9, 2.3 Hz, 1H), 5.04 (s, 2H), 4.33 (ddd, *J* = 11.5, 5.0, 1.8 Hz, 1H), 4.25 (ddd, *J* = 11.3, 2.4, 1.2 Hz, 1H), 3.87 (s, 3H), 3.21 (ddt, *J* = 16.6, 5.1, 1.1 Hz, 1H), 3.02–2.90 (m, 1H); ^{13}C NMR (125 MHz, $CDCl_3$) δ 166.1, 159.7, 158.7, 154.7, 137.2, 131.4, 130.6, 129.6, 128.8 (2), 128.2 (2), 127.7, 122.4, 119.7, 114.5, 111.4, 108.9, 102.7, 70.3, 67.1, 66.5, 55.6, 29.9. 7-(Benzyloxy)chroman-3-yl 3-methoxybenzoate (11 mg, 0.028 mmol) and palladium/carbon (10%) were suspended in tetrahydrofuran (2 mL) and stirred for 18 h under a hydrogen atmosphere. The suspension was filtered through a small pad of celite. The eluent was concentrated and the residue purified by flash chromatography (SiO_2, 1:1 EtOAc/hexanes) to give **21k** (7.5 mg, 89.4%) as a colorless oil: ^{1}H NMR (500 MHz, $CDCl_3$) δ 7.58 (dt, *J* = 7.7, 1.2 Hz, 1H), 7.52 (dd, *J* = 2.7, 1.5 Hz, 1H), 7.31 (t, *J* = 8.0 Hz, 1H), 7.09 (ddd, *J* = 8.2, 2.7, 1.0 Hz, 1H), 6.92 (dt, *J* = 8.2, 1.0 Hz, 1H), 6.43 (dd, *J* = 8.2, 2.5 Hz, 1H), 6.39 (d, *J* = 2.5 Hz, 1H), 5.49 (qd, *J* = 4.9, 2.3 Hz, 1H), 4.81

(brs, 1H), 4.32 (ddd, *J* = 11.5, 4.9, 1.9 Hz, 1H), 4.24 (ddt, *J* = 11.4, 1.8, 1.0 Hz, 1H), 3.84 (s, 3H), 3.19 (ddt, *J* = 16.7, 5.2, 1.2 Hz, 1H), 3.03–2.84 (m, 1H); ^{13}C NMR (125 MHz, $CDCl_3$) δ 166.2, 159.7, 155.3, 154.8, 131.4, 130.9, 129.6, 122.4, 119.8, 114.5, 111.3, 108.9, 103.5, 67.1, 66.5, 55.7, 29.9; IR (KBr) ν_{max} 3384, 2910, 2848, 1701, 1635, 1508, 1259, 1164, 1116, 667 cm^{-1}; HRMS (ESI+) *m*/*z* [M + H^+] calcd for $C_{17}H_{17}O_5$, 301.1076, found 301.1076.

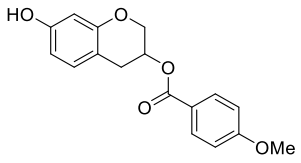

7-Hydroxychroman-3-yl 4-Methoxybenzoate (21l): A solution of **20b** (11 mg, 0.04 mmol) in dichloromethane (0.5 mL) was added to a stirred solution of 4-methoxybenzoic acid (12 mg, 0.08 mmol), *N*,*N*′-dicyclohexylcarbodiimide (17 mg, 0.08 mmol), and 4-dimethylaminopyridine (4.8 mg, 0.04 mmol) under argon at 0 °C. The resulting solution was stirred for 6 h at rt and then filtered. The eluent was diluted with dichloromethane (5 mL) and washed with 0.5 N HCl (2 × 4 mL) and then with saturated sodium bicarbonate (2 × 4 mL) solution. The combined organic layers were washed with saturated sodium chloride solution (4 mL), dried over anhydrous sodium sulfate, filtered and concentrated. The residue was purified by flash chromatography (SiO_2, 1:8 EtOAc/hexanes) to afford 7-(benzyloxy)chroman-3-yl 4-methoxybenzoate (15.5 mg, 79.2%) as a colorless oil, which was used as for hydrogenolysis: ^{1}H NMR (500 MHz, $CDCl_3$) δ 8.05–7.90 (m, 2H), 7.48–7.31 (m, 5H), 7.01–6.95 (m, 1H), 6.93–6.83 (m, 2H), 6.59 (dd, *J* = 8.4, 2.6 Hz, 1H), 6.53 (d, *J* = 2.6 Hz, 1H), 5.49 (qd, *J* = 4.8, 2.2 Hz, 1H), 5.04 (s, 2H), 4.32 (ddd, *J* = 11.4, 4.9, 1.9 Hz, 1H), 4.24 (ddd, *J* = 11.4, 2.3, 1.2 Hz, 1H), 3.85 (s, 3H), 3.20 (ddt, *J* = 16.7, 5.1, 1.1 Hz, 1H), 3.03–2.84 (m, 1H); ^{13}C NMR (125 MHz, $CDCl_3$) δ 166.0, 163.7, 158.6, 154.8, 137.2, 132.0, 130.7, 128.8 (2), 128.2, 127.7 (2), 122.5 (2), 113.8 (2), 111.6, 108.9, 102.7, 70.3, 67.2, 66.0, 55.6, 29.9.

7-(Benzyloxy)chroman-3-yl 4-methoxybenzoate (11 mg, 0.028 mmol) and palladium/carbon (10%) were suspended in tetrahydrofuran (2 mL) and stirred for 18 h under a hydrogen atmosphere. The suspension was filtered through a small pad of celite. The eluent was concentrated and the residue purified by flash chromatography (SiO_2, 1:1 EtOAc/hexanes) to give **21l** (8 mg, 94.3%) as a colorless oil: ^{1}H NMR (500 MHz, $CDCl_3$) δ 8.00–7.88 (m, 2H), 6.93 (dt, *J* = 8.3, 0.9 Hz, 1H), 6.91–6.87 (m, 2H), 6.43 (dd, *J* = 8.2, 2.5 Hz, 1H), 6.39 (d, *J* = 2.5 Hz, 1H), 5.48 (qd, *J* = 4.8, 2.2 Hz, 1H), 4.78 (br s, 1 H), 4.32 (ddd, *J* = 11.5, 4.9, 1.9 Hz, 1H), 4.23 (dtd, *J* = 11.5, 1.5, 0.8 Hz, 1H), 3.85 (s, 3H), 3.18 (ddt, *J* = 16.5, 5.0, 1.2 Hz, 1H), 2.95 (dtd, *J* = 16.7, 2.4, 1.3 Hz, 1H); ^{13}C NMR (125 MHz, $CDCl_3$) δ 166.0, 163.7, 155.3, 154.8, 132.0, 130.9 (2), 122.5 (2), 113.8, 111.5, 108.8, 103.5, 67.2, 66.0, 55.7, 29.9; IR (KBr) ν_{max} 3392, 2918, 2848, 1701, 1606, 1510, 1458, 1259, 1164, 1108, 1022 cm^{-1}; HRMS (ESI+) *m*/*z* [M + H$^+$] calcd for $C_{17}H_{17}O_5$, 301.1076, found 301.1071.

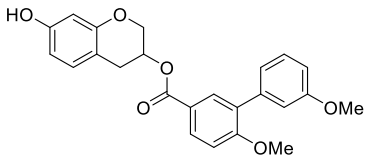

7-Hydroxychroman-3-yl 3′,6-Dimethoxy-[1,1′-biphenyl]-3-carboxylate (21m): A solution of **20b** (10 mg, 0.039 mmol) in dichloromethane (0.5 mL) was added to a stirred solution 4-methoxybenzoic acid (12 mg, 0.08 mmol), *N*,*N*′-dicyclohexylcarbodiimide (17 mg, 0.08 mmol), and 4-dimethylaminopyridine (4.8 mg, 0.04 mmol) under argon at 0 °C. The resulting solution was stirred for 6 h at rt and then filtered. The filtrate was diluted with dichloromethane (5 mL) and washed with 0.5 N HCl (2 × 4 mL) and then with saturated sodium bicarbonate (2 × 4 mL) solution. The combined organic layers were washed with saturated sodium chloride solution (4 mL), dried over anhydrous sodium sulfate, filtered, and concentrated. The residue was purified by flash

chromatography (SiO_2, 1:8 EtOAc/hexanes) to afford 7-(benzyloxy)chroman-3-yl 3′,6-dimethoxy-[1,1′-biphenyl]-3-carboxylate (17 mg, 87.4%) as a colorless oil, which was used further as obtained for hydrogenolysis): ^{1}H NMR (500 MHz, $CDCl_3$) δ 7.99 (d, *J* = 8.4 Hz, 2H), 7.48–7.42 (m, 2H), 7.42–7.36 (m, 2H), 7.37–7.31 (m, 2H), 7.08 (dt, *J* = 7.7, 1.2 Hz, 1H), 7.04 (dd, *J* = 2.6, 1.6 Hz, 1H), 6.99–6.95 (m, 2H), 6.91 (ddd, *J* = 8.2, 2.6, 0.9 Hz, 1H), 6.58 (dd, *J* = 8.4, 2.6 Hz, 1H), 6.53 (d, *J* = 2.5 Hz, 1H), 5.49 (qd, *J* = 5.0, 2.4 Hz, 1H), 5.03 (s, 2H), 4.31 (ddd, *J* = 11.4, 5.2, 1.7 Hz, 1H), 4.25 (ddd, *J* = 11.4, 2.5, 1.1 Hz, 1H), 3.21 (dd, *J* = 16.6, 5.1 Hz, 1H), 3.06–2.90 (m, 1H); ^{13}C NMR (125 MHz, $CDCl_3$) δ 166.0, 160.6, 159.5, 158.7, 154.8, 138.9, 137.2, 132.6, 131.3, 130.7, 130.6, 129.3, 128.8 (2), 128.2, 127.7 (2), 122.5, 122.2, 115.4, 113.1, 111.6, 110.7, 108.9, 102.7, 70.3, 67.2, 66.2, 56.0, 55.5, 30.0. 7-(Benzyloxy)chroman-3-yl 3′,6-dimethoxy-[1,1′-biphenyl]-3-carboxylate (12 mg, 0.024 mmol) and palladium/carbon (10%) were suspended in tetrahydrofuran (2 mL) and stirred for 18 h under a hydrogen atmosphere. The suspension was filtered through a small pad of celite. The eluent was concentrated and the residue purified by flash chromatography (SiO_2, 1:1 EtOAc/hexanes) to give **21m** (9 mg, 91.4%) as a colorless oil: ^{1}H NMR (500 MHz, $CDCl_3$) δ 8.01–7.94 (m, 2H), 7.34 (t, *J* = 7.9 Hz, 1H), 7.10–7.05 (m, 1H), 7.03 (dd, *J* = 2.6, 1.6 Hz, 1H), 6.97 (d, *J* = 8.6 Hz, 1H), 6.95–6.88 (m, 2H), 6.42 (dd, *J* = 8.2, 2.6 Hz, 1H), 6.38 (d, *J* = 2.5 Hz, 1H), 5.48 (qd, J = 5.0, 2.4 Hz, 1H), 4.73 (br s, 1 H), 4.31 (ddd, *J* = 11.4, 5.1, 1.8 Hz, 1H), 4.24 (ddd, *J* = 11.5, 2.4, 1.1 Hz, 1H), 3.87 (s, 3H), 3.84 (s, 3H), 3.19 (ddt, *J* = 16.6, 5.0, 1.2 Hz, 1H), 3.03–2.90 (m, 1H); ^{13}C NMR (125 MHz, $CDCl_3$) δ 166.0, 160.6, 159.5, 155.3, 154.8, 138.9, 132.7, 131.3, 130.9, 130.6, 129.3, 122.5, 122.2, 115.5, 113.1, 111.5, 110.8, 108.9, 103.5, 67.2, 66.2, 56.0, 55.5, 30.0; IR (KBr) ν_{max} 3411, 2921, 1701, 1598, 1510, 1278, 1224, 1155, 1116, 1043, 754 cm^{-1}; HRMS (ESI+) *m*/*z* [M + H^+] calcd for $C_{24}H_{23}O_6$, 407.1495, found 407.1475.

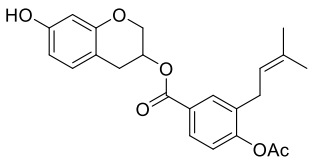

7-Hydroxychroman-3-yl 4-Acetoxy-3-(3-methylbut-2-en-1-yl)benzoate (21n): 4-Acetoxy-3-(3-methylbut-2-en-1-yl)benzoic acid (39 mg, 0.156 mmol) and thionyl chloride (38 μL, 0.312 mmol) in THF (5 mL) were heated at reflux for 3 h under argon, cooled to rt, and concentrated. The residue was dissolved in dichloromethane (0.5 mL) and added dropwise to a stirred solution of **20b** (20 mg, 0.078) in dichloromethane (0.7 mL) with trimethylamine (0.3 mL) under argon at 0 °C. The resulting mixture was stirred for 6 h at rt before solvent was removed. The residue was purified by flash chromatography (SiO_2 1:4 EtOAc/hexanes) to give 7-benzyloxychroman-3-yl 4-acetoxy-3-(3-methylbut-2-en-1-yl)benzoate (26 mg, 84%) as a colorless oil, which was used as for hydrogenolysis: ^{1}H NMR (400 MHz, $CDCl_3$) δ 7.90–7.82 (m, 2H), 7.48–7.37 (m, 4H), 7.37–7.31 (m, 1H), 7.06 (d, *J* = 8.4 Hz, 1H), 6.97 (dt, *J* = 8.3, 0.9 Hz, 1H), 6.59 (dd, *J* = 8.4, 2.6 Hz, 1H), 6.53 (d, *J* = 2.5 Hz, 1H), 5.49 (qd, *J* = 4.7, 2.2 Hz, 1H), 5.18 (dddd, *J* = 7.3, 5.8, 2.9, 1.5 Hz, 1H), 5.04 (s, 2H), 4.33 (ddd, *J* = 11.6, 4.8, 1.9 Hz, 1H), 4.28–4.16 (m, 1H), 3.87 (s, 3H), 3.84 (s, 3H), 3.21 (m, 3H), 3.04–2.90 (m, 1H), 2.32 (s, 3H), 1.72 (q, *J* = 1.3 Hz, 3H), 1.70–1.64 (m, 3H). A solution of palladium acetate (1.3 mg, 0.006 mg), trimethylamine (4 μL, 0.03 mmol), triethylsilane (24 μL, 0.15) in dichloromethane (0.8 mL) was stirred for 15 min under argon before the addition of a solution of 7-benzyloxychroman-3-yl 4-acetoxy-3-(3-methylbut-2-en-1-yl)benzoate (15 mg, 0.03 mmol) in dichloromethane (0.4 mL). The resulting mixture was stirred for 15 h, quenched with saturated ammonium chloride (2 mL) and extracted with ether (3 × 4 mL). The combined organic layers were washed with saturated sodium chloride solution, dried over anhydrous sodium sulfate, filtered and concentrated. The residue was purified by flash chromatography (SiO_2, 1:2

EtOAc/hexanes) to give **21n** (14.8 mg, 53.4%) as a colorless oil: ^{1}H NMR (500 MHz, $CDCl_3$) δ 7.88 (d, *J* = 2.1 Hz, 1H), 7.84 (dd, *J* = 8.4, 2.2 Hz, 1H), 7.06 (d, *J* = 8.4 Hz, 1H), 6.92 (dt, *J* = 8.3, 0.9 Hz, 1H), 6.46–6.40 (m, 1H), 6.38 (d, *J* = 2.5 Hz, 1H), 5.49 (qd, *J* = 4.7, 2.2 Hz, 1H), 5.17 (dddt, *J* = 7.3, 5.9, 2.9, 1.4 Hz, 1H), 4.63 (s, 1H), 4.32 (ddd, *J* = 11.5, 4.8, 1.9 Hz, 1H), 4.22 (dt, *J* = 11.4, 1.6 Hz, 1H), 3.24 (d, *J* = 7.2 Hz, 2H), 3.18 (ddt, *J* = 16.7, 5.1, 1.2 Hz, 1H), 2.94 (ddd, *J* = 16.5, 4.7, 1.8 Hz, 1H), 2.32 (s, 3H), 1.72 (q, *J* = 1.3 Hz, 3H), 1.67 (d, *J* = 1.3 Hz, 3H); ^{13}C NMR (125 MHz, $CDCl_3$) δ 167.8, 164.4, 154.0, 153.6, 151.7, 132.9, 130.9, 129.6 (2), 127.7, 126.7, 121.4, 119.7, 110.1, 107.6, 102.2, 65.8, 65.1, 28.7, 27.7, 24.6, 19.8, 16.8; IR (KBr) ν_{max} 3419, 2823, 2854, 1716, 1596, 1456, 1286, 1201, 1163, 1054, 796 cm^{-1}; HRMS (ESI+) *m*/*z* [M + H^+] calcd for $C_{23}H_{25}O_6$, 397.1651, found 397.1642.

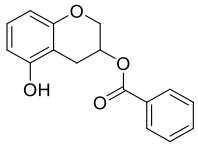

5-Hydroxychroman-3-yl Benzoate (21o): A solution of **20c** (9 mg, 0.035 mmol), in dichloromethane (0.5 mL) was added to a stirred solution of benzoic acid (8.6 mg, 0.07 mmol), N,N′-dicyclohexylcarbodiimide (23 mg, 0.11 mmol) and 4-dimethylaminopyridine (4.2 mg, 0.035 mmol) under argon at 0 °C. The resulting solution was stirred for 6 h at rt and then filtered. The filtrate was diluted with dichloromethane (5 mL) and washed with 0.5 N HCl (2 × 4 mL) and saturated sodium bicarbonate (2 × 4 mL) solution. The combined organic layers were washed with saturated sodium chloride solution (4 mL), dried over anhydrous sodium sulfate, filtered and concentrated. The residue was purified by flash chromatography (SiO_2, 1:9 EtOAc/hexanes) to give 5-(benzyloxy)chroman-3-yl benzoate (21 mg, 90%) as a colorless oil, which was used as is for hydrogenolysis: ^{1}H NMR (500 MHz, $CDCl_3$) δ 8.08–7.97 (m, 2H), 7.66–7.50 (m, 1H), 7.49–

7.28 (m, 7H), 7.12 (tt, *J* = 8.3, 0.8 Hz, 1H), 6.57 (ddd, *J* = 14.2, 8.3, 1.0 Hz, 2H), 5.56 (dtd, *J* = 5.3, 4.4, 2.2 Hz, 1H), 5.08 (s, 2H), 4.34 (ddd, *J* = 11.4, 4.9, 1.9 Hz, 1H), 4.23 (ddd, *J* = 11.4, 2.2, 1.1 Hz, 1H), 3.17 (ddt, *J* = 18.0, 5.7, 1.0 Hz, 1H), 3.03 (ddd, *J* = 17.8, 4.3, 1.7 Hz, 1H); ^{13}C NMR (125 MHz, $CDCl_3$) δ 166.2, 157.5, 155.0, 137.2, 133.3, 130.2, 130.0 (2), 128.8, 128.5 (2), 128.1 (2), 127.5 (2), 127.4, 109.8, 108.9, 103.9, 70.2, 66.8, 66.0, 25.7. 5-(Benzyloxy)chroman-3-yl benzoate (5 mg, 0.014 mmol) and palladium/carbon (10%) were suspended in tetrahydrofuran (2 mL) and stirred for 18 h under a hydrogen atmosphere The suspension was filtered through a small pad of celite. The eluent was concentrated and the residue purified by flash chromatography (SiO_2, 1:1 EtOAc/hexanes) to give **21o** (3 mg, 93%) as a colorless oil: ^{1}H NMR (500 MHz, $CDCl_3$) δ 8.10–7.92 (m, 2H), 7.62–7.47 (m, 1H), 7.47–7.35 (m, 2H), 7.01 (t, *J* = 8.1 Hz, 1H), 6.52 (dd, *J* = 8.2, 1.0 Hz, 1H), 6.38 (dd, *J* = 8.0, 1.0 Hz, 1H), 5.55 (tdd, *J* = 5.2, 4.4, 2.2 Hz, 1H), 4.84 (br s, 1 H), 4.33 (ddd, *J* = 11.4, 4.9, 1.9 Hz, 1H), 4.22 (dt, *J* = 11.6, 1.5 Hz, 1H), 3.12 (dd, *J* = 17.4, 5.5 Hz, 1H), 2.97 (ddd, *J* = 17.5, 4.3, 1.8 Hz, 1H); ^{13}C NMR (125 MHz, $CDCl_3$) δ 166.3, 155.3, 154.5, 133.4, 130.1, 130.0, 128.6 (2), 127.7 (2), 109.4, 107.4, 107.2, 66.8, 65.9, 25.3. IR (KBr) ν_{max} 3374, 2921, 1703, 1681,1476, 1098, 770 cm^{-1}; HRMS (ESI-) *m*/*z* [M – H$^+$] calcd for $C_{16}H_{13}O_4$, 269.0814, found 269.0804.

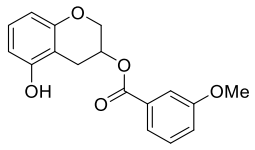

5-Hydroxychroman-3-yl 3-Methoxybenzoate (21p): A solution of **20c** (14 mg, 0.055 mmol) in dichloromethane (0.5 mL) was added to a stirred solution of 3-methoxybenzoic acid (17 mg, 0.11 mmol), N,N′-dicyclohexylcarbodiimide (23 mg, 0.11 mmol) and 4-dimethylaminopyridine (8 mg, 0.11 mmol) under argon at 0 °C. The resulting solution was stirred for 6 h at rt and then filtered.

The eluent was diluted with dichloromethane (5 mL) and washed with 0.5 N HCl (2 × 4 mL) and then with saturated sodium bicarbonate (2 × 4 mL) solution. The combined organic layers were washed with saturated sodium chloride solution (4 mL), dried over anhydrous sodium sulfate, and filtered and the solvent removed. The residue was purified by flash chromatography (SiO_2, 1:9 EtOAc/hexanes) to afford 5-(benzyloxy)chroman-3-yl 3-methoxybenzoate (19 mg, 90%) as a colorless oil, which was used as is for hydrogenolysis: ^{1}H NMR (400 MHz, $CDCl_3$) δ 7.61 (dt, *J* = 7.7, 1.3 Hz, 1H), 7.54 (dd, *J* = 2.7, 1.5 Hz, 1H), 7.47–7.29 (m, 6H), 7.15–7.05 (m, 2H), 6.57 (ddd, *J* = 10.7, 8.3, 1.0 Hz, 2H), 5.63–5.49 (m, 1H), 5.08 (s, 2H), 4.32 (ddd, *J* = 11.4, 5.1, 1.8 Hz, 1H), 4.26–4.18 (m, 1H), 3.83 (s, 3H), 3.17 (dd, *J* = 17.8, 5.5 Hz, 1H), 3.09–2.95 (m, 1H); ^{13}C NMR (125 MHz, $CDCl_3$) δ 166.1, 159.7, 157.5, 155.0, 137.2, 131.5, 129.6, 128.8 (2), 128.1, 127.6, 127.4 (2), 122.4, 119.7, 114.5, 109.8, 108.8, 103.9, 70.2, 66.7(2), 66.2, 55.7. 5-(Benzyloxy)chroman-3-yl 3-methoxybenzoate (18 mg, 0.044 mmol) and palladium/carbon (10%) were suspended in tetrahydrofuran (2 mL) and stirred for 18 h under a hydrogen atmosphere. The suspension was filtered through a small pad of celite. The eluent was concentrated and the residue purified by flash chromatography (SiO_2, 1:1 EtOAc/hexanes) to give **21p** (12.9 mg, 92.4%) as a colorless oil: ^{1}H NMR (500 MHz, $CDCl_3$) δ 7.53 (dt, *J* = 7.7, 1.3 Hz, 1H), 7.46 (dd, *J* = 2.7, 1.5 Hz, 1H), 7.24 (t, *J* = 8.0 Hz, 1H), 7.02 (ddd, *J* = 8.2, 2.7, 1.0 Hz, 1H), 6.93 (t, *J* = 8.1 Hz, 1H), 6.44 (dd, *J* = 8.3, 1.0 Hz, 1H), 6.31 (dd, *J* = 8.0, 1.0 Hz, 1H), 5.54–5.43 (m, 1H), 4.87 (s, 1H), 4.27–4.21 (m, 1H), 4.15 (dt, *J* = 11.4, 1.6 Hz, 1H), 3.75 (s, 3H), 3.06 (dd, *J* = 17.4, 5.5 Hz, 1H), 2.90 (ddd, *J* = 17.4, 4.6, 1.7 Hz, 1H); ^{13}C NMR (125 MHz, $CDCl_3$) δ 166.2, 159.7, 155.3, 154.5, 131.4, 129.6, 127.7, 122.4, 119.8, 114.5, 109.4, 107.4, 107.2, 66.8, 66.1, 55.7, 25.3. IR (KBr) ν_{max} cm^{-1} ; HRMS (ESI-) *m*/*z* [M – H^+] calcd for $C_{17}H_{15}O_5$, 299.0920, found 299.0934.

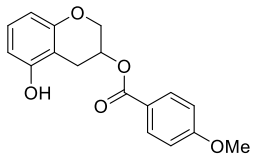

5-Hydroxychroman-3-yl 4-Methoxybenzoate (**21q**): A solution of **20c** (11 mg, 0.042 mmol) in dichloromethane (0.5 mL) was added to a stirred solution of 4-methoxybenzoic acid (13 mg, 0.09 mmol), N,N′-dicyclohexylcarbodiimide (18 mg, 0.085 mmol) and 4-dimethylaminopyridine (5 mg, 0.05 mmol) under argon at 0 °C. The resulting solution was stirred for 6 h at rt and then filtered. The filtrate was diluted with dichloromethane (5 mL) and washed with 0.5 N HCl (2 × 4 mL) and then with saturated sodium bicarbonate (2 × 4 mL) solution. The combined organic layers were washed with saturated sodium chloride solution (4 mL), dried over anhydrous Na_2SO_4, filtered, and concentrated. The residue was purified by flash chromatography (SiO_2, 1:9 EtOAc/hexanes) to give 5-(benzyloxy)chroman-4-yl 3-methoxybenzoate (15 mg, 91.5%) as a colorless oil, which was used as is for hydrogenolysis: ^{1}H NMR (500 MHz, $CDCl_3$) δ 8.09–7.85 (m, 2H), 7.50–7.30 (m, 5H), 7.11 (t, *J* = 8.2 Hz, 1H), 6.97–6.83 (m, 2H), 6.60–6.56 (m, 1H), 6.57–6.52 (m, 1H), 5.63–5.48 (m, 1H), 5.06 (s, 2H), 4.31 (ddd, *J* = 11.4, 5.0, 1.9 Hz, 1H), 4.27–4.17 (m, 1H), 3.85 (s, 3H), 3.16 (dd, *J* = 17.8, 5.5 Hz, 1H), 3.01 (ddd, *J* = 17.8, 4.4, 1.7 Hz, 1H); ^{13}C NMR (125 MHz, $CDCl_3$) δ 166.0, 163.7, 157.5, 155.1, 137.3, 132.1, 128.8 (2), 128.1 (2), 127.5 (2), 127.4, 122.6, 113.8 (2), 109.8, 109.0, 103.8, 70.2, 66.9, 65.7, 55.6, 25.7. 5-(Benzyloxy)chroman-4-yl 3-methoxybenzoate (5 mg, 0.014 mmol) and palladium/carbon (10%) were suspended in tetrahydrofuran (2 mL) and stirred for 18 h under a hydrogen atmosphere. The suspension was filtered through a small pad of celite. The eluent was concentrated and the residue purified by flash chromatography (SiO_2, 1:1 EtOAc/hexanes) to give **21q** (3.5 mg, 93%) as a colorless oil: ^{1}H NMR (500 MHz, $CDCl_3$) δ 8.10–7.92 (m, 2H), 7.64–7.49 (m, 1H), 7.49–7.38 (m, 2H), 7.02 (t, *J* = 8.1

Hz, 1H), 6.53 (dd, *J* = 8.2, 1.0 Hz, 1H), 6.40 (dd, *J* = 8.0, 1.0 Hz, 1H), 5.56 (tdd, *J* = 5.2, 4.4, 2.2 Hz, 1H), 4.86 (s, 1H), 4.35 (ddd, *J* = 11.4, 4.9, 1.9 Hz, 1H), 4.23 (dt, *J* = 11.6, 1.6 Hz, 1H), 3.14 (dd, *J* = 17.4, 5.5 Hz, 1H), 2.99 (ddd, *J* = 17.5, 4.3, 1.8 Hz, 1H); ^{13}C NMR (125 MHz, $CDCl_3$) δ 166.3, 155.3, 154.5 (2), 133.4 (2), 130.1, 130.0, 128.6, 127.7, 109.4 (2), 107.4, 107.2, 66.8, 65.9, 25.3; IR (KBr) ν_{max} 3384, 2921, 1701, 1683, 1606, 1471, 1259, 1168, 1099, 771 cm^{-1}; HRMS (ESI-) *m*/*z* [M – H^+] calcd for $C_{17}H_{15}O_5$, 299.0920, found 299.0928.

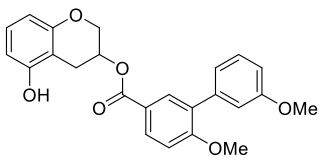

5-Hydroxychroman-3-yl 3′,6-Dimethoxy-[1,1′-biphenyl]-3-carboxylate (**21r**): A solution of **22c** (11 mg, 0.042 mmol), in dichloromethane (0.5 mL) was added to a stirred solution of 3′,6-dimethoxy-[1,1′-biphenyl]-3-carboxylic acid (22 mg, 0.085 mmol), *N*,*N*′-dicyclohexylcarbodiimide (18 mg, 0.085 mmol), and 4-dimethylaminopyridine (5 mg, 0.0042 mmol) under argon at 0 °C. The resulting solution was stirred for 6 h at rt and then filtered. The filtrate was diluted with dichloromethane (5 mL) and washed with 0.5 N HCl (2 × 4 mL) and saturated sodium bicarbonate (2 × 4 mL) solution. The combined organic layers were washed with saturated sodium chloride solution (4 mL), dried over anhydrous sodium sulfate, filtered, and concentrated. The residue was purified by flash chromatography (SiO_2, 1:8 EtOAc/hexanes) to afford 7-(benzyloxy)chroman-3-yl 3′,6-dimethoxy-[1,1′-biphenyl]-3-carboxylate (18 mg, 85%) as a colorless oil, which was used further as obtained: ^{1}H NMR (400 MHz, $CDCl_3$) δ 8.07–7.92 (m, 2H), 7.49–7.28 (m, 6H), 7.19–7.05 (m, 2H), 7.04 (dd, *J* = 2.7, 1.6 Hz, 1H), 6.97 (d, *J* = 8.5 Hz, 1H), 6.91 (ddd, *J* = 8.4, 2.7, 1.0 Hz, 1H), 6.60–6.54 (m, 2H), 5.54 (qd, *J* = 5.1, 2.4 Hz, 1H), 5.08 (s, 2H), 4.30 (ddd, *J* = 11.3, 5.2, 1.7 Hz, 1H), 4.23 (dd, *J* = 11.6, 2.1 Hz, 1H), 3.87 (s, 3H), 3.84 (s,

3H), 3.18 (dd, *J* = 17.7, 5.6 Hz, 1H), 3.10–2.90 (m, 1H); ^{13}C NMR (100 MHz, $CDCl_3$) δ 166.0, 160.5, 159.4, 157.5, 155.0, 138.9, 137.2, 132.6, 131.3, 130.6, 129.2, 128.7 (2), 128.1, 127.5 (2), 127.4, 122.6, 122.2, 115.4, 113.2, 110.7, 109.8, 109.0, 103.9, 70.2, 66.8, 65.9, 56.0, 55.5, 25.8. 7-(Benzyloxy)chroman-3-yl 3′,6-dimethoxy-[1,1′-biphenyl]-3-carboxylate (18 mg, 0.036 mmol) and palladium/carbon (10%) were suspended in tetrahydrofuran (2 mL) and stirred for 18 h under a hydrogen atmosphere. The suspension was filtered through a small pad of celite. The eluent was concentrated and the residue purified by flash chromatography (SiO_2, 1:1 EtOAc/hexanes) to give **21r** (13 mg, 88.2%) as a colorless oil: ^{1}H NMR (500 MHz, $CDCl_3$) δ 7.96–7.88 (m, 2H), 7.25 (t, *J* = 7.9 Hz, 1H), 7.00 (dt, *J* = 7.6, 1.2 Hz, 1H), 6.96 (dd, *J* = 2.6, 1.5 Hz, 1H), 6.94–6.87 (m, 2H), 6.83 (ddd, *J* = 8.3, 2.6, 1.0 Hz, 1H), 6.44 (dd, *J* = 8.3, 1.0 Hz, 1H), 6.31 (dd, *J* = 8.0, 1.1 Hz, 1H), 5.55–5.34 (m, 1H), 4.86 (br s, 1 H), 4.22 (ddd, *J* = 11.3, 5.2, 1.7 Hz, 1H), 4.16 (ddd, *J* = 11.4, 2.4, 1.2 Hz, 1H), 3.78 (s, 3H), 3.76 (s, 3H), 3.06 (dd, *J* = 17.3, 5.6 Hz, 1H), 2.92–2.83 (m, 1H); ^{13}C NMR (125 MHz, $CDCl_3$) δ 166.0, 160.6, 159.4, 155.3, 154.5, 138.9, 132.7, 131.3, 130.7, 129.3, 127.6, 122.5, 122.2, 115.4, 113.2, 110.7, 109.4, 107.4, 107.3, 66.9, 65.7, 56.0, 55.5, 25.4; IR (KBr) ν_{max} 3396, 2933, 2837, 1712, 1598, 1469, 1440, 1249, 1031, 771, 711 cm^{-1}; HRMS (ESI+) *m*/*z* [M + H$^+$] calcd for $C_{24}H_{23}O_6$, 407.1495, found 407.1482.

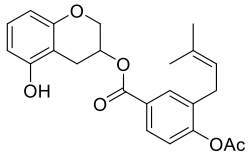

5-Hydroxychroman-3-yl 4-Acetoxy-3-(3-methylbut-2-en-1-yl)benzoate (21s): A solution of **20c** (10 mg, 0.04 mmol), in dichloromethane (0.5 mL) was added to a stirred solution of 4-acetoxy-3-(3-methylbut-2-en-1-yl)benzoic acid (20 mg, 0.08 mmol), *N*,*N*′-dicyclohexylcarbodiimide (16 mg, 0.08 mmol), and 4-dimethylaminopyridine (5 mg, 0.042 mmol) under argon at 0 °C. The

resulting solution was stirred for 6 h at rt and filtered. The filtrate was diluted with dichloromethane (5 mL) and washed with 0.5 N HCl (2 × 4 mL) and then with saturated sodium bicarbonate (2 × 4 mL) solution. The combined organic layers were washed with saturated sodium chloride solution (4 mL), dried over anhydrous sodium sulfate filtered and solvent was removed. The residue was purified by flash chromatography (SiO_2, 1:8 EtOAc/hexanes) to give 5-(benzyloxy)chroman-3-yl 4-acetoxy-3-(3-methylbut-2-en-1-yl)benzoate (13 mg, 72.2%) as a colorless oil, which was used as is in the next step: ^{1}H NMR (500 MHz, $CDCl_3$) δ 7.94–7.83 (m, 2H), 7.45–7.29 (m, 5H), 7.10 (t, *J* = 8.3 Hz, 1H), 7.06 (d, *J* = 8.4 Hz, 1H), 6.62–6.55 (m, 2H), 5.67–5.48 (m, 1H), 5.18 (dddd, *J* = 7.2, 5.8, 2.9, 1.4 Hz, 1H), 5.07 (s, 2H), 4.31 (ddd, *J* = 11.4, 4.9, 1.9 Hz, 1H), 4.26–4.17 (m, 1H), 3.25 (d, *J* = 7.1 Hz, 2H), 3.14 (dd, *J* = 17.8, 5.4 Hz, 1H), 3.01 (ddd, *J* = 17.8, 4.4, 1.8 Hz, 1H), 2.32 (s, 3H), 1.71 (q, *J* = 1.3 Hz, 3H), 1.67 (d, *J* = 1.3 Hz, 3H); ^{13}C NMR (125 MHz, $CDCl_3$) δ 169.0, 165.6, 157.5, 155.0, 152.9, 137.2, 134.1, 132.2, 129.0, 128.7 (2), 128.1, 128.0 (2), 127.5 (2), 127.4, 122.6, 121.0, 109.8, 108.8, 103.9, 70.2, 66.7, 66.0, 28.9, 25.9, 25.7, 21.1, 18.1. For benzyl group removal, a solution of palladium acetate (1 mg, 0.004 mmol), trimethylamine (4 μL, 0.025 mmol), and triethylsilane (19 μL, 0.0112) in DCM (0.8 mL) was stirred for 15 min under argon before the addition of a solution of 5-(benzyloxy)chroman-3-yl 4-acetoxy-3-(3-methylbut-2-en-1-yl)benzoate (12 mg, 0.025 mmol) in dichloromethane (0.2 mL) reaction was stirred for 15 h. The reaction mixture was quenched with saturated ammonium chloride (2 mL) and extracted with ether (3 × 4 mL). The combined organic layers were washed with saturated sodium chloride solution, dried over Na_2SO_4, filtered, and concentrated. The residue was purified by flash chromatography (SiO_2, 1:2 EtOAc/hexanes) to afford **21s** as colorless oil: ^{1}H NMR (500 MHz, $CDCl_3$) δ 8.02–7.67 (m, 2H), 7.05 (d, *J* = 8.3 Hz, 1H), 7.03–6.98 (m, 1H), 6.53 (dd, *J* = 8.3, 1.1 Hz, 1H), 6.43 (dd, *J* = 8.1, 1.0 Hz, 1H), 5.52 (tdd, *J* = 5.1, 4.2, 2.1 Hz, 1H), 5.17 (dddt, *J* = 7.3, 5.8, 2.9, 1.4 Hz, 1H), 4.31

(ddd, *J* = 11.5, 4.8, 2.0 Hz, 1H), 4.24–4.12 (m, 1H), 3.24 (d, *J* = 7.2 Hz, 2H), 3.05 (dd, *J* = 17.6, 5.3 Hz, 1H), 2.94 (ddd, *J* = 17.5, 4.4, 1.8 Hz, 1H), 2.32 (s, 3H), 1.71 (q, *J* = 1.3 Hz, 3H), 1.69–1.65 (m, 3H); ^{13}C NMR (125 MHz, $CDCl_3$) δ 168.8, 165.4, 155.0, 154.6, 152.7, 133.9, 131.9, 128.8, 127.8 (2), 127.1, 122.4, 120.8, 110.8, 110.5, 109.5, 66.4, 66.0, 28.7, 25.8, 25.7, 20.9, 17.8; IR (KBr) ν_{max} 3429, 2854, 1716, 1595, 1458, 1286, 1161, 1054 cm^{-1}; HRMS (ESI+) *m*/*z* [M + H^+] calcd for $C_{23}H_{25}O_6$, 397.1651, found 397.1662.

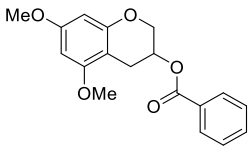

5,7-Dimethoxychroman-3-yl Benzoate (**25a**): A solution of **24** (10 mg, 0.04 mmol), in dichloromethane (0.5 mL) was added to a stirred solution of benzoic acid (12 mg, 0.1 mmol), *N*,*N*′-dicyclohexylcarbodiimide (20.6 mg, 0.1 mmol), and 4-dimethylaminopyridine (5 mg, 0.042 mmol) under argon at 0 °C . The resulting solution was stirred for 6 h at rt and then filtered. The filtrate was diluted with dichloromethane (5 mL) and washed with 0.5 N HCl (2 × 4 mL) and then with saturated sodium bicarbonate (2 × 4 mL) solution. The combined organic layers were washed with saturated sodium chloride solution (4 mL), dried over anhydrous sodium sulfate, filtered, and concentrated. The residue was purified by flash chromatography (SiO_2, 1:7 EtOAc/hexanes) to afford **25a** (13 mg, 90%) as a colorless oil: ^{1}H NMR (500 MHz, $CDCl_3$) δ 8.14–7.91 (m, 2H), 7.55 (ddt, *J* = 7.6, 6.8, 1.1 Hz, 1H), 7.47–7.37 (m, 2H), 6.11 (s, 2H), 5.52 (tdt, *J* = 5.5, 4.5, 1.9 Hz, 1H), 4.32 (dddd, *J* = 11.4, 4.9, 1.9, 0.9 Hz, 1H), 4.21 (ddd, *J* = 11.5, 2.2, 1.2 Hz, 1H), 3.79 (dd, *J* = 2.9, 0.9 Hz, 6H), 3.09–2.94 (m, 1H), 2.88 (ddd, *J* = 17.4, 4.3, 1.8 Hz, 1H); ^{13}C NMR (125 MHz, $CDCl_3$) δ 166.3, 159.8, 159.1, 155.3, 133.4, 130.3, 130.1 (2), 128.6 (2), 100.8, 93.4, 92.0, 67.1, 66.2, 55.7,

55.6, 25.1; IR (KBr) ν_{max} 2931, 1716, 1620, 1591, 1499, 1456, 1145, 1045, 754 cm^{-1}; HRMS (ESI+) *m*/*z* [M + H^+] calcd for $C_{18}H_{19}O_5$, 315.1232, found 315.1239.

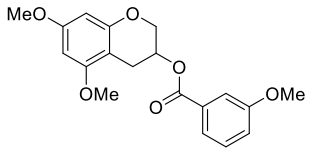

5,7-Dimethoxychroman-3-yl 3-Methoxybenzoate (25b): A solution of **24** (10 mg, 0.04 mmol), in dichloromethane (0.5 mL) was added to a stirred solution of 3-methoxybenzoic acid (15 mg, 0.1 mmol), *N*,*N*′-dicyclohexylcarbodiimide (20.6 mg, 0.1 mmol), and 4-dimethylaminopyridine (5 mg, 0.042 mmol) under argon at 0 °C. The resulting solution was stirred for 6 h at rt and then filtered. The filtrate was diluted with dichloromethane (5 mL) and washed with 0.5 N HCl (2 × 4 mL) and then with saturated sodium bicarbonate (2 × 4 mL) solution. The combined organic layers were washed with saturated sodium chloride solution (4 mL), dried over anhydrous sodium sulfate, filtered, and concentrated. The residue was purified by flash chromatography (SiO_2, 1:6 EtOAc/hexanes) to afford **25b** (13 mg, 80%) as a colorless oil: ^{1}H NMR (500 MHz, $CDCl_3$) δ 7.61 (dt, *J* = 7.7, 1.2 Hz, 1H), 7.54 (dd, *J* = 2.7, 1.5 Hz, 1H), 7.31 (t, *J* = 7.9 Hz, 1H), 7.09 (ddd, *J* = 8.3, 2.7, 1.1 Hz, 1H), 6.10 (d, *J* = 1.2 Hz, 2H), 5.69–5.42 (m, 1H), 4.30 (ddd, *J* = 11.4, 5.1, 1.8 Hz, 1H), 4.24–4.16 (m, 1H), 3.83 (s, 3H), 3.79 (s, 3H), 3.78 (s, 3H), 3.02 (ddd, *J* = 17.5, 5.6, 1.3 Hz, 1H), 2.86 (ddd, *J* = 17.4, 4.5, 1.7 Hz, 1H); ^{13}C NMR (125 MHz, $CDCl_3$) δ 166.2, 159.8, 159.7, 159.0, 155.3, 131.5, 129.6, 122.4, 119.6, 114.5, 100.7, 93.4, 92.0, 67.0, 66.3, 55.7, 55.6, 55.6, 25.1; IR (KBr) ν_{max} 2935, 2839, 1716, 1622, 1593, 1498, 1456, 1276, 1145, 1045, 754 cm^{-1}; HRMS (ESI+) *m*/*z* [M + H^+] calcd for $C_{19}H_{21}O_6$, 345.1338, found 345.1347.

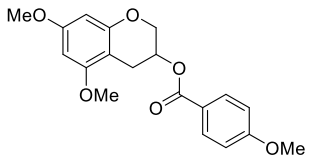

5,7-Dimethoxychroman-3-yl 4-Methoxybenzoate (25c): A solution of **24** (10 mg, 0.04 mmol), in dichloromethane (0.5 mL) was added to a stirred solution of 4-methoxybenzoic acid (15 mg, 0.1 mmol), *N*,*N*′-dicyclohexylcarbodiimide (20.6 mg, 0.1 mmol), and 4-dimethylaminopyridine (5 mg, 0.042 mmol) under argon at 0 °C. The resulting solution was stirred for 6 h at rt and then filtered. The filtrate was diluted with dichloromethane (5 mL) and washed with 0.5 N HCl (2 × 4 mL) and then with saturated sodium bicarbonate (2 × 4 mL) solution. The combined organic layers were washed with saturated sodium chloride solution (4 mL), dried over anhydrous sodium sulfate, filtered, and concentrated. The residue was purified by flash chromatography (SiO_2, 1:6 EtOAc/hexanes) to afford **25c** (14 mg, 86%) as a colorless oil: ^{1}H NMR (500 MHz, $CDCl_3$) δ 7.98 (ddd, *J* = 10.7, 5.1, 2.6 Hz, 2H), 7.27 (td, *J* = 4.5, 1.5 Hz, 1H), 6.89 (ddd, *J* = 8.5, 5.7, 2.6 Hz, 2H), 6.10 (m, 2H), 5.56–5.37 (m, 1H), 4.29 (m, 1H), 4.26–4.12 (m, 1H), 3.88–3.81 (s, 3H), 3.78 (s, 6H), 3.10–2.93 (m, 1H), 2.85 (dddd, *J* = 17.5, 5.7, 4.3, 2.3 Hz, 1H); ^{13}C NMR (125 MHz, $CDCl_3$) δ 166.0, 163.7, 159.8, 159.0, 155.3, 132.1 (2), 122.7, 113.8 (2), 100.9, 93.3, 91.9, 67.1, 65.8, 55.6, 55.6 (2), 25.1; IR (KBr) ν_{max} 2935, 1716, 1620, 1593, 1499, 1456, 1145, 1043 cm^{-1}; HRMS (ESI+) *m*/*z* [M + H$^+$] calcd for $C_{19}H_{21}O_6$, 345.1338, found 345.1347.

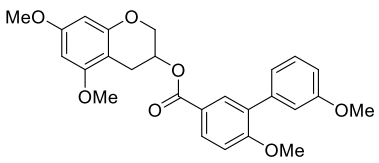

5,7-Dimethoxychroman-3-yl 3′,6-Dimethoxy-[1,1′-biphenyl]-3-carboxylate (**25d**): A solution of **24** (10 mg, 0.04 mmol), in dichloromethane (0.5 mL) was added to a stirred solution of 3′,6-

dimethoxy-[1,1′-biphenyl]-3-carboxylic acid (15 mg, 0.1 mmol), *N*,*N*′-dicyclohexylcarbodiimide (20.6 mg, 0.1 mmol), and 4-dimethylaminopyridine (5 mg, 0.042 mmol) under argon at 0 °C. The resulting solution was stirred for 6 h at rt and then filtered. The filtrate was diluted with dichloromethane (5 mL) and washed with 0.5 N HCl (2 × 4 mL) and then with saturated sodium bicarbonate (2 × 4 mL) solution. The combined organic layers were washed with saturated sodium chloride solution (4 mL), dried over anhydrous Na_2SO_4, filtered, and concentrated. The residue was purified by flash chromatography (SiO_2, 1:6 EtOAc/hexanes) to afford **25d** (18.4 mg, 82%) as a colorless oil: ^{1}H NMR (500 MHz, $CDCl_3$) δ 8.06–7.97 (m, 2H), 7.34 (t, *J* = 7.9 Hz, 1H), 7.08 (dt, *J* = 7.7, 1.2 Hz, 1H), 7.04 (dd, *J* = 2.6, 1.5 Hz, 1H), 6.97 (d, *J* = 8.6 Hz, 1H), 6.91 (ddd, *J* = 8.2, 2.6, 0.9 Hz, 1H), 6.10 (s, 2H), 5.54–5.42 (m, 1H), 4.28 (ddd, *J* = 11.3, 5.2, 1.7 Hz, 1H), 4.21 (ddd, *J* = 11.2, 2.3, 1.1 Hz, 1H), 3.87 (s, 3H), 3.84 (s, 3H), 3.79 (s, 3H), 3.78 (s, 3H), 3.02 (ddd, *J* = 17.4, 5.6, 1.2 Hz, 1H), 2.85 (ddd, *J* = 17.2, 4.6, 1.6 Hz, 1H); ^{13}C NMR (125 MHz, $CDCl_3$) δ 166.0, 160.5, 159.7, 159.4, 159.0, 155.3, 139.0, 132.6, 131.3, 130.6, 129.2, 122.7, 122.2, 115.4, 113.1, 110.7, 100.9, 93.3, 91.9, 67.1, 66.0, 56.0, 55.62, 55.6, 55.5, 25.2. IR (KBr) ν_{max} 2954, 2931, 1712, 1595, 1498, 1456, 1436, 1247, 1215, 1052, 813, 756 cm^{-1}; HRMS (ESI+) *m*/*z* [M + Na$^+$] calcd for $C_{26}H_{26}NaO_7$, 473.1576, found 473.1566.

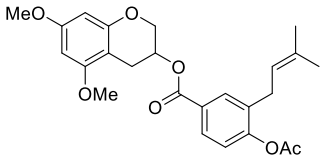

5,7-Dimethoxychroman-3-yl 4-Acetoxy-3-(3-methylbut-2-en-1-yl)benzoate (**25e**): A solution of **24** (20 mg, 0.08 mmol) in dichloromethane (1 mL) was added to a stirred solution of 4-acetoxy-3-(3-methylbut-2-en-1-yl)benzoic acid (48 mg, 0.19 mmol), *N*,*N*′-dicyclohexylcarbodiimide (40 mg, 0.19 mmol), and 4-dimethylaminopyridine (12 mg, 0.084 mmol) under argon at 0 °C. The

resulting solution was stirred for 6 h at rt and then filtered. The filtrate was diluted with dichloromethane (10 mL) and washed with 0.5 N HCl (2 × 8 mL) and then with saturated sodium bicarbonate (2 × 8 mL) solution. The combined organic layers were washed with saturated sodium chloride solution (8 mL), dried over anhydrous sodium sulfate, filtered, and concentrated. The residue was purified by flash chromatography (SiO_2, 1:7 EtOAc/hexanes) to afford **25e** (17 mg, 53%) as a colorless oil: ^{1}H NMR (500 MHz, $CDCl_3$) δ 7.90 (d, *J* = 2.1 Hz, 1H), 7.86 (dd, *J* = 8.4, 2.2 Hz, 1H), 7.06 (d, *J* = 8.4 Hz, 1H), 6.18 (s, 2H), 5.57–5.44 (m, 1H), 5.18 (dddd, *J* = 7.2, 5.8, 2.8, 1.4 Hz, 1H), 4.30 (ddd, *J* = 11.4, 4.9, 1.9 Hz, 1H), 4.25 – 4.02 (m, 1H), 3.79 (s, 3H), 3.78 (s, 3H), 3.25 (d, *J* = 7.2 Hz, 2H), 2.99 (ddd, *J* = 17.3, 5.4, 1.2 Hz, 1H), 2.86 (ddd, *J* = 17.4, 4.4, 1.8 Hz, 1H), 2.32 (s, 3H), 1.72 (q, *J* = 1.2 Hz, 3H), 1.69–1.63 (m, 3H); ^{13}C NMR (125 MHz, $CDCl_3$) δ 169.1, 165.7, 159.8, 159.0, 155.2, 152.9, 134.1 (2), 132.1, 129.0, 128.1, 122.6, 121.1, 100.7, 93.3, 91.9, 66.9, 66.2, 55.6, 55.6, 28.9, 25.9, 25.1, 21.1, 18.1; IR (KBr) ν_{max} 2937, 2844, 1737, 1622, 2595, 1242, 1218, 1201, 1145, 1128, 1058, 811 cm^{-1}; HRMS (ESI+) *m*/*z* [M + H$^+$] calcd for $C_{25}H_{29}O_7$, 441.1913, found 441.1894.

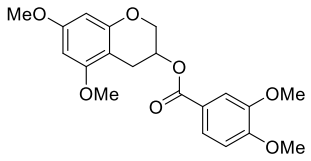

5,7-Dimethoxychroman-3-yl 3,4-Dimethoxybenzoate (**25f**): A solution of **24** (5 mg, 0.025 mmol) in dichloromethane (0.5 mL) was added to a stirred solution of 3,4-dimethoxybenzoic acid (9 mg, 0.05 mmol), *N*,*N*′-dicyclohexylcarbodiimide (10 mg, 0.05 mmol), and 4-dimethylaminopyridine (3 mg, 0.025 mmol) under argon at 0 °C. The resulting solution was stirred for 6 h at rt and then filtered. The filtrate was diluted with dichloromethane (5 mL) and washed with 0.5 N HCl (2 × 4 mL) and then with saturated sodium bicarbonate (2 × 4 mL) solution. The

combined organic layers were washed with saturated sodium chloride solution (4 mL), dried over anhydrous sodium sulfate, filtered, and concentrated. The residue was purified by flash chromatography (SiO_2, 1:6 EtOAc/hexanes) to afford **25f** (10 mg, 71.4%) as a colorless oil: ^{1}H NMR (500 MHz, $CDCl_3$) δ 7.65 (dd, *J* = 8.4, 2.0 Hz, 1H), 7.52 (d, *J* = 2.0 Hz, 1H), 6.85 (d, *J* = 8.5 Hz, 1H), 6.10 (s, 2H), 5.57–5.41 (m, 1H), 4.28 (ddd, *J* = 11.3, 5.1, 1.8 Hz, 1H), 4.21 (ddd, *J* = 11.3, 2.2, 1.1 Hz, 1H), 3.92 (d, *J* = 8.3 Hz, 6H), 3.79 (d, *J* = 4.1 Hz, 6H), 3.02 (ddd, *J* = 17.2, 5.5, 1.2 Hz, 1H), 2.86 (ddd, *J* = 17.3, 4.5, 1.6 Hz, 1H); ^{13}C NMR (125 MHz, $CDCl_3$) δ 159.9 (2), 159.5 (2), 155.4 (2), 138.5, 128.8, 128.3, 126.5, 100.5, 93.5, 92.4, 78.9, 66.6, 55.7 (2), 55.6 (2), 28.4; IR (KBr) ν_{max} 2931, 1701, 1558, 1458, 1419, 1271, 732 cm^{-1}; HRMS (ESI+) *m*/*z* [M + Na$^+$] calcd for $C_{20}H_{22}NaO_7$, 397.1263, found 397.1269.

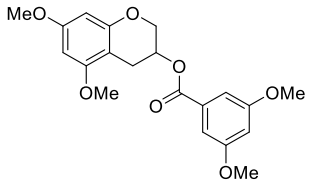

5,7-Dimethoxychroman-3-yl 3,5-Dimethoxybenzoate (**25g**): A solution of **24** (5 mg, 0.025 mmol) in dichloromethane (0.5 mL) was added to a stirred solution of 3,4-dimethoxybenzoic acid (9 mg, 0.05 mmol), *N*,*N*′-dicyclohexylcarbodiimide (10 mg, 0.05 mmol), and 4-dimethylaminopyridine (3 mg, 0.025 mmol) under argon at 0 °C. The resulting solution was stirred for 6 h at rt and then filtered. The filtrate was diluted with dichloromethane (5 mL) and washed with 0.5 N HCl (2 × 4 mL) and then with saturated sodium bicarbonate (2 × 4 mL) solution. The combined organic layers were washed with saturated sodium chloride solution (4 mL), dried over anhydrous sodium sulfate, filtered, and concentrated. The residue was purified by flash chromatography (SiO_2, 1:6 EtOAc/hexanes) to afford **25g** (11.9 mg, 85%) as a colorless oil: ^{1}H NMR (500 MHz, $CDCl_3$) δ 7.16 (d, *J* = 2.4 Hz, 2H), 6.64 (t, *J* = 2.4 Hz, 1H), 6.10 (s, 2H), 5.57–

5.43 (m, 1H), 4.28 (ddd, *J* = 11.3, 5.2, 1.7 Hz, 1H), 4.21 (ddd, *J* = 11.3, 2.4, 1.1 Hz, 1H), 3.85–3.73 (m, 12H), 3.02 (ddd, *J* = 17.3, 5.5, 1.2 Hz, 1H), 2.85 (ddd, *J* = 17.4, 4.7, 1.7 Hz, 1H); ^{13}C NMR (125 MHz, $CDCl_3$) δ 159.9 (2), 159.5 (2), 155.4 (2), 138.5, 128.8, 128.3, 126.5, 100.5 (2), 93.5, 92.4, 78.9, 66.6, 55.7, 55.6 (2), 28.4. IR (KBr) ν_{max} 2931, 1701, 1558, 1458, 1419, 1271, 732 cm^{-1}; HRMS (ESI+) *m*/*z* [M + Na^+] calcd for $C_{20}H_{22}NaO_7$, 397.1263, found 397.1269.

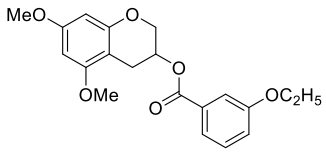

5,7-Dimethoxychroman-3-yl 3-Ethoxybenzoate (**25h**): A solution of **24** (10 mg, 0.04 mmol) in dichloromethane (0.5 mL) was added to a stirred solution of 3-ethoxybenzoic acid, *N*,*N*′-dicyclohexylcarbodiimide (20.6 mg, 0.1 mmol), and 4-dimethylaminopyridine (5 mg, 0.042 mmol) under argon at 0 °C. The resulting solution was stirred for 6 h and filtered. The filtrate was diluted with dichloromethane (5 mL) and washed with 0.5 N HCl (2 × 4 mL) and then with saturated sodium bicarbonate (2 × 4 mL) solution. The combined organic layers were washed with saturated sodium chloride solution (4 mL), dried over anhydrous sodium sulfate, filtered, and concentrated. The residue was purified by flash chromatography (SiO_2, 1:6 EtOAc/hexanes) to afford **25h** (14 mg, 82.3%) as a colorless oil: ^{1}H NMR (500 MHz, $(CD_3)_2CO$) δ 7.52 (ddd, *J* = 7.7, 1.5, 1.0 Hz, 1H), 7.46 (dd, *J* = 2.6, 1.5 Hz, 1H), 7.38 (t, *J* = 7.9 Hz, 1H), 7.16 (ddd, *J* = 8.2, 2.7, 1.0 Hz, 1H), 6.14 (d, *J* = 2.4 Hz, 1H), 6.06 (d, *J* = 2.4 Hz, 1H), 5.50–5.41 (m, 1H), 4.32 (ddd, *J* = 11.5, 4.5, 2.0 Hz, 1H), 4.22 (ddt, *J* = 11.5, 1.9, 0.9 Hz, 1H), 4.07 (q, *J* = 7.0 Hz, 2H), 3.79 (s, 3H), 3.76 (s, 3H), 2.99 (ddd, *J* = 17.3, 5.2, 1.1 Hz, 1H), 2.89–2.78 (m, 1H), 1.36 (t, *J* = 7.0 Hz, 3H); ^{13}C NMR (125 MHz, $(CD_3)_2CO$) δ 166.2, 160.7, 160.0, 159.8, 156.1, 132.5, 130.5, 122.3, 120.1, 115.9, 101.1, 94.2, 92.2, 67.3, 67.1, 64.3, 55.8, 55.5, 25.4, 15.0; IR (KBr) ν_{max} 2910, 1718, 1622,

1593, 1498, 1423, 1274, 1217, 1145, 1051, 754 cm^{-1}; HRMS (ESI+) *m*/*z* [M + H^+] calcd for $C_{20}H_{23}O_6$, 359.1495, found 359.1483.

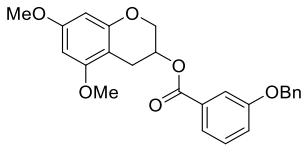

5,7-Dimethoxychroman-3-yl 3-(Benzyloxy)benzoate (**25i**): A solution of **24** (10 mg, 0.04 mmol), in dichloromethane (0.5 mL) was added to a stirred solution of 3-(benzyloxy)benzoic acid (23 mg, 0.1 mmol) (17 mg, 0.1 mmol), *N*,*N*′-dicyclohexylcarbodiimide (20.6 mg, 0.1 mmol), and 4-dimethylaminopyridine (5 mg, 0.042 mmol) under argon at 0 °C. The resulting solution was stirred for 6 h at rt then filterd. The filtrate was diluted with dichloromethane (5 mL) and washed with 0.5 N HCl (2 × 4 mL) and then with saturated sodium bicarbonate (2 × 4 mL) solution. The combined organic layers were washed with saturated sodium chloride solution (4 mL), dried over anhydrous sodium sulfate, filtered, and concentrated. The residue was purified by flash chromatography (SiO_2, 1:5 EtOAc/hexanes) to afford **25i** (18 mg, 90%) as a pale yellow amorphous solid: ^{1}H NMR (500 MHz, $CDCl_3$) δ 7.62 (dd, *J* = 7.2, 1.5 Hz, 2H), 7.48–7.36 (m, 4H), 7.37–7.27 (m, 2H), 7.19–7.12 (m, 1H), 6.11 (s, 2H), 5.50 (ddt, *J* = 5.3, 4.2, 2.5 Hz, 1H), 5.09 (s, 2H), 4.31 (ddd, *J* = 11.3, 4.9, 1.9 Hz, 1H), 4.20 (ddd, *J* = 11.4, 2.2, 1.2 Hz, 1H), 3.79 (s, 3H), 3.77 (s, 3H), 3.02 (ddd, *J* = 17.4, 5.5, 1.2 Hz, 1H), 2.87 (ddd, *J* = 17.4, 4.3, 1.8 Hz, 1H); ^{13}C NMR (125 MHz, $CDCl_3$) δ 166.1, 159.8, 159.0, 158.8, 155.3, 136.7, 131.6, 129.6 (2), 128.9 (2), 128.3, 127.8, 122.7, 120.4, 115.6, 100.7, 93.4, 92.0, 70.4, 67.0, 66.3, 55.6, 55.6, 25.1; IR (KBr) ν_{max} 2918, 1701, 1683, 1558, 15036, 1458, 1203, 1145, cm^{-1}; HRMS (ESI+) *m*/*z* [M + H^+] calcd for $C_{25}H_{25}O_6$, 421.1651, found 421.1637.

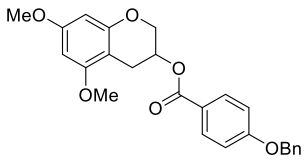

5,7-Dimethoxychroman-3-yl 4-(Benzyloxy)benzoate (**25j**): A solution of **24** (10 mg, 0.04 mmol) in dichloromethane (0.5 mL) was added to a stirred solution of 4-(benzyloxy)benzoic acid (23 mg, 0.1 mmol) (23 mg, 0.1 mmol), *N*,*N*′-dicyclohexylcarbodiimide (20.6 mg, 0.1 mmol), and 4-dimethylaminopyridine (5 mg, 0.042 mmol) under argon at 0 °C. The resulting solution was stirred for 6 h at rt and then filtered. The filtrate was diluted with dichloromethane (5 mL) and washed with 0.5 N HCl (2 × 4 mL) and then with saturated sodium bicarbonate (2 × 4 mL) solution. The combined organic layers were washed with saturated sodium chloride solution (4 mL), dried over anhydrous sodium sulfate, filtered, and concentrated. The residue was purified by flash chromatography (SiO_2, 1:5 EtOAc/hexanes) to afford **25j** (17 mg, 85%) as a colorless oil: ^{1}H NMR (500 MHz, $CDCl_3$) δ 7.62 (dd, *J* = 7.2, 1.5 Hz, 2H), 7.46–7.37 (m, 4H), 7.36–7.29 (m, 2H), 7.21–7.04 (m, 1H), 6.11 (s, 2H), 5.50 (ddt, *J* = 5.3, 4.2, 2.5 Hz, 1H), 5.09 (s, 2H), 4.31 (ddd, *J* = 11.3, 4.9, 1.9 Hz, 1H), 4.20 (ddd, *J* = 11.4, 2.2, 1.2 Hz, 1H), 3.81–3.78 (m, 6H), 3.02 (ddd, *J* = 17.4, 5.5, 1.2 Hz, 1H), 2.87 (ddd, *J* = 17.4, 4.3, 1.8 Hz, 1H); ^{13}C NMR (125 MHz, $CDCl_3$) δ 165.9, 162.8, 159.7, 159.0, 155.3, 136.4, 132.1 (2), 128.9 (2), 128.4, 127.7 (2), 122.9, 114.6 (2), 100.8, 93.3, 91.9, 70.3, 67.1, 65.8, 55.6, 55.6, 25.1. IR (KBr) ν_{max} 2918, 2817, 1701, 1683, 1558, 1503, 1458, 1203, 1145, 729 cm^{-1}; HRMS (ESI+) *m*/*z* [M + H$^+$] calcd for $C_{25}H_{25}O_6$, 421.1651, found 421.1666.

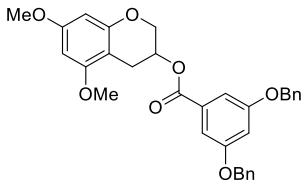

5,7-Dimethoxychroman-3-yl 3,5-Bis(benzyloxy)benzoate (**25k**): A solution of **24** (10 mg, 0.04 mmol), in dichloromethane (0.5 mL) was added to a stirred solution of 3,5-bis(benzyloxy)benzoic acid (33.4 mg, 0.1 mmol), *N*,*N*′-dicyclohexylcarbodiimide (20.6 mg, 0.1 mmol), and 4-dimethylaminopyridine (5 mg, 0.042 mmol) under argon at 0 °C. The resulting solution was stirred for 6 h at rt and then filtered. The filtrate was diluted with dichloromethane (5 mL) and washed with 0.5 N HCl (2 × 4 mL) and then with saturated sodium bicarbonate (2 × 4 mL) solution. The combined organic layers were washed with saturated sodium chloride solution (4 mL), dried over anhydrous sodium sulfate, filtered, and concentrated. The residue was purified by flash chromatography (SiO_2, 1:5 EtOAc/hexanes) to afford **25k** (22 mg, 88%) as an amorphous pale yellow solid: ^{1}H NMR (500 MHz, $CDCl_3$) δ 7.51–7.27 (m, 12H), 6.79 (t, *J* = 2.3 Hz, 1H), 6.11 (s, 2H), 5.47 (qd, *J* = 5.0, 2.2 Hz, 1H), 5.04 (s, 4H), 4.29 (ddd, *J* = 11.4, 5.0, 1.8 Hz, 1H), 4.25–4.12 (m, 1H), 3.79 (s, 3H), 3.77 (s, 3H), 3.01 (ddd, *J* = 17.4, 5.5, 1.1 Hz, 1H), 2.85 (ddd, *J* = 17.4, 4.5, 1.7 Hz, 1H); ^{13}C NMR (125 MHz, $CDCl_3$) δ 166.0, 159.9 (2), 159.8, 159.0, 155.3, 136.6 (2), 132.1, 128.9 (4), 128.4 (4), 127.9 (2), 108.8 (2), 107.3, 100.7, 93.4, 92.0, 70.5 (2), 66.9, 66.5, 55.6, 55.6, 25.1; IR (KBr) ν_{max} 2955, 2852, 1697, 1596, 1456, 1145, 1251, 1009, 769 cm^{-1}; HRMS (ESI+) *m*/*z* [M + H$^+$] calcd for $C_{32}H_{31}O_7$, 527.2070, found 527.2087.

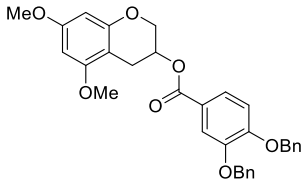

5,7-Dimethoxychroman-3-yl 3,4-Bis(benzyloxy)benzoate (25l): A solution of **24** (9 mg, 0.04 mmol), in dichloromethane (0.5 mL) was added to a stirred solution of 3,4-bis(benzyloxy)benzoic acid (33.4 mg, 0.1 mmol), *N*,*N*′-dicyclohexylcarbodiimide (20.6 mg, 0.1 mmol), and 4-dimethylaminopyridine (5 mg, 0.042 mmol) under argon at 0 °C. The resulting solution was stirred

for 6 h at rt and then filtered. The filtrate was diluted with dichloromethane (5 mL) and washed with 0.5 N HCl (2 × 4 mL) and then with saturated sodium bicarbonate (2 × 4 mL) solution. The combined organic layers were washed with saturated sodium chloride solution (4 mL), dried over anhydrous sodium sulfate, filtered, and concentrated. The residue was purified by flash chromatography (SiO_2, 1:5 EtOAc/hexanes) to afford **25l** (20.8 mg, 92%) as an amorphous pale yellow solid: ^{1}H NMR (500 MHz, $CDCl_3$) δ 7.61 (d, *J* = 2.0 Hz, 1H), 7.58 (dd, *J* = 8.4, 2.0 Hz, 1H), 7.48–7.40 (m, 4H), 7.40–7.29 (m, 6H), 6.88 (d, *J* = 8.4 Hz, 1H), 6.11 (s, 2H), 5.56–5.39 (m, 1H), 5.22 (s, 2H), 5.17 (s, 2H), 4.27 (ddd, J = 11.3, 4.9, 1.8 Hz, 1H), 4.22–4.14 (m, 1H), 3.79 (s, 3H), 3.78 (s, 3H), 2.98 (ddd, *J* = 17.3, 5.5, 1.2 Hz, 1H), 2.83 (ddd, *J* = 17.4, 4.3, 1.7 Hz, 1H); ^{13}C NMR (125 MHz, $CDCl_3$) δ 165.9, 159.8, 159.0, 155.3, 153.1, 148.4, 137.0, 136.7, 128.8 (3), 128.7, 128.2, 128.1, 127.7 (2), 127.3 (2), 124.4, 123.1, 115.8, 113.3, 100.8, 93.3, 91.9, 71.3, 71.0, 67.0, 65.9, 55.6, 55.6, 25.1. IR (KBr) ν_{max} 2921, 2848, 1699, 1618, 1510, 1454, 1290, 1203, 1058 cm^{-1}; HRMS (ESI+) *m*/*z* [M + H$^+$] calcd for $C_{32}H_{31}O_7$, 527.2070, found 527.2081.

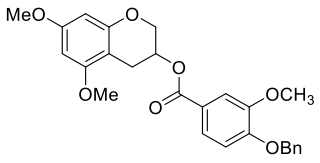

5**,7-Dimethoxychroman-3-yl 4-(Benzyloxy)-3-methoxybenzoate (25m)**: A solution of **24** (20 mg, 0.1 mmol), in dichloromethane (0.5 mL) was added to a stirred solution of 4-(benzyloxy)-3-methoxybenzoic acid (49 mg, 0.19 mmol), *N*,*N*′-dicyclohexylcarbodiimide (39 mg, 0.19 mmol), and 4-dimethylaminopyridine (12 mg, 0.1 mmol) under argon at 0 °C. The resulting solution was stirred for 6 h at rt and then filtered. The filtrate was diluted with dichloromethane (5 mL) and washed with 0.5 N HCl (2 × 4 mL) and then with saturated sodium bicarbonate (2 × 4 mL) solution. The combined organic layers were washed with saturated sodium chloride solution (4 mL), dried

over anhydrous sodium sulfate, filtered, and concentrated. The residue was purified by flash chromatography (SiO_2, 1:5 EtOAc/hexanes) to afford **25m** (34 mg, 81%) as an amorphous pale yellow solid: IR (KBr) ν_{max} 2921, 2848, 1699, 1618, 1510, 1454, 1290, 1203, 1058 cm^{-1}; HRMS (ESI+) *m*/*z* [M + H^+] calcd for $C_{26}H_{27}O_7$, 451.1757, found 451.1668.

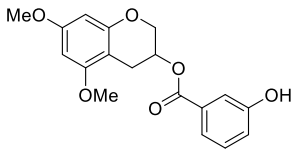

5,7-Dimethoxychroman-3-yl 3-Hydroxybenzoate (26a): Palladium/carbon (10%) and **25i** (18 mg, 0.03 mmol) were suspended in tetrahydrofuran (2 mL) and stirred for 18 h under a hydrogen atmosphere. The suspension was filtered through a small plug of celite. The eluent was concentrated and the residue purified by flash chromatography (SiO_2, 1:3 EtOAc/hexanes) to give **26a** (8.8 mg, 92.6%) as a colorless oil: ^{1}H NMR (500 MHz, CD_3CN) δ 7.41 (ddd, *J* = 7.7, 1.6, 1.0 Hz, 1H), 7.33 (dd, *J* = 2.6, 1.6 Hz, 1H), 7.29 (t, *J* = 7.9 Hz, 1H), 7.24–7.16 (m, 1H), 7.03 (ddd, *J* = 8.1, 2.6, 1.1 Hz, 1H), 6.14 (d, *J* = 2.3 Hz, 1H), 6.07 (d, *J* = 2.3 Hz, 1H), 5.52–5.36 (m, 1H), 4.30 (ddd, *J* = 11.7, 4.2, 2.1 Hz, 1H), 4.15 (ddt, *J* = 11.6, 1.9, 1.0 Hz, 1H), 3.77 (s, 3H), 3.74 (s, 3H), 2.92 (ddd, *J* = 17.4, 5.2, 1.1 Hz, 1H), 2.86–2.71 (m, 1H). ^{13}C NMR (125 MHz, CD_3CN) δ 166.5, 160.7, 159.9, 157.9, 156.1, 132.6, 130.8, 122.5, 121.9, 118.3, 117.0, 94.2, 92.4, 67.4, 67.0, 56.2, 55.9, 25.1. IR (KBr) ν_{max} 3335, 2918, 1701, 1683, 1558, 15036, 1458, 1203, 1145, cm^{-1}. HRMS (ESI+) *m*/*z* [M + H^+] calcd for $C_{18}H_{19}O_6$, 331.1182, found 331.1188.

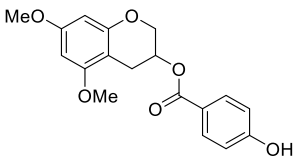

5,7-Dimethoxychroman-3-yl 4-Hydroxybenzoate (**26b**): Palladium/carbon (10%) and **25j** (12 mg, 0.028 mmol) were suspended in tetrahydrofuran (2 mL) and stirred for 18 h under a hydrogen atmosphere. The suspension was filtered through a small pad of celite. The eluent was concentrated and the residue purified by flash chromatography (SiO_2, 1:3 EtOAc/hexanes) to give the **26b** (9 mg, 90%) as a colorless oil: ^{1}H NMR (500 MHz, $(CD_3)_2CO$) δ 9.16 (s, 1H), 7.88–7.80 (m, 2H), 6.94–6.86 (m, 2H), 6.14 (d, *J* = 2.3 Hz, 1H), 6.05 (d, *J* = 2.3 Hz, 1H), 5.49–5.36 (m, 1H), 4.29 (ddd, *J* = 11.5, 4.6, 2.0 Hz, 1H), 4.24–4.14 (m, 1H), 3.79 (s, 3H), 3.75 (s, 3H), 2.97 (ddd, *J* = 17.3, 5.3, 1.1 Hz, 1H), 2.80 (ddd, *J* = 17.3, 4.0, 1.9 Hz, 1H); ^{13}C NMR (125 MHz, $(CD_3)_2CO$) δ 166.1, 162.7, 160.7, 159.8, 156.1, 132.5 (2), 122.4, 116.0 (2), 101.2, 94.2, 92.2, 67.4, 66.4, 55.8, 55.5, 25.5. IR (KBr) ν_{max} 3365, 2956, 2852, 1701, 1596, 1456, 1214, 1145, 1051, 767 cm^{-1}; HRMS (ESI+) *m*/*z* [M + Na$^+$] calcd for $C_{18}H_{18}NaO_6$, 353.1001, found 353.0991.

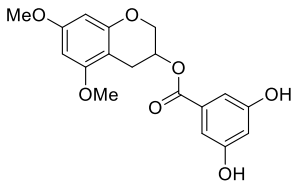

5,7-Dimethoxychroman-3-yl 3,5-Dihydroxybenzoate (**26c**): Palladium/carbon (10%) and **25k** (12 mg, 0.028 mmol) were suspended in tetrahydrofuran (2 mL) and stirred for 18 h under a hydrogen atmosphere. The suspension was filtered through a small pad of celite. The eluent was concentrated and the residue purified by flash chromatography (SiO_2, 1:1 EtOAc/hexanes) to give **26c** (12 mg, 91%) as a colorless oil: ^{1}H NMR (500 MHz, $(CD_3)_2CO$) δ 8.58 (s, 2H), 6.96 (d, *J* = 2.3 Hz, 2H), 6.56 (t, *J* = 2.3 Hz, 1H), 6.15 (d, *J* = 2.3 Hz, 1H), 6.05 (d, *J* = 2.3 Hz, 1H), 5.43 (dtd, *J* = 5.5, 4.1, 1.9 Hz, 1H), 4.31 (ddd, *J* = 11.6, 4.3, 2.1 Hz, 1H), 4.19 (ddt, *J* = 11.7, 1.9, 1.0 Hz, 1H), 3.79 (s, 3H), 3.75 (s, 3H), 2.97 (ddd, *J* = 17.6, 5.4, 1.2 Hz, 1H), 2.82–2.74 (m, 1H); ^{13}C NMR (125 MHz, $(CD_3)_2CO$) δ 166.2, 160.7, 159.8 (2), 159.4, 156.1, 133.1, 108.7, 108.1, 101.1, 94.2,

92.2, 67.3, 66.8, 55.8, 55.5 (2), 25.3. IR (KBr) ν_{max} 3365, 3330, 2956, 2850, 1697, 1596, 1456, 1361, 1145, 1054, 1004, 769, cm^{-1}; HRMS (ESI+) *m*/*z* [M + H^+] calcd for $C_{18}H_{19}O_7$, 347.1131, found 347.1134.

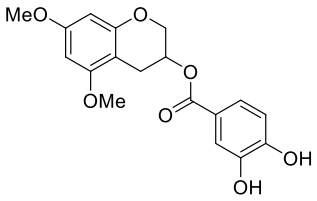

5,7-Dimethoxychroman-3-yl 3,4-Dihydroxybenzoate (**26d**): Palladium/carbon (10%) and **25l** (18 mg, 0.034 mmol) were suspended in tetrahydrofuran (2 mL) and stirred for 18 h under a hydrogen atmosphere. The suspension was filtered through a small pad of celite. The eluent was concentrated and the residue purified by flash chromatography (SiO_2, 1:3 EtOAc/hexanes) to give the desired product **26d** (11 mg, 92%) as a colorless oil: ^{1}H NMR (500 MHz, $(CD_3)_2$ CO) δ 7.45 (d, *J* = 2.1 Hz, 1H), 7.41 (dd, *J* = 8.3, 2.0 Hz, 1H), 6.88 (d, *J* = 8.3 Hz, 1H), 6.15 (d, *J* = 2.3 Hz, 1H), 6.10–6.04 (m, 1H), 5.49–5.38 (m, 1H), 4.29 (ddd, *J* = 11.5, 4.4, 2.0 Hz, 1H), 4.22–4.14 (m, 1H), 3.80 (s, 3H), 3.76 (s, 3H), 2.97 (ddd, *J* = 17.4, 5.5, 1.2 Hz, 1H); ^{13}C NMR (125 MHz, $(CD_3)_2$ CO)) δ 159.9, 160.2 (2), 158.1 (2), 123.6 (2), 122.85, 117.21, 115.9, 101.3, 94.3, 92.3, 67.47, 66.4, 55.9, 55.6, 25.5; IR (KBr) ν_{max} 3381, 3321, 2924, 2839, 1698, 16120, 1510, 1456, 1203, 1056, 728 cm^{-1}; HRMS (ESI+) *m*/*z* [M + H^+] calcd for $C_{18}H_{19}O_7$, 347.1131, found 347.1125:

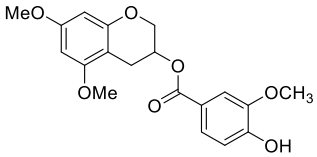

5,7-Dimethoxychroman-3-yl 4-Hydroxy-3-methoxybenzoate (**26e**): Palladium/carbon (10%) and **25m** (24 mg, 0.053 mmol) were suspended in tetrahydrofuran (2 mL) and stirred for 18 h

under a hydrogen atmosphere. The suspension was filtered through a small pad of Celite. The eluent was concentrated and the residue purified by flash chromatography (SiO_2, 1:3 EtOAc/hexanes) to give the desired product **26e** (17 mg, 91%) as a colorless oil: ^{1}H NMR (500 MHz, $CDCl_3$) δ 7.60 (dd, *J* = 8.4, 1.9 Hz, 1H), 7.52 (d, *J* = 1.9 Hz, 1H), 6.90 (d, *J* = 8.3 Hz, 1H), 6.10 (s, 2H), 6.07 (s, 1H), 5.47 (dq, *J* = 7.5, 2.6 Hz, 1H), 4.28 (ddd, *J* = 11.3, 5.1, 1.8 Hz, 1H), 4.24–4.16 (m, 1H), 3.92 (s, 3H), 3.78 (d, *J* = 3.5 Hz, 6H), 3.01 (ddd, *J* = 17.5, 5.6, 1.2 Hz, 1H), 2.85 (ddd, *J* = 17.3, 4.6, 1.7 Hz, 1H); ^{13}C NMR (125 MHz, $CDCl_3$) δ 165.8, 159.6, 158.2, 155.2, 150.2, 146.1, 124.5, 122.1, 114, 111.8, 100.6, 93.1, 91.7, 66.9, 65.8, 56.1, 55.4, 55.3, 24.9; IR (KBr) ν_{max} 3385, 2939, 2841, 1699, 1612, 1508, 1214, 1145, 729 cm^{-1}; HRMS (ESI+) *m*/*z* [M + H$^+$] calcd for $C_{19}H_{21}O_7$, 361.1287, found 361.1278.

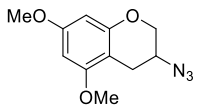

3-Azido-5,7-dimethoxychroman (**27**): A solution of **24** (75, 0.36 mmol) and triphenylphosphine (161 mg, 0.61) in tetrahydrofuran (2.5 mL) at 0 °C was treated with diisopropyl azodicarboxylate (120 μL, 0.61 mmol) and diphenylphosphoryl azide (130 μL, 0.61 mmol). The resulting mixture was stirred for 15 h at 25 °C before the solvent was removed. The residue was purified by flash chromatography (SiO_2, 1:20 EtOAc/hexanes) to give **27** (75 mg, 83.9%) as a light yellow oil: ^{1}H NMR (500 MHz, $CDCl_3$) δ 6.09 (d, *J* = 2.4 Hz, 1H), 6.06 (d, *J* = 2.4 Hz, 1H), 4.15 (ddd, *J* = 10.8, 2.6, 1.3 Hz, 1H), 4.02 (ddd, *J* = 10.9, 6.4, 1.5 Hz, 1H), 3.96 (qd, *J* = 6.0, 2.6 Hz, 1H), 3.80 (s, 3H), 3.76 (s, 3H), 2.95 (ddd, *J* = 16.7, 5.5, 1.4 Hz, 1H), 2.71 (ddd, *J* = 16.7, 6.0, 1.5 Hz, 1H). ^{13}C NMR (125 MHz, $CDCl_3$) δ 159.0, 157.9, 154.1, 99.3, 92.3, 91.2, 66.3, 54.7, 54.6, 52.4, 23.8; IR (KBr) ν_{max} 2931, 2847, 2113, 1558, 1456, 1276,811 cm^{-1}; HRMS (ESI+) *m*/*z* [M + H$^+$] calcd for $C_{11}H_{14}N_3O_3$, 236.1035, found 236.1028.

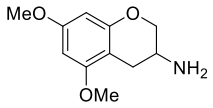

5,7-Dimethoxychroman-3-amine (**28**): To a solution of **27** and triphenylphosphine in THF (3 mL) was added water (22 μL, 0.93 mmol) and the solution stirred for 30 h at rt. The solvent was removed and the residue purified via flash chromatography (silica gel 3:97 MeOH/$CHCl_3$) to give **28** (55 mg, 83%) as a yellow oil: ^{1}H NMR (500 MHz, $CDCl_3$) δ 6.23–5.87 (m, 2H), 4.09 (ddd, *J* = 10.5, 2.8, 1.5 Hz, 1H), 3.84–3.79 (m, 1H), 3.78 (s, 3H), 3.76 (s, 3H), 3.34 (tdd, *J* = 6.8, 5.5, 2.9 Hz, 1H), 2.88 (ddd, *J* = 16.5, 5.5, 1.5 Hz, 1H), 2.36 (ddd, *J* = 16.4, 6.6, 1.2 Hz, 1H), 2.04 (d, *J* = 5.5 Hz, 2H); ^{13}C NMR (125 MHz, $CDCl_3$) δ 159.7, 159.1, 155.3, 101.7, 93.2, 91.8, 71.3, 55.6, 55.5, 44.0, 28.9; HRMS (ESI+) *m*/*z* [M + H^+] calcd for $C_{11}H_{16}NO_3$, 210.1130, found 210.1133.

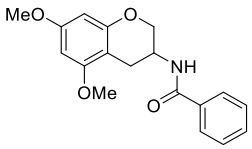

***N*-(5,7-Dimethoxychroman-3-yl)benzamide** (**29a**): Benzoic acid (15 mg, 0.12 mmol) and *N*-(3-dimethylaminopropyl)-N′-ethylcarbodiimide hydrochloride (19 mg, 0.14 mmol) were added to a solution of alcohol **28** (12 mg, 0.057 mmol) in dichloromethane (0.7 mL) with pyridine (0.3 mL). The resulting mixture was stirred for 16 h, and then the reaction mixture was diluted with dichloromethane (2 mL). The organic phase was washed with saturated sodium bicarbonate (2 × 2 mL) and saturated sodium chloride solution (3 mL). The organic layer was dried over anhydrous sodium sulfate, filtered, and concentrated. The residue was purified by flash chromatography (SiO_2, 1:2 Hexanes/EtOAc) to give **29a** (12 mg, 81%) as a pale yellow oil: ^{1}H NMR (500 MHz, $CDCl_3$) δ 7.78–7.66 (m, 2H), 7.54–7.46 (m, 1H), 7.41 (tt, *J* = 6.6, 1.4 Hz, 2H), 6.39 (d, *J* = 8.0 Hz, 1H), 6.17–5.90 (m, 2H), 4.70 (ddtd, *J* = 7.5, 5.5, 3.5, 1.8 Hz, 1H), 4.26 (ddd, *J* = 10.9, 3.8,

2.1 Hz, 1H), 4.15 (dd, *J* = 10.9, 1.8 Hz, 1H), 3.78 (d, *J* = 1.1 Hz, 6H), 2.91 (dd, *J* = 17.2, 5.7 Hz, 1H), 2.78 (ddd, *J* = 17.1, 3.2, 2.0 Hz, 1H); ^{13}C NMR (125 MHz, $CDCl_3$) δ 167.4, 159.9, 159.4, 155.3, 134.5, 131.8, 128.7 (2), 127.2 (2), 101.0, 93.5, 92.2, 68.3, 55.6, 55.6, 42.6, 25.6; IR (KBr) ν_{max} 3307, 2925, 2850, 1645, 1635, 1622, 1539, 1521, 1145, 1122, 813, 756 cm^{-1}; HRMS (ESI+) *m*/*z* [M + H^+] calcd for $C_{18}H_{20}NO_4$, 314.1392, found 314.1391.

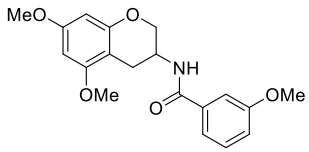

***N*-(5,7-Dimethoxychroman-3-yl)-3-methoxybenzamide** (**29b**): 3-Methoxybenzoic acid (15 mg, 0.12 mmol) and *N*-(3-dimethylaminopropyl)-N′-ethylcarbodiimide hydrochloride (19 mg, 0.14 mmol) were added to a solution of alcohol **28** (12 mg, 0.057 mmol) in dichloromethane (0.7 mL) with pyridine (0.3 mL). The resulting mixture was stirred for 16 h at rt, and then the reaction mixture was diluted with dichloromethane (2 mL). The organic phase was washed with saturated sodium bicarbonate (2 × 2 mL) and saturated sodium chloride solution (3 mL). The organic layer was dried over anhydrous sodium sulfate, filtered, and concentrated. The residue was purified by flash chromatography (SiO_2, 1:2 Hexanes/EtOAc) to give **29b** (12 mg, 70%) as a pale yellow oil: ^{1}H NMR (500 MHz, $CDCl_3$) δ 7.26 (dd, *J* = 2.6, 1.6 Hz, 1H), 7.22 (t, *J* = 7.9 Hz, 1H), 7.14 (dt, *J* = 7.7, 1.3 Hz, 1H), 6.94 (ddd, *J* = 8.2, 2.7, 1.0 Hz, 1H), 6.30 (d, *J* = 8.0 Hz, 1H), 6.02 (d, *J* = 2.4 Hz, 1H), 6.01 (d, *J* = 2.4 Hz, 1H), 4.60 (dtt, *J* = 7.7, 3.8, 1.8 Hz, 1H), 4.17 (ddd, *J* = 10.9, 3.9, 2.1 Hz, 1H), 4.11–4.01 (m, 1H), 3.77 (s, 3H), 3.70 (s, 6H), 2.83 (dd, *J* = 17.1, 5.7 Hz, 1H), 2.69 (ddd, *J* = 17.2, 3.4, 2.1 Hz, 1H); ^{13}C NMR (125 MHz, $CDCl_3$) δ 167.3, 160.0, 159.9, 159.4, 155.3, 136.0, 129.7, 119.0, 117.9, 112.7, 100.9, 93.5, 92.2, 68.2, 55.7, 55.6 (2), 42.6, 25.5; IR (KBr) ν_{max} 3363,

2921, 2850, 1712, 1681, 1498, 1454, 1272, 1145, 771 cm^{-1}; HRMS (ESI+) *m*/*z* [M + H^+] calcd for $C_{19}H_{22}NO_5$, 344.1498, found 344.1498.

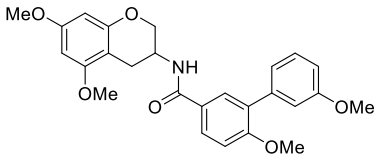

***N*-(5,7-Dimethoxychroman-3-yl)-3′,6-dimethoxy-[1,1′-biphenyl]-3-carboxamide** (**29c**): 3′,6-Dimethoxy-[1,1′-biphenyl]-3-carboxylic acid (25 mg, 0.1 mmol) and *N*-(3-dimethylaminopropyl)-*N*′-ethylcarbodiimide hydrochloride (19 mg, 0.12 mmol) were added to a solution of alcohol **28** (10 mg, 0.048 mmol) in dichloromethane (0.7 mL) with pyridine (0.3 mL). The resulting mixture was stirred for 16 h, and then the reaction mixture was diluted with dichloromethane (2 mL) and organic phase was washed with saturated sodium bicarbonate (2 × 2 mL) and saturated sodium chloride solution (2 mL). The organic layer was dried over anhydrous Na_2SO_4, filtered, and concentrated. The residue was purified by flash chromatography (SiO_2, 1:2 Hexanes/EtOAc) to give **29c** (19.3 mg, 90%) as an amorphous light yellow solid: ^{1}H NMR (500 MHz, $CDCl_3$) δ 7.76 (dd, *J* = 8.6, 2.4 Hz, 1H), 7.67 (d, *J* = 2.4 Hz, 1H), 7.39–7.30 (m, 1H), 7.08 (dt, *J* = 7.7, 1.1 Hz, 1H), 7.04 (dd, *J* = 2.6, 1.6 Hz, 1H), 6.98 (d, *J* = 8.6 Hz, 1H), 6.91 (ddd, *J* = 8.3, 2.6, 1.0 Hz, 1H), 6.32 (d, *J* = 7.9 Hz, 1H), 6.09 (d, *J* = 2.4 Hz, 1H), 6.08 (d, *J* = 2.4 Hz, 1H), 4.68 (ddt, *J* = 7.8, 3.9, 1.9 Hz, 1H), 4.24 (ddd, *J* = 10.8, 4.0, 2.0 Hz, 1H), 4.15 (dd, *J* = 10.7, 1.9 Hz, 1H), 3.84 (s, 6H), 3.77 (s, 6H), 2.92 (dd, *J* = 17.1, 5.7 Hz, 1H), 2.76 (ddd, *J* = 17.2, 3.5, 1.9 Hz, 1H); ^{13}C NMR (125 MHz, $CDCl_3$) δ 166.9, 159.8, 159.5, 159.3 (2), 155.3, 139.1, 130.7, 129.8, 129.3, 128.4, 126.9, 122.2, 115.4, 113.1, 110.9, 101.1, 93.5, 92.2, 68.3, 56.0, 55.6, 55.6, 55.5, 42.6, 25.6; IR (KBr) ν_{max} 3315, 2931 1620, 1596, 1531, 1498, 1249, 1201, 1249, 1215, 1145, 1051, 752 cm^{-1}; HRMS (ESI+) *m*/*z* [M + Na^+] calcd for $C_{26}H_{27}NaNO_6$, 472.1736, found 472.1738.

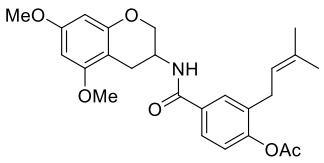

4-((5,7-Dimethoxychroman-3-yl)carbamoyl)-2-(3-methylbut-2-en-1-yl)phenyl Acetate (29d): 4-Acetoxy-3-(3-methylbut-2-en-1-yl)benzoic acid (47 mg, 0.19 mmol) and *N*-(3-dimethylaminopropyl)-*N*′-ethylcarbodiimide hydrochloride (37 mg, 0.24 mmol) were added to a solution of alcohol **28** (20 mg, 0.096 mmol), in dichlormethane (1.4 mL) with pyridine (0.6 mL). The resulting mixture was stirred for 16 h and then the reaction mixture was diluted with dichloromethane (4 mL). The organic phase was washed with saturated $NaHCO_3$ (2 × 4 mL) and saturated sodium chloride solution (4 mL). The organic layer was dried over anhydrous Na_2SO_4, filtered and concentrated. The residue was purified by flash chromatography (SiO_2, 1:2 Hexanes/EtOAc) to give **29d** (33 mg, 77%) as an amorphous light yellow solid: ^{1}H NMR (500 MHz, $CDCl_3$) δ 7.66 (d, *J* = 2.2 Hz, 1H), 7.54 (dd, *J* = 8.3, 2.3 Hz, 1H), 7.06 (d, *J* = 8.3 Hz, 1H), 6.34 (d, *J* = 8.0 Hz, 1H), 6.12 (d, *J* = 2.3 Hz, 1H), 6.10 (d, *J* = 2.3 Hz, 1H), 5.20 (dddd, *J* = 7.2, 5.8, 2.9, 1.4 Hz, 1H), 4.68 (dtt, *J* = 7.6, 3.6, 1.7 Hz, 1H), 4.26 (ddd, *J* = 10.9, 3.8, 2.1 Hz, 1H), 4.15 (dd, *J* = 10.8, 1.8 Hz, 1H), 3.80 (s, 6H), 3.27 (d, *J* = 7.2 Hz, 2H), 2.91 (dd, *J* = 17.1, 5.6 Hz, 1H), 2.86–2.71 (m, 1H), 2.33 (s, 3H), 1.74 (s, 3H), 1.72–1.66 (s, 3H); ^{13}C NMR (125 MHz, $CDCl_3$) δ 169.2, 166.9, 159.9, 159.4, 155.3, 151.5, 134.4, 134.0, 132.5, 129.6, 125.7, 122.6, 121.1, 100.9, 93.5, 92.2, 68.2, 55.6, 55.6, 42.6, 29.0, 25.9, 25.5, 21.1, 18.1; IR (KBr) ν_{max} 3325, 2932 1623, 1602, 1596, 1531, 1496, 1249, 1201, 1251, 1215, 1145, 749 cm^{-1}; HRMS (ESI+) *m*/*z* [M + Na$^+$] calcd for $C_{25}H_{29}NaNO_6$, 462.1893, found 462.1872

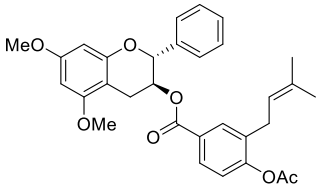

5,7-Dimethoxy-2-phenylchroman-3-yl 4-Acetoxy-3-(3-methylbut-2-en-1-yl)benzoate (**30**): A solution of **11a** (20 mg, 0.07 mmol) in dichloromethane (0.5 mL) was added to a solution of 4-acetoxy-3-(3-methylbut-2-en-1-yl)benzoic acid (36 mg, 0.14 mmol), N-(3-dimethylamino-propyl)-N′-ethylcarbodiimide hydrochloride (27 mg, 0.14 mmol) and 4-dimethylaminopyridine (25 mg, 0 0.21 mmol) in dichloromethane (1 mL) at 0 °C. The resulting mixture was stirred for 6 h at rt, diluted with dichloromethane (5 mL) and washed saturated sodium bicarbonate solution (2 × 4 mL). The organic layer was dried over anhydrous sodium sulfate, filtered and the solvent removed. The residue was purified via flash chromatography (SiO_2, 1:7 EtOAc/hexanes) to give the desired ester **30** (21 mg, 58.1 %) as a colorless oil: ^{1}H NMR (500 MHz, $CDCl_3$) δ 7.81 (d, *J* = 2.1 Hz, 1H), 7.77 (dd, *J* = 8.4, 2.2 Hz, 1H), 7.44 – 7.40 (m, 2H), 7.37 – 7.32 (m, 2H), 7.32 – 7.28 (m, 1H), 7.04 (d, *J* = 8.4 Hz, 1H), 6.22 (d, *J* = 2.3 Hz, 1H), 6.12 (d, *J* = 2.3 Hz, 1H), 5.54 (td, *J* = 6.5, 5.2 Hz, 1H), 5.27 (d, *J* = 6.4 Hz, 1H), 5.19 (tdt, *J* = 7.3, 2.9, 1.5 Hz, 1H), 3.79 (m, 6H), 3.23 (d, *J* = 7.3 Hz, 2H), 3.00 (dd, *J* = 16.8, 5.2 Hz, 1H), 2.81 (ddd, *J* = 16.7, 6.5, 0.9 Hz, 1H), 2.32 (s, 3H), 1.75 (q, *J* = 1.3 Hz, 3H), 1.68 (d, *J* = 1.4 Hz, 3H). ^{13}C NMR (125 MHz, $CDCl_3$) δ 169.0, 165.3, 160.0, 158.8, 155.0, 152.8, 138.2, 134.1, 134.0, 132.0, 128.9 (2), 128.8, 128.5, 128.0, 126.6 (2), 122.5, 121.0, 100.8, 93.2, 92.0, 78.7, 70.3, 55.6, 55.6, 28.8, 25.9, 24.0, 21.1, 18.0.IR (KBr) ν_{max} 2929, 1762, 1713, 1593, 1369, 1201, 1118, 816 cm^{-1}; HRMS (ESI+) *m*/*z* [M + H^+] calcd for $C_{31}H_{33}O_7$, 517.2226, found 517.2219.

II.9. References

1. Yang, C. S.; Wang, X.; Lu, G.; Picinich, S. C. Cancer prevention by tea: animal studies, molecular mechanisms and human relevance. *Nat Rev Cancer* **2009**, 9, 429-439.
2. Siddiqui, I. A.; Asim, M.; Hafeez, B. B.; Adhami, V. M.; Tarapore, R. S.; Mukhtar, H. Green tea polyphenol EGCG blunts androgen receptor function in prostate cancer. *FASEB J.* **2011**, 25, 1198-1207.
3. Wolfram, S. Effects of green tea and EGCG on cardiovascular and metabolic health. *J. Am. Coll. Nutri.* **2007**, 26, 373S-388S.
4. Cooper, R.; Morre, D. J.; Morre, D. M. Medicinal benefits of green tea: Part I. Review of noncancer health benefits. *J. Altern. Complement. Med.* **2005**, 11, 521-528.
5. Riegsecker, S.; Wiczynski, D.; Kaplan, M. J.; Ahmed, S. Potential benefits of green tea polyphenol EGCG in the prevention and treatment of vascular inflammation in rheumatoid arthritis. *Life Sci.* **2013**, 93, 307-312.
6. Khan, N.; Mukhtar, H. Modulation of signaling pathways in prostate cancer by green tea polyphenols. *Biochem. Pharmacol.* **2013**, 85, 667-672.
7. Khan, N.; Afaq, F.; Saleem, M.; Ahmad, N.; Mukhtar, H. Targeting multiple signaling pathways by green tea polyphenol (-)-epigallocatechin-3-gallate. *Cancer Res.* **2006**, 66, 2500-2505.
8. Katiyar, S.; Mukhtar, H. Tea in chemoprevention of cancer. *Int. J. Oncol.* **1996**, 8, 221-38.
9. Lecumberri, E.; Dupertuis, Y. M.; Miralbell, R.; Pichard, C. Green tea polyphenol epigallocatechin-3-gallate (EGCG) as adjuvant in cancer therapy. *Clin. Nutr.* **2013**, 32, 894-903.
10. Singh, B. N.; Shankar, S.; Srivastava, R. K. Green tea catechin, epigallocatechin-3-gallate (EGCG): mechanisms, perspectives and clinical applications. *Biochem. Pharmacol.* **2011**, 82, 1807-1821.
11. Xu, J. Z.; Yeung, S. Y.; Chang, Q.; Huang, Y.; Chen, Z. Y. Comparison of antioxidant activity and bioavailability of tea epicatechins with their epimers. *Br. J. Nutr.* **2004**, 91, 873-881.
12. Elbling, L.; Weiss, R. M.; Teufelhofer, O.; Uhl, M.; Knasmueller, S.; Schulte-Hermann, R.; Berger, W.; Micksche, M. Green tea extract and (-)-epigallocatechin-3-gallate, the major tea catechin, exert oxidant but lack antioxidant activities. *FASEB J.* **2005**, 19, 807-809.
13. Lambert, J. D.; Elias, R. J. The antioxidant and pro-oxidant activities of green tea polyphenols: a role in cancer prevention. *Arch. Biochem. Biophys.* **2010**, 501, 65-72.
14. Higdon, J. V.; Frei, B. Tea catechins and polyphenols: health effects, metabolism, and antioxidant functions. *Crit. Rev. Food Sci. Nutr.***2003**, 43, 89-143.
15. Kao, Y. H.; Chang, H. H.; Lee, M. J.; Chen, C. L. Tea, obesity, and diabetes. *Mol. Nutr. Food Res.* **2006**, 50, 188-210.
16. Cao, Y.; Cao, R. Angiogenesis inhibited by drinking tea. *Nature* **1999**, 398, 381.
17. Hwang, J. T.; Park, I. J.; Shin, J. I.; Lee, Y. K.; Lee, S. K.; Baik, H. W.; Ha, J.; Park, O. J. Genistein, EGCG, and capsaicin inhibit adipocyte differentiation process via activating AMP-activated protein kinase. *Biochem. Biophys. Res. Commun.* **2005**, 338, 694-699.
18. Zhang, T.; Zhang, J.; Derreumaux, P.; Mu, Y. Molecular mechanism of the inhibition of EGCG on the Alzheimer Abeta(1-42) dimer. *J. Phys. Chem. B* **2013**, 117, 3993-4002.

19. Dragicevic, N.; Smith, A.; Lin, X.; Yuan, F.; Copes, N.; Delic, V.; Tan, J.; Cao, C.; Shytle, R. D.; Bradshaw, P. C. Green tea epigallocatechin-3-gallate (EGCG) and other flavonoids reduce Alzheimer's amyloid-induced mitochondrial dysfunction. *J. Alzheimer's Dis.* **2011**, 26, 507-521.
20. Weinreb, O.; Mandel, S.; Amit, T.; Youdim, M. B. Neurological mechanisms of green tea polyphenols in Alzheimer's and Parkinson's diseases. *J.Nutr. Biochem.* **2004**, 15, 506-516.
21. Khan, N.; Bharali, D. J.; Adhami, V. M.; Siddiqui, I. A.; Cui, H.; Shabana, S. M.; Mousa, S. A.; Mukhtar, H. Oral administration of naturally occurring chitosan-based nanoformulated green tea polyphenol EGCG effectively inhibits prostate cancer cell growth in a xenograft model. *Carcinogenesis* **2014**, 35, 415-423.
22. Du, G. J.; Zhang, Z.; Wen, X. D.; Yu, C.; Calway, T.; Yuan, C. S.; Wang, C. Z. Epigallocatechin Gallate (EGCG) is the most effective cancer chemopreventive polyphenol in green tea. *Nutrients* **2012**, 4, 1679-1691.
23. Chen, D.; Pamu, S.; Cui, Q.; Chan, T. H.; Dou, Q. P. Novel epigallocatechin gallate (EGCG) analogs activate AMP-activated protein kinase pathway and target cancer stem cells. *Bioorg. Med. Chem.* **2012**, 20, 3031-3037.
24. Zhou, H.; Chen, J. X.; Yang, C. S.; Yang, M. Q.; Deng, Y.; Wang, H. Gene regulation mediated by microRNAs in response to green tea polyphenol EGCG in mouse lung cancer. *BMC genomics.* **2014**, 15 Suppl 11, S3.
25. Mereles, D.; Hunstein, W. Epigallocatechin-3-gallate (EGCG) for clinical trials: more pitfalls than promises? *Int. J. Mol. Sci.* **2011**, 12, 5592-5603.
26. Li, N.; Sun, Z.; Han, C.; Chen, J. The chemopreventive effects of tea on human oral precancerous mucosa lesions. *Proc. Soc. Exp. Biol. Med.* **1999**, 220, 218-224.
27. Tsao, A. S.; Liu, D.; Martin, J.; Tang, X. M.; Lee, J. J.; El-Naggar, A. K.; Wistuba, I.; Culotta, K. S.; Mao, L.; Gillenwater, A.; Sagesaka, Y. M.; Hong, W. K.; Papadimitrakopoulou, V. Phase II randomized, placebo-controlled trial of green tea extract in patients with high-risk oral premalignant lesions. *Cancer Prev. Res.* **2009**, 2, 931-941.
28. Hakim, I. A.; Harris, R. B.; Brown, S.; Chow, H. H.; Wiseman, S.; Agarwal, S.; Talbot, W. Effect of increased tea consumption on oxidative DNA damage among smokers: a randomized controlled study. *J. Nutr.* **2003**, 133, 3303S-3309S.
29. Luo, H.; Tang, L.; Tang, M.; Billam, M.; Huang, T.; Yu, J.; Wei, Z.; Liang, Y.; Wang, K.; Zhang, Z. Q.; Zhang, L.; Wang, J. S. Phase IIa chemoprevention trial of green tea polyphenols in high-risk individuals of liver cancer: modulation of urinary excretion of green tea polyphenols and 8-hydroxydeoxyguanosine. *Carcinogenesis* **2006**, 27, 262-268.
30. Bettuzzi, S.; Brausi, M.; Rizzi, F.; Castagnetti, G.; Peracchia, G.; Corti, A. Chemoprevention of human prostate cancer by oral administration of green tea catechins in volunteers with high-grade prostate intraepithelial neoplasia: a preliminary report from a one-year proof-of-principle study. *Cancer Res.* **2006**, 66, 1234-1240.
31. Jatoi, A.; Ellison, N.; Burch, P. A.; Sloan, J. A.; Dakhil, S. R.; Novotny, P.; Tan, W.; Fitch, T. R.; Rowland, K. M.; Young, C. Y.; Flynn, P. J. A phase II trial of green tea in the treatment of patients with androgen independent metastatic prostate carcinoma. *Cancer* **2003**, 97, 1442-1446.
32. Hamajima, N.; Tajima, K.; Tominaga, S.; Matsuura, A.; Kuwabara, M.; Okuma, K. Tea polyphenol intake and changes in serum pepsinogen levels. *Jpn. J. Cancer Res.* **1999,** 90, 136-143.

33. Zhou, D. H.; Wang, X.; Yang, M.; Shi, X.; Huang, W.; Feng, Q. Combination of low concentration of (-)-epigallocatechin gallate (EGCG) and curcumin strongly suppresses the growth of non-small cell lung cancer in vitro and in vivo through causing cell cycle arrest. *Int. J. Mol. Sci.* **2013,** 14, 12023-12036.
34. Chen, C.; Shen, G.; Hebbar, V.; Hu, R.; Owuor, E. D.; Kong, A. N. Epigallocatechin-3-gallate-induced stress signals in HT-29 human colon adenocarcinoma cells. *Carcinogenesis* **2003**, 24, 1369-1378.
35. Thangapazham, R. L.; Singh, A. K.; Sharma, A.; Warren, J.; Gaddipati, J. P.; Maheshwari, R. K. Green tea polyphenols and its constituent epigallocatechin gallate inhibits proliferation of human breast cancer cells in vitro and in vivo. *Cancer Lett.* **2007**, 245, 232-241.
36. Manthey, J. A.; Guthrie, N. Antiproliferative activities of citrus flavonoids against six human cancer cell lines. *J. Agric. Food. Chem.* **2002**, 50, 5837-5843.
37. Khafif, A.; Schantz, S. P.; Chou, T. C.; Edelstein, D.; Sacks, P. G. Quantitation of chemopreventive synergism between (-)-epigallocatechin-3-gallate and curcumin in normal, premalignant and malignant human oral epithelial cells. *Carcinogenesis* **1998**, 19, 419-424.
38. Mukhtar, E.; Adhami, V. M.; Khan, N.; Mukhtar, H. Apoptosis and autophagy induction as mechanism of cancer prevention by naturally occurring dietary agents. *Curr. Drug Targets.* **2012**, 13, 1831-1841.
39. Chen, Z. P.; Schell, J. B.; Ho, C. T.; Chen, K. Y. Green tea epigallocatechin gallate shows a pronounced growth inhibitory effect on cancerous cells but not on their normal counterparts. *Cancer Lett.* **1998**, 129, 173-179.
40. Fang, M. Z.; Wang, Y.; Ai, N.; Hou, Z.; Sun, Y.; Lu, H.; Welsh, W.; Yang, C. S. Tea polyphenol (-)-epigallocatechin-3-gallate inhibits DNA methyltransferase and reactivates methylation-silenced genes in cancer cell lines. *Cancer Res.* **2003**, 63, 7563-7570.
41. Singh, B. N.; Zhang, G.; Hwa, Y. L.; Li, J.; Dowdy, S. C.; Jiang, S. W. Nonhistone protein acetylation as cancer therapy targets. *Expert Rev. Anticancer Ther.* **2010**, 10, 935-954.
42. Lee, W. J.; Shim, J. Y.; Zhu, B. T. Mechanisms for the inhibition of DNA methyltransferases by tea catechins and bioflavonoids. *Mol. Pharmacol.* **2005**, 68, 1018-1030.
43. Kato, K.; Long, N. K.; Makita, H.; Toida, M.; Yamashita, T.; Hatakeyama, D.; Hara, A.; Mori, H.; Shibata, T. Effects of green tea polyphenol on methylation status of RECK gene and cancer cell invasion in oral squamous cell carcinoma cells. *Br. J. Cancer.* **2008**, 99, 647-654.
44. Volate, S. R.; Muga, S. J.; Issa, A. Y.; Nitcheva, D.; Smith, T.; Wargovich, M. J. Epigenetic modulation of the retinoid X receptor alpha by green tea in the azoxymethane-Apc Min/+ mouse model of intestinal cancer. *Mol. Carcinog.* **2009**, 48, 920-933.
45. Shankar, S.; Suthakar, G.; Srivastava, R. K. Epigallocatechin-3-gallate inhibits cell cycle and induces apoptosis in pancreatic cancer. *Frontiers in bioscience : a journal and virtual library* **2007**, 12, 5039-50.
46. Farabegoli, F.; Papi, A.; Bartolini, G.; Ostan, R.; Orlandi, M. (-)-Epigallocatechin-3-gallate downregulates Pg-P and BCRP in a tamoxifen resistant MCF-7 cell line. *Phytomedicine* **2010**, 17, 356-362.

47. Qiao, J.; Gu, C.; Shang, W.; Du, J.; Yin, W.; Zhu, M.; Wang, W.; Han, M.; Lu, W. Effect of green tea on pharmacokinetics of 5-fluorouracil in rats and pharmacodynamics in human cell lines in vitro. *Food Chem. Toxicol.* **2011**, 49, 1410-1415.
48. Chan, M. M.; Soprano, K. J.; Weinstein, K.; Fong, D. Epigallocatechin-3-gallate delivers hydrogen peroxide to induce death of ovarian cancer cells and enhances their cisplatin susceptibility. *J. Cell. Physiol.* **2006**, 207, 389-396.
49. Chen, T. C.; Wang, W.; Golden, E. B.; Thomas, S.; Sivakumar, W.; Hofman, F. M.; Louie, S. G.; Schonthal, A. H. Green tea epigallocatechin gallate enhances therapeutic efficacy of temozolomide in orthotopic mouse glioblastoma models. *Cancer Lett.* **2011**, 302, 100-108.
50. Kim, H. S.; Kim, M. H.; Jeong, M.; Hwang, Y. S.; Lim, S. H.; Shin, B. A.; Ahn, B. W.; Jung, Y. D. EGCG blocks tumor promoter-induced MMP-9 expression via suppression of MAPK and AP-1 activation in human gastric AGS cells. *Anticancer Res.* **2004**, 24, 747-53.
51. Masuda, M.; Suzui, M.; Weinstein, I. B. Effects of epigallocatechin-3-gallate on growth, epidermal growth factor receptor signaling pathways, gene expression, and chemosensitivity in human head and neck squamous cell carcinoma cell lines. *Clin. Cancer Res.* **2001**, 7, 4220-4229.
52. Gupta, S.; Hussain, T.; Mukhtar, H. Molecular pathway for (-)-epigallocatechin-3-gallate-induced cell cycle arrest and apoptosis of human prostate carcinoma cells. *Arch. Biochem. Biophys.* **2003**, 410, 177-185.
53. Choi, J. H.; Rhee, I. K.; Park, K. Y.; Park, K. Y.; Kim, J. K.; Rhee, S. J. Action of green tea catechin on bone metabolic disorder in chronic cadmium-poisoned rats. *Life Sci.* **2003,** 73, 1479-1489.
54. Bridges, E. M.; Harris, A. L. The angiogenic process as a therapeutic target in cancer. *Biochem. Pharmacol.* **2011**, 81, 1183-1191.
55. Senior, J. H.; Trimble, K. R.; Maskiewicz, R. Interaction of positively-charged liposomes with blood: implications for their application in vivo. *Biochim. Biophys. Acta.* **1991**, 1070, 173-179.
56. Ahmad, N.; Gupta, S.; Mukhtar, H. Green tea polyphenol epigallocatechin-3-gallate differentially modulates nuclear factor kappaB in cancer cells versus normal cells. *Arch. Biochem. Biophys.* **2000**, 376, 338-346.
57. Chandra, S.; De Mejia Gonzalez, E. Polyphenolic compounds, antioxidant capacity, and quinone reductase activity of an aqueous extract of Ardisia compressa in comparison to mate (Ilex paraguariensis) and green (Camellia sinensis) teas. *J. Agric. Food. Chem.* **2004**, 52, 3583-3589.
58. Ahmad, N.; Adhami, V. M.; Gupta, S.; Cheng, P.; Mukhtar, H. Role of the retinoblastoma (pRb)-E2F/DP pathway in cancer chemopreventive effects of green tea polyphenol epigallocatechin-3-gallate. *Arch. Biochem. Biophys.* **2002**, 398, 125-131.
59. Adhami, V. M.; Siddiqui, I. A.; Ahmad, N.; Gupta, S.; Mukhtar, H. Oral consumption of green tea polyphenols inhibits insulin-like growth factor-I-induced signaling in an autochthonous mouse model of prostate cancer. *Cancer Res.* **2004**, 64, 8715-8722.
60. Dong, Z.; Ma, W.; Huang, C.; Yang, C. S. Inhibition of tumor promoter-induced activator protein 1 activation and cell transformation by tea polyphenols, (-)-epigallocatechin gallate, and theaflavins. *Cancer Res.* **1997**, 57, 4414-4419.

61. Shankar, S.; Ganapathy, S.; Hingorani, S. R.; Srivastava, R. K. EGCG inhibits growth, invasion, angiogenesis and metastasis of pancreatic cancer. *Front. Biosci.* **2008**, 13, 440-52.
62. Masuda, M.; Suzui, M.; Lim, J. T.; Weinstein, I. B. Epigallocatechin-3-gallate inhibits activation of HER-2/neu and downstream signaling pathways in human head and neck and breast carcinoma cells. *Clin. Cancer Res.* **2003**, 9, 3486-3491.
63. Reiter, C. E.; Kim, J. A.; Quon, M. J. Green tea polyphenol epigallocatechin gallate reduces endothelin-1 expression and secretion in vascular endothelial cells: roles for AMP-activated protein kinase, Akt, and FOXO1. *Endocrinology* **2010,** 151, 103-114.
64. Meeran, S. M.; Mantena, S. K.; Elmets, C. A.; Katiyar, S. K. (-)-Epigallocatechin-3-gallate prevents photocarcinogenesis in mice through interleukin-12-dependent DNA repair. *Cancer Res.* **2006**, 66, 5512-5520.
65. Oku, N.; Matsukawa, M.; Yamakawa, S.; Asai, T.; Yahara, S.; Hashimoto, F.; Akizawa, T. Inhibitory effect of green tea polyphenols on membrane-type 1 matrix metalloproteinase, MT1-MMP. *Biol. Pharm. Bull.* **2003**, 26, 1235-1238.
66. Berger, S. J.; Gupta, S.; Belfi, C. A.; Gosky, D. M.; Mukhtar, H. Green tea constituent (--)-epigallocatechin-3-gallate inhibits topoisomerase I activity in human colon carcinoma cells. *Biochem. Biophys. Res. Commun.* **2001**, 288, 101-105.
67. Nandakumar, V.; Vaid, M.; Katiyar, S. K. (-)-Epigallocatechin-3-gallate reactivates silenced tumor suppressor genes, Cip1/p21 and p16INK4a, by reducing DNA methylation and increasing histones acetylation in human skin cancer cells. *Carcinogenesis* **2011**, 32, 537-544.
68. Khan, N.; Adhami, V. M.; Mukhtar, H. Apoptosis by dietary agents for prevention and treatment of prostate cancer. *Endocr. Relat. Cancer* **2010**, 17, R39-52.
69. Nam, S.; Smith, D. M.; Dou, Q. P. Ester bond-containing tea polyphenols potently inhibit proteasome activity in vitro and in vivo. *J. Biol. Chem.* **2001,** 276, 13322-13330.
70. Palermo, C. M.; Westlake, C. A.; Gasiewicz, T. A. Epigallocatechin gallate inhibits aryl hydrocarbon receptor gene transcription through an indirect mechanism involving binding to a 90 kDa heat shock protein. *Biochemistry* **2005**, 44, 5041-52.
71. Yin, Z.; Henry, E. C.; Gasiewicz, T. A. (-)-Epigallocatechin-3-gallate is a novel Hsp90 inhibitor. *Biochemistry* **2009**, 48, 336-45.
72. Ishino, N.; Yanase, E.; Nakatsuka, S. Epimerization of tea catechins under weakly acidic and alkaline conditions. *Biosci. Biotechnol. Biochem.* **2010**, 74, 875-877.
73. Sang, S.; Lee, M. J.; Hou, Z.; Ho, C. T.; Yang, C. S. Stability of tea polyphenol (-)-epigallocatechin-3-gallate and formation of dimers and epimers under common experimental conditions. *J. Agric. Food. Chem.* **2005**, 53, 9478-9484.
74. Wan, S. B.; Landis-Piwowar, K. R.; Kuhn, D. J.; Chen, D.; Dou, Q. P.; Chan, T. H. Structure-activity study of epi-gallocatechin gallate (EGCG) analogs as proteasome inhibitors. *Bioorg. Med. Chem.* **2005**, 13, 2177-2185.
75. Osanai, K.; Landis-Piwowar, K. R.; Dou, Q. P.; Chan, T. H. A para-amino substituent on the D-ring of green tea polyphenol epigallocatechin-3-gallate as a novel proteasome inhibitor and cancer cell apoptosis inducer. *Bioorg. Med. Chem.* **2007**, 15, 5076-5082.
76. Kazi, A.; Wang, Z.; Kumar, N.; Falsetti, S. C.; Chan, T. H.; Dou, Q. P. Structure-activity relationships of synthetic analogs of (-)-epigallocatechin-3-gallate as proteasome inhibitors. *Anticancer Res.* **2004**, 24, 943-954.

77. Suzuki, M.; Sano, M.; Yoshida, R.; Degawa, M.; Miyase, T.; Maeda-Yamamoto, M. Epimerization of tea catechins and O-methylated derivatives of (-)-epigallocatechin-3-O-gallate: relationship between epimerization and chemical structure. *J. Agric. Food. Chem.* **2003**, 51, 510-514.
78. Burlison, J. A.; Neckers, L.; Smith, A. B.; Maxwell, A.; Blagg, B. S. J. Novobiocin: Redesigning a DNA Gyrase Inhibitor for Selective Inhibitor of Hsp90. *J. Am. Chem. Soc.* **2006**, 128, 15529-15536.
79. Donnelly, A.; Blagg, B. S. J. Novobiocin and Additional Inhibitors of the hsp90 C-Terminal Nucleotide-Binding Pocket. *Curr. Med. Chem.* **2008**, 15, 2702-2717.
80. Kusuma, B. R.; Khandelwal, A.; Gu, W.; Brown, D.; Liu, W.; Vielhauer, G.; Holzbeierlein, J.; Blagg, B. S. J. Synthesis and Biological Evaluation of Coumarin Replacements of Novobiocin as Hsp90 Inhibitors. *Bioorg. Med. Chem.* **2014**, 22, 1441-1449.
81. Zhao, H.; Donnelly, A. C.; Kusuma, B. R.; Brandt, G. E. L.; Brown, D.; Rajewski, R. A.; Vielhauer, G.; Holzbeierlein, J.; Cohen, M. S.; Blagg, B. S. J. Engineering an Antibiotic to Fight Cancer: Optimization of the Novobiocin Scaffold to Produce Anti-Proliferative Agents. *J. Med. Chem.* **2011**, 54, 3839-3853.
82. Li, L.; Chan, T. H. Enantioselective synthesis of epigallocatechin-3-gallate (EGCG), the active polyphenol component from green tea. *Org. Lett.* **2001**, 3, 739-741.
83. Nicolaou, K. C.; Adsool, V. A.; Hale, C. R. An expedient procedure for the oxidative cleavage of olefinic bonds with PhI(OAc)2, NMO, and catalytic OsO4. *Org. Lett.* **2010**, 12, 1552-1555.
84. Zheng, T.; Narayan, R. S.; Schomaker, J. M.; Borhan, B. One-pot regio- and stereoselective cyclization of 1,2,n-triols. *J. Am. Chem. Soc.* **2005**, 127, 6946-6947.
85. Tuckmantel, W.; Kozikowski, A. P.; Romanczyk, L. J. Studies in polyphenol chemistry and bioactivity. 1. Preparation of building blocks from (+)-catechin. Procyanidin formation. Synthesis of the cancer cell growth inhibitor, 3-O-galloyl-(2R,3R)-epicatechin-4 beta,8-[3-O-galloyl-(2R,3R)-epicatechin]. *J. Am. Chem. Soc.* **1999**, 121, 12073-12081.
86. Coleman, R. S.; Shah, J. A. Chemoselective cleavage of benzyl ethers, esters, and carbamates in the presence of other easily reducible groups. *Synthesis* **1999**, 1399-1400.
87. Chen, W.; Yang, X. D.; Li, Y.; Yang, L. J.; Wang, X. Q.; Zhang, G. L.; Zhang, H. B. Design, synthesis and cytotoxic activities of novel hybrid compounds between dihydrobenzofuran and imidazole. *Org. Biomol. Chem.* **2011**, 9, 4250-4255.
88. Fairlamb, I. J.; Dickinson, J. M.; O'Connor, R.; Cohen, L. H.; van Thiel, C. F. Synthesis and antimicrobial evaluation of farnesyl diphosphate mimetics. *Bioorg. Chem.* **2003**, 31, 80-97.
89. Shi, Z.; He, C. An Au-catalyzed cyclialkylation of electron-rich arenes with epoxides to prepare 3-chromanols. *J. Am. Chem. Soc.* **2004**, 126, 5964-5965.
90. Klepper, F.; Jahn, E. M.; Hickmann, V.; Carell, T. Synthesis of the transfer-RNA nucleoside queuosine by using a chiral allyl azide intermediate. *Angew. Chem. Int. Ed. Engl.* **2007**, 46, 2325-2327.
91. Donnelly, A. C.; Mays, J. R.; Burlison, J. A.; Nelson, J. T.; Vielhauer, G.; Holzbeierlein, J.; Blagg, B. S. The design, synthesis, and evaluation of coumarin ring derivatives of the novobiocin scaffold that exhibit antiproliferative activity. *J. Org. Chem.* **2008**, 73, 8901-8920.

92. Khandelwal, A.; Hall, J. A.; Blagg, B. S. Synthesis and structure-activity relationships of EGCG analogues, a recently identified Hsp90 inhibitor. *J. Org. Chem.* **2013**, 78, 7859-7884.

Chapter III

The Development of Grp94-Selective Inhibitors

III.1. Introduction

Hsp90 is responsible for the conformational maturation of more than 200 substrates (client proteins).[1, 2] Many of which are associated with cell signaling, making it a highly sought after target for the development of antitumor agents, as multiple signaling nodes can be disrupted simultaneously through Hsp90 inhibition.[3, 4] There are four Hsp90 isoforms: Hsp90α and Hsp90β are located in the cytosol, Grp94 resides in the endoplasmic reticulum, and Trap1 is localized to mitochondria.[5, 6] Each of these isoforms forms a complex with various co-chaperones and partner proteins to fold individual substrate proteins.[7-10] There are currently 17 molecules undergoing clinical trials that bind the Hsp90 N-terminal ATP-binding site. Unfortunately, all of these molecules are *pan*-inhibitors and target all four Hsp90 isoforms with similar affinity.[11-13] *Pan*-inhibitory activity of current clinical candidates appears detrimental, as results from clinical trials have reported hepatotoxicity, cardiotoxicity, ocular toxicity, bone metastasis and peripheral neuropathy amongst other side effects.[14-18]

An additional problem associated with all *pan*-inhibitors of the Hsp90 N-terminal ATP-binding site is that they induce Hsp70 and Hsp90 expression (pro-survival heat shock response) at the same concentrations required for client protein degradation, making both scheduling and dosing of these drugs extremely difficult.[12, 19-21] Induction of the pro-survival heat shock response by *pan*-inhibitors requires the administration of drugs at higher doses and with an increased frequency, which pushes the patient towards toward the maximum tolerated dose, resulting in toxicity.[20] Consequently, alternative methods to inhibit the Hsp90 protein folding machinery are needed that do not induce this pro-survival heat shock response.[22-24] Selective inhibition of

individual isoforms represents one approach to overcome the detriments associated with *pan*-inhibition of all Hsp90's.[25-28]

The expression of Hsp90 isoforms can vary among cancers, suggesting an inherent dependence of cancer upon individual isoforms.[29-38] In addition, Hsp90 isoforms exhibit specificity for client proteins substrates via interactions with co-chaperones, which suggests that Hsp90 isoforms should be targeted individually.[32, 39, 40] Some isoform-specific clients have been identified and therefore, isoform-selective Hsp90 inhibitors are likely to provide a therapeutic opportunity that minimizes on-target toxicity by limiting the number of clients affected via *pan*-Hsp90 inhibition.[28, 41-44] Therefore, selective-inhibitors of individual isoforms are highly sought after and their development represents a new paradigm in Hsp90 research. This chapter focuses on the development of Grp94-selective inhibitors.

III.2. Grp94

Glucose-regulated protein 94 (Grp94) is encoded by the HSP90B1 gene and is located in the lumen of the endoplasmic reticulum. Grp94 is not expressed in unicellular organisms and is ubiquitously expressed in human cells.[6, 45, 46] Grp94 is responsible for the maturation and degradation of a client proteins associated with cell-to-cell signaling and immunity (innate and adaptive).[47-50] In addition, Grp94 plays a key role in cellular adhesion and migration through maintaining cell polarity and the intracellular-trafficking of integrins.[50-52] Unlike the cytosolic isoforms, Grp94 is not overexpressed via the heat shock response, it is upregulated following induction of ER stress (calcium imbalance, hypoxia, redox stress).[53] Grp94 is essential for embryonic development and stem cell maintenance as observed by siRNA knockdown studies.[54]

Grp94 is responsible for maturation and trafficking of a restricted number of proteins as shown in Table 1.[47] These client proteins include, Toll-like receptors (1, 2, 4, and 9), IGF-I, IGF-

II, integrins, and Her2. Many of these client proteins are implicated in various diseases, including liver cancer, multiple myeloma, rheumatoid arthritis and glaucoma.[55-58] In fact, small molecule inhibitors of Grp94 are therapeutically useful for the treatment of such diseases.[27, 55, 56, 58] As stated earlier, Grp94 is only essential during embryonic development, and therefore, its inhibition represents a non-toxic therapeutic application.

Grp94 is overexpressed in some cancers and is generally associated with more aggressive tumor growth and poor prognosis.[36, 59, 60] Recently, Hua and co-workers showed that Grp94 is required for the growth and survival of multiple myeloma cells.[61] Inhibition of Grp94, by a Grp94-selective inhibitor, WS-13, resulted in decreased cell proliferation. This response is mediated by LRP6, a Grp94 client, which is a co-receptor for the Wnt receptor, frizzled. Grp94 inhibition limits the LRP6 expression at the cell surface which blocks the Wnt/β-catenin signaling pathway, and results in decreased cell proliferation. Hence, Grp94 inhibition decreases cell proliferation, and induces apoptosis. Another client of Grp94 is Her2, which is a receptor tyrosine kinase and an oncogenic protein. Recent studies by Patel and co-workers showed that siRNA knockdown of Grp94 in Her2 overexpressing SkBr3 cells resulted in decreased expression of Her2 at the cell surface.[62] Additionally, Grp94 inhibitors successfully decreased the levels of Her2 in SkBr3 cell lysates.

Grp94's clientele includes some integrins (α2, α4, β7, αL, β2), which play a key role in cell adhesion and migration.[47] Grp94 is responsible for the maturation as well as intracellular trafficking of these proteins. Grp94 knockdown or pharmacological inhibition downregulates the expression of integrins, which results in decreased migration.[27, 52] Hence, Grp94 inhibitors represent a non-toxic approach for the treatment of cancer metastasis.

Table 9. Grp94 client proteins. (IP: immunoprecipitation, KO: Knock-out)

Grp94 Client Proteins	IP	Grp94KO/ RNAi	Grp94 Drug Inhibition
ADAMTS9	+	+	+
Apolipoprotein B	+		
Cartilage	+		
Collagen	+		+
EGF-R	+		+
Erb2			
Golgi apparatus casein Kinase	+		
Ig chains	+		
IGF-I		+	
IGF-II	+	+	+
IFN-γ	+		
IL-12p80	+	+	+
Insulin receptor IRS-1			+
Integrins CD49d, α4, β7, αL, β2		+	
MHC class II	+		
Bile-salt dependent lipase		+	+
Thrombospondin	+		
Thyroglobulin	+		
TLR1, TLR2, TLR4	+	+	
TLR9	+	+	
WFS1	+		
α–1 antitypsin	+		
Protein C	+		
HSV glycoprotein	+		

Grp94 inhibitors have also demonstrated efficacy in *in vivo* models of glaucoma, a disease caused by increased intraocular pressure caused by mutant myocilin aggregates.[27, 55, 56] Mutations

in myocilin cause it to accumulate in endoplasmic reticulum (ER) of trabecular meshwork cells leading to dysregulation of humor outflow, which results in elevated intraocular pressure and toxicity. Grp94 recognizes mutant myocilin aggregates as abnormal, but fails to promote their clearance via ERAD (Endoplasmic reticulum associated protein degradation). However, disruption of the Grp94-myocilin complex through knockdown or pharmacological inhibition results in the clearance of myocilin aggregates through autophagic mechanism. Grp94 inhibitors have been shown to downregulate the levels of various myocilin mutants that result in primary open angle glaucoma.[27, 56]

III.3. Ligand Occupation of Grp94 N-Terminal ATP-Binding Pocket

The N-terminal ATP binding site is highly identical amongst Hsp90 isoforms (Figure 20a).[63, 64] However, one key difference that is present in Grp94 and not in other Hsp90 isoforms is the insertion of 5-amino acid sequence into the primary sequence (182−186, Figure 20, highlighted in red). While this sequence does not comprise the binding pocket, its effect on the tertiary structure of Grp94 is significant. Grp94 adopts different conformations upon ligand binding, these conformations result in additional sub-pockets within the N-terminus (vide infra), which can be exploited for the development of Grp94-selective inhibitors.[65, 66]

III.3.1 Binding of Geldanamycin to Grp94

Geldanamycin (GDA), a *pan*-Hsp90 inhibitor that binds to both Hsp90α and Grp94 in similar binding modes (Figure 21) manifests interactions that are conserved amongst both isoforms.[66] The C-7 carbamate makes a hydrogen bond with Asp 149 (Asp93 in Hsp90α), while one oxygen of the quinone ring interacts with Asp110 (Asp54 in Hsp90α) and Lys 114 (Lys58 in Hsp90α). Additionally, GDA also provides favorable hydrophobic interactions with multiple residues including Met154, Leu163, Val197, and Phe199. The quinone binds in a *cis*-amide

conformation to both Grp94 and Hsp90α. The binding affinity of GDA for Grp94 (170 nM) is higher than for Hsp90α (~1 μM); this difference has not been rationalized.

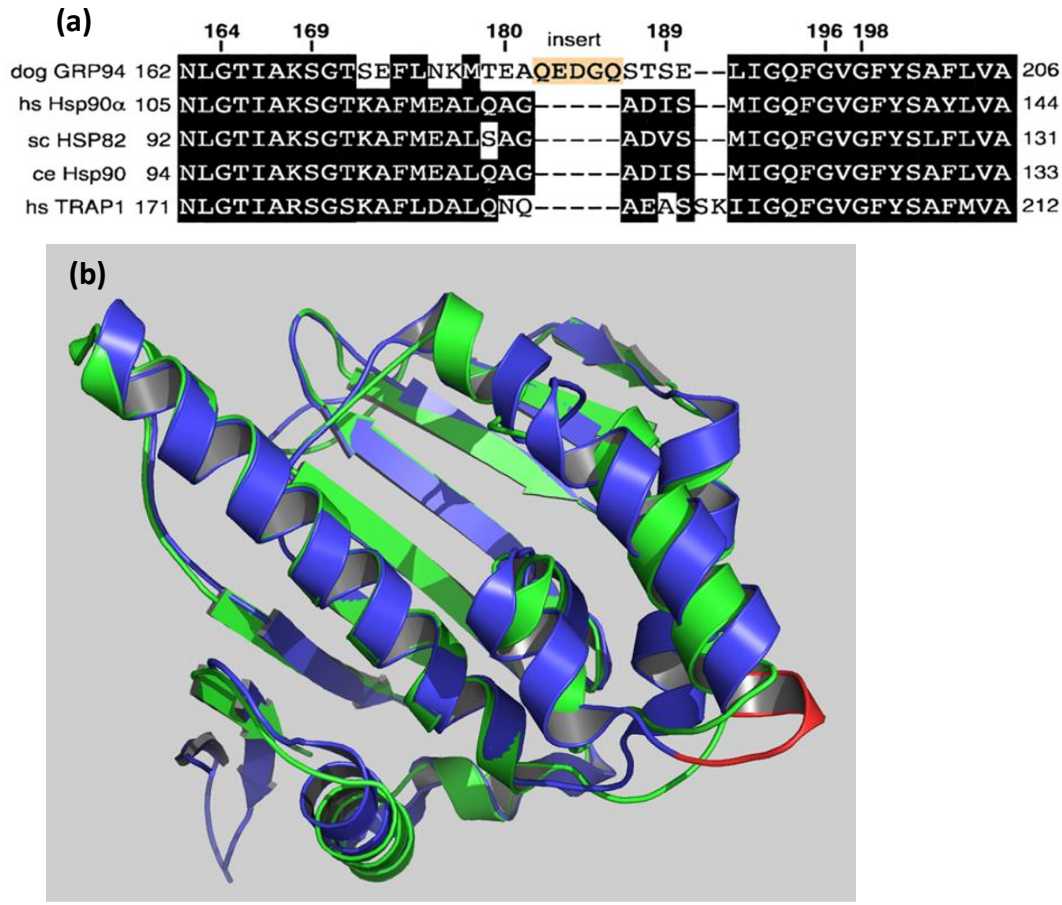

Figure 20. Differences between Hsp90α vs Grp94. (a) Sequence alignment of Hsp90 isoforms. (b) Overlay of apo-Hsp90 (colored in green) and apo-Grp94 (colored in blue and red). The loop containing the 5-amino acid insertion in Grp94 is highlighted in red.

III.3.2 Binding of NECA to Grp94

A broad spectrum adenosine A2 receptor agonist, 5'-Nethylcarboxamidoadenosine (NECA) was the first Grp94-selctive inhibitor identified (Figure22).[67] In order to understand NECA's interactions with Grp94, Gewirth and co-workers solved the co-crystal structure of NECA bound to Grp94. As expected, the adenine moiety of NECA exhibited similar interactions with Grp94 as observed in the ATP/Grp94 complex.[63, 68] Overlay of this co-crystal structure with

Hsp90α provided an explanation for the observed selectivity over Hsp90α. As mentioned previously, the 5-amino acid insertion alters the tertiary structure of Grp94, which leads to

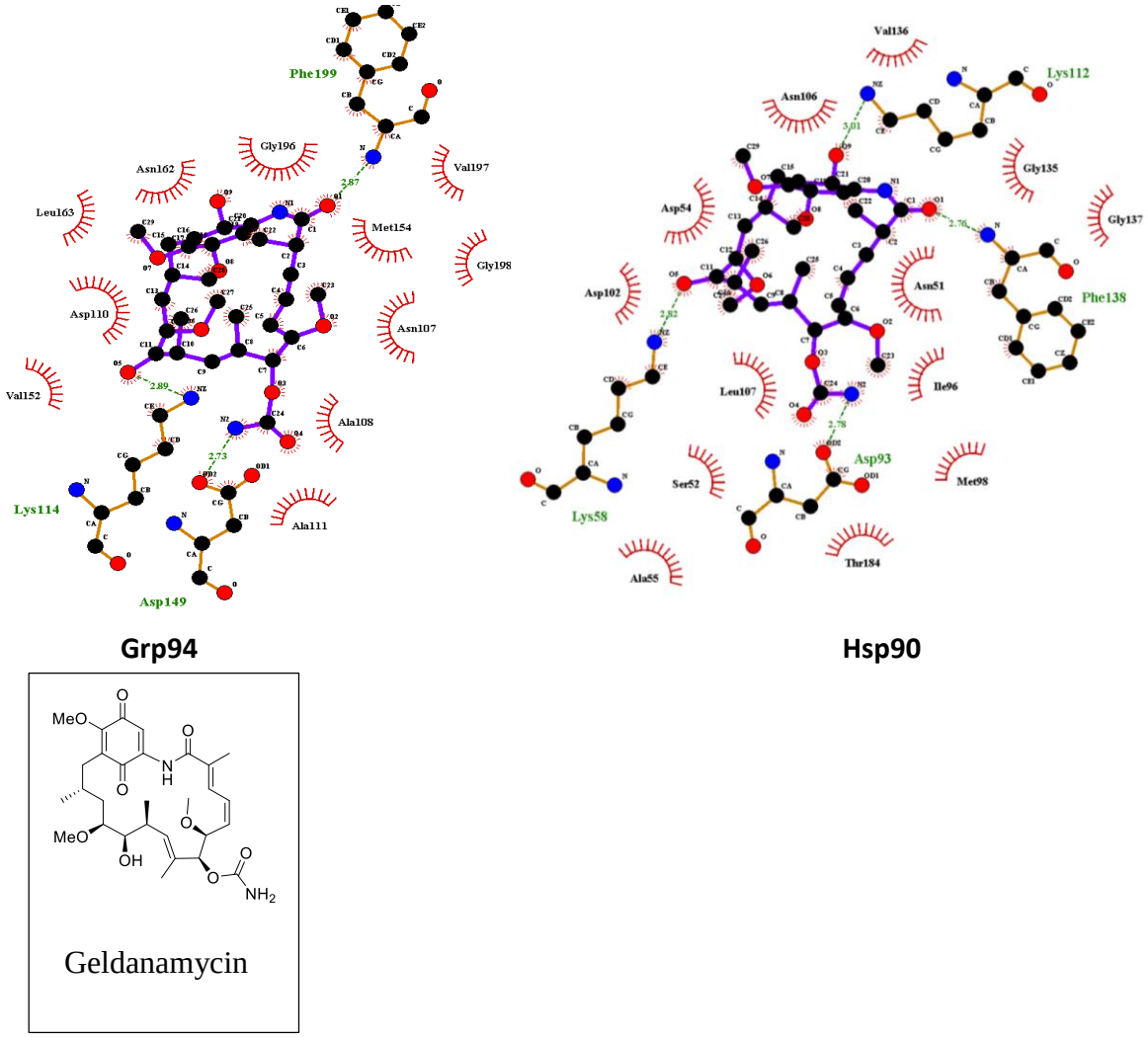

Figure 21. Binding of Geldanamycin to Grp94 (PDB: 2EXL) and Hsp90α (PDB: 1YET). Figures were generated using "ligplot plus" program.

repositioning of Ala167 and Lys168 within the binding pocket. These reorganizations induce a secondary binding pocket that is not present in Hsp90α. As shown in Figure 22b, the 5'-ethyl moiety of NECA projects into this region and make hydrophobic interactions with Val197 and

Tyr200. In Hsp90α, the 5' ethyl of NECA orients towards Gly121 which prevents NECA from binding Hsp90α.

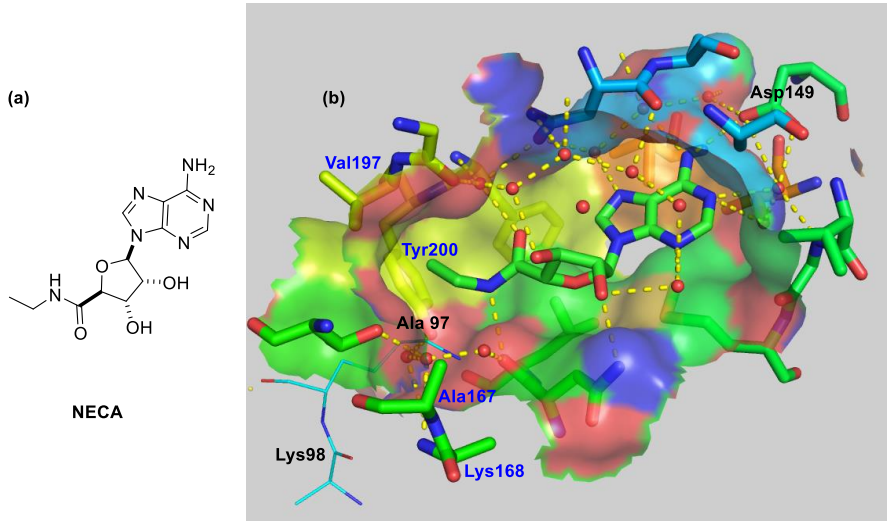

Figure 22. Binding of NECA to Grp94. (a) Structure of NECA; (b) NECA bound to Grp94 (PDB: 1QY5); putative position of Lys and Ala (represented as lines for Hsp90α) is labeled in black.

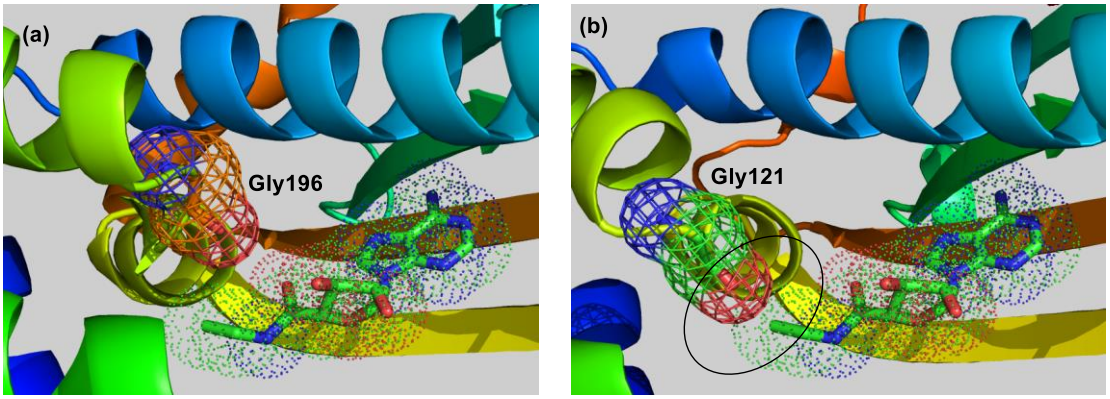

Figure 23. Rationale for observed selectivity of NECA for Grp94. (a) Co-crystal structure of NECA bound to Grp94 (PDB:1QY5); (b) NECA modeled in Hsp90α-binding pocket (PDB: 2FXS), steric interaction between Gly121 and ethyl group of NECA is circled.

III.3.3. Binding of Radamide Grp94

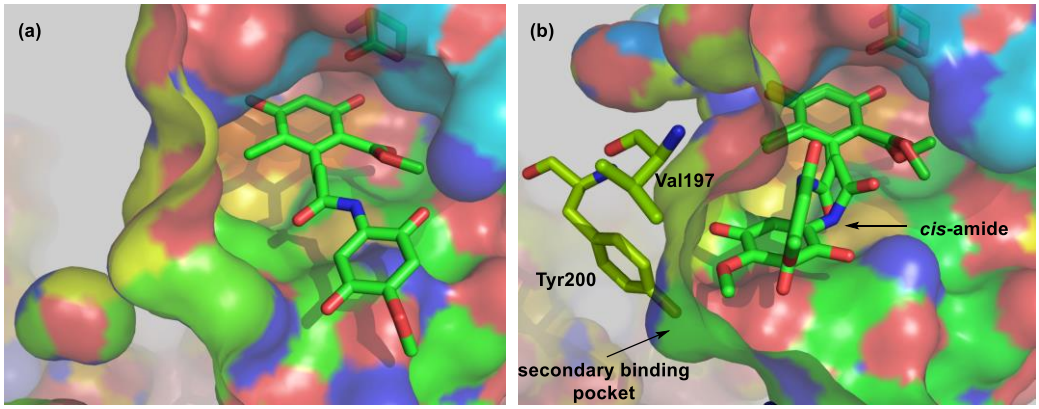

Figure 24. Binding of radamide to Grp94 versus Hsp90. Co-crystal structures of radamide (a) Hsc82 (PDB: 2FXS); (b) Grp94 (PDB: 2GFD).

Co-crystallization of radamide with Hsp90 demonstrated radamide to exist in a *trans*-amide conformation within the binding pocket (Figure 24a).[66] However, the co-crystal structure of radamide bound to Grp94 revealed the presence of two distinct conformations within the binding pocket (50% occupancy of each): the conformations contained a *cis*-amide or a *trans*-amide orientation (Figure 24b). The *cis*-amide conformation of radamide orients the quinone moiety directly towards the exclusive secondary binding pocket present in Grp94, and provides opportunity to develop Grp94-selctive inhibitors.

III.4. Development of Grp94-Selective Inhibitors

Prior studies in the Blagg laboratory have established that the quinone moiety is dispensable for Grp94 inhibition, which led to the development of compound **33** (Grp94 K_d = 20 μM). Structure-activity relationship studies were conducted on the phenyl ring. A summary of these prior studies is provided in Figure 25. Chloride substituents at the 2- and the 3-position were advantageous, and a bromide at the 4-position proved most beneficial. The 4-bromophenyl amide

was the best compound resulting from this series, which manifested an apparent K_d of 1.5 μM against Grp94.

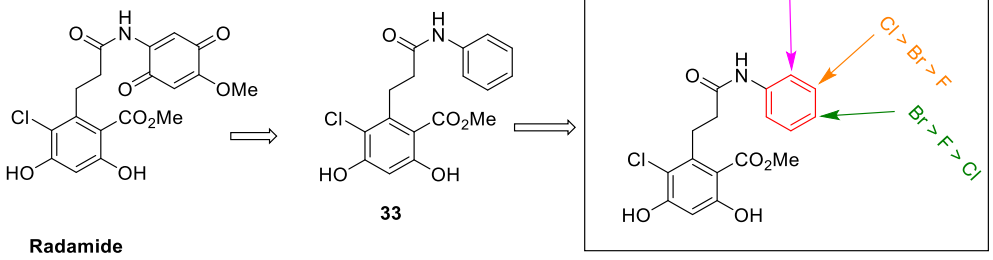

Figure 25. Summary of prior studies on radamide -derived Grp94 inhibitors.

Simultaneous studies in the Blagg laboratory led to the development of the first rationally designed Grp94-selective inhibitor, BnIm.[25] BnIm was developed by incorporation of a bioisosteric replacement (imidazole) of the cis-amide of radamide (Figure 25). Grp94-selective inhibition was determined in cells by a decrease in Grp94-mediated Toll-like receptor trafficking to the cell surface and the lack of cytosolic Hsp90 client protein degradation. BnIm manifested apparent K_d of 1.14 μM against Grp94. BnIm was co-crystallized with Grp94 and analysis of its co-crystal structure provided useful information about its binding interactions. Further development of BnIm analogues was pursued in parallel with radamide analogues.

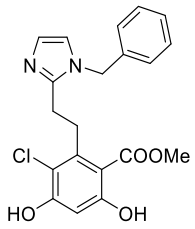

Figure 26. Structure of BnIm

III.4.1 Development of Radamide Analogues as Grp94 Inhibitors

Based on prior studies, the development of radamide and BnIm analogues was pursued for selective Grp94 inhibition. Additionally, a resorcinol-isoindoline scaffold was also sought. In an

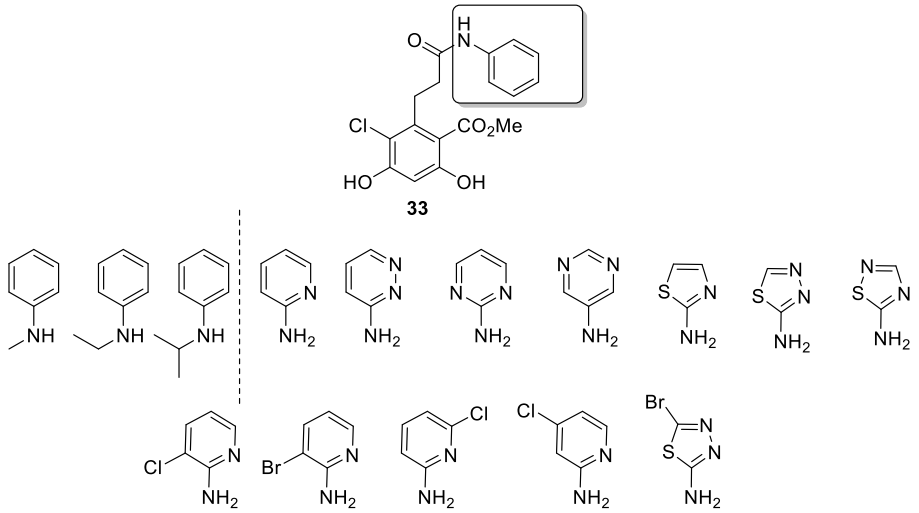

Figure 27. Proposed radamide analogues for improved Grp94-inhibiton.

effort to further improve Grp94-selective binding, tertiary amides were proposed (Figure 27), which were expected to favor the *cis*-amide conformation by making the *cis*-conformation lower in energy, and therefore providing Grp94-selectivity. In a second series of analogues, heterocyclic anilines were introduced in lieu of the phenyl ring. Due to the π-rich nature of the secondary binding pocket, replacement of the phenyl ring with heterocycles was hypothesized to improve π–π interactions and thereby improve affinity for Grp94. Additionally, electron withdrawing heterocycles were thought to enhance isomerization to the *cis*-amide conformation.

III.4.1.1. Synthesis of Radamide Analogues

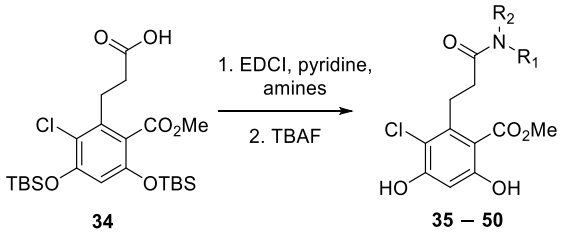

Scheme 6. Synthesis of radamide analogues.

The synthesis of proposed analogues started with previously reported **34**. 1-Ethyl-3-(3-dimethylaminopropyl) carbodiimide (EDCI) mediated coupling of **34**, with requisite anilines (Figure 27) gave the amide products, and subsequent removal of *tert*-butyldimethylsilyl ethers

utilizing tetra-n-butylammonium fluoride (TBAF) afforded the desired analogues, **35–50** (Scheme-6)

III.4.1.2. Evaluation of Radamide Analogues

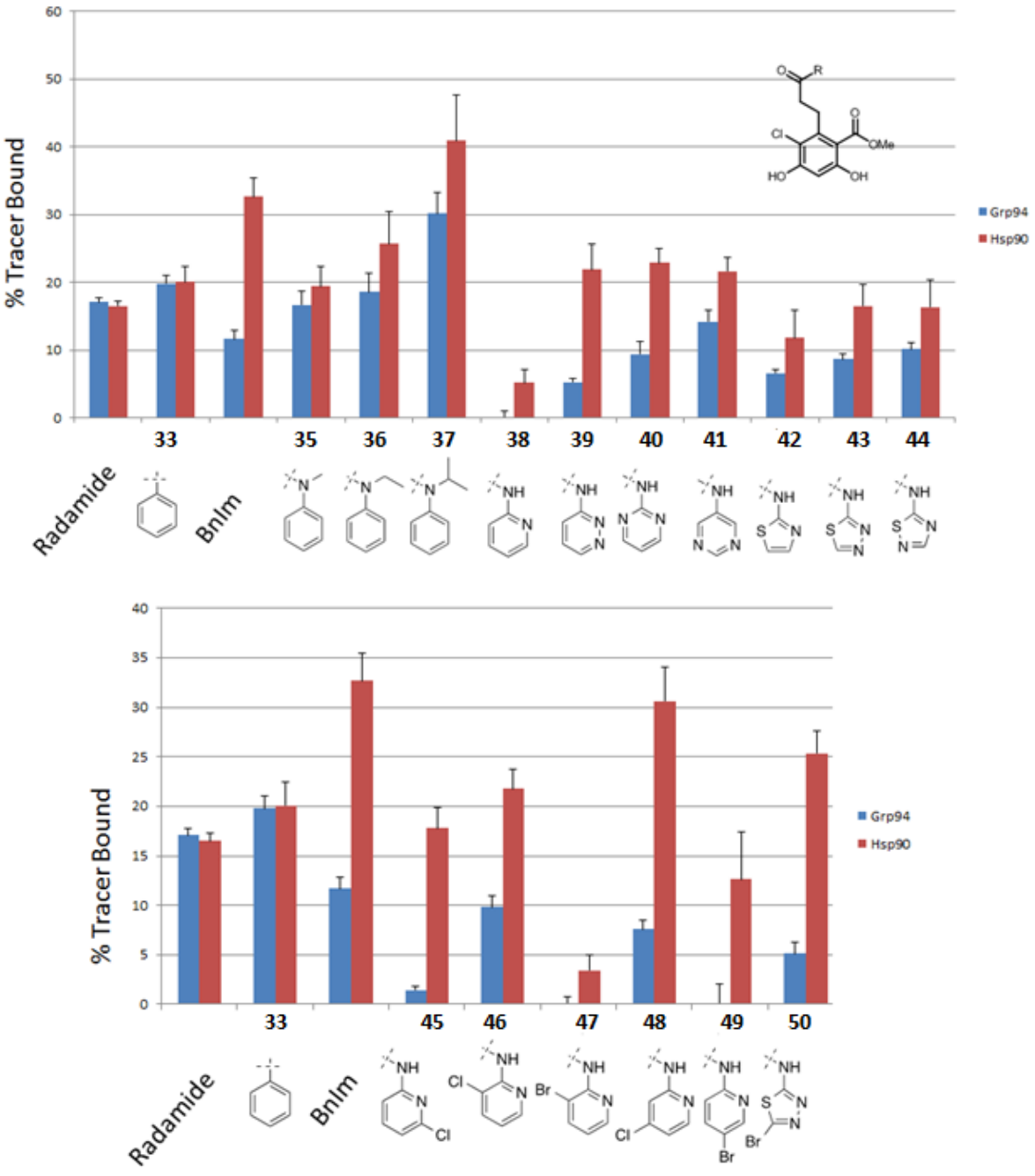

Figure 28. Evaluation of radamide analogues.

Once prepared, compounds **35–50** were evaluated via a fluorescence polarization assay at 25 μM. This fluorescence polarization assay is a competitive binding assay that utilizes FITC-labeled geldenamycin as a tracer.[69, 70] The compounds of interest were evaluated for their ability to displace this tracer (FITC-GDA).[69] The bound tracer is normalized to a DMSO control and is inversely proportional to the affinity of an inhibitor. For comparison, BnIm and compound **33** were used as positive controls. As shown in Figure 28, the tertiary amide containing compounds **35**–**37** did not exhibit selectivity. Introduction of 2-pyridine, 1,2-diazene, 1,6-diazene, 3,5-diazene, thiazole, 1,2,4-thiadiazole, and 1,3,4-thidiazole were beneficial, as these compounds exhibited improved binding affinity for Grp94 at 25 μM. The 2-pyridine containing analogue (**38)** was the best amongst this series and chosen for further development. As described earlier, halogen substitutions were beneficial on phenyl amide **33** and therefore, chloride and bromide substituents were incorporated onto the pyridine ring. Evaluation of compounds **45–50** provided **49**, which manifested affinity similar to **38** and provided a substantial improvement in selectivity for Grp94 versus Hsp90α.

III.4.2. The Development of BnIm Analogues as Grp94 Inhibitors

The binding of BnIm to Grp94 induced a conformational change in Grp94 compared to radamide bound Grp94.[66] As shown in Figure 29a, BnIm bound to Grp94 shifts the N-terminal "lid" to a partially closed conformation (green), which contrasts with the open conformation that is observed when radamide bound Grp94 (colored red). This closed "lid" orientation resulted in repositioning of key amino acid residues (Phe195, Val 197, Phe199, Tyr200, Trp223) (Figure 29b). As a result of this conformational change, the phenyl side chain of BnIm projected toward Trp223. Additionally, the resorcinol moiety of BnIm was oriented 180° compared to radamide. The phenyl ring of BnIm produced multiple hydrophobic contacts with Trp223, Phe197, Val197. When

evaluating the co-crystal structures, it was envisioned that substitution at the 4-position would be tolerated and would produce improved affinity. Additionally, replacement of the phenyl side chain with heterocycles could also enhance π–π interactions between the ligand and the protein due to the π-rich nature of this binding region (Scheme 7).

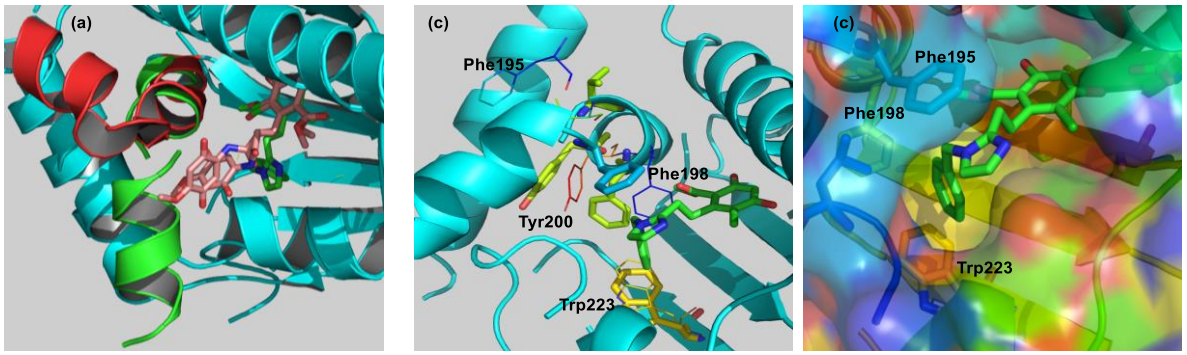

Figure 29. Binding of BnIm to Grp94. (a) Overlay of co-crystal structures of BnIm ("lid" is colored as green, Blagg and Gewirth, unpublished results) and radamide ("lid" is colored as red PDB: 2GFD) bound to Grp94. (b) reorientation of side chains (shown in sticks) in BnIm bound Grp94, the position of side chains in radamide bound Grp94 is shown in lines. (c) Hydrophobic environment around phenyl side chain of BnIm.

III.4.2.1. Synthesis of BnIm Analogues

The proposed compounds were synthesized by use of a multicomponent reaction.[25] Aldehyde (**51**) was prepared following a reported procedure, which upon treatment with the requisite benzyl amines, ammonium bicarbonate, and glyoxal produced the corresponding imidazole.[71] Cleavage of *tert*-butyldimethylsilyl ethers in presence of tetra-n-butylammonium fluoride gave the desired products, **52–60** (Scheme 7).

III.4.2.2. Evaluation of BnIm Analogues

At first, compounds **52–60** were evaluated at a 25 μM concentration in a fluorescence polarization assay. As shown in Figure 30, incorporation of the 4-methyl substituent significantly increased selectivity for Grp94 and maintained affinity compared to BnIm. However, the inclusion

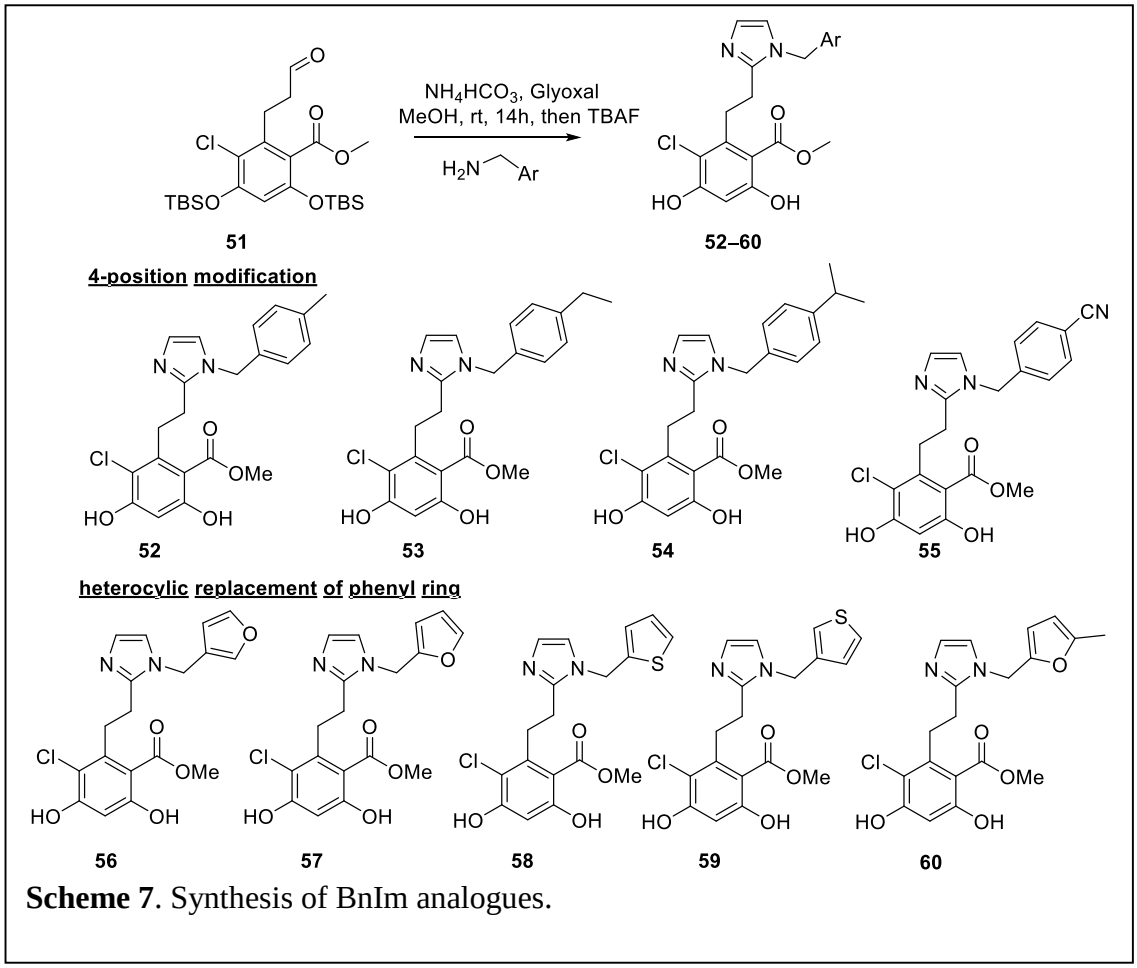

Scheme 7. Synthesis of BnIm analogues.

of extended alkyl chains were not tolerated and resulted in decreased affinity due to the steric clashes with the protein. Compound **52** was chosen from the 25 μM screening to determine its apparent K_d against Hsp90α and Grp94, which manifested an apparent K_d of 730 nM and 34-fold selectivity for Grp94. Replacement of the phenyl side chain with heterocycles was more beneficial. Compounds **57** and **58** improved affinities for Grp94 and maintained selectivity. Molecular modeling studies suggested that the selectivity of **57** could be improved by the inclusion of a methyl group onto the 5-position of a furan ring. The overlay of energy minimized structures, **52** and **57** indicated the 5-position of the furan to aligned similarly to the 4-position of phenyl ring

within the Grp94-binding pocket. Evaluation of the 5-methylfuran analogue confirmed this hypothesis, as **60** manifested ~41-fold selectivity for Grp94.

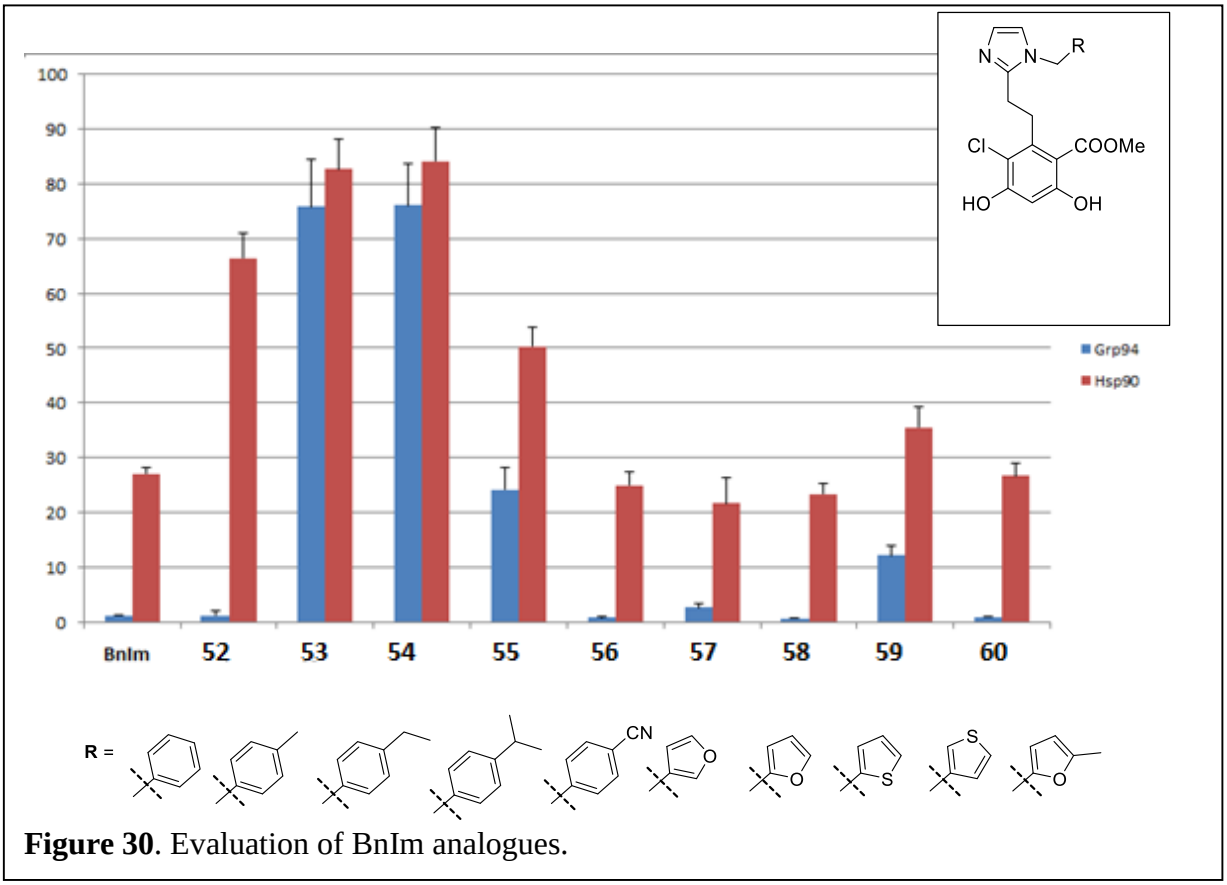

Figure 30. Evaluation of BnIm analogues.

Table 10. Apparent K_d of BnIm analogues

Compound	K_d Grp94 (μM)	K_d Hsp90α (μM)	Fold-selectivity for Grp94
BnIm	1.14 ± 0.1	13.1 ± 1.1	12
52	0.73 ± 0.1	25.2 ± 2.1	34
56	1.5 ± 0.1	3.77 ± 0.4	3
57	0.55 ± 0.06	5.91 ± 0.88	11
58	0.47 ± 0.07	3.92 ± 0.51	8
59	2.14 ± 0.22	6.54 ± 0.86	3
60	0.65 ± 0.1	26.6 ± 2.3	41

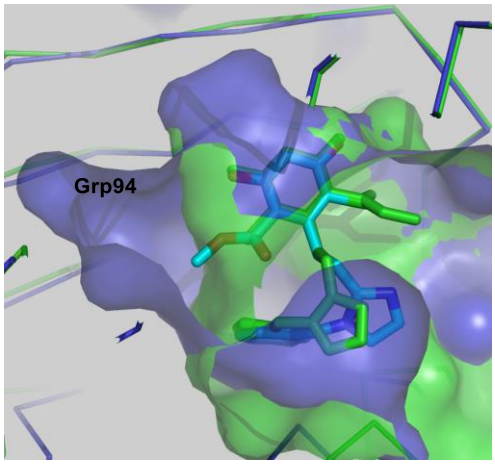

Figure 31. An overlay of co-crystal structure of BnIm bound to Hsp90α (green) and Grp94 (blue).

III.4.3. Development of Resorcinol-Isoindoline Class of Grp94 Inhibitors

As previously mentioned, the co-crystal structure of BnIm demonstrated a re-orientation of the protein, as well as a 180° rotation of the resorcinol ring. An overlay of BnIm's co-crystal structures with Grp94 and Hsp90α revealed the conformational change, which formed an exclusive sub-pocket near the ester of BnIm as shown in Figure 31. Based on these observations, it was hypothesized that ligands targeting this region of the Grp94 binding pocket would provide selectivity for Grp94 versus other Hsp90 isoforms. Therefore, in pursuit of more efficacious Grp94 inhibitors, modifications to the resorcinol ring were pursued.

Modifications at the 5-position of the resorcinol ring of BnIm were deemed difficult, and consequently an alternative scaffold was pursued to rapidly access analogues that bind to this unique sub-pocket. After careful consideration, the resorcinol-isoindoline compound **61** was chosen for the development of 5-resorcinol analogues. Compound **61** is derived from a known Hsp90 inhibitor, AT13387 (Figure 32a) and was synthesized following literature procedure.[72, 73] For selective Grp94-inhibiton, the incorporation of alkyl esters and aryl groups onto the 5-position was proposed, via the preparation of compounds **62–64** to gain understating of the binding pocket. Compounds **62** and **63** were designed to mimic ester moiety of BnIm, and compound **64** was proposed to produce hydrophobic interactions with the sub-pocket. In parallel to these studies, Patel and co-workers identified a purine-derived inhibitor PU-WS13 (Figure 32a) that also take advantage of this Grp94 sub-pocket.[44, 74] They screened a library of Hsp90 inhibitors against all

Hsp90 isoforms and identified, PU-WS13 as Grp94-selctive inhibitors. Compounds **62–65** were then proposed to confirm their findings as they encompass optimal aryl substitutions obtained from their studies.

III.4.3.1 Syntheses of Resorcinol-Isoindoline Analogues

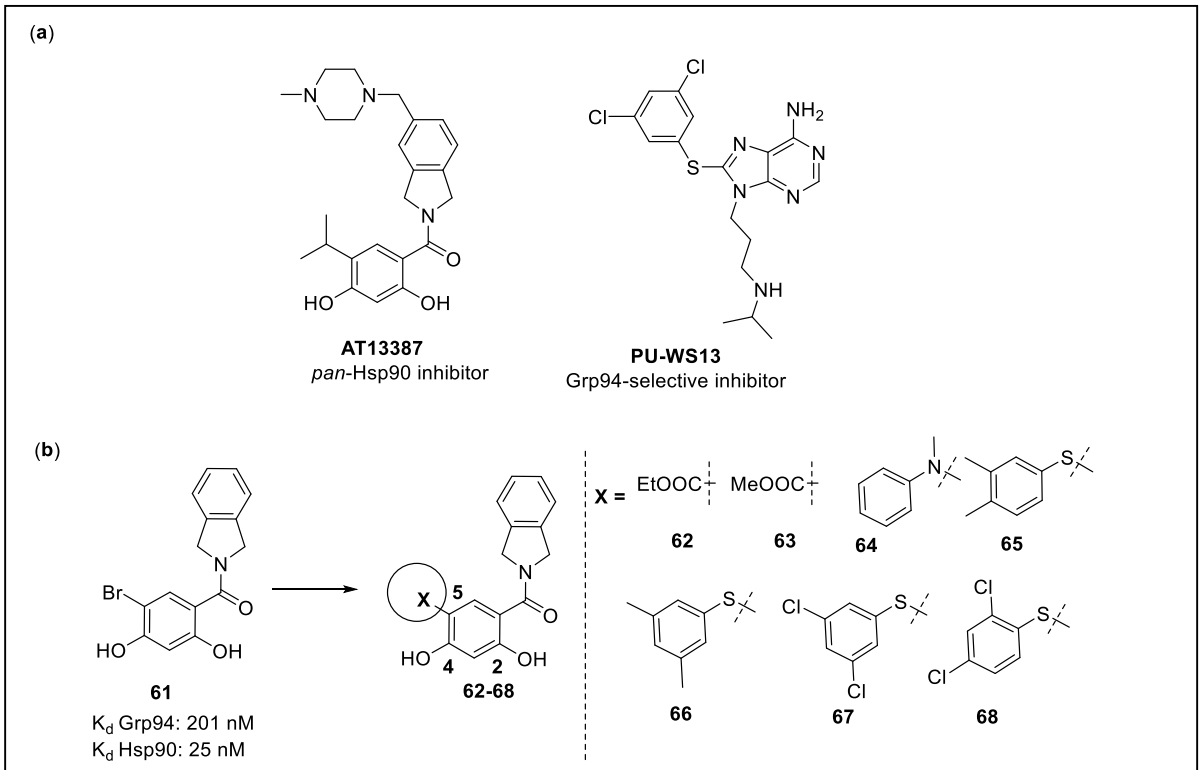

Figure 32. Development of resorcinol-isoindoline class of Grp94-selective inhibitors. (a) Structure of AT13387 and PU-WS13. (b) Proposed resorcinol-isoindoline compounds for selective Grp94 inhibition.

Synthesis of the proposed analogues began via the preparation of **69** following literature procedures.[75] As shown in Scheme 8, the proposed analogues were prepared via palladium catalyzed cross-coupling reactions with **69**. A palladium catalyzed decrboxylative coupling reaction of **69** enlisting ethyl potassium oxalate, palladium (II) trifluoroacetate, and 1,3-Bis(diphenylphosphino)propane (dppp), and subsequent cleavage of the benzyl ethers furnished the desired compound, **62**.[76] Transesterification of **62** in the presence of methanol gave methyl

ester, **63**. N-methyl aniline in **64** was coupled by the use of Tris(dibenzylideneacetone)dipalladium(0) ($Pd_2(dba)_{3)}$ in the presence of RuPhos.[77] For the syntheses of compounds **65–68**, the requisite thiols were coupled enlisting ($Pd_2(dba)_3$), sodium *tert*-butoxide, and XPhos to give corresponding thioethers.[78] However, this reaction did not work for synthesis of **68**, as 2,4-dichlorobenzethiol is sterically hindered and is an electronically disfavored coupling partner. Instead, synthesis of **65** was accomplished with palladium acetate ($Pd(OAc)_2$) and the Josiphos ligand.[79, 80] The benzyl ethers of these intermediates phenyl thioethers were cleaved via boron tribromide to furnish the corresponding resorcinol products **65–68**.

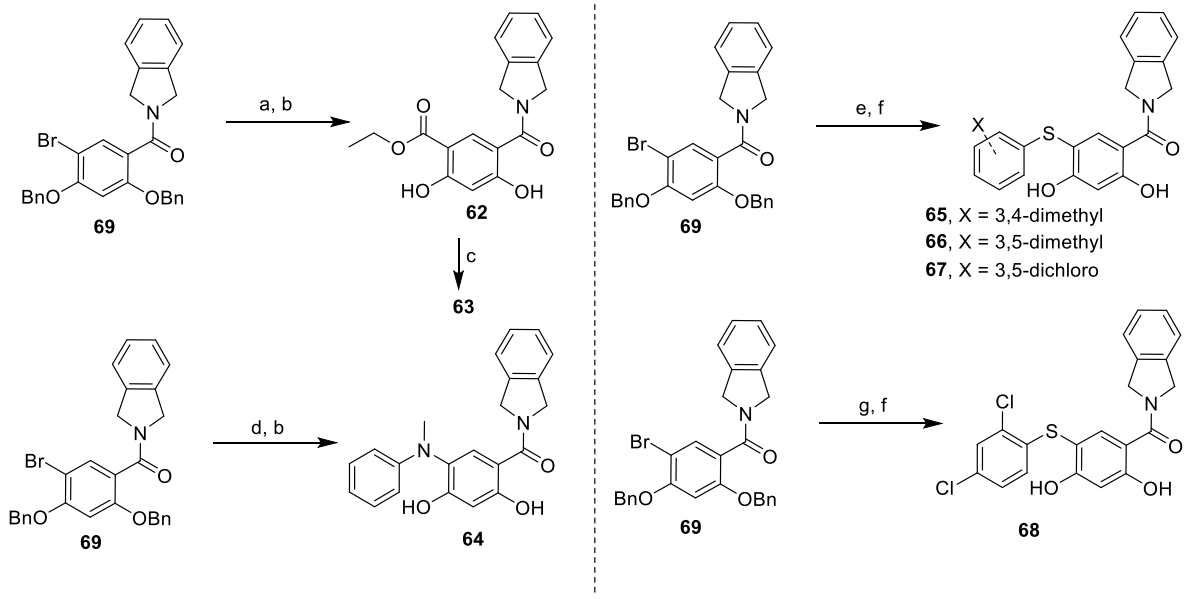

Scheme 8. Synthesis of resorcinol-isoindoline class of Grp94 inhibitors.

III.4.3.2. Evaluation of Resorcinol-Isoindoline Class of Grp94 Inhibitors

Binding affinity of compounds **62–68** were determined against Hsp90α and Grp94 in the FP assay and summarized in Table 11. Aryl thioether containing compounds, **65–68**, manifested

low nM affinity for Grp94. Surprisingly, these compounds did not manifest selectivity over Hsp90α. Similarly, N-methyl aniline containing **64** manifested apparent K_d of 17 nM against Grp94 and manifested only a two-fold selectivity over Hsp90α. The most selective compound of this series was the 2,4-dichlorophenyl thioether **68**, which manifested 8-fold selectivity for Grp94. Incorporation of a methyl ester (**63**) at the 5-position did not increase affinity for Hsp90α or Grp94. Conversely, the ethyl ester **62** manifested IC_{50} of 0.77 μM with 5-fold selectivity for Grp94.

Table 11. Evaluation of resorcinol-isoindoline class of Grp94 inhibitors

Compound	K_d Grp94 (μM)	K_d Hsp90α (μM)	Fold-selectivity for Grp94
BnIm	1.14 ± 0.1	13.1 ± 1.1	12
62	0.77 ± 0.1	3.52 ± 2.3	5
63	>10	>10	-
64	0.017 ± 0.003	0.034 ± 0.008	2
65	0.021 ± 0.003	0.066± 0.006	3
66	0.033 ± 0.002	0.075 ± 0.004	2
67	0.031 ± 0.003	0.029 ± 0.010	-
68	0.059 ± 0.006	0.460 ± 0.006	8

These results were unexpected as these compounds were predicted to selectively bind Grp94. The excellent binding affinities against Hsp90α indicate that these substitutions are also accommodated within the Hsp90α ATP-binding pocket. In depth analysis of various co-crystal structures of Hsp90α revealed that some purine-derived ligands induce an extra binding channel in Hsp90α, which is not usually induced with resorcinol derived inhibitors.[44, 81] Overlay of these purine-bound co-crystal structures with our resorcinol based inhibitors revealed this binding channel in Hsp90α expands about the 5-position of the resorcinol ring (Figure 33a and 33b). An overlay of two co-crystal structures of purine based inhibitors (PU-H36 and PU-H54) bound to Hsp90α (PDB: 3O0I) and Grp94 (PDB: 3O2F) suggests that the phenyl ring attached to a sulfanyl

linker can bind both Grp94 and Hsp90α.[74] As shown in Figure 33b, an 80° tortional rotation about the sulfanyl linker can project the 8-phenyl ring into the Hsp90α-specific binding channel from the Grp94-specific subpocket. When compound **65** was modeled in these co-crystal structures, the rotation about the sulfanyl linker indicated that the phenyl ring could be accommodated in both the Hsp90α and Grp94 binding pockets, resulting in no selectivity (Figure 33c & 33d).

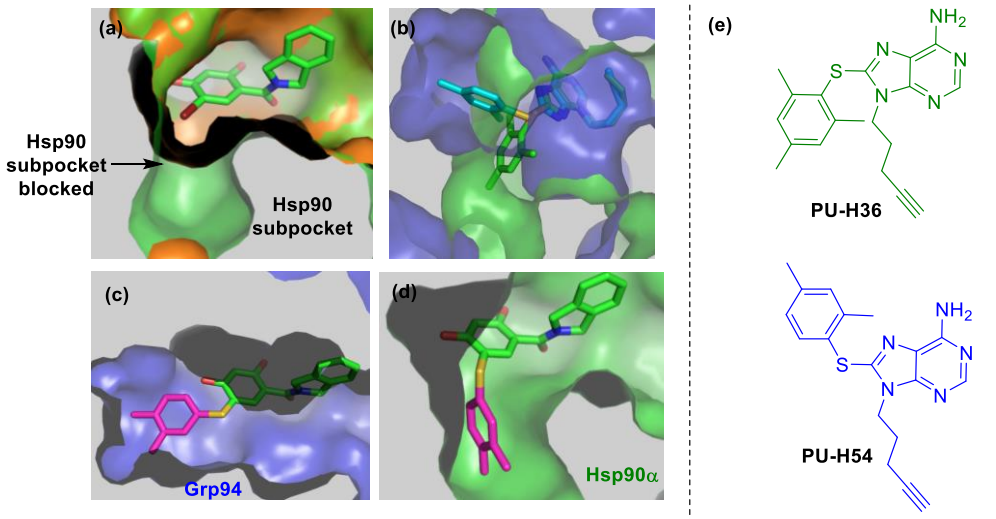

Figure 33. Binding modes of compound **61** and **65**. (a) Compound **61** modeled in different co-crystal structures of Hsp90, with and without additional binding pocket around 5-position of resorcinol ring. (green, PDB: 3O0I, orange, PDB: 2XAB). (b) Overlay of purine based-inhibitors bound to Hsp90α (Green PDB: 3O0I) and Grp94 (blue, PDB: 3O2F). (c) Proposed binding mode of **65** in Grp94; (d) Proposed binding mode of **65** in Hsp90α. (e) Structures of PU-H36 and PU-H54.

These results indicate that modification at the 5-position of the resorcinol may induce an opening of a binding channel that is similar to that observed with purine inhibitors, resulting in the inhibition of Grp94 and Hsp90α. For selective Grp94 inhibition, incorporation of a linker-less aryl group at the 5-position was therefore proposed. A linker appears to be required to project 5-aryl substituents towards the Hsp90α-specific binding pocket (Figure 33d) and hence, the omission of a nitrogen or sulfur linker would produce a molecule that induces a steric clash with Phe138 within the Hsp90α binding site. However, this modification should be accommodated in the Grp94-

binding pocket. To test this hypothesis, two molecules containing a phenyl and a furan attached to the 5-position of resorcinol ring were proposed. As shown in Figure 34, a furan will be accommodated in the Grp94 binding pocket as the oxygen would interact favorably with Asn107.

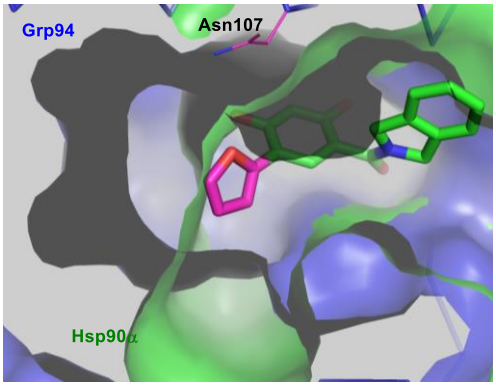

Figure 34. Overlay of proposed binding modes of **71**in Hsp90α (green, PDB 1UY6) and Grp94 (blue, PDB: 3O0I) binding pocket.

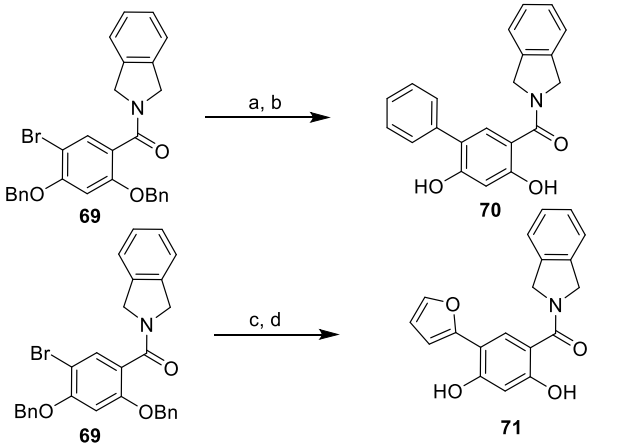

Reagents: (a) 1.PhB(OH)$_2$, Pd(dppf)Cl$_2$; (b) Pd/C, H$_2$; (c) Pd(PPh)$_3$, Cs$_2$CO$_3$,furan-2-ylboronic acid ; (d) Pd/C, cyclohexene

Scheme 9. Syntheses of compounds **70** and **71**.

Analogues **70** and **71** were synthesized via a Suzuki cross-coupling reaction between phenyl boronic acid or 2-furylboronic acid with **69,** followed by hydrogenolysis (Scheme 9). These molecules were evaluated via a fluorescence polarization assay for their affinity and selectivity (Table 12). Analogue **71** manifested an apparent K_d of 220 nM for Grp94 with 35-fold selectivity over Hsp90α. Unfortunately, **70** did not bind at the highest concentration tested (100 μM).

Table 12. Apparent K_d values of des-linker analogues **70** and **71**

Compound	K_d Grp94 (μM)	K_d Hsp90α (μM)	Fold-selectivity for Grp94
BnIm	1.14 ± 0.1	13.1 ± 1.1	12
70	>100	>100	-
71	0.22 ± 0.029	7.79 ± 1.02	35

III.5. Conclusions and Future Directions

The co-crystal structures of several *pan*-Hsp90 inhibitors bound to Hsp90α, Hsp90β, and Grp94 provided strong rationale for the structure-based design of Grp94-selective inhibitors. Three different scaffolds were evaluated during the pursuit of selective Grp94-selective inhibitors. Studies on the *pan*-Hsp90 inhibitor, radamide generated improved Grp94-selective inhibitors and modifications to the aryl side chain of BnIm provided a 40-fold selective analog with an apparent K_d of 650 nM. The resorcinol-isoindoline scaffold was also evaluated to probe the second exclusive sub-pocket of Grp94, which led to the identification of the highly efficacious Grp94-selective inhibitor **71**, which can serve as a starting point for the development of more potent inhibitors. Evaluation of compound **71** against Her2-positive cancer cells and multiple myeloma cells is currently underway. In collaboration with Chad Dickey's lab at the University of South Florida, compound **71** will be evaluated for the potential treatment of glaucoma. Together, these Grp94-selective inhibitors will enable identification of more Grp94-specific client proteins and lead to the further understanding of the Grp94-dependent processes.

III.6. Methods and Experiments

All reactions were performed in oven-dried glassware under argon atmosphere unless otherwise stated. Dichloromethane (DCM), tetrahydrofuran (THF), and toluene were passed through a column of activated alumina prior to use. Anhydrous methanol, acetonitrile, and *N*-methyl-2-pyrrolidone (NMP) were purchased and used without further purification. Flash column chromatography was performed using silica gel (40−63 μm particle size). The ^{1}H (500 and 400 MHz) and ^{13}C NMR (125 and 100 MHz) spectra were recorded on 500 and 400 MHz spectrometer. Data are reported as p = pentet, q = quartet, t = triplet, d = doublet, s = singlet, br s = broad singlet, m = multiplet; coupling constant(s) in Hz. Infrared spectra were obtained using FT/IR

spectrometer. High resolution mass spectral data were obtained on a time-of-flight mass spectrometer and analysis was performed using electrospray ionization.

Fluorescence Polarization Assay

The assay was performed in 96-well format in black, flat bottom plates (Santa Cruz Biotechnology) with a final volume of 100 μL. 25 μL of assay buffer (20 mM HEPES, pH 7.3, 50 mM KCl, 5 mM $MgCl_2$, 20 mM Na_2MoO_4, 2 mM DTT, 0.1 mg/mL BGG, and 0.01% NP-40) containing 6 nM FITC-GDA (fluorescent tracer, stock in DMSO and diluted in assay buffer) and 50 μL of assay buffer containing 10 nM of either Grp94 or Hsp90α were added to each well. Compounds were tested in triplicate wells (1% DMSO final concentration). For each plate, wells containing buffer only (background), tracer in buffer only (low polarization control), and protein and tracer in buffer with 1% DMSO (high polarization control) were included. Plates were incubated at 4 °C with rocking for 24 h. Polarization values (in mP units) was measured at 37 °C with an excitation filter at 485 nm and an emission filter at 528 nm. Polarization values were correlated to % tracer bound and compound concentrations. The concentration of inhibitor at which the tracer was 50% displaced represents apparent K_d.

General method for amide formation for compounds **35–36** and **38–50**

To a solution of acid **34** (0.05 mmol), EDCI·HCl (0.12 mmol), and pyridine (0.13 mmol) in dichloromethane (1 mL) was added the corresponding aniline (0.1 mmol) and stirred at room temperature under argon overnight. Upon complete consumption of acid **34**, the solvent was removed and the residue dissolved in THF (1 mL). The reaction mixture was then treated with TBAF (0.2 mmol) and stirred for 30 min, and upon completion saturated aqueous NH_4Cl was added and extracted with ethyl acetate. The combined organic layers were then dried over Na_2SO_4,

filtered, and concentrated to give a crude oil. The residue was purified via flash chromatography (SiO_2, 49:1 CH_2Cl_2/MeOH) to afford the desired amides.

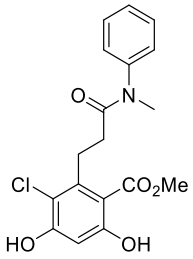

Methyl 3-chloro-4,6-dihydroxy-2-(3-(methyl(phenyl)amino)-3-oxopropyl)benzoate (35): 28 mg, 77% yield, white amorphous solid: ^{1}H NMR (400 MHz, $CDCl_3$–MeOD) δ 7.34 (dd, J = 8.4, 6.8 Hz, 2H), 7.31–7.23 (m, 2H), 7.15–7.08 (m, 2H), 6.33 (s, 1H), 3.87 (s, 3H), 3.25 (d, J = 7.5 Hz, 5H), 2.35–2.27 (m, 2H); ^{13}C NMR ($CDCl_3$–CH_3OH, 125 MHz) δ 172.9, 171.0, 162.1, 157.9, 143.7, 142.3, 130.0 (2), 128.1, 127.2 (2), 114.8, 106.0, 102.3, 52.4, 37.6, 33.4, 28.9; (ESI+) m/z [M+H$^+$] calcd for $C_{18}H_{19}ClNO_5$, 364.0952; found 364.0943.

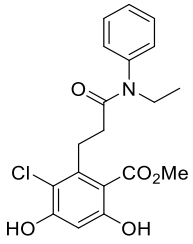

Methyl 3-chloro-2-(3-(ethyl(phenyl)amino)-3-oxopropyl)-4,6-dihydroxybenzoate (36): 30 mg, 79% yield, white amorphous solid: ^{1}H NMR (500 MHz, $CDCl_3$–CD_3OD) δ 7.34 (t, J = 7.7 Hz, 2H), 7.31–7.24 (m, 2H), 7.06 (dd, J = 7.3, 1.7 Hz, 2H), 6.33 (d, J = 4.0 Hz, 1H), 3.87 (d, J = 3.9 Hz, 3H), 3.70 (q, J = 7.1 Hz, 3H), 3.27–3.19 (m, 2H), 2.34–2.16 (m, 2H), 1.07 (td, J = 7.2, 3.4 Hz, 3H); ^{13}C NMR ($CDCl_3$– CD_3OD, 125 MHz) δ 172.3, 171.0, 162.0, 157.9, 142.3, 141.9, 129.9 (2), 128.3 (2), 128.2, 114.7, 106.1, 102.2, 52.4, 44.3, 33.7, 28.8, 13.0; (ESI+) m/z [M+H$^+$] calcd for $C_{19}H_{21}ClNO_5$, 378.1108; found 378.1108.

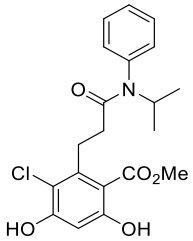

Methyl 3-chloro-4,6-dihydroxy-2-(3-(isopropyl(phenyl)amino)-3-oxopropyl)benzoate (37):

A solution of benzyl protected acid **1a** (100 mg, 0.22 mmol) in dichloromethane was treated with oxalyl chloride (23 μL, 0.33 mmol) under argon atmosphere and then stirred at room temperature for 2 h. The solvent was then removed and the residue was placed under high vacuum for 30 min to remove any unreacted oxalyl chloride. The residue was then re-dissolved in dry CH_2Cl_2 (3 mL), cooled to 0 °C, and was treated sequentially with diisopropylethyl amine (57 μL, 0.33 mmol) and *N*-isopropylaniline (72 μL, 0.33 mmol). The resulting mixture was stirred at room temperature overnight under Ar. The solvent was removed and the residue was passed through a short pad of silica (1:1, ethyl acetate/Hexanes) and was concentrated to afford the amide crude product, which was dissolved in methanol (5 mL) and treated with Pd/C (10%). The resulting suspension was charged with a hydrogen balloon and stirred under H_2 at room temperature for 16 h, filtered through celite, concentrated, and purified by flash chromatography (SiO_2, 1:1 EtOAc/Hexanes) to afford compound **51** (30 mg, 35% yield over 2 steps) as a white solid. ^{1}H NMR (400 MHz, $CDCl_3$): δ 7.45–7.27 (m, 13H), 7.06–7.12 (m, 2H), 6.41 (s, 1H), 5.07 (hept, J = 6.8 Hz, 1H), 5.04 (s, 2H), 4.98 (s, 2H), 3.88 (s, 3H), 3.03–2.93 (m, 2H), 2.30–2.21 (m, 2H), 1.08 (d, J = 6.8 Hz, 6 H). ^{13}C NMR (125 MHz, $CDCl_3$): δ 171.1, 167.5, 155.4, 154.5, 138.6, 138.3, 136.2, 135.9, 130.3, 129.2, 128.6, 128.5, 128.1, 127.9, 126.9, 126.8, 118.4, 115.5, 98.2, 70.9, 70.8, 52.4, 45.8, 34.4, 27.9, 21.0. HRMS (ESI+) *m/z* [M+Na$^+$] calcd for, $C_{20}H_{22}ClNO_5Na$, 414.1084; found 414.1076.

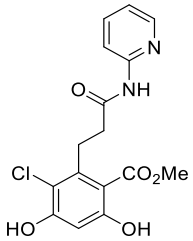

Methyl 3-chloro-4,6-dihydroxy-2-(3-oxo-3-(pyridin-2-ylamino)propyl)benzoate (38): 10 mg, 62 %, pale yellow amorphous solid:^{1}H NMR (500 MHz, $(CD_3)_2CO$) δ 8.39–8.07 (m, 2H), 7.80 (dd, J = 8.7, 7.4, 1.8 Hz, 1H), 7.10 (dd, J = 7.3, 4.8, 1.1 Hz, 1H), 6.55 (s, 1H), 3.99 (s, 3H), 3.57–3.42 (m, 2H), 2.98–2.77 (m, 2H). ^{13}C NMR (125 MHz, $(CD_3)_2CO$) δ 171.60, 162.34, 158.67, 153.19, 148.85, 143.11, 138.72, 120.02, 114.86, 114.29, 108.11, 103.12, 52.92, 36.62, 28.77. HRMS (ESI+) m/z [M+Na$^+$] calcd for $C_{16}H_{15}ClN_2O_5Na$, 373.0669; found, 373.0630.

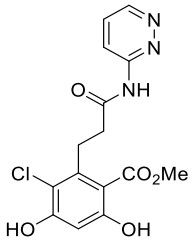

Methyl 3-chloro-4,6-dihydroxy-2-(3-oxo-3-(pyridazin-3-ylamino)propyl)benzoate (39): 26 mg, yield 74%, white amorphous solid: ^{1}H NMR (500 MHz, $(CD_3)_2CO$) δ 10.04 (s, 1H), 8.92 (dd, J = 4.7, 1.5 Hz, 1H), 8.47 (dd, J = 9.0, 1.5 Hz, 1H), 7.63 (dd, J = 9.0, 4.7 Hz, 1H), 6.52 (s, 1H), 3.94 (s, 3H), 3.54–3.38 (m, 2H), 2.99–2.84 (m, 2H); ^{13}C NMR (125 MHz, $(CD_3)_2CO$) δ 158.78, 149.10, 142.85, 128.79, 118.60, 118.54, 103.20, 52.93, 36.60, 28.60; HRMS (ESI+) m/z [M+Na$^+$] calcd for $C_{15}H_{14}ClN_3O_5Na$, 374.0520; found 374.0534.

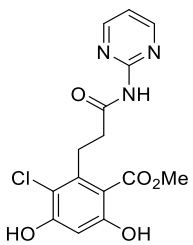

Methyl 3-chloro-4,6-dihydroxy-2-(3-oxo-3-(pyrimidin-2-ylamino)propyl)benzoate (40):

21 mg, yield 60%, white amorphous solid: ^{1}H NMR (500 MHz, $(CD_3)_2CO$) δ 9.04 (d, J = 1.3 Hz, 2H), 8.83 (s, 1H), 6.51 (s, 1H), 3.94 (s, 3H), 3.57–3.31 (m, 2H), 2.82–2.69 (m, 2H); ^{13}C NMR (125 MHz, $(CD_3)_2CO$): δ 171.7, 171.2, 158.6, 154.2, 148.0, 147.9, 142.7, 135.6, 135.5, 114.8, 108.3, 103.2, 52.9, 36.4, 28.7; HRMS (ESI+) m/z [M+Na$^+$] calcd for $C_{15}H_{14}ClN_3O_5Na$, 374.0520, found 374.0527.

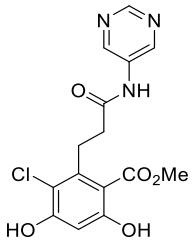

Methyl 3-chloro-4,6-dihydroxy-2-(3-oxo-3-(pyrimidin-5-ylamino)propyl)benzoate (41): 23 mg, 66% yield, white amorphous solid: ^{1}H NMR (400 MHz, $CDCl_3$– CD_3OD) δ 9.01 (s, 2H), 8.84 (s, 1H), 6.42 (s, 1H), 3.91 (s, 3H), 3.59–3.36 (m, 2H), 2.70–2.51 (m, 2H); ^{13}C NMR ($CDCl_3$, 125 MHz): δ 172.1, 170.9, 162.0, 158.1, 152.9, 147.6 (2), 141.8, 114.8 (2), 106.2, 102.6, 52.6, 35.7, 28.2; (ESI+) m/z [M+H$^+$] calcd for $C_{15}H_{15}ClN_3O_5$, 352.0712; found 352.0712.

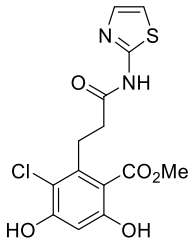

Methyl 3-chloro-4,6-dihydroxy-2-(3-oxo-3-(thiazol-2-ylamino)propyl)benzoate (42): 30 mg, 84% yield, white amorphous solid: ^{1}H NMR (500 MHz, $(CD_3)_2CO$) δ 7.40 (d, J = 3.6 Hz, 1H), 7.11 (d, J = 3.6 Hz, 1H), 6.52 (s, 1H), 3.94 (s, 3H), 3.57–3.34 (m, 2H), 2.98–2.78 (m, 2H); ^{13}C NMR ($(CD_3)_2CO$, 125 MHz) δ 171.3, 170.7, 162.4, 158.9, 158.7, 142.7, 138.5, 114.9, 113.9, 108.2, 103.3, 53.0, 35.4, 28.6. (ESI+) m/z [M+H$^+$] calcd for $C_{14}H_{14}ClN_2O_5S$, 357.0312; found 357.0323.

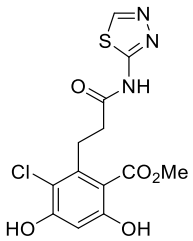

Methyl 2-(3-((1,3,4-thiadiazol-2-yl)amino)-3-oxopropyl)-3-chloro-4,6-dihydroxybenzoate (43): 28 mg, 78% yield, white amorphous solid: ^{1}H NMR (500 MHz, $CDCl_3$– CD_3OD) δ 8.79 (d, J = 0.9 Hz, 1H), 6.44 (d, J = 0.9 Hz, 1H), 3.89 (d, J = 0.9 Hz, 3H), 3.62–3.30 (m, 2H), 2.93–2.40 (m, 4H); ^{13}C NMR($CDCl_3$– CD_3OD, 125 MHz): 171.0, 170.9, 162.3, 159.5, 158.1, 148.0, 141.3, 114.9, 106.1, 102.8, 52.6, 34.9, 28.0. (ESI+) m/z [M+Na^+] calcd for $C_{13}H_{12}ClN_3O_5SNa$, 380.0084; found 380.0090.

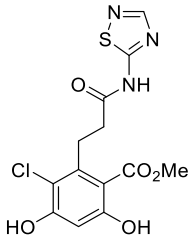

Methyl 2-(3-((1,2,4-thiadiazol-5-yl)amino)-3-oxopropyl)-3-chloro-4,6-dihydroxybenzoate (44): 19 mg, 53% yield, white amorphous solid: ^{1}H NMR (400 MHz, $CDCl_3$– CD_3OD) δ 8.19 (s, 1H), 7.72 (s, 1H), 6.36 (s, 1H), 3.83 (s, 3H), 3.50–3.32 (m, 2H), 2.91–2.69 (m, 2H); ^{13}C NMR ($CDCl_3$– CD_3OD, 125 MHz): δ 179.3, 176.3, 174.5, 163.0, 162.2.161.6, 144.8, 118.6, 110.2, 106.4, 56.3, 38.1, 33.5. (ESI+) m/z [M+Na^+] calcd for $C_{13}H_{12}ClN_3O_5SNa$, 380.0084; found 380.0078.

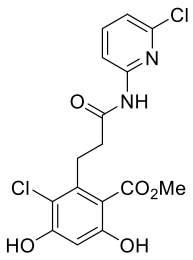

Methyl 3-chloro-2-(3-((6-chloropyridin-2-yl)amino)-3-oxopropyl)-4,6-dihydroxybenzoate (45): 27 mg, 70% yield, white amorphous solid: ^{1}H NMR (500 MHz, $(CD_3)_2CO$) δ 10.88 (1H, br s), 9.48 (1H, br s)8.09 (dd, J = 8.2, 1.8 Hz, 1H), 7.80–7.58 (m, 1H), 7.00 (dd, J = 7.9, 1.7 Hz, 1H), 6.63–6.10 (m, 1H), 3.93 (s, 3H), 3.46–3.10 (m, 2H), 2.91–2.55 (m, 2H); ^{13}C NMR (125 MHz, $(CD_3)_2CO$) δ 172.1, 171.5, 158.8, 153.3, 149.6, 143.1, 142.2, 119.9 (2), 115.0, 112.8, 108.3, 103.3, 53.1, 36.7, 28.8; (FAB) m/z [M+Na$^+$] calcd for $C_{16}H_{14}Cl_2N_2O_5Na$, 407.0174, found 407.0177.

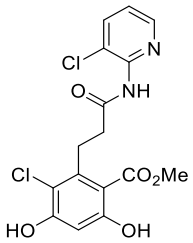

Methyl 3-chloro-2-(3-((3-chloropyridin-2-yl)amino)-3-oxopropyl)-4,6-dihydroxybenzoate (46): 21 mg, 55% yield, white amorphous solid: ^{1}H NMR (500 MHz, $(CD_3)_2CO$) δ 8.36 (dd, J = 4.7, 1.6 Hz, 1H), 7.92 (dd, J = 8.0, 1.6 Hz, 1H), 7.27 (ddd, J = 8.0, 4.7, 0.6 Hz, 1H), 6.52 (s, 1H), 3.97 (s, 3H), 3.55–3.39 (m, 2H), 3.00–2.76 (m, 2H). ^{13}C NMR (125 MHz, $(CD_3)_2CO$) δ 171.4, 171.28, 158.6, 149.3, 147.5, 143.2 (2), 139.3, 122.9 (2), 114.8, 108.14, 103.1, 52.9, 35.9, 28.8; (ESI+) m/z [M+Na$^+$] calcd for $C_{16}H_{14}Cl_2N_2O_5Na$, 407.0174; found 407.0174.

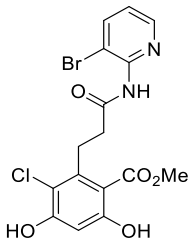

Methyl 2-(3-((3-bromopyridin-2-yl)amino)-3-oxopropyl)-3-chloro-4,6-dihydroxybenzoate (47): 31 mg, 71% yield, white amorphous solid: ^{1}H NMR (400 MHz, $CDCl_3$–MeOD) δ 8.47 (dd, J = 4.7, 1.6 Hz, 1H), 7.98 (dd, J = 8.0, 1.6 Hz, 1H), 7.27–7.22(m, 1H), 6.34 (s, 1H), 3.85 (s, 3H),

3.35–3.29 (m, 2H), 2.91–2.65 (m, 2H). ^{13}C NMR (125 MHz, $CDCl_3$,): δ 172.8, 170.0, 161.2, 156.9, 149.7, 147.8, 141.7, 140.6, 124.9, 120.3, 113.8, 105.0, 101.4, 51.6, 36.3, 26.6. (ESI+) *m*/*z* [M+Na^+] calcd for $C_{16}H_{14}BrClN_2O_5Na$, 450.9672; found 450.9677.

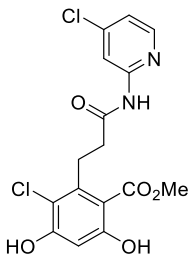

Methyl 3-chloro-2-(3-((4-chloropyridin-2-yl)amino)-3-oxopropyl)-4,6-dihydroxybenzoate (48): 31 mg, 71% yield, white amorphous solid: ^{1}H NMR (400 MHz, $CDCl_3$– CD_3OD) δ 8.47 (dd, *J* = 4.7, 1.6 Hz, 1H), 7.98 (dd, *J* = 8.0, 1.6 Hz, 1H), 7.27–7.22(m, 1H), 6.34 (s, 1H), 3.85 (s, 3H), 3.35–3.29 (m, 2H), 2.91–2.65 (m, 2H). ^{13}C NMR (125 MHz, $CDCl_3$,): δ 172.8, 170.0, 161.2, 156.9, 149.7, 147.8, 141.7, 140.6, 124.9, 120.3, 113.8, 105.0, 101.4, 51.6, 36.3, 26.6. (ESI+) *m*/*z* [M+Na^+] for $C_{16}H_{14}BrClN_2O_5Na$, 450.9672; found 450.9677.

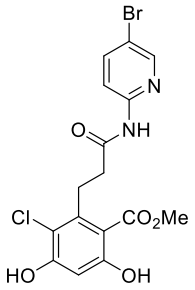

Methyl 2-(3-((5-bromopyridin-2-yl)amino)-3-oxopropyl)-3-chloro-4,6-dihydroxybenzoate (49): 29 mg, 68% yield, white amorphous solid: ^{1}H NMR (500 MHz, $CDCl_3$–MeOD) δ 8.31–8.19 (m, 1H), 8.19–8.05 (m, 1H), 7.84–7.71 (m, 1H), 6.54–6.28 (m, 1H), 3.94 (s, 3H), 3.42–3.35 (m, 2H), 2.63 (dq, *J* = 12.7, 3.8, 2.1 Hz, 2H); ^{13}C NMR ($CDCl_3$– CD_3OD, 125 MHz): δ 171.5, 170.9, 162.1, 158.2, 150.2, 148.6, 141.6, 141.0, 115.5, 114.8, 114.5, 106.1, 102.6, 52.6, 36.4, 28.3. (FAB) *m*/*z* [M+Na^+] calcd for $C_{16}H_{14}BrClN_2O_5Na$, 450.9672; found 450.9681.

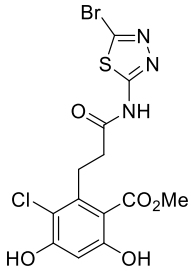

Methyl 2-(3-((5-bromo-1,3,4-thiadiazol-2-yl)amino)-3-oxopropyl)-3-chloro-4,6-dihydroxy benzoate (50): 12 mg, 28% yield, gray amorphous solid: ^{1}H NMR (500 MHz, $(CD_3)_2CO$) δ 6.53 (s, 1H), 3.94 (s, 4H), 3.59–3.43 (m, 2H), 3.05–2.84 (m, 2H). ^{13}C NMR (125 MHz, $(CD_3)_2CO$): δ 171.7, 161.6, 158.7, 142.2, 134.8, 130.6, 114.9, 108.1, 103.3, 79.3, 53.0, 35.2, 21.1. HRMS (ESI+) *m*/*z* [M+H$^+$] calcd for $C_{13}H_{12}BrClN_3O_5S$: 435.9370; found 435.9377.

General procedure for multicomponent cyclization reaction:

Requisite benzyl amines (0.26 mmol, 1.0 eq.) were added to a stirred solution of **9** (125 mg, 0.26 mmol, 1.0 eq.) in wet methanol (2 mL) and stirring continued for 30 min at rt before the addition of NH_4HCO_3 (0.26 mmol) and glyoxal (0.26 mmol). After stirring for 12 h, tetrabutylammonium fluoride (0.52 mL of 1 M solution in THF, 0.52 mmol) was added and then stirred for 30 min before the reaction was quenched with saturated ammonium chloride solution (10 mL) and extracted with ethyl acetate (3 × 10 mL). The organic layers were combined, dried (Na_2SO_4), filtered, and concentrated. The residue was purified via flash chromatography (SiO_2, 1:49 MeOH:dichloromethane) to afford the desired product as amorphous solids.

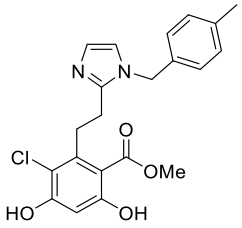

Methyl 3-chloro-4,6-dihydroxy-2-(2-(1-(4-methylbenzyl)-1H-imidazol-2-yl)ethyl)benzoate (52): 44 mg (43%), off-white amorphous solid. ^{1}H NMR (500 MHz, CD_3OD) δ 7.15 (d, *J* = 7.9

Hz, 2H), 7.03 (d, *J* = 1.4 Hz, 1H), 7.00–6.96 (m, 2H), 6.94 (d, *J* = 1.5 Hz, 1H), 6.39 (s, 1H), 5.05 (s, 2H), 3.77 (s, 3H), 3.37–3.30 (m, 2H), 2.97–2.89 (m, 2H), 2.31 (s, 3H). ^{13}C NMR(125 MHz, MeOD) δ 171.3, 160.9, 159.0, 148.8, 141.5, 138.9, 135.1, 130.5 (2), 127.9 (2), 127.1, 121.8, 115.0, 110.1, 103.3, 52.8, 50.1, 31.5, 27.3, 21.1. HRMS (ESI+) *m*/*z* $[M + H]^+$ for $C_{21}H_{22}ClN_2O_4$, 401.1268; found 401.1266.

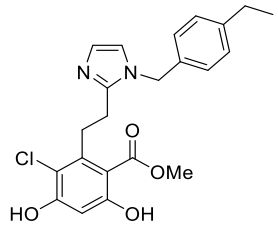

Methyl 3-chloro-2-(2-(1-(4-ethylbenzyl)-1H-imidazol-2-yl)ethyl)-4,6-dihydroxybenzoate (53):37 mg (39%), off white amorphous solid. ^{1}H NMR (500 MHz, $CDCl_3$, CD_3OD) δ 7.14 (d, *J* = 8.1 Hz, 2H), 7.11–7.08 (m, 1H), 6.98–6.91 (m, 2H), 6.85 (d, *J* = 1.5 Hz, 1H), 6.44 (s, 1H), 4.96 (s, 3H), 3.54–3.45 (m, 2H), 3.04 (t, *J* = 7.9 Hz, 2H), 2.59 (q, *J* = 7.6 Hz, 2H), 1.17 (td, *J* = 7.6, 1.0 Hz, 3H). ^{13}C NMR (125 MHz, $CDCl_3$, CD_3OD) δ 170.6, 162.1, 158.2, 147.2, 145.0, 140.9, 132.1, 128.8 (2), 127.2 (2), 124.2, 120.6, 114.9, 106.2, 103.0, 50.0, 49.9, 30.7, 28.6, 25.6, 15.6. HRMS (ESI+) *m*/*z* $[M + H]^+$ for $C_{22}H_{24}ClN_2O_4$, 415.1425; found 415.1432.

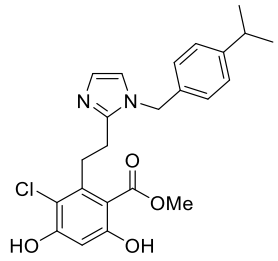

Methyl 3-chloro-4,6-dihydroxy-2-(2-(1-(4-isopropylbenzyl)-1H-imidazol-2 yl)ethyl)benzoate (54): 25 mg (22%), white amorphous solid. ^{1}H NMR (500 MHz, $CDCl_3$) δ 7.13 (d, *J* = 8.1 Hz, 2H), 7.03 (s, 1H), 6.90 (d, *J* = 8.2 Hz, 2H), 6.80 (d, *J* = 1.5 Hz, 1H), 6.49 (s, 1H), 4.95 (s, 2H), 3.79 (s, 3H), 3.50 (t, *J* = 7.9 Hz, 2H), 3.00–2.92 (m, 2H), 2.82 (hept, *J* = 6.9 Hz, 1H), 1.16 (d, *J* =

7.0 Hz, 6H). ^{13}C NMR (125 MHz, $CDCl_3$) δ 170.63, 162.91, 157.32, 149.25, 147.18, 127.20 (2), 126.81 (2), 120.19, 114.50, 106.24, 103.00, 99.98, 52.76, 49.56, 33.81, 30.77, 29.72, 23.93 (2). HRMS (ESI+) *m*/*z* $[M + H]^+$ calcd for $C_{23}H_{26}ClN_2O_4$, 429.1581; found 429.1588.

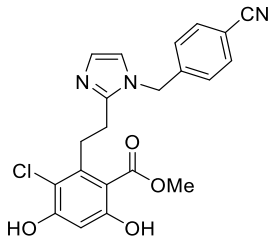

Methyl 3-chloro-2-(2-(1-(4-cyanobenzyl)-1H-imidazol-2-yl)ethyl)-4,6-dihydroxybenzoate (55): 37 mg (39%), off white amorphous solid. ^{1}H NMR (500 MHz, $CDCl_3$) δ 7.79 (q, *J* = 7.8, 6.0 Hz, 2H), 7.61–7.36 (m, 2H), 7.20–7.12 (m, 1H), 7.05 (s, 1H), 6.57 (s, 1H), 5.44–5.25 (m, 2H), 4.00 (s, 3H), 3.57 (q, *J* = 7.7 Hz, 2H), 3.02 (t, *J* = 7.9 Hz, 2H). ^{13}C NMR (125 MHz, $CDCl_3$): 170.4, 161.5, 158.0, 147.8, 142.0, 141.2, 132.8, (2), 127.7, 127.4, 127.0 (2), 120.2, 118.2, 114.5, 111.6, 102.4, 52.4, 52.3, 30.8, 26.0. HRMS (ESI+) *m*/*z* $[M + H]^+$ for $C_{21}H_{19}ClN_3O_4$, 412.1064; found 412.1049.

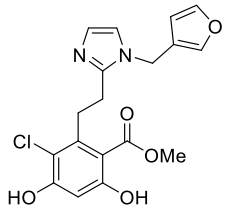

Methyl 3-chloro-2-(2-(1-(furan-3-ylmethyl)-1H-imidazol-2-yl)ethyl)-4,6 Dihydroxybenzoate (56): 40 mg (41%), off-white amorphous solid. ^{1}H NMR (500 MHz, $CDCl_3$, CD_3OD) δ 7.30 (d, *J* = 1.6 Hz, 1H), 7.20 (s, 1H), 6.84 (dd, *J* = 2.7, 1.4 Hz, 1H), 6.78 (d, *J* = 1.4 Hz, 1H), 6.36 (d, *J* = 2.0 Hz, 1H), 6.15 (d, *J* = 1.9 Hz, 1H), 4.80 (s, 2H), 3.78 (d, *J* = 1.9 Hz, 3H), 3.39 (tt, *J* = 8.9, 2.5 Hz, 2H), 2.95–2.80 (m, 2H). ^{13}C NMR (125 MHz, $CDCl_3$, CD_3OD): δ 170.8, 161.8, 158.1, 147.3,

144.1, 141.6, 141.6, 140.1, 126.7, 121.0, 119.6, 114.7, 109.4, 106.2, 102.5, 52.4, 41.0, 30.8, 26.1. HRMS (ESI+) *m/z* $[M + H]^+$ for $C_{18}H_{18}ClN_2O_5$, 377.0904; found 377.0905.

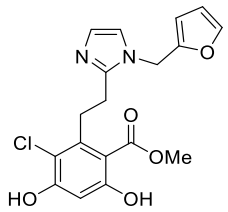

Methyl 3-chloro-2-(2-(1-(furan-2-ylmethyl)-1H-imidazol-2-yl)ethyl)-4,6-dihydroxybenzoate (57): 44 mg (45%), off-white amorphous solid. ^{1}H NMR (500 MHz, $CDCl_3$, CD_3OD) δ 7.31 (dt, *J* = 2.4, 1.2 Hz, 1H), 6.87 (dd, *J* = 2.4, 1.4 Hz, 1H), 6.83 (d, *J* = 1.5 Hz, 1H), 6.40 (d, *J* = 1.8 Hz, 1H), 6.26 (dt, *J* = 3.5, 1.7 Hz, 1H), 6.18 (d, *J* = 3.3 Hz, 1H), 4.94 (d, *J* = 1.6 Hz, 2H), 3.82 (d, *J* = 1.9 Hz, 3H), 3.46 (ddd, *J* = 10.2, 6.1, 2.0 Hz, 2H), 2.95 (ddd, *J* = 9.8, 5.9, 1.5 Hz, 2H). ^{13}C NMR (125 MHz, $CDCl_3$, CD_3O) δ 170.9, 162.0, 158.2, 149.1, 147.4, 143.2, 141.8, 126.9, 119.7, 114.8, 110.6, 108.8, 106.2, 102.6, 52.6, 42.6, 30.8, 26.1. HRMS (ESI+) *m/z* $[M + H]^+$ for $C_{18}H_{18}ClN_2O_5$, 377.0904; found 377.0911.

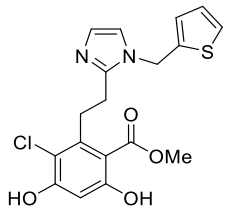

Methyl 3-chloro-4,6-dihydroxy-2-(2-(1-(thiophen-2-ylmethyl)-1H-imidazol-2-yl)ethyl) benzoate (58): 37 mg (37%), yellow amorphous solid. ^{1}H NMR (400 MHz, $CDCl_3$, CD_3OD) δ 7.23 (dd, *J* = 5.1, 1.3 Hz, 1H), 6.95 (d, *J* = 1.5 Hz, 1H), 6.92 (dd, *J* = 5.1, 3.5 Hz, 1H), 6.87 (dd, *J* = 3.5, 1.9 Hz, 2H), 6.43 (s, 1H), 5.17 (d, *J* = 0.9 Hz, 2H), 3.84 (s, 3H), 3.56–3.44 (m, 2H), 3.01–2.92 (m, 2H). ^{13}C NMR (125 MHz, $CDCl_3$, CD_3OD) δ 170.9, 162.1, 158.2, 147.3, 141.7, 138.5, 127.2, 126.9, 126.4, 126.2, 119.7, 114.9, 106.2, 102.7, 52.6, 44.7, 30.9, 26.2. HRMS (ESI+) *m/z* $[M + H]^+$ for $C_{18}H_{18}ClN_2O_4S$, 393.0676; found 393.0674.

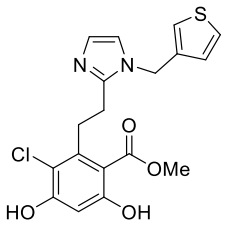

Methyl 3-chloro-4,6-dihydroxy-2-(2-(1-(thiophen-3-ylmethyl)-1H-imidazol-2-yl)ethyl) benzoate (59): 8 mg (27%), yellow amorphous solid. ^{1}H NMR (400 MHz, $CDCl_3$, CD_3OD) δ 7.25 (d, *J* = 4.8 Hz, 1H), 6.98–6.92 (m, 2H), 6.83 (d, *J* = 1.5 Hz, 1H), 6.81–6.78 (m, 1H), 6.37 (s, 1H), 4.97 (s, 2H), 3.79 (s, 3H), 3.43–3.37 (m, 2H), 2.95–2.88 (m, 2H). ^{13}C NMR (126 MHz, $CDCl_3$, CD_3OD) δ 174.48, 165.67, 162.02, 151.06, 145.03, 140.31, 131.26, 130.04, 129.39, 126.69, 124.00, 118.61, 110.15, 106.53, 56.40, 49.27, 34.49, 29.68. HRMS (ESI+) *m*/*z* $[M + H]^+$ for $C_{18}H_{18}ClN_2O_4S$, 393.0676; found 393.0693.

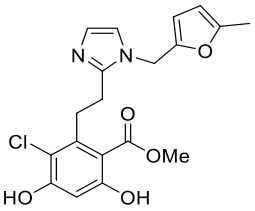

Methyl 3-chloro-4,6-dihydroxy-2-(2-(1-((5-methylfuran-2-yl)methyl)-1H-imidazol-2-yl) ethyl)benzoate (60): 46 mg (46%), off white amorphous solid. ^{1}H NMR (400 MHz, $CDCl_3$, CD_3OD) δ 6.87 (d, *J* = 1.4 Hz, 1H), 6.84 (d, *J* = 1.4 Hz, 1H), 6.41 (s, 1H), 6.08 (d, *J* = 3.1 Hz, 1H), 5.84 (dd, *J* = 3.0, 1.2 Hz, 1H), 4.88 (s, 2H), 3.84 (s, 3H), 3.49–3.42 (m, 2H), 3.08–2.93 (m, 2H), 2.18 (d, *J* = 1.0 Hz, 3H). ^{13}C NMR (125 MHz, $CDCl_3$, CD_3OD) δ 171.0, 162.2, 158.3, 153.1, 147.3, 147.1, 141.9, 126.7, 119.7, 114.9, 109.7, 106.5, 106.1, 102.6, 52.6, 42.7, 30.9, 26.2, 13.5. HRMS (ESI+) *m*/*z* $[M + H]^+$ for $C_{19}H_{20}ClN_2O_5$, 391.1061; found 391.1066.

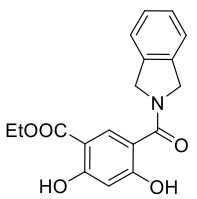

Ethyl 2,4-dihydroxy-5-(isoindoline-2-carbonyl)benzoate (62): A biotage microwave vial was charged with **69** (150mg, 0.29 mmol, 1 eq.), ethyl potassium oxalate (68 mg, 0.44 mmol, 1.5 eq.), 1,3-Bis(diphenylphosphino)propane (9mg, 0.021 mmol, 0.075 eq.), and palladium (II) trifluoroacetate (5mg, 0.015 mmol, 0.05 eq.). The tube was sealed with a cap lined with a disposable Teflon septum. The tube was evacuated and purged with nitrogen (3 times), before the addition of N-methyl 2-pyrrolidone (0.7 mL) by syringe. The resulting mixture was heated at 150 °C for 24 h, cooled to rt, and filtered through a small pad of celite (elution with ethyl acetate). Solvent was removed and the residue purified by flash chromatography (SiO_2, 1:3 ethyl acetate/hexanes) to give the corresponding 5-ester product, which was used further as obtained, and taken in dichloromethane (2 mL), cooled to 0 °C before the addition of 1 M solution of boron tribromide (0.6 mL). The resulting mixture was stirred for 6 h, quenched with saturated sodium bicarbonate solution (5 mL) and extracted with dichloromethane (2 × 10 mL). The combined organic layers were washed with saturated sodium chloride solution (15 mL), dried over anhydrous sodium sulfate, filtered, and concentrated. The residue purified with flash chromatography (SiO_2, 1:2 ethyl acetate/hexanes) to give the desired product **62** as white amorphous solid (15 mg, 15 %). ^{1}H NMR (500 MHz, $CDCl_3$) δ 12.21 (s, 1H), 11.19 (s, 1H), 8.29 (s, 1H), 7.34 (s, 4H), 6.54 (s, 1H), 5.12 (s, 4H), 4.45 (q, *J* = 7.1 Hz, 2H), 1.44 (t, *J* = 7.1 Hz, 3H). ^{13}C NMR (125 MHz, $CDCl_3$) δ 170.2, 169.6, 167.4, 165.6, 135.9 (2), 131.8 (2), 128.2 (2), 122.8, 109.7, 105.0, 104.6, 55.4, 53.8, 61.7, 14.5. HRMS (ESI+) *m*/*z* [M+H$^+$] calcd for $C_{18}H_{18}NO_5$, 328.1185, found 328.1187.

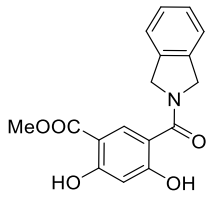

Methyl 2,4-dihydroxy-5-(isoindoline-2-carbonyl)benzoate (63): A solution of **62** (20 mg, 0.06 mmol, 1.0 eq.) in methanol was heated at 80 °C for 14 h in presence of 1,8 Diazabicyclo[5.4.0]undec-7-ene (2 μL, 0.012 mmol, 0.2 eq.). The solvent was removed and the residue purified with flash chromatography (SiO_2, 1:2 ethyl acetate/hexanes) to give the desired product **63** as white amorphous solid (14 mg, 73%). ^{1}H NMR (400 MHz, $CDCl_3$ δ 12.27 (s, 1H), 11.13 (s, 1H), 8.28 (s, 1H), 7.34 (s, 4H), 6.55 (d, *J* = 0.7 Hz, 1H), 5.12 (s, 4H), 3.99 (d, *J* = 0.7 Hz, 3H). ^{13}C NMR (125 MHz, $CDCl_3$) δ 170.2, 169.6, 167.4, 165.6, 135.9 (2), 131.8 (2), 128.2 (2), 122.8, 109.9, 105.2, 104.8, 55.4, 53.8, 52.7. HRMS (ESI+) *m*/*z* [M+H$^+$] calcd for $C_{17}H_{16}NO_5$, 314.1028, found, 314.1023.

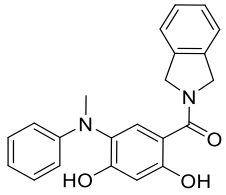

(2-Hydroxy-5-(methyl(phenyl)amino)phenyl)(isoindolin-2-yl)methanone (64): A biotage microwave vial was charged with **69** (180mg, 0.35 mmol, 1 eq.), N-methylaniline (45 μL, 0.42 mmol, 1.2 eq.), RuPhos (7 mg, 0.014 mmol, 0.04 eq), Tris(dibenzylideneacetone)dipalladium(0) (16mg, 0.017 mmol, 0.05 eq.), sodium *tert*-butoxide (40 mg, 0.53 mmol, 1.5 eq.). The tube was sealed with a cap lined with a disposable Teflon septum. The tube was evacuated and purged with nitrogen (3 times), before the addition of toluene (3.0 mL) by syringe. The resulting mixture was heated at 120 °C for 18 h, cooled to rt, and filtered through a small pad of celite (elution with ethyl acetate). Solvent was removed and the residue purified by flash chromatography (SiO_2, 1:3 ethyl acetate/hexanes) to give the corresponding 5-substituted product, which was used further as obtained, and taken in dichloromethane (2 mL), cooled to 0 °C before the addition of 1 M solution of boron tribromide (0.6 mL). The resulting mixture was stirred for 6 h, quenched with saturated

sodium bicarbonate solution (5 mL) and extracted with dichloromethane (2 × 10 mL). The combined organic layers were washed with saturated sodium chloride solution (15 mL), dried over anhydrous sodium sulfate, filtered, and concentrated. The residue purified with flash chromatography (SiO_2, 1:2 ethyl acetate/hexanes) to give the desired product **64** as white amorphous solid (47 mg, 38 %). ^{1}H NMR (500 MHz, $CDCl_3$) δ 11.59 (s, 1H), 7.38 (s, 1H), 7.33 – 7.21 (m, 6H), 6.90 (tt, *J* = 7.3, 1.1 Hz, 1H), 6.81 – 6.75 (m, 2H), 6.70 (s, 1H), 6.43 (s, 1H), 4.97 (s, 4H), 3.23 (s, 3H). ^{13}C NMR (125 MHz, $CDCl_3$) δ 170.2, 161.5, 149.6, 157.1, 135.7 (2), 129.3 (3), 127.8 (2), 127.3, 127.1, 122.5 (2), 119.5, 114.7, 110.1, 103.7, 54.7, 53.8, 40.3. HRMS (ESI-) *m*/*z* [M–H$^+$] calcd for $C_{22}H_{19}NO_5$, 359.1396, found 359.1387.

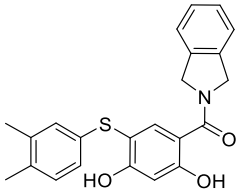

(5-((3,4-Dimethylphenyl)thio)-2,4-dihydroxyphenyl)(isoindolin-2-yl)methanone (65): A biotage microwave vial was charged with **69** (180mg, 0.35 mmol, 1 eq.), 3,4-dimethylbenzenethiol (54 mg, 0.38 mmol, 1.1 eq.), 1,1 ferrocenediyl-bis(diphenylphosphine) (20 mg, 0.035 mmol, 0.1 eq), Tris(dibenzylideneacetone)dipalladium(0) (17mg, 0.018 mmol, 0.05 eq.), *N*,*N*-diisopropylethylamine (67 μL, 0.39 mmol, 1.1 eq.). The tube was sealed with a cap lined with a disposable Teflon septum. The tube was evacuated and purged with nitrogen (3 times), before the addition of toluene (3.0 mL) by syringe. The resulting mixture was heated at 120 °C for 18 h, cooled to rt, and filtered through a small pad of celite (elution with ethyl acetate). Solvent was removed and the residue purified by flash chromatography (SiO_2, 1:3 ethyl acetate/hexanes) to give the corresponding 5-substituted product, which was used further as obtained, and taken in dichloromethane (2 mL), cooled to 0 °C before the addition of 1 M solution of boron tribromide

(0.6 mL). The resulting mixture was stirred for 6 h, quenched with saturated sodium bicarbonate solution (5 mL) and extracted with dichloromethane (2 × 10 mL). The combined organic layers were washed with saturated sodium chloride solution (15 mL), dried over anhydrous sodium sulfate, filtered, and concentrated. The residue purified with flash chromatography (SiO_2, 1:2 ethyl acetate/hexanes) to give the desired product **65** as white amorphous solid (34 mg, 25 %). ^{1}H NMR (500 MHz, $CDCl_3$) δ 12.06 (s, 1H), 7.90 (s, 1H), 7.38 – 7.29 (m, 3H), 7.04 (d, *J* = 7.9 Hz, 1H), 6.92 (d, *J* = 2.1 Hz, 1H), 6.87 – 6.81 (m, 2H), 6.70 (s, 1H), 5.08 (s, 4H), 2.28 – 2.13 (m, 6H). ^{13}C NMR (125 MHz, $CDCl_3$) δ 170.0, 165.2, 161.1, 138.2, 137.5, 135.4, 132.7, 130.8, 128.1 (2), 128.1 (2), 124.5 (2), 122.8, 111.1, 107.0, 104.1, 55.7, 53.8, 20.1, 19.5. HRMS (ESI+) *m*/*z* [M+H$^+$] calcd for $C_{23}H_{22}NO_3S$, 392.1320, found 392.1317.

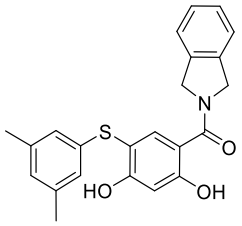

(5-((3,5-Dimethylphenyl)thio)-2,4-dihydroxyphenyl)(isoindolin-2-yl)methanone (66): A biotage microwave vial was charged with **69** (180mg, 0.35 mmol, 1 eq.), 3,5-dimethylbenzenethiol (54 mg, 0.38 mmol, 1.1 eq.), 1,1′-ferrocenediyl-bis(diphenylphosphine) (20 mg, 0.035 mmol, 0.1 eq.), Tris(dibenzylideneacetone)dipalladium(0) (17mg, 0.018 mmol, 0.05 eq.), *N*,*N*'-diisopropylethylamine (67 μL, 0.39 mmol, 1.1 eq.). The tube was sealed with a cap lined with a disposable Teflon septum. The tube was evacuated and purged with nitrogen (3 times), before the addition of toluene (3.0 mL) by syringe. The resulting mixture was heated at 120 °C for 18 h, cooled to rt, and filtered through a small pad of celite (elution with ethyl acetate). Solvent was removed and the residue purified by flash chromatography (SiO_2, 1:3 ethyl acetate/hexanes) to

give the corresponding 5-substituted product, which was used further as obtained, and taken in dichloromethane (2 mL), cooled to 0 °C before the addition of 1 M solution of boron tribromide (0.6 mL). The resulting mixture was stirred for 6 h, quenched with saturated sodium bicarbonate solution (5 mL) and extracted with dichloromethane (2 × 10 mL). The combined organic layers were washed with saturated sodium chloride solution (15 mL), dried over anhydrous sodium sulfate, filtered, and concentrated. The residue purified with flash chromatography (SiO_2, 1:2 ethyl acetate/hexanes) to give the desired product **66** as white amorphous solid (42 mg, 31 %). ^{1}H NMR (500 MHz, $CDCl_3$ δ 12.09 (s, 1H), 7.83 (s, 1H), 7.31 (dt, *J* = 6.4, 3.3 Hz, 3H), 7.05 – 7.02 (m, 1H), 6.93 – 6.87 (m, 1H), 6.80 (s, 1H), 6.71 (s, 1H), 6.64 (d, *J* = 8.0 Hz, 1H), 5.04 (s, 4H), 2.44 (s, 3H), 2.29 (s, 3H). ^{13}C NMR (125 MHz, $CDCl_3$) δ 169.9, 165.1, 161.1, 137.4 (2), 136.2, 135.5 (2), 131.8 (2), 131.6 (2), 127.8 (2), 126.0 (2), 111.2, 106.2, 104.2, 55.7, 53.8, 21.0, 20.1. HRMS (ESI-) *m*/*z* [M−H$^+$] calcd for $C_{23}H_{22}NO_3S$, 390.1164, found 390.1151.

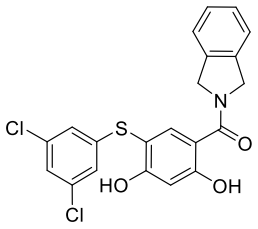

(5-((3,5-Dichlorophenyl)thio)-2,4-dihydroxyphenyl)(isoindolin-2-yl)methanone (67): A biotage microwave vial was charged with **69** (150 mg, 0.29 mmol, 1 eq.), 3,5-dichlorobenzenethiol (52 mg, 0.29 mmol, 1.0 eq.), 1,1′-ferrocenediyl-bis(diphenylphosphine) (16 mg, 0.029 mmol, 0.1 eq.), Tris(dibenzylideneacetone)dipalladium(0) (13mg, 0.015 mmol, 0.05 eq.), *N*,*N*'-diisopropylethylamine (55 μL, 0.39 mmol, 1.1 eq.). The tube was sealed with a cap lined with a disposable Teflon septum. The tube was evacuated and purged with nitrogen (3 times), before the addition of toluene (3.0 mL) by syringe. The resulting mixture was heated at 120 °C for 18 h,

cooled to rt, and filtered through a small pad of celite (elution with ethyl acetate). Solvent was removed and the residue purified by flash chromatography (SiO_2, 1:3 ethyl acetate/hexanes) to give the corresponding 5-substituted product, which was used further as obtained, and taken in dichloromethane (2 mL), cooled to 0 °C before the addition of 1 M solution of boron tribromide (0.5 mL). The resulting mixture was stirred for 6 h, quenched with saturated sodium bicarbonate solution (5 mL) and extracted with dichloromethane (2 × 10 mL). The combined organic layers were washed with saturated sodium chloride solution (15 mL), dried over anhydrous sodium sulfate, filtered, and concentrated. The residue purified with flash chromatography (SiO_2, 1:2 ethyl acetate/hexanes) to give the desired product **67** as white amorphous solid (23 mg, 18 %). ^{1}H NMR (500 MHz, $CDCl_3$) δ 12.11 (s, 1H), 7.88 (s, 1H), 7.35 – 7.30 (m, 4H), 7.18 (t, *J* = 1.8 Hz, 1H), 6.93 (d, *J* = 1.8 Hz, 2H), 6.75 (s, 1H), 6.60 (s, 1H), 5.10 (s, 4H). ^{13}C NMR (125 MHz, $CDCl_3$) δ 169.7, 166.0, 161.2, 140.4, 138.0 (2), 136.1(2), 128.2 (2), 126.6 (2), 124.1 (2), 122.8 (2), 111.8, 104.7, 103.8, 54.9, 53.8. HRMS (ESI+) *m/z* [M+H$^+$] for $C_{21}H_{16}Cl_2NO_3S$, 433.0306, found 433.0317.

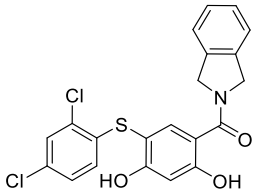

(5-((2,4-Dichlorophenyl)thio)-2,4-dihydroxyphenyl)(isoindolin-2-yl)methanone (68): A biotage microwave vial was charged with **69** (150 mg, 0.29 mmol, 1 eq.), 2,4-dichlorobenzenethiol (52 mg, 0.29 mmol, 1.0 eq.), JosiPhos (4 mg, 0.001 mmol, 0.02 eq.), palladium (II) acetate (7 mg, 0.029 mmol, 0.1 eq.), sodium *tert*-butoxide (41 mg, 0.32 mmol, 1.1 eq.). The tube was sealed with a cap lined with a disposable Teflon septum. The tube was evacuated and purged with nitrogen (3 times), before the addition of toluene (1.0 mL) by syringe. The resulting mixture was heated at 120 °C for 18 h, cooled to rt, and filtered through a small pad of celite (elution with ethyl acetate).

Solvent was removed and the residue purified by flash chromatography (SiO_2, 1:3 ethyl acetate/hexanes) to give the corresponding 5-substituted product, which was used further as obtained, and taken in dichloromethane (2 mL), cooled to 0 °C before the addition of 1 M solution of boron tribromide (0.5 mL). The resulting mixture was stirred for 6 h, quenched with saturated sodium bicarbonate solution (5 mL) and extracted with dichloromethane (2 × 10 mL). The combined organic layers were washed with saturated sodium chloride solution (15 mL), dried over anhydrous sodium sulfate, filtered, and concentrated. The residue purified with flash chromatography (SiO_2, 1:2 ethyl acetate/hexanes) to give the desired product **68** as white amorphous solid (17 mg, 14 %). ^{1}H NMR (400 MHz, $CDCl_3$) δ 12.21 (s, 1H), 7.89 (s, 1H), 7.42 (d, *J* = 2.1 Hz, 1H), 7.32 (s, 5H), 7.11 (dd, *J* = 8.6, 2.2 Hz, 1H), 6.74 (s, 1H), 6.61 (s, 1H), 6.58 (s, 1H), 5.09 (s, 4H). HRMS (ESI+) *m*/*z* [M+H$^+$] calcd for $C_{21}H_{16}Cl_2NO_3S$, 433.0306, found 433.0310.

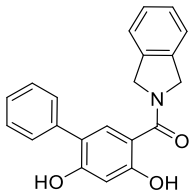

(4,6-Dihydroxy-[1,1'-biphenyl]-3-yl)(isoindolin-2-yl)methanone (70): A biotage microwave vial was charged with 69 (100 mg, 0.19 mmol, 1 eq.), phenyl boronic acid (549 mg, 0.39 mmol, 2.0 eq.), and [1,1′-Bis(diphenylphosphino)ferrocene]dichloropalladium (27 mg, 0.038 mmol, 0.2 eq). The tube was sealed with a cap lined with a disposable Teflon septum. The tube was evacuated and purged with nitrogen (3 times), before the addition of a solvent mixture of toluene (1.0 mL), ethanol (1.0 mL), and saturated sodium bicarbonate solution (1.0 mL) by syringe. The resulting mixture was heated at 80 °C for 14 h, cooled to rt, and filtered through a small pad of celite (elution with ethyl acetate). Solvent was removed and the residue purified by flash chromatography (SiO_2,

1:3 ethyl acetate/hexanes) to give the corresponding 5-substituted product, which was used further as obtained, and taken in dichloromethane (2 mL), cooled to 0 °C before the addition of 1 M solution of boron tribromide (0.5 mL). The resulting mixture was stirred for 6 h, quenched with saturated sodium bicarbonate solution (5 mL) and extracted with dichloromethane (2 × 10 mL). The combined organic layers were washed with saturated sodium chloride solution (15 mL), dried over anhydrous sodium sulfate, filtered, and concentrated. The residue purified with flash chromatography (SiO_2, 1:3 ethyl acetate/hexanes) to give the desired product **70** as white amorphous solid (31 mg, 49 %). ^{1}H NMR (500 MHz, $CDCl_3$) δ 11.67 (s, 1H), 7.57 (s, 1H), 7.56 – 7.41 (m, 5H), 7.34 – 7.28 (m, 4H), 6.63 (s, 1H), 5.78 (s, 1H), 5.11 (s, 4H). ^{13}C NMR (125 MHz, $CDCl_3$) δ 170.7, 162.6, 156.8, 136.6, 136.0 (2), 130.4, 129.7 (4), 128.1 (3), 128.0, 122.8, 119.7, 110.4, 104.5, 55.2, 53.4. HRMS (ESI-) *m*/*z* [M–H$^+$] calcd for $C_{21}H_{16}NO_3$, 330.1130, found 330.1124.

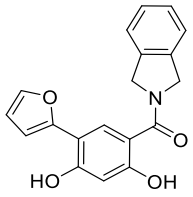

(5-(furan-2-yl)-2,4-dihydroxyphenyl)(isoindolin-2-yl)methanone (71): A biotage microwave vial was charged with **69** (100 mg, 0.19 mmol, 1 eq.), 2-furanylboronic acid (43mg, 0.39 mmol, 2.0 eq.), tetrakis(triphenylphosphine)palladium (0) (67 mg, 0.06 mmol, 0.3 eq), and cesium carbonate (76 mg, 0.23 mmol, 1.2 eq.). The tube was sealed with a cap lined with a disposable Teflon septum. The tube was evacuated and purged with nitrogen (3 times), before the addition of a solvent mixture of toluene (1.5 mL) and methanol (0.5 mL) by syringe. The resulting mixture was heated at 110 °C for 1 h under microwave heating. The reaction mixture was filtered through a small pad of celite (elution with ethyl acetate). Solvent was removed and the residue purified by

flash chromatography (SiO_2, 1:3 ethyl acetate/hexanes) to give the corresponding 5-substituted product, which was subjected to hydrogenolysis as obtained. The residue was dissolved in a solvent mixture of ethyl acetate (1.5 mL) and ethanol (0.5 mL), followed by the addition of 10% palladium on carbon and cyclohexene (0.2 mL). The resulting mixture was heated at 100 °C for 14 h, filtered through a pad of celite (elution with ethyl acetate), and concentrated. The residue purified with flash chromatography (SiO_2, 1:2 ethyl acetate/hexanes) to give the desired product **71** as white amorphous solid (13 mg, 14 %). ^{1}H NMR (400 MHz, $CDCl_3$) δ 11.51 (s, 1H), 7.84 (s, 1H), 7.45 (dd, *J* = 1.8, 0.8 Hz, 1H), 7.20 – 7.24 (m, 4H), 6.97 (s, 1H), 6.60 – 6.56 (m, 1H), 6.50 (br s, 1H), 6.48 (dd, *J* = 3.4, 1.9 Hz, 1H), 5.07 (s, 4H). ^{13}C NMR (100 MHz, $CDCl_3$) δ 170.6, 162.4, 156.7, 151.6, 141.3 (3), 128.1 (2), 127.0 (2), 122.8, 112.0, 110.5, 109.1, 106.1, 105.3, 54.0 (2). HRMS (ESI+) *m*/*z* [M+H$^+$] calcd for $C_{19}H_{16}NO_4$, 322.1079, found 322.1086.

III.7. References

1. Whitesell, L.; Lindquist, S. L. HSP90 and the Chaperoning of Cancer. *Nat. Rev. Cancer* **2005**, 5, 761-772.
2. Whitesell, L.; Lin, N. U. HSP90 as a platform for the assembly of more effective cancer chemotherapy. *Biochimi. Biophys. Acta*. **2012**, 1823, 756-766.
3. Bagatell, R.; Whitesell, L. Altered Hsp90 function in cancer: a unique therapeutic opportunity. *Mol. Cancer Ther*. **2004**, 3, 1021-1030.
4. Workman, P. Combinatorial attack on multistep oncogenesis by inhibiting the Hsp90 molecular chaperone. *Cancer Lett*. **2004**, 206, 149-157.
5. Chen, B.; Piel, W. H.; Gui, L.; Bruford, E.; Monteiro, A. The HSP90 family of genes in the human genome: insights into their divergence and evolution. *Genomics* **2005**, 86, 627-637.
6. Sreedhar, A. S.; Kalmár, É.; Csermely, P.; Shen, Y.-F. Hsp90 Isoforms: Functions, Expression and Clinical Importance. *FEBS Lett.* **2004**, 562, 11-15.
7. Zuehlke, A.; Johnson, J. L. Hsp90 and co-chaperones twist the functions of diverse client proteins. *Biopolymers* **2010**, 93, 211-217.
8. Riggs, D. L.; Cox, M. B.; Cheung-Flynn, J.; Prapapanich, V.; Carrigan, P. E.; Smith, D. F. Functional specificity of co-chaperone interactions with Hsp90 client proteins. *Crit. Rev. Biochem. Mol. Biol.* **2004**, 39, 279-295.

9. Connell, P.; Ballinger, C. A.; Jiang, J.; Wu, Y.; Thompson, L. J.; Hohfeld, J.; Patterson, C. The co-chaperone CHIP regulates protein triage decisions mediated by heat-shock proteins. *Nat. Cell Biol.* **2001**, 3, 93-96.
10. Chadli, A.; Felts, S. J.; Toft, D. O. GCUNC45 is the first Hsp90 co-chaperone to show α/β isoform specificity. *J. Biol. Chem.* **2008**, 283, 9509-9512.
11. Barrott, J. J.; Haystead, T. A. J. Hsp90, an Unlikely Ally in the War on Cancer. *FEBS J.* **2013**, 280, 1381-1396.
12. Jhaveri, K.; Taldone, T.; Modi, S.; Chiosis, G. Advances in the clinical development of heat shock protein 90 (Hsp90) inhibitors in cancers. *Biochim. Biophys. Acta*. **2012**, 1823, 742-755.
13. Khandelwal, A.; Crowley, V. M.; Blagg, B. S. Natural Product Inspired N-Terminal Hsp90 Inhibitors: From Bench to Bedside? *Med. Res. Rev.* **2016**, 36, 92-118.
14. Neckers, L.; Workman, P. Hsp90 Molecular Chaperone Inhibitors: Are We There Yet? *Clin. Cancer Res.* **2012**, 18, 64-76.
15. Holzbeierlein, J. M.; Windsperger, A.; Vielhauer, G. Hsp90: A Drug Target? *Curr. Oncol. Rep.* **2010,** 12, 95-101.
16. Biamonte, M. A.; Van de Water, R.; Arndt, J. W.; Scannevin, R. H.; Perret, D.; Lee, W. C. Heat shock protein 90: inhibitors in clinical trials. *J. Med. Chem.* **2010**, 53, 3-17.
17. Hong, D. S.; Banerji, U.; Tavana, B.; George, G. C.; Aaron, J.; Kurzrock, R. Targeting the molecular chaperone heat shock protein 90 (HSP90): lessons learned and future directions. *Cancer Treat. Rev.* **2013**, 39, 375-387.
18. Garcia-Carbonero, R.; Carnero, A.; Paz-Ares, L. Inhibition of HSP90 molecular chaperones: moving into the clinic. *The Lancet. Oncol.* **2013**, 14, e358-369.
19. Morimoto, R. I. The heat shock response: systems biology of proteotoxic stress in aging and disease. *Cold Spring Harb. Symp. Quant. Biol.* **2011**, 76, 91-99.
20. Bagatell, R.; Paine-Murrieta, G. D.; Taylor, C. W.; Pulcini, E. J.; Akinaga, S.; Benjamin, I. J.; Whitesell, L. Induction of a heat shock factor 1-dependent stress response alters the cytotoxic activity of hsp90-binding agents. *Clin. Cancer Res.***2000**, 6, 3312-3318.
21. Jolly, C.; Morimoto, R. I. Role of the heat shock response and molecular chaperones in oncogenesis and cell death. *J. Natl. Cancer Inst.* **2000**, 92, 1564-1572.
22. Powers, M. V.; Workman, P. Inhibitors of the heat shock response: biology and pharmacology. *FEBS Lett.* **2007**, 581, 3758-3769.
23. Brandt, G. E. L.; Blagg, B. S. J. Alternate Strategies of Hsp90 Modulation for the Treatment of Cancer and Other Diseases. *Curr. Top. Med. Chem.* **2009**, 9, 1447-1461.
24. Hall, J. A.; Forsberg, L. K.; Blagg, B. S. Alternative approaches to Hsp90 modulation for the treatment of cancer. *Future Med. Chem.* **2014,** 6, 1587-1605.
25. Duerfeldt, A. S.; Peterson, L. B.; Maynard, J. C.; Ng, C. L.; Eletto, D.; Ostrovsky, O.; Shinogle, H. E.; Moore, D. S.; Argon, Y.; Nicchitta, C. V.; Blagg, B. S. Development of a Grp94 inhibitor. *J. Am. Chem. Soc.* **2012**, 134, 9796-9804.
26. Ernst, J. T.; Neubert, T.; Liu, M.; Sperry, S.; Zuccola, H.; Turnbull, A.; Fleck, B.; Kargo, W.; Woody, L.; Chiang, P.; Tran, D.; Chen, W.; Snyder, P.; Alcacio, T.; Nezami, A.; Reynolds, J.; Alvi, K.; Goulet, L.; Stamos, D. Identification of novel HSP90α/β isoform selective inhibitors using structure-based drug design. demonstration of potential utility in treating CNS disorders such as Huntington's disease. *J. Med. Chem.* **2014**, 57, 3382-3400.
27. Crowley, V. M.; Khandelwal, A.; Mishra, S.; Stothert, A. R.; Huard, D. J.; Zhao, J.; Muth, A.; Duerfeldt, A. S.; Kizziah, J. L.; Lieberman, R. L.; Dickey, C. A.; Blagg, B. S.

Development of Glucose Regulated Protein 94-Selective Inhibitors Based on the BnIm and Radamide Scaffold. *J. Med. Chem.* **2016**, 59, 3471-3488.
28. Liu, W.; Vielhauer, G. A.; Holzbeierlein, J. M.; Zhao, H.; Ghosh, S.; Brown, D.; Lee, E.; Blagg, B. S. KU675, a Concomitant Heat-Shock Protein Inhibitor of Hsp90 and Hsc70 that Manifests Isoform Selectivity for Hsp90α in Prostate Cancer Cells. *Mol. Pharmacol.* **2015**, 88, 121-130.
29. Milicevic, Z.; Bogojevic, D.; Mihailovic, M.; Petrovic, M.; Krivokapic, Z. Molecular characterization of hsp90 isoforms in colorectal cancer cells and its association with tumour progression. *Int. J. Oncol.* **2008**, 32, 1169-1178.
30. Chang, Y. S.; Lo, C. W.; Sun, F. C.; Chang, M. D.; Lai, Y. K. Differential expression of Hsp90 isoforms in geldanamycin-treated 9L cells. *Biochem. Biophys. Res. Comm.* **2006**, 344, 37-44.
31. McDowell, C. L.; Bryan Sutton, R.; Obermann, W. M. Expression of Hsp90 chaperone proteins in human tumor tissue. *Int. J. Biol. Macromol.* **2009**, 45, 310-314.
33. Wang, Q.; He, Z.; Zhang, J.; Wang, Y.; Wang, T.; Tong, S.; Wang, L.; Wang, S.; Chen, Y. Overexpression of endoplasmic reticulum molecular chaperone GRP94 and GRP78 in human lung cancer tissues and its significance. *Cancer Detect. Preven.* **2005**, 29, 544-551.
34. Dejeans, N.; Glorieux, C.; Guenin, S.; Beck, R.; Sid, B.; Rousseau, R.; Bisig, B.; Delvenne, P.; Buc Calderon, P.; Verrax, J. Overexpression of GRP94 in breast cancer cells resistant to oxidative stress promotes high levels of cancer cell proliferation and migration: implications for tumor recurrence. *Free Radic. Biol. Med.* **2012**, 52, 993-1002.
35. Wang, Q.; An, L.; Chen, Y.; Yue, S. Expression of endoplasmic reticulum molecular chaperon GRP94 in human lung cancer tissues and its clinical significance. *Chin. Med. J.* **2002**, 115, 1615-1619.
36. Takahashi, H.; Wang, J. P.; Zheng, H. C.; Masuda, S.; Takano, Y. Overexpression of GRP78 and GRP94 is involved in colorectal carcinogenesis. *Histol. Histopathol.* **2011**, 26, 663-671.
37. Chatterjee, M.; Jain, S.; Stuhmer, T.; Andrulis, M.; Ungethum, U.; Kuban, R. J.; Lorentz, H.; Bommert, K.; Topp, M.; Kramer, D.; Muller-Hermelink, H. K.; Einsele, H.; Greiner, A.; Bargou, R. C. STAT3 and MAPK signaling maintain overexpression of heat shock proteins 90α and β in multiple myeloma cells, which critically contribute to tumor-cell survival. *Blood* **2007**, 109, 720-728.
38. Li, C. F.; Huang, W. W.; Wu, J. M.; Yu, S. C.; Hu, T. H.; Uen, Y. H.; Tian, Y. F.; Lin, C. N.; Lu, D.; Fang, F. M.; Huang, H. Y. Heat shock protein 90 overexpression independently predicts inferior disease-free survival with differential expression of the α and β isoforms in gastrointestinal stromal tumors. *Clin. Cancer Res.* **2008**, 14, 7822-7831.
39. Gao, Y.; Yechikov, S.; Vazquez, A. E.; Chen, D.; Nie, L. Distinct roles of molecular chaperones HSP90α and HSP90β in the biogenesis of KCNQ4 channels. *PloS one* **2013,** 8, e57282.
40. Karagoz, G. E.; Rudiger, S. G. Hsp90 interaction with clients. *Trends Biochem. Sci.* **2015**, 40, 117-125.
41. Prince, T. L.; Kijima, T.; Tatokoro, M.; Lee, S.; Tsutsumi, S.; Yim, K.; Rivas, C.; Alarcon, S.; Schwartz, H.; Khamit-Kush, K.; Scroggins, B. T.; Beebe, K.; Trepel, J. B.; Neckers, L. Client Proteins and Small Molecule Inhibitors Display Distinct Binding Preferences for Constitutive and Stress-Induced HSP90 Isoforms and Their Conformationally Restricted Mutants. *PloS one* **2015**, 10, e0141786.

42. Didelot, C.; Lanneau, D.; Brunet, M.; Bouchot, A.; Cartier, J.; Jacquel, A.; Ducoroy, P.; Cathelin, S.; Decologne, N.; Chiosis, G.; Dubrez-Daloz, L.; Solary, E.; Garrido, C. Interaction of heat-shock protein 90β isoform (HSP90β) with cellular inhibitor of apoptosis 1 (c-IAP1) is required for cell differentiation. *Cell Death Differ.* **2008**, *15*, 859-866.
43. Peterson, L. B.; Eskew, J. D.; Vielhauer, G. A.; Blagg, B. S. The hERG channel is dependent upon the Hsp90α isoform for maturation and trafficking. *Mol. Pharmacol.* **2012,** 9, 1841-6.
44. Patel, P. D.; Yan, P.; Seidler, P. M.; Patel, H. J.; Sun, W.; Yang, C.; Que, N. S.; Taldone, T.; Finotti, P.; Stephani, R. A.; Gewirth, D. T.; Chiosis, G. Paralog-selective Hsp90 inhibitors define tumor-specific regulation of HER2. *Nat. Chem. Biol.* **2013**, 9, 677-684.
45. Little, E.; Ramakrishnan, M.; Roy, B.; Gazit, G.; Lee, A. S. The glucose-regulated proteins (GRP78 and GRP94): functions, gene regulation, and applications. *Crit. Rev. Eukaryot. Gene Expr.* **1994**, 4, 1-18.
46. Yang, Y.; Liu, B.; Dai, J.; Srivastava, P. K.; Zammit, D. J.; Lefrancois, L.; Li, Z. Heat shock protein gp96 is a master chaperone for toll-like receptors and is important in the innate function of macrophages. *Immunity* **2007**, 26, 215-226.
47. McLaughlin, M.; Vandenbroeck, K. The endoplasmic reticulum protein folding factory and its chaperones: new targets for drug discovery? *Br. J. Pharmacol.* **2011**, 162, 328-345.
48. Randow, F.; Seed, B. Endoplasmic reticulum chaperone gp96 is required for innate immunity but not cell viability. *Nat. Cell Biol.* **2001**, 3, 891-896.
49. Liu, B.; Staron, M.; Hong, F.; Wu, B. X.; Sun, S.; Morales, C.; Crosson, C. E.; Tomlinson, S.; Kim, I.; Wu, D.; Li, Z. Essential roles of grp94 in gut homeostasis via chaperoning canonical Wnt pathway. *Proc. Natl. Acad. Sci.* **2013**, 110, 6877-6882.
50. Zhu, G.; Lee, A. S. Role of the unfolded protein response, GRP78 and GRP94 in organ homeostasis. *J. Cell. Physiol.* **2015**, 230, 1413-1420.
51. Marzec, M.; Eletto, D.; Argon, Y. GRP94: An HSP90-like protein specialized for protein folding and quality control in the endoplasmic reticulum. *Biochim. Biophys. Acta.* **2012**, 1823, 774-87.
52. Ghosh, S.; Shinogle, H. E.; Galeva, N. A.; Dobrowsky, R. T.; Blagg, B. S. Endoplasmic Reticulum-resident Heat Shock Protein 90 (HSP90) Isoform Glucose-regulated Protein 94 (GRP94) Regulates Cell Polarity and Cancer Cell Migration by Affecting Intracellular Transport. *J. Biol. Chem.* **2016**, 291, 8309-8323.
53. Eletto, D.; Dersh, D.; Argon, Y. GRP94 in ER quality control and stress responses. *Semin. Cell Dev. Biol.* **2010,** 21, 479-485.
54. Randow, F.; Seed, B. Endoplasmic reticulum chaperone gp96 is required for innate immunity but not cell viability. *Nat. Cell Biol.* **2001**, 3, 891-896.
55. Stothert, A. R.; Suntharalingam, A.; Huard, D. J.; Fontaine, S. N.; Crowley, V. M.; Mishra, S.; Blagg, B. S.; Lieberman, R. L.; Dickey, C. A. Exploiting the interaction between Grp94 and aggregated myocilin to treat glaucoma. *Hum. Mol. genet.* **2014**, 23, 6470-6480.
56. Suntharalingam, A.; Abisambra, J. F.; O'Leary, J. C., 3rd; Koren, J., 3rd; Zhang, B.; Joe, M. K.; Blair, L. J.; Hill, S. E.; Jinwal, U. K.; Cockman, M.; Duerfeldt, A. S.; Tomarev, S.; Blagg, B. S.; Lieberman, R. L.; Dickey, C. A. Glucose-regulated protein 94 triage of mutant myocilin through endoplasmic reticulum-associated degradation subverts a more efficient autophagic clearance mechanism. *J. Biol. Chem.* **2012**, 287, 40661-40669.
57. Huang, Q. Q.; Sobkoviak, R.; Jockheck-Clark, A. R.; Shi, B.; Mandelin, A. M., 2nd; Tak, P. P.; Haines, G. K., 3rd; Nicchitta, C. V.; Pope, R. M. Heat shock protein 96 is elevated

in rheumatoid arthritis and activates macrophages primarily via TLR2 signaling. *J. Immunol.* **2009**, 182, 4965-4973.
58. Hua, Y.; White-Gilbertson, S.; Kellner, J.; Rachidi, S.; Usmani, S. Z.; Chiosis, G.; Depinho, R.; Li, Z.; Liu, B. Molecular chaperone gp96 is a novel therapeutic target of multiple myeloma. *Clin. Cancer Res.* **2013,** 19, 6242-6251.
59. Chen, X.; Ding, Y.; Liu, C. G.; Mikhail, S.; Yang, C. S. Overexpression of glucose-regulated protein 94 (Grp94) in esophageal adenocarcinomas of a rat surgical model and humans. *Carcinogenesis* **2002**, 23, 123-130.
60. Dejeans, N.; Glorieux, C.; Guenin, S.; Beck, R.; Sid, B.; Rousseau, R.; Bisig, B.; Delvenne, P.; Buc Calderon, P.; Verrax, J. Overexpression of GRP94 in breast cancer cells resistant to oxidative stress promotes high levels of cancer cell proliferation and migration: implications for tumor recurrence. *Free Radic. Biol. Med.* **2012,** 52, 993-1002.
61. Hua, Y.; White-Gilbertson, S.; Kellner, J.; Rachidi, S.; Usmani, S. Z.; Chiosis, G.; Depinho, R.; Li, Z.; Liu, B. Molecular chaperone gp96 is a novel therapeutic target of multiple myeloma. *Clin. Cancer Res.* **2013,** 19, 6242-51.
62. Patel, P. D.; Yan, P.; Seidler, P. M.; Patel, H. J.; SUn, W.; Yang, C.; Que, N. S.; Taldone, T.; Finotti, P.; Stephani, R. A.; Gewirth, D. T.; Chiosis, G. Paralog-Selective Hsp90 Inhibitors Define Tumor-Specific Regulation of HER2. *Nat.Chem. Biol.* **2013**, *9*, 677-684.
63. Rosser, M. F.; Nicchitta, C. V. Ligand interactions in the adenosine nucleotide-binding domain of the Hsp90 chaperone, GRP94. I. Evidence for allosteric regulation of ligand binding. *J. Biol. Chem.* **2000**, 275, 22798-22805.
64. Wassenberg, J. J.; Reed, R. C.; Nicchitta, C. V. Ligand interactions in the adenosine nucleotide-binding domain of the Hsp90 chaperone, GRP94. II. Ligand-mediated activation of GRP94 molecular chaperone and peptide binding activity. *J. Biol. Chem.* **2000**, 275, 22806-22814.
65. Immormino, R. M.; Dollins, D. E.; Shaffer, P. L.; Soldano, K. L.; Walker, M. A.; Gewirth, D. T. Ligand-induced conformational shift in the N-terminal domain of GRP94, an Hsp90 chaperone. *J. Biol. Chem.* **2004**, 279, 46162-46171.
66. Immormino, R. M.; Metzger, L. E. t.; Reardon, P. N.; Dollins, D. E.; Blagg, B. S.; Gewirth, D. T. Different poses for ligand and chaperone in inhibitor-bound Hsp90 and GRP94: implications for paralog-specific drug design. *J. Mol. Biol.* **2009**, 388, 1033-1042.
67. Hutchison, K. A.; Nevins, B.; Perini, F.; Fox, I. H. Soluble and membrane-associated human low-affinity adenosine binding protein (adenotin): properties and homology with mammalian and avian stress proteins. *Biochemistry* **1990**, 29, 5138-44.
68. Soldano, K. L.; Jivan, A.; Nicchitta, C. V.; Gewirth, D. T. Structure of the N-terminal domain of GRP94. Basis for ligand specificity and regulation. *J. Biol. Chem.* **2003**, 278, 48330-48338.
69. Kim, J.; Felts, S.; Llauger, L.; He, H.; Huezo, H.; Rosen, N.; Chiosis, G. Development of a fluorescence polarization assay for the molecular chaperone Hsp90. *J. Biolmol. Screen.* **2004**, 9, 375-381.
70. Howes, R.; Barril, X.; Dymock, B. W.; Grant, K.; Northfield, C. J.; Robertson, A. G.; Surgenor, A.; Wayne, J.; Wright, L.; James, K.; Matthews, T.; Cheung, K. M.; McDonald, E.; Workman, P.; Drysdale, M. J. A fluorescence polarization assay for inhibitors of Hsp90. *Anal. Biochem.* **2006**, 350, 202-213.

71. Duerfeldt, A. S.; Brandt, G. E.; Blagg, B. S. Design, synthesis, and biological evaluation of conformationally constrained cis-amide Hsp90 inhibitors. *Org. Lett.* **2009**, 11, 2353-2356.
72. Murray, C. W.; Carr, M. G.; Callaghan, O.; Chessari, G.; Congreve, M.; Cowan, S.; Coyle, J. E.; Downham, R.; Figueroa, E.; Frederickson, M.; Graham, B.; McMenamin, R.; O'Brien, M. A.; Patel, S.; Phillips, T. R.; Williams, G.; Woodhead, A. J.; Woolford, A. J. Fragment-based drug discovery applied to Hsp90. Discovery of two lead series with high ligand efficiency. *J. Med. Chem.* **2010**, 53, 5942-5955.
73. Woodhead, A. J.; Angove, H.; Carr, M. G.; Chessari, G.; Congreve, M.; Coyle, J. E.; Cosme, J.; Graham, B.; Day, P. J.; Downham, R.; Fazal, L.; Feltell, R.; Figueroa, E.; Frederickson, M.; Lewis, J.; McMenamin, R.; Murray, C. W.; O'Brien, M. A.; Parra, L.; Patel, S.; Phillips, T.; Rees, D. C.; Rich, S.; Smith, D. M.; Trewartha, G.; Vinkovic, M.; Williams, B.; Woolford, A. J. Discovery of (2,4-dihydroxy-5-isopropylphenyl)-[5-(4-methylpiperazin-1-ylmethyl)-1,3-dihydrois oindol-2-yl]methanone (AT13387), a novel inhibitor of the molecular chaperone Hsp90 by fragment based drug design. *J. Med. Chem.* **2010**, 53, 5956-5969.
74. Patel, H. J.; Patel, P. D.; Ochiana, S. O.; Yan, P.; Sun, W.; Patel, M. R.; Shah, S. K.; Tramentozzi, E.; Brooks, J.; Bolaender, A.; Shrestha, L.; Stephani, R.; Finotti, P.; Leifer, C.; Li, Z.; Gewirth, D. T.; Taldone, T.; Chiosis, G. Structure-activity relationship in a purine-scaffold compound series with selectivity for the endoplasmic reticulum Hsp90 paralog Grp94. *J. Med. Chem.* **2015**, 58, 3922-3943.
75. Woodhead, A. J.; Angove, H.; Carr, M. G.; Chessari, G.; Congreve, M.; Coyle, J. E.; Cosme, J.; Graham, B.; Day, P. J.; Downham, R.; Fazal, L.; Feltell, R.; Figueroa, E.; Frederickson, M.; Lewis, J.; McMenamin, R.; Murray, C. W.; O'Brien, M. A.; Parra, L.; Patel, S.; Phillips, T.; Rees, D. C.; Rich, S.; Smith, D. M.; Trewartha, G.; Vinkovic, M.; Williams, B.; Woolford, A. J. Discovery of (2,4-dihydroxy-5-isopropylphenyl)-[5-(4-methylpiperazin-1-ylmethyl)-1,3-dihydrois oindol-2-yl]methanone (AT13387), a novel inhibitor of the molecular chaperone Hsp90 by fragment based drug design. *J. Med. Chem.* **2010**, 53, 5956-5969.
76. Shang, R.; Fu, Y.; Li, J. B.; Zhang, S. L.; Guo, Q. X.; Liu, L. Synthesis of aromatic esters via Pd-catalyzed decarboxylative coupling of potassium oxalate monoesters with aryl bromides and chlorides. *J. Am. Chem. Soc.* **2009**, 131, 5738-5739.
77. Maiti, D.; Fors, B. P.; Henderson, J. L.; Nakamura, Y.; Buchwald, S. L. Palladium-Catalyzed Coupling of Functionalized Primary and Secondary Amines with Aryl and Heteroaryl Halides: Two Ligands Suffice in Most Cases. *Chem. Sci.***2011**, 2, 57-68.
78. Bang-Andersen, B.; Ruhland, T.; Jorgensen, M.; Smith, G.; Frederiksen, K.; Jensen, K. G.; Zhong, H.; Nielsen, S. M.; Hogg, S.; Mork, A.; Stensbol, T. B. Discovery of 1-[2-(2,4-dimethylphenylsulfanyl)phenyl]piperazine (Lu AA21004): a novel multimodal compound for the treatment of major depressive disorder. *J. Med. Chem.* **2011**, 54, 3206-3221.
79. Hartwig, J. F. Evolution of a fourth generation catalyst for the amination and thioetherification of aryl halides. *Acc. Chem. Res.* **2008**, 41, 1534-1544.
80. Fernandez-Rodriguez, M. A.; Shen, Q.; Hartwig, J. F. A general and long-lived catalyst for the palladium-catalyzed coupling of aryl halides with thiols. *J. Am. Chem. Soc.* **2006**, 128, 2180-2181.

81. He, H.; Zatorska, D.; Kim, J.; Aguirre, J.; Llauger, L.; She, Y.; Wu, N.; Immormino, R. M.; Gewirth, D. T.; Chiosis, G. Identification of potent water soluble purine-scaffold inhibitors of the heat shock protein 90. *J. Med. Chem.* **2006**, 49, 381-390.

Chapter IV

Development of the First Hsp90β-Selective N-Terminal Inhibitor

IV.1 Introduction

Heat shock protein 90 (Hsp90) is responsible for maintaining cellular homeostasis by assisting in the maturation of nascent polypeptides and the rematuration of the denatured proteins into their biologically active conformations.[1-5] There are more than 200 protein substrates (clients) that are dependent upon Hsp90 for their maturation and proper function. Many of these client proteins are signaling proteins that can lead to tumor initiation, tumor progression, and metastasis.[6-8] In fact, Hsp90's clients are associated with all 10 hallmarks of cancer; hence, Hsp90 facilitates cancer cell growth and survival.[9, 10] Hsp90 also folds many of the oncogenic and mutant client proteins, which helps to explain the increased dependency of tumor cells on Hsp90.[11, 12] Increased dependency on Hsp90 correlates directly with increased Hsp90 levels in most cancers.[13-16] As shown previously, Hsp90 exists primarily in an activated heteroprotein complex in cancer cells, which exhibits >200-fold higher affinity for ATP than the homodimer in normal cells.[17] Similarly the heteroprotein complex also exhibits greater ATPase activity.[17] Unlike conventional chemotherapy agents that target a single oncogene, enzyme, or receptor, Hsp90 inhibition simultaneously disrupts of multiple signaling nodes essential to cancer, and thus, mimics combination therapy through a single target.[18-21] Since Hsp90 inhibitors accumulate in tumor cells more effectively than normal tissues, Hsp90 inhibitors can exhibit a broad therapeutic window. As a result, Hsp90 has become a highly sought after target for the development of anti-tumor agents, and has led to 17 clinical candidates.[21-23] However, the clinical progress of these inhibitors has been hampered by modest efficacy, escalated dosing, and adverse effects that include cardiotoxicity, hepatotoxicity, bone metastasis, and ocular toxicity.[24-28]

All of the Hsp90 inhibitors under clinical investigation bind the N-terminal nucleotide binding pocket and exhibit *pan*-Hsp90 inhibitory activity against all four Hsp90 isoforms; Hsp90α (cytosolic and inducible), Hsp90β (cytosolic and constitutively expressed), Grp94 (endoplasmic reticulum located) and TRAP1 (mitochondria localized).[29, 30]

This simplistic model of *pan*-Hsp90 inhibition for the treatment of cancer requires significant modification to address the detriments associated with current Hsp90 inhibitors.[31, 32] The expression of Hsp90 isoforms can vary among cancers, which suggests that a cancer's dependence upon individual isoforms also varies.[33-36] In addition, Hsp90 isoforms exhibit specificity for client protein substrates and interacts with co-chaperones, which suggests that Hsp90 isoforms could be targeted individually.[37-41] Consequently, isoform-selective Hsp90 inhibitors are likely to provide a therapeutic opportunity to minimize off-target toxicity by limiting the number of clients affected via Hsp90 inhibition. Among the four isoforms, some specific roles for Grp94 and the consequences of Grp94-inhibition have been reported. Isoform-dependent clients of Grp94 (e.g. mutant myocilin, immunoglobulins, TLR1, TLR2, TLR9, IGF-1, IGF-2) have been identified and Grp94 inhibitors have shown efficacy for the potential treatment of glaucoma, multiple myeloma, and cancer metastasis.[42-46] The two cytosolic isoforms, Hsp90α and Hsp90β, are the most relevant for the treatment of cancer as majority of oncogenic proteins are dependent upon them for proper function.[47] Some isoform-selective clients of the two cytosolic isoforms have recently been identified, and proteomic studies have identified survivin, Raf, and the hERG channel as Hsp90α-dependent clients. c-IAP1 and $CXCR_4$ are dependent upon Hsp90β.[24, 34, 43, 48] However, they have not been confirmed via pharmacological studies. Collectively, these prior studies establish that both cytosolic isoforms modulate substrates associated with different oncogenic pathways, supporting the hypothesis that selective inhibition

of each Hsp90 isoform represents a new approach to improve the therapeutic potential of Hsp90 inhibitors. Since the hERG channel is dependent upon the Hsp90α isoform, Hsp90β-selective inhibitors may avoid the cardiotoxicity often observed in clinical trials with some *pan*-Hsp90 inhibitors. In addition, Hsp90β-specific inhibitors would enable the identification of Hsp90β-selective clients and provide data to identify the cancers that are driven by Hsp90β-dependent substrates.

IV.1.1. Hsp90β

The Hsp90β isoform is located in the cytosol along with the Hsp90α isoform and is encoded by the HSPAB1 gene.[29, 49] Hsp90β is constitutively expressed, and its expression can be induced, but to a lesser extent than Hsp90α.[49] Overexpression of Hsp90β has been associated with chronic tumors.[33, 50-54] Most studies do not differentiate between the roles of these two cytosolic isoforms but some biochemical and functional differences have been reported.[24, 29, 49, 55] The Hsp90β-isoform plays a key role in early embryonic development, germ cell maturation, cytoskeleton stabilization, cellular transformation, and long term cellular adaptation.[55-61] Hsp90α is involved with growth promotion, cell cycle regulation, and stress-induced cytoprotection.[62, 63] Hsp90β interacts with P-glycoproteins, therefore, its expression has been associated with drug-resistance.[64] A few Hsp90β-dependent oncogenic clients have been identified, including $CXCR_4$ and CDK6 (unpublished data). Client proteins, co-chaperones and partner proteins interacts differently with each cytosolic isoform. For example, the Hsp90 co-chaperone, GCUNC45, interacts preferentially with Hsp90β.[65] Recently, Neckers and co-workers studied ligand and client protein binding to Hsp90β and Hsp90α.[40] Using various Hsp90 mutants, they showed that Hsp90 clients manifest different affinity for both cytosolic isoforms.

Collectively, these prior studies establish specific roles of Hsp90β in carcinogenesis and underline the need to develop Hsp90β-selective inhibitors.

IV.2. Differences in N-Terminal ATP-Binding Pocket of Hsp90 Isoforms

Greater than 85% identity is shared between in the N-terminal ATP-binding sites of the Hsp90 isoforms, which has limited the development of isoform-selective inhibitors.[29, 49] Since Grp94 shares the least identity amongst the Hsp90 isoforms, it was the first sought for the development of isoform-selective inhibitors. Grp94-selctive inhibitors have been developed and are currently being evaluated for various therapeutic applications.[21, 44, 45, 66, 67] However, Hsp90α and Hsp90β are >95% identical within the N-terminal binding site, suggesting that selective inhibition of these isoforms would be more challenging. Sequence alignment of the N-terminal domain of the Hsp90 isoforms reveals (Figure 35A) that there are only two amino acids that differ between Hsp90α versus Hsp90β. As shown in Figure 35B, there is a network of water-mediated hydrogen bonds that align at the bottom of the pocket surrounding the phenols of radicicol bound to each Hsp90 isoform. The carbonyl and 4-phenol make hydrogen bonds with Thr184 and Asp93 (numbered for Hsp90β) through these water molecules, which are conserved amongst the majority of Hsp90 co-crystal structures and mediate hydrogen bonding interactions between ligands and Hsp90 isoforms. Leu48, Lys58, Asp93, Ile96, Gly97, Met98, Leu107, Thr109, Phe138, Tyr139, Trp162, and Thr184 (numbered for Hsp90β) represent the key amino acids within the N-terminal ATP-binding pocket and are conserved amongst the four isoforms. Overlay of the Hsp90α and Hsp90β co-crystal structures revealed that the ATP binding pocket in Hsp90β contains Ala52 and Leu91, in lieu of Ser52and Ile91, which are present in Hsp90α. The Grp94 and Trap1 binding pockets contain Val147 and Ile156 in lieu of Leu91, respectively. Based on these observations, we hypothesized that an Hsp90β-selective inhibitor should exhibit substitutions at the 4-position of

the resorcinol ring that creates a unfavorable steric interactions with the bulkier side chains present in Hsp90α, Grp94, and Trap-1.

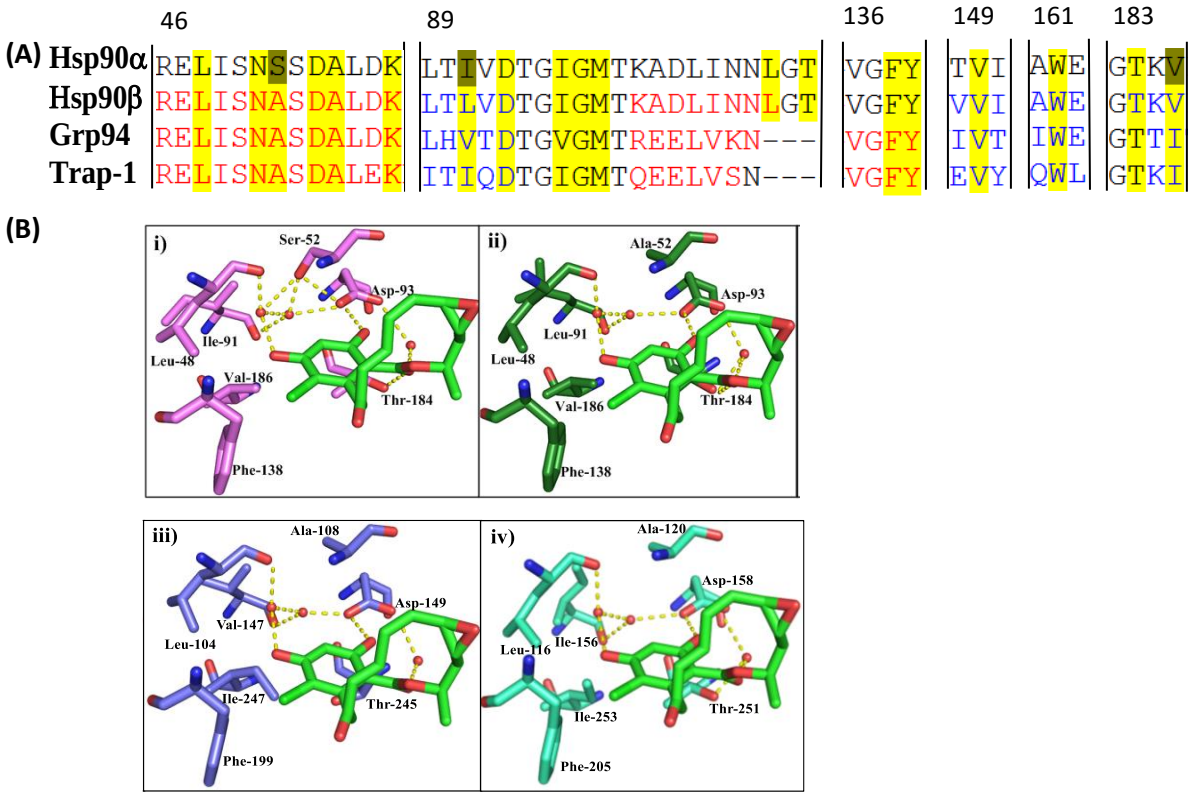

Figure 35. Differences amongst Hsp90 Isoforms. (**A**) Sequence alignment of Hsp90 isoforms. Key residues comprising N-terminal binding pocket are highlighted in yellow. Residues in blue boxes indicate the amino acid difference between Hsp90 isoforms (**B**) Modeling of Radicicol into N-terminal ATP binding site of Hsp90 isoforms: i) Hsp90α (PDB code: 2XAB) ii) Hsp90β (PDB code: 1UYM) iii) Grp94 (PDB code: 4NH9) iv) Trap-1(PDB code: 4Z1F).

IV.3. Development of Resorcinol Analogues Modified at the 4-Position

IV.3.1. Design of Resorcinol Analogues Modified at the 4-Position for Selective Hsp90β-Inhibition

To probe the subtle differences about the 3- and the 4-position of the resorcinol ring, modifications to the 4-position were pursued. Based on prior experience with the resorcinol-isoindoline scaffold (Chapter III), it was chosen for the development of new Hsp90β-selective

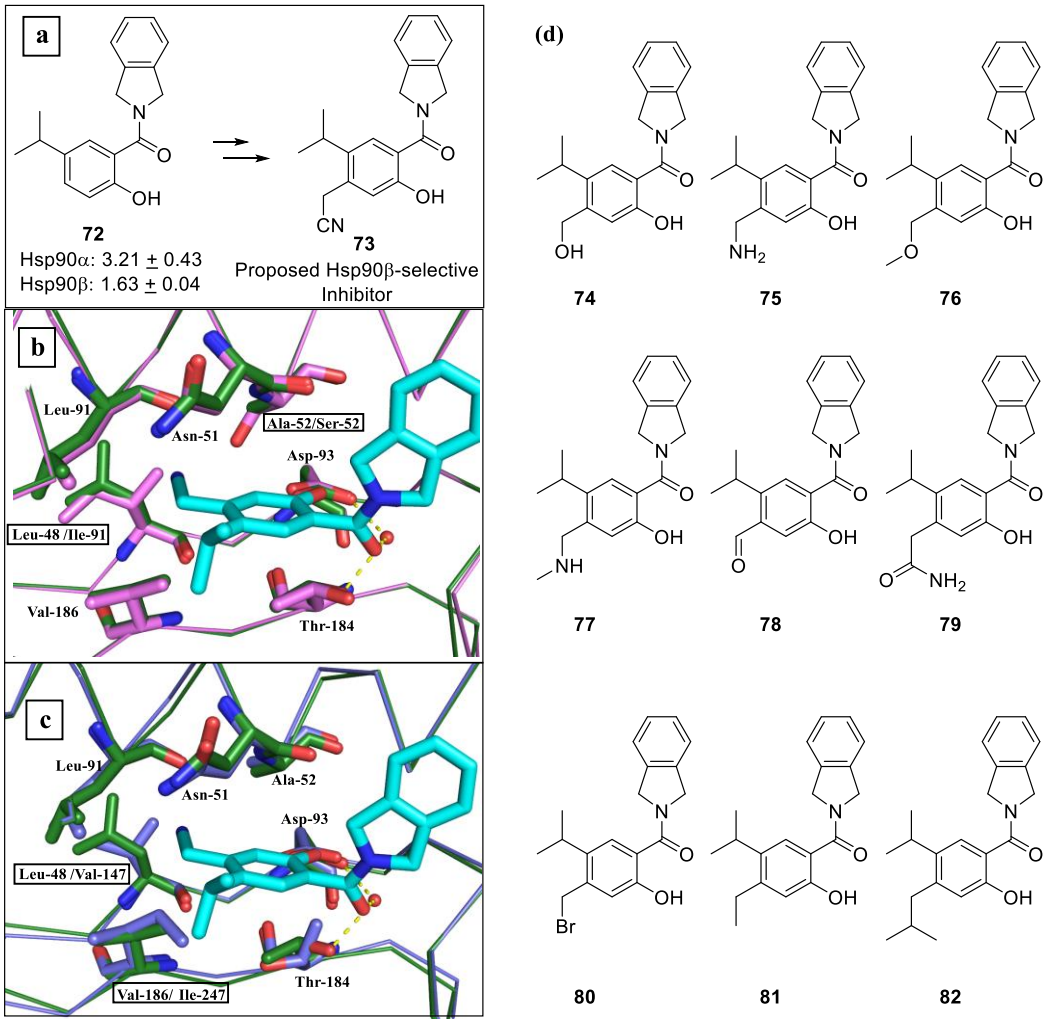

Figure 36. Proposed Hsp90β-selective molecules. (a) a new scaffold for Hsp90β-selective inhibition; Overlay of **73** docked into Hsp90β (PDB code 1UYM, colored green) with N-terminal ATP binding site of (b) Hsp90α (PDB code: 2XAB) and with (c) Grp94 (PDB code: 4NH9 colored blue) (d) Proposed modification at the 4-position **72**.

inhibitors. Since modification at the 4-position were sought, initial investigation began with compound **72** (Figure 36a), which lacks the 4-phenol. Hsp90β inhibitory activity of compound **72** was confirmed via a fluorescence polarization assay and manifested an apparent K_d of 1.63 μM against Hsp90β. The 2-phenol and the amide moiety of compound **72** mimic the corresponding 2-

phenol and lactone present in radicicol. The 5-isopropyl produces hydrophobic interactions with Phe138 and Val186.

Molecular modeling studies suggested that the incorporation of bulky substituents at the 4-position would impart greater selectivity for Hsp90β. Therefore, **73–82** were proposed to investigate the differences between Hsp90β and other Hsp90 isoforms. As shown in Figure 36b & 36c, 4-cyanomethylene (**73**) was proposed to accommodate within the ATP-binding pocket of Hsp90β. The cyanomethyl would not be tolerated in the case of Hsp90α and Grp94, due to unfavorable steric interactions with Ile91 in Hsp90α (Figure 36b), and Val187 in Grp94 (Figure 36c). In addition, the nitrile appears to displace a conserved water molecule in Hsp90, which would increase the entropy of binding and thereby enhance affinity. The conserved water molecules are located in a semi-hydrophobic environment comprising of Leu48, Leu91, Ala52 and Val186.

IV.3.2. Synthesis of 4-Modified Resorcinol Analogues

IV.3.2.1. Synthesis of Compound 72

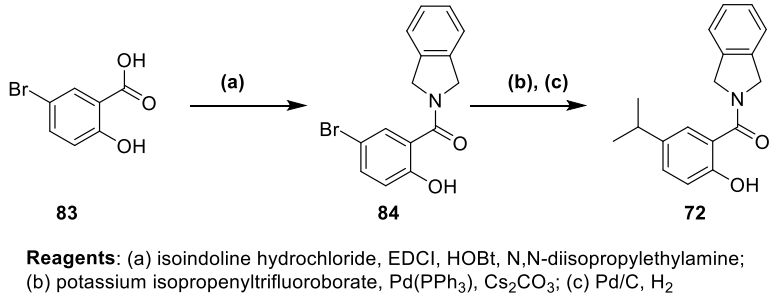

Reagents: (a) isoindoline hydrochloride, EDCI, HOBt, N,N-diisopropylethylamine; (b) potassium isopropenyltrifluoroborate, $Pd(PPh_3)$, Cs_2CO_3; (c) Pd/C, H_2

Scheme 10. Synthesis of compound 72.

Compound **72** was synthesized starting from commercially available 5-bromo salicylic acid, **83**.[68, 69] Carbodiimide coupling of the acid with isoindoline produced intermediate **84** (Scheme 10). The isopropyl group at the 5-position was introduced via a Suzuki coupling reaction of **84** with potassium isopropenyl trifluoroborate and subsequent reduction of the olefin afforded **72**.

IV.3.2.2 Syntheses of 73–82

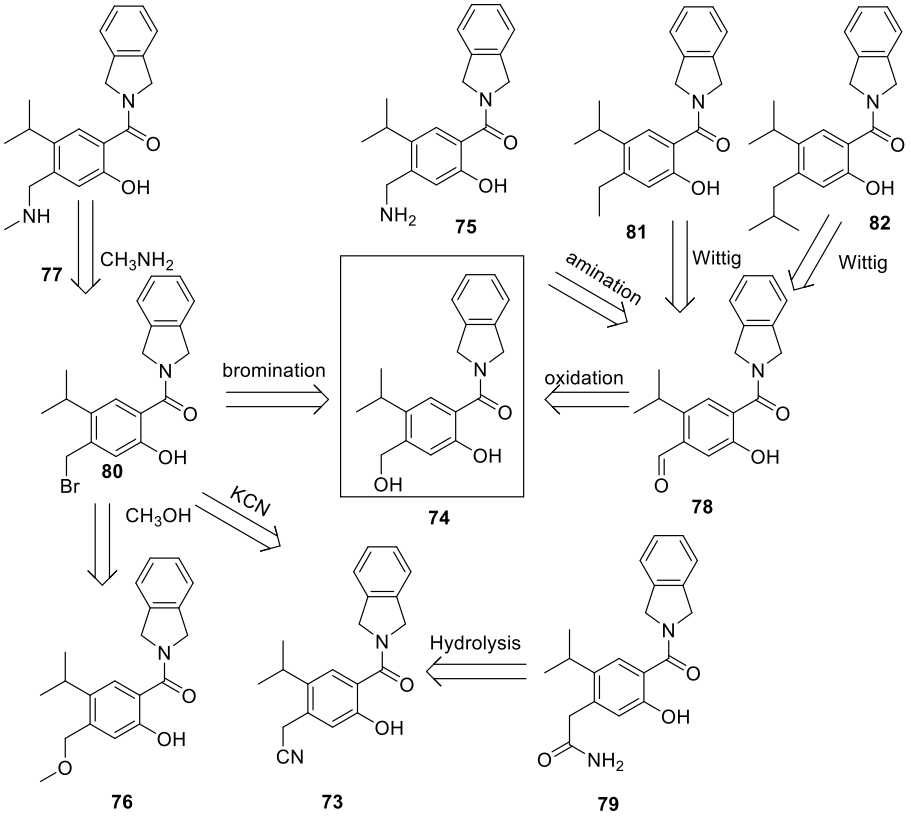

Scheme 11. Proposed retro-syntheses of resorcinol analogues modified at the 4-position.

For the synthesis of compounds **73–82**, a revised synthetic scheme allowed for late stage diversification to access the desired analogues (Scheme 11). Compound **74** was envisioned as a common intermediate to **73**, and **75–82**. As Shown in Scheme 11, bromination of **74** would yield the corresponding benzylic bromide (**80**), which would undergo nucleophilic displacement with the requisite nucleophiles to give **73**, **77**, and **76**. Hydrolysis of the nitrile present in **73** would give access to the corresponding amide, **79**. Oxidation of the benzylic alcohol (**74**), would generate the corresponding aldehyde (**78**), which could be modified to afford analogues **81** and **82** via Wittig olefination and reduction. In addition, reductive amination of **78** would afford **75.**

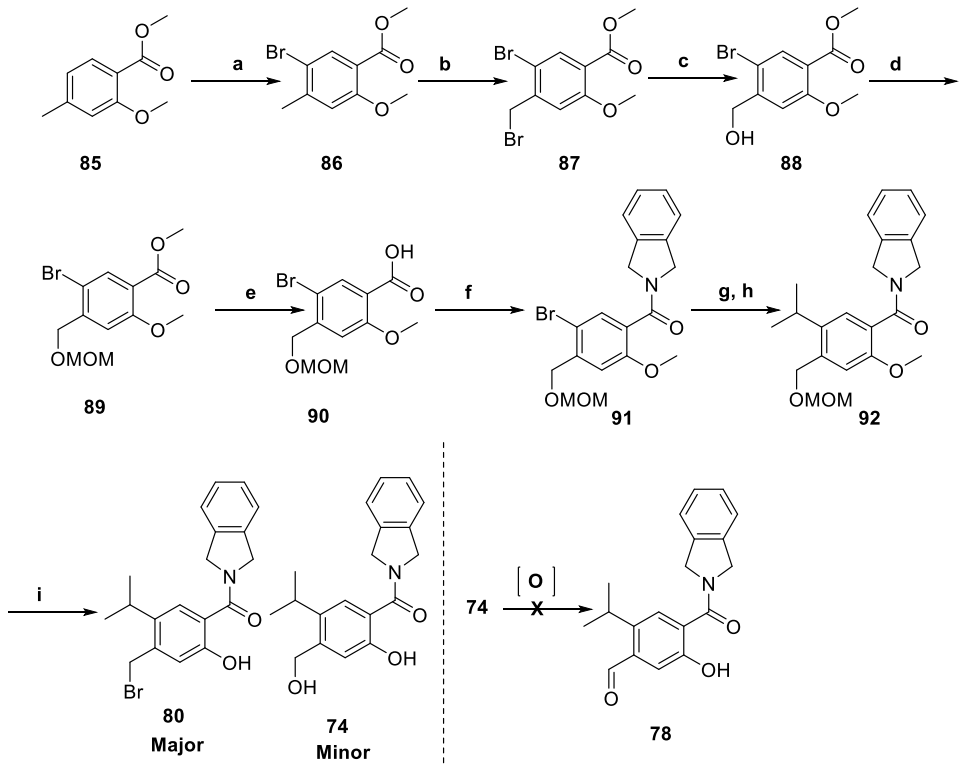

Reagents: (a) Br_2 ; (b) NBS, AIBN; (c) $CaCO_3$; (d) MOMCl, N,N-diisopropylethylamine; (e) LiOH; (f) isoindoline hydrochloride, EDCI, HOBt, N,N-diisopropylethylamine; (g) potassium isopropenyltrifluoroborate, $Pd(PPh_3)_4$, Cs_2CO_3; (h) Pd/C,H_2; (i) BBr_3.

Scheme 12. Syntheses of resorcinol analogues modified at the 4-position.

Synthesis of **74** commenced with bromination of methyl 2-methoxy-4-methylbenzoate (**85**, Scheme 12), which occurred in a regioselective manner to give the corresponding 5-bromo product, **86**. Benzylic bromination of **86** with N-bromosuccinimide and azaisobutyronitrile afforded **87**. Subsequent hydrolysis of the benzyl bromide (**87**) using calcium carbonate gave the corresponding benzylic alcohol, **88**.[70] **88** was converted to methoxy methyl ether (**89**) using methoxymethyl chloride, and *N*,*N*-diisopropylethylamine. Ester **89** was hydrolyzed under basic conditions to provide the corresponding acid, **90**, which upon 1-ethyl-3-(3-dimethylaminopropyl) carbodiimide (EDCI)-mediated coupling with isoindoline gave **91**. isopropyl group at the 5-

position was introduced as described previously. Demethylation of **92** enlisting boron tribromide gave the bromomethyl containing compound **80**, as the major product, the corresponding benzylic alcohol, **74**, was also isolated as a minor product during this transformation. Nucleophilic displacement of the benzylic bromide in **80** with methyl amine and methanol gave **76** and **77**, respectively (Scheme 13). Similarly, **80** was further modified via potassium cyanide and 18-crown-6 to furnish **73**, which upon basic hydrolysis gave the amide, **79**.

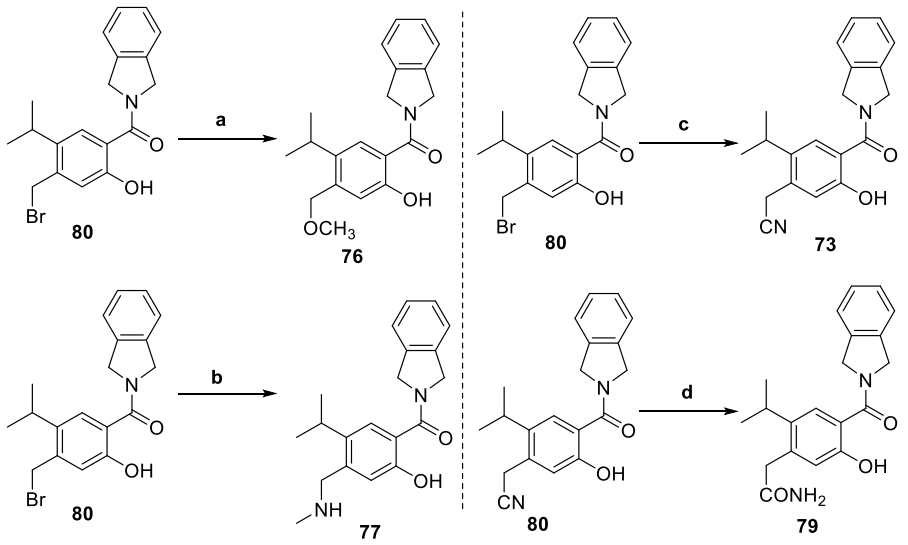

(a) CH_3OH; (b) CH_3NH_2 in THF; (c) KCN, 18-crown-6; (d) H_2O_2,

Scheme 13. Modification of benzyl bromide analogue **80**.

Oxidation of the benzylic alcohol (**74**) to the corresponding benzaldehyde did not work (using Dess-Martin periodinane, tetrapropylammonium perruthenate, manganese dioxide), because the benzylic positions of the isoindoline were also readily oxidized (Scheme 12). Therefore, an alternative route was devised, and oxidation of the benzylic alcohol was accomplished before introduction of the isoindoline (Scheme 14). Intermediate **88** was coupled with potassium isopropyl trifluoroborate as previously described, to give **93**. Compound **93** was

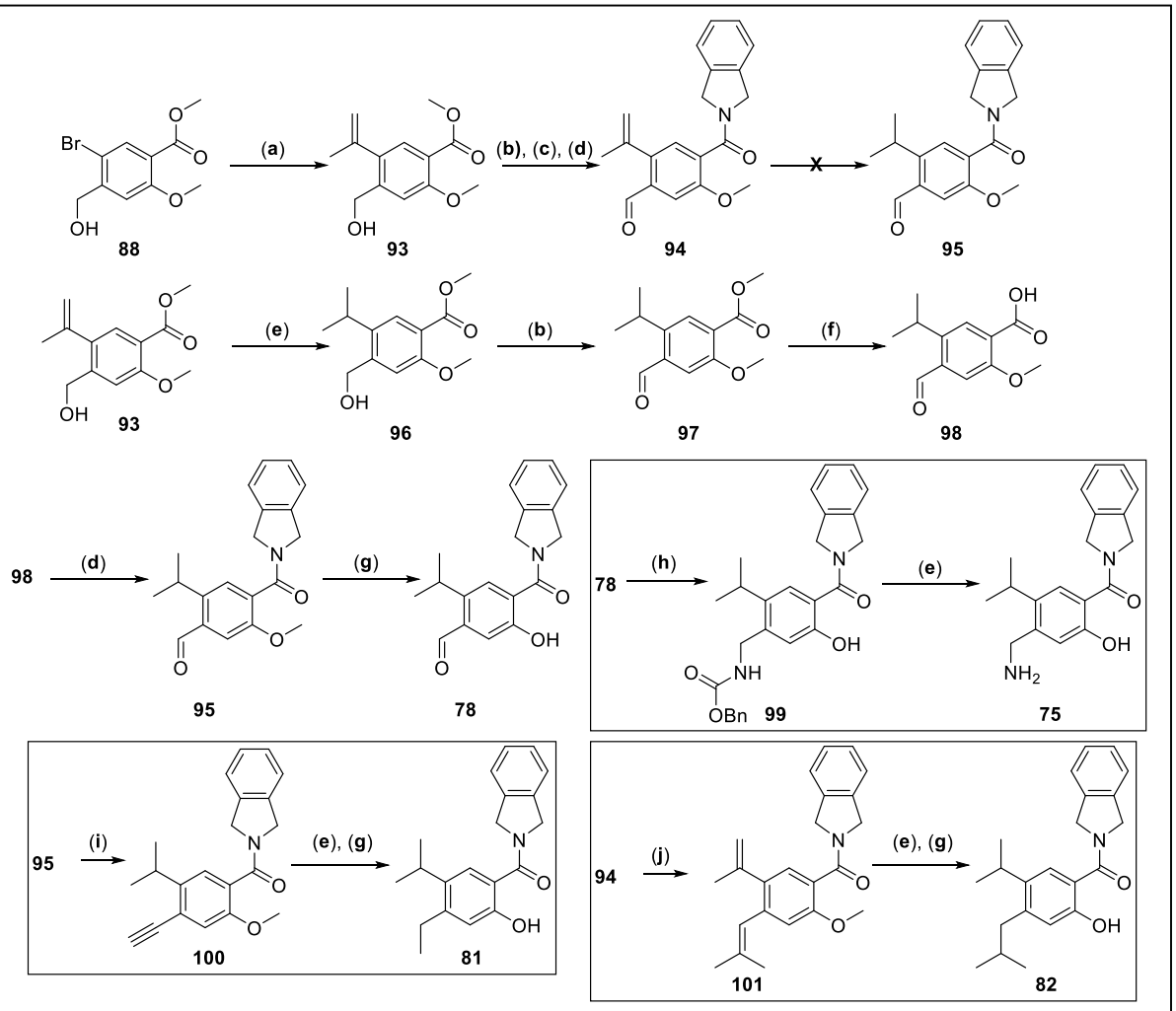

Reagents: (a) potassium isopropenyltrifluoroborate, $Pd(PPh_3)$, Cs_2CO_3; (b) MnO_2; (c) LiOH;(d) isoindoline hydrochloride, EDCI, HOBt, N,N-diisopropylethylamine; (e) Pd/C, H_2; (f) Me_3SnOH;(g) BBr_3; (h) benzyl carbamate,TFA,Et_3SiH; (i) Bestmann reagent, K_2CO_3 (j) isopropyltriphenyl phosphonium iodide, BuLi;

Scheme 14. Synthesis of compound **78** and its derivatives.

oxidized using manganese dioxide (MnO_2) to give the corresponding aldehyde, which upon hydrolysis of ester followed by carbodiimide coupling with isoindoline afforded **94**. Hydrolysis of ester **93** and subsequent coupling with isoindoline furnished aldehyde, **94**. However, chemoselective reduction of the alkene using diphenyl sulfide did not provide the desired product. Therefore, reduction of the alkene prior to oxidation of the alcohol was sought out. The desired intermediate **97** was obtained in three steps from alcohol **88**. The isopropyl group was incorporated

as previously described to give benzyl alcohol, **96**, which underwent oxidation via manganese dioxide to give aldehyde **97**.

Hydrolysis of the ester present in **97** did not proceed under basic conditions. Analysis of the side products revealed the likely generation of a carbanion that results from deprotonation of the benzylic hydrogen at the 5-position. Consequently, a milder condition was used to hydrolyze the ester of **97**. Prior studies by Nicolaou and co-workers have demonstrated that trimethyl tinhydride can hydrolyze aromatic esters in the presence of other base sensitive moieties.[71] Therefore, the methyl ester **97** was subjected to these conditions, which provided the corresponding acid, **98**, in good yield. Carbodiimide coupling of the acid gave **95**, which upon cleavage of the methyl ether using boron tribromide furnished the desired analogue, **78**. Aldehyde **95** served as a common intermediate for the syntheses of the analogues **75**, **81**, and **82** (Scheme 14). Treatment of **95** with benzyl carbamate, trifluoroacetic acid, and triethylsilane gave the corresponding carbamate, which upon hydrogenolysis under a hydrogen atmosphere and in the presence of palladium on carbon, afforded the desired benzyl amine. For the preparation of **81**, the aldehyde (**95**) was converted to the corresponding alkyne via utilization of the Bestmann-Ohira reagent. Hydrogenation of the alkyne followed by methyl ether cleavage furnished the 4-ethyl analogue, **81**. Similarly, the *iso*-butyl analogue was synthesized from aldehyde **94** by a Wittig reaction enlisting isopropyl triphenylphosphonium iodide and butyl lithium, followed by reduction of the corresponding alkene.

IV.3.3. Evaluation of 4-Modified Resorcinol Analogues

The synthesized analogues were evaluated via a fluorescence polarization assay. Analogue **73** exhibited an apparent K_d of 2.27 μM and 0.97 μM against Hsp90α and Hsp90β, respectively (Table 13). The selectivity and potency of benzaldehyde, **78**, was better than the corresponding

benzyl alcohol **74** and benzyl amine **75**. The benzaldehyde analogue a manifested an apparent K_d of 240 nM for Hsp90β and 5-fold selectivity versus Hsp90α. This data suggests that aldehyde may act as a hydrogen bond accepter. The methoxy methyl ether **76** did not bind Hsp90β. Interestingly, benzyl bromide **80** manifested increased affinity and selectivity for the Hsp90β. Its bioisosteric replacement by an isopropyl group (**82**) decreased affinity. Overall, some analogues did maintain or improve affinity for Hsp90β compared to compound **72**. The lack of selectivity of **72** versus Hsp90α was surprising. Collectively, these results suggested the potential of alternative binding modes for these analogues. To better understand the binding interactions of **73** and **78** with Hsp90β; co-crystal structures of these compounds bound to Hsp90β were solved in collaboration with Dr. Robert Matts at Oklahoma State University. Examination of the co-crystal structures revealed some rationale for the poor selectivity manifested by these molecules.

Table 13. The Evaluation of 4-resorcinol analogues

Compound	**K_d Hsp90α** (μM)	**K_d Hsp90β** (μM)	**Fold-selectivity for Hsp90β**
72	3.21 ± 0.43	1.63 ± 0.04	2
73	2.28 ± 0.12	0.97 ± 0.03	3
74	4.21 ± 0.62	1.97 ± 0.07	-
75	>50	>50	-
76	>50	>50	-
77	>100	23.19 ± 1.07	4
78	0.24 ± 0.08	1.21 ± 0.12	-
79	15.21 ± 1.15	5.50 ± 0.51	3
80	4.98 ± 0.97	0.73 ± 0.11	7
81	>50	>50	-
82	>50	>50	-

As shown in Figure 37a, the cyanomethylene (**73**) side chain adopts a backward conformation instead of the expected forward orientation, which is attributed to the free rotation of the methylene group within the binding pocket. This binding mode could not be predicted in the original molecular modeling studies, as it would have caused a steric clash with the Asn46

residue. The co-crystal structure revealed that the side chain of Asn46 shifts 0.6 Å to accommodate the cyanomethylene group (Figure 37c and 37d) to produce a hydrogen bond. The carbonyl of **78** also binds in a similar conformation and interacts favorably with Asn46. The 2-phenol of both compounds maintained interactions with Asp88 and Thr179. Only two other co-crystal structures of Hsp90β exist (none with the resorcinol core). Therefore, the co-crystal structure of **73** and **79** were highly beneficial and subsequently used for the design of new Hsp90β-selective inhibitors.

IV.4. Development of a 3-Modified Resorcinol Analogue

IV.4.1. Design of a 3-Substituted Resorcinol Analogues for Selective Hsp90β-Inhibition

Unfortunately, modification of the 4-position did not increase selectivity, and therefore, an alternative strategy was devised based on the newly obtained co-crystal structures of **73** and **78** bound to Hsp90β. It was proposed that the introduction of the substituents at the 3-position would allow for exploitation of both the amino acids that differ between Hsp90α (Ser52, Ile91) and Hsp90β (Ala, Leu) and manifest increased selectivity while simultaneously projecting substituents to the small exclusive sub-pocket present in Hsp90β. Molecular modeling studies suggested that the inclusion of a hydroxymethylene group at the 3-position would produce selectivity for Hsp90β. The methylene group would sterically clash with Ser52 in Hsp90α, while the hydoroxyl group would produce a steric clash with Ile91 in Hsp90α. Similarly, the introduction of a hydroxymethylene group would produce unfavorable interactions with Val148 and prohibit Grp94 binding. In addition, the hydroxyl group would likely displace a conserved water molecule in this region, and therefore provide an entropic driving force.

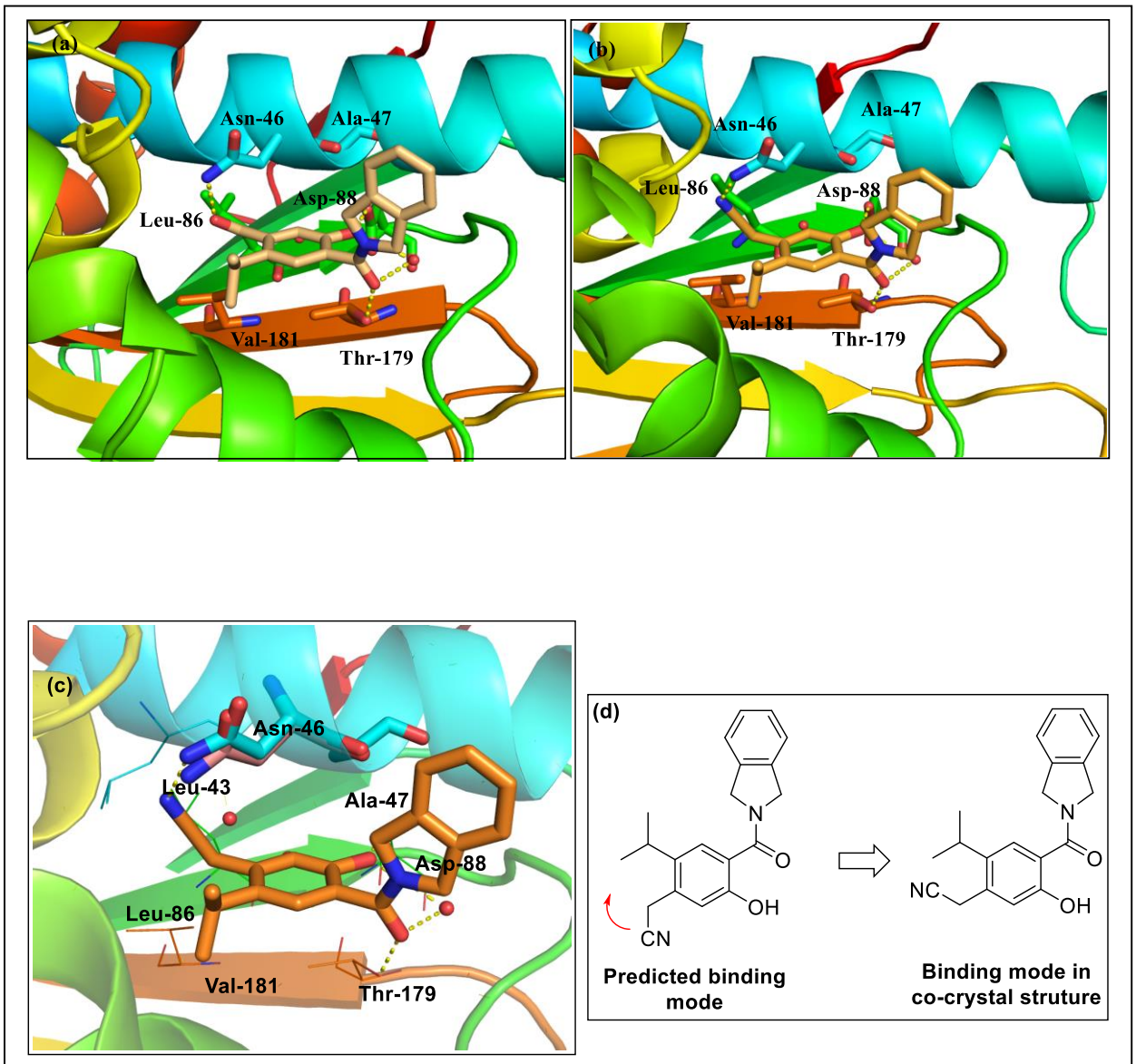

Figure 37. Co-crystallization of 4-modified resorcinol analogues. (a) Co-crystal structure of **73** bound Hsp90β; (b) co-crystal structure of **79** bound Hsp90β; (c) Movement of Asn46 allows for backward bending of nitrile, Previous position of Asn46 is represented in pink. Asn46 in co-crystal structure of **73** is represented in blue. (d) two-dimensional representation of binding modes of **73**.

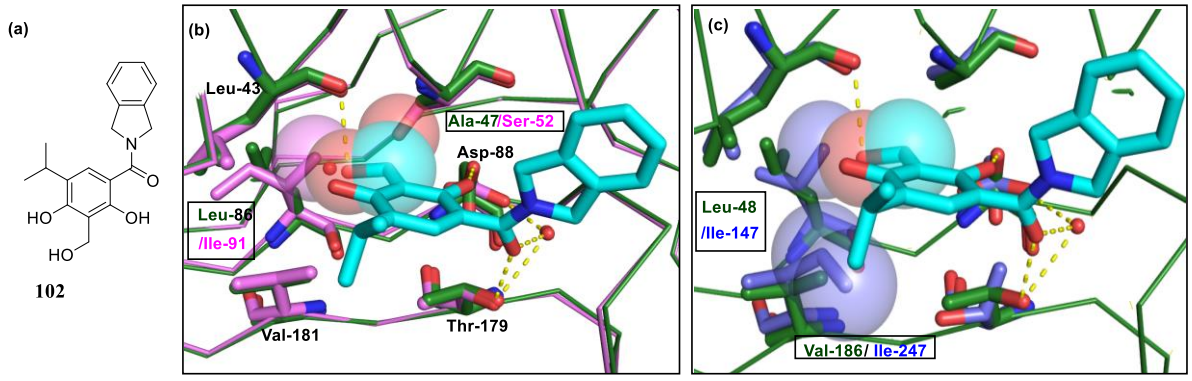

Figure 38. Proposed modification at the 3-position of resorcinol. (a) Structure of 102. Docking pose of compound **102** in Hsp90β (colored green) overlaid with (b) Hsp90α N-terminal ATP- binding site (colored pink) and with (c) Grp94 N-terminal ATP binding site. The highlighted water molecule is conserved in all 4 isoforms and 102 was predicted to displace it.

IV.4.2. Synthesis of a 3-Substituted Resorcinol Analogue

Synthesis of the proposed analogue **102** commenced via **103**, which was prepared following a literature procedure. Formylation of **103** via the Duff reaction gave the 3-formyl resorcinol intermediate, **104** (Scheme 15). Reduction of aldehyde **104** with sodium borohydride furnished the desired product **102**.

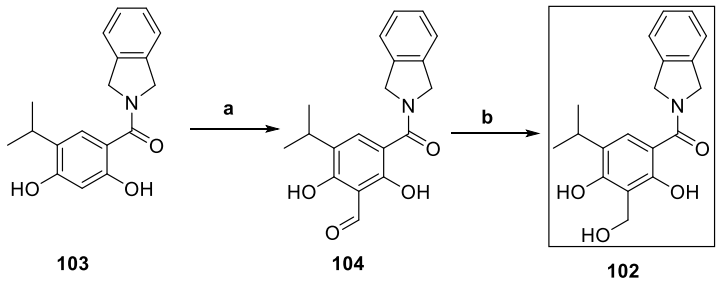

Scheme 15. Synthesis of **102**.

IV.4.3. Evaluation and Co-Crystallization of 102

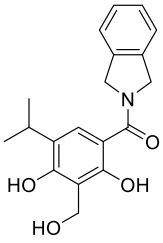

102

Hsp90α: > 100 μM
Hsp90β: = 4.27 ± 0.19 μM
Grp94: > 100 μM
>24-fold selectivity for Hsp90β

Figure 39. Apparent K_d of analogue **102** (**KUNB30**).

Upon preparation of analogue **102**, it was evaluated via a fluorescence polarization and found to manifest an apparent K_d of 4.27 μM for Hsp90β. More importantly, it manifested selectivity (>24-fold) over other isoforms (Figure 39). The co-crystal structure of the compound **102** (**KUNB30**) bound to Hsp90β was then solved in collaboration with Dr. Robert Matts, which suggested that the benzyl alcohol has displaced a conserved water molecule. The benzylic alcohol made hydrogen bonding interactions with the backbone of Leu43.

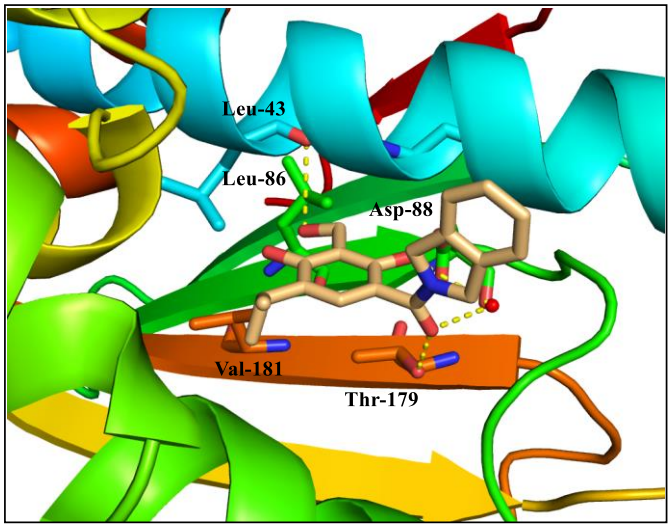

Figure 40. Co-crystal structure of **KUNB30** bound to Hsp90β.

IV.5. Development of KUNB31

IV.5.1 Design of KUNB31

Flexibility associated with the hydroxymethylene group in **KUNB30** exhibits a significant entropic penalty upon binding. Therefore, it was proposed that the introduction of a ring constrained variant would reduce the entropic penalty and enhanced binding affinity. Using the co-crystal structure of **KUNB30**, it was envisioned that introduction of a heterocyclic ring system that joined the 3- and 4-positions of the resorcinol ring would illicit such properties. Therefore, benzoisoxazole **105** was designed and sought after for biological evaluation.

IV.5.2. Synthesis and Evaluation of KUNB31

Analogue **105** was synthesized from **104** enlisting triflic acid and sodium azide (Scheme 16).[72] The two regeoisomeric isooxazole products were separated by column chromatography, and the structure of **105** was confirmed by X-ray crystallography. Analogue **105** (**KUNB31**) manifested an apparent K_d of 180 nM against Hsp90β, and exhibited ~50-fold selectivity versus Hsp90α and Grp94.

IV.6. Cellular Studies

IV.6.1. Anti-Proliferation Activity

Once the Hsp90β-selective inhibitors, **KUNB30** and **KUNB31**, were identified, cellular studies commenced to evaluate the effect of Hsp90β-inhibition on cancer cell lines (Table 14). Growth inhibitory activity manifested by these compounds was evaluated against NCI-H23 (lung cancer), MCF-7 (breast cancer), and SkBr3(breast cancer) cells. **KUNB31** manifested an IC_{50}'s of

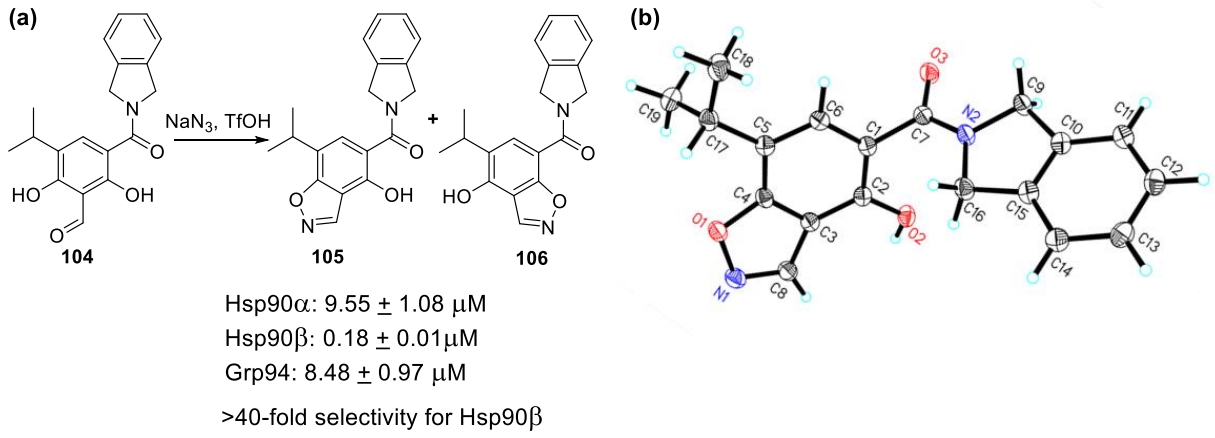

Scheme 16. (a) Synthesis, evaluation; and (b) X-ray crystal structure of **KUNB31**.

6.74 ± 1.10μM, 28.27 ± 1.47μM and 38.21 ± 2.75 μM against NCI H23, MCF-7, and Skbr3 cells, respectively. **KUNB30** was more efficacious in cells and manifested an IC_{50} of 3.90 ± 0.33, 13.67 ± 1.46, 9.13 ± 1.03 against NCI H23, MCF-7, and Skbr3 cells, respectively. These studies

confirmed that selective inhibition of the Hsp90β isoform manifests growth inhibitory activity against cancer cells.

Table 14. Anti-proliferative activity of **KUNB30** and **KUNB31** against cancer cells

Cancer Cell Line	**KUNB30** (μM)	**KUNB31** (μM)
NCI-H23	3.90 ± 0.33	6.74 ± 1.10
MCF-7	13.67 ± 1.46	28.27 ± 1.47
SkBr3	9.13 ± 1.03	38.21 ± 2.75

IV.6.2. Western Blot Analyses

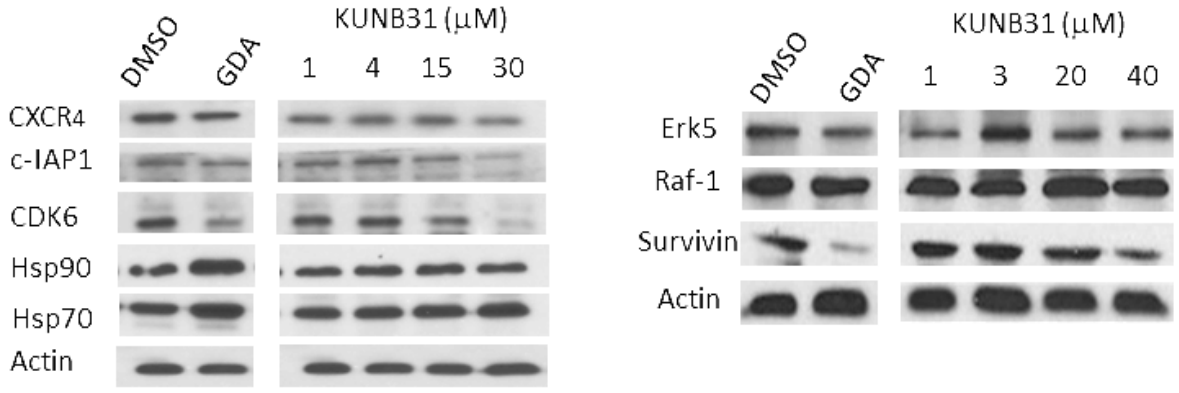

Figure 41. Western blot analyses of **KUNB31** in NCI-H23 cell line.

After determination of anti-proliferation activity, western blot analyses were conducted on NCI-H23 cell lysates that were treated with **KUNB31**. Since, Hsp90 inhibition induces the degradation of client proteins via ubiquitin-proteasome pathway, levels of Hsp90-dependent clients were evaluated upon administration of **KUNB31** in NCI-H23 cells. Additionally, immunoblots for Hsp90 and Hsp70 were also obtained to evaluate the induction of the heat-shock response. As shown in Figure 41, **KUNB31** induced the degradation of Hsp90β–dependent clients c-IAP1, $CXCR_4$, and CDK6 without the induction of Hsp70 and Hsp90 levels. Similar to genetic knockdown studies, Hsp90α-dependent clients Raf and survivin were less sensitive to Hsp90β-

inhibition. Degradation of non-selective client Erk5 was also observed. These results suggest that Hsp90β inhibition limits the detrimental induction of the heat shock response, and hence, represents an alternative approach to *pan*-Hsp90 inhibition.

IV.7. Conclusions and Future Directions

Using a structure-based design, the first small molecule N-terminal inhibitors of the Hsp90β isoform have been developed. These inhibitors manifest anti-proliferation activity against cancer cell lines, and induce the degradation of Hsp90 client proteins. Hence, Hsp90β inhibitors represent a new class of Hsp90 inhibitors for the treatment of cancer. In addition, Hsp90β-selective inhibitors will serve as useful probes to identify of Hsp90β-dependent clients and enable the identification of specific roles played by individual isoforms.

Induction of the pro-survival heat shock response has limited the clinical success of current *pan*-Hsp90 inhibitors. Induction of heat shock response results in higher levels of Hsp90, which leads to decreased occupancy of the target by such inhibitors. Consequently, the induction of heat shock response results in poor efficacy by Hsp90 inhibitors and leads to dosing and scheduling complications. In our preliminary studies, Hsp90β-inhibitors did not exhibit these detrimental activities, which suggests that selective Hsp90β inhibition is a useful alternative to *pan*-Hsp90 inhibition.

Prior to this work, there were only two other co-crystal structure of Hsp90β bound to an inhibitor reported. This work produced co-crystal structures of three inhibitors bound to Hsp90β, which can be used to design future isoform-selective inhibitors. The Co-crystal structure of **KUNB30** bound to Hsp90β represents the first co-crystal structure of a resorcinol based inhibitor bound to Hsp90β. Co-crystallization of **KUNB31** is underway in collaboration with the Robert Matts Laboratory, at Oklahoma State University.

IV.8. Methods and Experiments

All reactions were performed in oven-dried glassware under argon atmosphere unless otherwise stated. Dichloromethane (DCM), tetrahydrofuran (THF), and toluene were passed through a column of activated alumina prior to use. Anhydrous methanol, acetonitrile, *N*,*N*-dimethylformamide (DMF), and carbon tetrachloride (CCl_4) were purchased and used without further purification. Flash column chromatography was performed using silica gel (40−63 μm particle size). The ^{1}H (500 and 400 MHz) and ^{13}C NMR (125 and 100 MHz) spectra were recorded on 500 and 400 MHz spectrometer. Data are reported as p = pentet, q = quartet, t = triplet, d = doublet, s = singlet, br s = broad singlet, m = multiplet; coupling constant(s) in Hz. Infrared spectra were obtained using FT/IR spectrometer. High resolution mass spectral data were obtained on a time-of-flight mass spectrometer and analysis was performed using electrospray ionization.

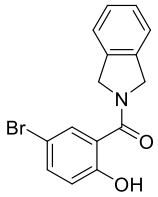

(5-Bromo-2-hydroxyphenyl)(isoindolin-2-yl)methanone (84): 1-Ethyl-3-(3-dimethylaminopropyl)carbodiimide (5.20 g, 27.64 mmol, 2.0 eq.) was added to a stirred solution of **83** (3.0 g, 13.82 mmol, 1 eq.), isoindoline hydrochloride (3.22 g, 20.73 mmol, 1.5 eq.), 1-hydroxybenzotriazole (3.73 g, 27.64 mmol, 2 eq.) *N*,*N*-diisopropylethylamine (4.81 mL, 27.64 mmol, 2.0 eq.) in dichloromethane (150 mL) at 0 °C. The resulting solution was stirred at rt for 14 h before quenching with saturated sodium bicarbonate solution (120 mL). The organic layer was washed with 1 M hydrochloric acid solution (120 mL) and saturated sodium chloride solution (120 mL), dried over sodium sulfate, filtered, and concentrated. The residue was purified by flash chromatography (SiO_2, 1:4 hexanes/ethyl acetate) to afford **84** (3.24 g,77.9 %) as a white

amorphous solid. ^{1}H NMR (400 MHz, $CDCl_3$) δ 10.92 (s, 1H), 7.73 (d, *J* = 2.2 Hz, 1H), 7.48 (dd, *J* = 8.8, 2.4 Hz, 1H), 7.34 (s, 4H), 6.94 (d, *J* = 8.8 Hz, 1H), 5.10 (s, 4H). ^{13}C NMR (100MHz, $CDCl_3$) δ 169.4, 159.4, 136.1 (2), 134.8, 130.5, 128.2 (2), 122.8 (2), 120.2, 118.7 110.2, 55.8, 53.3. HRMS (ESI+) *m/z* [M + H^+] calcd for $C_{15}H_{13}BrNO_2$, 318.0130, found 318.0119.

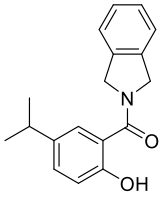

(2-Hydroxy-5-isopropylphenyl)(isoindolin-2-yl)methanone (72): A biotage microwave vial was charged with **84** (1.0 g, 3.42 mmol, 1 eq.), triethylamine (0.62 mL, 4.44 mmol, 1.3 eq.), [1,1′ Bis(diphenylphosphino)ferrocene]dichloropalladium(II) (278 mg, 0.34 mmol, 0.1 eq.), potassium isopropenyltrifluoroborate (604 mg, 4.10 mmol, 1.2 eq.). The tube was sealed with a cap lined with a disposable Teflon septum. The tube was evacuated and purged with nitrogen (3 times), before the addition of 2-propanol (17 mL) by syringe. The resulting mixture was heated at 100 °C for 6 h, cooled to rt, and filtered through a small pad of celite (elution with ethyl acetate). Solvent was removed and the residue purified by flash chromatography (SiO_2, 1:4 ethyl acetate/hexanes) to afford (2-hydroxy-5-(prop-1-en-2-yl)phenyl)(isoindolin-2-yl)methanone, which was used further as obtained. Palladium on carbon (10%) was added to a solution of (2-hydroxy-5-(prop-1-en-2-yl)phenyl)(isoindolin-2-yl)methanone in ethyl acetate (25 mL). The suspension was stirred for 16 h under a hydrogen atmosphere before it was filtered through a pad of celite and eluted with EtOAc (20 mL). The eluent was concentrated to afford **72** (652 mg, 67.5 %) as a white amorphous solid. ^{1}H NMR (400 MHz, $CDCl_3$) δ 10.44 (s, 1H), 7.40 (d, *J* = 2.2 Hz, 1H), 7.28 (s, 4H), 6.92 (d, *J* = 8.5 Hz, 1H), 5.06 (s, 4H), 2.88 (hept, *J* = 7.0 Hz, 1H), 1.24 (d, *J* = 6.9 Hz, 6H). ^{13}C NMR (100 MHz, $CDCl_3$) δ 171.4, 157.9, 138.8, 136.1 (2), 131.5, 128.0 (2), 125.7, 122.8 (2), 118.0, 117.1,

55.8, 53.5, 33.6, 24.4 (2). HRMS (ESI+) *m/z* [M + H^+] calcd for $C_{18}H_{20}NO_2$, 282.1494, found 282.1483.

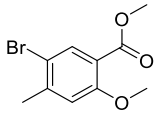

Methyl 5-bromo-2-methoxy-4-methylbenzoate (86): A solution of bromine in chloroform was added dropwise to a solution of **85** (10.0 g, 55.4 mmol, 1.0 eq.) in chloroform at 0 °C (250 mL). The resulting mixture was stirred at rt for 4 h before quenching with 10% aqueous solution of sodium thiosulfate (200 mL). The organic layer was washed with saturated sodium bicarbonate solution (2 × 200 mL) and saturated sodium chloride solution (200 mL), dried over anhydrous sodium sulfate, filtered, and concentrated. The residue was purified by flash chromatography (SiO_2, 1:9 ethyl acetate/hexanes) to afford **86** (12.81 g, 89.2 %) as a light brown amorphous solid. ^{1}H NMR (400 MHz, $CDCl_3$) δ 7.93 (dt, *J* = 7.1, 4.0 Hz, 1H), 6.82 (t, *J* = 4.0 Hz, 1H), 3.97 – 3.76 (m, 6H), 2.38 (dt, *J* = 6.5, 4.0 Hz, 3H). ^{13}C NMR (125 MHz, $CDCl_3$) δ 165.2, 158.5, 144.0, 135.2, 118.9, 114.8, 114.6, 56.3, 52.2, 23.7. HRMS (ESI+) *m/z* [M + H^+] calcd for $C_{10}H_{12}BrO_3$, 258.9969, found 258.9973.

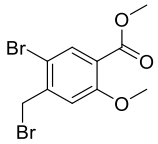

Methyl 5-bromo-4-(bromomethyl)-2-methoxybenzoate (87): A solution of **86** (12.8g, 48.8 mmol), N-bromosuccinimide (9.68 g, 54.78 mmol, 1.1 eq.), azobisisobutyronitrile (1.64 g, 9.96 mmol, 0.2 eq.) in carbon tetrachloride was heated at 70 °C. After 14 h, solvent was removed and the residue purified by flash chromatography (SiO_2, 1:9 ethyl acetate/hexanes) to afford **87** (13.92 g, 71.3 %) as a white amorphous solid. ^{1}H NMR (500 MHz, $CDCl_3$) δ 7.91 (s, 1H), 7.60 (s, 1H), 7.00 (s, 1H), 3.99 (s, 3H), 3.90 (s, 3H). ^{13}C NMR (125 MHz, $CDCl_3$) δ 164.7, 159.0, 144.8, 135.5,

123.0, 114.6, 109.5, 56.7, 52.7, 39.3. HRMS (ESI+) *m/z* [M + H^+] calcd for $C_{10}H_{11}Br_2O_3$, 336.9075, found 336.9079.

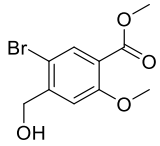

Methyl 5-bromo-4-(hydroxymethyl)-2-methoxybenzoate (88): Calcium carbonate (11.3 g, 113.4 mmol, 3 eq.) was added to a solution of **87** (12.8 g, 37.8 mmol, 1 eq.) in dioxane (100 mL) and water (100 mL). The resulting mixture was heated at 120 °C in a sealed tube for 16 h. The reaction mixture was cooled to rt, filtered, and concentrated. The residue was purified by flash chromatography (SiO_2, 1:5 ethyl acetate/hexanes) to afford **88** (8.2 g, 79.2%) as a colorless amorphous solid. ^{1}H NMR (500 MHz, $CDCl_3$) δ 7.9 (s, 1H), 7.2 (d, *J* = 0.9 Hz, 1H), 4.7 (dd, *J* = 5.7, 1.0 Hz, 2H), 3.9 (s, 3H), 3.9 (s, 3H). ^{13}C NMR (125 MHz, $CDCl_3$) δ 165.5, 159.0, 145.7, 135.3, 120.0, 111.9, 111.3, 64.8, 56.5, 52.5. HRMS (ESI+) *m/z* [M + H^+] calcd for $C_{10}H_{12}BrO_4$, 274.9919, found 274.9923.

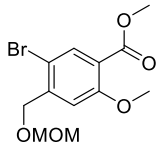

Methyl 5-bromo-2-methoxy-4-((methoxymethoxy)methyl)benzoate (89): A solution of **88** (3.2 g, 11.63 mmol, 1.0 eq.) in dichloromethane (116 mL) was cooled to 0 °C before the addition of *N*,*N*-diisopropylethylamine (12.13 mL, 69.79 mmol, 6.0 eq.) and 6M solution of chloromethoxymethyl ether (11.8 ml, 69.79 mmol, 6.0 eq.). The reaction was allowed to reach at rt and stirred for 14 h before quenching with saturated sodium bicarbonate solution (60 mL). The aqueous layer was extracted with dichloromethane (2 × 60 mL) and the combined organic layers were washed with saturated sodium chloride solution (150 ml), dried over anhydrous sodium sulfate, filtered, and concentrated. The residue was purified by flash chromatography (SiO_2, 1:49

acetone/dichloromethane) to afford **89** (2.82 g, 76.1%) as a colorless oil. ^{1}H NMR (400 MHz, $CDCl_3$) δ 7.97 (s, 1H), 7.18 (d, *J* = 0.9 Hz, 1H), 4.80 (s, 2H), 4.64 (d, *J* = 0.9 Hz, 2H), 3.93 (s, 3H), 3.89 (s, 3H), 3.44 (s, 3H). ^{13}C NMR (100 MHz, $CDCl_3$) δ 165.4, 158.9, 143.4, 135.4, 120.3, 112.4, 111.8, 96.6, 68.9, 56.6, 55.9, 52.4. HRMS (ESI+) *m/z* [M + H^+] calcd for $C_{12}H_{16}BrO_5$, 319.0181, found 319.0187.

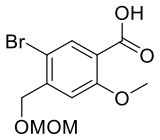

5-Bromo-2-methoxy-4-((methoxymethoxy)methyl)benzoic acid (90): Lithium hydroxide monohydrate (5.37 g, 128.0 mmol, 10.0 eq.) was added to a solution of **89** (4.08 g, 12.8 mmol, 1 eq.) in a solvent mixture of tetrahydrofuran (43 mL), water (43 mL), methanol (43 mL). The resulting mixture was stirred at rt for 16 h and concentrated. The residue was treated with 1 M hydrochloric acid and pH was adjusted to 2. The resulting suspension was extracted with ethyl acetate (3 × 100 mL), the combined organic layers were washed with saturated sodium chloride solution, dried over anhydrous sodium sulfate, filtered and concentrated to afford **90** (3.26 g, 83.2 %) as a light brown solid. ^{1}H NMR (500 MHz, $CDCl_3$) δ 10.59 (s, 1H), 8.33 (s, 1H), 7.30 (s, 1H), 4.83 (s, 2H), 4.67 (d, *J* = 0.9 Hz, 2H), 4.12 (s, 3H), 3.46 (s, 3H). ^{13}C NMR (125 MHz, $CDCl_3$) δ 164.1, 157.5, 145.5, 137.1, 117.8, 113.9, 111.6, 96.7, 68.7, 57.3, 56.0. HRMS (ESI+) *m/z* [M + H^+] calcd for $C_{11}H_{14}BrO_5$, 305.0025, found 305.0028.

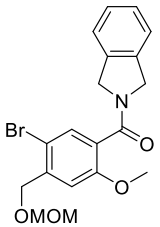

(5-Bromo-2-methoxy-4-((methoxymethoxy)methyl)phenyl)(isoindolin-2-yl)methanone (91): 1-Ethyl-3-(3-dimethylaminopropyl)carbodiimide (1.25g, 6.54 mmol, 2.0 eq.) was added to a

stirred solution of **90** (1.0 g, 3.27 mmol, 1 eq.), isoindoline hydrochloride (663 mg, 4.26 mmol, 1.3 eq.), 1-hydroxybenzotriazole (1.0 g, 6.54 mmol, 2 eq.) N-,N-diisopropylethylamine (1.72 mL, 9.81 mmol, 3.0 eq.) in dichloromethane (33 mL) at 0 °C. The resulting solution was stirred at rt for 14 h before quenching with saturated sodium bicarbonate solution (30 mL). The organic layer was washed with 1 M hydrochloric acid solution (30 mL) and saturated sodium chloride solution (30 mL), dried over sodium sulfate, filtered and concentrated. The residue was purified by flash chromatography (SiO_2, 1:3 hexanes/ethylacetate) to afford **91** (1.22 g, 91.8%) as a colorless oil. ^{1}H NMR (400 MHz, $CDCl_3$) δ 7.50 (s, 1H), 7.37 – 7.26 (m, 3H), 7.19 – 7.12 (m, 2H), 4.99 (s, 2H), 4.82 (s, 2H), 4.68 (s, 2H), 4.62 (s, 2H), 3.88 (s, 3H), 3.48 (s, 3H). HRMS (ESI+) *m/z* [M + H^+] calcd for $C_{11}H_{14}BrO_5$, 452.1072, found 452.1066.

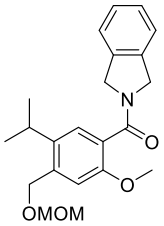

Isoindolin-2-yl(5-isopropyl-2-methoxy-4-((methoxymethoxy)methyl)phenyl)methanone (92): A biotage microwave vial was charged with **91** (1.0 g, 2.46 mmol, 1 eq.), Tetrakis(triphenylphosphine)palladium (0) (277 mg, 0.24 mmol, 0.1 eq.), cesium carbonate (2.4 g, 7.4 mmol, 3 eq.), and potassium isopropenyltrifluoroborate (427 mg, 2.88 mmol, 1.2 eq.). The tube was sealed with a cap lined with a disposable Teflon septum. The tube was evacuated and purged with nitrogen (3 times), before the addition of tetrahydrofuran (10.8 mL) and water (1.2 mL) by syringe. The resulting mixture was heated at 100 °C for 24 h, cooled to rt, and filtered through a small pad of celite (elution with ethyl acetate). Solvent was removed and the residue purified by flash chromatography (SiO_2, 1:3 ethyl acetate/hexanes) to afford isoindolin-2-yl(2-methoxy-4-((methoxymethoxy)methyl)-5-(prop-1-en-2-yl)phenyl)methanone, which was used further as

obtained. Palladium on carbon (10%) was added to a solution of Isoindolin-2-yl(2-methoxy-4-((methoxymethoxy)methyl)-5-(prop-1-en-2-yl)phenyl)methanone in ethyl acetate (25 mL). The suspension was stirred for 16 h under a hydrogen atmosphere before it was filtered through a pad of celite and eluted with EtOAc (20 mL). The eluent was concentrated to afford **92** (530 mg, 58.3 %) as a light brown amorphous solid. ^{1}H NMR (400 MHz, $CDCl_3$) δ 7.76 (d, *J* = 7.6 Hz, 1H), 7.60 (td, *J* = 7.6, 1.1 Hz, 1H), 7.48 (d, *J* = 7.7 Hz, 1H), 7.41 (t, *J* = 7.5 Hz, 1H), 7.21 (s, 1H), 6.94 (s, 1H), 4.94 (s, 2H), 4.67 (s, 2H), 4.63 (s, 2H), 3.70 (s, 3H), 3.37 (s, 3H), 3.05 (h, *J* = 6.8 Hz, 1H), 1.15 (s, 3H). ^{13}C NMR (100 MHz, $CDCl_3$) δ 168.7, 166.3, 155.0, 141.6, 139.0, 138.4, 134.1, 131.6, 128.7, 125.7, 125.4, 125.2, 123.7, 111.2, 96.0, 66.8, 56.1, 55.7, 48.7, 28.4, 24.0 (2). HRMS (ESI+) *m/z* [M + Na^+] calcd for $C_{22}H_{27}NO_4Na$, 392.1838, found 392.1838.

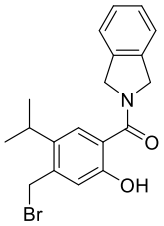

(4-(Bromomethyl)-2-hydroxy-5-isopropylphenyl)(isoindolin-2-yl)methanone (80): 1 M solution of boron tribromide (1.22 mmol, 1.22 mL, 2 eq.), was added to a solution of **92** (200 mg, 0.61 mmol) in anhydrous dichloromethane (6.1 ml) at 0 ^{o}C. The resulting mixture was stirred at rt for 14 h before quenching with saturate sodium bicarbonate solution (5 mL). The aqueous layer was extracted with dichloromethane (2 × 10 mL). The combined organic layers were washed with saturated sodium chloride solution (20 mL), dried over anhydrous sodium sulfate, filtered, and concentrated. The residue was purified by flash chromatography (SiO_2, 1:50 acetone/dichloromethane) to afford **80** (98 mg, 43.7 %) as a white solid. Additionally, compound **74** (38 mg, 20%) was also isolated. ^{1}H NMR (500 MHz, CD_2Cl_2) δ 7.53 (s, 1H), 7.32 (s, 4H), 6.94 (s, 1H), 5.07 (s, 5H), 4.53 (s, 2H), 3.27 (p, *J* = 6.8 Hz, 1H), 1.31 (d, *J* = 6.8 Hz, 5H). ^{13}C NMR

(125 MHz, CD_2Cl2) δ 170.5, 157.3, 139.9 (2), 138.1 (2), 128.1, 126.3, 123.0, 119.4 (2), 119.1 (2), 118.5, 55.9 (2), 31.0, 24.3 (2). HRMS (ESI+) *m/z* [M + Na^+] calcd for $C_{19}H_{20}BrNO_2Na$, 374.756, found 374.0769.

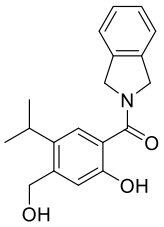

(2-Hydroxy-4-(hydroxymethyl)-5-isopropylphenyl)(isoindolin-2-yl)methanone (74): 1 M solution of boron tribromide (1.22 mmol, 1.22 mL, 2 eq.), was added to a solution of **92** (200 mg, 0.61 mmol) in anhydrous dichloromethane (6.1 ml) at 0 ^oC. The resulting mixture was stirred at rt for 14 h before quenching with saturate sodium bicarbonate solution (5 mL). The aqueous layer was extracted with dichloromethane (2 × 10 mL). The combined organic layers were washed with saturated sodium chloride solution (20 mL), dried over anhydrous sodium sulfate, filtered, and concentrated. The residue was purified by flash chromatography (SiO_2, 1:3 ethyl acetate/hexanes) to afford **74** (38 mg, 20%) as a colorless solid. Additionally, compound **80** (98 mg, 43.7 %) was also isolated as a colorless solid. ^1H NMR (400 MHz, $CDCl_3$) δ 10.53 (s, 1H), 7.53 (s, 1H), 7.32 (s, 4H), 7.07 (s, 1H), 5.10 (s, 4H), 4.76 (s, 2H), 3.17 – 3.22 (m, 1H), 1.26 – 1.30 (m, 6H). ^{13}C NMR (125 MHz, $CDCl_3$) δ 171.0, 158.0, 150.2, 143.1, 136.7, 136.4, 129.9, 129.1, 126.8, 126.6, 125.2, 116.9, 116.6, 62.9, 55.8, 53.4, 30.2, 24.5 (2). HRMS (ESI+) *m/z* [M + H^+] calcd for $C_{19}H_{22}NO_3$, 312.1600, found 312.1604.

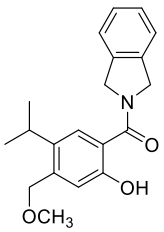

(2-Hydroxy-5-isopropyl-4-(methoxymethyl)phenyl)(isoindolin-2-yl)methanone (76): Sodium methoxide (10.8 mg, 0.20 mmol, 2.5 eq.) was added to a solution of **80** (30 mg, 0.08 mmol, 1 eq.) in anhydrous methanol. The resulting mixture was heated at 60 ^{o}C for 8h, before quenching with 1 M hydrochloric acid (2 mL), extracted with ethyl acetate (3 × 3 mL). The combined organic layers were washed with saturated sodium chloride solution, dried over sodium sulfate, filtered, and concentrated. The residue was purified by flash chromatography (SiO_2, 3:10 ethyl acetate/hexanes) to afford **76** (13 mg, 49.9 %) as a colorless oil. ^{1}H NMR (400 MHz, $CDCl_3$) δ 10.45 (s, 1H), 7.52 (s, 1H), 7.29 (d, *J* = 19.5 Hz, 4H), 7.02 (s, 1H), 5.09 (s, 4H), 4.50 (s, 2H), 3.43 (s, 3H), 3.14 – 3.46 (m, 1H), 1.28 (d, *J* = 6.9 Hz, 7H). ^{13}C NMR (100 MHz, $CDCl_3$) δ 170.8, 157.4, 140.4 (2), 137.0 (2), 127.8, 124.9(2), 122.6, 117.8 (2), 116.6, 72.1, 58.3 (3), 28.0, 24.2 (2). HRMS (ESI+) *m/z* [M + Na^+] calcd for $C_{20}H_{23}NO_3Na$, 348.1576, found 346.1567.

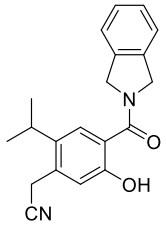

2-(5-Hydroxy-4-(isoindoline-2-carbonyl)-2-isopropylphenyl)acetonitrile (73): Potassium cyanide (43 mg, 0.66 mmol, 5.0 eq.) was added to a solution of **80** (50 mg, 0.14 mmol, 1.0 eq.) and 18-crown-6 (71 mg, 0.27 mmol, 2.0 eq.) in *N*,*N*-dimethylformamide (2.0 mL) at rt. The reaction was stirred for 2 h, diluted with water (20 mL), extracted with ethyl acetate (2 × 20 mL). The combined organic layers were washed with saturated sodium chloride solution (30 mL), dried over anhydrous sodium sulfate, filtered, and concentrated. The residue was purified by flash chromatography (SiO_2, 1:3 ethyl acetate/hexanes) to afford **73** (39.9 mg, 92.5 %) as colorless oil. ^{1}H NMR (400 MHz, $CDCl_3$) δ 10.53 (s, 1H), 7.54 (s, 1H), 7.32 (d, *J* = 4.6 Hz, 4H), 7.03 (s, 1H), 5.09 (s, 4H), 3.74 (s, 2H), 3.07 (hept, *J* = 6.9 Hz, 1H), 1.32 (d, *J* = 6.8 Hz, 6H). ^{13}C NMR (100

MHz, $CDCl_3$) δ 170.5, 158.0, 136.5, 135.85 (2) 132.4, 128.1, 125.7 (2), 122.8, 118.6, 117.7, 117.5, 56.2 (2), 29.0, 24.1(2), 21.7. HRMS (ESI+) *m/z* [M + H^+] calcd for $C_{20}H_{21}N_2O_2$, 321.1603, found 321.1610.

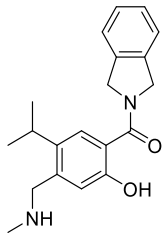

(2-Hydroxy-5-isopropyl-4-((methylamino)methyl)phenyl)(isoindolin-2-yl)methanone (77): 2.0 M methyl amine in tetrahydrofuran (0.1 mL, 0.20 mmol, 2.5 eq.) was added to a solution of **80** (30 mg, 0.08 mmol, 1 eq.) in tetrahydrofuran (1 mL). The resulting mixture was stirred at rt for 6 h, and concentrated. The residue was purified by flash chromatography (SiO_2, 1:10 methanol/dichloromethane) to afford **77** (8 mg, 28 %) as a colorless oil. ^{1}H NMR (500 MHz, $CDCl_3$) δ 7.43 (s, 1H), 7.32 (d, *J* = 4.7 Hz, 4H), 6.97 (s, 1H), 5.07 (s, 5H), 3.78 (s, 2H), 3.21 (p, *J* = 6.8 Hz, 1H), 2.54 (s, 3H), 1.27 (d, *J* = 6.8 Hz, 7H). ^{13}C NMR (125 MHz, $CDCl_3$) δ 171.1, 157.4, 142.4, 137.2, 136.2, 128.0 (2), 125.0 (2), 122.8 (2), 118.7, 118.1, 55.5, 53.3, 52.7, 36.5, 28.2, 24.4 (2). HRMS (ESI+) *m/z* [M + H^+] calcd for $C_{20}H_{25}N_2O_2$, 325.1916, found 325.1904.

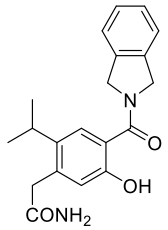

2-(5-Hydroxy-4-(isoindoline-2-carbonyl)-2-isopropylphenyl)acetamide (79): 30 % Hydrogen peroxide (0.10 mL, 0.19 mmol, 3.0 eq.) and 2M solution of sodium hydroxide (95 µl, 0.19 mmol, 3.0 eq.) was added to a solution of **73** (20 mg, 0.062 mmol, 1.0 eq.) in a solvent mixture of ethanol (0.5 mL) and dimethyl sulfoxide (0.2 mL). The resulting mixture was stirred for 1 h before the

addition of water (3 mL). The resulting mixture was extracted with ethyl acetate (3 × 5 mL). The combined organic layers were washed with saturated sodium chloride solution (10 mL), dried over anhydrous sodium sulfate, filtered, and concentrated The residue was purified by preparatory TLC (SiO_2, 1:9 acetone/dichloromethane) to give **79** as a colorless amorphous solid (12 mg. 54.4 %). ^{1}H NMR (500 MHz, $CDCl_3$) δ 10.6 (s, 1H), 7.6 (s, 1H), 7.3 (d, *J* = 5.0 Hz, 4H), 6.9 (s, 1H), 5.4 (s, 2H), 5.1 (s, 4H), 3.6 (s, 2H), 3.1 (hept, *J* = 6.8 Hz, 1H), 1.3 (d, *J* = 6.8 Hz, 7H). ^{13}C NMR (125 MHz, $CDCl_3$) δ 172.7, 170.7, 158.0, 137.9 (2), 137.7, 135.9, 128.2, 126.0 (2), 122.9, 119.8(2), 117.2, 55.9, 53.5, 41.3, 28.9, 24.4 (2). HRMS (ESI+) *m/z* [M + H^+] calcd for $C_{20}H_{22}N_2O_3$, 339.1709, found 339.1699.

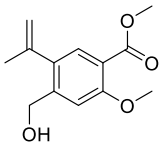

Methyl 4-formyl-2-methoxy-5-(prop-1-en-2-yl)benzoate (93): A biotage microwave vial was charged with **88** (0.75 g, 2.7 mmol, 1 eq.), tetrakis(triphenylphosphine)palladium(0) (312 mg, 0.27 mmol, 0.1 eq.), cesium carbonate (2.68 g, 8.25 mmol, 3 eq.), and potassium isopropenyltrifluoroborate (440 mg, 2.97 mmol, 1.2 eq.). The tube was sealed with a cap lined with a disposable teflon septum. The tube was evacuated and purged with nitrogen (3 times), before the addition of tetrahydrofuran (21.6 mL) and water (2.4 mL) by syringe. The resulting mixture was heated at 100 °C for 24 h, cooled to rt, and filtered through a small pad of celite (elution with ethyl acetate). Solvent was removed and the residue was purified by flash chromatography (SiO_2, 1:3 ethyl acetate/hexanes) to afford **93** as a colorless amorphous solid (580 mg, 90 %). ^{1}H NMR (400 MHz, $CDCl_3$) δ 7.57 (s, 1H), 7.14 (s, 1H), 5.19 (p, *J* = 1.7 Hz, 1H), 4.82 – 4.76 (m, 1H), 4.69 (s, 2H), 3.84 (d, *J* = 3.0 Hz, 6H), 2.72 (s, 1H), 2.06 – 1.94 (m, 3H). ^{13}C NMR

(100 MHz, $CDCl_3$) δ 166.7, 158.4, 144.0, 143.3, 134.2, 131.3, 118.1, 116.1, 110.9, 62.5, 56.1, 52.1, 24.8. HRMS (ESI+) *m/z* [M + H^+] calcd for $C_{13}H_{17}O_4$, 237.1126, found 237.1122.

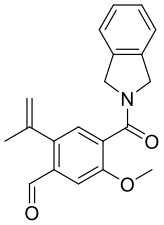

4-(Isoindoline-2-carbonyl)-5-methoxy-2-(prop-1-en-2-yl)benzaldehyde (94): Manganese dioxide (2.80 g, 24.0 mol, 10.0 eq.) was added to a solution of **93** (550 mg, 2.40 mmol, 1.0 eq.) in dichloromethane (120 mL) at rt. The resulting mixture was stirred at rt for 16 h, filtered through a small pad of celite, eluted with ethyl acetate, and concentrated. Solvent was removed to give the corresponding aldehyde which was used further as obtained. Lithium hydroxide monohydrate (1.0 g, 24.0 mmol) was added to a solution of the aldehyde in methanol (8 mL), tetrahydrofuran (8 mL), and water (8 mL). The resulting mixture was stirred for 14 h at rt. The residue was treated with 1 M hydrochloric acid and pH was adjusted to 2. The resulting suspension was extracted with ethyl acetate (3 × 50 mL), the combined organic layers were washed with saturated sodium chloride solution (100 mL), dried over anhydrous sodium sulfate, filtered, and concentrated to afford the corresponding acid as off-white solid which was used further as obtained. 1-Ethyl-3-(3-dimethylaminopropyl)carbodiimide (1.53 g, 4.80 mmol) was added to a stirred solution of the acid, isoindoline hydrochloride (485 mg, 3.12 mmol), 1-hydroxybenzotriazole (735 mg, 4.8 mmol), *N*,*N*-diisopropylethylamine (1.25 mL, 7.20 mmol) in dichloromethane (24 mL) at 0 °C. The resulting solution was stirred at rt for 14 h before quenching with saturated sodium bicarbonate solution (20 mL). The organic layer was washed with 1 M hydrochloric acid solution (15 mL) and saturated sodium chloride solution (20 mL), dried over anhydrous sodium sulfate, filtered, and concentrated. The residue was purified by flash chromatography (SiO_2, 1:3 hexanes/ethyl acetate)

to afford **94** as a light brown amorphous solid (331 mg, 43%). HRMS (ESI+) m/z [M + H^+] calcd for $C_{20}H_{20}NO_3$, 322.1443, found 322.1449

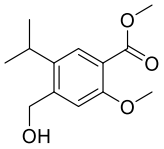

Methyl 4-(hydroxymethyl)-5-isopropyl-2-methoxybenzoate (96): Palladium on carbon (10%,) was added to a solution of **93** (500 mg, 2.11 mmol) in ethyl acetate (6 mL). The suspension was stirred for 16 h under a hydrogen atmosphere before it was filtered through a pad of celite and eluted with EtOAc (20 mL). The eluent was concentrated to afford **96** (476 mg, 94.2 %) as a colorless amorphous solid. ^{1}H NMR (400 MHz, $CDCl_3$) δ 7.71 (s, 1H), 7.06 (s, 1H), 4.78 (s, 2H), 3.88 (s, 3H), 3.84 (s, 3H), 3.06 (hept, *J* = 6.9 Hz, 1H), 1.22 (d, *J* = 6.8 Hz, 6H). ^{13}C NMR (100 MHz, $CDCl_3$) δ 167.1, 157.5, 143.7, 137.9, 128.9, 118.9, 111.1, 62.5, 56.3, 52.2, 28.0, 23.9 (2). HRMS (ESI+) *m/z* [M + Na^+] calcd for $C_{13}H_{18}O_4Na$, 261.1103, found 261.1091

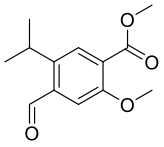

Methyl 4-formyl-5-isopropyl-2-methoxybenzoate (97): Manganese dioxide (1.64 g, 18.8 mmol, 10.0 eq.) was added to a solution of **96** (450 mg, 1.88 mmo0l, 1.0 eq.) in dichloromethane at rt. The resulting mixture was stirred at rt for 16 h, filtered through a small pad of celite, eluted with ethyl acetate, and concentrated. The residue was purified by flash chromatography (SiO_2, 1:6 ethyl acetate/hexanes) to afford **97** (367.3 mg, 82.7 %) as a yellow colorless solid. ^{1}H NMR (400 MHz, $CDCl_3$) δ 10.44 (s, 1H), 7.77 (s, 1H), 7.40 (s, 1H), 3.91 (d, *J* = 3.5 Hz, 6H), 3.84 – 3.75 (m, 1H), 1.30 (d, *J* = 6.9 Hz, 6H). ^{13}C NMR (100 MHz, $CDCl_3$) δ 190.9, 166.5, 156.8, 143.2, 136.1, 129.6,

125.6, 112.0, 56.4, 52.5, 27.2, 24.2 (2). HRMS (ESI+) m/z [M + H^+] calcd for $C_{13}H_{17}O_4$, 237.1127, found 237.1117.

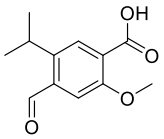

4-Formyl-5-isopropyl-2-methoxybenzoic acid (98): Trimethyltinhydroxide (3.63 g, 20.1 mmol, 4.0 eq.) was added to solution of **97** (1.12 g, 5.03 mmol, 1.0 eq.) in 1,2 dichloroethane (25 mL). The resulting mixture was heated at 75 °C for 50 h, cooled to rt, and concentrated. The residue was suspended in ethyl acetate (100 mL), washed with 1 M hydrochloric acid (3 × 60 mL) and saturated sodium chloride solution (100 mL). The solvent was removed to afford **98** (952 mg, 85.1 %) as a colorless amorphous solid. ^{1}H NMR (400 MHz, $CDCl_3$) δ 10.74 (br s, 1H), 10.52 (s, 1H), 8.27 (s, 1H), 7.53 (s, 1H), 4.13 (s, 3H), 3.79 – 4.13 (m, 1H), 1.36 (d, *J* = 6.8 Hz, 6H). ^{13}C NMR (100 MHz, $CDCl_3$) δ 190.4, 164.9, 156.2, 145.1, 137.5, 132.6, 122.3, 111.5, 57.3, 27.4, 24.3. HRMS (ESI-) *m/z* [M – H^+] calcd for $C_{12}H_{13}O_4$, 221.0814, found 221.0809.

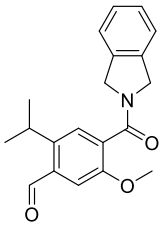

4-(Isoindoline-2-carbonyl)-2-isopropyl-5-methoxybenzaldehyde (95): 1-Ethyl-3-(3-dimethylaminopropyl) carbodiimide (1.63 g, 8.54 mmol, 2.0 eq.) was added to a stirred solution of **98** (950 mg, 4.27 mmol, 1 eq.), isoindoline hydrochloride (731 mg, 4.70 mmol, 1.1 eq.), 1-hydroxybenzotriazole (635 mg, 4.70 mmol, 1.1 eq.) *N*,*N*-diisopropylethylamine (3.26 mL, 18.8 mmol, 4.4 eq.) in dichloromethane 42 mL) at 0 °C. The resulting solution was stirred at rt for 14 h before quenching with saturated sodium bicarbonate solution (30 mL). The organic layer was washed with 1 M hydrochloric acid solution (30 mL) and saturated sodium chloride solution (30

mL), dried over anhydrous sodium sulfate, filtered and concentrated. The residue was purified by flash chromatography (SiO_2, 3:10 hexanes/ethyl acetate) to afford **95** (1.22 g, 91.8%) as a white amorphous solid. ^{1}H NMR (400 MHz, $CDCl_3$) δ 10.47 (s, 1H), 7.48 – 7.21 (m, 5H), 7.15 (d, *J* = 7.4 Hz, 1H), 5.01 (s, 2H), 4.58 (s, 2H), 4.02 – 3.76 (m, 4H), 1.32 (d, *J* = 6.8 Hz, 7H). ^{13}C NMR (100 MHz, $CDCl_3$) δ 190.8, 167.6, 153.7, 144.9, 136.4, 136.4, 134.4, 132.5, 128.0, 127.7, 126.1, 123.3, 122.7, 111.2, 56.1, 53.4, 52.3, 27.3, 24.4 (2). HRMS (ESI+) *m/z* [M + Na^+] calcd for $C_{20}H_{21}NO_3Na$, 346.1419, found 346.1404.

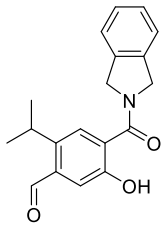

5-Hydroxy-4-(isoindoline-2-carbonyl)-2-isopropylbenzaldehyde (78): 1 M solution of boron tribromide (1.22 mmol, 1.22 mL, 2 eq.), was added to a solution of **95** (200 mg, 0.61 mmol) in anhydrous dichloromethane (6.1 ml) at 0 ^{o}C. The resulting mixture was stirred at rt for 14 h before quenching with saturate sodium bicarbonate solution (5 mL). The aqueous layer was extracted with dichloromethane (2 × 10 mL). The combined organic layers were washed with saturated sodium chloride solution (20 mL), dried over sodium sulfate, filtered and concentrated. The residue was purified by flash chromatography (SiO_2, 1:50 acetone/dichloromethane) to afford **78** (121.8 mg, 63.7 %) as a colorless solid. ^{1}H NMR (400 MHz, $CDCl_3$) δ 10.31 (s, 1H), 10.11 (s, 1H), 7.64 (s, 1H), 7.43 (s, 1H), 7.37 – 7.29 (m, 4H), 5.08 (s, 5H), 3.93 (h, *J* = 6.9 Hz, 1H), 1.34 (d, *J* = 6.7 Hz, 6H). HRMS (ESI-) m/z [M – H^+] calcd for $C_{19}H_{18}NO_3$, 308.1287, found 308.1282.

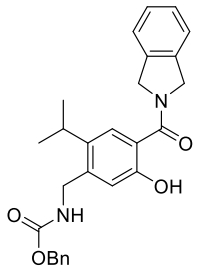

Benzyl (4-(isoindoline-2-carbonyl)-2-isopropyl-5-methoxybenzyl)carbamate (99): Benzyl carbamate (109 mg, 0.72 mmol, 3.0 eq.), triethyl silane (114 µl, 0.72 mmol, 3.0 eq.) and trifluoroacetic acid (36 µl, 0.48 mmol. 2.0 eq.) were added to a solution of **78** (75 mg, 0.24 mmol, 1.0 eq.) in acetonitrile (2.5 mL). The resulting mixture was stirred for 24 h before quenching with saturated sodium bicarbonate solution (10 mL). The aqueous layer was extracted with ethyl acetate (2 × 10 mL). The combined organic layers were washed with saturated sodium chloride solution (15 mL), dried over sodium sulfate, filtered and concentrated. The residue was purified by flash chromatography (SiO_2, 1:2 ethyl acetate/hexanes) to afford **99** (93.7 mg, 87.9 %) as a colorless oil. ^{1}H NMR (400 MHz, $CDCl_3$) δ 10.52 (s, 1H), 7.50 (s, 1H), 7.41 – 7.27 (m, 9H), 6.92 (s, 1H), 5.15 (s, 3H), 5.06 (s, 4H), 4.45 (d, *J* = 5.9 Hz, 2H), 3.20 – 3.05 (m, 1H), 1.27 (d, *J* = 6.8 Hz, 6H). ^{13}C NMR (100 MHz, $CDCl_3$) δ 170.8, 157.7, 156.4, 136.7, 136.6, 136.0, 128.7(3), 128.3 (2), 128.3 (2), 128.0, 125.3 (2), 122.8 (2), 117.0, 116.8, 67.1, 55.6, 55.3, 42.4, 28.2, 24.3 (2). HRMS (ESI+) *m/z* [M + H^+] calcd for $C_{27}H_{29}N_2O_4$, 445.2127, found 445.2131.

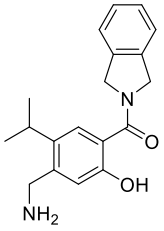

(4-(Aminomethyl)-2-hydroxy-5-isopropylphenyl) (isoindolin-2-yl)methanone (75): Palladium on carbon (10%) was added to a solution of **99** (93 mg, 0.21 mmol) in ethyl acetate (5 mL). The suspension was stirred for 16 h under a hydrogen atmosphere before it was filtered through a pad

of celite and eluted with EtOAc (20 mL). The eluent was concentrated to afford **75** (36 mg, 55.6 %) as a colorless oil. ^{1}H NMR (400 MHz, $CDCl_3$) δ 7.48 (s, 1H), 7.31 (s, 4H), 6.99 (s, 1H), 5.08 (s, 4H), 3.91 (s, 2H), 3.17 (hept, *J* = 6.8 Hz, 1H), 1.28 (d, *J* = 6.8 Hz, 6H). ^{13}C NMR (100 MHz, $CDCl_3$) δ 171.0, 157.7, 145.4, 136.4, 136.1 (2), 128.0 (2), 125.1, 122.8 (2), 116.6, 116.4, 53.6 (2), 43.4, 28.1, 24.5 (2). HRMS (ESI+) *m/z* [M + H^+] calcd for $C_{19}H_{23}N_2O_2$, 311.1760, found 311.1774.

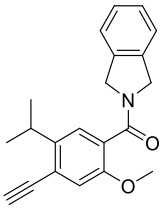

(4-Ethynyl-5-isopropyl-2-methoxyphenyl)(isoindolin-2-yl)methanone (100): Dimethyl-1-diazo-2-oxopropylphosphonate (60 µL, 0.40 mmol, 1.2 eq.) was added to a stirred solution of aldehyde **95** (100 mg, 0.31 mmol, 1.0 eq.) and potassium carbonate (86 mg, 0.62 mmol, 2.0 eq.) in methanol (3.1 mL). The resulting mixture was stirred for 24 h at rt and diluted with ethyl acetate (10 mL). The organic layer was washed with saturated sodium bicarbonate solution (10 mL), dried over anhydrous sodium sulfate, filtered and concentrated. The residue was purified by flash chromatography (SiO_2, 1:3 ethyl acetate/hexanes) to afford **100** (77.1 mg, 78.1 %) as a colorless oil. ^{1}H NMR (400 MHz, $CDCl_3$) δ 7.35 – 7.23 (m, 3H), 7.21 (s, 1H), 7.13 (d, *J* = 7.4 Hz, 1H), 7.05 (s, 1H), 4.98 (s, 2H), 4.58 (s, 2H), 3.81 (d, *J* = 1.3 Hz, 3H), 3.82 – 3.40 (m, 1H), 3.33 (s, 1H), 1.24 (d, *J* = 7.1 Hz, 6H). ^{13}C NMR (100 MHz, $CDCl_3$) δ 168.1, 152.9, 144.3, 136.7, 136.5, 127.9, 127.8, 127.6, 124.7, 123.2, 122.9, 122.7, 115.5, 82.0, 81.8, 56.0, 53.4, 52.2, 31.0, 23.3 (2). HRMS (ESI+) *m/z* [M + H^+] calcd for $C_{21}H_{22}NO_2$, 320.1651, found 320.1660.

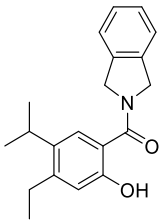

(4-Ethyl-5-isopropyl-2-methoxyphenyl)(isoindolin-2-yl)methanone (81): Palladium on carbon (10%) was added to a solution of **95** (75 mg, 0.23 mmol) in ethyl acetate (10 mL). The suspension was stirred for 16 h under a hydrogen atmosphere before it was filtered through a pad of celite and eluted with EtOAc (20 mL). The eluent was concentrated to afford (4-ethyl-5-isopropyl-2-methoxyphenyl)(isoindolin-2-yl)methanone (72.1 mg, 97.6 %) as a colorless amorphous solid. ^{1}H NMR (400 MHz, $CDCl_3$) δ 7.37 – 7.24 (m, 3H), 7.19 (s, 1H), 7.14 (d, *J* = 7.4 Hz, 1H), 6.75 (s, 1H), 5.00 (s, 2H), 4.63 (s, 2H), 3.83 (s, 3H), 3.11 – 3.18 (m, 1H), 2.71 (q, *J* = 7.5 Hz, 2H), 1.21 – 1.27 (m, 9H). ^{13}C NMR (100 MHz, $CDCl_3$) δ 168.1, 152.9, 144.3, 136.7, 136.5, 127.9, 127.8, 127.6, 124.7, 123.2, 122.9, 122.7, 115.5, 82.0, 81.8, 56.0, 53.4, 52.2, 31.0, 23.3 (2). HRMS (ESI+) m/z [M + H^+] calcd for $C_{21}H_{26}NO_2$, 324.1963, found 324.1969. 1 M solution of boron tribromide (0.38 mmol, 0.38 mL, 2 eq.), was added to a solution of (4-ethyl-5-isopropyl-2-methoxyphenyl)(isoindolin-2-yl)methanone (60 mg, 0.19 mmol) in anhydrous dichloromethane (2 mL) at 0 ^{o}C. The resulting mixture was stirred at rt for 14 h before quenching with saturate sodium bicarbonate solution (5 mL). The aqueous layer was extracted with dichloromethane (2 × 10 mL). The combined organic layers were washed with saturated sodium chloride solution (20 mL), dried over anhydrous sodium sulfate, filtered, and concentrated. The residue was purified by flash chromatography (SiO_2, 1:2 ethyl acetate/hexanes) to afford **81** (33.2 mg, 56.7 %) as a pale yellow oil. ^{1}H NMR (400 MHz, $CDCl_3$) δ 10.54 (s, 1H), 7.40 (s, 1H), 7.30 – 7.18 (m, 4H), 6.75 (s, 1H), 5.02 (s, 4H), 3.09 (hept, *J* = 6.7 Hz, 1H), 2.61 (q, *J* = 7.6 Hz, 2H), 1.15 – 1.21 (m, 9H). ^{13}C NMR (100 MHz, $CDCl_3$) δ 171.3, 157.9, 147.3, 136.7, 136.2 (2), 128.0, 124.9, 122.8 (2), 117.5 (2), 115.0, 56.1 (2),28.2, 25.8, 24.5 (2), 15.4. HRMS (ESI+) *m/z* [M + H^+] calcd for $C_{20}H_{24}NO_2$, 310.1807, found 310.1794.

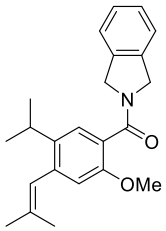

Isoindolin-2-yl(5-isopropyl-2-methoxy-4-(2-methylprop-1-en-1-yl)phenyl)methanone (101): 1.6 M Solution of *n*-butyl lithium in hexanes (0.32 mL, 0.5 mmol, 2.0 eq.) was added to a suspension of isopropyltriphenylphosphonium iodide (216 mg, 0.5 mmol, 1.0 eq.) in tetrahydrofuran (1 mL) at 0 ^{o}C. The resulting mixture was stirred for 30 min before the addition of a solution of **95** (80 mg, 0.25 mmol, 1.0 eq.) in tetrahydrofuran (1 mL) at 0 ^{o}C. The reaction was warmed to rt and stirred for 5 h before quenching with water (10 mL). The aqueous layer was extracted with ethyl acetate (2 × 10 mL). The combined organic layers were washed with saturated sodium chloride solution (20 mL), dried over sodium sulfate, filtered and concentrated. The residue was purified by flash chromatography (SiO_2, 1:5 ethyl acetate/hexanes) to afford **101** (66.6 mg, 75.9 %) as a pale yellow oil. ^{1}H NMR (400 MHz, $CDCl_3$) δ 7.37 – 7.24 (m, 4H), 7.16 (d, *J* = 5.1 Hz, 2H), 6.78 (s, 1H), 6.25 (s, 1H), 5.14 – 5.12 (m, 1H), 5.01 (s, 2H), 4.93 – 4.85 (m, 1H), 4.67 (s, 2H), 3.84 (s, 3H), 1.99 (s, 3H), 1.91 (s, 3H), 1.81 (s, 3H). ^{13}C NMR (100 MHz, $CDCl_3$) δ 168.6, 153.8, 144.8, 138.8, 136.9, 136.7, 136.5, 135.7, 127.8, 127.6, 127.5, 125.0, 124.6, 123.3, 122.7, 115.7, 113.0, 56.0, 53.6, 52.2, 26.4, 24.2, 19.7. HRMS (ESI+) *m/z* [M + H^+] calcd for $C_{23}H_{26}NO_2$, 310.1807, found 310.1794.

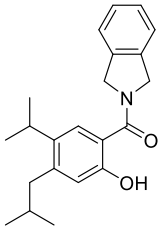

(2-Hydroxy-4-isobutyl-5-isopropylphenyl)(isoindolin-2-yl)methanone (82): Palladium on carbon (10%) was added to a solution of **101** (60 mg, 0.17 mmol) in ethyl acetate (5 mL). The suspension was stirred for 16 h under a hydrogen atmosphere before it was filtered through a pad of celite and eluted with EtOAc (20 mL). The eluent was concentrated to afford (4-isobutyl-5-isopropyl-2-methoxyphenyl)(isoindolin-2-yl)methanone (56.3 mg, 94.2 %) as a colorless amorphous solid. ^{1}H NMR (400 MHz, $CDCl_3$) δ 7.38 – 7.22 (m, 3H), 7.20 (s, 1H), 7.14 (d, *J* = 7.3 Hz, 1H), 6.67 (s, 1H), 5.00 (s, 2H), 4.62 (s, 2H), 3.81 (s, 3H), 3.13 (hept, *J* = 6.9 Hz, 1H), 2.54 (d, *J* = 7.2 Hz, 2H), 1.85 (dp, *J* = 13.6, 6.8 Hz, 1H), 1.20 (d, *J* = 6.8 Hz, 6H), 0.97 (d, *J* = 6.6 Hz, 6H). ^{13}C NMR (100 MHz, $CDCl_3$) δ 169.2, 152.8, 141.3, 139.8, 137.0, 136.8, 127.8, 127.5, 124.9, 124.8, 123.2, 122.7, 113.2, 55.9, 53.5, 52.2, 42.6, 30.4, 28.4, 24.4 (2), 22.8 (2). HRMS (ESI+) *m/z* [M + H^+] calcd for $C_{23}H_{30}NO_2$, 352.2277, found 352.2275. 1 M solution of boron tribromide (0.34 mmol, 0.34 mL, 2 eq.), was added to a solution of (4-isobutyl-5-isopropyl-2-methoxyphenyl)(isoindolin-2-yl)methanone (60 mg, 0.17 mmol) in anhydrous dichloromethane (2 mL) at 0 ^{o}C. The resulting mixture was stirred at rt for 14 h before quenching with saturate sodium bicarbonate solution (5 mL). The aqueous layer was extracted with dichloromethane (2 × 10 mL). The combined organic layers were washed with saturated sodium chloride solution (20 mL), dried over sodium sulfate, filtered and concentrated. The residue was purified by flash chromatography (SiO_2, 1:3 ethyl acetate/hexanes) to afford **82** (33.2 mg, 56.7 %) as a colorless amorphous solid. ^{1}H NMR (500 MHz, $CDCl_3$) δ 10.60 (s, 1H), 7.48 (s, 1H), 7.32 (s, 4H), 6.77 (s, 1H), 5.10 (s, 4H), 3.16 (hept, *J* = 6.8 Hz, 1H), 2.51 (d, *J* = 7.2 Hz, 2H), 1.87 (dt, *J* = 13.5, 6.8 Hz, 1H), 1.26 (d, *J* = 6.8 Hz, 7H), 0.96 (d, *J* = 6.6 Hz, 6H). ^{13}C NMR (125 MHz, $CDCl_3$) δ 171.3, 157.4, 144.8, 137.3, 136.2 (2), 128.0, 125.1, 122.8, 119.1, 115.2, 55.9, 53.5, 42.2, 30.1, 28.3, 24.7 (2), 22.9 (2). HRMS (ESI+) *m/z* [M + H^+] calcd for $C_{22}H_{28}NO_2$, 338.2120, found 338.2125.

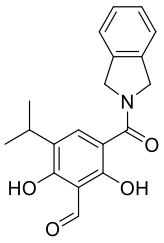

2,6-Dihydroxy-3-(isoindoline-2-carbonyl)-5-isopropylbenzaldehyde (104): A solution of **103** (400 mg, 1.34 mmol, 1 eq.), hexamethylenetetramine (376 mg, 2.68 mmol, 2.0 eq.) in trifluoroacetic acid was heated at 100 °C for 14 h in a sealed tube, cooled to rt, and solvent was removed. The residue was treated with 3 M hydrochloric acid and the resulting mixture was heated at 60 ^{o}C for 3 h. The mixture was cooled to rt, diluted with water (20 ml), extracted with ethyl acetate (2 × 20 mL). The organic layer was washed with water (30 ml), saturated sodium bicarbonate solution (30 mL), and saturated sodium chloride solution (30 mL), dried over anhydrous sodium sulfate, filtered, and concentrated. The residue was purified by flash chromatography (SiO_2, 1:9 ethyl acetate/hexanes) to afford **104** (312.2 mg, 71.8 %) as a pale yellow amorphous solid. ^{1}H NMR (500 MHz, $CDCl_3$) δ 13.06 (s, 1H), 12.74 (s, 1H), 10.44 (s, 1H), 7.74 (s, 1H), 7.34 (d, *J* = 2.2 Hz, 4H), 5.12 (s, 4H), 3.36 – 3.27 (m, 1H), 1.28 (d, *J* = 6.9 Hz, 6H). ^{13}C NMR (125 MHz, $CDCl_3$) δ 195.1, 170.7, 165.0, 164.0, 135.7, 133.5 (2), 128.2 (2), 126.2, 122.8 (2), 110.1, 106.9, 54.8 (2), 26.1, 22.7 (2). HRMS (ESI+) *m/z* [M + H^+] calcd for $C_{19}H_{20}NO_4$, 338.2120, found 338.2117.

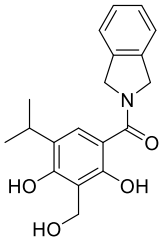

(2,4-Dihydroxy-3-(hydroxymethyl)-5-isopropylphenyl)(isoindolin-2-yl)methanone (102): Sodium borohydride (2.8 mg, 0.06 mmol) was added to a solution of **104** (20 mg, 0.07 mmol, 2.0

eq.) in a solvent mixture of tetrahydrofuran (1.5 mL) and methanol (0.5 mL) at ^{o}C. The resulting mixture was stirred at rt for 1 h before the addition of 1 M hydrochloric acid (2 mL). The aqueous layer was extracted with ethyl acetate (2 × 5 mL), and the combined organic layers washed with saturated sodium chloride solution, dried over anhydrous sodium sulfate, filtered, and concentrated. The residue was purified by preparatory TLC (SiO_2, 1:3 ethyl acetate/hexanes) to give **102** as a colorless amorphous solid (14.2 mg, 72.2 %). ^{1}H NMR (500 MHz, $CDCl_3$) δ 11.72 (s, 1H), 8.76 (s, 1H), 7.43 (s, 1H), 7.32 (s, 4H), 5.11 (s, 6H), 3.34 – 3.24 (m, 1H), 2.31 (s, 1H), 1.28 (d, *J* = 6.9 Hz, 6H). ^{13}C NMR (125 MHz, $CDCl_3$) δ 171.7, 158.6, 157.1, 136.2 (2), 128.0, 126.3 (2), 125.5, 122.8 (2), 111.4, 108.3, 59.3, 54.2 (2), 26.6, 23.1 (2). HRMS (ESI+) m/z [M + H^+] calcd for $C_{19}H_{21}NO_4$, 328.1549, found 328.1543.

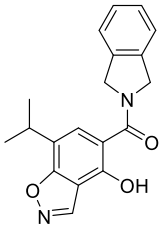

(4-Hydroxy-7-isopropylbenzo[d]isoxazol-5-yl)(isoindolin-2-yl)methanone (105): Triflic acid (79 µL, 0.90 mmol, 6.0 eq.) and sodium azide (15 mg, 0.23 mmol, 1.5 eq.) were added to a solution of **104** (50 mg, 0.15 mmol, 1.0 eq.) in acetonitrile (1.5 mL) at rt. The resulting mixture was stirred for 5 min and concentrated. The residue was treated with water (2 mL) and ethyl acetate (3 mL). The aqueous layer was extracted with ethyl acetate (2 × 3 mL) and the combined organic layers washed with saturated sodium chloride solution (6 mL), dried over anhydrous sodium sulfate, filtered, and concentrated. The residue was purified using preparatory TLC (SiO_2, 1:3 ethyl acetate/hexanes) to afford **105** as a white amorphous solid. (18.3 mg, 37.8 %). Additionally, **106** (13.1, 27.1 %) was also isolated as a white amorphous solid. ^{1}H NMR (400 MHz, $CDCl_3$) δ 12.42 (s, 1H), 8.86 (d, *J* = 1.3 Hz, 1H), 7.65 (s, 1H), 7.34 (s, 4H), 5.14 (s, 4H), 3.40 (hept, *J* = 7.0 Hz,

1H), 1.45 (d, *J* = 7.1 Hz, 6H). ^{13}C NMR (100 MHz, $CDCl_3$) δ 171.1, 163.7, 156.1, 145.2, 135.9, 128.2 (2), 126.5 (2), 122.8 (2), 121.6, 112.9, 110.4, 54.2 (2), 29.4, 22.7 (2). HRMS (ESI+) m/z [M + H^+] calcd for $C_{19}H_{19}N_2O_3$, 323.1396, found 323.1392.

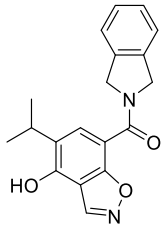

(4-Hydroxy-5-isopropylbenzo[d]isoxazol-7-yl)(isoindolin-2-yl)methanone (106): ^{1}H NMR (400 MHz, $CDCl_3$; δ 9.59 (s, 1H), 9.10 (s, 1H), 7.60 (s, 1H), 7.45 – 7.26 (m, 3H), 7.16 (d, *J* = 7.4 Hz, 1H), 5.17 (s, 2H), 4.91 (s, 2H), 3.18 (h, *J* = 7.0 Hz, 1H), 1.06 (d, *J* = 6.9 Hz, 6H). ^{13}C NMR (101 MHz, $CDCl_3$) δ 167.9, 157.9, 151.0, 145.2, 136.5, 135.8, 130.0, 129.4, 128.1, 127.9, 123.1, 122.8, 112.6, 109.5, 53.9, 53.3, 26.4, 22.9 (2). HRMS (ESI+) m/z [M + H^+] calcd for $C_{19}H_{19}N_2O_3$, 323.1396, found 323.1399.

IV.9. References

1. Chiosis, G.; Dickey, C. A.; Johnson, J. L. A Global View of Hsp90 Functions. *Nat. Struc. Mol. Biol.* **2013**, 20, 1-4.
2. Csermely, P.; Schnaider, T.; Sőti, C.; Prohászka, Z.; Nardai, G. The 90-k-Da Molecular Chaperone Family: Structure, Function, and Clinical Applications. A Comprehensive Reveiw. *Pharmacol. Ther.* **1998**, 79, 129-168.
3. Johnson, J. L. Evolution and function of diverse Hsp90 homologs and cochaperone proteins. *Biochim. Biophys. Acta.* **2012**, 1823, 607-613.
4. Rohl, A.; Rohrberg, J.; Buchner, J. The chaperone Hsp90: changing partners for demanding clients. *Trends Biochem. Sci.* **2013**, 38, 253-262.
5. Saibil, H. Chaperone Machines for Protein Folding, Unfolding and Disaggregation. *Nat. Rev. Mol. Cell Biol.* **2013**, 14, 630-642.
6. Peterson, L. B.; Blagg, B. S. To fold or not to fold: modulation and consequences of Hsp90 inhibition. *Future Med. Chem.* **2009**, 1, 267-283.
7. Whitesell, L.; Lindquist, S. L. HSP90 and the chaperoning of cancer. *Nat. Rev. Cancer* **2005**, 5, 761-772.
8. Whitesell, L.; Mimnaugh, E. G.; De Costa, B.; Myers, C. E.; Neckers, L. M. Inhibition of heat shock protein HSP90-pp60v-src heteroprotein complex formation by benzoquinone ansamycins: essential role for stress proteins in oncogenic transformation. *Proc. Natl. Acad. Sci. U.S.A.* **1994**, 91, 8324-8328.

9. Hanahan, D.; Weinberg, R. A. The hallmarks of cancer. *Cell* **2000**, 100, 57-70.
10. Hanahan, D.; Weinberg, R. A. Hallmarks of cancer: the next generation. *Cell* **2011**, 144, 646-674.
11. Trepel, J.; Mollapour, M.; Giaccone, G.; Neckers, L. Targeting the dynamic HSP90 complex in cancer. *Nat. Rev. Cancer* **2010**, 10, 537-549.
12. Miyata, Y.; Nakamoto, H.; Neckers, L. The therapeutic target Hsp90 and cancer hallmarks. *Curr. Pharm. Des.* **2013**, 19, 347-365.
13. Goetz, M. P.; Toft, D. O.; Ames, M. M.; Erlichman, C. The Hsp90 Chaperone Complex as a Novel Target for Cancer Therapy. *Ann. Oncol.* **2003**, 14, 1169-1176.
14. Whitesell, L.; Lindquist, S. L. HSP90 and the Chaperoning of Cancer. *Nat. Rev.* ***2005****, 5,* 761-772.
15. Bagatell, R.; Whitesell, L. Altered Hsp90 function in cancer: a unique therapeutic opportunity. *Mol. Cancer Ther.* **2004,** 3, 1021-1030.
16. Taipale, M.; Jarosz, D. F.; Lindquist, S. HSP90 at the hub of protein homeostasis: emerging mechanistic insights. *Nat. Rev. Mol. Cell Biol.* **2010,** 11, 515-528.
17. Kamal, A.; Thao, L.; Sensintaffar, J.; Zhang, L.; Boehm, M. F.; Fritz, L. C.; Burrows, F. J. A high-affinity conformation of Hsp90 confers tumour selectivity on Hsp90 inhibitors. *Nature* **2003**, 425, 407-410.
18. Vilenchik, M.; Solit, D.; Basso, A.; Huezo, H.; Lucas, B.; He, H.; Rosen, N.; Spampinato, C.; Modrich, P.; Chiosis, G. Targeting wide-range oncogenic transformation via PU24FCl, a specific inhibitor of tumor Hsp90. *Chem. Biol.* **2004,** 11, 787-797.
19. Prodromou, C. Strategies for Stalling Malignancy-Targeting Cancer's Addiction to Hsp90. *Curr. Top. Med. Chem.* **2009**, 9, 1352-1368.
20. Workman, P.; Burrows, F.; Neckers, L.; Rosen, N. Drugging the cancer chaperone HSP90: combinatorial therapeutic exploitation of oncogene addiction and tumor stress. *Ann. N.Y. Acad. Sci.* **2007,** 1113, 202-216.
21. Khandelwal, A.; Crowley, V. M.; Blagg, B. S. Natural Product Inspired N-Terminal Hsp90 Inhibitors: From Bench to Bedside? *Med. Res. Rev.* **2016**, 36, 92-118.
22. Neckers, L.; Workman, P. Hsp90 molecular chaperone inhibitors: are we there yet? *Clin. Cancer Res.* **2012**, 18, 64-76.
23. Neckers, L.; Trepel, J. B. Stressing the development of small molecules targeting HSP90. *Clin. Cancer Res.* **2014**, 20, 275-277.
24. Peterson, L. B.; Eskew, J. D.; Vielhauer, G. A.; Blagg, B. S. J. The hERG Channel is Dependent Upon the Hsp90a Isoform for Maturation and Trafficking. *Mol. Pharm.* **2012**, 9, 1841-1846.
25. Holzbeierlein, J. M.; Windsperger, A.; Vielhauer, G. Hsp90: A Drug Target? *Curr. Oncol. Rep.* **2010**, 12, 95-101.
26. Biamonte, M. A.; Van de Water, R.; Arndt, J. W.; Scannevin, R. H.; Perret, D.; Lee, W. C. Heat shock protein 90: inhibitors in clinical trials. *J. Med. Chem.* **2010**, 53, 3-17.
27. Garcia-Carbonero, R.; Carnero, A.; Paz-Ares, L. Inhibition of HSP90 Molecular Chaperones: Moving into the Clinic. *Lancet. Oncol.* **2013**, 14, e358-e369.
28. Powers, M. V.; Workman, P. Inhibitors of the heat shock response: biology and pharmacology. *FEBS Lett.* **2007**, 581, 3758-3769.
29. Chen, B.; Piel, W. H.; Gui, L.; Bruford, E.; Monteiro, A. The HSP90 family of genes in the human genome: insights into their divergence and evolution. *Genomics* **2005**, 86, 627-637.

30. Sreedhar, A. S.; Kalmar, E.; Csermely, P.; Shen, Y. F. Hsp90 isoforms: functions, expression and clinical importance. *FEBS Lett.* **2004**, 562, 11-15.
31. Bagatell, R.; Paine-Murrieta, G. D.; Taylor, C. W.; Pulcini, E. J.; Akinaga, S.; Benjamin, I. J.; Whitesell, L. Induction of a heat shock factor 1-dependent stress response alters the cytotoxic activity of hsp90-binding agents. *Clin. Cancer Res.* **2000,** 6, 3312-3318.
32. Hong, D. S.; Banerji, U.; Tavana, B.; George, G. C.; Aaron, J.; Kurzrock, R. Targeting the molecular chaperone heat shock protein 90 (HSP90): lessons learned and future directions. *Cancer Treat. Rev.* **2013**, 39, 375-387.
33. Milicevic, Z.; Bogojevic, D.; Mihailovic, M.; Petrovic, M.; Krivokapic, Z. Molecular characterization of hsp90 isoforms in colorectal cancer cells and its association with tumour progression. *Int. J. Oncol.* **2008**, 32, 1169-1178.
34. Liu, W.; Vielhauer, G. A.; Holzbeierlein, J. M.; Zhao, H.; Ghosh, S.; Brown, D.; Lee, E.; Blagg, B. S. KU675, a Concomitant Heat-Shock Protein Inhibitor of Hsp90 and Hsc70 that Manifests Isoform Selectivity for Hsp90a in Prostate Cancer Cells. *Mol. Pharmacol.* **2015**, 88, 121-130.
35. McDowell, C. L.; Bryan Sutton, R.; Obermann, W. M. Expression of Hsp90 chaperone proteins in human tumor tissue. *Int. J. Biol. Macromol.* **2009**, 45, 310-314.
36. Wang, Q.; He, Z.; Zhang, J.; Wang, Y.; Wang, T.; Tong, S.; Wang, L.; Wang, S.; Chen, Y. Overexpression of endoplasmic reticulum molecular chaperone GRP94 and GRP78 in human lung cancer tissues and its significance. *Cancer Detect. Prev.* **2005**, 29, 544-551.
37. Li, C. F.; Huang, W. W.; Wu, J. M.; Yu, S. C.; Hu, T. H.; Uen, Y. H.; Tian, Y. F.; Lin, C. N.; Lu, D.; Fang, F. M.; Huang, H. Y. Heat shock protein 90 overexpression independently predicts inferior disease-free survival with differential expression of the a and b isoforms in gastrointestinal stromal tumors. *Clin. Cancer Res.***2008**, 14, 7822-7831.
38. Gao, Y.; Yechikov, S.; Vazquez, A. E.; Chen, D.; Nie, L. Distinct roles of molecular chaperones HSP90a and HSP90b in the biogenesis of KCNQ4 channels. *PloS one* **2013**, 8, e57282.
39. Karagoz, G. E.; Rudiger, S. G. Hsp90 interaction with clients. *Trends Biochem. Sci* **2015**, 40, 117-125.
40. Prince, T. L.; Kijima, T.; Tatokoro, M.; Lee, S.; Tsutsumi, S.; Yim, K.; Rivas, C.; Alarcon, S.; Schwartz, H.; Khamit-Kush, K.; Scroggins, B. T.; Beebe, K.; Trepel, J. B.; Neckers, L. Client Proteins and small molecule inhibitors display distinct binding Preferences for Constitutive and Stress-Induced HSP90 Isoforms and Their conformationallyrRestricted mutants. *PloS one* **2015**, 10, e0141786.
41. Peterson, L. B.; Eskew, J. D.; Vielhauer, G. A.; Blagg, B. S. The hERG channel is dependent upon the Hsp90a isoform for maturation and trafficking. *Mol. Pharm.* **2012**, 9, 1841-1846.
42. McLaughlin, M.; Vandenbroeck, K. The endoplasmic reticulum protein folding factory and its chaperones: new targets for drug discovery? *Br. J. Pharmacol.* **2011**, 162, 328-345.
43. Stothert, A. R.; Suntharalingam, A.; Huard, D. J.; Fontaine, S. N.; Crowley, V. M.; Mishra, S.; Blagg, B. S.; Lieberman, R. L.; Dickey, C. A. Exploiting the interaction between Grp94 and aggregated myocilin to treat glaucoma. *Hum. Mol. Genet.* **2014**, *23*, 6470-6480.
44. Patel, P. D.; Yan, P.; Seidler, P. M.; Patel, H. J.; SUn, W.; Yang, C.; Que, N. S.; Taldone, T.; Finotti, P.; Stephani, R. A.; Gewirth, D. T.; Chiosis, G. Paralog-Selective Hsp90 inhibitors define tumor-specific regulation of HER2. *Nat. Chem. Biol.* **2013**, *9*, 677-684.

45. Muth, A.; Crowley, V.; Khandelwal, A.; Mishra, S.; Zhao, J.; Hall, J.; Blagg, B. S. Development of radamide analogs as Grp94 inhibitors. *Bioorg. Med. Chem.* **2014,** 22, 4083-4098.
46. Lee, A. S. Glucose-regulated proteins in cancer: molecular mechanisms and therapeutic potential. *Nat. Rev. Cancer* **2014,** 14, 263-276.
47. Ernst, J. T.; Neubert, T.; Liu, M.; Sperry, S.; Zuccola, H.; Turnbull, A.; Fleck, B.; Kargo, W.; Woody, L.; Chiang, P.; Tran, D.; Chen, W.; Snyder, P.; Alcacio, T.; Nezami, A.; Reynolds, J.; Alvi, K.; Goulet, L.; Stamos, D. Identification of novel HSP90a/b isoform selective inhibitors using structure-based drug design. demonstration of dotential utility in treating CNS disorders such as Huntington's disease. *J. Med. Chem.* **2014**, 57, 3382-3400.
48. Didelot, C.; Lanneau, D.; Brunet, M.; Bouchot, A.; Cartier, J.; Jacquel, A.; Ducoroy, P.; Cathelin, S.; Decologne, N.; Chiosis, G.; Dubrez-Daloz, L.; Solary, E.; Garrido, C. Interaction of heat-shock protein 90 b-isoform with cellular inhibitor of apoptosis 1 (c-IAP1) is required for cell differentiation. *Cell Death Differ.* **2008**, 15, 859-866.
49. Sreedhar, A. S.; Kalmar, E.; Csermely, P.; Shen, Y. F. Hsp90 isoforms: functions, expression and clinical importance. *FEBS Lett.* **2004,** 562, 11-15.
50. Rong, B.; Zhao, C.; Liu, H.; Ming, Z.; Cai, X.; Gao, W.; Yang, S. Identification and verification of Hsp90-b
as a potential serum biomarker for lung cancer. *Am. J. Cancer Res.* **2014**, 4, 874-885.
51. Biaoxue, R.; Xiling, J.; Shuanying, Y.; Wei, Z.; Xiguang, C.; Jinsui, W.; Min, Z. Upregulation of Hsp90b and annexin A1 correlates with poor survival and lymphatic metastasis in lung cancer patients. *J. Exp.Clin. Cancer Res.* **2012**, 31, 70-83.
52. Wu, Y.; Huang, B.; Liu, Q.; Liu, Y. Heat shock protein 90b over-expression is associated with poor survival in stage I lung adenocarcinoma patients. *Int. J. Clin. Exp.Pathol.* **2015**, 8, 8252-8259.
53. Andrulis, M.; Chatterjee, M.; Jain, S.; Stuhmer, T.; Ungethum, U.; Kuban, R. J.; Lorentz, H.; Bommert, K.; Topp, M.; Kramer, D.; Muller-Hermelinks, H. K.; Einsele, H.; Bargou, R. C.; Greiner, A. Heat shock protein 90a and b are overexpressed in multiple myeloma cells and critically contribute to survival. *Verhandlungen der Deutschen Gesellschaft fur Pathologie* **2007**, 91, 330-337.
54. Chatterjee, M.; Jain, S.; Stuhmer, T.; Andrulis, M.; Ungethum, U.; Kuban, R. J.; Lorentz, H.; Bommert, K.; Topp, M.; Kramer, D.; Muller-Hermelink, H. K.; Einsele, H.; Greiner, A.; Bargou, R. C. STAT3 and MAPK signaling maintain overexpression of heat shock proteins 90a and b in multiple myeloma cells, which critically contribute to tumor-cell survival. *Blood* **2007**, 109, 720-728.
55. Shinozaki, F.; Minami, M.; Chiba, T.; Suzuki, M.; Yoshimatsu, K.; Ichikawa, Y.; Terasawa, K.; Emori, Y.; Matsumoto, K.; Kurosaki, T.; Nakai, A.; Tanaka, K.; Minami, Y. Depletion of hsp90b induces multiple defects in B cell receptor signaling. *J. Biol. Chem.* **2006**, 281, 16361-16369.
56. Liu, X.; Ye, L.; Wang, J.; Fan, D. Expression of heat shock protein 90b in human gastric cancer tissue and SGC7901/VCR of MDR-type gastric cancer cell line. *Chin. Med. J.* **1999**, 112, 1133-1137.
57. Sreedhar, A. S.; Csermely, P. Heat shock proteins in the regulation of apoptosis: new strategies in tumor therapy: a comprehensive review. *Pharmacol. Ther.* **2004**, 101, 227-257.

58. Gruppi, C. M.; Zakeri, Z. F.; Wolgemuth, D. J. Stage and lineage-regulated expression of two hsp90 transcripts during mouse germ cell differentiation and embryogenesis. *Mol. Reprod. Dev.* **1991**, 28, 209-217.
59. Vanmuylder, N.; Werry-Huet, A.; Rooze, M.; Louryan, S. Heat shock protein HSP86 expression during mouse embryo development, especially in the germ-line. *Anat. Embryol.* **2002**, 205, 301-306.
60. Dugyala, R. R.; Claggett, T. W.; Kimmel, G. L.; Kimmel, C. A. HSP90a, HSP90b, and p53 expression following in vitro hyperthermia exposure in gestation day 10 rat embryos. *Toxicol. Sci.* **2002**, 69, 183-190.
61. Cambiazo, V.; Gonzalez, M.; Isamit, C.; Maccioni, R. B. The b-isoform of heat shock protein hsp-90 is structurally related with human microtubule-interacting protein Mip-90. *FEBS Lett.* **1999**, 457, 343-347.
62. Zuehlke, A. D.; Beebe, K.; Neckers, L.; Prince, T. Regulation and function of the human HSP90AA1 gene. *Gene* **2015**, 570, 8-16.
63. Yufu, Y.; Nishimura, J.; Nawata, H. High constitutive expression of heat shock protein 90a in human acute leukemia cells. *Leuk. Res.* **1992**, 16, 597-605.
64. Bertram, J.; Palfner, K.; Hiddemann, W.; Kneba, M. Increase of P-glycoprotein-mediated drug resistance by hsp90b. *Anticancer Drugs* **1996**, 7, 838-845.
65. Chadli, A.; Felts, S. J.; Toft, D. O. GCUNC45 is the first Hsp90 co-chaperone to show a/b isoform specificity. *J. Biol. Chem.* **2008**, 283, 9509-9512.
66. Hua, Y.; White-Gilbertson, S.; Kellner, J.; Rachidi, S.; Usmani, S. Z.; Chiosis, G.; Depinho, R.; Li, Z.; Liu, B. Molecular chaperone gp96 is a novel therapeutic target of multiple myeloma. *Clin. Cancer Res.* **2013**, 19, 6242-6251.
67. Crowley, V. M.; Khandelwal, A.; Mishra, S.; Stothert, A. R.; Huard, D. J.; Zhao, J.; Muth, A.; Duerfeldt, A. S.; Kizziah, J. L.; Lieberman, R. L.; Dickey, C. A.; Blagg, B. S. Development of Glucose Regulated Protein 94-Selective Inhibitors Based on the BnIm and Radamide Scaffold. *J. Med. Chem.* **2016**, 59, 3471-3488.
68. Woodhead, A. J.; Angove, H.; Carr, M. G.; Chessari, G.; Congreve, M.; Coyle, J. E.; Cosme, J.; Graham, B.; Day, P. J.; Downham, R.; Fazal, L.; Feltell, R.; Figueroa, E.; Frederickson, M.; Lewis, J.; McMenamin, R.; Murray, C. W.; O'Brien, M. A.; Parra, L.; Patel, S.; Phillips, T.; Rees, D. C.; Rich, S.; Smith, D. M.; Trewartha, G.; Vinkovic, M.; Williams, B.; Woolford, A. J. Discovery of (2,4-dihydroxy-5-isopropylphenyl)-[5-(4-methylpiperazin-1-ylmethyl)-1,3-dihydrois oindol-2-yl]methanone (AT13387), a novel inhibitor of the molecular chaperone Hsp90 by fragment based drug design. *J. Med. Chem.* **2010**, 53, 5956-5969.
69. Woodhead, A. J.; Angove, H.; Carr, M. G.; Chessari, G.; Congreve, M.; Coyle, J. E.; Cosme, J.; Graham, B.; Day, P. J.; Downham, R.; Fazal, L.; Feltell, R.; Figueroa, E.; Frederickson, M.; Lewis, J.; McMenamin, R.; Murray, C. W.; O'Brien, M. A.; Parra, L.; Patel, S.; Phillips, T.; Rees, D. C.; Rich, S.; Smith, D. M.; Trewartha, G.; Vinkovic, M.; Woolford, A. J. Discovery of (2,4-dihydroxy-5-isopropylphenyl)-[5-(4-methylpiperazin-1-ylmethyl)-1,3-dihydrois oindol-2-yl]methanone (AT13387), a novel inhibitor of the molecular chaperone Hsp90 by fragment based drug design. *J. Med. Chem.* **2010**, 53, 5956-5969.
70. Itoh, Y.; Kitaguchi, R.; Ishikawa, M.; Naito, M.; Hashimoto, Y. Design, synthesis and biological evaluation of nuclear receptor-degradation inducers. *Bioorg. Med. Chem.* **2011**, 19, 6768-6778.

71. Nicolaou, K. C.; Estranda, A. A.; Zak, Mark.; Lee, S. H.; Safina, B. S. A Mild and Selective Method for the Hydrolysis of Esters with Trimethyltin Hydroxide. *Angew. Chem. Int. Ed*. **2005**, *44*, 1378-1382.
72. Rokade, B. V.; Prabhu, K. R. Chemoselective Schmidt Reaction Mediated by Triflic Acid: Selective Synthesis of Nitriles from Aldehydes. *J. Org. Chem.* **2012**, *77*, 5364-5370.

Chapter V

The Development of Hsp90α-Selective Inhibitors

V.1. Introduction

The development of isoform-selective inhibitors of the Hsp90 protein folding machinery represents a new paradigm for anti-cancer drug discovery.[1-8] The limited success of *pan*-inhibitors in clinical trials warrants the development of alternative strategies to modulate Hsp90.[9-11] Isoform-selective inhibitors represent one such approach as individual Hsp90 isoforms have been associated with oncogenesis and genetic knockdowns of individual isoforms resulted in depletion of selected oncogenic proteins.[2, 12-15] Towards this objective, Grp94-selective inhibitors (**BnIm**, **KUNG29**, **WS-13**) have been identified and are currently under investigation for the potential treatment of breast, blood, and liver cancer.[5, 8, 16, 17] Additionally, Grp94 inhibitors are being investigated for the treatment of glaucoma and metastatic cancer.[13] Chapter IV described development of the first Hsp90β-selective inhibitor (**KUNB31**) and preliminary studies show that Hsp90β-inhibition induced the degradation of client proteins without induction of Hsp90 and Hsp70 levels. Hence, Hsp90β-selective inhibitors may overcome the detriments of the heat-shock response, which is one of the major concerns associated with *pan*-Hsp90 inhibitors. While a Trap-1-selective inhibitor has yet to be identified, selective inhibition of Trap-1 has been accomplished by mitochondrial targeting methods.[4] Hence, for complete deconvolution of all Hsp90-isoforms, the development of Hsp90α-selective inhibitors was pursued and is described in this chapter.

V.1.1. Hsp90α Isoform

The Hsp90α isoform resides in the cytosol and is encoded by the HSP90AA1 gene.[18, 19] The primary amino acid sequence in Hsp90α is 86% identical and 93% similar to Hsp90β, while the N-terminal ATP binding site is more than 95% identical between these two isoforms.[20, 21] Prior

studies have identified only few biochemical differences between Hsp90α and Hsp90β.[22–25] Hsp90α readily dimerizes when compared to Hsp90β. Unlike Hsp90β, Hsp90α does not interact with microtubules. Hsp90α is more inducible than Hsp90β and its cellular roles involve growth promotion, cell cycle regulation, and stress-induced cytoprotection. Hsp90α knockout in mice was shown non-lethal and resulted in dysfunctional spermocytes in male mice.[26-28] Hsp90β-knockout in mice exhibit compromised cellular differentiation.[29] These studies suggest that unlike Hsp90β, Hsp90α is not essential for survival. However, Hsp90α has tissue specific roles that cannot be compensated by Hsp90β. Hsp90α is overexpressed in cancers and has been associated with poor prognosis of breast cancer, pancreatic carcinoma, and leukemia.[30-36] Prior studies have shown that genetic knockdown of Hsp90α results in the degradation several oncogenic client proteins. Therefore, the administration of an Hsp90α-selective inhibitors could selectively inhibit some cancers.

Hsp90α is responsible for the proliferation and metastasis of many cancers. Hsp90α is also responsible for hERG channel maturation and trafficking.[3] siRNA knockdown of Hsp90α disrupts hERG maturation, which may cause the cardiotoxicity observed with *pan*-Hsp90 inhibitors in the clinic. Despite this problems, selective inhibition of Hsp90α is of interest as a chemical probe to further delineate the biological impact of isoform-selective inhibition and to validate that small molecule inhibition of Hsp90α does in fact lead to the cardiotoxicity observed with its genetic knockdown. Maturation of Hsp90α client hERG channel occurs within the cell, while extracellular Hsp90α has been implicated as an anti-cancer target.[30, 34, 37, 38] Extracellular Hsp90α activates MMP-2 and promote tumor invasion .[39-41] Both the intra and extracellular functioning of Hsp90α

highlight the advantages of its selective inhibition, and studies to produce Hsp90α-selective inhibitors may be useful for anti-cancer applications.

V.2. Identification of a Lead Compound for the Development of Hsp90α-Selective Inhibitors

V.2.1. Binding of Radicicol and PU3 with Hsp90α versus Hsp90β

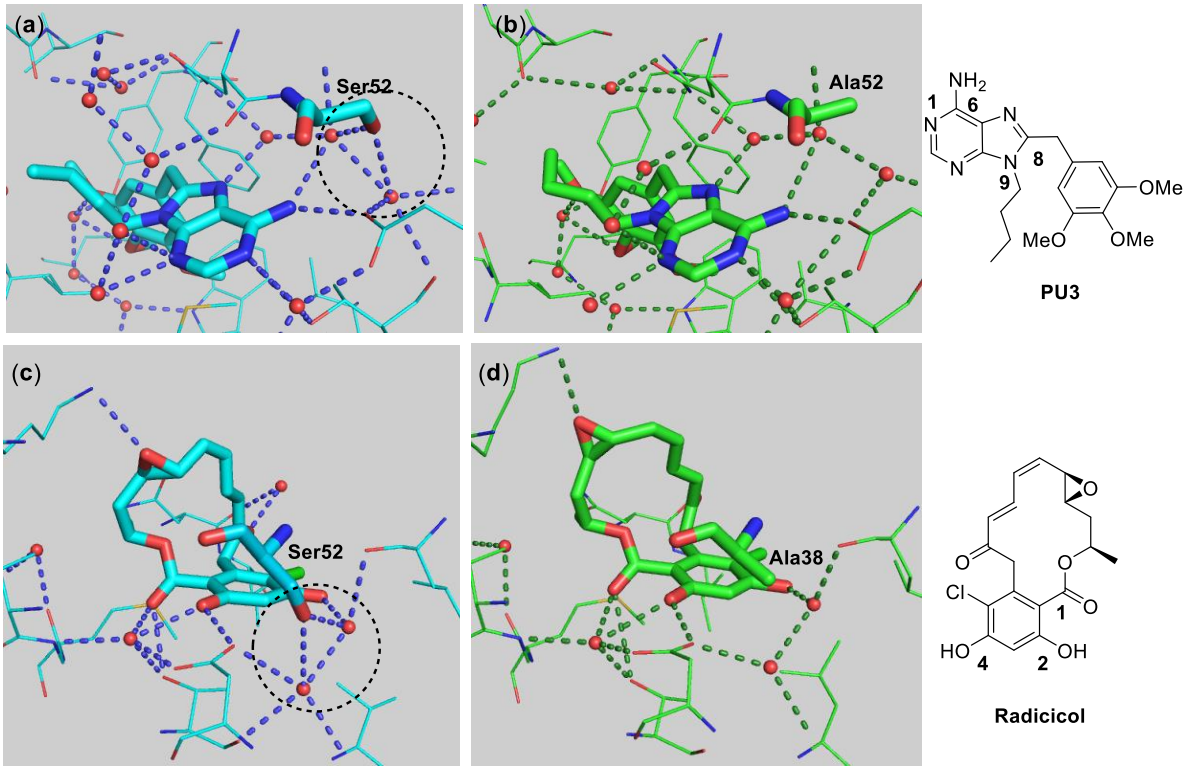

Figure 42. Differences in binding of ligands between Hsp90α and Hsp90β. (a) co-crystal structure of PU3 bound to Hsp90α (PDB: 1UY6); (b) co-crystal structure of PU3 bound to Hsp90β (PDB: 1UYM); (C) co-crystal structure of radicicol bound to Hsp90α (PDB: 4EKG); (d) co-crystal structure of radicicol bound to Hsc82 (PDB: 1BGQ).

Hsp90α and Hsp90β share more than 95% similarity in their N-terminal ATP-binding pocket. As described in chapter IV, only two amino acids differ in the ATP-binding pocket of Hsp90α (Ser52, Ile91) and Hsp90β (Ala52, Leu91). The bulkier side chains of Ser52 and Ile91 in Hsp90α produced a steric clash with Hsp90β-selective inhibitor, **KUNB31**, providing selectivity for Hsp90β. For the development of an Hsp90α-selective inhibitor, these steric interactions would

not be relevant. Hence, the hydrogen bonding interactions manifested by the phenols with Ser52 (Ala in other three isoforms) were sought for further evaluation.

Purine derived compound, **PU3**, is the only known Hsp90 inhibitor that has been co-crystallized with both Hsp90α and Hsp90β (PDB: 1UYM and 1UY6). A comparison of the two co-crystal structures revealed that **PU3** binds to both isoforms similarly.[42] The only difference in binding is the interaction between the N-6 amine and Ser52 (Figure 42a & 42b) in Hsp90α. The N-6 amine produces two additional water-mediated hydrogen bonding interactions with Ser52 of Hsp90α. These interactions are not present in Hsp90β due to the presence of Ala52. Similar to purine-derived inhibitors, resorcinol-based inhibitors also produce a stronger hydrogen bonding network with Hsp90α. Radicicol has never been co-crystallized with Hsp90β; its co-crystal structures with Hsp90α and Hsc82 (yeast homologue of Hsp90) have been solved.[43] Comparison of the primary sequences of these proteins shows that Hsc82 contains Ala38, in lieu of Ser52 in Hsp90α, and Ala52 in Hsp90β, and is more similar to Hsp90β (Table 15). Evaluation of the co-crystal structure of radicicol bound to Hsp90α shows that the presence of Ser52 (Figure 42c & 42d), as opposed to Ala52 in Hsp90β, results in a stronger hydrogen bonding network. Conserved water molecules in Hsp90α coordinate with Ser52, whereas in Hsp90β/Hsc82, Ala52 alters this spatial arrangement.

Table 15. Difference in Hsp90α, Hsp90β, and yeast Hsp90 (Hsc82) ATP binding pocket

Protein	**Residues (numbered for Hsp90α)**				
	52	**91**	**92**	**141**	**154**
Hsp90α	Ser	IlE	Val	Ala	His
Hsp90β	Ala	Leu	Val	Ala	His
Hsc82	Ala	Ile	Ile	Arg	Ser

Interestingly, these additional hydrogen bonds result in only 3-fold selectivity for Hsp90α versus Hsp90β as radicicol manifested an apparent K_d of 4 nM for Hsp90α versus 15 nM for Hsp90β in a thermal shift calorimetry assay.[20] Prior studies by Vilma and co-workers have provided insights into the differences in binding of radicicol to both cytosolic isoforms. The intrinsic enthalpy of binding (ΔH) for radicicol is 10 kJ higher for Hsp90α than Hsp90β, which should result in a greater difference in dissociation constants (K_d). However, binding of radicicol to Hsp90β results in greater entropy when compared to Hsp90α, which accounts for the observed difference in dissociation constants. This observation can be rationalized by greater hydrophobicity with Hsp90β when compared to Hsp90α (Table 16), and consequently radicicol produces more hydrophobic interactions within the Hsp90β binding pocket and results in greater entropy contribution.[44] Collectively, these studies suggest that the interactions manifested by the ligand with Ser52 are critical for the development of an Hsp90α-selective inhibitor.

Table 16. Relative hydrophobicity of Hsp90 isoforms

Protein	Hydrophobic	Hydrophilic	Ratio
Hsp90α	1.46	0.97	1.5
Hsp90β	1.73	0.82	2
Grp94	2.98	0.63	5
Trap-1	2.2	0.72	3

V.2.2. Synthesis and Evaluation of 4-Amino 2-Phenol Analogues

The development of Hsp90α-selective inhibitors commenced via optimization of the 5-bromo resorcinol compound, **61** (Chapter III) to probe the hydrogen bonding interactions with Ser52. At first, conversion of the 4-phenol to the aniline was proposed. The 5-bromo substituent was replaced with an isopropyl group, and analogues with electron withdrawing groups on the nitrogen were also evaluated. Syntheses of the proposed analogues (**109**, **111–113**, Scheme 17)

commenced via bromination of the 4-amino-2-methoxybenzoic acid (**107**) to give **108**. Carbodiimide coupling of the acid (**108**) with isoindoline gave **109**, which upon methyl ether cleavage using boron tribromide gave the desired product, **110**. Suzuki coupling of **109** with potassium isopropenyl trifluoroborate, followed by palladium-catalyzed hydrogenation under a hydrogen atmosphere furnished the 5-isopropyl intermediate **111**, which upon treatment with boron tribromide gave **112**. The aniline was modified to the corresponding cyanamide by enlisting cyanogen bromide.

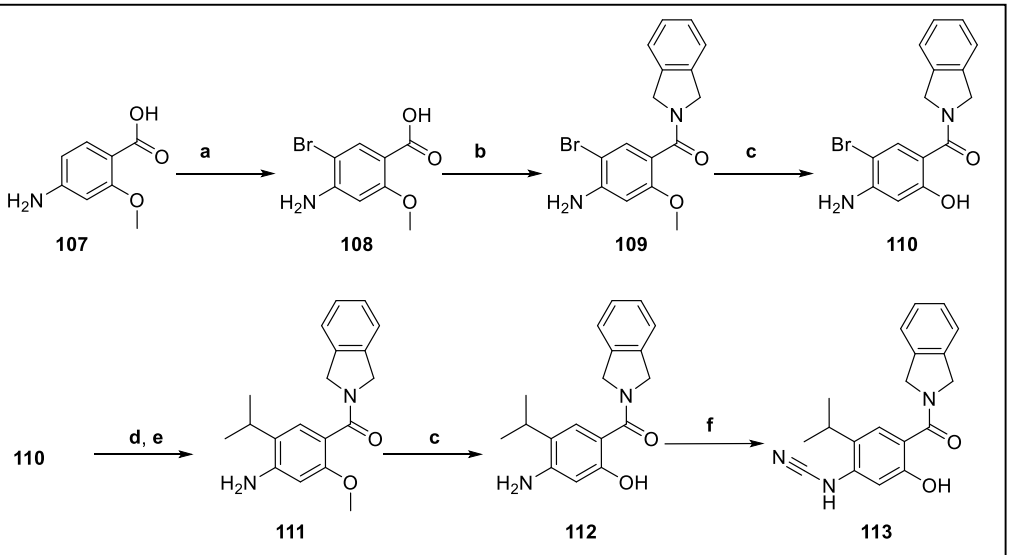

Reagents: (a) Br_2; (b) isoindoline hydrochloride, EDCI, HOBt, N,N-diisopropylethylamine; (c) BBr_3; (d) potassium isopropenyltrifluoroborate, $Pd(PPh_3)$, Cs_2CO_3; (e) Pd/C, H_2; (f) CNBr

Scheme 17. Syntheses of 4-amino-2-phenol analogues.

The 4-amino-2-phenol analogues **110**, **112**, and **113** were evaluated in a fluorescence polarization assay and did not exhibit selectivity for Hsp90α (Table 17). These analogues were less efficacious than the corresponding 4-phenol (**61**). This data suggested that the 4-phenol is producing more efficacious interactions with Ser52 than the corresponding aniline.

Table 17. Evaluation of 4-amino-2-phenol analogues

Compound	Apparent K_d Hsp90α (μM)	Apparent K_d Hsp90β (μM)	Selectivity for Hsp90α
61	0.025 ± 0.01	0.033 ± 0.01	-
110	0.22±0.01	0.50±0.01	2
112	0.46±0.22	0.71±013	1.5
113	0.18 ± 0.01	0.42 ± 0.05	2

In a parallel, additional scaffolds were also evaluated for selective Hsp90α inhibition. As shown in Figure 43, the 3-position of resorcinol moiety was modified to improved interactions with Ser52 (**KUNA01**, **KUNA02**). Unfortunately, an Hsp90α-selective inhibitor could not be identified. Research groups from academia and industry screened several known Hsp90 inhibitors to identify isoform-selective inhibitors but these efforts were not productive.[2, 45, 46]

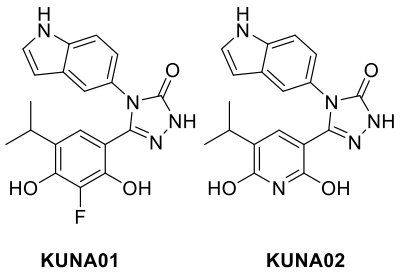

Figure 43. Additional studies towards selective Hsp90α-inhibition.

V.2.3. Identification of the Monophenol-Isoindoline Scaffold for Selective Hsp90α-Inhibition

After these failed attempts, a different strategy was devised to exploit the hydrogen bonding network that surrounds the resorcinol ring. As previously mentioned, only the 4-phenol of the resorcinol interacts with Ser52 in Hsp90α (Ala in Hsp90β, Grp94, and Trap1). Hence it should drive selectivity for Hsp90α. The 2-phenol interacts similarly with both the Hsp90α and Hsp90β ATP-binding pockets (Figure 42). While collectively the resorcinol moiety results in 3-fold selectivity for

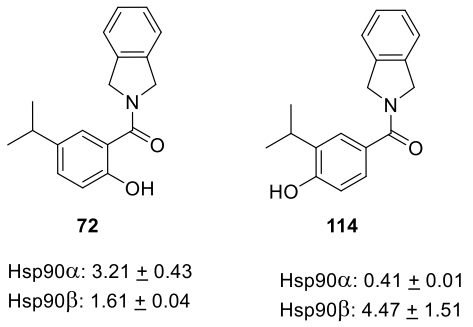

Figure 44. Apparent K_d of monophenol analogues.

Hsp90α, the individual contribution of each phenol had never been evaluated for binding with individual isoforms. Therefore, compounds that lacks the 4-phenol were considered for evaluation. We had access to compound **72**, that lacks 4-phenol (Chapter IV). Additionally, compound **114**, which lacks the 2-phenol was synthesized using a reported procedure.[47] These compounds were evaluated in a fluorescence polarization assay and their binding affinities for Hsp90α and Hsp90β were determined. While compound, **72** manifested 2-fold selectivity for Hsp90β, compound **114** bound Hsp90α with 10-fold selectivity. The selectivity of **114** confirmed our hypothesis that exclusive interactions of the 4-phenol with Ser52 could lead to an Hsp90α-selective inhibitor. Therefore, further development of **114** was pursued.

V.3. Development of the Monophenol-Isoindoline Scaffold for Selective Hsp90α Inhibition

It was proposed that substituents at the 4- and 5-positions may change the electronic nature and spatial arrangement of the 4-phenol and alter its hydrogen bonding interactions with Ser52. Therefore, two different series were proposed for investigation of **114** analogues: (1) replacements of the 4-phenol, and (2) Modification of the 5-position of the resorcinol. Initially, replacement of the 4-phenol with the corresponding aniline and meothoxy group were proposed, as well as heterocycles adjoining the 4- and the 5-positions (Series I, Figure 45). In a second series, modifications of the 5-position were also pursued (Series II, Figure 45)

V.3.1. Syntheses of Series I and Series II Analogues

Compound **115**, **121**, and **126** were synthesized following a literature procedure.[47] The synthesis of **116** commenced with 4-amino benzoic acid, which upon electrophilic bromination and subsequent carbodiimide coupling with isoindoline gave **132**. Suzuki coupling of **132** with isopropenyl trifluoroborate and subsequent hydrogenation of the olefin gave the desired analogue **116**.[48] Analogues **117–120** were synthesized by an EDCI-mediated coupling of isoindoline with

commercially available appropriate heterocyclic carboxylic acids. Analogues **129–130** were synthesized from **128**, which upon treatment with sodium borohydride and methyl magnesium bromide gave **129** and **130**, respectively (Scheme 18).

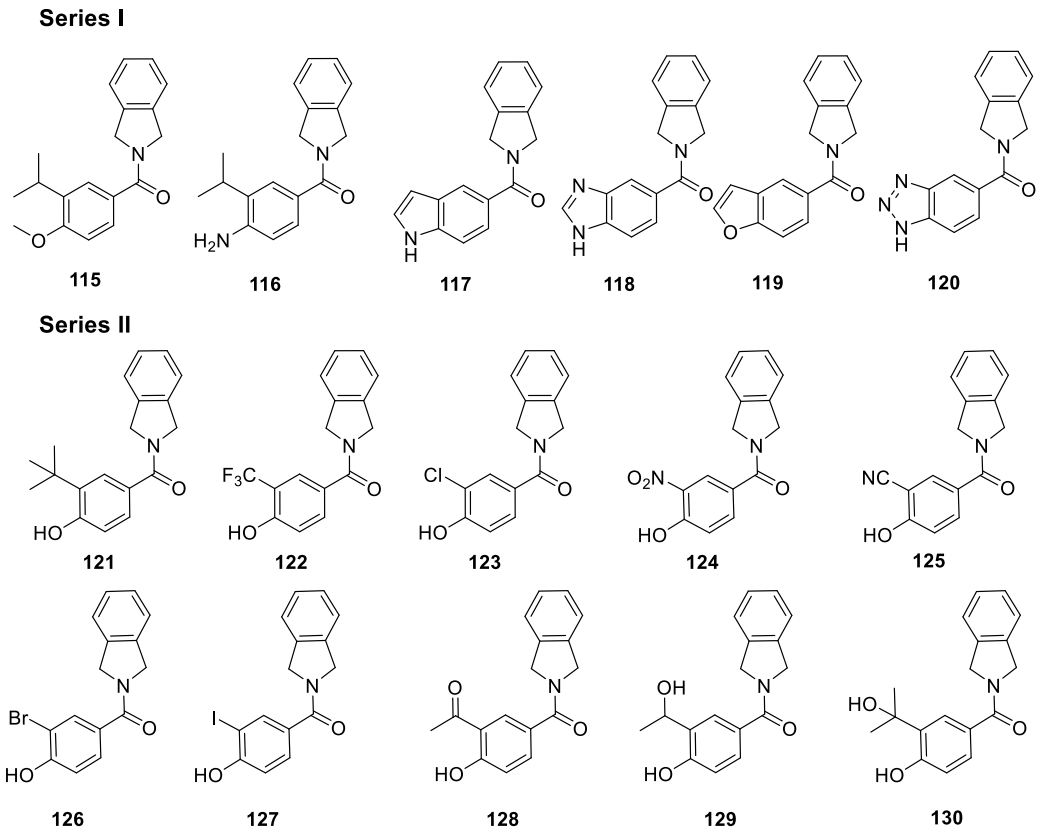

Figure 45. Proposed modifications on monophenol-isoindoline scaffold.

V.3.2. Evaluation of Series I and Series II Analogues

Upon preparation, compounds **115–130** were evaluated in a fluorescence polarization assay. As shown in Table 18, replacement of the 4-phenol with an aniline (**116**) or methyl ether (**115**) decreased affinity, which suggested that the 4-phenol acts as a hydrogen bond donor. The heterocycles were also inactive, which suggests that spatial arrangement of the hydrogen bond donor at the 4-position is important. Replacement of the isopropyl with a chlorine, bromine, or *tert*-butyl substituents enhanced selectivity for Hsp90α. Analogue **130** manifested the highest

affinity for Hsp90α, which indicated potential interactions of the tertiary alcohol with Asn84. Compound **126** was chosen for further optimization based on these observed trends.

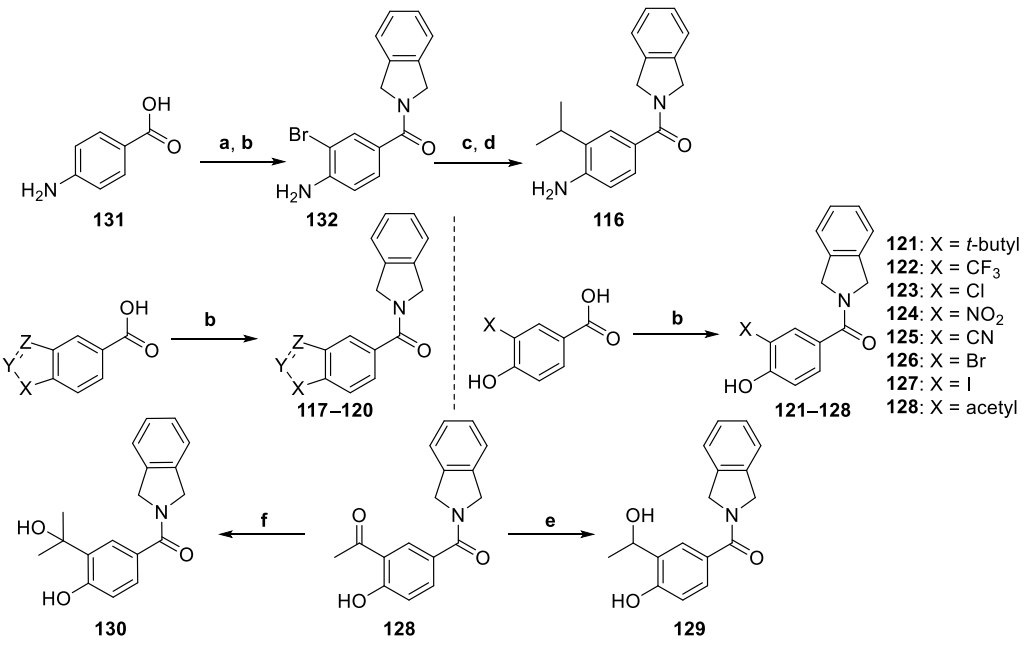

Reagents: (a) NBS; (b) isoindoline hydrochloride, EDCI, HOBt, N,N-diisopropylethylamine; (c) potassium isopropenyltrifluoroborate, $Pd(dppf)Cl_2$, Et_3N (d) Pd/C, H_2; (e) $NaBH_4$; (f) MeMgBr

Scheme 18. Syntheses of Series I and Series II analogues for selective Hsp90α-inhibition

V.4. Modification to the Isoindoline Core of 126

Prior studies on the resorcinol-isoindoline scaffold have shown that modifications to the 5-position of the isoindoline ring system modulate Hsp90 affinity and cellular efficacy.[47, 48] The co-crystal structure of compound **121** bound to Hsp90α has been reported previously, which shows that the benzene ring of the isoindoline projects towards the solvent exposed region of the N-terminal ATP-binding site (Figure 46a).[47] Substituents at the 5-position of the isoindoline may interact with the surrounding hydrophilic residues (Asp54, Lys58, Figure 46a). Therefore,

compounds **133–138** were proposed (Figure 46b). Additionally, an analogue containing a 2,3-dihydro-1H-pyrrolo[3,4-c]pyridine in lieu of isoindoline was also sought.

Table 18. The evaluation of Series-I and Series-II analogues

Compound	Apparent K_d Hsp90α (μM)	Apparent K_d Hsp90β (μM)	Selectivity for Hsp90α
115	68.09 ± 3.96	>100	2-fold
116	>100	>100	-
117	>100	>100	-
118	>100	>100	-
119	>100	>100	-
120	>100	>100	-
121	2.62 ± 0.08	>200	>75-fold
122	7.90 ± 1.18	>200	>25-fold
123	4.69 ± 0.27	>200	>42-fold
124	>100	>100	-
125	>100	>100	-
126	2.73 ± 0.19	>200	>73-fold
127	>100	>100	-
128	>100	>100	-
129	7.11 ± 0.42	57.17 ± 0.88	8-fold
130	0.65 ± 0.04	12.92 ± 1.92	19-fold

V.4.1. Synthesis of Analogues with Modification to the Isoindoline Core

The proposed analogues **133–138** were prepared via an EDCI-mediated coupling of 3-bromo-4-hydroxybenzoic acid (Scheme 19) with the requisite isodindolines. **138** was prepared by methyl ether cleavage of **137** using boron tribromide.

V.4.2 Evaluation of Analogues with Modification to the Isoindoline Core

The isoindoline analogues **133–139** were evaluated in a fluorescence polarization assay**.** Incorporation of bulkier substituents on the isoindoline ring did not improve Hsp90α affinity

(Table 19). However, introduction of a fluorine, chlorine or phenol substituents was tolerated at the 5-position. The inclusion of a bulkier bromine and methyl ester decreased affinity.

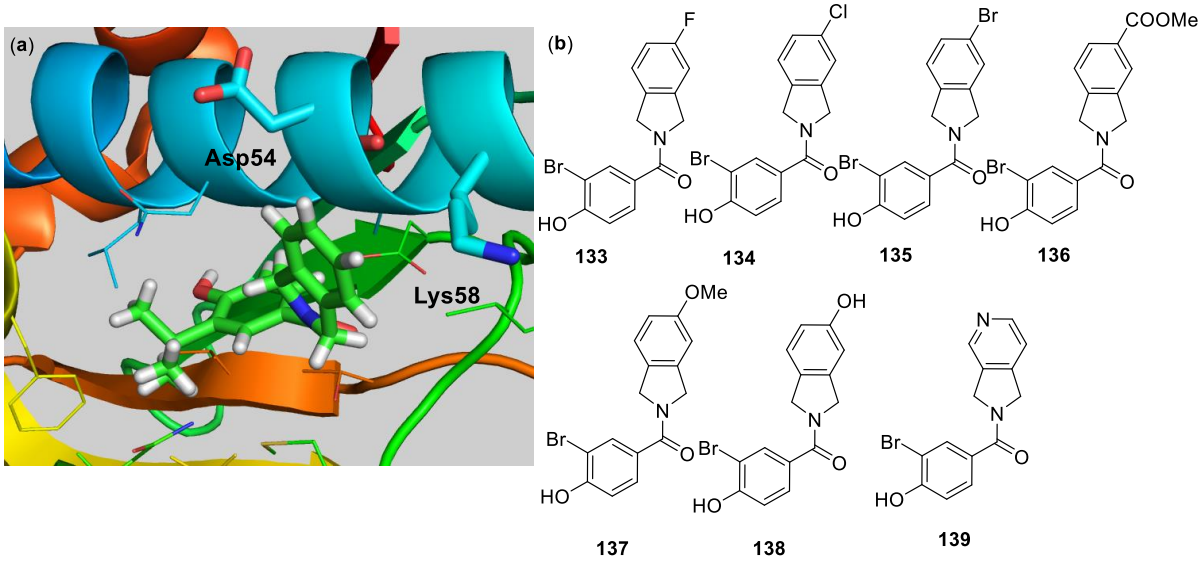

Figure 46. Proposed modification to isoindoline core. (a) Previously reported co-crystal structure of **121** (PDB: 3XHX) (b) Proposed isoindoline analogues

V.5. Preliminary Studies to Probe the Inducible Binding Pocket

Prior studies demonstrated conformational flexibility in amino acid residues **104–111** of Hsp90α/Hsp90β, as they can adopt various conformations (α-helix, closed loop, and open loop) upon binding to an inhibitor.[45] These conformational variations produce an additional binding pocket within the Hsp90α/Hsp90β ATP binding site, which can produce beneficial interactions with inhibitors.[49, 50] A survey of the co-crystal structures bound to various ligands provided further insights. The purine and benzamide class of Hsp90 inhibitors induced this additional binding pocket, whereas the resorcinol and ansamycin classes of inhibitors did not. Structurally, induction of this additional binding pocket has been associated with three-dimensional conformations of the amino acid residues 104–111.[51-54] As shown in Figure 47, these residues adopt an α-helix

(BIIB021), an open loop (17-DMAG), or a closed loop (AUY-922) conformation. The additional binding pocket is induced only when these residues adopt the α-helix conformation in the case of BIIB021bound to Hsp90α. However, when these residues adopt an open or a closed loop conformation, the binding pocket is blocked by Phe124. Recently, Shen and co-workers obtained a co-crystal structure of resorcinol-derived inhibitor that demonstrated an additional binding pocket about the 5-position of the resorcinol ring.[55] In the co-crystal structure, the residues 104–111 were shown to adopt a α-helix conformation. This was the first time when a resorcinol-based compound, similar to purine-based inhibitors, was shown to induce the additional binding pocket about the 5-position of resorcinol ring.

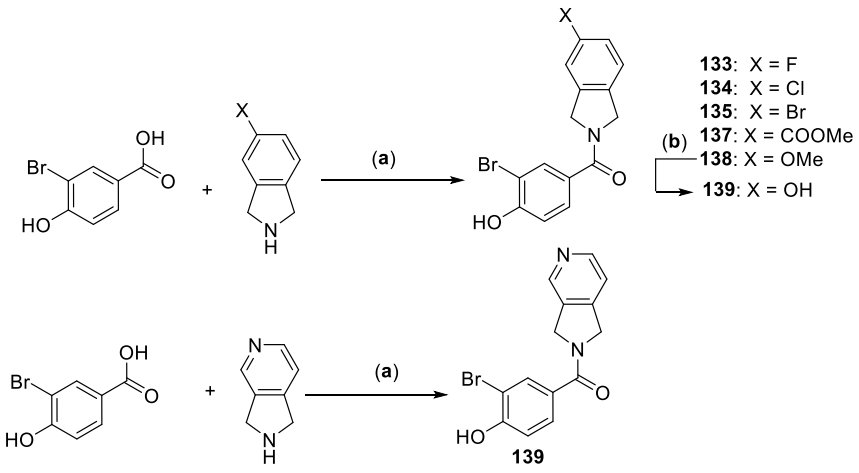

Scheme 19. Modifications to the isoindoline core.

As shown in Chapter III, our resorcinol based inhibitors were expected to induce a similar binding pocket as the incorporation of benzyl thioethers (**65–68**) and phenyl amines (**64**) were more beneficial than the corresponding 5-bromo containing compound (**61**). To determine whether a similar binding pocket can be induced with the monophenol **126**, two analogues **140** and **141** were proposed (Scheme 20). Preparation of these analogues is described in Scheme 20. The 4-

phenol on 3-bromo-4-hydroxybenzic acid was modified to the corresponding benzyl ether, which upon carbodiimide coupling with isoindoline afforded **142**. Subsequent palladium-catalyzed coupling of **142** with thiophenol or N-methyl aniline, followed by cleavage of benzyl ethers using boron tribromide afforded **140** and **141**, respectively. Analogue **141** manifested a 3-fold improvement in affinity as compared to **126**, whereas thiophenyl ether **140** manifested similar affinity as **126**.

Table 19. Evaluation of isoindoline analogues in FP assay

Compound	Hsp90α	Hsp90β	Selectivity for Hsp90α
133	8.04 ± 0.15	>200	>24-fold
134	6.17 ± 1.24	>200	>32-fold
135	>200	>200	-
136	94.47 ± 27.31	>200	>2-fold
137	11.59 ± 2.62	>200	>17-fold
138	13.25 ± 3.20	>200	>15-fold
139	8.21 ± 0.59	>200	>24-fold

This data suggests that the thiophenyl ether and the N-phenylamine substituents are tolerated at the 5-position. Therefore, modification to the 5-position of **126** induces this conformational change and creates the additional binding pocket. While these analogues maintained high selectivity for Hsp90α over Hsp90β-isoform, their selectivity over Grp94 was only ~5-fold, due to the binding of these substituents in adjacent Grp94-exclusive binding pocket (discussed in Chapter III). These findings are highly important and suggests this sub-pocket can be probed for to attain better Hsp90α inhibitors.

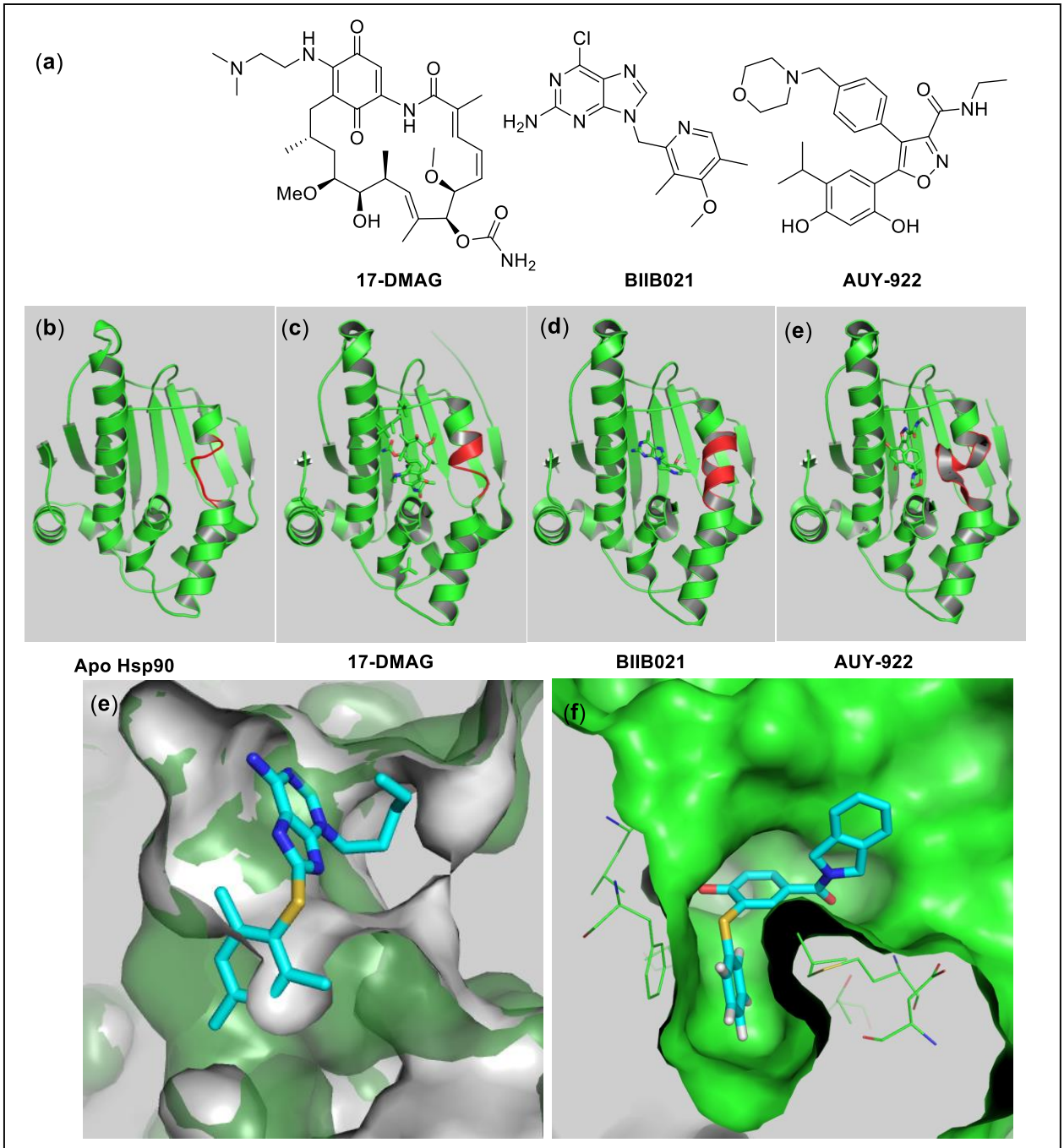

Figure 47. Binding modes of ligands in Hsp90α N-terminal binding pocket. (a)Structure of 17-DMAG, BII021, and AUY 922; (b) Apo-Hsp90α (PDB: 1YER); (b) 17-DMAG (PDB: 1OSF); (c) BII021 (PDB: 3qdd); (d)AUY922 (PDB: 2VCI); (e) Overlay of co-crystal structure of Apo-Hsp90α (gray)with BIIB021 bound to Hsp90α (green); (f) Proposed binding mode of **140** in Hsp90α binding pocket.

V.6. Cellular Efficacy of Hsp90α-Selective Inhibitors

Once the Hsp90α-selective inhibitors were identified, cellular studies commenced to evaluate the effect of Hsp90α-inhibition on the growth of breast cancer cell lines (MCF-7 and SkBr3). The anti-proliferation activities are summarized in Table 19. **126** manifested an IC_{50} of 48.34 ± 5.64 μM and 40 ± 3.21 μM against the MCF-7 and Skbr3 cancer cell lines, respectively.

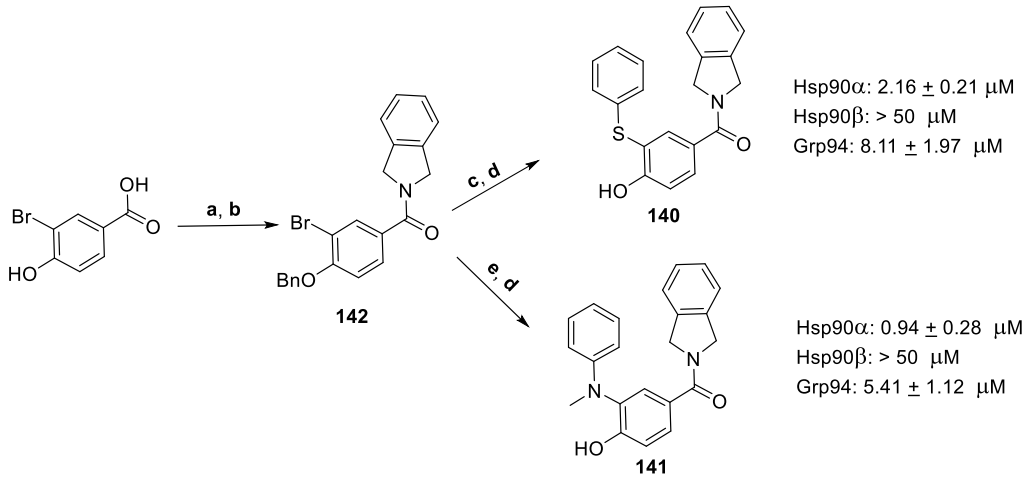

Reagents: (a) (i)BnBr, K_2CO_3, (ii) NaOH; (b) EDCI, HOBt, Isoindoline; (c) thiophenol, $Pd_2(dba)_3$, Hunig's base, DPPF; (d) BBr_3; (e) N-methyl aniline, $Pd_2(dba)_3$, NaO^tBu, RuPhos.

Scheme 20. Syntheses and evaluation of compounds **140** and **141**.

Interestingly, 5-*tert* butyl analogue, **121**, manifested a 6-fold improvement in cellular efficacy. Incorporation of a fluorine or a chlorine substituent at the 5-position of the isoindoline also improved anti-proliferation activity. Similarly, the thiophenyl ether analogue **140** was also more efficacious, and manifested an IC_{50} of 11.57 ± 1.16 μM and 12.96 ± 1.67 μM against the MCF-7 and SKBr3 cell lines, respectively.

V.7. Western Blot Analyses of Compound 126

Prior studies in the Blagg laboratory have led to the identification of a few Hsp90α-selective and Hsp90β-selective clients via genetic knockdown of individual isoforms in PC3 cells (Figure 48). These studies identified $CXCR_4$ and CDK6 as Hsp90β-dependent clients, whereas

survivin, Raf, c-Src, and hERG were identified as the Hsp90α-dependent client proteins. Additionally, Erk5, and Akt were degraded upon knockdown of either Hsp90α or Hsp90β, indicating an overlapping roles for both isoforms. To verify these findings, western blot analyses were conducted on PC cell lysates that were treated with the Hsp90α-selective inhibitor **126**. As shown in Figure 46, **126** induced the degradation of Hsp90α client protein Raf. Additionally, levels of Akt and Her2 were also degraded. In contrast to genetic knock down studies, levels of CDK6 were also depleted, which indicates a difference between the genetic knockdown and pharmacological studies.

Table 20. Evaluation of Hsp90α-selective inhibitors in MTS assay

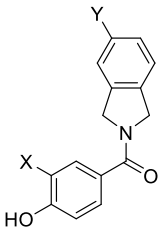

121: X = *tert*-butyl, Y = H
126: X = Br, Y = H
130: X = 4-hydroxy-3-(2-hydroxypropan-2-yl, Y = H
133: X = Br, Y = F
134: X = Br, Y = Cl
140: X = thiophenyl, Y = H
141: X= methyl phenylamino, Y = H

Compound	MCF-7	SKBr3
121	7.32 ± 1.19	8.87 ± 2.23
126	48.34 ± 5.64	40 ± 3.21
130	20.51± 3.93	22.29 ± 2.61
133	22.36 ± 2.76	5.17 ± 1.16
134	9.69 ± 1.71	7.28 ± 2.68
140	11.57 ± 1.16	12.96 ± 1.67
141	11.77 ± 1.05	10.22 ± 2.10

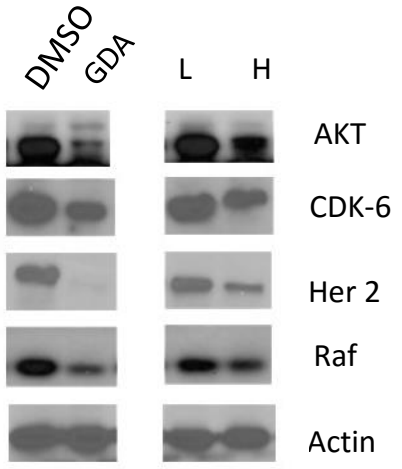

Figure 48. Western Blot analyses of **126** in PC3-MM2 cell. "H" represents a concentration 3 × IC_{50}; while "L" represents a concentration of 0.5 × IC_{50}. IC_{50} of KUNA21 was determines as 72 μM in PC3-MM2 cells.

V.8. Evaluation of Compound 126 and KUNB31 in NCI-60 Cell Panel

The isoform selective-inhibitors **126** and **KUNB31** were also evaluated in a NCI-60 panel to evaluate the dependence of different cancers upon individual Hsp90 isoforms. The screening results showed that isoform-selective inhibitors affect cancer cell lines differently that *pan*-inhibitors. While the Hsp90α selective inhibitor, compound **126**, was more efficacious against A549, NCI-H322, HT29, and OVCAR-5 cancer cell lines (Figure 49), the Hsp90β-selective inhibitor, **KUNB31**, manifested higher efficacy against MOLT-4, NCI-H23, SNB-75, MCF-7, and MDA-MB231 cells (Figure 50). These studies confirm that isoform-selective inhibitors modulate different cancer pathways and provide a more selective approach to treat various cancers.

V.9. Conclusions and Future Directions

By taking advantage of the hydrogen boding network that aligns at the bottom of the Hsp90 ATP-biding pocket, the first Hsp90α-selective inhibitors have been identified. We have shown that the hydrogen bonding interaction manifested by the 4-phenol of the resorcinol-based Hsp90 inhibitors with Ser52 provides selectivity for Hsp90α. Modification of **126** resulted in analogues that potentially change the conformation of Hsp90α and open an extended binding pocket near the 5-position of the resorcinol ring. These compounds showed growth inhibitory activity against the

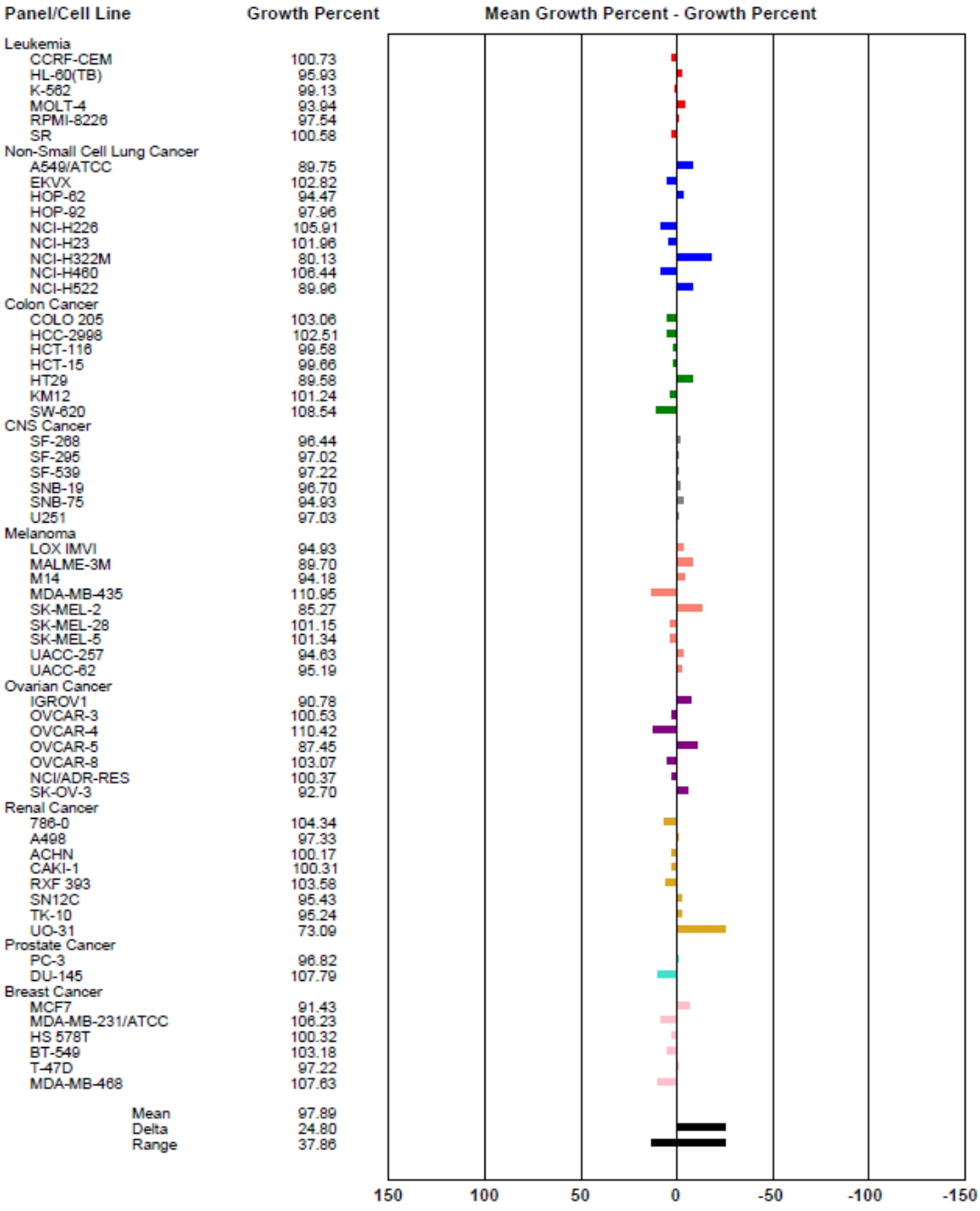

Figure 49. Evaluation of compound **126** in NCI-60 cell panel.

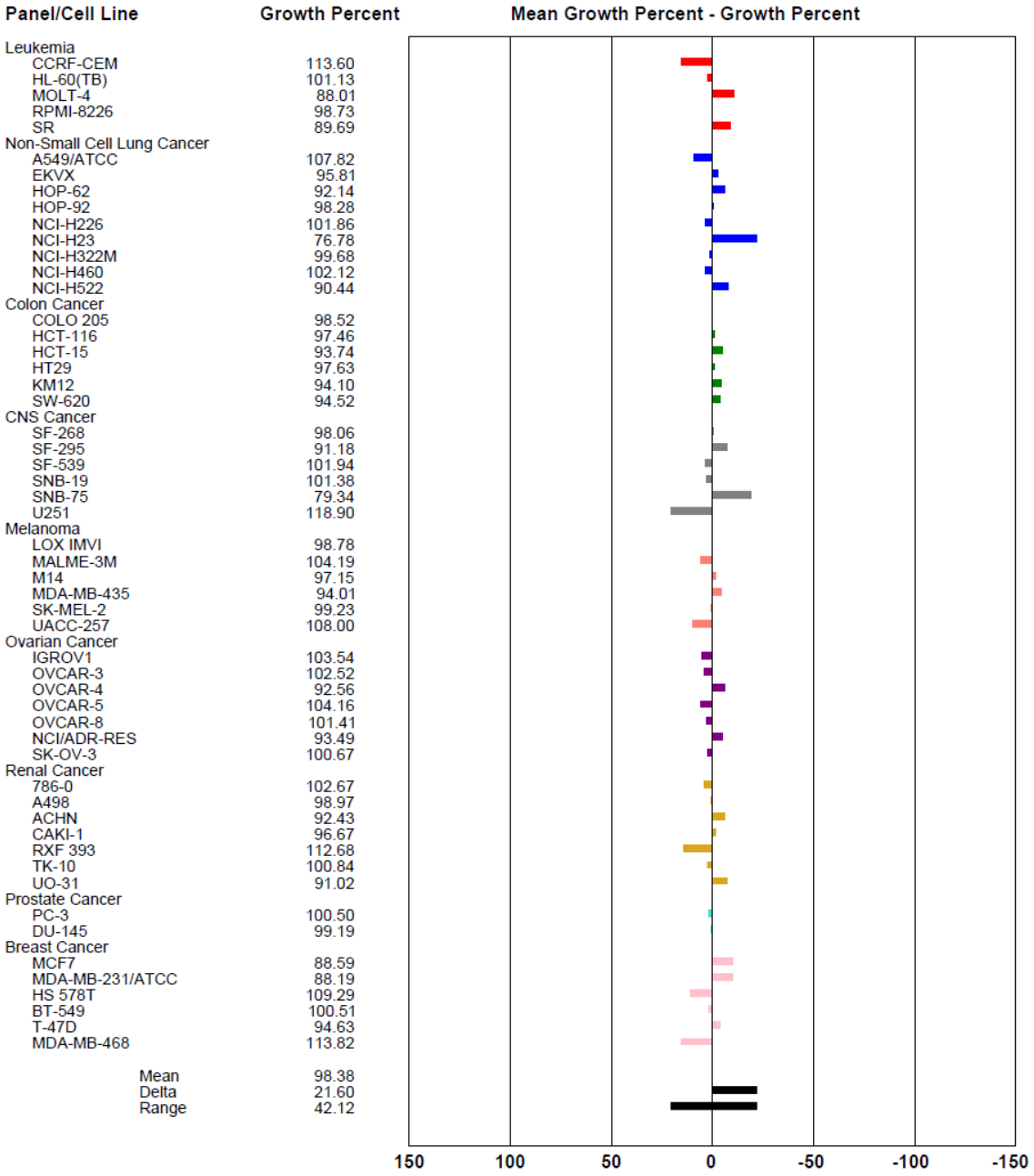

Figure 50. Evaluation of **KUNB31** in NCI-60 cell panel.

MCF-7 and SkBr3 cell lines and represent a new class of Hsp90 inhibitors for the treatment of cancer. Co-crystallization of these inhibitors is currently in progress in collaboration with Dr. Robert Matts at the Oklahoma State University.

Isoform-selective inhibition of Hsp90 represents an innovative approach that has the potential to overcome the detriments associated with current *pan*-Hsp90 inhibitors. Our efforts have provided isoform-selective inhibitors for three of the four Hsp90 isoforms. NCI-60 panel screening of compound **126** and **KUNB31** identified cancer cell lines that are more sensitive to inhibition of the Hsp90α and Hsp90β isoforms, respectively. These findings provide a clinical potential for each class of Hsp90 isoform-selective inhibitor. In addition, future studies that utilize Hsp90α-, Hsp90β-, and Grp94-selective inhibitors will also enhance our understanding of the dependence of client proteins upon each isoform and may provide opportunities to target a more selective group of cancers.

V.10. Methods and Experiments

All reactions were performed in oven-dried glassware under argon atmosphere unless otherwise stated. Dichloromethane (DCM), tetrahydrofuran (THF), and toluene were passed through a column of activated alumina prior to use. Anhydrous methanol, acetonitrile, and *N*-methyl-2-pyrrolidone (NMP) were purchased and used without further purification. Flash column chromatography was performed using silica gel (40−63 μm particle size). The ^{1}H (500 and 400 MHz) and ^{13}C NMR (125 and 100 MHz) spectra were recorded on 500 and 400 MHz spectrometer. Data are reported as p = pentet, q = quartet, t = triplet, d = doublet, s = singlet, br s = broad singlet, m = multiplet; coupling constant(s) in Hz. Infrared spectra were obtained using FT/IR spectrometer. High resolution mass spectral data were obtained on a time-of-flight mass spectrometer and analysis was performed using electrospray ionization.

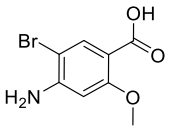

4-Amino-5-bromo-2-methoxybenzoic acid (108): N-bromosuccinimide (2.79 g, 15.7 mmol, 1.05 eq.) was added to a solution of **107** (2.5 g, 14.9 mmol, 1.0 eq.) in acetonitrile (75 mL). The resulting mixture was heated at 60 ^{o}C for 14 h, cooled to rt, diluted with water (100 mL), and extracted with ethyl acetate (3 × 100 mL). The combined organic layers were washed with saturated sodium chloride solution, dried over sodium sulfate, filtered, and concentrated to give 4-amino-5-bromo-2-methoxybenzoic acid (2.80 g, 77.1 %) as light brown amorphous solid. ^{1}H NMR (500 MHz, DMSO-d_6) δ 11.87 (s, 1H), 7.73 (s, 1H), 6.44 (s, 1H), 6.04 (s, 2H), 3.72 (s, 3H). ^{13}C NMR (125 MHz, DMSO) δ 165.3, 160.2, 150.8, 135.9, 108.2, 97.7, 97.0, 55.5. HRMS (ESI–) m/z [M – H^{+}] calcd for $C_9H_7BrNO_3$, 255.9609, found 255.9604.

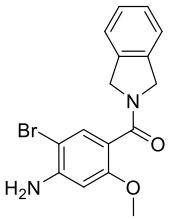

(4-Amino-5-bromo-2-methoxyphenyl)(isoindolin-2-yl)methanone (109): 1-Ethyl-3-(3-dimethylaminopropyl)carbodiimide (3.89 g, 20.32 mmol, 2.0 eq.) was added to a stirred solution of **108** (2.5 g, 10.16 mmol, 1 eq.), isoindoline hydrochloride (2.05 mg, 13.20 mmol, 1.3 eq.), 1-hydroxybenzotriazole (3.11 g, 20.32 mmol, 2 eq.) *N*,*N*-diisopropylethylamine (5.30 mL, 30.48 mmol, 3.0 eq.) in dichloromethane (100 mL) at 0 °C. The resulting solution was stirred at rt for 14 h before quenching with saturated sodium bicarbonate solution (100 mL). The organic layer was washed sodium chloride solution (100 mL), dried over sodium sulfate, filtered and concentrated. The residue was purified by flash chromatography (SiO_2, 1:3 hexanes/ethyl acetate) to afford **109**

(2.31 g, 65.7%) as a colorless oil. ^{1}H NMR (500 MHz, $CDCl_3$) δ 7.38 (s, 1H), 7.35 – 7.25 (m, 3H), 7.18 – 7.13 (m, 1H), 6.35 (s, 1H), 4.96 (s, 2H), 4.66 (s, 2H), 4.29 (s, 2H), 3.78 (s, 3H). ^{13}C NMR (125 MHz, $CDCl_3$) δ 167.5, 156.2, 146.3, 136.9, 136.7, 131.9, 127.8, 127.6, 123.2, 122.7, 118.4, 99.9, 98.6, 56.0, 53.6, 52. HRMS (ESI+) m/z [M + H^+] calcd for $C_{16}H_{16}BrN_2O_2$, 347.0395, found 347.0398.

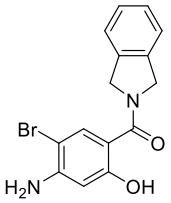

(4-Amino-5-bromo-2-hydroxyphenyl)(isoindolin-2-yl)methanone (110): 1 M solution of boron tribromide (0.60 mmol, 0.60 mL, 2 eq.), was added to a solution of **109** (104.2 mg, 0.30 mmol) in anhydrous dichloromethane (6 mL) at 0 °C. The resulting mixture was stirred at rt for 14 h before quenching with saturate sodium bicarbonate solution (5 mL). The aqueous layer was extracted with dichloromethane (2 × 10 mL). The combined organic layers were washed with saturated sodium chloride solution (20 mL), dried over sodium sulfate, filtered and concentrated. The residue was purified by flash chromatography (SiO_2, 1:6 ethyl acetate/hexanes) to afford **110** (67.7, mg, 67.81 %) as a colorless amorphous solid. ^{1}H NMR (500 MHz, $CDCl_3$) δ 11.88 (s, 1H), 7.73 (s, 1H), 7.33 (s, 4H), 6.36 (s, 1H), 5.10 (s, 4H). ^{13}C NMR (125 MHz, $CDCl_3$) δ 170.0, 162.3, 148.4, 136.0 (2), 132.4 (2), 128.0, 122.8 (2), 108.5, 102.8, 97.8, 55.1 (2). HRMS (ESI+) m/z [M + H^+] calcd for $C_{15}H_{14}BrN_2O_2$, 333.0239, found 333.0238.

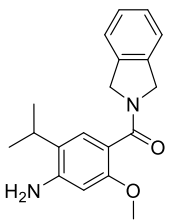

(4-Amino-5-isopropyl-2-methoxyphenyl)(isoindolin-2-yl)methanone (111): A biotage microwave vial was charged with **110** (1.0 g, 2.46 mmol, 1 eq.), [1,1′-Bis(diphenylphosphino)ferrocene]dichloropalladium(II), complex with dichloromethane (251 mg, 0.32 mmol, 0.2 eq.), triethylamine (289 µl, 2.1 mmol, 1.3 eq.), and potassium isopropenyltrifluoroborate (309 mg, 2.10 mmol, 1.3 eq.). The tube was sealed with a cap lined with a disposable Teflon septum. The tube was evacuated and purged with nitrogen (3 times), before the addition of 2-propanol (8 mL) by syringe. The resulting mixture was heated at 100 °C for 6 h, cooled to rt, and filtered through a small pad of celite (elution with ethyl acetate). Solvent was removed and the residue purified by flash chromatography (SiO_2, 1:3 ethyl acetate/hexanes) to afford (4-amino-2-methoxy-5-(prop-1-en-2-yl)phenyl)(isoindolin-2-yl)methanone, which was used as obtained and dissolved in ethyl acetate (15 mL). Palladium on carbon (10%) was added to this solution and the suspension was stirred for 16 h under a hydrogen atmosphere before it was filtered through a pad of celite and eluted with ethyl acetate (20 mL). The eluent was concentrated to afford **111** (318.3 mg, 64.9 %) as a colorless amorphous solid. ^{1}H NMR (500 MHz $CDCl_3$) δ 7.34 – 7.23 (m, 3H), 7.16 – 7.12 (m, 1H), 7.10 (s, 1H), 6.27 (s, 1H), 4.99 (s, 2H), 4.66 (s, 2H), 3.92 – 3.81 (m, 2H), 3.78 (s, 3H), 2.83 (hept, *J* = 6.8 Hz, 1H), 1.24 (d, *J* = 6.8 Hz, 6H). ^{13}C NMR (125 MHz, $CDCl_3$) δ 169.4, 154.6, 145.9, 137.3, 136.9, 127.7, 127.5, 125.7, 124.9, 123.2, 122.6, 117.3, 98.8, 55.8, 53.6, 52.3, 27.4, 22.5 (2). HRMS (ESI+) m/z [M + H^+] calcd for $C_{19}H_{23}N_2O_2$, 311.1760, found 311.1745.

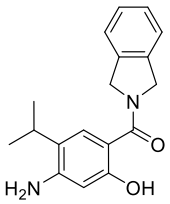

(4-Amino-2-hydroxy-5-isopropylphenyl)(isoindolin-2-yl)methanone (112): 1 M solution of boron tribromide (0.32 mmol, 0.60 mL, 2 eq.), was added to a solution of **111** (50 mg, 0.16 mmol) in anhydrous dichloromethane (3 mL) at 0 °C. The resulting mixture was stirred at rt for 14 h before quenching with saturate sodium bicarbonate solution (5 mL). The aqueous layer was extracted with dichloromethane (2 × 10 mL). The combined organic layers were washed with saturated sodium chloride solution (20 mL), dried over sodium sulfate, filtered and concentrated. The residue was purified by flash chromatography (SiO_2, 1:6 ethyl acetate/hexanes) to afford **112** (59.3 mg, 28.1 %) as a colorless amorphous solid. ^{1}H NMR (500 MHz, $CDCl_3$) δ 11.52 (s, 1H), 7.42 (d, *J* = 0.6 Hz, 1H), 7.31 (s, 4H), 6.26 (s, 1H), 5.10 (s, 4H), 4.08 (d, *J* = 45.9 Hz, 2H), 2.90 – 2.81 (m, 1H), 1.31 (d, *J* = 6.8 Hz, 6H). ^{13}C NMR (125 MHz, $CDCl_3$) δ 171.6, 160.8, 148.5, 136.4, 127.9 (2), 126.0 (2), 122.7 (2), 107.3, 102.8, 54.8 (2), 27.4, 22.8 (2). HRMS (ESI+) m/z [M + H^+] calcd for $C_{18}H_{21}N_2O_2$, 297.1603, found 297.1609.

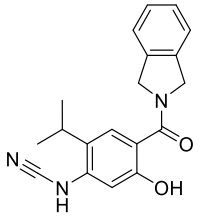

N-(5-Hydroxy-4-(isoindoline-2-carbonyl)-2-isopropylphenyl)cyanamide (113): Cyanogen bromide (35 mg, 0.32 mmol, 2eq.) was added to a solution of **112** (50 mg, 0.16 mmol, 1 eq.) in diethyl ether at ^{o}C. The resulting mixture stirred for 14h at rt, diluted with ethyl acetate (10 mL), washed with water (10 mL) and saturated sodium chloride solution (10 mL). The organic layer was dried over sodium sulfate, filtered and concentrated. The residue was taken in dichloromethane (2 mL) and 1M solution of boron tribromide (0.32 mL, 0.32 mmol, 2.0 eq.) was added at 0 ^{o}C. The resulting mixture was stirred at rt for 14 h before quenching with saturate sodium bicarbonate solution (5 mL). The aqueous layer was extracted with dichloromethane (2 ×

10 mL). The combined organic layers were washed with saturated sodium chloride solution (15 mL), dried over sodium sulfate, filtered and concentrated. The residue was purified by flash chromatography (SiO_2, 1:6 ethyl acetate/hexanes) to afford **113** (25.0 mg, 48.6 %) as a colorless amorphous solid. ^{1}H NMR (500 MHz, Methylene Chloride-d_2) δ 11.38 (s, 1H), 7.54 (s, 1H), 7.32 (s, 4H), 6.83 (s, 1H), 6.03 (s, 1H), 5.08 (s, 5H), 2.80 (hept, *J* = 6.8 Hz, 1H), 1.30 (d, *J* = 6.8 Hz, 7H). ^{13}C NMR (125 MHz, CD_2Cl_2) δ 170.6, 160.6, 139.0 (2), 128.1, 126.6 (3), 124.3, 122.9, 112.7, 110.2, 104.3 (2), 54.9 (2), 27.4, 22.9 (2). HRMS (ESI+) m/z [M + H^+] calcd for $C_{20}H_{20}N_3O_2$, 334.1556, found 334.1565.

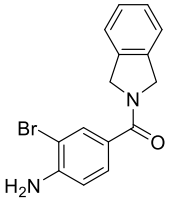

(4-Amino-3-bromophenyl)(isoindolin-2-yl)methanone (132): 1-Ethyl-3-(3-dimethylaminopropyl)carbodiimide (4.32 g, 37.02 mmol, 2.0 eq.) was added to a stirred solution of 4-amino-3-bromobenzoic acid (4.0 g, 18.51 mmol, 1 eq.), isoindoline hydrochloride (4.32 g, 27.77 mmol, 1.5 eq.), 1-hydroxybenzotriazole (5.0 g, 37.02 mmol, 2 eq.) N-,N-diisopropylethylamine (6.44 mL, 37.02 mmol, 2.0 eq.) in dichloromethane (200 mL) at 0 °C. The resulting solution was stirred at rt for 14 h before quenching with saturated sodium bicarbonate solution (150 mL). The organic layer was washed sodium chloride solution (150 mL), dried over sodium sulfate, filtered and concentrated. The residue was purified by flash chromatography (SiO_2, 1:2 hexanes/ethyl acetate) to afford **132** (4.33 g, 73.8 %) as a colorless oil. ^{1}H NMR (400 MHz, $CDCl_3$) δ 7.74 (d, *J* = 1.9 Hz, 1H), 7.41 (dd, *J* = 8.2, 1.9 Hz, 1H), 7.36 – 7.25 (m, 3H), 7.19 (d, *J* = 7.3 Hz, 1H), 6.79 (d, *J* = 8.3 Hz, 1H), 5.00 (s, 2H), 4.86 (s, 2H), 4.38 (br s, 2H). ^{13}C NMR (100

MHz, $CDCl_3$) δ 169.1, 146.1, 136.7, 136.6, 132.3, 128.1, 128.0, 127.7, 127.2, 123.1, 122.6, 114.9, 108.5, 55.4, 52.9. HRMS (ESI+) m/z [M + H^+] calcd for $C_{15}H_{14}BrN_2O$, 318.1243, found 318.1241.

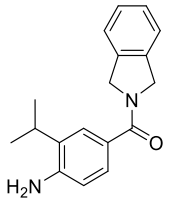

(4-Amino-3-isopropylphenyl)(isoindolin-2-yl)methanone (116): A biotage microwave vial was charged with **132** (1.0 g, 3.15 mmol, 1 eq.), [1,1′-Bis(diphenylphosphino)ferrocene]dichloropalladium(II), complex with dichloromethane (251 mg, 0.32 mmol, 0.2 eq.), triethylamine (289 µl, 2.1 mmol, 1.3 eq.), and potassium isopropenyltrifluoroborate (309 mg, 2.10 mmol, 1.3 eq.). The tube was sealed with a cap lined with a disposable Teflon septum. The tube was evacuated and purged with nitrogen (3 times), before the addition of 2-propanol (8 mL) by syringe. The resulting mixture was heated at 100 °C for 6 h, cooled to rt, and filtered through a small pad of celite (elution with ethyl acetate). Solvent was removed and the residue purified by flash chromatography (SiO_2, 1:3 ethyl acetate/hexanes) to afford (4-amino-2-methoxy-5-(prop-1-en-2-yl)phenyl)(isoindolin-2-yl)methanone, which was used as obtained and dissolved in ethyl acetate (15 mL). Palladium on carbon (10%) was added to this solution and the suspension was stirred for 16 h under a hydrogen atmosphere before it was filtered through a pad of celite and eluted with ethyl acetate (20 mL). The eluent was concentrated to afford **116** (318.3 mg, 64.9 %) as a colorless amorphous solid. ^{1}H NMR (400 MHz, CD_2Cl_2) δ 7.40 (d, *J* = 1.9 Hz, 1H), 7.35 – 7.12 (m, 5H), 6.69 (dd, *J* = 8.2, 1.2 Hz, 1H), 4.94 – 4.83 (m, 4H), 4.05 (br s, 2H), 2.95 – 2.88 (m, 1H), 1.27 (d, *J* = 6.9 Hz, 6H). ^{13}C NMR (100 MHz, CD_2Cl2) δ 170.6, 145.6, 137.2, 131.8, 127.5, 126.6, 126.1, 125.3, 122.8, 122.5, 114.6, 55.2, 52.5, 27.7, 22.0. ^{13}C NMR (100 MHz, CD_2Cl2) δ 170.6, 145.6, 137.2 (2), 131.8, 127.5, 126.6, 126.1 (2), 125.3 (2),

122.8, 122.5, 114.6, 55.2, 52.5, 27.7, 22.0. HRMS (ESI+) m/z [M + H^+] calcd for $C_{18}H_{21}N_2O$, 281.1654, found 281.1642.

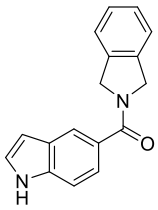

(1H-Indol-5-yl)(isoindolin-2-yl)methanone (117): 1-Ethyl-3-(3-dimethylaminopropyl) carbodiimide (142 mg, 0.74 mmol, 2.0 eq.) was added to a stirred solution of *1H*-indole-5-carboxylic acid (59 mg, 0.37 mmol, 1 eq.), isoindoline hydrochloride (87 mg, 0.46 mmol, 1.5 eq.), 1-hydroxybenzotriazole (100 mg, 0.74 mmol, 2 eq.) N-,N-diisopropylethylamine (0.141 mL, 0.81 mmol, 2.2 eq.) in dichloromethane (4 mL) at 0 °C. The resulting solution was stirred at rt for 14 h before the addition of saturated sodium bicarbonate solution (4 mL). The organic layer was washed with 1 N HCl (2 × 3 mL) and saturated sodium chloride solution (3 mL), dried over anhydrous sodium sulfate, filtered, and concentrated. The residue was purified by flash chromatography (SiO_2, 1:3 hexanes/ethyl acetate) to afford **117** (56 mg, 57.8 %) as a colorless oil. ^{1}H NMR (400 MHz, $CDCl_3$) δ 8.61 (s, 1H), 7.91 (s, 1H), 7.43 (s, 2H), 7.14 (d, *J* = 7.5 Hz, 1H), 6.62 (t, *J* = 2.4 Hz, 1H), 5.09 (s, 2H), 4.88 (s, 2H). ^{13}C NMR (125 MHz, $CDCl_3$) δ 172.0, 137.0, 136.8, 128.4, 127.9, 127.6, 127.5, 125.7 (2), 123.1, 122.6, 121.4, 120.2, 111.4, 103.4, 55.6, 52.8. HRMS (ESI+) m/z [M + H^+] calcd for $C_{17}H_{15}N_2O$, 263.1184 found, 263.1182

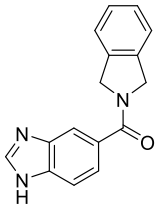

(1H-benzo[d]imidazol-5-yl)(isoindolin-2-yl)methanone (118): 1-Ethyl-3-(3-dimethylaminopropyl) carbodiimide (142 mg, 0.74 mmol, 2.0 eq.) was added to a stirred solution

of *1H*-benzo[d]imidazole-5-carboxylic acid (60 mg, 0.37 mmol, 1 eq.), isoindoline hydrochloride (87 mg, 0.46 mmol, 1.5 eq.), 1-hydroxybenzotriazole (100 mg, 0.74 mmol, 2 eq.) N-,N-diisopropylethylamine (0.141 mL, 0.81 mmol, 2.2 eq.) in dichloromethane (4 mL) at 0 °C The resulting solution was stirred at rt for 14 h before the addition of saturated sodium bicarbonate solution (4 mL). The organic layer was washed with 1 N HCl (2 × 3 mL) and saturated sodium chloride solution (3 mL), dried over anhydrous sodium sulfate, filtered, and concentrated. The residue was purified by flash chromatography (SiO_2, 1:3 hexanes/ethyl acetate) to afford **118** (60 mg, 61.3 %) as a colorless oil.^{1}H NMR (400 MHz, $CDCl_3$) δ 8.06 (s, 1H), 7.93 (s, 1H), 7.67 (d, *J* = 8.5 Hz, 1H), 7.47 (d, *J* = 8.3 Hz, 1H), 7.41 – 7.24 (m, 3H), 7.14 (d, *J* = 7.4 Hz, 1H), 5.06 (s, 2H), 4.82 (s, 2H). ^{13}C NMR (125 MHz, $CDCl_3$) δ 167.5, 142.9, 141.7, 136.5, 136.2, 134.5, 131.2, 128.9, 128.0, 127.8, 125.5, 124.4, 123.7, 123.1, 54.0, 52.9. HRMS (ESI+) m/z [M + H^+] calcd for $C_{16}H_{14}N_3O$, 264.1137 found, 264.1129.

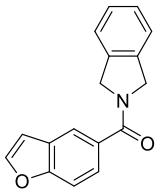

Benzofuran-5-yl(isoindolin-2-yl)methanone (119): 1-Ethyl-3-(3-dimethylaminopropyl) carbodiimide (142 mg, 0.74 mmol, 2.0 eq.) was added to a stirred solution of benzofuran-5-carboxylic acid (60 mg, 0.37 mmol, 1 eq.), isoindoline hydrochloride (87 mg, 0.46 mmol, 1.5 eq.), 1-hydroxybenzotriazole (100 mg, 0.74 mmol, 2 eq.) N-,N-diisopropylethylamine (0.141 mL, 0.81 mmol, 2.2 eq.) in dichloromethane (4 mL) at 0 °C. The resulting solution was stirred at rt for 14 h before the addition of saturated sodium bicarbonate solution (4 mL). The organic layer was washed with 1 N HCl (2 × 3 mL) and saturated sodium chloride solution (3 mL), dried over anhydrous sodium sulfate, filtered, and concentrated. The residue was purified by flash chromatography

(SiO_2, 1:3 hexanes/ethyl acetate) to afford **119** (60 mg, 67.4 %) as a colorless oil. ^{1}H NMR (500 MHz, $CDCl_3$) δ 7.85 (dd, *J* = 1.7, 0.7 Hz, 1H), 7.71 (d, *J* = 2.2 Hz, 1H), 7.58 (dt, *J* = 8.5, 0.9 Hz, 1H), 7.54 (dd, *J* = 8.5, 1.7 Hz, 1H), 7.39 – 7.27 (m, 3H), 7.15 (d, *J* = 7.5 Hz, 1H), 6.85 (dd, *J* = 2.2, 0.9 Hz, 1H), 5.07 (s, 2H), 4.82 (s, 2H). ^{13}C NMR (125 MHz, $CDCl_3$) δ 170.9, 155.7, 146.3, 136.7, 136.6, 131.8, 128.0, 127.7, 127.6, 123.7, 123.2, 122.6, 120.6, 111.7, 107.1, 55.5, 52.8. HRMS (ESI+) m/z [M + H^+] calcd for $C_{17}H_{14}NO_2$, 264.1025 found, 264.1021

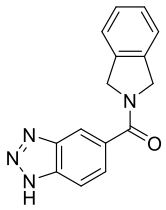

(1H-benzo[d][1,2,3]triazol-5-yl)(isoindolin-2-yl)methanone (120): 1-Ethyl-3-(3-dimethylaminopropyl) carbodiimide (142 mg, 0.74 mmol, 2.0 eq.) was added to a stirred solution of *1H*-benzo[d][1,2,3]triazole-5-carboxylic acid (60 mg, 0.37 mmol, 1 eq.), isoindoline hydrochloride (87 mg, 0.46 mmol, 1.5 eq.), 1-hydroxybenzotriazole (100 mg, 0.74 mmol, 2 eq.) N-,N-diisopropylethylamine (0.141 mL, 0.81 mmol, 2.2 eq.) in dichloromethane (4 mL) at 0 °C The resulting solution was stirred at rt for 14 h before the addition of saturated sodium bicarbonate solution (4 mL). The organic layer was washed with 1 N HCl (2 × 3 mL) and saturated sodium chloride solution (3 mL), dried over anhydrous sodium sulfate, filtered, and concentrated. The residue was purified by flash chromatography (SiO_2, 1:3 hexanes/ethyl acetate) to afford **120** (53 mg, 56.4 %) as a colorless oil. ^{1}H NMR (400 MHz, $CDCl_3$-CD_3OD δ 8.12 (s, 1H), 7.88 (d, *J* = 8.6 Hz, 1H), 7.63 (dd, *J* = 8.5, 1.4 Hz, 1H), 7.42 – 7.28 (m, 3H), 7.15 (d, *J* = 7.4 Hz, 1H), 5.09 (s, 2H), 4.82 (s, 2H). ^{13}C NMR (100 MHz, $CDCl_3$) δ 170.2, 147.7, 136.2 (2), 136.1(2), 128.2, 127.9 (2), 123.2, 122.6, 115.9, 114.7, 55.4, 52.9. HRMS (ESI+) m/z [M + H^+] calcd for $C_{15}H_{13}N_4O$, 265.1089 found, 265.1081.

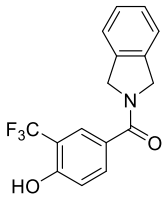

(4-Hydroxy-3-(trifluoromethyl)phenyl)(isoindolin-2-yl)methanone (122): 1-Ethyl-3-(3-dimethylaminopropyl) carbodiimide (192 mg, 2.0 mmol, 2.0 eq.) was added to a stirred solution of 4-hydroxy-3-(trifluoromethyl)benzoic acid (206 mg, 1.0 mmol, 1 eq.), isoindoline hydrochloride (233 mg, 1.5 mmol, 1.5 eq.), 1-hydroxybenzotriazole (306 mg, 2.0 mmol, 2 eq.) N-,N-diisopropylethylamine (0.39 mL, 2.2 mmol, 2.2 eq.) in dichloromethane (10 mL) at 0 °C The resulting solution was stirred at rt for 14 h before the addition of saturated sodium bicarbonate solution (10 mL). The organic layer was washed with 1 N HCl (2 × 10 mL) and saturated sodium chloride solution (10 mL), dried over anhydrous sodium sulfate, filtered, and concentrated. The residue was purified by flash chromatography (SiO_2, 1:3 hexanes/ethyl acetate) to afford **122** (164 mg, 53.8 %) as a colorless oil. ^{1}H NMR (500 MHz, $CDCl_3$) δ 7.72 (d, *J* = 2.2 Hz, 1H), 7.55 (dd, *J* = 8.4, 2.2 Hz, 1H), 7.21 (s, 6H), 7.12 (d, *J* = 7.4 Hz, 1H), 6.90 (d, *J* = 8.4 Hz, 1H), 4.94 (s, 2H), 4.76 (s, 2H). ^{13}C NMR (125 MHz, $CDCl_3$) δ 168.3, 155.9, 135.1, 135.0, 131.4, 126.9, 126.6, 126.1, 125.3 (q, *J* = 5.2 Hz), 123.6 (q, *J* = 269 Hz), 121.9, 121.4, 116.0, 115.8 (q, *J* = 30.2 Hz), 54.1, 51.7. ^{19}F NMR (376 MHz, $CDCl_3$) δ -63.0. HRMS (ESI+) m/z [M + H^+] calcd for $C_{16}H_{13}F_3NO_2$, 306.0742 found, 306.0754.

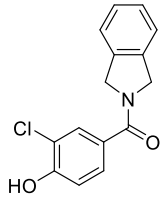

(3-Chloro-4-hydroxyphenyl)(isoindolin-2-yl)methanone (123): 1-Ethyl-3-(3-dimethylaminopropyl) carbodiimide (149 mg, 1.16 mmol, 2.0 eq.) was added to a stirred solution

of 3-chloro-4-hydroxybenzoic acid (100 mg, 0.55 mmol, 1 eq.), isoindoline hydrochloride (128 mg, 0.82 mmol, 1.5 eq.), 1-hydroxybenzotriazole (211 mg, 1.10 mmol, 2 eq.) N-,N-diisopropylethylamine (0.21 mL, 1.21 mmol, 2.2 eq.) in dichloromethane (6 mL) at 0 °C The resulting solution was stirred at rt for 14 h before the addition of saturated sodium bicarbonate solution (5 mL). The organic layer was washed with 1 N HCl (2 × 5 mL) and saturated sodium chloride solution (5 mL), dried over anhydrous sodium sulfate, filtered, and concentrated. The residue was purified by flash chromatography (SiO_2, 1:3 hexanes/ethyl acetate) to afford **123** (82 mg, 54.6 %) as a colorless oil. ^{1}H NMR (400 MHz, $CDCl_3$) δ 7.64 (d, *J* = 2.0 Hz, 1H), 7.47 (d, *J* = 8.4 Hz, 1H), 7.36 – 7.28 (m, 3H), 7.19 (d, *J* = 7.3 Hz, 1H), 7.10 (d, *J* = 8.4 Hz, 1H), 5.02 (s, 2H), 4.84 (s, 2H).^{13}C NMR (125 MHz, $CDCl_3$-CD_3OD) δ 169.2, 153.8, 136.4, 136.3, 129.3, 128.9, 128.1, 127.8, 127.6, 123.1, 122.6, 120.4, 116.4, 55.3, 52.9. HRMS (ESI+) m/z [M + H^+] calcd for $C_{15}H_{13}ClNO_2$, 274.0635 found 274.0640.

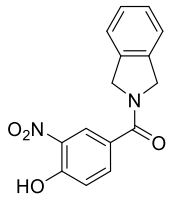

(4-hydroxy-3-nitrophenyl)(isoindolin-2-yl)methanone (124): 1-Ethyl-3-(3-dimethylaminopropyl) carbodiimide (192 mg, 2.0 mmol, 2.0 eq.) was added to a stirred solution of 4-hydroxy-3-nitrobenzoic acid (183 mg, 1.0 mmol, 1 eq.), isoindoline hydrochloride (233 mg, 1.5 mmol, 1.5 eq.), 1-hydroxybenzotriazole (306 mg, 2.0 mmol, 2 eq.) N-,N-diisopropylethylamine (0.39 mL, 2.2 mmol, 2.2 eq.) in dichloromethane (10 mL) at 0 °C The resulting solution was stirred at rt for 14 h before the addition of saturated sodium bicarbonate solution (10 mL). The organic layer was washed with 1 N HCl (2 × 10 mL) and saturated sodium chloride solution (10 mL), dried over anhydrous sodium sulfate, filtered, and concentrated. The

residue was purified by flash chromatography (SiO_2, 1:3 hexanes/ethyl acetate) to afford **124** (207 mg, 72.8 %) as a colorless oil. ^{1}H NMR (500 MHz, $CDCl_3$) δ 8.40 (d, *J* = 2.2 Hz, 1H), 7.86 (dd, *J* = 8.7, 2.2 Hz, 1H), 7.37 – 7.11 (m, 5H), 5.02 (s, 2H), 4.86 (s, 2H).^{13}C NMR (125 MHz, $CDCl_3$) δ 167.6, 156.4, 136.7 (2), 136.1, 136.0, 128.6, 128.3, 127.9, 124.5, 123.2, 122.7, 120.7, 55.3, 53.1. HRMS (ESI+) m/z [M - H^+] calcd for $C_{15}H_{11}NO_2$, 283.0719, found 283.0725.

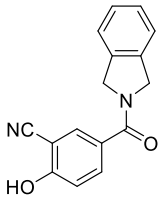

2-Hydroxy-5-(isoindoline-2-carbonyl)benzonitrile (125): 1-Ethyl-3-(3-dimethylaminopropyl) carbodiimide (586 mg, 3.06 mmol, 2.0 eq.) was added to a stirred solution of 4-hydroxy-3-nitrobenzoic acid (250 mg, 1.53 mmol, 1 eq.), isoindoline hydrochloride (356 mg, 3.06 mmol, 1.5 eq.), 1-hydroxybenzotriazole (470 mg, 3.06 mmol, 2 eq.) N-,N-diisopropylethylamine (1.12 mL, 6.42 mmol, 4.2 eq.) in dichloromethane (16 mL) at 0 °C The resulting solution was stirred at rt for 14 h before the addition of saturated sodium bicarbonate solution (15 mL). The organic layer was washed with 1 N HCl (2 × 15 mL) and saturated sodium chloride solution (15 mL), dried over anhydrous sodium sulfate, filtered, and concentrated. The residue was purified by flash chromatography (SiO_2, 1:3 hexanes/ethyl acetate) to afford **125** (162 mg, 61.5 %) as a colorless oil. ^{1}H NMR (500 MHz, $CDCl_3$- CD_3OD) δ 7.72 (dd, *J* = 9.3, 2.2 Hz, 1H), 7.62 (ddd, *J* = 10.9, 8.0, 2.2 Hz, 1H), 7.31–7.23 (m, 3H), 7.16 (t, *J* = 8.7 Hz, 1H), 6.97 (t, *J* = 8.6 Hz, 1H), 4.95 (d, *J* = 11.5 Hz, 2H), 4.80 (d, *J* = 9.1 Hz, 2H). ^{13}C NMR (125 MHz, $CDCl_3$) δ 168.8, 162.0, 136.0, 135.9, 133.8, 132.4, 128.1, 127.8, 127.5, 123.0, 122.6, 116.6, 116.4, 99.8, 55.3, 52.9. HRMS (ESI+) m/z [M + H^+] calcd for $C_{16}H_{13}NO_2$, 265.0977, found 265.0984.

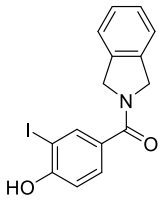

(4-hydroxy-3-iodophenyl)(isoindolin-2-yl)methanone (127): 1-Ethyl-3-(3-dimethylaminopropyl) carbodiimide (192 mg, 2.0 mmol, 2.0 eq.) was added to a stirred solution of 4-hydroxy-3-iodobenzoic acid (264 mg, 1.0 mmol, 1 eq.), isoindoline hydrochloride (233 mg, 1.5 mmol, 1.5 eq.), 1-hydroxybenzotriazole (306 mg, 2.0 mmol, 2 eq.) N-,N-diisopropylethylamine (0.39 mL, 2.2 mmol, 2.2 eq.) in dichloromethane (10 mL) at 0 °C The resulting solution was stirred at rt for 14 h before the addition of saturated sodium bicarbonate solution (25 mL) and ethyl acetate (50 mL). The organic layer was washed with 1 N HCl (2 × 25 mL) and saturated sodium chloride solution (50 mL), dried over anhydrous sodium sulfate, filtered, and concentrated. The residue was triturated with dichloromethane to afford **127** (166 mg, 45.6 %) as an off-white amorphous solid. ^{1}H NMR (400 MHz, DMSO-d_6) δ 11.29 – 11.14 (br s, 1H), 7.64 (d, J = 7.3 Hz, 1H), 7.46 – 7.27 (m, 5H), 6.92 (dd, J = 11.1, 1.6 Hz, 1H), 4.82 (s, 2H), 4.64 (s, 2H). ^{13}C NMR (100 MHz, DMSO-d_6) δ 163.3, 157.7, 136.4, 135.9, 132.1, 132.0, 127.5, 127.4, 123.0, 122.9, 117.3,104.7, 103.8, 51.7 (2). HRMS (ESI+) m/z [M + H^+] calcd for $C_{15}H_{13}INO_2$, 365.9991, found 365.9998.

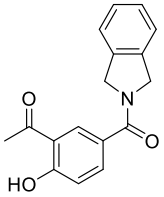

1-(2-Hydroxy-5-(isoindoline-2-carbonyl)phenyl)ethan-1-one (128): 1-Ethyl-3-(3-dimethylaminopropyl) carbodiimide (4.26 g, 22.20 mmol, 2.0 eq.) was added to a stirred solution of 3-chloro-4-hydroxybenzoic acid (2.0 g, 11.10 mmol, 1 eq.), isoindoline hydrochloride (2.59 g,

16.7 mmol, 1.5 eq.), 1-hydroxybenzotriazole (2.99 g, 22.2 mmol, 2 eq.) N-,N-diisopropylethylamine (8.12 mL, 46.62 mmol, 4.2 eq.) in dichloromethane (110 mL) at 0 °C The resulting solution was stirred at rt for 14 h before the addition of saturated sodium bicarbonate solution (100 mL). The organic layer was washed with 1 N HCl (2 × 100 mL) and saturated sodium chloride solution (100 mL), dried over anhydrous sodium sulfate, filtered, and concentrated. The residue was purified by flash chromatography (SiO_2, 1:3 hexanes/ethyl acetate) to afford **128** (2.12 g, 67.8 %) as a colorless oil. ^{1}H NMR (500 MHz, $CDCl_3$) δ 12.49 (s, 1H), 8.09 (d, *J* = 2.1 Hz, 1H), 7.75 (dd, *J* = 8.6, 2.1 Hz, 1H), 7.39 – 7.28 (m, 3H), 7.20 (d, *J* = 7.5 Hz, 1H), 7.06 (d, *J* = 8.6 Hz, 1H), 5.05 (s, 2H), 4.86 (s, 2H), 2.69 (s, 3H). ^{13}C NMR (125 MHz, $CDCl_3$) δ 204.7, 169.2, 163.9, 136.4 (2), 134.9, 131.1, 128.2, 127.8, 127.5, 123.2, 122.6, 119.6, 118.5, 55.4, 53.0, 27.0. HRMS (ESI+) m/z [M + H^+] calcd for $C_{17}H_{16}NO_3$, 282.1130, found 282.1135.

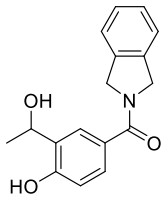

(4-Hydroxy-3-(1-hydroxyethyl)phenyl)(isoindolin-2-yl)methanone (129): Sodium borohydride (12 mg, 0.35 mmol, 1.5 eq.) was added to a solution of **128** (56 mg, 0.2 mmol, 1.0 eq.) in a solvent mixture of tetrahydrofuran (0.5 mL) and methanol (1.5 mL) at 0 °C. The resulting mixture was stirred for 1 h at rt before the addition of saturated ammonium chloride solution (2 mL). The aqueous layer was extracted with ethyl acetate (2 × 3 mL). The combined organic layers were washed with saturated sodium chloride solution (5 mL), dried over anhydrous sodium sulfate, filtered, and concentrated. The residue was purified by flash chromatography (SiO_2, 1:2 hexanes/ethyl acetate) to afford **129** (25 mg, 45.22 %) as a colorless oil. ^{1}H NMR (400 MHz, CD_3OD) δ 7.65 (d, *J* = 2.2 Hz, 1H), 7.42 – 7.33 (m, 2H), 7.33 – 7.20 (m, 3H), 6.85 (d, *J* = 8.3 Hz,

1H), 5.18 (q, *J* = 6.4 Hz, 1H), 4.94 (s, 2H), 1.45 (d, *J* = 6.4 Hz, 3H). ^{13}C NMR (100 MHz, CD_3OD) δ 172.9, 157.5, 137.9, 137.1, 133.7, 128.8, 128.6, 128.4, 128.1, 126.4, 123.8, 123.6, 115.9, 66.3, 56.3, 53.6, 24.1. HRMS (ESI+) m/z [M + H^+] calcd for 284.1287, $C_{17}H_{18}NO_3$, found 284.1281.

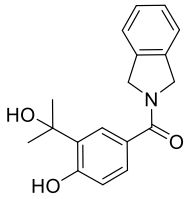

(4-Hydroxy-3-(2-hydroxypropan-2-yl)phenyl)(isoindolin-2-yl)methanone (130): 1 M solution of methyl magnesium bromide in tetrahydrofuran (0.24mL, 0.24 mmol, 1.2 eq.) was added to a solution of **128** (56 mg, 0.2 mmol, 1.0 eq.) in tetrahydrofuran (2.0 mL) 0 °C. The resulting mixture was stirred for 1 h at 0 °C before the addition of saturated ammonium chloride solution (2 mL). The aqueous layer was extracted with ethyl acetate (2 × 3 mL). The combined organic layers were washed with saturated sodium chloride solution (5 mL), dried over anhydrous sodium sulfate, filtered, and concentrated. The residue was purified by flash chromatography (SiO_2, 1:2 hexanes/ethyl acetate) to afford **130** (19 mg, 33.2 %) as a colorless oil. ^{1}H NMR (400 MHz, $CDCl_3$) δ 9.83 (s, 1H), 7.35 – 7.25 (m, 5H), 7.16 (d, *J* = 7.3 Hz, 1H), 6.82 (d, *J* = 8.3 Hz, 1H), 4.98 (s, 2H), 4.80 (s, 2H), 4.59 (br s, 1H), 1.62 (s, 6H). ^{13}C NMR (100 MHz, $CDCl_3$) δ 171.1, 158.0, 136.6, 136.4, 132.1, 128.0, 127.7, 127.6, 127.0, 125.3, 123.1, 122.6, 117.3, 75.4, 55.4, 52.9, 31.1, 30.2. HRMS (ESI+) m/z [M - H^+] calcd 296.1287 for $C_{18}H_{18}NO_3$, found, 296.1278.

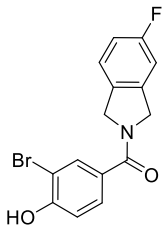

(3-Bromo-4-hydroxyphenyl)(5-fluoroisoindolin-2-yl)methanone (133): 1-Ethyl-3-(3-dimethylaminopropyl) carbodiimide (88 mg, 0.46 mmol, 2.0 eq.) was added to a stirred solution of 3-bromo-4-hydroxybenzoic acid (50 mg, 0.23 mmol, 1 eq.), 5-fluoroisoindoline hydrochloride (48 mg, 0.28 mmol, 1.2 eq.), 1-hydroxybenzotriazole (62 mg, 0.46 mmol, 2 eq.) N-,N-diisopropylethylamine (0.17 mL, 0.97 mmol, 4.2 eq.) in dichloromethane 3.0 mL) at 0 °C The resulting solution was stirred at rt for 14 h before the addition of saturated sodium bicarbonate solution (3 mL). The organic layer was washed with 1 N HCl (2 × 3 mL) and saturated sodium chloride solution (3 mL), dried over anhydrous sodium sulfate, filtered, and concentrated. The residue was purified by flash chromatography (SiO_2, 1:3 hexanes/ethyl acetate) to afford **133** (58 mg, 76.1 %) as a light gray amorphous solid. ^{1}H NMR (400 MHz, $CDCl_3$) δ 10.48 (s, 1H), 7.45 (d, *J* = 2.2 Hz, 1H), 7.35-7.25 (m, 3H), 7.27 – 7.24 (m, 2H), 6.97 (d, *J* = 8.5 Hz, 1H), 5.10 (s, 4H), 2.92 (hept, *J* = 7.0 Hz, 1H), 1.29 (d, *J* = 6.9 Hz, 6H). ^{19}F NMR (376 MHz, $CDCl_3$) δ -114.55. ^{13}C NMR (125 MHz, $CDCl_3$) δ 172.6, 167.1 (d, *J* = 120 Hz), 160.9, 144.7, 143.6, 138.3, 137.7, 133.5, 129.7, 121.0, 119.6 (d, *J* = 23 Hz), 115.2 (d, *J* = 23 Hz), 114.1, 59.3, 57.1. HRMS (ESI+) m/z [M + H^+] calcd for $C_{15}H_{12}BrFNO_2$, 336.0035, found 336.0042.

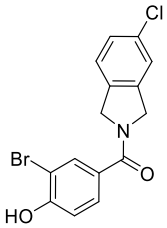

(3-Bromo-4-hydroxyphenyl)(5-chloroisoindolin-2-yl)methanone (134): 1-Ethyl-3-(3-dimethylaminopropyl) carbodiimide (47 mg, 0.24 mmol, 2.0 eq.) was added to a stirred solution of 3-bromo-4-hydroxybenzoic acid (25 mg, 0.12 mmol, 1 eq.), 5-chloroisoindoline hydrochloride (26 mg, 0.13 mmol, 1.2 eq.), 1-hydroxybenzotriazole (38 mg, 0.24 mmol, 2 eq.) N-,N-diisopropylethylamine (0.09 mL, 0.51 mmol, 4.2 eq.) in dichloromethane (2.0 mL) at 0 °C The

resulting solution was stirred at rt for 14 h before the addition of saturated sodium bicarbonate solution (15 mL) and ethyl acetate (15 mL). The organic layer was washed with 1 N HCl (2 × 10 mL) and saturated sodium chloride solution (10 mL), dried over anhydrous sodium sulfate, filtered, and concentrated. The residue was triturated with dichloromethane (5 mL) to afford **134** (26 mg, 65.0 %) as a white amorphous solid. ^{1}H NMR (500 MHz, CD_3OD) δ 8.08 – 7.46 (m, 3H), 7.29 – 7.05 (m, 2H), 6.77 (d, *J* = 8.4 Hz, 1H), 4.77 – 4.67 (m, 4H). ^{13}C NMR (125 MHz, CD_3OD) δ 169.2, 153.4, 138.7, 135.3, 131.8, 131.1, 127.5, 127.2, 124.3, 124.0, 123.9, 122.7, 115.6, 54.2, 52.0. HRMS (ESI+) m/z [M + H^+] calcd for $C_{15}H_{12}ClBrNO_2$, 351.9740, found 351.9747.

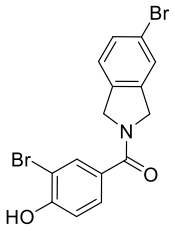

(3-Bromo-4-hydroxyphenyl)(5-bromoisoindolin-2-yl)methanone (135): 1-Ethyl-3-(3-dimethylaminopropyl) carbodiimide (44 mg, 0.23 mmol, 2.0 eq.) was added to a stirred solution of 3-bromo-4-hydroxybenzoic acid (25 mg, 0.12 mmol, 1 eq.), 5-bromoisoindoline hydrochloride (33 mg, 0.14 mmol, 1.2 eq.), 1-hydroxybenzotriazole (31 mg, 0.23 mmol, 2 eq.) N-,N-diisopropylethylamine (0.09 mL, 0.48 mmol, 4.2 eq.) in dichloromethane (2.0 mL) at 0 °C The resulting solution was stirred at rt for 14 h before the addition of saturated sodium bicarbonate solution (15 mL) and ethyl acetate (15 mL). The organic layer was washed with 1 N HCl (2 × 10 mL) and saturated sodium chloride solution (10 mL), dried over anhydrous sodium sulfate, filtered, and concentrated. The residue was purified by flash chromatography (SiO_2, 1:19 acetone/dichloromethane) to afford **135** (27 mg, 58.4 %) as a colorless oil. ^{1}H NMR (500 MHz, $CDCl_3$-CD_3OD) δ 7.86 – 7.76 (m, 1H), 7.52 – 7.37 (m, 2H), 7.27 – 7.14 (m, 1H), 6.97 (d, *J* = 8.5 Hz, 1H), 4.96 – 4.86 (m, 4H). ^{13}C NMR (125 MHz, CD_3OD) δ 170.7, 157.4, 139.3, 136.4, 133.3,

131.7, 128.9, 128.8, 126.8, 125.3, 122.1, 116.7, 110.6, 55.6, 53.2. HRMS (ESI+) m/z [M + H^+] calcd for $C_{15}H_{12}Br_2NO_2$, 395.9235, found 395.9251.

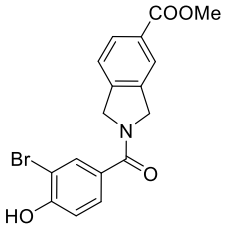

Methyl 2-(3-bromo-4-hydroxybenzoyl)isoindoline-5-carboxylate (136): 1-Ethyl-3-(3-dimethylaminopropyl) carbodiimide (88 mg, 0.46 mmol, 2.0 eq.) was added to a stirred solution of 3-bromo-4-hydroxybenzoic acid (50 mg, 0.23 mmol, 1 eq), methyl isoindoline-5-carboxylate hydrochloride (58 mg, 0.27 mmol, 1.2 eq.), 1-hydroxybenzotriazole (62 mg, 0.46 mmol, 2 eq.) N-,N-diisopropylethylamine (0.17 mL, 0.97 mmol, 4.2 eq.) in dichloromethane (3.0 mL) at 0 °C The resulting solution was stirred at rt for 14 h before the addition of saturated sodium bicarbonate solution (15 mL) and ethyl acetate (15 mL). The organic layer was washed with 1 N HCl (2 × 10 mL) and saturated sodium chloride solution (10 mL), dried over anhydrous sodium sulfate, filtered, and concentrated. The residue was triturated with dichloromethane (5 mL) to afford **136** (42 mg, 47.9 %) as a pale yellow amorphous solid. ^{1}H NMR (500 MHz, CD_3OD) δ 8.04 – 7.91 (m, 2H), 7.81 (d, *J* = 2.1 Hz, 1H), 7.53 – 7.35 (m, 2H), 6.99 (d, *J* = 8.4 Hz, 1H), 5.00 – 4.95 (m, 4H), 3.91 – 3.89 (m, 3H). ^{13}C NMR (125 MHz), CD_3OD δ 171.0, 168.2, 157.8, 143.1, 138.3, 133.7 (2), 131.2, 130.5, 129.7, 129.1, 125.1, 124.1, 110.8, 56.0, 53.6, 52.7. HRMS (ESI+) m/z [M + H^+] calcd for $C_{17}H_{15}BrNO_4$, 377.0263, found 377.0277.

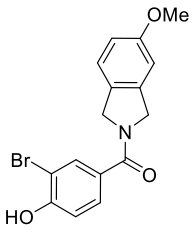

(3-Bromo-4-hydroxyphenyl)(5-methoxyisoindolin-2-yl)methanone (137): 1-Ethyl-3-(3-dimethylaminopropyl) carbodiimide (88 mg, 0.46 mmol, 2.0 eq.) was added to a stirred solution of 3-bromo-4-hydroxybenzoic acid (50 mg, 0.23 mmol, 1 eq.), 5-methoxyisoindoline hydrochloride (52 mg, 0.28 mmol, 1.2 eq.), 1-hydroxybenzotriazole (62 mg, 0.46 mmol, 2 eq.) N-,N-diisopropylethylamine (0.17 mL, 0.97 mmol, 4.2 eq.) in dichloromethane (3.0 mL) at 0 °C The resulting solution was stirred at rt for 14 h before the addition of saturated sodium bicarbonate solution (15 mL) and ethyl acetate (15 mL). The organic layer was washed with 1 N HCl (2 × 10 mL) and saturated sodium chloride solution (10 mL), dried over anhydrous sodium sulfate, filtered, and concentrated. The residue was triturated with dichloromethane (5 mL) to afford **137** (32 mg, 41.3 %) as a white amorphous solid. ^{1}H NMR (500 MHz, CD_3OD) δ 7.58 (d, *J* = 2.0 Hz, 1H), 7.28 (dd, *J* = 8.4, 2.1 Hz, 1H), 7.05–6.93 (m, 1H), 6.94 (d, *J* = 8.4 Hz, 1H), 6.78–6.59 (m, 2H), 4.66 – 4.57 (m, 4H), 3.60–3.57 (m, 3H).^{13}C NMR (125 MHz, CD_3OD) δ 169.6, 159.9, 156.3, 137.8, 137.0, 132.2, 127.8, 127.6, 123.1, 115.4, 113.9, 109.4, 107.1, 53.6, 54.4, 52.1. HRMS (ESI+) m/z [M - H^+] calcd for $C_{16}H_{13}BrNO_3$, 346.0079 found 346.0089.

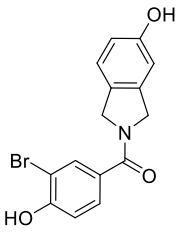

(3-Bromo-4-hydroxyphenyl)(5-hydroxyisoindolin-2-yl)methanone (138): Boron tribromide (1M solution in dichloromethane, 0.12 mL, 0.12 mmol, 2.0 eq.) was added to a solution of **136** (20 mg, 0.-06 mmol, 1.0 eq.) at 0 C. the resulting mixture was stirred at rt for 6 h before the addition of saturated sodium bicarbonate solution (10 mL) and ethyl acetate (10 mL). The organic layer was washed with saturated sodium chloride solution (10 mL), dried over anhydrous sodium sulfate,

filtered, and concentrated. The residue was triturated with dichloromethane (2 mL) to afford **138** (14 mg, 70.2 %) as pale yellow amorphous solid. ^{1}H NMR (500 MHz, Methanol-d_4) δ 7.78 (d, J = 2.0 Hz, 1H), 7.48 (dd, J = 8.4, 2.1 Hz, 1H), 7.16 – 7.04 (m, 1H), 6.98 (dd, J = 8.4, 1.3 Hz, 1H), 6.81 – 6.64 (m, 2H), 4.86 – 4.77(m, 4H). ^{13}C NMR (125 MHz, CD_3OD) δ 171.0, 158.6, 157.6, 138.7, 133.6, 129.7, 129.0, 127.9, 124.5, 116.8, 116.2, 110.7, 110.2, 56.0, 53.5. HRMS (ESI+) m/z [M + H^+] calcd for $C_{15}H_{13}BrNO_3$, 334.0079, found 334.0094.

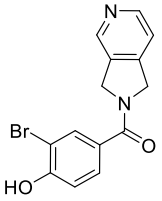

(3-Bromo-4-hydroxyphenyl)(1,3-dihydro-2H-pyrrolo[3,4-c]pyridin-2-yl)methanone (139):

1-Ethyl-3-(3-dimethylaminopropyl) carbodiimide (47 mg, 0.24 mmol, 2.0 eq.) was added to a stirred solution of 3-bromo-4-hydroxybenzoic acid (25 mg, 0.12 mmol, 1 eq), 2,3-dihydro-1H-pyrrolo[3,4-c]pyridine dihydrobromide (37 mg, 0.13 mmol, 1.2 eq.), 1-hydroxybenzotriazole (38 mg, 0.24 mmol, 2 eq.) N-,N-diisopropylethylamine (0.09 mL, 0.51 mmol, 4.2 eq.) in dichloromethane (2.0 mL) at 0 °C The resulting solution was stirred at rt for 14 h before the addition of saturated sodium bicarbonate solution (15 mL) and ethyl acetate (15 mL). The organic layer was washed with 1 N HCl (2 × 10 mL) and saturated sodium chloride solution (10 mL), dried over anhydrous sodium sulfate, filtered, and concentrated. The residue was triturated with dichloromethane (5 mL) to afford **139** (21 mg, 54.3 %) as a white amorphous solid. ^{1}H NMR (500 MHz, Methanol-d_4) δ 8.62 – 8.43 (m, 2H), 7.81 (d, J = 2.1 Hz, 1H), 7.52 – 7.33 (m, 2H), 6.97 (d, J = 8.4 Hz, 1H), 5.03 – 4.95 (m, 4H). ^{13}C NMR (125 MHz, CD_3OD) δ 171.1, 158.5, 148.9, 148.5, 145.0, 135.1, 133.7, 129.2, 128.8, 119.9, 117.1, 111.1, 55.0, 52.7. HRMS (ESI+) m/z [M + H^+] calcd for $C_{14}H_{12}N_2O_2$, 319.0082, found 319.0079.

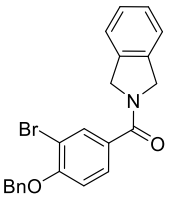

(4-(Benzyloxy)-3-bromophenyl)(isoindolin-2-yl)methanone (142): **)**: Potassium carbonate (10.22 g, 73.6 mmol, 4 eq) was added to a solution of 3-Bromo-4-hydroxybenzoic acid (4 g, 18.4 mmol, 1.0 eq) of acetonitrile (150 mL). Subsequently, benzyl bromide (4.37 mL, 4.05 mmol, 2.2 eq) was added dropwise, and the reaction was heated at 80 °C for 14 h. Upon cooling, the reaction mixture was filtered, the residue washed with ethyl acetate (100 mL), and concentrated. The resulting white solid (7.0 g, 17.8 mmol, 1 eq) was then suspended in a solvent mixture of tertrahydrofuran (60 mL), water (20 mL) and methanol (20 mL) and lithium hydroxide (1.29 g, 53.4 mmol, 3 eq) was added. The reaction stirred for 16 hours at room temperature, and concentrated. The residue was treated with 1 M hydrochloric acid solution and pH was adjusted to 2. The resulting mixture was extracted with ethyl acetate (3 × 100 mL). The combined organic layers were washed with saturated sodium chloride solution (200 mL), dried over anhydrous sodium sulfated, and concentrated. The resulting acid (5.19 g, 16.9 mmol, 1 eq) was added to a stirred solution of isoindoline hydrochloride (3.22 g, 25.35 mmol, 1.5 eq.), 1-hydroxybenzotriazole (3.73 g, 33.8 mmol, 2 eq.) *N*,*N*-diisopropylethylamine (4.81 mL, 33.8 mmol, 2.0 eq.) in dichloromethane (170 mL) at 0 °C. The resulting solution was stirred at rt for 14 h before quenching with saturated sodium bicarbonate solution (120 mL). The organic layer was washed with 1 M hydrochloric acid solution (120 mL) and saturated sodium chloride solution (120 mL), dried over anhydrous sodium sulfate, filtered, and concentrated. The residue was purified by flash chromatography (SiO2, 1:4 hexanes/ethyl acetate) to afford **142** (3.24 g, 43 %) as a light brown amorphous solid. ^{1}H NMR (400 MHz, $CDCl_3$) δ 7.85 (d, *J* = 2.0 Hz, 1H), 7.55 – 7.47 (m,

3H), 7.42 (t, *J* = 7.5 Hz, 2H), 7.33 (dq, *J* = 14.0, 6.8 Hz, 4H), 7.19 (d, *J* = 7.3 Hz, 1H), 6.99 (d, *J* = 8.5 Hz, 1H), 5.23 (s, 2H), 5.01 (s, 2H), 4.83 (s, 2H). ^{13}C NMR (100 MHz, $CDCl_3$) δ 168.8, 156.6, 136.4, 136.2 (2), 132.7, 130.5, 128.9 (2), 128.3, 128.1, 128.0, 127.8 (2), 127.2, 123.2, 122.7, 113.3, 112.5, 71.1, 55.3, 52.9. HRMS (ESI+) m/z [M + H^+] calcd for $C_{22}H_{19}BrNO_2$, 408.0599, found 408.0591.

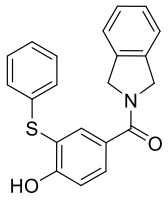

(4-Hydroxy-3-(phenylthio)phenyl)(isoindolin-2-yl)methanone (140): A biotage microwave vial was charged with **142** (100 mg, 0.25 mmol, 1 eq.), thiophenol (42 μl, 0.45 mmol, 1.9 eq.), 1,1′-ferrocenediyl-bis(diphenylphosphine) (45 mg, 0.05 mmol, 0.2 eq.), Tris(dibenzylideneacetone)dipalladium(0) (31 mg, 0.05 mmol, 0.2 eq.), *N*,*N*'-diisopropylethylamine (79 μL, 0.46 mmol, 1.9 eq.). The tube was sealed with a cap lined with a disposable Teflon septum. The tube was evacuated and purged with nitrogen (3 times), before the addition of toluene (3.0 mL) by syringe. The resulting mixture was heated at 120 °C for 18 h, cooled to rt, and filtered through a small pad of celite (elution with ethyl acetate). Solvent was removed and the residue purified by flash chromatography (SiO_2, 1:3 ethyl acetate/hexanes) to give the corresponding 5-substituted product, which was used further as obtained, and taken in dichloromethane (2 mL), cooled to 0 °C before the addition of 1 M solution of boron tribromide (0.6 mL). The resulting mixture was stirred for 6 h, quenched with saturated sodium bicarbonate solution (5 mL) and extracted with dichloromethane (2 × 10 mL). The combined organic layers were washed with saturated sodium chloride solution (15 mL), dried over anhydrous sodium

sulfate, filtered, and concentrated. The residue purified with flash chromatography (SiO_2, 1:2 ethyl acetate/hexanes) to give the desired product **140** as white amorphous solid (36 mg, 41 ^{1}H NMR (400 MHz, $CDCl_3$) δ 7.83 (d, *J* = 2.1 Hz, 1H), 7.66 (dd, *J* = 8.4, 2.2 Hz, 1H), 7.36 – 7.25 (m, 4H), 7.23 – 7.11 (m, 5H), 6.82 (s, 1H), 5.01 (s, 2H), 4.82 (s, 2H). ^{13}C NMR (100 MHz, $CDCl_3$) δ 169.2, 158.8, 136.6, 136.5, 136.0, 135.2, 131.7, 129.8, 129.6 (2), 128.1, 127.8, 127.7, 126.9 (2), 123.1, 122.6, 117.4, 115.8, 55.3, 52.9. HRMS (ESI+) m/z [M + H^+] calcd for $C_{21}H_{18}NO_2S$, 348.1058, found 348.1051.

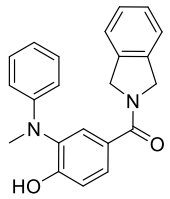

(4-hydroxy-3-(methyl(phenyl)amino)phenyl)(isoindolin-2-yl)methanone: A biotage microwave vial was charged with **142** (100 mg, 0.25 mmol, 1 eq.), N-methyl aniline (44 μl, 0.36 mmol, 1.5 eq.), RuPhos (10 mg, 0.02 mmol, 0.08 eq.), Tris(dibenzylideneacetone)dipalladium(0) (22 mg, 0.02 mmol, 0.1 eq.), sodium *tert*-butoxide (35 mg, 0.36 mmol, 1.5 eq.). The tube was sealed with a cap lined with a disposable Teflon septum. The tube was evacuated and purged with nitrogen (3 times), before the addition of toluene (3.0 mL) by syringe. The resulting mixture was heated at 120 °C for 18 h, cooled to rt, and filtered through a small pad of celite (elution with ethyl acetate). Solvent was removed and the residue purified by flash chromatography (SiO_2, 1:3 ethyl acetate/hexanes) to give the corresponding 5-substituted product, which was used further as obtained, and taken in dichloromethane (2 mL), cooled to 0 °C before the addition of 1 M solution of boron tribromide (0.6 mL). The resulting mixture was stirred for 6 h, quenched with saturated sodium bicarbonate solution (5 mL) and extracted with dichloromethane (2 × 10 mL). The combined organic layers were washed with saturated sodium chloride solution (15 mL), dried over

anhydrous sodium sulfate, filtered, and concentrated. The residue purified with flash chromatography (SiO_2, 1:2 ethyl acetate/hexanes) to give the desired product **141** as white amorphous solid (36 mg, 41 %). ^{1}H NMR (400 MHz, $CDCl_3$) δ 7.49 (dd, *J* = 8.4, 2.1 Hz, 1H), 7.41 (d, *J* = 2.1 Hz, 1H), 7.30 (dd, *J* = 9.9, 4.3 Hz, 3H), 7.25 – 7.22 (m, 1H), 7.17 (d, *J* = 7.3 Hz, 1H), 7.12 (d, *J* = 8.4 Hz, 1H), 6.89 (tt, *J* = 7.3, 1.0 Hz, 1H), 6.79 – 6.74 (m, 2H), 6.35 (s, 1H), 4.98 (s, 2H), 4.80 (s, 2H), 3.24 (s, 3H).^{13}C NMR (101 MHz, $CDCl_3$) δ 169.7, 154.6, 149.2, 136.6 (2), 135.9, 129.9, 129.5 (2), 128.0, 127.7, 127.5, 126.9, 123.1, 122.6, 120.0, 115.5, 115.4 (2), 55.3, 52.8, 40.3. HRMS (ESI+) m/z [M + H^+] calcd for $C_{22}H_{21}N_2O_2$, 345.1603, found 345.1612.

V.11. References

1. Duerfeldt, A. S.; Peterson, L. B.; Maynard, J. C.; Ng, C. L.; Eletto, D.; Ostrovsky, O.; Shinogle, H. E.; Moore, D. S.; Argon, Y.; Nicchitta, C. V.; Blagg, B. S. Development of a Grp94 inhibitor. *J. Am. Chem. Soc.* **2012**, 134, 9796-9804.
2. Patel, P. D.; Yan, P.; Seidler, P. M.; Patel, H. J.; SUn, W.; Yang, C.; Que, N. S.; Taldone, T.; Finotti, P.; Stephani, R. A.; Gewirth, D. T.; Chiosis, G. Paralog-Selective Hsp90 Inhibitors Define Tumor-Specific Regulation of HER2. *Nat. Chem. Biol.* **2013**, *11*, 677-684.
3. Peterson, L. B.; Eskew, J. D.; Vielhauer, G. A.; Blagg, B. S. The hERG channel is dependent upon the Hsp90α isoform for maturation and trafficking. *Mol. Pharmacol.* **2012**, 9, 1841-1846.
4. Lee, C.; Park, H. K.; Jeong, H.; Lim, J.; Lee, A. J.; Cheon, K. Y.; Kim, C. S.; Thomas, A. P.; Bae, B.; Kim, N. D.; Kim, S. H.; Suh, P. G.; Ryu, J. H.; Kang, B. H. Development of a mitochondria-targeted Hsp90 inhibitor based on the crystal structures of human TRAP1. *J. Am. Chem. Soc.* **2015**, 137, 4358-4367.
5. Crowley, V. M.; Khandelwal, A.; Mishra, S.; Stothert, A. R.; Huard, D. J.; Zhao, J.; Muth, A.; Duerfeldt, A. S.; Kizziah, J. L.; Lieberman, R. L.; Dickey, C. A.; Blagg, B. S. Development of Glucose Regulated Protein 94-Selective Inhibitors Based on the BnIm and Radamide Scaffold. *J. Med. Chem.* **2016**, 59, 3471-3488.
6. Muth, A.; Crowley, V.; Khandelwal, A.; Mishra, S.; Zhao, J.; Hall, J.; Blagg, B. S. Development of radamide analogs as Grp94 inhibitors. *Bioorg. Med. Chem.* **2014**, 22, 4083-4098.
7. Gewirth, D. T. Paralog specific Hsp90 Inhibitors - a brief history and a bright future. *Curr.Top. Med. Chem.* **2016**, PMID: 27072700.
8. Ansa-Addo, E. A.; Thaxton, J.; Hong, F.; Wu, B. X.; Zhang, Y.; Fugle, C. W.; Metelli, A.; Riesenberg, B.; Williams, K.; Gewirth, D. T.; Chiosis, G.; Liu, B.; Li, Z. Clients and Oncogenic Roles of Molecular Chaperone gp96/grp94. *Curr. Top. Med. Chem.* **2016**, PMID: 27072698.

9. Neckers, L.; Workman, P. Hsp90 molecular chaperone inhibitors: are we there yet? *Clin. Cancer Res.* **2012**, 18, 64-76.
10. Klietmann, W.; Focht, J.; Nosner, K. [Comparative in vitro study of the antimicrobial activity of ceftazidime against clinical isolates]. *Infection* **1987**, 15 Suppl 4, S145-149.
11. Soga, S.; Akinaga, S.; Shiotsu, Y. Hsp90 inhibitors as anti-cancer agents, from basic discoveries to clinical development. *Curr. Pharm. Des.* **2013**, 19, 366-376.
12. Liu, W.; Vielhauer, G. A.; Holzbeierlein, J. M.; Zhao, H.; Ghosh, S.; Brown, D.; Lee, E.; Blagg, B. S. KU675, a Concomitant Heat-Shock Protein Inhibitor of Hsp90 and Hsc70 that Manifests Isoform Selectivity for Hsp90α in Prostate Cancer Cells. *Mol. Pharmacol.* **2015**, 88, 121-130.
13. Stothert, A. R.; Suntharalingam, A.; Huard, D. J.; Fontaine, S. N.; Crowley, V. M.; Mishra, S.; Blagg, B. S.; Lieberman, R. L.; Dickey, C. A. Exploiting the interaction between Grp94 and aggregated myocilin to treat glaucoma. *Hum Mol. Genet.* **2014**, 23, 6470-6480.
14. Suntharalingam, A.; Abisambra, J. F.; O'Leary, J. C., 3rd; Koren, J., 3rd; Zhang, B.; Joe, M. K.; Blair, L. J.; Hill, S. E.; Jinwal, U. K.; Cockman, M.; Duerfeldt, A. S.; Tomarev, S.; Blagg, B. S.; Lieberman, R. L.; Dickey, C. A. Glucose-regulated protein 94 triage of mutant myocilin through endoplasmic reticulum-associated degradation subverts a more efficient autophagic clearance mechanism. *J. Biol. Chem.* **2012**, 287, 40661-40669.
15. Didelot, C.; Lanneau, D.; Brunet, M.; Bouchot, A.; Cartier, J.; Jacquel, A.; Ducoroy, P.; Cathelin, S.; Decologne, N.; Chiosis, G.; Dubrez-Daloz, L.; Solary, E.; Garrido, C. Interaction of heat-shock protein 90β isoform HSP90β with cellular inhibitor of apoptosis 1 (c-IAP1) is required for cell differentiation. *Cell Death Differ.* **2008**, *15*, 859-866.
16. Muth, A.; Crowley, V.; Khandelwal, A.; Mishra, S.; Zhao, J.; Hall, J.; Blagg, B. S. Development of radamide analogs as Grp94 inhibitors. *Bioorg. Med. Chem.* **2014**, 22, 4083-4098.
17. Patel, H. J.; Patel, P. D.; Ochiana, S. O.; Yan, P.; Sun, W.; Patel, M. R.; Shah, S. K.; Tramentozzi, E.; Brooks, J.; Bolaender, A.; Shrestha, L.; Stephani, R.; Finotti, P.; Leifer, C.; Li, Z.; Gewirth, D. T.; Taldone, T.; Chiosis, G. Structure-activity relationship in a purine-scaffold compound series with selectivity for the endoplasmic reticulum Hsp90 paralog Grp94. *J. Med. Chem.* **2015**, 58, 3922-3943.
18. Sreedhar, A. S.; Kalmar, E.; Csermely, P.; Shen, Y. F. Hsp90 isoforms: functions, expression and clinical importance. *FEBS Lett.* **2004**, 562, 11-15.
19. Csermely, P.; Schnaider, T.; Soti, C.; Prohaszka, Z.; Nardai, G. The 90-kDa molecular chaperone family: structure, function, and clinical applications. A comprehensive review. *Pharmacol. Ther.* **1998**, 79, 129-168.
20. Zubriene, A.; Gutkowska, M.; Matuliene, J.; Chaleckis, R.; Michailoviene, V.; Voroncova, A.; Venclovas, C.; Zylicz, A.; Zylicz, M.; Matulis, D. Thermodynamics of radicicol binding to human Hsp90 α and β isoforms. *Biophys. Chem.* **2010**, 152, 153-163.
21. Chen, B.; Piel, W. H.; Gui, L.; Bruford, E.; Monteiro, A. The HSP90 family of genes in the human genome: insights into their divergence and evolution. *Genomics* **2005**, 86, 627-637.
22. Pepin, K.; Momose, F.; Ishida, N.; Nagata, K. Molecular cloning of horse Hsp90 cDNA and its comparative analysis with other vertebrate Hsp90 sequences. *J. Vet. Med. Sci.* **2001**, 63, 115-124.

23. Yamada, T.; Hashiguchi, A.; Fukushima, S.; Kakita, Y.; Umezawa, A.; Maruyama, T.; Hata, J. Function of 90-kDa heat shock protein in cellular differentiation of human embryonal carcinoma cells. *In Vitro Cell Dev. Biol. Anim.* **2000**, 36, 139-146.
24. Lele, Z.; Hartson, S. D.; Martin, C. C.; Whitesell, L.; Matts, R. L.; Krone, P. H. Disruption of zebrafish somite development by pharmacologic inhibition of Hsp90. *Dev. Biol.* **1999**, 210, 56-70.
25. Prince, T. L.; Kijima, T.; Tatokoro, M.; Lee, S.; Tsutsumi, S.; Yim, K.; Rivas, C.; Alarcon, S.; Schwartz, H.; Khamit-Kush, K.; Scroggins, B. T.; Beebe, K.; Trepel, J. B.; Neckers, L. Client Proteins and Small Molecule Inhibitors Display Distinct Binding Preferences for Constitutive and Stress-Induced HSP90 Isoforms and Their Conformationally Restricted Mutants. *PloS one* **2015**, 10, e0141786.
26. Grad, I.; Cederroth, C. R.; Walicki, J.; Grey, C.; Barluenga, S.; Winssinger, N.; De Massy, B.; Nef, S.; Picard, D. The molecular chaperone Hsp90α is required for meiotic progression of spermatocytes beyond pachytene in the mouse. *PloS one* **2010**, 5, e15770.
27. Kajiwara, C.; Kondo, S.; Uda, S.; Dai, L.; Ichiyanagi, T.; Chiba, T.; Ishido, S.; Koji, T.; Udono, H. Spermatogenesis arrest caused by conditional deletion of Hsp90α in adult mice. *Biology open* **2012**, 1, 977-982.
28. Saribek, B.; Jin, Y.; Saigo, M.; Eto, K.; Abe, S. HSP90β is involved in signaling prolactin-induced apoptosis in newt testis. *Biochem. Biophys. Res. Comm.* **2006,** 349, 1190-1197.
29. Voss, A. K.; Thomas, T.; Gruss, P. Mice lacking HSP90β fail to develop a placental labyrinth. *Development* **2000**, 127, 1-11.
30. Bohonowych, J. E.; Hance, M. W.; Nolan, K. D.; Defee, M.; Parsons, C. H.; Isaacs, J. S. Extracellular Hsp90 mediates an NF-kappaB dependent inflammatory stromal program: implications for the prostate tumor microenvironment. *The Prostate* **2014**, 74, 395-407.
31. Zuehlke, A. D.; Beebe, K.; Neckers, L.; Prince, T. Regulation and function of the human HSP90AA1 gene. *Gene* **2015**, 570, 8-16.
32. Ammirante, M.; Rosati, A.; Gentilella, A.; Festa, M.; Petrella, A.; Marzullo, L.; Pascale, M.; Belisario, M. A.; Leone, A.; Turco, M. C. The activity of hsp90α promoter is regulated by NF-kappa B transcription factors. *Oncogene* **2008**, 27, 1175-1178.
33. Jiang, H.; Duan, B.; He, C.; Geng, S.; Shen, X.; Zhu, H.; Sheng, H.; Yang, C.; Gao, H. Cytoplasmic HSP90α expression is associated with perineural invasion in pancreatic cancer. *Int. J. Clin. Exp. Pathol.* **2014**, 7, 3305-3311.
34. Chen, W. S.; Chen, C. C.; Chen, L. L.; Lee, C. C.; Huang, T. S. Secreted heat shock protein HSP90α induces nuclear factor-kappaB-mediated TCF12 protein expression to down-regulate E-cadherin and to enhance colorectal cancer cell migration and invasion. *J. Biol. Chem.* **2013**, 288, 9001-9010.
35. Yufu, Y.; Nishimura, J.; Nawata, H. High constitutive expression of heat shock protein 90 α in human acute leukemia cells. *Leuk. Res.* **1992**, 16, 597-605.
36. Yano, M.; Naito, Z.; Yokoyama, M.; Shiraki, Y.; Ishiwata, T.; Inokuchi, M.; Asano, G. Expression of hsp90 and cyclin D1 in human breast cancer. *Cancer Lett.* **1999**, 137, 45-51.
37. Tsutsumi, S.; Neckers, L. Extracellular heat shock protein 90: a role for a molecular chaperone in cell motility and cancer metastasis. *Cancer Sci.* **2007**, 98, 1536-1539.
38. Gopal, U.; Bohonowych, J. E.; Lema-Tome, C.; Liu, A.; Garrett-Mayer, E.; Wang, B.; Isaacs, J. S. A novel extracellular Hsp90 mediated co-receptor function for LRP1 regulates EphA2 dependent glioblastoma cell invasion. *PloS one* **2011**, 6, e17649.

39. Eustace, B. K.; Sakurai, T.; Stewart, J. K.; Yimlamai, D.; Unger, C.; Zehetmeier, C.; Lain, B.; Torella, C.; Henning, S. W.; Beste, G.; Scroggins, B. T.; Neckers, L.; Ilag, L. L.; Jay, D. G. Functional proteomic screens reveal an essential extracellular role for hsp90α in cancer cell invasiveness. *Nat. Cell. Biol.* **2004**, 6, 507-514.
40. Song, X.; Wang, X.; Zhuo, W.; Shi, H.; Feng, D.; Sun, Y.; Liang, Y.; Fu, Y.; Zhou, D.; Luo, Y. The regulatory mechanism of extracellular Hsp90α on matrix metalloproteinase-2 processing and tumor angiogenesis. *J. Biol. Chem.* **2010**, 285, 40039-40049.
41. Li, W.; Tsen, F.; Sahu, D.; Bhatia, A.; Chen, M.; Multhoff, G.; Woodley, D. T. Extracellular Hsp90 (eHsp90) as the actual target in clinical trials: intentionally or unintentionally. *Int. Rev. Cell Mol. Biol.* **2013**, 303, 203-235.
42. Wright, L.; Barril, X.; Dymock, B.; Sheridan, L.; Surgenor, A.; Beswick, M.; Drysdale, M.; Collier, A.; Massey, A.; Davies, N.; Fink, A.; Fromont, C.; Aherne, W.; Boxall, K.; Sharp, S.; Workman, P.; Hubbard, R. E. Structure-activity relationships in purine-based inhibitor binding to HSP90 isoforms. *Chem. Biol.* **2004**, 11, 775-785.
43. Roe, S. M.; Prodromou, C.; O'Brien, R.; Ladbury, J. E.; Piper, P. W.; Pearl, L. H. Structural basis for inhibition of the Hsp90 molecular chaperone by the antitumor antibiotics radicicol and geldanamycin. *J. Med. Chem.* **1999**, 42, 260-266.
44. Patel, P. D.; Yan, P.; Seidler, P. M.; Patel, H. J.; Sun, W.; Yang, C.; Que, N. S.; Taldone, T.; Finotti, P.; Stephani, R. A.; Gewirth, D. T.; Chiosis, G. Paralog-selective Hsp90 inhibitors define tumor-specific regulation of HER2. *Nat. Chem. Biol.* **2013**, 9, 677-684.
45. Ernst, J. T.; Neubert, T.; Liu, M.; Sperry, S.; Zuccola, H.; Turnbull, A.; Fleck, B.; Kargo, W.; Woody, L.; Chiang, P.; Tran, D.; Chen, W.; Snyder, P.; Alcacio, T.; Nezami, A.; Reynolds, J.; Alvi, K.; Goulet, L.; Stamos, D. Identification of Novel HSP90α/β Isoform Selective Inhibitors Using Structure-Based Drug Design. Demonstration of Potential Utility in Treating CNS Disorders such as Huntington's Disease. *J. Med. Chem.* **2014**, 57, 3382-3400.
46. Sun, J.; Lin, C.; Qin, X.; Dong, X.; Tu, Z.; Tang, F.; Chen, C.; Zhang, J. Synthesis and biological evaluation of 3,5-disubstituted-4-alkynylisoxozales as a novel class of HSP90 inhibitors. *Bioorg. Med. Chem.* **2015**, 25, 3129-3134.
47. Murray, C. W.; Carr, M. G.; Callaghan, O.; Chessari, G.; Congreve, M.; Cowan, S.; Coyle, J. E.; Downham, R.; Figueroa, E.; Frederickson, M.; Graham, B.; McMenamin, R.; O'Brien, M. A.; Patel, S.; Phillips, T. R.; Williams, G.; Woodhead, A. J.; Woolford, A. J. Fragment-based drug discovery applied to Hsp90. Discovery of two lead series with high ligand efficiency. *J. Med. Chem.* **2010**, 53, 5942-5955.
48. Woodhead, A. J.; Angove, H.; Carr, M. G.; Chessari, G.; Congreve, M.; Coyle, J. E.; Cosme, J.; Graham, B.; Day, P. J.; Downham, R.; Fazal, L.; Feltell, R.; Figueroa, E.; Frederickson, M.; Lewis, J.; McMenamin, R.; Murray, C. W.; O'Brien, M. A.; Parra, L.; Patel, S.; Phillips, T.; Rees, D. C.; Rich, S.; Smith, D. M.; Trewartha, G.; Vinkovic, M.; Williams, B.; Woolford, A. J. Discovery of (2,4-dihydroxy-5-isopropylphenyl)-[5-(4-methylpiperazin-1-ylmethyl)-1,3-dihydrois oindol-2-yl]methanone (AT13387), a novel inhibitor of the molecular chaperone Hsp90 by fragment based drug design. *J. Med Chem.* **2010**, 53, 5956-5969.
49. He, H.; Zatorska, D.; Kim, J.; Aguirre, J.; Llauger, L.; She, Y.; Wu, N.; Immormino, R. M.; Gewirth, D. T.; Chiosis, G. Identification of potent water soluble purine-scaffold inhibitors of the heat shock protein 90. *J. Med. Chem.* **2006**, 49, 381-390.

50. Chiosis, G.; Lucas, B.; Shtil, A.; Huezo, H.; Rosen, N. Development of a purine-scaffold novel class of Hsp90 binders that inhibit the proliferation of cancer cells and induce the degradation of Her2 tyrosine kinase. *Bioorg. Med. Chem.* **2002**, 10, 3555-3564.
51. Barta, T. E.; Veal, J. M.; Rice, J. W.; Partridge, J. M.; Fadden, R. P.; Ma, W.; Jenks, M.; Geng, L.; Hanson, G. J.; Huang, K. H.; Barabasz, A. F.; Foley, B. E.; Otto, J.; Hall, S. E. Discovery of benzamide tetrahydro-4H-carbazol-4-ones as novel small molecule inhibitors of Hsp90. *Bioorg. Med. Chem. Lett.* **2008**, 18, 3517-3521.
52. Stebbins, C. E.; Russo, A. A.; Schneider, C.; Rosen, N.; Hartl, F. U.; Pavletich, N. P. Crystal structure of an Hsp90-geldanamycin complex: targeting of a protein chaperone by an antitumor agent. *Cell* **1997**, 89, 239-250.
53. Brough, P. A.; Aherne, W.; Barril, X.; Borgognoni, J.; Boxall, K.; Cansfield, J. E.; Cheung, K. M.; Collins, I.; Davies, N. G.; Drysdale, M. J.; Dymock, B.; Eccles, S. A.; Finch, H.; Fink, A.; Hayes, A.; Howes, R.; Hubbard, R. E.; James, K.; Jordan, A. M.; Lockie, A.; Martins, V.; Massey, A.; Matthews, T. P.; McDonald, E.; Northfield, C. J.; Pearl, L. H.; Prodromou, C.; Ray, S.; Raynaud, F. I.; Roughley, S. D.; Sharp, S. Y.; Surgenor, A.; Walmsley, D. L.; Webb, P.; Wood, M.; Workman, P.; Wright, L. 4,5-diarylisoxazole Hsp90 chaperone inhibitors: potential therapeutic agents for the treatment of cancer. *J. Med. Chem.* **2008**, 51, 196-218.
54. Shi, J.; Van de Water, R.; Hong, K.; Lamer, R. B.; Weichert, K. W.; Sandoval, C. M.; Kasibhatla, S. R.; Boehm, M. F.; Chao, J.; Lundgren, K.; Timple, N.; Lough, R.; Ibanez, G.; Boykin, C.; Burrows, F. J.; Kehry, M. R.; Yun, T. J.; Harning, E. K.; Ambrose, C.; Thompson, J.; Bixler, S. A.; Dunah, A.; Snodgrass-Belt, P.; Arndt, J.; Enyedy, I. J.; Li, P.; Hong, V. S.; McKenzie, A.; Biamonte, M. A. EC144 is a potent inhibitor of the heat shock protein 90. *J. Med. Chem.* **2012**, 55, 7786-7795.
55. Ren, J.; Li, J.; Wang, Y.; Chen, W.; Shen, A.; Liu, H.; Chen, D.; Cao, D.; Li, Y.; Zhang, N.; Xu, Y.; Geng, M.; He, J.; Xiong, B.; Shen, J. Identification of a new series of potent diphenol HSP90 inhibitors by fragment merging and structure-based optimization. *Bioorg. Med. Chem. Lett.* **2014,** 24, 2525-9.